EPIGENETIC MECHANISMS AND POST-TRANSLATIONAL MODIFICATIONS AS NOVEL THERAPEUTIC TARGETS IN CANCER

EDITED BY: Yi-Chao Zheng, Zhi Shi, Ning Wang and Yingjie Zhang

PUBLISHED IN: Frontiers in Pharmacology

frontiers Research Topics

frontiers

ISSN 1664-8714
ISBN 978-2-88976-983-4
DOI 10.3389/978-2-88976-983-4

About Frontiers

Frontiers is more than just an open-access publisher of scholarly articles: it is a pioneering approach to the world of academia, radically improving the way scholarly research is managed. The grand vision of Frontiers is a world where all people have an equal opportunity to seek, share and generate knowledge. Frontiers provides immediate and permanent online open access to all its publications, but this alone is not enough to realize our grand goals.

Frontiers Journal Series

The Frontiers Journal Series is a multi-tier and interdisciplinary set of open-access, online journals, promising a paradigm shift from the current review, selection and dissemination processes in academic publishing. All Frontiers journals are driven by researchers for researchers; therefore, they constitute a service to the scholarly community. At the same time, the Frontiers Journal Series operates on a revolutionary invention, the tiered publishing system, initially addressing specific communities of scholars, and gradually climbing up to broader public understanding, thus serving the interests of the lay society, too.

Dedication to Quality

Each Frontiers article is a landmark of the highest quality, thanks to genuinely collaborative interactions between authors and review editors, who include some of the world's best academicians. Research must be certified by peers before entering a stream of knowledge that may eventually reach the public - and shape society; therefore, Frontiers only applies the most rigorous and unbiased reviews.
Frontiers revolutionizes research publishing by freely delivering the most outstanding research, evaluated with no bias from both the academic and social point of view. By applying the most advanced information technologies, Frontiers is catapulting scholarly publishing into a new generation.

What are Frontiers Research Topics?

Frontiers Research Topics are very popular trademarks of the Frontiers Journals Series: they are collections of at least ten articles, all centered on a particular subject. With their unique mix of varied contributions from Original Research to Review Articles, Frontiers Research Topics unify the most influential researchers, the latest key findings and historical advances in a hot research area! Find out more on how to host your own Frontiers Research Topic or contribute to one as an author by contacting the Frontiers Editorial Office: frontiersin.org/about/contact

EPIGENETIC MECHANISMS AND POST-TRANSLATIONAL MODIFICATIONS AS NOVEL THERAPEUTIC TARGETS IN CANCER

Topic Editors:
Yi-Chao Zheng, Zhengzhou University, China
Zhi Shi, Jinan University, China
Ning Wang, The University of Hong Kong, Hong Kong, SAR China
Yingjie Zhang, Shandong University, China

Citation: Zheng, Y.-C., Shi, Z., Wang, N., Zhang, Y., eds. (2022). Epigenetic Mechanisms and Post-translational Modifications as Novel Therapeutic Targets in Cancer. Lausanne: Frontiers Media SA. doi: 10.3389/978-2-88976-983-4

Table of Contents

frontiers | Frontiers in Pharmacology

TYPE Editorial
PUBLISHED 08 August 2022
DOI 10.3389/fphar.2022.988334

OPEN ACCESS

EDITED AND REVIEWED BY
Heike Wulff,
University of California, Davis,
United States

*CORRESPONDENCE
Zhi Shi,
tshizhi@jnu.edu.cn
Ning Wang,
ckwang@hku.hk
Ying-Jie Zhang,
zhangyingjie@sdu.edu.cn
Yi-Chao Zheng,
yichaozheng@zzu.edu.cn

SPECIALTY SECTION
This article was submitted to Experimental Pharmacology and Drug Discovery,
a section of the journal
Frontiers in Pharmacology

RECEIVED 07 July 2022
ACCEPTED 08 July 2022
PUBLISHED 08 August 2022

CITATION
Shi Z, Wang N, Zhang Y-J and Zheng Y-C (2022), Editorial: Epigenetic mechanisms and post-translational modifications as novel therapeutic targets in cancer.
Front. Pharmacol. 13:988334.
doi: 10.3389/fphar.2022.988334

Editorial: Epigenetic mechanisms and post-translational modifications as novel therapeutic targets in cancer

Zhi Shi[1]*, Ning Wang[2]*, Ying-Jie Zhang[3]* and Yi-Chao Zheng[4,5,6]*

[1]Department of Cell Biology & Institute of Biomedicine, National Engineering Research Center of Genetic Medicine, MOE Key Laboratory of Tumor Molecular Biology, Guangdong Provincial Key Laboratory of Bioengineering Medicine, College of Life Science and Technology, Jinan University, Guangzhou, Guangdong, China, [2]School of Chinese Medicine, The University of Hong Kong, Hong Kong, China, [3]MOE Key Laboratory of Chemical Biology, Department of Medicinal Chemistry, School of Pharmaceutical Sciences, Cheeloo College of Medicine, Shandong University, Jinan, China, [4]Collaborative Innovation Centre of New Drug Research and Safety Evaluation, Zhengzhou, Henan Province, China, [5]Key Laboratory of Advanced Drug Preparation Technologies, Zhengzhou University, Zhengzhou, Henan Province, China, [6]MOE Key Laboratory of Henan Province for Drug Quality and Evaluation, School of Pharmaceutical Sciences, Zhenghzou University, Zhengzhou, Henan Province, China

KEYWORDS

cancer, targets, epigenetic mechanisms, post-translational modifications, methylation

Editorial on the Research Topic
Epigenetic mechanisms and post-translational modifications as novel therapeutic targets in cancer

This Research Topic "*Epigenetic mechanisms and post-translational modifications as novel therapeutic targets in cancer*" collected 11 articles on epigenetic mechanisms, post-translational modifications, cell cycle and signaling pathways related to tumorigenesis and development. Our aim is to provide new research directions for targeted cancer therapies and drug development.

Epigenetic modifications affect genetic expression without the sequence change of DNA, and its disorders are closely related to the occurrence and progression of cancer. Methylation is a widely studied form of epigenetic modification. Zhou et al. summarized the role and mechanism of the modification related enzymes "Writers" and "Erasers" in cancer, providing a basis for the development of anti-tumor epigenetic drugs. Tang et al. assessed the causal relationship between smoking-related DNA methylation and breast cancer risk by Mendelian randomization. The results suggest that DNA methylation plays an important role in linking smoking to breast cancer, especially the subtype of ER^+ breast cancer. Zeng et al. evaluated pyroptosis-related genes in esophageal adenocarcinoma and found that the expressions of GSDMB and ZBP1 were influenced by DNA methylation levels. Huo et al. focused on the role of RNA modification in cancer. They summarized the molecular mechanism of RNA modification in the occurrence and development of head

and neck squamous cell carcinoma and discussed the related treatment options. Jing et al. demonstrated that hypoxia induced upregulation of ELFN1-AS1 expression in colorectal cancer cells. As a potential target of competing endogenous RNA, ELFN1-AS1 relieved the inhibition of TRIM14 by sponging miR-191-5p, thus promoting the proliferation and invasion of colorectal cancer cells. Lu et al. elucidated the role of acetylation modification in tumor immunity by focusing on histone acetyltransferases and deacetylases, and discussed the clinical application of acetylation-modified drugs in tumor therapy.

Post-translational modifications increase the protein diversity and play critical roles in regulating the protein activity, localization, and interaction with other molecules. Hou et al. provided evidence that low expression of USP47 in the primary colorectal cancer was associated with disease-free survival. USP47 deubiquitinated and stabilized the expression of transcription elongation factor A3 (TCEA3). Knockdown of UPS47 or TCEA3 can enhance doxorubicin-induced apoptosis and pyrotosis of colorectal cancer cells, which provides a potential target for the treatment of colorectal cancer.

In normal cells, cell cycle and signal transduction are strictly regulated, and their dysregulation and abnormal activation lead to various diseases including cancer. Xia et al. identified aminoquinoline as a novel multi-kinase inhibitor of CDK4/6 and PI3K/AKT for the treatment of hepatocellular carcinoma. Zhao et al. revealed that lysophosphatidic acid induced transactivation of EGFR through MMP-dependent pathway, which upregulated geminin expression and promoted DNA replication in gastric cancer cells. Guo et al. found that a natural microbial product, Ilicicolin A, as a novel EZH2 antagonist, inhibited the EZH2-mediated signaling pathway to enhance the sensitivity of castration-resistant prostate cancer cells to enzalutamide. Yang et al. investigated the role of kinesin family member 2C (KIF2C) in cervical cancer. KIF2C expression was significantly upregulated in cervical cancer, promoted cervical cancer cells proliferation, invasion, and migration. Knockdown of KIF2C inhibited the development of cervical cancer by activating p53 signaling pathway, providing a new target for the treatment of cervical cancer.

In conclusion, the "*Epigenetic mechanisms and post-translational modifications as novel therapeutic targets in cancer*" Research Topic emphasizes that epigenetic and post-translational modification provide new targets for the development of anti-cancer drugs and bring new strategies for treatment of cancer.

Author contributions

All authors listed have made a substantial, direct, and intellectual contribution to the work and approved it for publication.

Funding

ZS was supported by funds from the National Key Research and Development Program of China No. 2017YFA0505104 and the Science and Technology Program of Guangzhou No. 202206010081.

Conflict of interest

The authors declare that the research was conducted in the absence of any commercial or financial relationships that could be construed as a potential conflict of interest.

Publisher's note

frontiers in Pharmacology

REVIEW
published: 03 June 2021
doi: 10.3389/fphar.2021.690057

Methylation Landscape: Targeting Writer or Eraser to Discover Anti-Cancer Drug

Wen-min Zhou[1†], Bin Liu[2†], Amin Shavandi[3], Lu Li[4], Hang Song[4]* and Jian-ye Zhang[1]**

[1]Key Laboratory of Molecular Target & Clinical Pharmacology and the State Key Laboratory of Respiratory Disease, School of Pharmaceutical Sciences & the Fifth Affiliated Hospital, Guangzhou Medical University, Guangzhou, China, [2]Department of Cellular and Molecular Biology, Beijing Chest Hospital, Capital Medical University/Beijing Tuberculosis and Thoracic Tumor Research Institute, Beijing, China, [3]BioMatter Unit, École Polytechnique de Bruxelles, Université Libre de Bruxelles (ULB), Brussels, Belgium, [4]Department of Biochemistry and Molecular Biology, School of Integrated Chinese and Western Medicine, Anhui University of Chinese Medicine, Hefei, China

OPEN ACCESS

Edited by:
Yi-Chao Zheng,
Zhengzhou University, China

Reviewed by:
Faming Wang,
Blood Center of Wisconsin, United States
Fazhi Yu,
University of Science and Technology of China, China

***Correspondence:**
Lu Li
deerlyee@hotmail.com
Hang Song
tosonghang@sina.com
Jian-ye Zhang
jianyez@163.com

[†]These authors have contributed equally to this work

Specialty section:
This article was submitted to Experimental Pharmacology and Drug Discovery, a section of the journal Frontiers in Pharmacology

Received: 02 April 2021
Accepted: 18 May 2021
Published: 03 June 2021

Citation:
Zhou W-m, Liu B, Shavandi A, Li L, Song H and Zhang J-y (2021) Methylation Landscape: Targeting Writer or Eraser to Discover Anti-Cancer Drug. Front. Pharmacol. 12:690057. doi: 10.3389/fphar.2021.690057

Cancer is a major global health challenge for our health system, despite the important pharmacological and therapeutic discoveries we have seen since past 5 decades. The increasing prevalence and mortality of cancer may be closely related to smoking, exposure to environmental pollution, dietary and genetic factors. Despite significant promising discoveries and developments such as cell and biotechnological therapies a new breakthrough in the medical field is needed to develop specific and effective drugs for cancer treatment. On the development of cell therapies, anti-tumor vaccines, and new biotechnological drugs that have already shown promising effects in preclinical studies. With the continuous enrichment and development of chromatin immunoprecipitation sequencing (ChIP-seq) and its derivative technologies, epigenetic modification has gradually become a research hotspot. As key ingredients of epigenetic modification, Writers, Readers, Erasers have been gradually unveiled. Cancer has been associated with epigenetic modification especially methylation and therefore different epigenetic drugs have been developed and some of those are already undergoing clinical phase I or phase II trials, and it is believed that these drugs will certainly assist the treatment in the near future. With respect to this, an overview of anti-tumor drugs targeting modified enzymes and de-modified enzymes will be performed in order to contribute to future research.

Keywords: epigenetics, writers, readers, erasers, cancer, epigenetic drugs

INTRODUCTION

The epigenetic modification will affect gene expression. The genetic changes in gene expression or cell phenotype can happen without the sequence change of DNA. The phenomenon is called the epigenetic phenomenon, which can be stably inherited and may be reversible during embryonic development and cell proliferation (Harvey et al., 2018). The core of epigenetics includes various covalent modifications of histones and nucleic acids, which coordinately regulate chromatin structure and gene expression. Disorders of the epigenetic processes will drive abnormal transcription programs and promote the occurrence and progression of cancer (Sapienza and Issa, 2016; Nebbioso et al., 2018). According to the current research results, the regulatory mechanisms of epigenetic modification mainly include DNA methylation (Skvortsova et al., 2019), RNA interference (Holoch and Moazed, 2015), histone modification (Stoll et al., 2018),

chromatin remodeling (Dawson and Kouzarides, 2012), and nucleosome localization (Allis and Jenuwein, 2016).

Currently, DNA methylation is the most fully studied form of epigenetic modification, which mainly involves adding a methyl group to the C5 position of the cytosine base to produce 5-methylcytosine. Normal methylation is necessary for maintaining cell growth and metabolism, while abnormal DNA methylation can cause diseases (such as cancers). The reason for the occurrence of this event may be that, on the one hand, abnormal methylation may prevent the transcription of tumor suppressor genes, and on the other hand, it may cause genome instability. Therefore, the study of DNA methylation is very helpful for understanding biological growth and disease treatment (Koch et al., 2018). In the cell nucleus, DNA is wrapped around histones and packaged to form a chromatin structure, and the tightness of chromatin packaging determines the activity of gene expression. Studies have confirmed that chromatin can switch between the "on and off" states by regulating the chemical modification of histones (Bannister and Kouzarides, 2011; Calo and Wysocka, 2013). Non-coding RNA refers to a functional RNA molecule that cannot be translated into protein and has a regulatory effect, and it plays a very important role in regulating gene expression. The regulation of non-coding RNA is the regulation of gene transcription through certain mechanisms, such as RNA interference (Holoch and Moazed, 2015).

Chromatin remodeling involves a series of biological processes mediated by the chromatin remodeling complex, which is characterized by nucleosome changes in chromatin, and it was considered to be an important epigenetic mechanism (Nacev et al., 2020). Studies have suggested that nucleosomes were barriers to gene transcription, and DNA tightly wound on histones cannot bind to many transcription factors and activation factors. In each type of cell, several specific genes are activated while others inhibited; thus, resulting in a variety of gene expression patterns. Therefore, changes in the position of nucleosomes in the genome have an important impact on regulating gene expression. With the development of life cycle activities, such as DNA replication, recombination, repair, and transcriptional regulation, the positioning of nucleosomes in chromatin has undergone dynamic changes. This continuous change requires participation of a series of chromatin remodeling complexes (Dawson and Kouzarides, 2012).

So far, researchers have identified four different types of cytosine residue modifications in DNA, including methylation, hydroxymethylation, formylation, and carboxylation (Biswas and Rao, 2018). In addition, more than ten different types of histone modifications have been identified; and among them, methylation and acetylation are the most stable and suitable. With continuous progress in the research on epigenetics, the key roles associated with these modifications are gradually being deciphered. They are as follows: 1) the writers-a large number of enzymes that can modify nucleotide bases and specific amino acid residues in histones, 2) the erasers-a group of enzymes proficient in removing these markers, and 3) the readers -a series of different proteins that possess specific domains that can recognize specific epigenetic marks in a locus. Together, these enzymes and protein domains constitute epigenetic tools (Biswas and Rao, 2018; Zaccara et al., 2019). The modification of DNA and histones occurs by adding various chemical groups using a variety of enzymes. We will focus on the most extensive study of epigenetic modifications, namely methylation. Both DNA and histones are prone to methylation, and this modification usually controls gene expression in cells through changes in transcription activation or inhibition. Here, the epigenetic writers, which we intend to focus on include DNA methyltransferase, histone lysine methyltransferase, and protein arginine methyltransferase (Biswas and Rao, 2018). Depending on the requirements of the cell to modify the expression state of the locus, epigenetic marks formed by histone post-translational modification and DNA covalent modification can be removed. To achieve this purpose, a group of enzymes called erasers can counter the writer's activities. The eraser can catalyze the removal of epigenetic marks, thereby reducing the effect of epigenetic marks on transcription; thus, leading to regulation of gene expression. The key difference between genetic mutation and epigenetic modification is that epigenetic changes are reversible, which makes them attractive drug targets. On the whole, the ultimate goal of research on tumor-related epigenetic mechanisms is to apply them to clinical diagnosis and preventive treatment (**Figure 1**).

WRITERS

Modifications of DNA and histone proteins occur through the additions of various chemical groups utilizing numerous enzymes. Although a plethora of modifications are possible, we have focused on the two most widely studied epigenetic alterations, methylation and acetylation. Both DNA and histone proteins are prone to methylation, while acetylation is associated only with histones. These two modifications frequently govern the gene expression pattern in a cell by switching between transcriptional activation or repression. Changes in global DNA methylation and individual gene methylation patterns are distinguishing features of cancer cells, which are governed by DNMT: DNA methyltransferase. Global DNA hypomethylation and hypermethylation of the promoter regions of tumor suppressor genes have been reported in malignant cells (Kulis and Esteller, 2010). These modifications are caused by DNMT providing a viable target for developing drugs against these enzymes.

Abnormal DNA methylation at the C5 position of the cytosine catalyzed by DNMTs is not only related to silencing of many tumor suppressor genes, but also to other diseases. Small molecule inhibitors of DNMTs are the most widely used epigenetic therapies for cancer treatment, mainly for the treatment of myelodysplastic syndrome (MDS) and acute myeloid leukemia (AML) (Khan et al., 2013; Du et al., 2020). DNMT is usually overexpressed in various cancer tissues and cell lines. Since DNA methylation is reversible, DNMT is considered an important epigenetic target for drug development. DNMT inhibitors are categorized into nucleosides and non-nucleosides. Among these inhibitors, the nucleoside analogue azacytidine and its deoxy derivative decitabine are both irreversible DNMT inhibitors and have been approved for the treatment of bone marrow hyperplastic syndrome (Zhou et al., 2018b). Studies have

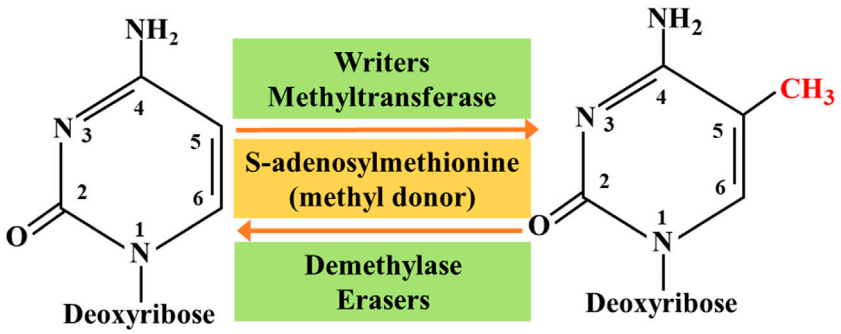

FIGURE 1 | Methylation interactions between writers and erasers.

shown that DNMTs can up-regulate the immune signal in ovarian cancer through the viral defense pathway (Chiappinelli et al., 2015).

Inhibitors of poly (ADP-ribose) polymerase 1 (PARP1) have shown promise for targeting cancer cells harboring mutations in the double-strand break (DSB) repair breast cancer genes, BRCA1 and BRCA2, where these drugs induce synthetic lethality. Studies have shown that PARP1 and DNMTs have shown an unexpected benefit in the combined treatment of non-small cell lung cancer (NSCLC). Chemoradiation is the main treatment method for NSCLC. Interestingly, combined treatment with PARP1 and DNMTs can make NSCLC cells very sensitive to ionizing radiation both *in vitro* and *in vivo*. With respect to the key mechanism, DNMTs may produce a BRCA-like phenotype by down-regulating the expression of key homologous recombination and non-homologous end joining genes (Abbotts et al., 2019).

The enhancer of Zeste homolog 2 (EZH2) is histone methyltransferase, and it catalyzes the methylation of histone 3 lysine 27, which is a sign of transcriptional inhibition. Many studies have clarified the complex role of EZH2 in normal biology and tumorigenesis. The effect of EZH2 on tumorigenesis is attributed to direct gene overexpression and point mutations leading to gain or loss of function. To a large extent, point mutations can increase the function of lymphoma and inactivate mutations in myeloid malignancies, and overexpression is the main manifestation of epithelial malignancies and specific lymphoma subtypes. Interestingly, EZH2 may have a dual function, and based on the dynamic expression of EZH2 in cell differentiation and cell cycle progression, it has the ability to act as both an oncogene and a tumor suppressor. Tazemetostat is the first EZH2 inhibitor, and it has shown enhanced clinical activity in mutant follicular lymphoma and diffuse large B-cell lymphoma. A new treatment strategy is required not only for the treatment of lymphoma, but it may also be beneficial in the treatment of many other malignant tumors (Lue and Amengual, 2018).

Another *in vivo* clinical study on tazemetostat published in 2018 reported that it showed good safety and anti-tumor activity in refractory B-cell non-Hodgkin's lymphoma and advanced solid tumors, including epithelioid sarcoma. Further clinical studies of tazemetostat monotherapy are ongoing in phase 2 trials in adults and phase 1 trials in children. A total of 64 patients (21 cases of B-cell non-Hodgkin's lymphoma and 43 cases of advanced solid tumors) received treatment with tazemetostat. No treatment-related deaths occurred. A durable objective response was observed in 21 patients with B-cell non-Hodgkin's lymphoma (Italiano et al., 2018) (NCT01897571).

Excellent efficacy of EZH2 inhibitors in cancer is likely to cause the problem of drug resistance. Studies have confirmed that the role of Forkhead box transcription factor-1 (FOXO1) is linked to the role of EZH2 inhibitors in cancer. It is believed that the FOXO1 gene is a new inhibitory target of EZH2 and FOXO1 is a key mediator of EZH2 inhibition and induction of prostate cancer cell death. Phosphatase and tension homolog (PTEN) is a well-known tumor suppressor and FOXO1 is a key downstream effector of PTEN in inhibiting cell growth and survival. Further studies have proved that EZH2 inhibitors cannot effectively induce PTEN-deficient cancer cell death, but they can be overcome by combination therapy with taxanes. The following mechanism is likely: EZH2 inhibits FOXO1 expression and may serve as a target of EZH2 inhibitors, which can be used to overcome EZH2 inhibitor resistance in PTEN mutant cancers or to treat PTEN-deficient prostate cancer in combination with taxane. A new inhibitory target and FOXO1 is a key mediator of EZH2 inhibition to induce prostate cancer cell death. Further studies have proved that EZH2 inhibitors cannot effectively induce PTEN-deficient cancer cell death, but they can be overcome by combination therapy with taxanes (Ma et al., 2019). Furthermore, Bitler et al. believe that inhibition of EZH2 methyltransferase can lead to regression of ARID1A mutant tumors in mouse models of ovarian cancer. This is because PIK3IPI is the target of ARID1A and EZH2, which up-regulates PIK3IPI by inhibiting EZH2, and ultimately inhibits the oncogenic PI3K/Akt signal (Bitler et al., 2015).

DOT1L is the only known histone 3 lysine 79 (H3K79) methyltransferase, while AML or acute lymphocytic leukemia (ALL) is a malignant clonal disease of hematopoietic stem cells, and without any special treatment, these patients can only survive for about 3 months. Some of these patients can even die within a few days after the diagnosis. Both these diseases are associated with aberration in mixed lineage leukemia (MLL) gene (also known as KMT2A) translocation at chromosome 11q23, and both show a poor prognosis. If DOT1L can become an attractive target for the treatment of acute leukemia, it will be of great benefit to the medical field. Pinometostat (EPZ-5676) is a small

molecule inhibitor of DOT1L histone methyltransferase interference. In an *in vivo* clinical trial, the DOT1L inhibitor pinometostat can reduce H3K79 methylation and has moderate clinical activity in adult acute leukemia. This study demonstrates the therapeutic potential of DOT1L in the mixed lineage leukemia (MLL) gene rearrangement of leukemia and lays the foundation for future combination therapy in this patient population (Stein et al., 2018) (NCT01684150).

In another study, convincing evidence was obtained by using DOT1L inhibitors as targeted therapy for MLL. EPZ004777 is a potent and selective inhibitor of DOT1L. According to the reports, MLL cells treated with EPZ004777 can selectively inhibit H3K79 methylation and can effectively block the expression of leukemia-associated genes. In addition, *in vitro* experiments showed that EPZ004777 has a selective killing effect on leukemia cells translocated by the MLL gene, and it has minimal effect on non-MLL translocated cells. *In vivo* experiments also showed a good performance; i.e., by administering EPZ004777 to a mouse xenograft model of MLL, the survival period can be significantly extended (Daigle et al., 2011).

It is undeniable that effective inhibitors of DOT1L have achieved many surprising results in targeting leukemia with MLL gene rearrangement. Research on this subject will continue in the future. In a document published in 2019, it has been confirmed that pinometostat as a DOT1L inhibitor has entered a phase 1 clinical trial to treat children with relapsed/refractory leukemia with MLL gene rearrangement Patient (NCT02141828). It has also been confirmed that pinometostat is undergoing a phase 1/2 clinical trial for evaluating the combination of pinometostat and standard chemotherapy for the treatment of newly diagnosed MLL rearranged leukemia in children and adults (NCT03724084) (Lonetti et al., 2019).

Different from the leukemia mechanism of MLL gene translocation, DOT1L is also believed to play an important role in the occurrence and development of breast cancer. Studies have suggested that DOT1L can target the gene expression of epithelial-mesenchymal transition (EMT) promoters by cooperating with the c-Myc/p300 transcriptional activity complex, thereby playing an important role in the occurrence and development of breast cancer, which suggests that DOT1L is a potential therapeutic target for invasive breast cancer (Lee and Kong, 2015).

Similarly, the new psammaplin A analogue (PsA-3091) is considered as a new template for DOT1L inhibitors, and it shows an effective inhibitory effect on DOT1L-mediated H3K79 methylation. As already known, triple-negative breast cancer (TNBC) is the most difficult disease to treat among women and has a high risk of metastasis. According to reports, PsA-3091 has a significant inhibitory effect on the proliferation, migration, and invasion of TNBC cells, and it can significantly enhance the expression of E-cadherin and inhibit the expression of N-cadherin, ZEB1, and vimentin. In addition, by developing an orthotopic mouse model, it has been suggested that PsA-3091 can effectively inhibit lung metastasis and tumor growth by regulating DOT1L activity and EMT biomarkers. *In vivo* and *in vitro* studies have confirmed that PsA-3091 exhibits excellent anti-tumor and anti-metastasis effects, and it can be speculated as a promising potential target for the treatment of patients with metastatic breast cancer (Byun et al., 2019). In addition, DOT1L inhibitors have also shown surprising performance in neuroblastoma (Wong et al., 2017) and colorectal cancer (Huang et al., 2017).

In recent years, abundant research evidence has shown that PRMT5, as an oncogene, can play an indispensable regulatory role in the pathological progression of various human cancers by promoting the proliferation, invasion, and metastasis of cancer cells. This indicates that PRMT5 may become a potential biomarker or therapeutic target for cancer. Regulation of epigenetics may be one of the main mechanisms by which PRMTs affect cell activities. Currently, PRMT1 and PRMT5 inhibitors have entered the first phase of clinical trials; thus, opening up a new path for the treatment of solid tumors and hematological malignancies (Jarrold and Davies, 2019) (NCT03666988) (**Table 1** and **Figure 2**).

ERASERS

In recent years, the regulatory role of epigenetic modifications in the occurrence and development of malignant tumors has received extensive attention. It is obvious that some epigenetic markers, whether in the form of post-translational modifications of histones or equivalent modifications of DNA, have proven to be non-permanent; i.e., removable. An enzyme called eraser appears immediately, which can remove these genetic markers, thereby resisting the writer's activity and leading to the regulation of gene expression (Biswas and Rao, 2018).

In the past few decades, with the rise of RNA epigenetics, the focus of N6-methyladenosine (m6A) RNA modification has gradually become a research hotspot in the field of biological sciences. In the early days, due to the incompatibility of technology and information, research on epigenetic modification was focused on the DNA and protein levels. Currently, the RNA epigenetic modification based on m6A has dynamic and reversible characteristics, and it is the most common mRNA epigenetic modification that exists in all higher eukaryotes. It involves fine regulation of many complex cellular processes, such as RNA processing, transportation, localization, translation, and degradation. Studies have shown that m6A can dynamically regulate RNA transport, localization, translation, and degradation through the abnormal expression of "writing", "erasing", and "reading" related factors. It can play a role in tumor development through a variety of mechanisms, including promotion or inhibition. Here, we mainly introduce the eraser, which can encode m6A demethylase to remove the m6A modification in the RNA molecule, which is the key to the reversibility of the m6A modification process (Roundtree et al., 2017). Currently, the identified "erasers" are mainly fat mass and obesity associated (FTO) protein and AlkB homolog 5 (ALKBH5) (Zou et al., 2016; Zhang et al., 2017). Although these two erasers have similar functions, they have different processes.

Studies have proved that FTO is not only limited to playing a major role in obesity-related diseases, but is also involved in the occurrence, development, and prognosis of a variety of cancers,

TABLE 1 | Describe the author and eraser mechanism in cancer.

Component	Disease	Target	Function	Regulation	Refs
METTL3	AML	Promoter	Writers	Downregulation of it leads to cell cycle arrest and leukemia cell differentiation	Barbieri et al. (2017)
METTL3	CRC	SOX2	Writers	Promote the progression of CRC through m6A-IGF2BP2-dependent mechanism	Li et al. (2019b)
METTL14	CRC	XIST	Writers	Inhibit the proliferation and metastasis of CRC by down-regulating XIST	Yang et al. (2020)
METTL14	CRC	SOX4	Writers	Inhibit the migration, invasion and metastasis of CRC cells through SOX4	Chen et al. (2020b)
WTAP	HCC	ETS1	Writers	Promotes the progression of HCC through m6A-HuR-dependent epigenetic silencing of ETS1	Chen et al. (2019)
DNMT	CML	MNC bone marrow	Writers	The expression level of DNMT mRNA is related to the disease progression of CML.	Li et al. (2015)
DNMT1	GC	PCDH10	Writers	By interacting with HOTAIR and miR-148b, it leads to the methylation of PCDH10, thereby promoting the development of GC	Seo et al. (2021)
DNMT1	HCC	miR-148a-3p	Writers	Block the negative regulation between miR-148a-3p, thereby inhibiting the stem cell characteristics of HCC cells	Li et al. (2020)
EZH2	PTEN-mutated cancer	FOXO1	Writers	Inhibition of FOXO1 can treat PTEN-proficient cancers	Ma et al. (2019)
EZH2	EOC	PRMT4	Writers	The activity of EZH2 determines the level of PRMT4 expression in EOC	Karakashev et al. (2018)
WTAP	SaOS	HMBOX1	Writers	Inhibit the expression of HMBOX1 in an m6A-dependent manner to promote the occurrence of SaOS.	Chen et al. (2020a)
FTO	AML	FB23 FB23–2	Erasers	Inhibit proliferation and promote differentiation/apoptosis of AML cell lines	Huang et al. (2019)
FTO	Leuke-mia	LILRB4	Erasers	Inhibit the maintenance and immune escape of cancer stem cells	Su et al. (2020)
FTO	NSCLC	USP7	Erasers	Promote the growth of NSCLC by regulating the m6A level of USP7 mRNA	Li et al. (2019a)
FTO	Cervical cancer	E2F1 Myc	Erasers	Overexpression of E2F1 or Myc can make up for the lack of FTO, thereby reducing cell proliferation and migration	Zou et al. (2019)
FTO	Breast tumor	BNIP3	Erasers	Promote breast tumor progression by inhibiting BNIP3	Niu et al. (2019)
ALKBH2	Bladder cancer	MUC1	Erasers	Promote the development of bladder cancer by regulating the expression of MUC1	Fujii et al. (2013)
ALKBH5	EOC	MiR-7 BCL-2	Erasers	Inhibition of autophagy in epithelial ovarian cancer through miR-7 and BCL-2	Zhu et al. (2019)
ALKBH5	PC	PER1	Erasers	Prevents the progression of pancreatic cancer through the post-transcriptional activation of PER1 that depends on m6A-YTHDF2	Guo et al. (2020)
ALKBH5	AML	LSCs LICs	Erasers	Selectively promote tumorigenesis and cancer stem cell self-renewal in AML	Shen et al. (2020)

METTL3, methyltransferase-like 3; CRC, Colorectal carcinoma; SOX2, sex determining region Y-box 2; XIST, X inactivate-specific transcript; SOX4, SRY-related high-mobility-group box; WTAP, Wilms tumor 1-associated protein; HCC, hepatocellular carcinoma; ETS1, ETS proto-oncogene 1; SaOS, osteosarcoma; CML, Chronic Myeloid Leukemia; PCDH10, Protocadherin 10; FOXO1, Forkhead box transcription factor-1; PRMT, protein arginine methyltransferase; EOC, Epithelial ovarian cancer; NSCLC, non-small cell lung cancer; Erasers, ubiquitin-specific protease; EOC, epithelial ovarian cancer; LSCs/LICs, leukemia stem/initiating cells.

including AML, glioblastoma, and breast cancer (Chen and Du, 2019; Lan et al., 2020). Long-term studies have shown that m6A modification is related to tumorigenesis, proliferation, invasion, and metastasis, and it acts as an oncogene or tumor suppressor gene in malignant tumors (Sun et al., 2019). Rhein, meclofenamic acid (MA), MO-I-500, fluorescein, and R-2-hydroxyglutarate (R-2HG) belong to a group of specific or non-specific FTO inhibitors that have been identified. Briefly, these small molecules are limited in their clinical applications due to their weak biological functions and low sensitivity and/or specificity (Huang et al., 2019).

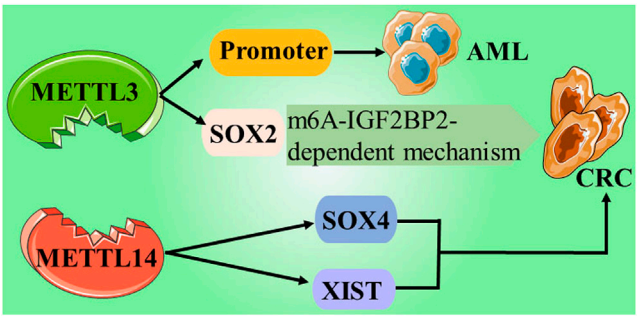

FIGURE 2 | Give examples of the role and mechanisms involved writers in cancers.

Su et al. developed two highly effective FTO inhibitors, CS1 and CS2. Compared with the two previously reported FTO inhibitors (FB23–2 and MO-I-500), CS1 and CS2 showed better performance in inhibiting the viability of AML cells. Su et al. obtained a set of up- or down-regulated pathways through global gene set enrichment analysis (GSEA). Surprisingly, in the up-regulated pathway, CS1, CS2, and FTO shared most of the abundant signaling pathways and core genes. Among the down-regulated pathways, the pathways inhibited by FTO are also widely present in the pathways inhibited by CS1 or CS2. The results showed that CS1 and CS2 may be able to exhibit high-efficiency performance by regulating the basic signal pathway of FTO. Interestingly, further *in vivo* experiments showed that CS2 treatment significantly reduced leukemic infiltration and doubled overall survival. However, CS1 treatment did not exert any significant effect. Further analysis showed that poor solubility and absorption of CS1 may be the reason for its inability to function in the body, and Su et al. subsequently solved this problem. However, it is undeniable that the FTO inhibitors CS1 and CS2 with anti-tumor and low side effects derived from the data have great

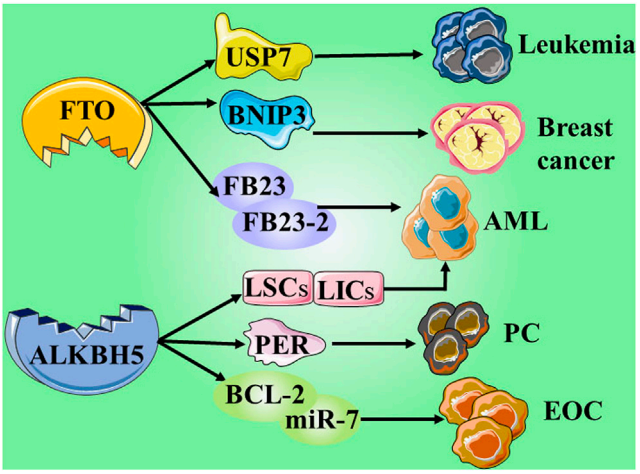

FIGURE 3 | Give examples of the role and mechanisms involved erasers in cancers.

potential in clinical applications (Su et al., 2020). Su et al. also found that R-2HG can display anti-tumor activity by targeting the FTO/m6A/MYC/CEPPA signaling pathway. In terms of the mechanism, R-2HG inhibits the increase in fat mass and the expression of FTO, thereby increasing the modification of m6A RNA in leukemia cells sensitive to R-2HG; thus, leading to further reduction in the stability of MYC/CEPPA transcripts, and ultimately suppressing the related pathways (Su et al., 2018).

It is recognized that ubiquitin-specific protease 7 (USP7) has a wide range of substrates, and most of the substrates, such as p53, PTEN, and FOXO4, are related to tumor suppression, DNA repair, or immune response. Therefore, USP7 is a potential cancer treatment target. Studies have found that FTO can promote the expression of USP7 through demethylation and can increase the stability of USP7, which is expected to become a potential target for the treatment of human lung cancer (Li J. et al., 2019). FTO can directly interact with oncogenic factors E2F1 and Myc. Experiments showed that by inhibiting FTO, the translation function of the two factors can be disrupted, thereby inhibiting the proliferation and migration of cervical cancer cells. But the study also revealed an interesting point, i.e., the overexpression of oncogenic factors E2F1 and Myc can also counteract the proliferation or migration of cervical cancer cells induced by the lack of FTO, and weaken its inhibitory effect (Zou et al., 2019). Similarly, some studies have shown that the expression of FTO is related to the occurrence and prognosis of gastric cancer. Experimental data have shown that FTO in a low expression state has the ability to inhibit the proliferation, migration, and invasion of gastric cancer. However, high expression of FTO exerts an opposite result, which promotes the activity of gastric cancer cells (Xu et al., 2017). FTO also provided deep insights in AML (Li Z. et al., 2017; Huang et al., 2019), breast cancer (Niu et al., 2019; Xu et al., 2020), and melanoma (Yang et al., 2019).

ALKBH5, another m6A demethylase of messenger RNA (mRNA) in higher eukaryotes, has also shown impressive performance. However, compared with the research on FTO, the research on ALKBH5 is still not thorough and abundant. In a study published in 2021, it was reported that the expression of ALKBH5 can be activated by Myc, and that the expression can reduce the m6A level in some selected Myc suppressor genes. Further experiments have also found that inhibiting the overexpression of ALKBH5 or selected Myc inhibitor genes can effectively inhibit the growth of Myc-mediated B-cell lymphoma *in vivo* and *in vitro* (Wu et al., 2021). In another study on osteosarcoma, ALKBH5 was also found to inhibit the occurrence and development of tumors through m6A-dependent epigenetic silencing of the pre-miR-181b-1/YAP signal axis present in osteosarcoma (Yuan et al., 2021). It is worth mentioning a recent novel discovery that ALKBH5 is not involved in DNA repair, but studies have found that demethylation of ALKBH5 may play a supporting role in maintaining genome integrity. In terms of the mechanism, the overexpression of ALKBH5 reduces the level of 3-methylcytosine in genomic DNA and the cytotoxic effect of the DNA-damaging alkylating agent methyl methanesulfonate (Akula et al., 2021) (**Table 1** and **Figure 3**; ; Fujii et al., 2013; Li et al., 2015; Barbieri et al., 2017; Karakashev et al., 2018; Ma et al., 2019; Chen et al. (2019); Li et al. (2019b); Niu et al. (2019); Zhu et al., 2019; Li et al. (2019a); Zou et al. (2019); Yang et al., 2020; Chen et al., 2020b; Li et al., 2020; Chen et al., 2020a; Huang et al., 2019; Su et al., 2020; Guo et al., 2020; Shen et al., 2020; Seo et al., 2021)

INTERACTION

Epigenetic modification is not a static entity, but it develops in a way dependent on the cellular environment and dynamically changes to cope with a complex environment. It can be simply understood as follows: epigenetic modifications undergo dynamic changes. Under a certain physiological environment, certain modifications will be added, and when external factors or physiological environments change, these newly added modifications will be removed. As mentioned earlier, epigenetic writers and erasers have proven to be ubiquitous in cancer, and epigenetic changes at different types and sites usually represent different meanings. This also provides many potential targets for cancer research and treatment. A large number of small molecule drugs are currently being developed mainly to target these epigenetic regulatory factors. Although only a few epigenetic drugs have been certified by the FDA for cancer treatment, a large number of excellent epigenetic drugs have gone through clinical research on cancer treatment and have achieved remarkable results (Ganesan et al., 2019). The above discussion has already been involved. However, there is no research linking epigenetic drugs and cancer treatment to prove whether there is a certain synergy. This point will be elaborated subsequently.

Enhancement of Chemotherapy Sensitivity

Chemotherapy is one of the most important methods for the treatment of malignant tumors. However, the resistance of tumor cells to chemotherapeutic drugs often leads to failure of chemotherapy. Therefore, it is particularly important to resensitize

the patients to chemotherapy-resistant drugs. Among the existing writers, DNMT decitabine can resensitize the patients with ovarian cancer to platinum-based drugs, and its mechanism may involve demethylation and re-expression in DNA repair and immune activation pathways (Fang et al., 2018). Sara et al. also strongly agreed with this finding and believed that epigenetic therapy has great potential in ovarian cancer (Moufarrij et al., 2019).

In breast cancer, Ye et al. found that the restoration of Spalt-like transcription factor 2 (SALL2) is mediated by DNMT inhibition, which can make tamoxifen-resistant breast cancer sensitive to tamoxifen therapy again. This discovery reveals and represents a potential clinical target that can be used for the treatment of tamoxifen-resistant breast cancer. These patients can benefit from the combination therapy of tamoxifen and DNMT inhibitors (Ye et al., 2019).

In colorectal cancer, Wei et al. confirmed that zebularine, a DNMT inhibitor with low toxicity, overcomes hypoxia-induced resistance to oxaliplatin in HCT116 cells by down-regulating the expression of hypoxia-inducible factor-1α (HIF-1α). It also provides a new strategy for the treatment of colorectal cancer, which is to overcome the resistance to oxaliplatin by increasing the hydroxylation of HIF-1α (Wei et al., 2020).

Similarly, in gefitinib-resistant PC9/AB2 cells, the combination of the EZH2 inhibitor GSK343 and gefitinib could significantly inhibit the activity of drug-resistant cells, reduce the migration ability of the cells, and induce the apoptosis of drug-resistant cells (Gong et al., 2019). EZH2 also showed surprising results in reversing the chemotherapy resistance of cervical cancer cells (Cai et al., 2016), cisplatin resistance in epithelial ovarian cancer (Liu et al., 2014), melanoma resistance to immunotherapy (Emran et al., 2019), and resistance of prostate cancer (Shankar et al., 2020), and it can be described as the gospel for patients.

Not only the writer, but the eraser is also excellent at improving the resistance to chemicals (Xiang et al., 2020). Zhou et al. demonstrated for the first time that FTO with elevated gene levels in cervical squamous cell carcinoma (CSCC) tissues can enhance the resistance of CSCC to radiotherapy and chemotherapy. The mechanism may be upregulation of β-catenin and subsequent activation of excision repair cross-complementation group 1 (ERCC1), and ultimately it was attributed to the demethylation of FTO (Zhou et al., 2018a). According to a report in 2020, malignant glioma is one of the deadly primary brain tumors in adults. Li et al. found that the inhibition of FTO can enhance the anti-tumor effect of the chemotherapeutic drug temozolomide in malignant glioma, and its mechanism may involve the MYC-miR-155/23a cluster-MXI1 feedback loop (Xiao et al., 2020). Compared with the well-researched FTO, there are relatively few studies on the resistance of ALKBH. Alkylating agents have broad-spectrum effects. It has been reported that it has anti-tumor, immunosuppressive, and other therapeutic effects, as well as carcinogenic, teratogenic, mutagenic, and bone marrow suppressive effects. Although alkylating agents have high toxicity and carcinogenic potential, they are still important first-line anti-tumor drugs for many highly aggressive and metastatic cancers (Sauter and Gillingham, 2020). Tran et al. inhibited the DNA repair activity of the ALKBH enzyme by targeting glutamine metabolism, leading to the accumulation of DNA alkylation damage, thereby increasing the sensitivity of cells to alkylating agents (Tran et al., 2017). The combination of drugs has achieved the effect of improving the efficacy and reducing the side effects of alkylating agents, which can be considered as a new strategy. In addition, the glutaminase inhibitor CB-839 has entered clinical trials for determining its safety and activity (Riess et al., 2021).

Inhibition of Proliferation and Promotion of Apoptosis

As a DNMT inhibitor, RG108 has been proven to effectively inhibit the proliferation of endometrial cancer cells and block the G2/M phase of the cell cycle to induce apoptosis, and it can be regarded as a promising drug candidate for endometrial cancer patients (Yang et al., 2017). Coincidentally, zebularine, another DNMT inhibitor, is thought to induce apoptosis in gastric cancer cells through the mitochondrial pathway (Tan et al., 2013). In addition, zebularine has also been shown to inhibit the proliferation of lung cancer A549 cells and HeLa cervical cancer cells through cell cycle arrest and apoptosis (You and Park, 2012; You and Park, 2014). Zhang et al. also stated that the combined application of DNMT and mTOR signals can inhibit the formation and proliferation of colorectal cancer (Zhang et al., 2009).

Kazuya Ishiguro et al. discussed the role of DOT1L in the development of multiple myeloma, and they believed that the inhibitory effect of DOT1L may be a new therapy for myeloma. Further experiments showed that the use of DOT1L inhibitors in multiple myeloma can induce cell cycle arrest and apoptosis, and can strongly inhibit cell proliferation *in vitro* (Ishiguro et al., 2019). Li et al. explored the effects of DOT1L inhibitor EPZ-5676 in combination with chemotherapy drugs on the proliferation and apoptosis of human ALL cells, and they concluded that the combination of these drugs has a synergistic inhibitory effect on proliferation, and low concentrations of EPZ-5676 combined with different chemotherapy drugs cause synergistic induction of apoptosis and have pro-apoptotic effects (Li LH. et al., 2017). However, the achievements of EZH2 in inhibiting proliferation and promoting apoptosis are countless, and they have been observed in colorectal cancer (Xu et al., 2018; Li X. et al., 2019), breast cancer (Han et al., 2018), and bladder cancer (Chen et al., 2019).

Similarly, FTO and ALKBH, the only known erasers, also have great potential in inhibiting proliferation and promoting apoptosis. In the study by Tang et al., it was suggested that FTO is necessary for the proliferation of pancreatic cancer cells by using RNA interference and knocking out FTO. With respect to its basic mechanism, Tang et al. believed that FTO is related to the interaction of MYC proto-oncogene and BHLH transcription factor (Tang et al., 2019). In the review of FTO by Wang et al., they believed that FTO is involved in a variety of biological processes, such as cancer cell apoptosis, proliferation, migration, metastasis, and stem cell self-renewal in human cancer. These modulations mainly rely on the communication between FTO and specific signal pathways, including PI3K/AKT, MAPK and mTOR signal pathways (Wang et al., 2020).

With respect to another type of eraser, ALKBH5, studies have found that silencing of ALKBH5 can significantly increase the proliferation, migration, and invasion of pancreatic cancer cells, and its overexpression will cause the opposite effect (Tang et al., 2020). In the study by Jin et al., it is believed that effective inhibition of the m6A modification of ALKBH5 may constitute a potential treatment strategy for lung cancer. Further experiments showed that ALKBH5 inhibited tumor proliferation and metastasis by reducing YTHDFs-mediated YAP expression and inhibiting miR-107/LATS2-mediated YAP activity in NSCLC (Jin et al., 2020). In general, both the writer and the eraser have their own unique advantages, attracting the attention of researchers.

CONCLUSION

Epigenetic modification is becoming a significant topic for research. With the development of next-generation sequencing technology, it will be possible explore more unknown areas for the world. As an important part of it. The resulting drugs that target epigenetic modifications will also be closely related to diseases, especially cancer. The change of epigenetic factors in cancer provides new targets for the development of cancer drugs, not only limited to a single therapy, but combined drugs that can achieve the desired efficacy. As with the emergence of any other new therapies, the fever of epigenetic modification is also essential to bring about adverse reactions. In the study of Allen et al., epigenetics affects gene expression, which may lead to adverse reactions of statins and have long-term effects on the health of statin users (Allen and Mamotte, 2017). In addition, the general public's attitude toward new therapies is not very positive. Paradoxically, any new thing is also pursued by the public. In the endless research on epigenetic modification, a large number of options will bring the dawn on cancer and even more refractory diseases.

AUTHOR CONTRIBUTIONS

J-yZ and HS designed and managed this article. HS, W-mZ and BL wrote the original manuscript. LL, HS, AS, and J-yZ reviewed this manuscript.

FUNDING

This work is supported by the National Natural Science Foundation of China (U1903126, 81773888 and 81802103), the Natural Science Foundation of Guangdong Province (2020A1515010605) and Project of High-Level Talents in AHUTCM (2019rcZD001).

SUPPLEMENTARY MATERIAL

The Supplementary Material for this article can be found online at: https://www.frontiersin.org/articles/10.3389/fphar.2021.690057/full#supplementary-material

REFERENCES

Abbotts, R., Topper, M. J., Biondi, C., Fontaine, D., Goswami, R., Stojanovic, L., et al. (2019). DNA Methyltransferase Inhibitors Induce a BRCAness Phenotype that Sensitizes NSCLC to PARP Inhibitor and Ionizing Radiation. *Proc. Natl. Acad. Sci. USA* 116 (45), 22609–22618. doi:10.1073/pnas.1903765116

Akula, D., O'Connor, T. R., and Anindya, R. (2021). Oxidative Demethylase ALKBH5 Repairs DNA Alkylation Damage and Protects against Alkylation-Induced Toxicity. *Biochem. Biophysical Res. Commun.* 534, 114–120. doi:10.1016/j.bbrc.2020.12.017

Allen, S. C., and Mamotte, C. D. S. (2017). Pleiotropic and Adverse Effects of Statins-Do Epigenetics Play a Role? *J. Pharmacol. Exp. Ther.* 362 (2), 319–326. doi:10.1124/jpet.117.242081

Allis, C. D., and Jenuwein, T. (2016). The Molecular Hallmarks of Epigenetic Control. *Nat. Rev. Genet.* 17 (8), 487–500. doi:10.1038/nrg.2016.59

Bannister, A. J., and Kouzarides, T. (2011). Regulation of Chromatin by Histone Modifications. *Cell Res* 21 (3), 381–395. doi:10.1038/cr.2011.22

Barbieri, I., Tzelepis, K., Pandolfini, L., Shi, J., Millán-Zambrano, G., and Robson, S. C. (2017). Promoter-Bound METTL3 Maintains Myeloid Leukaemia by m(6)A-Dependent Translation Control. *Nature* 552, 126–131. doi:10.1038/nature24678

Biswas, S., and Rao, C. M. (2018). Epigenetic Tools (The Writers, the Readers and the Erasers) and Their Implications in Cancer Therapy. *Eur. J. Pharmacol.* 837, 8–24. doi:10.1016/j.ejphar.2018.08.021

Bitler, B. G., Aird, K. M., Garipov, A., Li, H., Amatangelo, M., Kossenkov, A. V., et al. (2015). Synthetic Lethality by Targeting EZH2 Methyltransferase Activity in ARID1A-Mutated Cancers. *Nat. Med.* 21 (3), 231–238. doi:10.1038/nm.3799

Byun, W. S., Kim, W. K., Han, H. J., Chung, H.-J., Jang, K., Kim, H. S., et al. (2019). Targeting Histone Methyltransferase DOT1L by a Novel Psammaplin A Analog Inhibits Growth and Metastasis of Triple-Negative Breast Cancer. *Mol. Ther. - Oncolytics* 15, 140–152. doi:10.1016/j.omto.2019.09.005

Cai, L., Wang, Z., and Liu, D. (2016). Interference with Endogenous EZH2 Reverses the Chemotherapy Drug Resistance in Cervical Cancer Cells Partly by Up-Regulating Dicer Expression. *Tumor Biol.* 37 (5), 6359–6369. doi:10.1007/s13277-015-4416-9

Calo, E., and Wysocka, J. (2013). Modification of Enhancer Chromatin: what, How, and Why? *Mol. Cel* 49 (5), 825–837. doi:10.1016/j.molcel.2013.01.038

Chen, J., and Du, B. (2019). Novel Positioning from Obesity to Cancer: FTO, an m6A RNA Demethylase, Regulates Tumour Progression. *J. Cancer Res. Clin. Oncol.* 145 (1), 19–29. doi:10.1007/s00432-018-2796-0

Chen, Z., Du, Y., Liu, X., Chen, H., Weng, X., Guo, J., et al. (2019). EZH2 Inhibition Suppresses Bladder Cancer Cell Growth and Metastasis via the JAK2/STAT3 Signaling Pathway. *Oncol. Lett.* 18 (1), 907–915. doi:10.3892/ol.2019.10359

Chen, S., Li, Y., Zhi, S., Ding, Z., Wang, W., and Peng, Y. (2020a). WTAP Promotes Osteosarcoma Tumorigenesis by Repressing HMBOX1 Expression in an m(6)A-Dependent Manner. *Cell Death Dis.* 11, 659. doi:10.1038/s41419-020-02847-6

Chen, X., Xu, M., Xu, X., Zeng, K., Liu, X., and Pan, B. (2020b). METTL14-Mediated N6-Methyladenosine Modification of SOX4 mRNA Inhibits Tumor Metastasis in Colorectal Cancer. *Mol. Cancer* 19, 106. doi:10.1186/s12943-020-01220-7

Chiappinelli, K. B., Strissel, P. L., Desrichard, A., Li, H., Henke, C., Akman, B., et al. (2015). Inhibiting DNA Methylation Causes an Interferon Response in Cancer via dsRNA Including Endogenous Retroviruses. *Cell* 162 (5), 974–986. doi:10.1016/j.cell.2015.07.011

Daigle, S. R., Olhava, E. J., Therkelsen, C. A., Majer, C. R., Sneeringer, C. J., Song, J., et al. (2011). Selective Killing of Mixed Lineage Leukemia Cells by a Potent Small-Molecule DOT1L Inhibitor. *Cancer Cell* 20 (1), 53–65. doi:10.1016/j.ccr.2011.06.009

Dawson, M. A., and Kouzarides, T. (2012). Cancer Epigenetics: from Mechanism to Therapy. *Cell* 150 (1), 12–27. doi:10.1016/j.cell.2012.06.013

Du, W., Xu, A., Huang, Y., Cao, J., Zhu, H., Yang, B., et al. (2020). The Role of Autophagy in Targeted Therapy for Acute Myeloid Leukemia. *Autophagy*, 1–15. doi:10.1080/15548627.2020.1822628

Emran, A. A., Chatterjee, A., Rodger, E. J., Tiffen, J. C., Gallagher, S. J., Eccles, M. R., et al. (2019). Targeting DNA Methylation and EZH2 Activity to Overcome Melanoma Resistance to Immunotherapy. *Trends Immunol.* 40 (4), 328–344. doi:10.1016/j.it.2019.02.004

Fang, F., Cardenas, H., Huang, H., Jiang, G., Perkins, S. M., Zhang, C., et al. (2018). Genomic and Epigenomic Signatures in Ovarian Cancer Associated with Resensitization to Platinum Drugs. *Cancer Res.* 78 (3), 631–644. doi:10.1158/0008-5472.Can-17-1492

Fujii, T., Shimada, K., Anai, S., Fujimoto, K., Konishi, N., et al. (2013). ALKBH2, a Novel AlkB Homologue, Contributes to Human Bladder Cancer Progression by Regulating MUC1 Expression. *Cancer Sci.* 104, 321–327. doi:10.1111/cas.12089

Ganesan, A., Arimondo, P. B., Rots, M. G., Jeronimo, C., and Berdasco, M. (2019). The Timeline of Epigenetic Drug Discovery: from Reality to Dreams. *Clin. Epigenet* 11 (1), 174. doi:10.1186/s13148-019-0776-0

Gong, H., Yuan, Y., Li, Y., Zhang, H., Li, Y., Li, W., et al. (2019). [Role of EZH2 Inhibitor Combined with Gefitinib in EGFR-TKIs Resistant Lung Cancer Cells]. *Zhongguo Fei Ai Za Zhi* 22 (5), 255–263. doi:10.3779/j.issn.1009-3419.2019.05.01

Guo, X., Li, K., Jiang, W., Hu, Y., Xiao, W., Huang, Y., et al. (2020). RNA demethylase ALKBH5 Prevents Pancreatic Cancer Progression by Posttranscriptional Activation of PER1 in an m6A-YTHDF2-Dependent Manner. *Mol. Cancer* 19, 91. doi:10.1186/s12943-020-01158-w

Han, L., Zhang, H.-C., Li, L., Li, C.-X., Di, X., and Qu, X. (2018). Downregulation of Long Noncoding RNA HOTAIR andEZH2Induces Apoptosis and Inhibits Proliferation, Invasion, and Migration of Human Breast Cancer Cells. *Cancer Biother. Radiopharm.* 33 (6), 241–251. doi:10.1089/cbr.2017.2432

Harvey, Z. H., Chen, Y., and Jarosz, D. F. (2018). Protein-Based Inheritance: Epigenetics beyond the Chromosome. *Mol. Cel* 69 (2), 195–202. doi:10.1016/j.molcel.2017.10.030

Holoch, D., and Moazed, D. (2015). RNA-mediated Epigenetic Regulation of Gene Expression. *Nat. Rev. Genet.* 16 (2), 71–84. doi:10.1038/nrg3863

Huang, T., Lin, C., Zhong, L. L. D., Zhao, L., Zhang, G., Lu, A., et al. (2017). Targeting Histone Methylation for Colorectal Cancer. *Therap Adv. Gastroenterol.* 10 (1), 114–131. doi:10.1177/1756283x16671287

Huang, Y., Su, R., Sheng, Y., Dong, L., Dong, Z., Xu, H., et al. (2019). Small-Molecule Targeting of Oncogenic FTO Demethylase in Acute Myeloid Leukemia. *Cancer Cell* 35 (4), 677–691. doi:10.1016/j.ccell.2019.03.006

Ishiguro, K., Kitajima, H., Niinuma, T., Ishida, T., Maruyama, R., Ikeda, H., et al. (2019). DOT1L Inhibition Blocks Multiple Myeloma Cell Proliferation by Suppressing IRF4-MYC Signaling. *Haematologica* 104 (1), 155–165. doi:10.3324/haematol.2018.191262

Italiano, A., Soria, J.-C., Toulmonde, M., Michot, J.-M., Lucchesi, C., Varga, A., et al. (2018). Tazemetostat, an EZH2 Inhibitor, in Relapsed or Refractory B-Cell Non-hodgkin Lymphoma and Advanced Solid Tumours: a First-In-Human, Open-Label, Phase 1 Study. *Lancet Oncol.* 19 (5), 649–659. doi:10.1016/s1470-2045(18)30145-1

Jarrold, J., and Davies, C. C. (2019). PRMTs and Arginine Methylation: Cancer's Best-Kept Secret? *Trends Mol. Med.* 25 (11), 993–1009. doi:10.1016/j.molmed.2019.05.007

Jin, D., Guo, J., Wu, Y., Yang, L., Wang, X., Du, J., et al. (2020). m6A Demethylase ALKBH5 Inhibits Tumor Growth and Metastasis by Reducing YTHDFs-Mediated YAP Expression and Inhibiting miR-107/lats2-Mediated YAP Activity in NSCLC. *Mol. Cancer* 40 (1), 1–24. doi:10.1186/s12943-020-01161-1

Karakashev, S., Zhu, H., Wu, S., Yokoyama, Y., Bitler, B. G., Park, P. H., et al. (2018). CARM1-Expressing Ovarian Cancer Depends on the Histone Methyltransferase EZH2 Activity. *Nat. Commun.* 9, 631. doi:10.1038/s41467-018-03031-3

Khan, H., Vale, C., Bhagat, T., and Verma, A. (2013). Role of DNA Methylation in the Pathogenesis and Treatment of Myelodysplastic Syndromes. *Semin. Hematol.* 50 (1), 16–37. doi:10.1053/j.seminhematol.2013.01.001

Koch, A., Joosten, S. C., Feng, Z., de Ruijter, T. C., Draht, M. X., Melotte, V., et al. (2018). Analysis of DNA Methylation in Cancer: Location Revisited. *Nat. Rev. Clin. Oncol.* 15 (7), 459–466. doi:10.1038/s41571-018-0004-4

Kulis, M., and Esteller, M. (2010). DNA Methylation and Cancer. *Adv. Genet.* 70, 27–56. doi:10.1016/b978-0-12-380866-0.60002-2

Lan, N., Lu, Y., Zhang, Y., Pu, S., Xi, H., Nie, X., et al. (2020). FTO - A Common Genetic Basis for Obesity and Cancer. *Front. Genet.* 559138, 1–12. doi:10.3389/fgene.2020.559138

Lee, J.-Y., and Kong, G. (2015). DOT1L: a New Therapeutic Target for Aggressive Breast Cancer. *Oncotarget* 6 (31), 30451–30452. doi:10.18632/oncotarget.5860

Li, J., Han, Y., Zhang, H., Qian, Z., Jia, W., Gao, Y., et al. (2019a). The m6A Demethylase FTO Promotes the Growth of Lung Cancer Cells by Regulating the m6A Level of USP7 mRNA. *Biochem. Biophysical Res. Commun.* 512 (3), 479–485. doi:10.1016/j.bbrc.2019.03.093

Li, L. H., Wang, J., and Ke, X. Y. (2017a). [Effects of DOT1L Inhibitor EPZ-5676 Combined with Chemotherapeutic Drugs on Prolifiration and Apoptosis of RS 4;11 Cells]. *Zhongguo Shi Yan Xue Ye Xue Za Zhi* 25 (5), 1334–1341. doi:10.7534/j.issn.1009-2137.2017.05.010

li, X., Wang, L., Cao, X., Zhou, L., Xu, C., Cui, Y., et al. (2020). Casticin Inhibits Stemness of Hepatocellular Carcinoma Cells Via Disrupting The Reciprocal Negative Regulation Between DNMT1 and miR-148a-3p. *Toxicol. Appl. Pharmacol.* 396, 114998. doi:10.1016/j.taap.2020.114998

Li, X., Xing, J., Wang, H., and Yu, E. (2019b). The SLC34A2-ROS-HIF-1-Induced Up-Regulation of EZH2 Expression Promotes Proliferation and Chemo-Resistance to Apoptosis in Colorectal Cancer. *Biosci. Rep.* 112 (5), 1–15. doi:10.1042/bsr20180268

Li, L. H., Liu, X. D., Guo, X. F., Liu, X., Luo, J. M., and Zhang, Y. X. (2015). Expression and Clinical Significance of DNMT in Patients With Chronic Myeloid Leukemia. *Zhongguo Shi Yan Xue Ye Xue Za Zhi* 23, 1547–1550. doi:10.7534/j.issn.1009-2137.2015.06.003

Li, Z., Weng, H., Su, R., Weng, X., Zuo, Z., Li, C., et al. (2017b). FTO Plays an Oncogenic Role in Acute Myeloid Leukemia as a N 6 -Methyladenosine RNA Demethylase. *Cancer Cell* 31 (1), 127–141. doi:10.1016/j.ccell.2016.11.017

Liu, L., Guo, J., Yu, L., Cai, J., Gui, T., Tang, H., et al. (2014). miR-101 Regulates Expression of EZH2 and Contributes to Progression of and Cisplatin Resistance in Epithelial Ovarian Cancer. *Tumor Biol.* 35 (12), 12619–12626. doi:10.1007/s13277-014-2585-6

Lonetti, A., Pession, A., and Masetti, R. (2019). Targeted Therapies for Pediatric AML: Gaps and Perspective. *Front. Pediatr.* 7, 463. doi:10.3389/fped.2019.00463

Lue, J. K., and Amengual, J. E. (2018). Emerging EZH2 Inhibitors and Their Application in Lymphoma. *Curr. Hematol. Malig Rep.* 13 (5), 369–382. doi:10.1007/s11899-018-0466-6

Ma, L., Yan, Y., Bai, Y., Yang, Y., Pan, Y., Gang, X., et al. (2019). Overcoming EZH2 Inhibitor Resistance by Taxane in PTEN-Mutated Cancer. *Theranostics* 9 (17), 5020–5034. doi:10.7150/thno.34700

Moufarrij, S., Dandapani, M., Arthofer, E., Gomez, S., Srivastava, A., Lopez-Acevedo, M., et al. (2019). Epigenetic Therapy for Ovarian Cancer: Promise and Progress. *Clin. Epigenet* 11 (1), 7. doi:10.1186/s13148-018-0602-0

Nacev, B. A., Jones, K. B., Intlekofer, A. M., Yu, J. S. E., Allis, C. D., Tap, W. D., et al. (2020). The Epigenomics of Sarcoma. *Nat. Rev. Cancer* 20 (10), 608–623. doi:10.1038/s41568-020-0288-4

Nebbioso, A., Tambaro, F. P., Dell'Aversana, C., and Altucci, L. (2018). Cancer Epigenetics: Moving Forward. *Plos Genet.* 14 (6), e1007362. doi:10.1371/journal.pgen.1007362

Niu, Y., Lin, Z., Wan, A., Chen, H., Liang, H., Sun, L., et al. (2019). RNA N6-Methyladenosine Demethylase FTO Promotes Breast Tumor Progression through Inhibiting BNIP3. *Mol. Cancer* 18 (1), 46. doi:10.1186/s12943-019-1004-4

Riess, J. W., Frankel, P., Shackelford, D., Dunphy, M., Badawi, R. D., Nardo, L., et al. (2021). Phase 1 Trial of MLN0128 (Sapanisertib) and CB-839 HCl (Telaglenastat) in Patients with Advanced NSCLC (NCI 10327): Rationale and Study Design. *Clin. Lung Cancer* 22 (1), 67–70. doi:10.1016/j.cllc.2020.10.006

Roundtree, I. A., Evans, M. E., Pan, T., and He, C. (2017). Dynamic RNA Modifications in Gene Expression Regulation. *Cell* 169 (7), 1187–1200. doi:10.1016/j.cell.2017.05.045

Sapienza, C., and Issa, J.-P. (2016). Diet, Nutrition, and Cancer Epigenetics. *Annu. Rev. Nutr.* 36, 665–681. doi:10.1146/annurev-nutr-121415-112634

Sauter, B., and Gillingham, D. (2020). DNA Damaging Agents in Chemical Biology and Cancer. *chimia (aarau)* 74 (9), 693–698. doi:10.2533/chimia.2020.693

Seo, S. I., Yoon, J. H., Byun, H. J., Lee, S. K., et al. (2021). HOTAIR Induces Methylation of PCDH10, a Tumor Suppressor Gene, by Regulating DNMT1 and Sponging with miR-148b in Gastric Adenocarcinoma. *Yonsei Med J* 62, 118–128. doi:10.3349/ymj.2021.62.2.118

Shankar, E., Franco, D., Iqbal, O., Moreton, S., Kanwal, R., and Gupta, S. (2020). Dual Targeting of EZH2 and Androgen Receptor as a Novel Therapy for Castration-Resistant Prostate Cancer. *Toxicol. Appl. Pharmacol.* 404, 115200. doi:10.1016/j.taap.2020.115200

Shen, C., Sheng, Y., Zhu, A. C., Robinson, S., Jiang, X., Dong, L., et al. (2020). RNA Demethylase ALKBH5 Selectively Promotes Tumorigenesis and Cancer Stem Cell Self-Renewal in Acute Myeloid Leukemia. *Cell Stem Cell* 27, 64–80.e69. doi:10.1016/j.stem.2020.04.009

Skvortsova, K., Stirzaker, C., and Taberlay, P. (2019). The DNA Methylation Landscape in Cancer. *Essays Biochem.* 63 (6), 797–811. doi:10.1042/ebc20190037

Stein, E. M., Garcia-Manero, G., Rizzieri, D. A., Tibes, R., Berdeja, J. G., Savona, M. R., et al. (2018). The DOT1L Inhibitor Pinometostat Reduces H3K79 Methylation and Has Modest Clinical Activity in Adult Acute Leukemia. *Blood* 131 (24), 2661–2669. doi:10.1182/blood-2017-12-818948

Stoll, S., Wang, C., and Qiu, H. (2018). DNA Methylation and Histone Modification in Hypertension. *Ijms* 19 (4), 1174. doi:10.3390/ijms19041174

Su, R., Dong, L., Li, C., Nachtergaele, S., Wunderlich, M., Qing, Y., et al. (2018). R-2HG Exhibits Anti-tumor Activity by Targeting FTO/m6A/MYC/CEBPA Signaling. *Cell* 172 (1-2), 90–105. doi:10.1016/j.cell.2017.11.031

Su, R., Dong, L., Li, Y., Gao, M., Han, L., Wunderlich, M., et al. (2020). Targeting FTO Suppresses Cancer Stem Cell Maintenance and Immune Evasion. *Cancer Cell* 38 (1), 79–96. doi:10.1016/j.ccell.2020.04.017

Sun, T., Wu, R., and Ming, L. (2019). The Role of m6A RNA Methylation in Cancer. *Biomed. Pharmacother.* 112, 108613. doi:10.1016/j.biopha.2019.108613

Tan, W., Zhou, W., Yu, H.-g., Luo, H.-S., and Shen, L. (2013). The DNA Methyltransferase Inhibitor Zebularine Induces Mitochondria-Mediated Apoptosis in Gastric Cancer Cells *In Vitro* and *In Vivo*. *Biochem. Biophysical Res. Commun.* 430 (1), 250–255. doi:10.1016/j.bbrc.2012.10.143

Tang, B., Yang, Y., Kang, M., Wang, Y., Wang, Y., Bi, Y., et al. (2020). m6A Demethylase ALKBH5 Inhibits Pancreatic Cancer Tumorigenesis by Decreasing WIF-1 RNA Methylation and Mediating Wnt Signaling. *Mol. Cancer* 19 (1), 3. doi:10.1186/s12943-019-1128-6

Tang, X., Liu, S., Chen, D., Zhao, Z., and Zhou, J. (2019). The Role of the Fat Mass and Obesity-associated P-rotein in the P-roliferation of P-ancreatic C-ancer C-ells. *Oncol. Lett.* 17 (2), 2473–2478. doi:10.3892/ol.2018.9873

Tran, T. Q., Ishak Gabra, M. B., Lowman, X. H., Yang, Y., Reid, M. A., Pan, M., et al. (2017). Glutamine Deficiency Induces DNA Alkylation Damage and Sensitizes Cancer Cells to Alkylating Agents through Inhibition of ALKBH Enzymes. *Plos Biol.* 15 (11), e2002810. doi:10.1371/journal.pbio.2002810

Wang, J.-y., Chen, L.-j., and Qiang, P. (2020). The Potential Role of N6-Methyladenosine (m6A) Demethylase Fat Mass and Obesity-Associated Gene (FTO) in Human Cancers. *Ott* 13, 12845–12856. doi:10.2147/ott.S283417

Wei, T.-T., Lin, Y.-T., Tang, S.-P., Luo, C.-K., Tsai, C.-T., Shun, C.-T., et al. (2020). Metabolic Targeting of HIF-1α Potentiates the Therapeutic Efficacy of Oxaliplatin in Colorectal Cancer. *Oncogene* 39 (2), 414–427. doi:10.1038/s41388-019-0999-8

Wong, M., Tee, A. E. L., Milazzo, G., Bell, J. L., Poulos, R. C., Atmadibrata, B., et al. (2017). The Histone Methyltransferase DOT1L Promotes Neuroblastoma by Regulating Gene Transcription. *Cancer Res.* 77 (9), 2522–2533. doi:10.1158/0008-5472.Can-16-1663

Wu, G., Suo, C., Yang, Y., Shen, S., Sun, L., Li, S. T., et al. (2021). MYC Promotes Cancer Progression by Modulating M 6 A Modifications to Suppress Target Gene Translation. *EMBO Rep.* 22, e51519. doi:10.15252/embr.202051519

Xiang, M., Liu, W., Tian, W., You, A., and Deng, D. (2020). RNA N-6-Methyladenosine Enzymes and Resistance of Cancer Cells to Chemotherapy and Radiotherapy. *Epigenomics* 12 (9), 801–809. doi:10.2217/epi-2019-0358

Xiao, L., Li, X., Mu, Z., Zhou, J., Zhou, P., Xie, C., et al. (2020). FTO Inhibition Enhances the Antitumor Effect of Temozolomide by Targeting MYC-miR-155/23a Cluster-MXI1 Feedback Circuit in Glioma. *Cancer Res.* 80 (18), 3945–3958. doi:10.1158/0008-5472.Can-20-0132

Xu, D., Shao, W., Jiang, Y., Wang, X., Liu, Y., and Liu, X. (2017). FTO Expression Is Associated with the Occurrence of Gastric Cancer and Prognosis. *Oncol. Rep.* 38 (4), 2285–2292. doi:10.3892/or.2017.5904

Xu, M., Chen, X., Lin, K., Zeng, K., Liu, X., Pan, B., et al. (2018). The Long Noncoding RNA SNHG1 Regulates Colorectal Cancer Cell Growth through Interactions with EZH2 and miR-154-5p. *Mol. Cancer* 17 (1), 141. doi:10.1186/s12943-018-0894-x

Xu, Y., Ye, S., Zhang, N., Zheng, S., Liu, H., Zhou, K., et al. (2020). The FTO/miR-181b-3p/ARL5B Signaling Pathway Regulates Cell Migration and Invasion in Breast Cancer. *Cancer Commun.* 40 (10), 484–500. doi:10.1002/cac2.12075

Yang, L., Hou, J., Cui, X. H., Suo, L. N., and Lv, Y. W. (2017). RG108 Induces the Apoptosis of Endometrial Cancer Ishikawa Cell Lines by Inhibiting the Expression of DNMT3B and Demethylation of HMLH1. *Eur. Rev. Med. Pharmacol. Sci.* 21 (22), 5056–5064. doi:10.26355/eurrev_201711_13818

Yang, S., Wei, J., Cui, Y.-H., Park, G., Shah, P., Deng, Y., et al. (2019). m6A mRNA Demethylase FTO Regulates Melanoma Tumorigenicity and Response to Anti-PD-1 Blockade. *Nat. Commun.* 10 (1), 2782. doi:10.1038/s41467-019-10669-0

Yang, X., Zhang, S., He, C., Xue, P., Zhang, L., and He, Z. (2020). METTL14 Suppresses Proliferation and Metastasis of Colorectal Cancer by Down-Regulating Oncogenic Long Non-Coding RNA XIST. *Mol. Cancer* 19, 46. doi:10.1186/s12943-020-1146-4

Ye, L., Lin, C., Wang, X., Li, Q., Li, Y., Wang, M., et al. (2019). Epigenetic Silencing of SALL 2 Confers Tamoxifen Resistance in Breast Cancer. *EMBO Mol. Med.* 11 (12), e10638. doi:10.15252/emmm.201910638

You, B. R., and Park, W. H. (2014). Zebularine Inhibits the Growth of A549 Lung Cancer Cells via Cell Cycle Arrest and Apoptosis. *Mol. Carcinog.* 53 (11), 847–857. doi:10.1002/mc.22042

You, B. R., and Park, W. H. (2012). Zebularine Inhibits the Growth of HeLa Cervical Cancer Cells via Cell Cycle Arrest and Caspase-dependent Apoptosis. *Mol. Biol. Rep.* 39 (10), 9723–9731. doi:10.1007/s11033-012-1837-z

Yuan, Y., Yan, G., He, M., Lei, H., Li, L., Wang, Y., et al. (2021). ALKBH5 Suppresses Tumor Progression via an m6A-dependent Epigenetic Silencing of Pre-miR-181b-1/YAP Signaling axis in Osteosarcoma. *Cell Death Dis* 12 (1), 60. doi:10.1038/s41419-020-03315-x

Zaccara, S., Ries, R. J., and Jaffrey, S. R. (2019). Reading, Writing and Erasing mRNA Methylation. *Nat. Rev. Mol. Cel Biol* 20 (10), 608–624. doi:10.1038/s41580-019-0168-5

Zhang, S., Zhao, B. S., Zhou, A., Lin, K., Zheng, S., Lu, Z., et al. (2017). m 6 A Demethylase ALKBH5 Maintains Tumorigenicity of Glioblastoma Stem-like Cells by Sustaining FOXM1 Expression and Cell Proliferation Program. *Cancer Cell* 31 (4), 591–606. doi:10.1016/j.ccell.2017.02.013

Zhang, Y.-J., Zhao, S.-L., Tian, X.-Q., Sun, D.-F., Xiong, H., Dai, Q., et al. (2009). Combined Inhibition of Dnmt and mTOR Signaling Inhibits Formation and Growth of Colorectal Cancer. *Int. J. Colorectal Dis.* 24 (6), 629–639. doi:10.1007/s00384-009-0664-8

Zhou, S., Bai, Z.-L., Xia, D., Zhao, Z.-J., Zhao, R., Wang, Y.-Y., et al. (2018a). FTO Regulates the Chemo-Radiotherapy Resistance of Cervical Squamous Cell Carcinoma (CSCC) by Targeting β-catenin through mRNA Demethylation. *Mol. Carcinogenesis* 57 (5), 590–597. doi:10.1002/mc.22782

Zhou, Z., Li, H.-Q., and Liu, F. (2019b). DNA Methyltransferase Inhibitors and Their Therapeutic Potential. *Ctmc* 18 (28), 2448–2457. doi:10.2174/1568026619666181120150122

Zhu, H., Gan, X., Jiang, X., Diao, S., Wu, H., Hu, J., et al. (2019). ALKBH5 Inhibited Autophagy of Epithelial Ovarian Cancer Through miR-7 and BCL-2. *J Exp. Clin. Cancer* 38, 163. doi:10.1186/s13046-019-1159-2

Zou, D., Dong, L., Li, C., Yin, Z., Rao, S., and Zhou, Q. (2019). The m6A Eraser FTO Facilitates Proliferation and Migration of Human Cervical Cancer Cells. *Cancer Cel Int* 19, 321. doi:10.1186/s12935-019-1045-1

Zou, S., Toh, J. D. W., Wong, K. H. Q., Gao, Y.-G., Hong, W., and Woon, E. C. Y. (2016). N6-Methyladenosine: a Conformational Marker that Regulates the Substrate Specificity of Human Demethylases FTO and ALKBH5. *Sci. Rep.* 6, 25677. doi:10.1038/srep25677

Conflict of Interest: The authors declare that the research was conducted in the absence of any commercial or financial relationships that could be construed as a potential conflict of interest.

frontiers in Pharmacology

ORIGINAL RESEARCH
published: 15 July 2021
doi: 10.3389/fphar.2021.691769

Discovery of a New CDK4/6 and PI3K/AKT Multiple Kinase Inhibitor Aminoquinol for the Treatment of Hepatocellular Carcinoma

Zhong-Kun Xia[1†], Wei Wang[1†], Jian-Ge Qiu[1], Xi-Nan Shi[2,3]*, Hong-Jian Li[4], Rong Chen[5], Kun-Bin Ke[6], Chao Dong[7], Ying Zhu[8], Shi-Guo Wu[9], Rong-Ping Zhang[10], Zhuo-Ran Meng[2], Hui Zhao[6], Peng Gu[6], Kwong-Sak Leung[11], Man-Hon Wong[11], Xiao-Dong Liu[6], Feng-Mei Zhou[1], Jian-Ying Zhang[1], Ya-Ting Yao[1], Si-Jia Wang[1], Chun-Yang Zhang[12], Yan-Ru Qin[13], Marie Chia-mi Lin[1] and Bing-Hua Jiang[14]*

[1]School of Basic Medical Sciences, Academy of Medical Science, Zhengzhou University, Zhengzhou, China, [2]Department of Pathology, Yunnan University of Chinese Medicine, Kunming, China, [3]XingYi People' Hospital, Xingyi, China, [4]CUHK-SDU Joint Laboratory on Reproductive Genetics, School of Biomedical Sciences, Chinese University of Hong Kong, Hong Kong, China, [5]Department of Physiology, Yunnan University of Chinese Medicine, Kunming, China, [6]Department of Urology, The First Affiliated Hospital of Kunming Medical University, Kunming, China, [7]Department of the Second Medical Oncology, The Third Affiliated Hospital of Kunming Medical University, Yunnan Tumor Hospital, Kunming, China, [8]Department of Cadre Medical Branch, The Third Affiliated Hospital of Kunming Medical University, Kunming, China, [9]Department of Teaching and Research Section of Formulas of Chinese Medicine, Yunnan University of Chinese Medicine, Kunming, China, [10]School of Chinese Materia Medica and Yunnan Key Laboratory of Southern Medicinal Utilization, Yunnan University of Chinese Medicine,Kunming, China, [11]Department of Computer Science and Engineering, Chinese University of Hong Kong, Hong Kong, China, [12]College of Chemistry, Chemical Engineering and Materials Science, Shandong Normal University, Jinan, China, [13]Department of Oncology, The First Affiliated Hospital of Zhengzhou University, Zhengzhou, China, [14]Department of Pathology, Anatomy and Cell Biology, Thomas Jefferson University, Philadelphia, PA, United States*

OPEN ACCESS

Edited by:
Yingjie Zhang,
Shandong University, China

Reviewed by:
Lily Yang,
Emory University, United States
Xiaowen Hu,
University of Pennsylvania, United States

***Correspondence:**
Jian-Ge Qiu
jiangeqiu@zzu.edu.cn
Xi-Nan Shi
xilancixiang@163.com

†These authors have contributed equally to this work

Specialty section:
This article was submitted to Experimental Pharmacology and Drug Discovery, a section of the journal Frontiers in Pharmacology

Received: *07 April 2021*
Accepted: *25 June 2021*
Published: *15 July 2021*

Citation:
Xia Z-K, Wang W, Qiu J-G, Shi X-N, Li H-J, Chen R, Ke K-B, Dong C, Zhu Y, Wu S-G, Zhang R-P, Meng Z-R, Zhao H, Gu P, Leung K-S, Wong M-H, Liu X-D, Zhou F-M, Zhang J-Y, Yao Y-T, Wang S-J, Zhang C-Y, Qin Y-R, Lin MC and Jiang B-H (2021) Discovery of a New CDK4/6 and PI3K/AKT Multiple Kinase Inhibitor Aminoquinol for the Treatment of Hepatocellular Carcinoma. Front. Pharmacol. 12:691769. doi: 10.3389/fphar.2021.691769

Background: Hepatocellular carcinoma (HCC) is a lethal malignancy lacking effective treatment. The Cyclin-dependent kinases 4/6 (CDK4/6) and PI3K/AKT signal pathways play pivotal roles in carcinogenesis and are promising therapeutic targets for HCC. Here we identified a new CDK4/6 and PI3K/AKT multi-kinase inhibitor for the treatment of HCC.

Methods: Using a repurposing and ensemble docking methodology, we screened a library of worldwide approved drugs to identify candidate CDK4/6 inhibitors. By MTT, apoptosis, and flow cytometry analysis, we investigated the effects of candidate drug in reducing cell-viability,inducing apoptosis, and causing cell-cycle arrest. The drug combination and thermal proteomic profiling (TPP) method were used to investigate whether the candidate drug produced antagonistic effect. The *in vivo* anti-cancer effect was performed in BALB/C nude mice subcutaneously xenografted with Huh7 cells.

Results: We demonstrated for the first time that the anti-plasmodium drug aminoquinol is a new CDK4/6 and PI3K/AKT inhibitor. Aminoquinol significantly decreased cell viability, induced apoptosis, increased the percentage of cells in G1 phase. Drug combination screening indicated that aminoquinol could produce antagonistic effect with the PI3K inhibitor LY294002. TPP analysis confirmed that aminoquinol significantly stabilized CDK4, CDK6, PI3K and AKT proteins. Finally, *in vivo* study in Huh7 cells xenografted nude mice demonstrated that aminoquinol exhibited strong anti-tumor activity, comparable to that of

the leading cancer drug 5-fluorouracil with the combination treatment showed the highest therapeutic effect.

Conclusion: The present study indicates for the first time the discovery of a new CDK4/6 and PI3K/AKT multi-kinase inhibitor aminoquinol. It could be used alone or as a combination therapeutic strategy for the treatment of HCC.

Keywords: aminoquinol, hepatocellular carcinoma, CDK4/6, RB, PI3K

INTRODUCTION

Hepatocellular carcinoma (HCC) is the most common type of liver cancer, with only 30–40% of the patients eligible for curative treatments at the time of disease diagnosis (Liu et al., 2015). Surgical resection is the first line treatment, followed by liver transplantation and percutaneous ablation. However, there is a high frequency of tumor recurrence (Yang et al., 2015).

Targeted therapy for advanced HCC is a promising strategy, and HCC displays multiple drug targets. The multi-kinase inhibitor sorafenib has been used as the first-line agent in clinical practice since 2007. Recently, another multiple kinase inhibitor lenvatinib was approved to be the first line treatment. In addition, regorafenib and cabozantinib were recommended as second-line treatment for patients with advanced HCC who are resistant to sorafenib (Kudo 2020). However, most HCCs are resistant to currently available conventional chemotherapy and radiotherapy. Therefore, the development of new and more effective therapies against HCC is urgently needed.

Cyclin-dependent kinases (CDK) belongs to the family of serine/threonine protein kinase, which play pivotal roles in cell cycle regulation (Malumbres 2014), transcription, metabolism, neuro-physiological processes, cell differentiation and development (Asghar et al., 2015). In tumors cells, elevated CDK activities directly or indirectly increase cell proliferation, genomic instability (DNA mutations and chromosome deletion, etc.) and chromosome instability (chromosome number changes), that are critical for the development and progression of cancer (Malumbres and Barbacid 2009). Among them, CDK4/6 activities are necessary for the regulation of cell cycle in G1 phase. It has been well documented that the expression levels of CDK4/6 are significantly higher in many tumors (Yamamoto et al., 1995; Kim et al., 2000; Cohen 2002; Li et al., 2002). In HCC, 66.7% of patients were reported to have elevated CDK4 (Kim et al., 2000) and 46% have elevated CDK6 (Che et al., 2012).

PI3K/AKT signal pathway is one of the major intracellular signaling pathways which regulates diverse cellular functions, including cell proliferation, differentiation, translation regulation of protein synthesis, cell migration, and angiogenesis. PI3K-AKT-mTOR usually promotes survival by inhibiting pro-apoptotic factors and activating anti-apoptotic factors (Miricescu et al., 2020). The expressions of PI3K and AKT are elevated in HCC, and are significantly associated with reduced overall survival. Therefore, drugs targeting both CDK4/6 and PI3K/AKT signal pathways should be an excellent therapeutic strategy for HCC.

In this study, we applied a mixed computational and experimental strategy to repurpose approved small molecule drugs to identify inhibitor of CDK4/6 for HCC (Berman et al., 2000; Irwin and Shoichet 2005; Irwin et al., 2012; Li et al., 2012; Li et al., 2014; Huang and Wong 2016). We discovered aminoquinol as a new CD4/6 inhibitor with high anti-cancer activities in human liver cancer HepG2 and Huh7 cells. In addition, it also exhibited significant activity in Hep3B cells which lacks functional Rb gene, suggesting that it has other anti-cancer mechanisms in addition to CDK4/6. Through drug combination screening, we found that aminoquinol could produce weak synergistic effects with 5-Fu and the multi-kinase inhibitor soranfenib, however, clearly displayed antagonistic effects with the PI3K inhibitor LY294002. These results strongly suggested that it may also inhibited PI3K activity. Using Western blotting analysis, we demonstrated that aminoquinol treatment significantly decreased the expressions of key proteins in the CDK4/6 as well as the PI3K/AKT pathways. Thermal proteome profiling (TPP) (Jafari et al., 2014) analysis further suggested that proteins in both CDK4/6 and PI3K/AKT pathways are the binding targets of aminoquinol. Finally, in BALB/C nude mice subcutaneously xenografted with Huh7 cells, we demonstrated the *in vivo* anti-cancer effects by aminoquinol. Taken together, the present study indicates for the first time that aminoquinol is a new CDK4/6 and PI3K/AKT multi-kinase inhibitor and a potential candidate drug for the treatment of human HCC.

MATERIALS AND METHODS

Ethics Statement

This study was approved by the laboratory animal ethics committees of Zhengzhou University.

Chemicals and Anti-Bodies

Lifibrate, Nizofenone, Pimozide, Trifluperidol, Tosufloxacin, Cloricromene, Sulconazole, Sertindole, Aminoquinol, 5-Fuwere purchased from Sigma-Aldrich. Anti-cyclinD, anti-CDK2/4/6, anti-Rb, phosphorylated (pho)-CDK4/6, pho-Rb, AKT, pho-AKT and GAPDH were obtained from Cell Signaling Technology, Inc (Danvers, MA, United States). PI3K, mTOR, pho-mTOR were obtained from ZEN BIO.

Cell Lines and Cell Culture Experimental Conditions

The human liver cancer Huh7, HepG2 and Hep3B cell lines were obtained from the American Type Culture Collection (Manassas,

VA, United States). These cell lines were cultured in DMEM medium (GE Healthcare Life Sciences, Shanghai, China) containing 10% fetal bovine serum (FBS) (Invitrogen Life Technologies, Carlsbad, CA, United States) at 37°C in 5% CO2 and 95% humidified air. Cells were plated in 96-well, 24-well, or 6-well plates (Corning Incorporated, Corning, NY, United States) with medium containing 0.125% FBS for 24 h and then treated with medium containing 10% FBS and the test compounds at various concentrations and incubated for various times as indicated.

MTT and CCK-8 Assays

For the MTT assay (Sigma-Aldrich), cells were plated at an initial density of 9×10^3 cells/well in 96-well plates and incubated with 0.5 mg/ml MTT (Sigma-Aldrich) for 4 h. The medium was then discarded and 200 μl dimethylsulfoxide (Sigma-Aldrich) was added to dissolve the formed formazan crystals. The absorbance was measured at 570 nm with a Synergy 2 microplate reader (Bio-Tek Instruments, Inc., Winooski, VT, United States) according the standard protocol. CCK-8 assay was performed as described in the CCK-8 Kit (Dojindo Laboratories). Cells were seeded in 96-well plate, treated with various drugs for indicated time prior to the addition of CCK-8 solution and OD values were measured at 450 nm using a microplate reader.

Cell Cycle Analysis

Cells (4×10^4) were seeded in 24-well plates in DMEM medium containing 0.125% FBS for 24 h, and then treated with DMEM medium containing 10% FBS and various dose of aminoquinol for indicated time at 37°C. At the end of experiments, cells were fixed in ice-cold 70% ethanol and stained using a Coulter DNA-Prep Reagents kit (Beckman Coulter, Brea, CA, United States). Cellular DNA content of 1×10^4 cells from each sample was determined using an EPICS xL4 flow cytometer (Beckman Coulter). The cell cycle phase distribution was analyzed using ModFit LT 2.0 software (Verity Software House, Topsham, ME, United States). All data were obtained from two separate experiments of which each was performed in triplicate.

Cell Apoptosis Analysis

Cells were plated at 24-well plates with DMEM containing 0.125% FBS for 24 h and then treated with 10% FBS medium containing aminoquinol at concentrations 5 and 10 μM for 48 h. To quantify the apoptosis, the occurrence of apoptotic cells was determined by staining cells with both annexinV and propidium iodide (PI) Following manufacturer's instructions (Life Technologies). Briefly, cells were trypsinized with 0.25% trypsin in the absence of ethylenediaminetetraacetic acid (EDTA), washed with PBS twice, and resuspended in 500 μl of binding buffer at a concentration of 2×10^5–10^6 cells/ml. Two microliters of annexin V-EGFP and 5 μl of PI were added to the suspension followed by 5–15 min of incubation in the dark, and the cells were analyzed using flow cytometry (CyFlow Space/Partec, Germany).

Western Blot Analysis

Cells were plated on 6-well plates in DMEM medium containing 0.125% FBS for 24 h, and then treated with medium containing 10% FBS medium and various concentrations of aminoquinol for 6 h. Cells were harvested and the protein concentration was measured using a bicinchoninic acid Protein Assay kit (Thermo Fisher Scientific, Waltham, MA, United States). Equal amounts (10 μg protein) of cell lysates were resolved using 10% SDS-PAGE and transferred onto nitrocellulose membranes (Sigma-Aldrich). After blocking with 5% skim milk, blots were treated with the primary antibody at 4°C overnight, then with horseradish peroxidase-labeled secondary antibody. The proteins were measured using enhanced chemiluminescence detection system (Thermo Fisher scientific, United States). The primary antibodies were purchased commercially: anti-cyclin D1 (CST, no.2978), anti-CDK2 (CST, no.2546), anti-CDK4 (CST, no.12790), anti-phospho-CDK4 (CST, no.5884), anti-CDK6 (Abcam, no.13331), anti-phospho-CDK6 (ZEN BIO, no.530326), anti-Rb (CST, no.9313), anti-phospho-Rb (CST, no.9301), anti-KRAS (Proteintech, no.12063-1-AP), anti-NRAS (Proteintech, no.10724-AP), anti-c-Raf (CST, no.9422), anti-MEK1/2 (ZEN BIO, no.200424), anti-ERK1/2 (ZEN BIO, no.340750), anti-PI3K (ZEN BIO, no.380849), anti-AKT (CST, no.4685S), anti-phospho-AKT (CST, no.4060S), anti-mTOR (ZEN BIO, no.385034), anti-phospho-mTOR (ZEN BIO, no.385033), anti-GAPDH (CST, no.5174). All of the antibodies were diluted by 1: 1,000 dilution.

Quantitate the Synergy of Drug Combination

We quantitated the synergy of drug combination according to the Chou-Talalay method (Chou, 2011). Huh7 cells (5×10^3cells/well) were plated in 96-well plates, cells were treated with indicated concentrations of aminoquinol and 5-Fu (Wang et al., 2018), sorafenib (Bollard et al., 2017), or LY294002 (Teo et al., 2017) for 72 h. Cell viability was determined by CCK-8 assay and the absorbance values measured at 450 nm using microplate reader. The combined effect was analyzed by CompuSyn software (www.combosyn. com), and the multiple drug dose-effect were calculated using the Median Effects methods described by Chou and Talalay to determine the fraction affected (Fa), and the combination index (CI). The fraction affected Fa = 1- (average OD value of experimental group/average OD value of control group), which represents the inhibition rate. The combination index CI = (D)1/(Dx)1+(D)2/(Dx)2, Dosage as a single drug (D), Dosage used in the combination drug (Dx). The definitions of CI are the following: 1) CI = 1 represents additive effect, 2) CI < 1 represents synergistic effect, and 3) CI > 1 represents antagonism (Chou, 2006; Chou, 2010; Chou, 2011).

Thermal Proteome Profiling Analysis

TPP analysis were conducted as described previously (Jafari et al., 2014) (Franken et al., 2015). Huh7 cells were plated on 6-well plates in DMEM medium containing 10% FBS medium. After

washing with PBS, cells were scraped off, suspended in the lysis buffer, then lysed with three freeze thaw cycles using liquid nitrogen. The lysate was centrifuged at 10800×*g* for 20 min in 4°C, the supernatant collected, and adjusted to 1 mg ml^{-1} (by BCA assay). The lysates were treated with 100 μM aminoquinol or DMSO at 25°C for 20 min with gentle mixing, and divided into 10 fractions for thermal profiling. Fractions were heated at the indicated temperatures (35–75°C) for 3 min, incubated for 3 min at room temperature, centrifuged at 15,000×*g* for 5 min at room temperature, and the supernatants were analyzed by Western blots.

Evaluation of the Anti-cancer Activity of Aminoquinol *in vivo* in Nude Mice Xenografted With Huh7 Cells

Female BALB/C nude mice (n = 20, 4–5 weeks old; weighing 15 g; Vital River Laboratory Technology Co. Ltd., Beijing, China), were housed under pathogen-free conditions with a 12 h light/dark cycle, in an environment containing 50–80% humidity at 15–27°C, and cared for in accordance with the guidelines of the laboratory animal ethics committee of Zhengzhou University (Zhengzhou, China). The cages, food, and water of the mice were sterilized. To establish the xenograft model, 1 × 10^6 Huh7 cells in 0.2 ml phosphate-buffered saline were injected subcuta-neously into the right flank of the mice (n = 5) and the tumor size was measured every day using a caliper. One week after inoculation, when the tumors grew to a volume of 80–100 mm^3, mice were randomly divided into four groups (5 mice/group) and intraperitioneal injected with PBS (control), aminoquinol (35 mg/kg), 5-Fu (10 mg/kg), or aminoquinol (35 mg/kg) + 5-Fu (10 mg/kg), daily for 21 days. Tumor volume was calculated using formula V = ab^2/2 (a = longest axis; b = shortest axis). At 21 days, mice were sacrificed by cervical dislocation, tumors excised and weighed, their images captured, and the tissues fixed for immunohistochemistry studies.

Immunohistochemistry

Tumor tissues were fixed in 10% formalin, embedded in paraffin, sliced into 4 μm sections, deparaffinized, dehydrated, antigen retrieved, blocked with 5% goat serum, and incubated with the primary antibodies: anti-RB1 (CST, no.9313, 1: 500), anti-CDK4 (CST, no.12790, 1: 500), anti-CDK6 (CST, no.13331, 1: 500), anti-PI3K (ZEN BIO, no.220742, 1: 500), anti-AKT (CST, no.4685S, 1: 500), anti-phospho-AKT (CST, no.4060S, 1: 500), anti-phospho-mTOR (ZENBIO, no.380411, 1: 500) and anti-ki67 (SAB, no.48871, 1: 500). The slides were washed and incubated with biotinylated anti-mouse or anti-rabbit secondary antibodies. The peroxidase reaction was visualized using 3, 3′-diaminobenzidine tetrahydrochloride (DAB) and counterstained with hematoxylin. To quantitate the staining intensity, five random fields were chosen, and the numbers of total cells and positive cells were counted in each section under a microscope at 400× magnification. The percentage of positive cell populations from the five random fields was analyzed for statistical significance.

Statistical Analysis

Data were obtained from at least three experiments. Values are expressed as the mean ± standard deviation. Statistical analysis was performed by Student's t-test, and the results were analyzed using SPSS 16.0. $p < 0.05$ was considered to indicate a statistically significant difference between values.

RESULTS

Discovery of Aminoquinol as a CDK4/6 Inhibitor and Determined Its Activity in Reducing the Viability of HepG2 and Huh7 Cells

To identify candidate CDK4/6 inhibitors, we used structure-based virtual screening method to screen for CDK4/6 inhibitor as described previously (Shi et al., 2018). Briefly, five X-ray crystallographic structures of CDK4 and eight X-ray crystallographic structures of CDK6 in complex with ligands were collected from the Protein Data Bank (PDB) (Berman et al., 2000; Huang and Wong 2016). A total of 3,167 drugs that have been approved by worldwide authorities were selected to constitute a library of compounds to screen, and their structures were collected from the ZINC database (Irwin and Shoichet 2005) (Irwin et al., 2012). These drugs were individually docked to the ATP binding pocket of CDK4/6, and sorted in the ascending order of their predicted binding free energy. The free and open-source docking software idock v2.2.1 (Li et al., 2014) developed by our group was applied to dock all of the compounds onto all of the CDK4/6 structures to predict their binding conformations as well as their binding affinities. The compounds were sorted in an ascending order according to their average predicted binding free energy, and the high-scoring compounds were manually examined based on in silico estimations of binding strength, appropriate molecular weight and other drug-like properties, complementary matching of molecular shape, plus some sense of intuition from a computational chemist's experience. Finally, high-scoring compounds were shortlisted and 10 commercially available compounds (**Supplementary Table 1**) (Bueno 1965; Janssen et al., 1968; Ross 1970; Arnold et al., 1979; Dejana et al., 1982; Lassus et al., 1983; Fujimaki et al., 1988; Matsumoto et al., 1994; Muscatello et al., 2014) were purchased for subsequent wet-lab validations.

These ten compounds (Lifibrate, Nizofenone, Pimozide, TRIFLUPERIDOL, Tosufloxacin, Cloricromene, Sulconazole, Sertindole, Rafoxanide and Aminoquinol) were tested for their ability to decrease the viability of Huh7 (**Figure 1A**) and HepG2 (**Figure 1B**) cells. Aminoquinol was found to be the most effective drug in both cell lines. Aminoquinol reduced cell viability significantly ($p < 0.05$) in a dose and time dependent manner (**Figure 1C** and **Figure 1D**), with IC50 value equal to 1.47 μM for HepG2 and 2.13 μM for Huh7 cells. The predicted two-dimensional chemical structure of aminoquinol is shown in **Figure 1E**. Aminoquinol was stabilized through specific interactions such as hydrogen bonding, as well as nonspecific interactions such as hydrophobic interactions with residues in the drug-binding pocket of CDK4 and CDK6. Computer docking

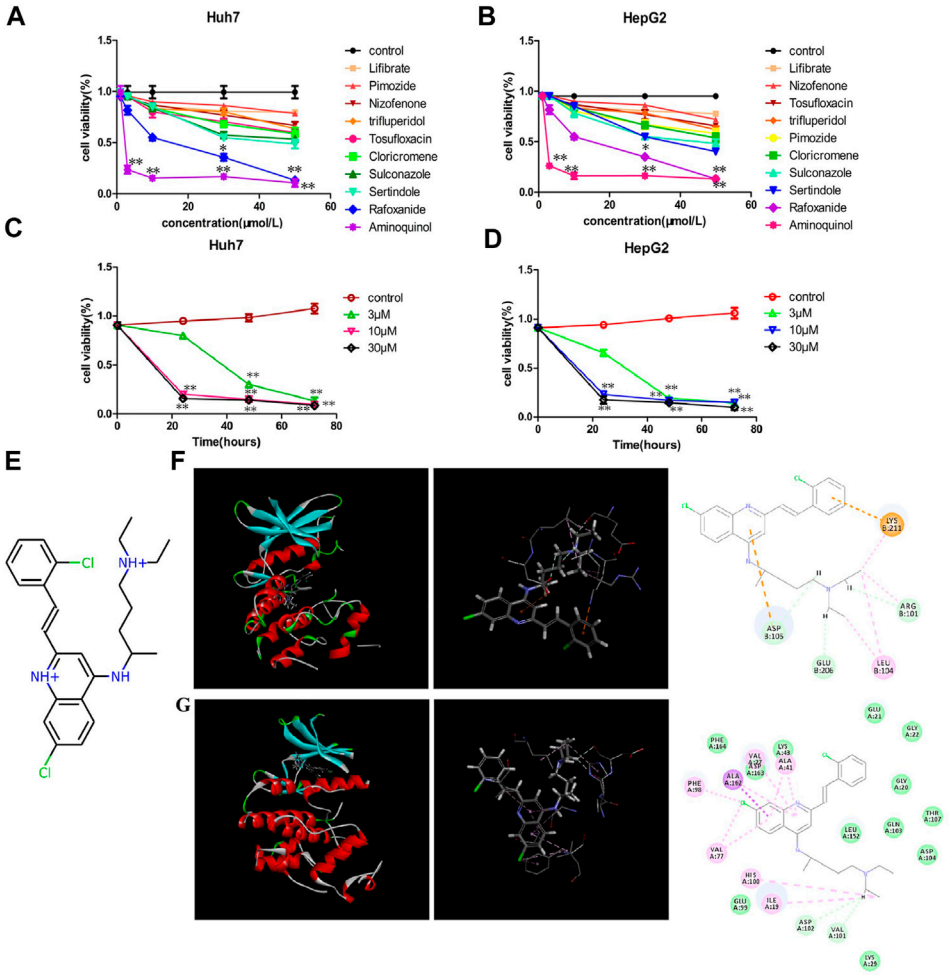

FIGURE 1 | The effect of aminoquinol on the cell viability in human hepatocarcinoma Huh7 and HepG2 cell lines **(A)** The effect of ten candidate compounds on the cell viability in Huh7 cells and **(B)** in HepG2 cells **(C)** Time-response curves for different doses of aminoquinol in Huh7 cells and **(D)** in HepG2 cells **(E)** The predicted two-dimensional chemical structure of aminoquinol **(F)** Computer docking analysis of the interaction of aminoquinol with CDK4 and **(G)** with CDK6 *, ** indicate significant difference at $p < 0.05$, $p < 0.01$, respectively.

analysis predicted that aminoquinol interact with CDK4 (**Figure 1F**) through three hydrogen bonds with ARG101, ASP105 and GLU206, two π–π stacking with ASP105 and LYS211, and one hydrophobic contact with LEU104. It interacts with CDK6 (**Figure 1G**) through four hydrophobic contacts with ILE19, ALA41, VAL77 and ALA162, two hydrogen bonds with VAL101 and ASP102, and two salt bridges with VAL77 and PHE98.

Aminoquinol Caused Cell Cycle Arrest in G1 Phase and Induced Cell Apoptosis

To assess the effects of aminoquinol on cell-cycle progression, cells were treated with aminoquinol (3, 5, 10 μM) for 6, 12 or 24 h, and its effects on the cell cycle profile were determined by flow cytometry. Aminoquinol induced the accumulation of cells in G1 phase as compared to the control group in a dose-and time-dependent manner in Huh7 (**Figure 2A**) and HepG2 (**Figure 2B**) cells. At 24 h after treatment, it significantly ($p < 0.05$) increased cell populations in the G1 phase and decreased the cell populations in S-phase in both Huh7 and HepG2 cells (**Figure 2C** and **Figure 2D**). We also investigated whether aminoquinol could induce cell apoptosis as tumors often re-grow after stop dosing with cell cycle inhibitor. As shown in **Figure 2E** and **Figure 2F**, aminoquinol (10 μM) significantly increased the percentage of both early and late apoptosis in Huh7 (**Figure 2E**) and HepG2 (**Figure 2F**) cells as compared to the control ($p < 0.05$), at 48 h after treatment.

Aminoquinol Treatment Decreased the Expression of CDK4/6, Rb, CyclinD, Pho-Rb, Pho-CDK4/6, but Not CDK2 in HepG2 and Huh7 Cells

To support the notion that aminoquinol is a CDK4/6 inhibitor, western blot analysis (**Figure 3A**) was used to verify the effects of

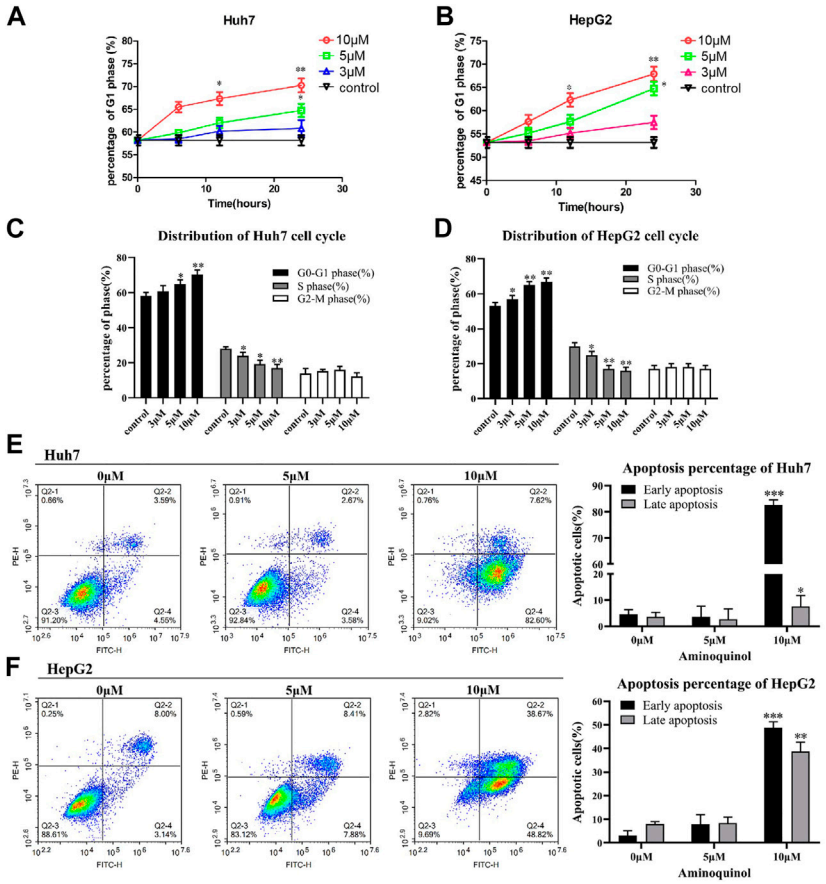

FIGURE 2 | Aminoquinol treatment caused cell cycle G1 arrest and induced apoptosis in Huh7 and HepG2 cells **(A)** Aminoquinol (3, 10 and 30 μM) treatment induced the accumulation of cells in G1 phase in a dose-and time-dependent manner in Huh7 and **(B)** HepG2 cells **(C)** At 24 h after treatment, aminoquinol significantly ($p < 0.05$) increased cell populations in the G1 phase and decreased the cell populations in S-phase in Huh7 and **(D)** HepG2 cells **(E)** At 48 h after treatment. aminoquinol (10 μM) significantly increased the percentage of early and late apoptosis in Huh7 and **(F)** HepG2 cells as compared to the control ($p < 0.05$), *, ** indicate significant difference at $p < 0.05$, $p < 0.01$, respectively.

aminoquinol (0, 2, 4, 6, 8, 10 μM) on the expressions of key proteins involved in cell cycle progression in Huh7 and HepG2 cells after 6 h of treatment. Amninoquinol dose-dependently decreased the expressions of CDK4 (**Figure 3D**), pho-CDK4 (**Figure 3E**), CDK6 (**Figure 3F**), pho-CDK6 (**Figure 3G**), cyclinD (**Figure 3C**), Rb (**Figure 3H**), and pho-Rb (**Figure 3I**), while it did not cause significant change in CDK2 (**Figure 3B**) expression. Quantitatively, aminoquinol appears to be most effective for reducing the expression of CDK4 (**Figure 3D**). These results suggested that amninoquinol inhibited CDK4/6 phosphorylation, reduced their complex with cyclinD, subsequently led to the reduction of Rb phosphorylation and the activation of E2F, and effectively inhibited the transition of G1 to S phase.

The Synergy of Aminoquinol Combined With 5-Fu, Sorfafenib and LY294002 in Reducing Cell Viability

The actions of CDK inhibitors on cell cycle arrest requires an intact functional RB. We found that aminoquinol could effectively reduce the viability of the Rb negative Hep3B cells (IC50 = 5.34 μM), suggesting that it has other anti-cancer mechanisms in addition to CDK4/6. To identify the additional mechanisms, Chou-Talalay method were used to evaluate the antagonistic or synergistic effect of aminoquinol (0, 1, 3, 5 μM) in combination with 5-Fu (0, 1, 3, 10, 30, 100 μM), the multi-kinase inhibitor sorfafenib (0, 1, 3, 10, 30, 100 μM), and the PI3K inhibitor LY294002 (0, 1, 3, 10, 30, 100 μM). Briefly, Huh7 (**Figures 4A, B**) and HepG2 (**Figures 4C, D**) cells were plated in 96-well plates (5×10^3cells/well), and treated with indicated concentrations of aminoquinol plus 5-Fu, sorafenib or LY294002 for 72 h. Cell viability was determined by the CCK-8 assay (**Figures 4A–D** left figure). The specific combination index (CI) values of the drug combination are shown in **Supplementary Table 2–7**. In aminoquinol and 5-Fu (**Figure 4A**, **Figure 4C**, right figure) or sorafenib (**Supplementary Figure 2A, B**, right figure) combination treatments, most of the fraction affected-combination index (Fa) and CI plot, the CI values were less than 1, suggesting a weak synergistic effect. Importantly, we found that the fraction

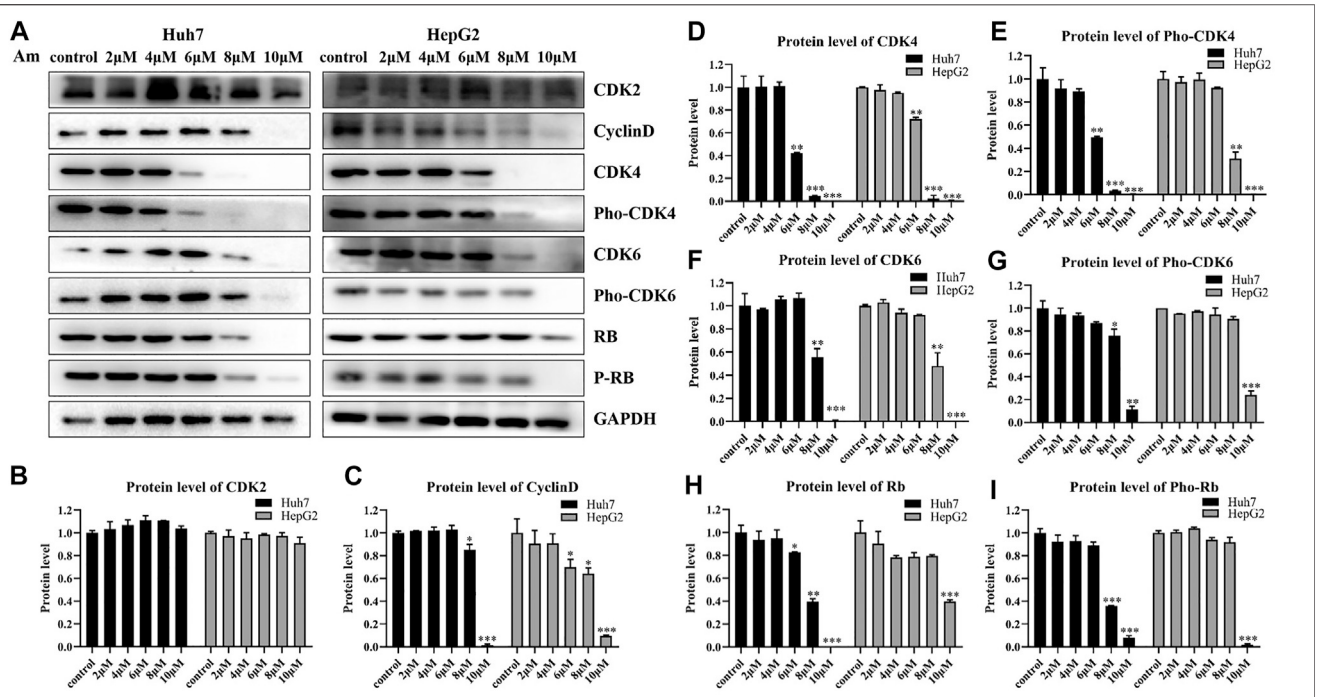

FIGURE 3 | Aminoquinol treatment decreased the expressions of CDK4/6, Rb, cyclinD, pho-Rb, pho-CDK4/6, but not CDK2 in HepG2 and Huh7 cells **(A)** The western blot analysis of Huh7 and HepG2 cells treated with different concentrations of aminoquinol (0, 2, 4, 6, 8, 10 μM) for 6 h **(B–I)** The quantified data of protein expressions for **(B)** CDK2, **(C)** CyclinD, **(D)** CDK4, **(E)** pho-CDK4, **(F)** CDK6, **(G)** pho-CDK6, **(E)** Rb and **(I)** pho-Rb. Data were presented as means ± standard deviation.*$p < 0.05$, **$p < 0.01$, ***$p < 0.001$, significantly different from the control group.

affected-combination index (Fa) and CI plot in the aminoquinol and LY294002 combination, indicated a clear antagonistic effect with all of the CI > 1 in Huh7 (**Figure 4B**, right figure) and HepG2 (**Figure 4D**, right figure) cells. These results strongly suggested that aminoquinol itself may possess PI3K inhibitor activity.

Aminoquinol Reduced the Expressions of Key Proteins in the PI3K/AKT/mTOR Pathway

To validate the effect of aminoquinol on the PI3K signal pathway, western blot analysis (**Figure 5A**) was conducted. Our results showed that aminoquinol (0, 4, 6, 8, 10 μM) treatment significantly and dose dependently decreased the protein expressions of PI3K (**Figure 5B**), AKT (**Figure 5C**), pho-AKT (**Figure 5D**), mTOR (**Figure 5E**), and pho-mTOR (**Figure 5F**), in Huh7 and HepG2 cells. Meanwhile, it had no significant effect on the expressions of Ras, Raf, MEK and ERK (**Supplementary Figure 3**). These results were consistent with what is expected of an PI3K/AKT inhibitor.

Thermal Proteome Profiling Analysis Suggested the Binding of Aminoquinol With CDK4/6, PI3K and AKT in Huh7 Cells

To further validate the molecular targets of aminoquinol, thermal proteome profiling (TPP) analysis were performed. Huh7 cells were lysed and treated for 20 min with vehicle (DMSO) or 100 μM aminoquinol to ensure a complete saturation of ligand binding and maximizes the shift in detected protein denaturation, and then heated at temperatures ranging from 35 to 75°C to denature and precipitate unbound proteins, as protein which bound to aminoquinol will be more stable and could not be precipitated at high temperature. The thermally aggregated proteins were then removed by centrifugation, and soluble protein fraction which contains ligand-bound proteins were collected and analyzed by western blot analysis. As shown in **Figure 6**, aminoquinol significantly improved the thermal stability of its main targets CDK4 (**Figure 6A**), CDK6 (**Figure 6B**), PI3K (**Figure 6C**), and pho-AKT (**Figure 6E**), suggesting direct bindings of aminoquinol and these proteins. The thermal stability of AKT (**Figure 6D**), mTOR (**Figure 6F**), and pho-mTOR (**Figure 6G**) showed weak increases, suggesting weak binding or indirect interaction with aminoquinol (Franken et al., 2015).

Aminoquinol Reduced the Tumor Growth *in vivo* in BALB/C Nude Mice Xenografted With Huh7 Cells

The *in vivo* anti-tumor activity of aminoquinol were evaluated in BALB/C nude mice xenografted with Huh7 cells. Huh7 cells were subcutaneously injected into the armpits of BALB/C nude mice. When the tumors grew to 80–100 mm^3 (7 days after inoculation), mice were randomly divided into four groups (5 mice/group), and treated with daily intraperitoneal administration of 1) control (PBS),

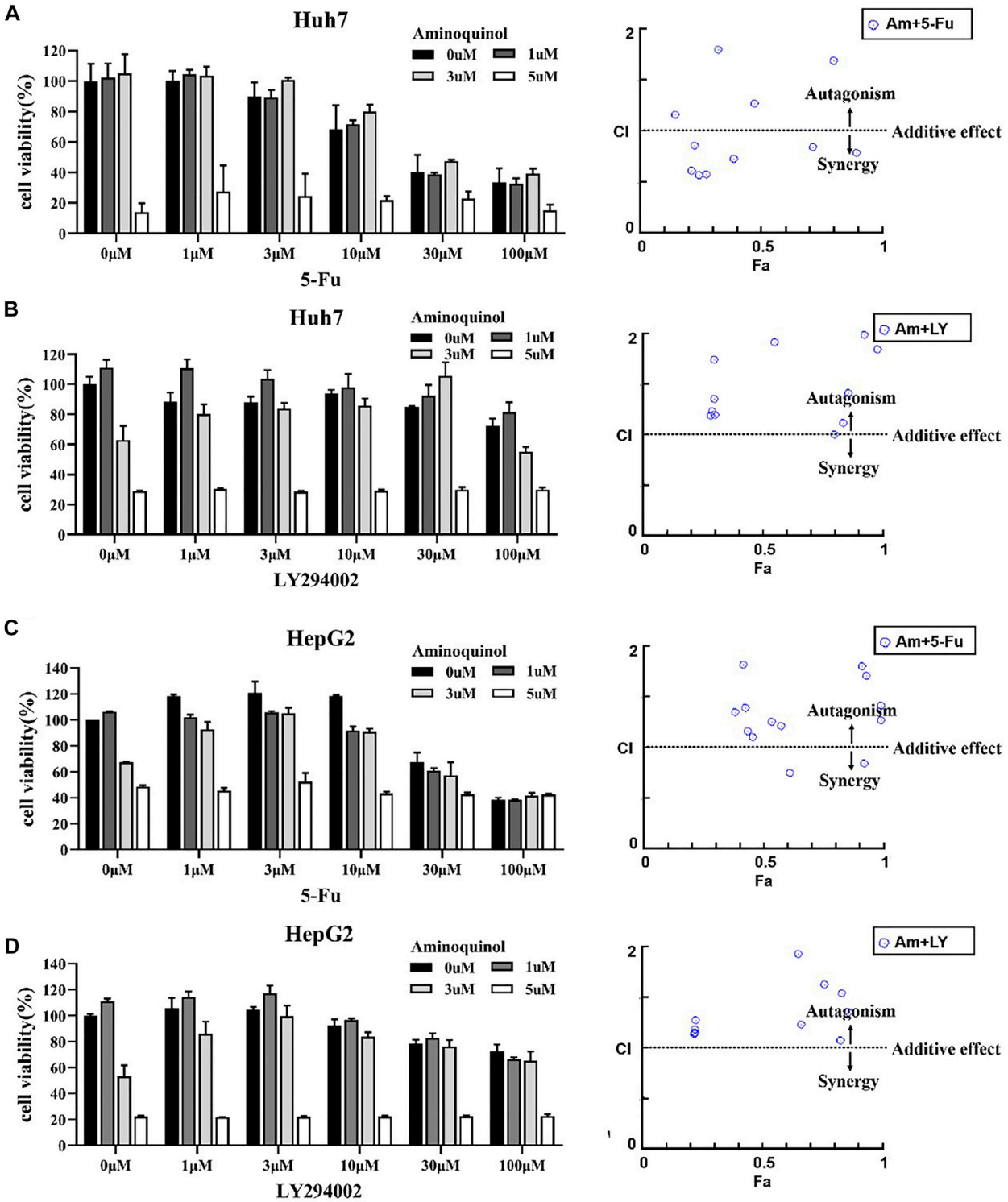

FIGURE 4 | The antagonistic or synergistic effect of combinating aminoquinol with 5-Fu, sorfafenib, and LY294002 in reducing cell viability in HCC cells **(A, B)**, left figures) Huh7 cells or **(C, D)**, left figures) HepG2 cells were treated for 72 h with aminoquinol (0, 1, 3, 5 μM) in combination with 5-Fu (0, 1, 3, 10, 30, 100 μM), or the PI3K inhibitor LY294002 (0, 1, 3, 10, 30, 100 μM), and cell viability determined **(A–D)**, right figures) The fraction affected (Fa)-combination index (CI) plots of aminoquinol in combination with 5-Fu or LY294002. The combined effects and the specific combination index (CI) were analyzed by CompuSyn software. CI > 1 indicated the antagonistic effect, CI = 1 indicated additive effect, and CI < 1 indicated synergistic effect.

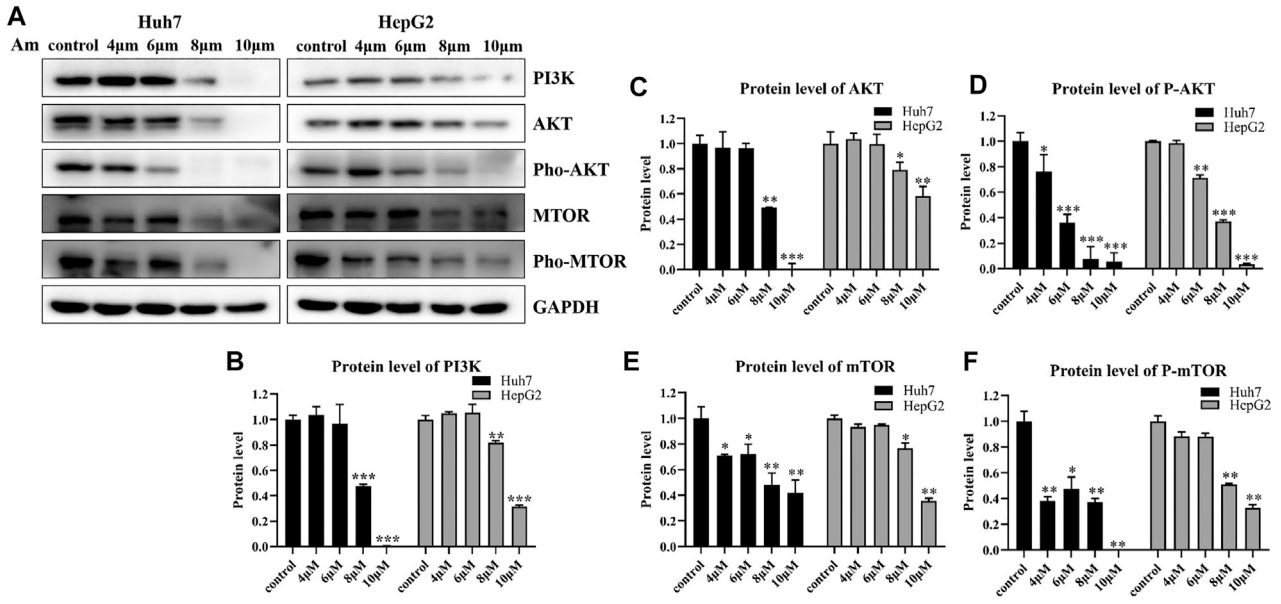

FIGURE 5 | Aminoquinol reduced the expressions of key proteins in the PI3K/AKT/mTOR pathway **(A)** Western blot analysis of Huh7 and HepG2 cells treated with indicated concentrations of aminoquinol for 6 h **(B–F)** The quantified data of **(B)** PI3K, **(C)** AKT, **(D)** p-AKT, **(E)** mTOR, and **(F)** p-mTOR. Data were presented as means ± standard deviation. $^{*}p < 0.05$, $^{**}p < 0.01$, $^{***}p < 0.001$, significantly different from the control group.

2) aminoquinol (35 mg/kg, i. p.), 3) 5-Fu (10 mg/kg, i. p.), and aminoquinol (35 mg/kg, i. p.) plus five- Fu (10 mg/kg, i. p.) for 21 days, and the tumor volume recorded. At the end of the experiment, mice were sacrificed by cervical dislocation, tumor tissues excised, weighed, images captured, and immunohistochemistry analysis performed. Aminoquinol and 5-Fu treatments significantly reduced tumor weight (**Figure 7A**) and tumor volume (**Figure 7B**), with comparable curative effects. Of note, administration of combined aminoquinol plus 5-Fu produced the highest therapeutic effect. At the same time, all treatments had no significant effect on the body weight of the mice during the whole experiment (**Figure 7C**). Immunohistochemistry staining of tumor tissues showed that aminoquinol treatment significantly reduced the expressions of Rb, CDK4, CDK6, PI3K, pho-AKT and pho-mTOR (**Figures 7D–K**), as compared to the control group. The 5-Fu treatment did not produce any obvious effect.

Clinical Significance

Taken together, our results suggested that aminoquinol acted through direct binding to CDK4/6 and PI3K/p-AKT (**Figure 8**). We analyzed the expressions of CDK4/6 and PI3K/AKT/mTOR in normal human tissues and liver cancer patient tissues through ualcan. As shown in **Supplementary Figure 1A, B**, in liver cancer tissues, the expressions of CDK4 (p = 1E-12) and CDK6 (p = 5.74E-14) were significantly increased. Kaplan-Meier analysis indicated that only elevated expression of CDK4 (**Supplementary Figure 1C**) is significantly associated with reduced overall patient survival (OS) (p = 6.20E-07), but there was no significant difference in CDK6 (**Supplementary Figure 1D**). For the PI3K/AKT/mTOR pathway, significantly elevated expression of the PI3K (p = 1.62E-12) (**Supplementary Figure 1E**), AKT (p = 0.0049) (**Supplementary Figure 1F**) and mTOR (p = 1E-12) (**Supplementary Figure 1G**) were observed in liver cancer patient tissues as compared to normal liver tissues. Kaplan-Meier analysis indicated that the elevated expressions of PI3K (p = 0.0025) (**Supplementary Figure 1H**) and AKT (p = 0.0025) (**Supplementary Figure 1I**) are significantly associated with reduced overall survival in liver cancer patients, while mTOR levels had no significant association with survival (**Supplementary Figure 1J**).

DISCUSSION

Cell cycle progression is regulated in a sequential and highly organized manner through the interaction of CDKs and cyclins (Malumbres and Barbacid 2009). During the G1 to S phase transition, the cyclinD-CDK4/6 complexes are sequentially activated and the retinoblastoma gene (Rb) is hyper-phosphorylated (Reed 1997; Cobrinik 2005), then releases the transcription factor E2F, which in turn facilitates the transcription of numerous cell cycle-related genes and make cells enter the S phase (Meraldi et al., 1999). The expressions of CDK4/6 are often elevated in many tumors (Yamamoto et al., 1995; Kim et al., 2000; Cohen 2002; Li et al., 2002; Che et al., 2012). Theoretically, CDK inhibitor should be a broad spectrum and effective therapeutic drug for HCC as well as many other cancers. However, the efficacy of CDK4/6 inhibitor to HCC and other cancers are very limited (Sherr et al., 2016; Bollard et al., 2017). The discovery of more effective and less toxic CDK inhibitors, or drugs that targeting both CDKs and other major molecular targets are urgently needed.

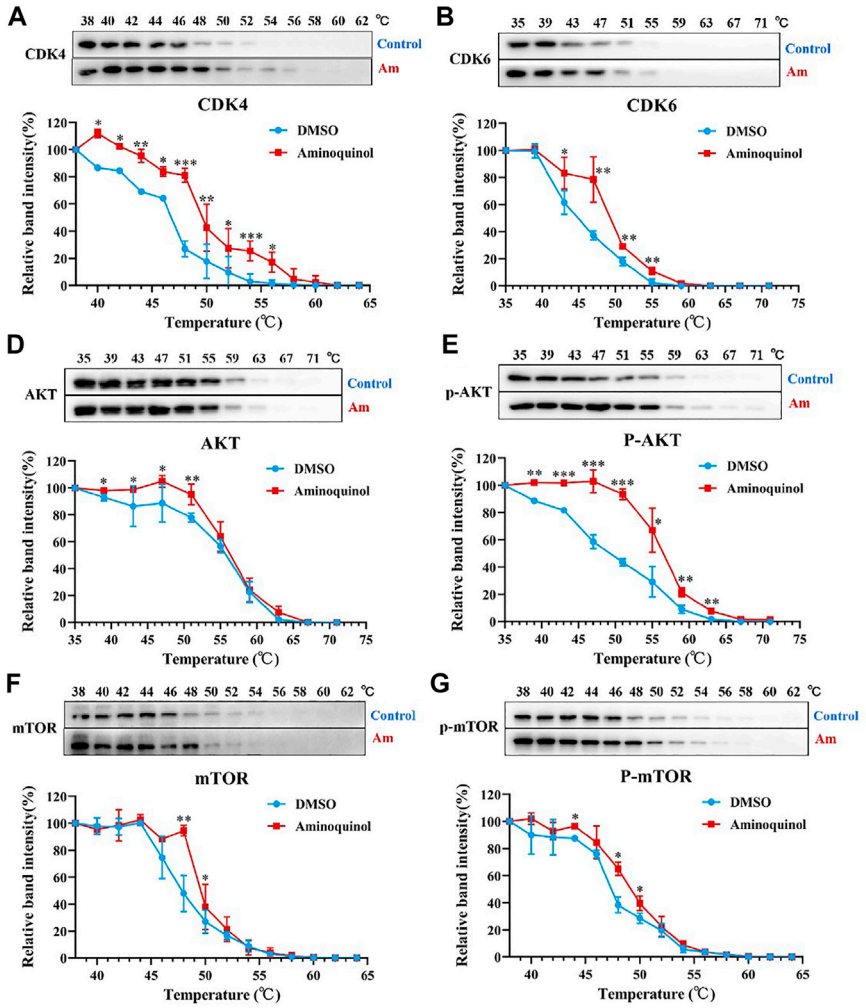

FIGURE 6 | Thermal proteome profiling (TPP) analysis suggested the binding of aminoquinol with CDK4/6, PI3K and p-AKT in Huh7 cells. Huh7 cell lysate was treated with aminoquinol (100 μM) or vehicle (DMSO) for 20 min and incubated at temperatures ranging from 35 to 75°C. Proteins from each fraction were analyzed via western blotting. Quantification was based on the intensity of bands. Thermal denaturation curves were obtained from all proteins in control (blue) and aminoquinol-treated (red) samples **(A–C, E)** The representative pictures of western blotting and thermal denaturation curves of **(A)** CDK4, **(B)** CDK6, **(C)** PI3K and **(E)** p-AKT, indicating thermal stabilization **(D, F–G)** The thermal stability of **(D)** AKT, **(F)** mTOR and **(G)** p-mTOR, indicating weak increases in thermal stability. All experiments were performed in triplicate, and data were given as the AVE ± SEM. *$p < 0.05$, **$p < 0.01$, ***$p < 0.001$, significantly different from the control group.

Currently, the combination of CDK 4/6 inhibitor palbociclib and fulvestant is FDA approved (Vidula and Rugo, 2016) clinically for the treatment of hormone receptor-positive and HER2-negative metastatic breast cancer (Lin et al., 2005). Palbociclib is a highly selective inhibitor of CDK4 and CDK6 kinases (Fry et al., 2004) in cells with functionally intact RB (Matsushime et al., 1992; Ewen et al., 1993; Kato et al., 1993), but not in RB absent Hep3B and BT549 (Asghar et al., 2015; Sherr et al., 2016). Results from an extensive preclinical study (Bollard et al., 2017) supports the use of palbociclib, alone or in combination with sorafenib, for HCC treatment. The adverse side effects of Palbociclib included neutropenia, infections, fatigue and gastrointestinal toxicity, which limited capacity of Palbociclib for the treatment of HCC (Bollard et al., 2017).

To discover more effective and less toxic CDK inhibitors, we have used computer-aided strategy to discover two CDK2 inhibitors, Adapaline and Fluspirilene for liver cancer and colon cancer (Shi et al., 2015a; Shi et al., 2015b), a CDK4/6 inhibitor Rafoxanide for skin cancer but not very effective for HCC (**Figures 1A, B**) (Shi et al., 2018). In addition, we have recently identified a CDK2/4/6 triple inhibitor (manuscript in preparation). In this study, we reported that aminoquinol is a new CDK4/6 inhibitor. Furthermore, it also inhibited the PI3K/AKT signal pathways, making it the first reported CDK4/6 plus PI3K/AKT muti-kinase inhibitor. Recent data indicated that the PI3K-AKT-mTOR signaling pathway plays an important role in the self-renewal of cancer stem cells and resistance to chemotherapy or radiation therapy (Park et al., 2020; Hou et al., 2021). Therefore, aminoquinol may be more effective for HCC and other cancers.

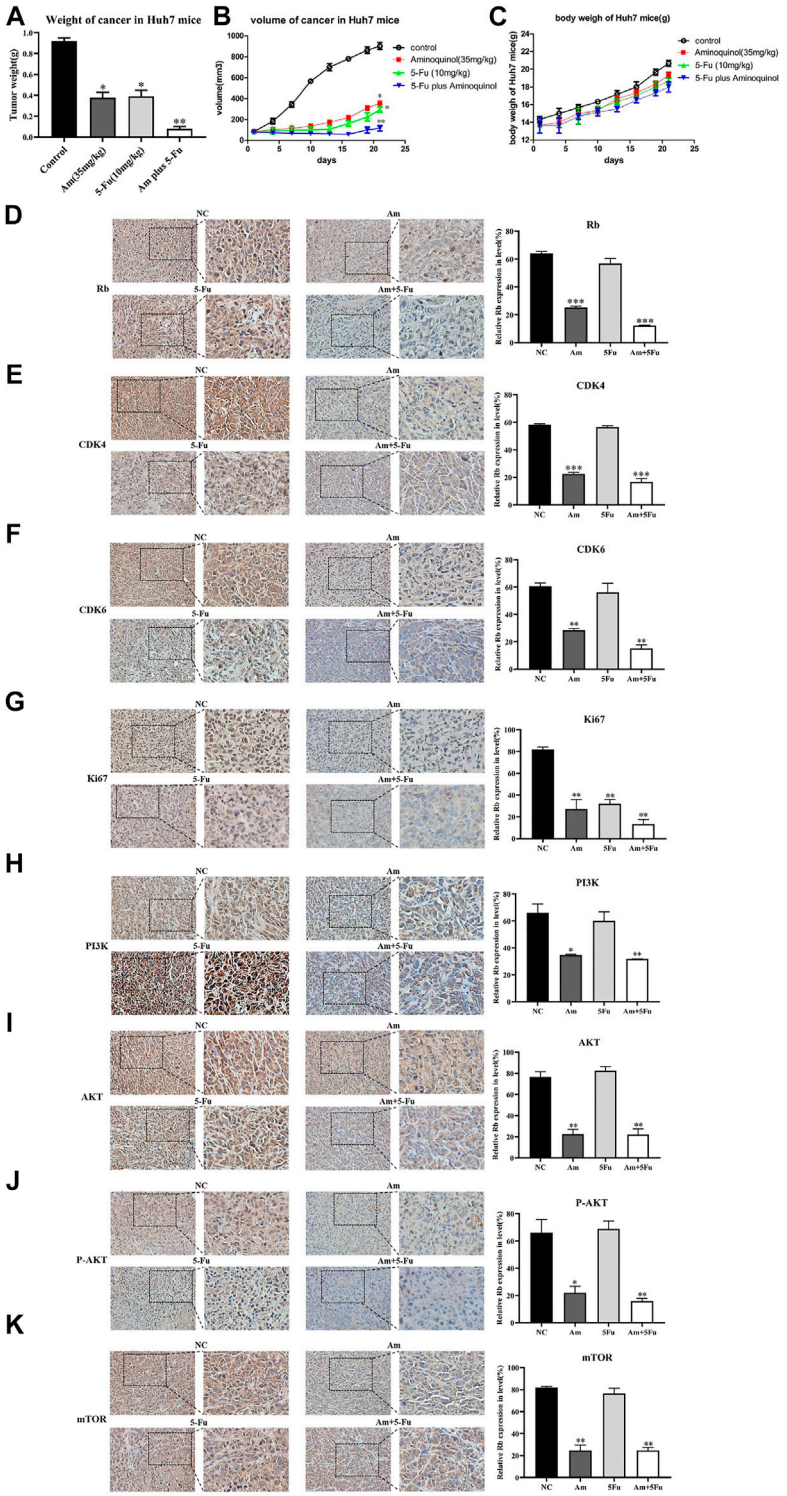

FIGURE 7 | Aminoquinol treatment inhibited tumor growth *in vivo* in BALB/C nude mice xenografted with Huh7 cells. BALB/C nude mice xenografted with Huh7 cells were treated with aminoquinol (35 mg/kg), 5-Fu (10 mg/kg), aminoquinol (35 mg/kg) plus 5-Fu (10 mg/kg) and PBS for 21 days daily by intraperitoneal injection **(A)** Tumor weight at 21 days after treatment **(B)** Tumor volumes during the experiment **(C)** The body weight of the mice during the experiment **(D–K)** The representative pictures and quantified data of immunohistochemistry staining of the xenografted tumor tissues for the expressions of **(D)** Rb, **(E)** CDK4, **(F)** CDK6, **(G)** ki67, **(H)** PI3K, **(I)** AKT, **(J)** P-AKT, and **(K)** mTOR. Data are expressed as the mean ± SD. $^{*}p < 0.05$, $^{**}p < 0.01$, $^{***}p < 0.001$, significantly different from the control PBS treatment group.

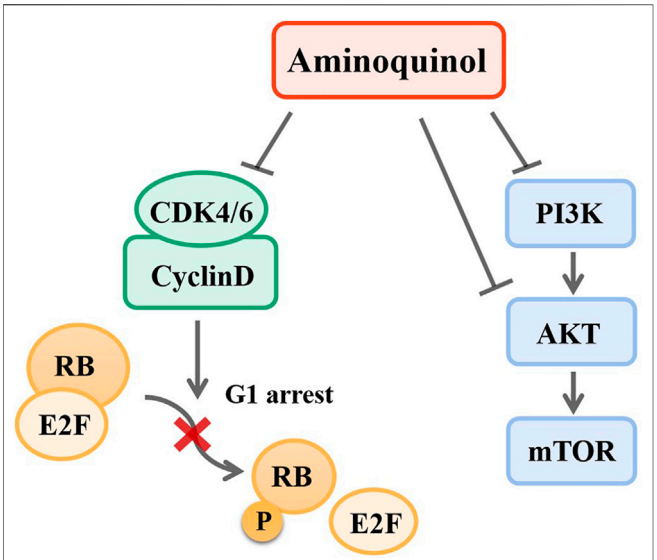

FIGURE 8 | Mechanisms of aminoquinol. Aminoquinol inhibited CDK4/6 phosphorylation and the complex with cyclinD, blocked the phosphorylation of RB and the releases of pRB via its association with transcription factor E2F, and subsequently inhibited the cell cycle to proceed from G1 to S-phase. In addition, aminoquinol also suppressed the signal pathway PI3K/AKT/mTOR, therefore inhibited cell proliferation and promoted apoptosis.

Considering the diverse genomic dysregulations observed in HCC, the combination of CDK inhibitor with inhibitors of multiple additional molecular targets should be more effective in the treatment of HCC and other cancers (Sobhani et al., 2019). As the loss of RB constituted the main mechanism of inherent drug resistance and acquired resistance in human liver cancer (Rivadeneira et al., 2010; Bollard et al., 2017). The observation that aminoquinol is equally effective on liver cancer cells which lack RB gene, may make it clinically more effectively against drug resistance.

Furthermore, aminoquinol displayed synergistic effect when used in combination with 5-Fu and sorfafenib (targets VEGFR-1, 2, 3, RET/PTC, and BRAF). (Bollard et al., 2017; Teo et al., 2017; Wang et al., 2018). 5-Fluorouracil (5-Fu) is a widely employed antineoplastic agent that acts as anti-metabolite (Wang et al., 2018; Moracci et al., 2021). Sorafenib has been used as a first-line drug in clinical practice for patients with advanced liver cancer for more than a decade (Bollard et al., 2017; Kudo 2020). Further studies will optimize the best combination of aminoquinol with sorafenib and other targeted drugs to provide additional synergistic efficacy against HCC and other cancers.

At present, aminoquinol is consider as an antiprotozoal drug, mainly used for acute necrotising form of cutaneous leishmaniasis (Shmushovich 1967). Originally used as an anti-plasmodium drug approved by FDA, aminoquinol it is relatively safe in the therapy of human. In our study, we did not observe significant changes in the body weight of the BALB/C nude mice administered (i.p.) with aminoquinol (35 mg/kg) for 21 days. The reported LD50 of aminoquinol equals to 125 mg/kg (i.p.) in mice (Keithly 1982). In comparison, mice received (150 mg/kg, oral) palbociclib showed a slight loss in body weight in the Huh7 xenograft model, with LD50 of Palbociclib in rats equal to 369 mg/kg (oral) (Flaherty et al., 2012). Aminoquinol has been reported to have acute oral toxicity and poor solubility. Further studies are required to improve efficacy and reduce toxicity. These strategies include the use of biodegradable materials as a carrier for targeted drug delivery to cancer cells, or combining with other small molecule drugs to reduce the dosage.

Taken together, as a new CDK4/6 and PI3K/AKT multi-kinase inhibitor, aminoquinol is a potential drug for HCC treatment alone or in combination with 5-Fu, sorafenib and potentially other targeted anti-cancer drugs. Optimization of best treatment combinations for the treatment of HCC and other cancers warrant further investigations.

DATA AVAILABILITY STATEMENT

The original contributions presented in the study are included in the article/**Supplementary Material**, further inquiries can be directed to the corresponding authors.

AUTHOR CONTRIBUTIONS

Z-KX, YZ, K-BK, H-JL, R-PZ, Z-RM and F-MZ carried out the samples collection and performed the experiments. WW, CD, X-DL, RC and SG Wu revised the manuscript. HZ, PG, K-SL, M-HW, J-GQ, X-NS and Y-TY designed the studies. J-YZ, B-HJ, J-GQ, X-NS, S-JW, C-YZ, Y-RQ and MC-mL wrote the manuscript.

ETHICS STATEMENT

The animal study was reviewed and approved by laboratory animal ethics committee of Zhengzhou University.

FUNDING

The present study was supported by grants from the Scientific Research Fund Project of Department of Education of Yunnan Province (No. 2017ZZX289, No. 2018JS208), Yunnan Applied Basic Res of Combined Foundation of Yunnan Province Science and Technology Dept. and Kunming Medical University Joint Fund for Fundamental Research (2017FE467(-186), 2018FE001(-069), 2019FE001(-064)), Yunnan Applied Basic Res. of Combined Foundation of Yunnan Province Science and Technology Department, Yunnan University of Chinese Medicine (2018FF001 (-026), 2019FF002 (-050,-040), 2018FF001 (-016), 2018FF001 (-079)), and the National Natural Science Foundation of China (No. 82060862, 81960835, No. 81802548, No. 81860451).

SUPPLEMENTARY MATERIAL

The Supplementary Material for this article can be found online at: https://www.frontiersin.org/articles/10.3389/fphar.2021.691769/full#supplementary-material

REFERENCES

Arnold, A., McAuliff, J. P., and Beyler, A. L. (1979). Metabolic Effects of a New Hypolipidemic Agent, Ciprofibrate. *J. Pharm. Sci.* 68, 1557–1558. Epub 1979/12/01. doi:10.1002/jps.2600681227

Asghar, U., Witkiewicz, A. K., Turner, N. C., and Knudsen, E. S. (2015). The History and Future of Targeting Cyclin-dependent Kinases in Cancer Therapy. *Nat. Rev. Drug Discov.* 14, 130–146. Epub 2015/01/31. doi:10.1038/nrd4504

Berman, H. M., Westbrook, J., Feng, Z., Gilliland, G., Bhat, T. N., Weissig, H., et al. (2000). The Protein Data Bank. *Nucleic Acids Res.* 28, 235–242. Epub 1999/12/11. doi:10.1093/nar/28.1.235

Bollard, J., Miguela, V., Ruiz de Galarreta, M., Venkatesh, A., Bian, C. B., Roberto, M. P., et al. (2017). Palbociclib (PD-0332991), a Selective CDK4/6 Inhibitor, Restricts Tumour Growth in Preclinical Models of Hepatocellular Carcinoma. *Gut* 66, 1286–1296. Epub 2016/11/17. doi:10.1136/gutjnl-2016-312268

Bueno, J. R. (1965). Therapeutic Evaluation of R2498 (Triperidol) in Hospitalized Schizophrenic Patients. *J. Bras Psiquiatr.* 14, 81–91. Epub 1965/01/01.

Che, Y., Ye, F., Xu, R., Qing, H., Wang, X., Yin, F., et al. (2012). Co-expression of XIAP and Cyclin D1 Complex Correlates with a Poor Prognosis in Patients with Hepatocellular Carcinoma. *Am. J. Pathol.* 180, 1798–1807. Epub 2012/03/21. doi:10.1016/j.ajpath.2012.01.016

Chou, T.-C. (2010). Drug Combination Studies and Their Synergy Quantification Using the Chou-Talalay Method. *Cancer Res.* 70, 440–446. Epub 2010/01/14. doi:10.1158/0008-5472.can-09-1947

Chou, T.-C. (2006). Theoretical Basis, Experimental Design, and Computerized Simulation of Synergism and Antagonism in Drug Combination Studies. *Pharmacol. Rev.* 58, 621–681. Epub 2006/09/14. doi:10.1124/pr.58.3.10

Chou, T. C. (2011). The Mass-Action Law Based Algorithm for Cost-Effective Approach for Cancer Drug Discovery and Development. *Am. J. Cancer Res.* 1, 925–954. doi:10.1158/1538-7445.am2013-5526

Cobrinik, D. (2005). Pocket Proteins and Cell Cycle Control. *Oncogene* 24, 2796–2809. Epub 2005/04/20. doi:10.1038/sj.onc.1208619

Cohen, P. (2002). Protein Kinases - the Major Drug Targets of the Twenty-First century?. *Nat. Rev. Drug Discov.* 1, 309–315. Epub 2002/07/18. doi:10.1038/nrd773

Dejana, E., de Castellarnau, C., Balconi, G., Rotilio, D., Pietra, A., and de Gaetano, G. (1982). AD 6, A Coronary Dilating Agent, Stimulates PGI2 Production in Rat Aorta *Ex Vivo* and in Human Endothelial Cells in Culture. *Pharmacol. Res. Commun.* 14, 719–724. Epub 1982/09/01. doi:10.1016/s0031-6989(82)80077-5

Ewen, M. E., Sluss, H. K., Sherr, C. J., Matsushime, H., Kato, J.-y., and Livingston, D. M. (1993). Functional Interactions of the Retinoblastoma Protein with Mammalian D-type Cyclins. *Cell* 73, 487–497. Epub 1993/05/07. doi:10.1016/0092-8674(93)90136-e

Flaherty, K. T., Lorusso, P. M., Demichele, A., Abramson, V. G., Courtney, R., Randolph, S. S., et al. (2012). Phase I, Dose-Escalation Trial of the Oral Cyclin-dependent Kinase 4/6 Inhibitor PD 0332991, Administered Using a 21-day Schedule in Patients with Advanced Cancer. *Clin. Cancer Res.* 18, 568–576. Epub 2011/11/18. doi:10.1158/1078-0432.ccr-11-0509

Franken, H., Mathieson, T., Childs, D., Sweetman, G. M. A., Werner, T., Tögel, I., et al. (2015). Thermal Proteome Profiling for Unbiased Identification of Direct and Indirect Drug Targets Using Multiplexed Quantitative Mass Spectrometry. *Nat. Protoc.* 10, 1567–1593. Epub 2015/09/18. doi:10.1038/nprot.2015.101

Fry, D. W., Harvey, P. J., Keller, P. R., Elliott, W. L., Meade, M., Trachet, E.., et al. (2004). Specific Inhibition of Cyclin-dependent Kinase 4/6 by PD 0332991 and Associated Antitumor Activity in Human Tumor Xenografts. *Mol. Cancer Ther.* 3, 1427–1438. Epub 2004/11/16.

Fujimaki, K., Noumi, T., Saikawa, I., Inoue, M., and Mitsuhashi, S. (1988). *In Vitro* and *In Vivo* Antibacterial Activities of T-3262, a New Fluoroquinolone. *Antimicrob. Agents Chemother.* 32, 827–833. Epub 1988/06/01. doi:10.1128/aac.32.6.827

Hou, Y., Sun, B., Liu, W., Yu, B., Shi, Q., Luo, F., et al. (2021). Targeting of Glioma Stem-like Cells with a Parthenolide Derivative ACT001 through Inhibition of AEBP1/PI3K/AKT Signaling. *Theranostics* 11, 555–566. Epub 2021/01/05. doi:10.7150/thno.49250

Huang, Z., and Wong, C. F. (2016). Inexpensive Method for Selecting Receptor Structures for Virtual Screening. *J. Chem. Inf. Model.* 56, 21–34. Epub 2015/12/15. doi:10.1021/acs.jcim.5b00299

Irwin, J. J., Sterling, T., Mysinger, M. M., Bolstad, E. S., and Coleman, R. G. (2012). ZINC: A Free Tool to Discover Chemistry for Biology. *J. Chem. Inf. Model.* 23 (52), 1757–1768. Epub 2012/05/17. doi:10.1021/ci3001277

Irwin, J. J., and Shoichet, B. K. (2005). ZINC − A Free Database of Commercially Available Compounds for Virtual Screening. *J. Chem. Inf. Model.* 45, 177–182. Epub 2005/01/26. doi:10.1021/ci049714+

Jafari, R., Almqvist, H., Axelsson, H., Ignatushchenko, M., Lundbäck, T., Nordlund, P., et al. (2014). The Cellular thermal Shift Assay for Evaluating Drug Target Interactions in Cells. *Nat. Protoc.* 9, 2100–2122. Epub 2014/08/08. doi:10.1038/nprot.2014.138

Janssen, P. A., Niemegeers, C. J., Schellekens, K. H., Dresse, A., Lenaerts, F. M., Pinchard, A., et al. (1968). Pimozide, a Chemically Novel, Highly Potent and Orally Long-Acting Neuroleptic Drug. I. The Comparative Pharmacology of Pimozide, Haloperidol, and Chlorpromazine. *Arzneimittelforschung* 18, 261–279. Epub 1968/03/01.

Kato, J., Matsushime, H., Hiebert, S. W., Ewen, M. E., and Sherr, C. J. (1993). Direct Binding of Cyclin D to the Retinoblastoma Gene Product (pRb) and pRb Phosphorylation by the Cyclin D-dependent Kinase CDK4. *Genes Dev.* 7, 331–342. Epub 1993/03/01. doi:10.1101/gad.7.3.331

Keithly, J. S. (1982). Testing Experimental Compounds against American Cutaneous and Mucocutaneous Leishmaniasis. *ResearchGate*. doi:10.21236/ada157956

Kim, H., Lee, M. J., Kim, M. R., Chung, I. P., Kim, Y. M., Lee, J. Y., et al. (2000). Expression of Cyclin D1, Cyclin E, Cdk4 and Loss of Heterozygosity of 8p, 13q, 17p in Hepatocellular Carcinoma: Comparison Study of Childhood and Adult Hepatocellular Carcinoma. *Liver Int.* 20, 173–178. Epub 2000/06/10. doi:10.1034/j.1600-0676.2000.020002173.x

Kudo, M. (2020). Recent Advances in Systemic Therapy for Hepatocellular Carcinoma in an Aging Society: 2020 Update. *Liver Cancer* 9, 640–662. doi:10.1159/000511001

Lassus, A., Forström, S., and Salo, O. (1983). A Double-Blind Comparison of Sulconazole Nitrate 1% Cream with Clotrimazole 1% Cream in the Treatment of Dermatophytoses. *Br. J. Dermatol.* 108, 195–198. Epub 1983/02/01. doi:10.1111/j.1365-2133.1983.tb00062.x

Li, H., Leung, K. S., Ballester, P. J., and Wong, M. H. (2014). Istar: a Web Platform for Large-Scale Protein-Ligand Docking. *PLoS One* 9, e85678, 2014. Epub 2014/01/30. doi:10.1371/journal.pone.0085678

Li, H., Leung, K. S., and Wong, M. H. (2012). "Idock: A Multithreaded Virtual Screening Tool for Flexible Ligand Docking," in 2012 IEEE Symposium on Computational Intelligence in Bioinformatics and Computational Biology (CIBCB), San Diego, CA, USA, May 9-12 2012, 77–84.

Li, K. K. W., Ng, I. O. L., Fan, S. T., Albrecht, J. H., Yamashita, K., and Poon, R. Y. C. (2002). Activation of Cyclin-dependent Kinases CDC2 and CDK2 in Hepatocellular Carcinoma. *Liver* 22, 259–268. Epub 2002/07/09. doi:10.1046/j.0106-9543.2002.01629.x

Lin, R.-x., Tuo, C.-w., Lü, Q.-j., Zhang, W., and Wang, S.-q. (2005). Inhibition of Tumor Growth and Metastasis with Antisense Oligonucleotides (Cantide) Targeting hTERT in an *In Situ* Human Hepatocellular Carcinoma Model. *Acta Pharmacol. Sin.* 26, 762–768. Epub 2005/05/27. doi:10.1111/j.1745-7254.2005.00762.x

Liu, Y., Buil, A., Collins, B. C., Gillet, L. C., Blum, L. C., Cheng, L. Y.., et al. (2015). Quantitative Variability of 342 Plasma Proteins in a Human Twin Population. *Mol. Syst. Biol.* 4 (11), 786, 2015. Epub 2015/02/06. doi:10.15252/msb.20145728

Malumbres, M., and Barbacid, M. (2009). Cell Cycle, CDKs and Cancer: a Changing Paradigm. *Nat. Rev. Cancer* 9, 153–166. Epub 2009/02/25. doi:10.1038/nrc2602

Malumbres, M. (2014). Cyclin-dependent Kinases. *Genome Biol.* 15, 122, 2014. Epub 2014/09/03. doi:10.1186/gb4184

Matsumoto, Y., Aihara, K., Kamata, T., and Goto, N. (1994). Nizofenone, a Neuroprotective Drug, Suppresses Glutamate Release and Lactate Accumulation. *Eur. J. Pharmacol.* 262, 157–161. Epub 1994/09/01. doi:10.1016/0014-2999(94)90039-6

Matsushime, H., Ewen, M. E., Strom, D. K., Kato, J.-Y., Hanks, S. K., Roussel, M. F., et al. (1992). Identification and Properties of an Atypical Catalytic Subunit (p34PSK-J3/cdk4) for Mammalian D Type G1 Cyclins. *Cell* 71, 323–334. Epub 1992/10/16. doi:10.1016/0092-8674(92)90360-o

Meraldi, P., Lukas, J., Fry, A. M., Bartek, J., and Nigg, E. A. (1999). Centrosome Duplication in Mammalian Somatic Cells Requires E2F and Cdk2-Cyclin A. *Nat. Cel. Biol.* 1, 88–93. Epub 1999/11/13. doi:10.1038/10054

Miricescu, D., Totan, A., Stanescu-Spinu, I. I., Badoiu, S. C., Stefani, C., and Greabu, M. (2020). PI3K/AKT/mTOR Signaling Pathway in Breast Cancer: From Molecular Landscape to Clinical Aspects. *Int. J. Mol. Sci.* 22, 173, 2020. Epub 2020/12/31. doi:10.3390/ijms22010173

Moracci, L., Crotti, S., Traldi, P., and Agostini, M. (2021). Mass Spectrometry in the Study of Molecular Complexes between 5-fluorouracil and Catechins. *J. Mass. Spectrom.* 56, e4682, 2021. Epub 2021/01/16. doi:10.1002/jms.4682

Muscatello, M. R. A., Bruno, A., Micali Bellinghieri, P., Pandolfo, G., and Zoccali, R. A. (2014). Sertindole in Schizophrenia: Efficacy and Safety Issues. *Expert Opin. Pharmacother.* 15, 1943–1953. Epub 2014/08/02. doi:10.1517/14656566.2014.947960

Park, S. R., Kim, S. R., Hong, I. S., and Lee, H. Y. (2020). A Novel Therapeutic Approach for Colorectal Cancer Stem Cells: Blocking the PI3K/Akt Signaling Axis with Caffeic Acid. *Front. Cel. Dev. Biol.* 8, 585987, 2020. Epub 2021/01/12. doi:10.3389/fcell.2020.585987

Reed, S. I. (1997). Control of the G1/S Transition. *Cancer Surv.* 29, 7–23. Epub 1997/01/01.

Rivadeneira, D. B., Mayhew, C. N., Thangavel, C., Sotillo, E., Reed, C. A., Graña, X., et al. (2010). Proliferative Suppression by CDK4/6 Inhibition: Complex Function of the Retinoblastoma Pathway in Liver Tissue and Hepatoma Cells. *Gastroenterology* 138, 1920–1930, 2010. Epub 2010/01/27. doi:10.1053/j.gastro.2010.01.007

Ross, D. B. (1970). Treatment of Experimental Fasciola Hepatica Infection of Sheep with Rafoxanide. *Vet. Rec.* 25 (87), 110–111. Epub 1970/07/25. doi:10.1136/vr.87.4.110

Sherr, C. J., Beach, D., and Shapiro, G. I. (2016). Targeting CDK4 and CDK6: From Discovery to Therapy. *Cancer Discov.* 6, 353–367. Epub 2015/12/15. doi:10.1158/2159-8290.cd-15-0894

Shi, X., Li, H., Shi, A., Yao, H., Ke, K., Dong, C.., et al. (2018). Discovery of Rafoxanide as a Dual CDK4/6 Inhibitor for the Treatment of Skin Cancer. *Oncol. Rep.* 40, 1592–1600. Epub 2018/06/30. doi:10.3892/or.2018.6533

Shi, X.-N., Li, H., Yao, H., Liu, X., Li, L., Leung, K.-S., et al. (2015a). Adapalene Inhibits the Activity of Cyclin-dependent Kinase 2 in Colorectal Carcinoma. *Mol. Med. Rep.* 12, 6501–6508. Epub 2015/09/24. doi:10.3892/mmr.2015.4310

Shi, X. N., Li, H., Yao, H., Liu, X., Li, L., Leung, K. S., et al. (2015b). In Silico Identification and *In Vitro* and *In Vivo* Validation of Anti-Psychotic Drug Fluspirilene as a Potential CDK2 Inhibitor and a Candidate Anti-Cancer Drug. *PLoS One* 10, e0132072. Epub 2015/07/07. doi:10.1371/journal.pone.0132072

Shmushovich, M. N. (1967). On the Problem of the Comparative Effectiveness of Aminoquinol and Acriouine Therapy in Lambliasis. *Sov. Med.* 30, 117–119. Epub 1967/02/01.

Sobhani, N., D'Angelo, A., Pittacolo, M., Roviello, G., Miccoli, A., Corona, S. P., et al. (2019). Updates on the CDK4/6 Inhibitory Strategy and Combinations in Breast Cancer. *Cells* 8, 321, 2019. Epub 2019/04/10. doi:10.3390/cells8040321

Teo, Z. L., Versaci, S., Dushyanthen, S., Caramia, F., Savas, P., Mintoff, C. P.., et al. (2017). Combined CDK4/6 and PI3Kα Inhibition Is Synergistic and Immunogenic in Triple-Negative Breast Cancer. *Cancer Res.* 15 (77), 6340–6352. Epub 2017/09/28. doi:10.1158/0008-5472.can-17-2210

Vidula, N., and Rugo, H. S. (2016). Cyclin-Dependent Kinase 4/6 Inhibitors for the Treatment of Breast Cancer: A Review of Preclinical and Clinical Data. *Clin. Breast Cancer* 16 (1), 8–17. doi:10.1016/j.clbc.2015.07.005

Wang, D., Sun, Y., Li, W., Ye, F., Zhang, Y., Guo, Y., et al. (2018). Antiproliferative Effects of the CDK6 Inhibitor PD0332991 and its Effect on Signaling Networks in Gastric Cancer Cells. *Int. J. Mol. Med.* 41, 2473–2484. Epub 2018/02/14. doi:10.3892/ijmm.2018.3460

Yamamoto, H., Monden, T., Ikeda, K., Izawa, H., Fukuda, K., Fukunaga, M., et al. (1995). Coexpression of Cdk2/cdc2 and Retinoblastoma Gene Products in Colorectal Cancer. *Br. J. Cancer* 71, 1231–1236. Epub 1995/06/01. doi:10.1038/bjc.1995.238

Yang, X., Xie, X., Xiao, Y.-F., Xie, R., Hu, C.-J., Tang, B., et al. (2015). The Emergence of Long Non-coding RNAs in the Tumorigenesis of Hepatocellular Carcinoma. *Cancer Lett.* 360, 119–124. Epub 2015/02/28. doi:10.1016/j.canlet.2015.02.035

Conflict of Interest: The authors declare that the research was conducted in the absence of any commercial or financial relationships that could be construed as a potential conflict of interest.

frontiers in Pharmacology

ORIGINAL RESEARCH
published: 23 September 2021
doi: 10.3389/fphar.2021.713322

USP47-Mediated Deubiquitination and Stabilization of TCEA3 Attenuates Pyroptosis and Apoptosis of Colorectal Cancer Cells Induced by Chemotherapeutic Doxorubicin

Xiaodan Hou[1†], Jun Xia[2†], Yuan Feng[1], Long Cui[3], Yili Yang[1,4], Peng Yang[2*] and Xin Xu[1,4*]*

[1]Suzhou Institute of Systems Medicine, Center for Systems Medicine, Chinese Academy of Medical Sciences, Suzhou, China, [2]Department of Emergency Medicine, the First Affiliated Hospital of Soochow University, Suzhou, China, [3]Department of Colorectal and Anal Surgery, Xinhua Hospital, Shanghai Jiao Tong University School of Medicine, Shanghai, China, [4]China Regional Research Centre, International Centre of Genetic Engineering and Biotechnology, Taizhou, China

The ubiquitin–proteasome system regulates a variety of cellular processes including growth, differentiation and apoptosis. While E1, E2, and E3 are responsible for the conjugation of ubiquitin to substrates, deubiquitinating enzymes (DUBs) reverse the process to remove ubiquitin and edit ubiquitin chains, which have profound effects on substrates' degradation, localization, and activities. In the present study, we found that the deubiquitinating enzyme USP47 was markedly decreased in primary colorectal cancers (CRC). Its reduced expression was associated with shorter disease-free survival of CRC patients. In cultured CRC cells, knockdown of USP47 increased pyroptosis and apoptosis induced by chemotherapeutic doxorubicin. We found that USP47 was able to bind with transcription elongation factor a3 (TCEA3) and regulated its deubiquitination and intracellular level. While ectopic expression of USP47 increased cellular TCEA3 and resistance to doxorubicin, the effect was markedly attenuated by TCEA3 knockdown. Further analysis showed that the level of pro-apoptotic Bax was regulated by TCEA3. These results indicated that the USP47-TCEA3 axis modulates cell pyroptosis and apoptosis and may serve as a target for therapeutic intervention in CRC.

Keywords: USP47, TCEA3, pyroptosis, apoptosis, colorectal cancer

OPEN ACCESS

Edited by:
Ning Wang,
The University of Hong Kong,
Hong Kong, SAR China

Reviewed by:
Kohsuke Tsuchiya,
Kanazawa University, Japan
Hoi Leong Xavier Wong,
Hong Kong Baptist University,
Hong Kong, SAR China

***Correspondence:**
Yili Yang
yangyl@ism.pumc.edu.cn
Peng Yang
yangpeng@suda.edu.cn
Xin Xu
zitanxu@163.com

[†]These authors have contributed equally to this work.

Specialty section:
This article was submitted to Experimental Pharmacology and Drug Discovery, a section of the journal Frontiers in Pharmacology

Received: *22 May 2021*
Accepted: *10 September 2021*
Published: *23 September 2021*

Citation:
Hou X, Xia J, Feng Y, Cui L, Yang Y, Yang P and Xu X (2021) USP47-Mediated Deubiquitination and Stabilization of TCEA3 Attenuates Pyroptosis and Apoptosis of Colorectal Cancer Cells Induced by Chemotherapeutic Doxorubicin. Front. Pharmacol. 12:713322. doi: 10.3389/fphar.2021.713322

INTRODUCTION

Ubiquitination regulates the level, localization, and activity of target proteins and affects diverse cellular processes, including cell growth, differentiation and apoptosis (Melino 2005; Bernassola et al., 2008). The modification usually requires the sequential actions of ubiquitin-activating enzyme (E1), ubiquitin-conjugating enzyme (E2), and ubiquitin ligase enzyme (E3), leading to the conjugation of the ubiquitin to a lysine (K) residue of the target protein and to the lysine residue of pre-conjugated ubiquitin (Varshavsky 1997). Therefore, the substrate protein could be attached by a single ubiquitin molecule at one lysine residue (referred as mono-ubiquitination), at multiple lysines (multi-ubiquitination), or conjugated with ubiquitin chains (poly-ubiquitination). While the K48-linked poly-ubiquitin chain usually targets proteins to proteasomal degradation, alternative linkages (e.g., K-63) are often associated with intracellular signal transduction (Glickman

and Ciechanover 2002). Interestingly, the ubiquitination status of cellular proteins is also determined by a large family of proteases that remove ubiquitin and edit polyubiquitin chain (Nijman et al., 2005). These deubiquitinating enzymes (DUBs) thus affect the degradation and function of many substrates, regulating most, if not all cellular processes (Hoeller and Dikic 2009; Hussain et al., 2009).

Based on their catalytic characteristic and structural similarity, DUBs are divided into a number of classes, among which, the largest group is the ubiquitin-specific proteases (USPs) family that includes 54 members. USPs contain the characteristic catalytic domains and various ubiquitin-interacting domains and zinc-finger domains (Komander et al., 2009). Of note, it has been shown that mutations and altered expression of USPs are often associated with human cancers, indicating that it is important to characterize and understand each USP's criticality indifferent cancers (Everett et al., 1997; Henry et al., 2003; Kennedy and D'Andrea 2006; Oliveira et al., 2004). USP47 is a 1375 amino-acid cysteine protease that contains the characteristic His and Cys catalytic domains for USPs and four ubiquitin-like domains (Piao et al., 2015). A number of studies have shown that it deubiquitinated and stabilized various substrates, including MAPK, DNA polymerase β, E-cadherin, β-catenin, SNAIL, YAP, SATB1 and β-TrCP (Parsons et al., 2011; Sako-Kubota et al., 2014; Ashton-Beaucage et al., 2016; Choi et al., 2017; Bufalieri et al., 2019; Yu et al., 2019; Pan et al., 2020). Consequently, it participates in the regulation of DNA damage repair, inflammasome activation, epithelial-mesenchymal transition, and affects proliferation and apoptosis of cancer cells, including these colorectal carcinomas (CRC).

CRC is one of the most common malignancies in both man and woman worldwide and a leading cause of cancer death (Markowitz and Bertagnolli 2009). It has been found that multiple USPs, including USP1, USP4, USP5, USP11 and USP21, were significantly increased in CRCs. They promote tumor cell growth and survival through regulating DNA damage response (Xu et al., 2019b), WNT/β-catenin pathway (Yun et al., 2015), and specific substrates such as Fos-related-antigen-1 (Yun et al., 2020), Tu translation elongation factor (Xu et al., 2019a), and protein phosphatase one catalytic subunit α (Sun et al., 2019). We found in the present study that USP47 was markedly decreased in CRCs and its reduced expression was associated with poor prognosis of CRC patients. We further identified that USP47 interacted with transcription elongation factor a3 (TCEA3, also known as TFIIS. h), and promoted its deubiquitination and stabilization. While USP47 knockdown sensitized cancer cells to anti-cancer drugs, its enforced expression increased cellular TCEA3 and chemoresistance, which was markedly attenuated by TCEA3 knockdown. Thus, USP47 functions as an effective modulator of cell death in CRC.

MATERIALS AND METHODS

Cell Culture, Tissues and Reagents

The HEK293T cell line and human CRC cell line HCT116 were cultured in DMEM/High Glucose medium (Hyclone, Shanghai, China) supplemented with 10% of fetal bovine serum (Gibco, Shanghai, China), 100 U/ml of penicillin, 100 μg/ml of streptomycin at 37°C in a humidified incubator containing 5% CO_2, 95% air atmosphere. The GSDME-knockout HCT116 (GSDME-KO) cells were generated by using the CRISPR-Cas9 system with lenti-CRISPR-v2 vector as previously described (PMID: 24157548). The sequence of the guide RNA was as follow: 5′-AAGTTTGCAAACCACGTGAG-3′. The 21 pairs of CRC and para-cancerous normal tissues were collected with informed consensus from patients enrolled into the First Affiliated Hospital of Soochow University, Suzhou, China. The study was approved by the Ethical Review Board of the First Affiliated Hospital of Soochow University. The tissue array was made from 136 CRC tissues collected with informed consensus from surgical specimens of patients enrolled into in the Department of Colorectal and Anal Surgery, Xinhua Hospital, Shanghai Jiaotong University School of Medicine, from January 2008 to December 2016. The collection was approved by Xinhua Hospital Ethics Committee. The clinicopathological information of these patients were shown in **Table 1**. Doxorubicin, MG132 and P22077 were purchased from Selleck Chemicals (Shanghai, China).

TABLE 1 | Case information.

Clinical parameters		Case (%)
Gender	Male	69 (50.7)
	Female	67 (49.3)
Age (year)	≤65	66 (48.5)
	>65	70 (51.5)
Stage	I	15 (11.0)
	II	95 (69.9)
	III	26 (19.1)
T	1	2 (1.5)
	2	15 (11.0)
	3	46 (33.8)
	4	73 (53.7)
N	0	68 (50.0)
	1	41 (30.1)
	2	27 (19.9)
M	0	125 (91.9)
	1	11 (8.1)
USP47	High	77 (56.6)
	Low	59 (43.4)

Plasmid Construction and siRNA Sequences

The pLVX-Flag-USP47 plasmid was purchased from GeneCopoeia (Guangzhou, China). TCEA3 cDNA (GenBank accession number: NM_003196.3) was amplified and cloned into pcDNA3.1. The sequences of siRNAs targeting USP47 were as follows: siRNA#1 sense: 5-GCUGUCGCCUUGUUA AAUATT-3, antisense: 5- UAUUUAACAAGGCGACAGCTT-3; siRNA#2 sense: 5-GGCGUCAAGUCAACAUAUATT-3,

antisense: UAUAUGUUGACUUGACGCCTT-3; siRNA#3 sense: 5-CCAGCAAUCAAGAGUUUGATT, antisense: 5-UCA AACUCUUGAUUGCUGGTT-3. The sequences of siRNAs targeting TCEA3 were as follows: siRNA#2 sense: 5-GGGACA AGUGUGUGGAGAUTT-3, antisense: 5- AUCUCCACACAC UUGUCCCTT-3; siRNA#3 sense: 5-CCUCUUCCAGUGCAG CAAATT-3, antisense: 5-UUUGCUGCACUGGAAGAGGTT-3.

Immunoblotting and Antibodies

The cultured cells and the human tissues were lysed with the appropriate amount of RIPA lysis buffer (Beyotime, Shanghai, China) containing 1 ×protease inhibitor mixture (Roche) and PMSF (Beyotime, Shanghai, China). The proteins in the supernatants were subjected to SDS-PAGE and immunoblotting as described previously (Hou et al., 2019). The antibodies used were as follows: anti-PARP (Cell Signaling Technology), GSDME (Abcam), USP47 (Santa Cruz), GAPDH (Abgent Biotechnology), β-actin (Santa Cruz), α-Tubulin (Santa Cruz), Flag (Medical and Biological Laboratories), Myc (Medical and Biological Laboratories), Ub (Santa Cruz), Bax (Santa Cruz).

RNA Extraction and RT-qPCR

Total RNA was extracted using the TRIzol reagent (X. Hou et al., 2019). First Strand cDNA Synthesis Kit and Fast-Start universal SYBR Green master mix were purchased from TakaraBio (Dalian, China). The following primers were used for real-time PCR: USP47, sense: 5-CAGTGGGATTCCTTTGGATG -3, antisense: 5-GGCCAGACATTCAGGGTAGA -3; and TCEA3, sense: 5-TCGCTGGAAGTTCTGCTGATGG -3, antisense: 5- ATTCTC CAATTAGGCTCCCCCA -3; β-actin, sense: 5- GCGGGAAAT CGTGCGTGACATT -3, antisense: 5- GATGGAGTTGAAGGT AGTTTCG -3; Bax, sense: 5- CATGGGCTGGACATTGGACT -3, antisense: 5- AAAGTAGGAGAGGAGGCCGT -3. The mRNA levels of the target genes were normalized to β-actin. Data were analyzed using GraphPad Prism 5.

Immunoprecipitation (IP) and Silver Staining

The cultured cells were lysed with the appropriate amounts of IP lysis buffer (50 mm HEPES at pH 7.5, 150 mm NaCl, 1.5 mm $MgCl_2$, 10 mm NaF, 1 mm EGTA, 1% Triton X-100, 10% Glycerol) containing 1× protease inhibitor mixture (Roche) and PMSF (Beyotime, Shanghai, China). The lysates were incubated with appropriate amount of primary antibody overnight at 4°C and then mixed with protein A/G-Sepharose beads (Santa Cruz) for 2 h. After 5 times of washing, the beads were boiled in 2 × SDS loading buffer for 10 min and subjected to SDS-PAGE. Following careful washing with clean water, silver staining of the gel was performed according to the manufacturer's instructions (Roche). The visible differential protein bands were excised and prepared for analyzing with LC-MS/MS, which was conducted by ProtTech (Wuhan, China).

Immunohistochemistry

The immunostaing of the CRC tissue array was performed with a anti-USP47 Ab (Santa Cruz). The staining intensity was graded as follows: 0, negative; 1, weak; 2, moderate; and 3, strong; and the percentage of positively stained cells was recorded as follows: 0, <5%; 1, 5–25%; 2, 26–50%; 3, 51–75%; and 4, >75% (Wei et al., 2018). Five fields were randomly selected in each section. The score was calculated by multiplying the staining intensity number with the percentage of positively stained cells' number. Total immunohistochemical scores of 0–six were considered to be low, whereas scores of 7–12 were considered to be high.

Statistical Analysis

Statistical analyses were performed using the GraphPad Prism. Data were presented as the means ± standard deviation (SD). The paired, two-tailed Student's t-test or one-way ANOVA were used to assess the significance between two groups. All reported differences were $^{*}p < 0.05$, $^{**}p < 0.01$, $^{***}p < 0.001$ unless otherwise stated.

RESULTS

USP47 Expression Is Reduced in Primary CRC and Associated With Disease-Free Survival of CRC Patients

We retrieved the data of USP47 expression measured by RNAseq from the public database: Gene expression profiling interactive analysis (GEPIA). As shown in **Figure 1A**, the TPM (Transcripts per kilobase of exon model per million mapped reads) of USP47 was significantly reduced in colon adenocarcinoma (n = 275) than the normal tissues (n = 349). We also collected 21 pairs of surgical excised tumor and adjacent normal tissues from patients with CRC. The levels of USP47 mRNA were quantified by using RT-qPCR with GAPDH as a control. Comparing that of non-cancerous tissues, the relative mRNA level of USP47 was markedly decreased in 14 cases of CRC tissues (66.7%). Only two cases showed increased expression of USP47 (9.5%), 5 cases had no significant changes in CRC (23.8%) (**Figure 1B**). The decreased level of USP47 in colorectal cancer was also evident when examined by immunohistochemistry (**Figure 1C**). Analyses of a tissue array containing 136 CRC specimens showed that 77 specimens had a high score (7–12), and 59 had a low score (0–6) (**Figure 1D**; **Table 1**). Patients with low expression of USP47 had a shorter disease-free survival compared with those with higher level (**Figure 1E**). In addition, USP47 expression was significantly associated with disease stages, but not patients' gender and age (**Table 2**). Thus, while increased expression of USP1, USP4, USP5, USP11, and USP21 promote CRC development (Xu et al., 2019b), decreased USP47 is associated with the development of CRC.

USP47 Regulates CRC Cell Death Induced by Doxorubicin

As found in primary CRCs, some colorectal cancer cell lines expressed detectable USP47. To assess the function of USP47, HCT116 cells were transfected with siRNAs targeting USP47 in the absence or presence of anti-cancer drug doxorubicin (Dox). While knockdown of USP47 alone did not have notable effects on HCT116 in 24 h, Dox-induced cell death was markedly enhanced (**Supplementary Figure S1A**). Of note, the number of "bubble-like" dead cells in Dox-treated culture was significant increased

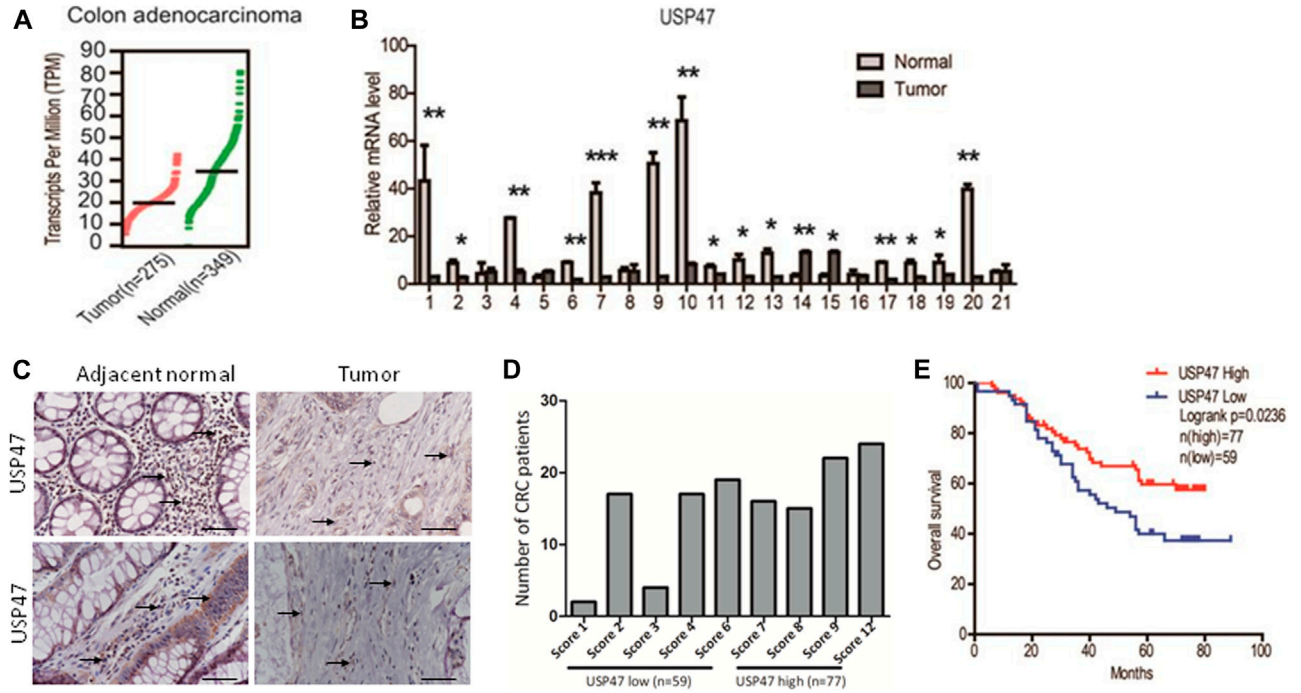

FIGURE 1 | Decreased expression of USP47 is associated with shorter disease-free survival time of CRC patients. **(A)** USP47 expression levels in colon adenocarcinoma and adjacent normal tissues retrieved from GEPIA database. Log2 (TPM+1) transformed data was used in the plot. **(B)** The mRNA levels of USP47 in 21 pairs of CRC and adjacent normal tissues were quantitated by RT-qPCR. The relative levels of the target genes were normalized to that of β-actin. The data were independently repeated three times and presented as the means ± SD, $^{*}p < 0.05$, $^{**}p < 0.01$. **(C)** Anti-USP47 immunohistochemistry of CRC and adjacent normal tissues. **(D, E)** Analyses of anti-USP47 immunostaining scores **(D)** and the disease-free survival of CRC patients **(E)**. CRC, colorectal cancer.

TABLE 2 | Correlation between USP47 levels in CRC patients and their clinicopathologic characteristics.

Tissues	Cases(N)	USP47 expression		*p*
		Low	High	
Gender				
Male	69	29	40	0.6537
Female	67	30	37	
Age (year)				
≤65	66	28	38	0.7616
>65	70	31	39	
Stage				
I + II	110	50	60	0.0376*
III	26	9	17	

*p < *0.05 was considered statistically significant.*

upon USP47 knockdown (**Supplementary Figure S1B**). As the appearance of "bubble-like" may be associated with pyroptosis, we examined the activation of gasdermin (GSDME), a marker of pyroptosis, in the HCT116 cells exposed to various treatments. As shown in **Figure 2A**, GSDME cleavages were markedly increased in cells treated with Dox and USP47-trageting siRNAs. Interestingly, the cleavages of PARP, a marker of apoptosis, were also significantly enhanced, suggesting that these cells died by both pyroptosis and apoptosis (**Figure 2A**). We then transfected HCT116 cells with USP47-expressing vector and examined their responses to the stimuli. As shown in **Figure 2B**, overexpression of USP47 decreased effectively the changes of the markers for pyroptosis and apoptosis. To further assess the role of GSDME, GSDME-KO cells were generated, and these cells were more resistant to Dox, manifested as reduced PARP cleavages and cell viability reduction (**Figures 2C,D**). Moreover, enforced expression of USP47 did not significantly reduce the cytotoxicity of Dox in GSDME-KO cells (**Figures 2E–G**). Above results indicated that USP47 mediated the pyroptosis and apoptosis induced by Dox in CRC.

USP47 Regulates the Expression of TCEA3

The effects of USP47 on CRC cell death propelled us to explore the underlying mechanisms. We transfected 293T cells with vector expressing Flag or Flag-USP47 and immunoprecipitated with an anti-Flag antibody to find potential substrate proteins. The immunoprecipitates were separated by SDS-PAGE and subjected to silver staining. Three visible differential bands were then excised and prepared for GC-MS (**Figure 3A**). Interestingly, TCEA3 (transcription elongation factor a3) was identified as one of the proteins in band 2. When HCT116 cells were transfected with indicated amounts of USP47-expressing vectors, the level of TCEA3 was increased markedly and dose-dependently (**Figures 3B,C**). On the other hand, both USP47 knockdown and USP47 inhibitor P22077 reduced the expression

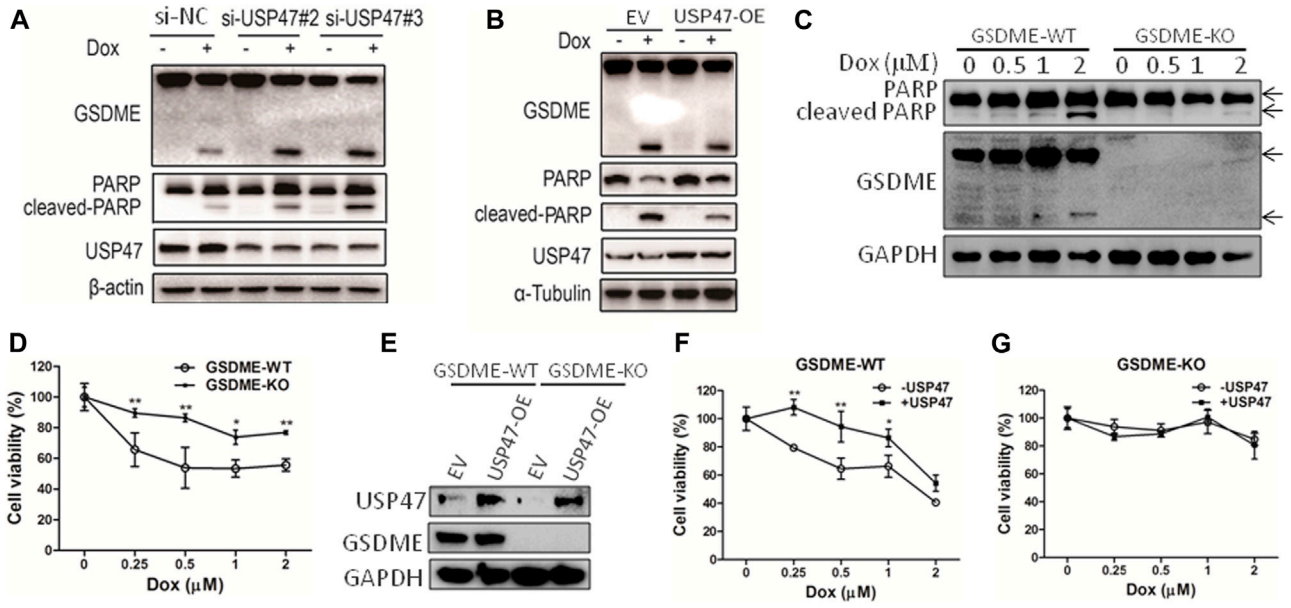

FIGURE 2 | USP47 regulates the cell death of CRC cells induced by doxorubicin. **(A)** Immunoblotting of GSDME, PARP and USP47 in HCT116 cells transfected with siRNAs for USP47 and treated with 1 μM Dox, doxorubicin. **(B)** Immunoblotting of GSDME, PARP and USP47 in HCT116 cells overexpressing USP47 and treated with 1 μM. **(C, D)** The wild-type (GSDME-WT) and GSDME-knockout (GSDME-KO) HCT116 cells were incubated with indicated Dox overnight, and cells were prepared for immunoblotting **(C)** and CCK-8 assay **(D)**. $^{*}p < 0.05$, $^{**}p < 0.01$. **(E)** The overexpressing efficacy of USP47. **(F, G)** GSDME-WT **(F)** or GSDME-KO **(G)** HCT116 cells were transfected with empty vector or USP47-overexpressing plasmids for 24 h, and then transfected cells were incubated with indicated Dox overnight, followed by CCK-8 assay. $^{*}p < 0.05$, $^{**}p < 0.01$.

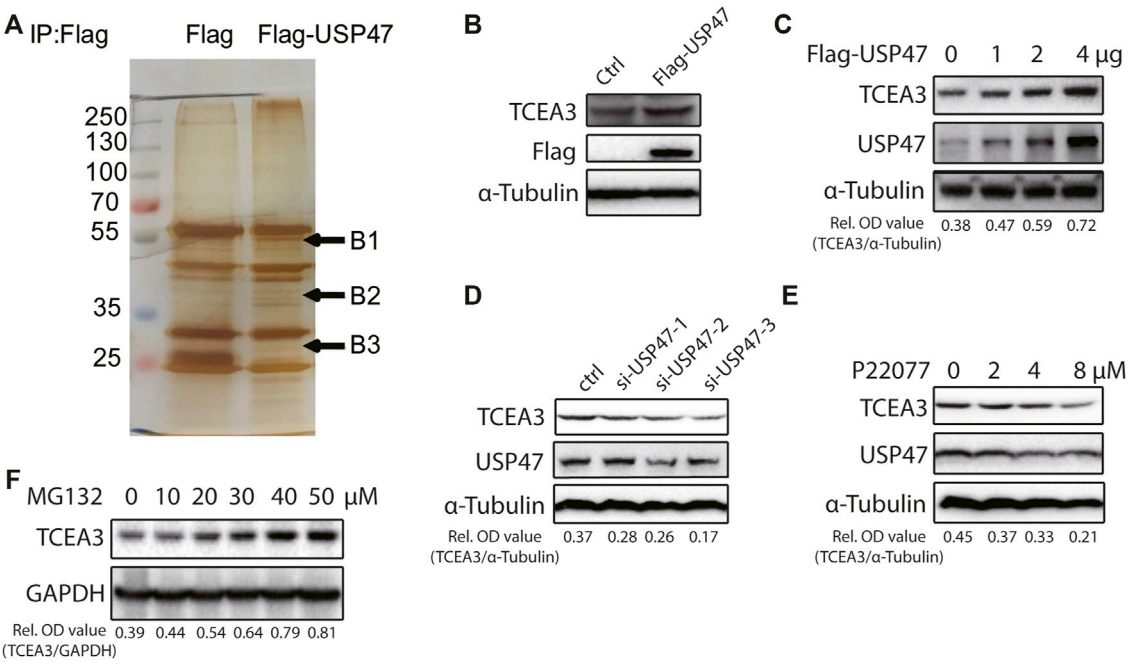

FIGURE 3 | USP47 regulated the expression of TCEA3. **(A)** Silver staining of lysates from HEK293T cells transfected with Flag-USP47-expressing vector for 48 h. **(B)** Anti-Flag immunoblotting of HCT116 cells transfected with Flag-USP47-expressing vector for 48 h. **(C)** The expression of USP47 and TCEA3 in HCT116 cells transfected with indicated amounts of USP47-expressing plasmid. **(D)** The expression of TCEA3 in USP47 HCT116 cells transfected with siRNAs against USP47. **(E)** Immunoblotting of TCEA3 in HCT116 cells treated with indicated amounts of USP47 inhibitor P22077 for 24 h. **(F)** Immunoblotting of TCEA3 in HCT116 cells treated with indicated amounts of MG132 for 6 h.

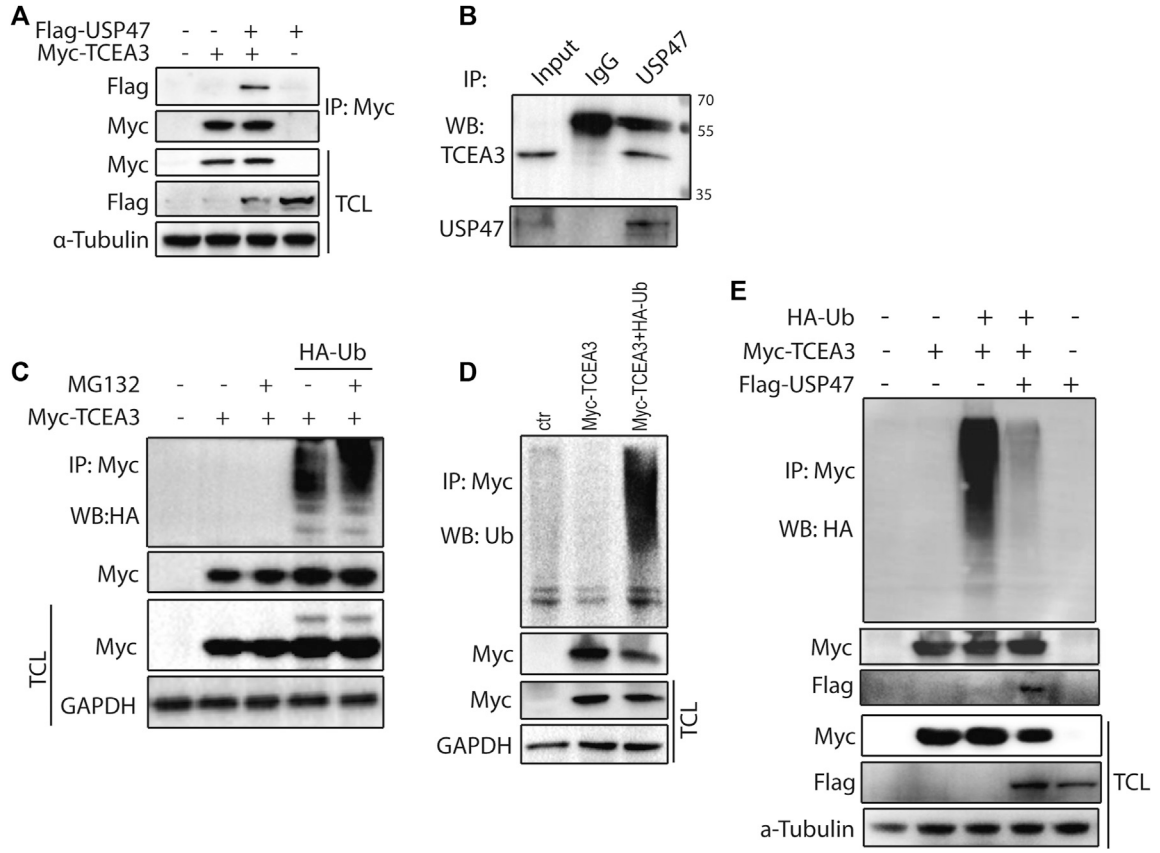

FIGURE 4 | USP47 acts as a deubiquitinating enzyme of TCEA3. **(A)** co-immunoprecipitation of overexpressed USP47 and TCEA3. Flag-USP47 and Myc-TCEA3-expressing plasmids were transfected into HEK293T cells for 48 h. Total cell lysate was immunoprecipitated with anti-Myc antibody and blot with anti-Flag antibody. Total cell lysates were also directly blotted with the antibodies. **(B)** The interaction of endogenous USP47 and TCEA3. Lysates from HCT116 cells were immunoprecipitated with anti-USP47 antibody and blotted with anti-TCEA3 antibody **(C, D)** The ubiquitination of TCEA3. Myc-TCEA3 and HA-Ub plasmids were transfected into HEK293T cells for 48 h. After exposed to 20 μM of MG132 for 6 h, the cells were harvested, immunoprecipitated with anti-Myc antibody, and blotted with anti-HA **(C)** or anti-Ub antibodies **(D)**. **(E)** USP47 decreased the ubiquitiantion of TCEA3. Flag-USP47, Myc-TCEA3 and HA-Ub plasmids were transfected into HEK293T cells for 48 h. Following treatment with 20 μM of MG132 for 6 h, cell lysates were immunoprecipitated with anti-Myc antibody and blotted with anti-HA, anti-Myc or anti-Flag antibody.

of TCEA3 (**Figures 3D,E**). Furthermore, proteasome inhibitor MG132 treatment increased the level of TCEA3 dose-dependently (**Figure 3F**). These results indicated that TCEA3 undergoes proteasomal degradation in CRC cells, which could be regulated by USP47.

USP47 Deubiquitinates and Stabilizes TCEA3

To further understand how USP47 regulated TCEA3, we co-tranfected vectors expressing Myc-TCEA3 and Flag-USP47 into HEK293T cells and performed immunoprecipitation with the anti-Myc antibody. As shown in **Figure 4A**, Flag-tag protein USP47 was effectively pulled down by the anti-Myc antibody when Myc-tagged protein TCEA3 was co-expressed. Furthermore, an anti-USP47 antibody was able to immunoprecipitated endogenous USP47 as well as TCEA3 in HCT116 (**Figure 4B**). These data demonstrated that USP47 and TCEA3 interacted in CRC cells. As USP47 is a DUB, we transfected cells with vector expressing HA-Ub and Myc-TCEA3 for 24 h and treated the cells with proteasome inhibitor MG132 for 6 h. Following IP with the anti-Myc antibody, poly-ubiquitination of TCEA3 was detected with both anti-HA (**Figure 4C**) and anti-Ub antibodies (**Figure 4D**), especially in cells exposed to MG132, indicating that TCEA3 undergoes ubiquitination and proteasomal degradation in HCT116 cells. Interestingly, co-transfection of USP47 with TCEA3 significantly reduced the ubiquitiantion of TCEA3 (**Figure 4E**), demonstrating that USP47 was capable of deubiquitinating TCEA3.

USP47 Regulates the Pyroptosis and Apoptosis Through the Substrate TCEA3

To assess the potential role of TCEA3 in USP47-meidated pyroptosis and apoptosis of CRC, we transfected vector expressing TCEA3 or siRNA targeting TCEA3 into CRC cells. While overexpression of TCEA3 attenuated the cleavages of

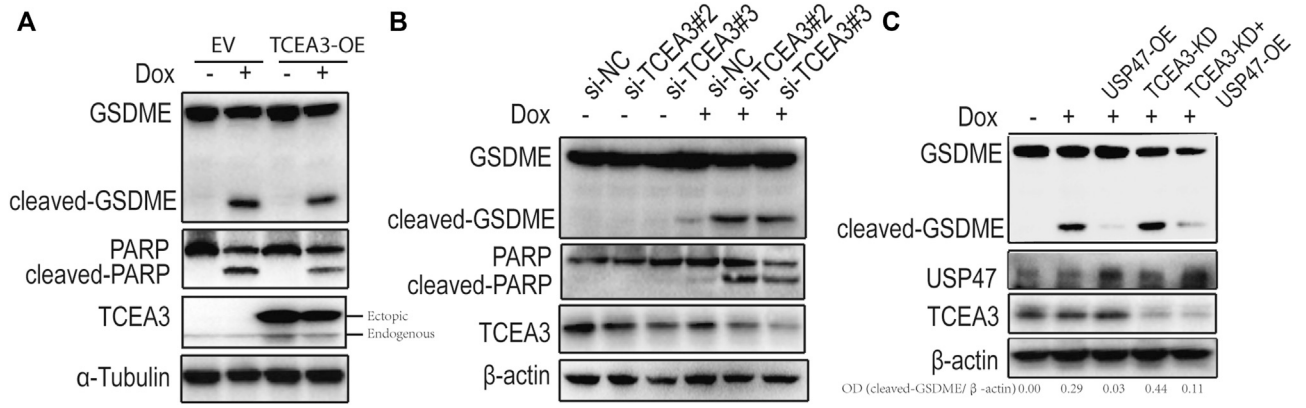

FIGURE 5 | TCEA3 mediated USP47-induced enhancement of pyroptosis and apoptosis. **(A)** GSDME, PARP and TCEA3 in HCT116 cells over-expressing TCEA3. After transfected with TCEA3-expressing plasmid for 1 day, the HCT116 cells were treated with 1 μM of Dox for 24 h and examined by immunoblotting. **(B)** GSDME, PARP and TCEA3 in HCT116 cells with TCEA3 knockdown. **(C)** Examination of GSDME, USP47 and TCEA3 in HCT116 cells treansfected with siRNA targeting TCEA3 and plasmid expressing USP47. TCEA3-OE, TCEA3-overexpressing plasmid; USP47-OE, USP47-overexpressing plasmid; TCEA3-KD, siRNA targeting TCEA3 (si-TCEA3#3).

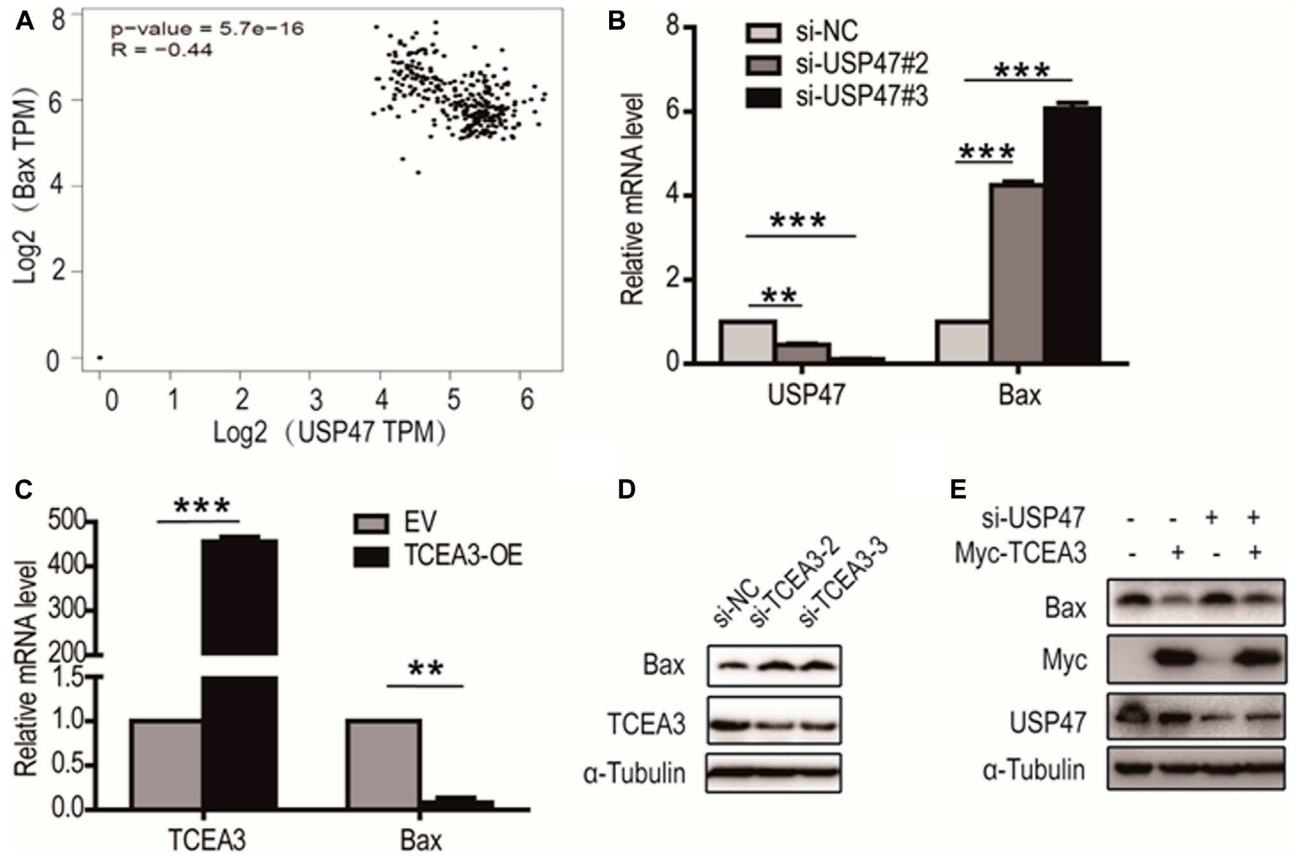

FIGURE 6 | Regulation of Bax transcription by TCEA3. **(A)** USP47 and Bax expressions were correlated. Data were retrieved from GEPIA database. **(B)** Bax mRNA level in HCT116 cells was increased after the transfection of USP47-targeted siRNAs for 24 h $^{**}p < 0.01$, $^{***}p < 0.001$. **(C)** The mRNA level of Bax was reduced in HCT116 cells after the transfected of TCEA3-expressing plasmid for 24 h $^{**}p < 0.01$, $^{***}p < 0.001$. **(D)** Bax was increased in HCT116 cells following transfection with TCEA3-targeted siRNAs for 48 h as examined by anti-Bax immunoblotting. **(E)** The expression of Bax in HCT116 cells transfected with TCEA3-expressing plasmid and/or USP47-targeted siRNAs for 48 h.

GSDME and PARP induced by Dox (**Figure 5A**), TCEA3 knockdown increased the cleavages of GSDME and PARP (**Figure 5B**). We then knocked down TCEA3 in USP47-overexpressing CRC cells. As shown in **Figure 5C**, USP47 overexpression reduced Dox-induced GSDME cleavages (Lane 3), which were mitigated by TCEA3 knockdown (Lane 5). These data indicated that TCEA3 was an important mediator for the action of USP47 on pyroptosis and apoptosis induced by Dox.

Bax Is Involved in the Pyroptosis and Apoptosis Regulated by TCEA3

From analyzing USP47-associating genes involved in pyroptosis and apoptosis in GEPIA database, it was found that Bax, a predominant pro-apoptotic molecule, was one of the proteins negatively correlated with USP47 expression (**Figure 6A**). We therefore examined whether USP47 affected the expression of Bax in CRC cells. As shown in **Figure 6B**, knockdown of USP47 resulted in a marked up raise of Bax mRNA as determined by RT-qPCR. Whereas enforced expression of TCEA3 led to a significant reduction of Bax mRNA (**Figure 6C**). Immunoblotting analyses also revealed that TCEA3 knockdown increased cellular Bax (**Figure 6D**), and TCEA3 overexpression decreased Bax at protein level (**Figure 6E**). Furthermore, when USP47 was silenced, the inhibitory of TCEA3 overexpression on Bax expression was mitigated (**Figure 6E**, Lane 4). These results demonstrated that the expression of Bax was regulated by USP47 through TCEA3. Thus, USP47-TCEA3-Bax axis was an effective regulator for the pyroptosis and apoptosis of CRC cells, and may be served as a novel target for effective chemotherapy.

DISCUSSION

Transcription of many human genes is dependent on the action of RNA polymerase II, a multiple subunits complex. TCEA3 is one of three transcription elongation factors in vertebrates, which promotes the mRNA cleavage by enhancing the intrinsic nuclease activity of RNA polymerase II (Kettenberger et al., 2003). TCEA3 has been found to be highly expressed in embryonic stem cells to regulate the differentiation of the cells (Park et al., 2013). More recent studies showed that it is also expressed in many tissues, including muscle, adrenal prostrate, ovary, colon, and liver. It has been also found that TCEA3 was downregulated in a variety of cancers types, and the lower TCEA3 expression is associated shorter overall survival of cancer patients (Kazim et al., 2020). Our finding in this study that USP47 is able to deubiquitinate and stabilize TCEA3 indicates that the reduced expression of USP47 may play a significant role in the reduction of TCEA3 in cancers, and it is of great interesting to further identify the E2 and E3 that ubiquitinate TCEA3 in the future. Interestingly, it has been reported that the mRNA level of USP47 was increased in a small group of colon mucosae from early onset CRC patients (Pan et al., 2020). USP47 was also found deubiquitinating YAP in the same study, suggesting that the deubiquitinating enzyme may also affect cell growth and tumor initiation under certain circumstances.

The relationship between TCEA3 and cell death appears complicated. Knockout of TCEA in mice is embryonic lethal, likely due to the dramatic increase of apoptotic cells, which was found in the fetal liver and other tissues (Ito et al., 2006). It has also been shown that knockdown of TCEA3 inhibited the proliferation of breast cancer cells and induces apoptosis (Hubbard et al., 2008), indicating that the protein is required for the survival of cells. However, it has also been found that enforced expression of TCEA3 inhibited proliferation and induced apoptosis in a number lines of cancer cells, including RMS, HeLa, PC3, MCF7, and MDA-321 (Kazim et al., 2020). In these cells, TCEA3 activated both intrinsic and extrinsic pathways of apoptosis. Of note, they all derived from tissues expressing high level TCEA3, suggesting that TCEA3 is likely suppressed during tumor development to block apoptosis. In our study of colon cancer cells, TECA3 knockdown or overexpression alone did not affect cell death markedly. When the cells were exposed to cytotoxic agent Dox, TCEA3 as well as USP47 protect them from apoptosis and pyrotosis, whereas knockdown of TCEA3 enhances Dox-induced cell death. Taking together, these results indicate that the effects of TCEA3 on cell death is highly cell type-dependent. Given the protein as a transcription elongation factor, it is conceivable that its influence on cells depends on driving mutations in cancer cells, status of the cell death machinery, and the damage of drug on the cells.

Pyroptosis is a form of programmed cell death characterized by cleavage of gasdermin family members, cell swelling, and formation of bubble-like protrusions (Shi et al., 2017). While pyroptosis holds back tumor development, it also provokes inflammation, which often provides a favorable environment for tumor initiation and progression. Therefore, a variety of efforts have been made to find agents that induce pyroptosis as anti-cancer therapeutics, which might overcome the resistance to apoptosis that occurred in many cancer cells. It has also become evident that effective anti-tumor chemotherapies often depend on their toxic action on tumor cells as well as host immune response (Hou et al., 2020). Recent studies further demonstrated that pyroptosis of tumor cells and the release of HMGB1 are able to induce effective antitumor immunity (Wang et al., 2020). Moreover, induction of pyroptosis in tumor cells sensitized tumors to immune checkpoint blockade. In this study, we found that the apoptosis and pyroptosis were both induced in CRC cells by Dox, and knockdown of USP47 or TCEA3 enhanced markedly pyroptotic cell death. Intriguingly, USP47 knockdown enhanced Dox-induced GSDME cleavages, which has been shown to be mediated by caspase 3, but we did not found markedly increased activated caspase three in the system. It was conceivable that the substrates of USP47 were able to protect GSDME from cleavages by caspase 3. The activity of caspase-3 may be increased by knockdown of USP47 or TCEA3 indirectly. Thus, this is an interesting system to explore the mechanisms of pyroptosis induction in tumor cells in our future work. Further, it is conceivable that inhibitors of USP47 and TCEA3 might be effective agents to enhance various chemotherapeutics-induced pyroptosis

and increase the effectiveness of anti-tumor therapies. These results indicated that the USP47-TCEA3 axis may modulate cell pyroptosis and apoptosis and could be served as a target for therapeutic intervention in CRC.

DATA AVAILABILITY STATEMENT

The original contributions presented in the study are included in the article/**Supplementary Material**, further inquiries can be directed to the corresponding authors.

ETHICS STATEMENT

This study was approved by the Review Board and Ethical Committee of the First Affiliated Hospital of Soochow University. The patients/participants provided their written informed consent to participate in this study.

AUTHOR CONTRIBUTIONS

XH, JX, YF, and XX performed the experiments. LC and PY analyzed the results. YY, XX, and XH wrote and edited the manuscript. YY and PY designed the research project. YY and XX revised the manuscript.

FUNDING

This work was supported by the funding of National Natural Science Foundation of China (Grant Nos. 81572378, 81973358).

SUPPLEMENTARY MATERIAL

The Supplementary Material for this article can be found online at: https://www.frontiersin.org/articles/10.3389/fphar.2021.713322/full#supplementary-material

REFERENCES

Ashton-Beaucage, D., Lemieux, C., Udell, C. M., Sahmi, M., Rochette, S., and Therrien, M. (2016). The Deubiquitinase USP47 Stabilizes MAPK by Counteracting the Function of the N-End Rule Ligase POE/UBR4 in Drosophila. *Plos Biol.* 14, e1002539. doi:10.1371/journal.pbio.1002539

Bernassola, F., Karin, M., Ciechanover, A., and Melino, G. (2008). The HECT Family of E3 Ubiquitin Ligases: Multiple Players in Cancer Development. *Cancer Cell* 14, 10–21. doi:10.1016/j.ccr.2008.06.001

Bufalieri, F., Infante, P., Bernardi, F., Caimano, M., Romania, P., Moretti, M., et al. (2019). ERAP1 Promotes Hedgehog-dependent Tumorigenesis by Controlling USP47-Mediated Degradation of βTrCP. *Nat. Commun.* 10, 3304. doi:10.1038/s41467-019-11093-0

Choi, B. J., Park, S. A., Lee, S. Y., Cha, Y. N., and Surh, Y. J. (2017). Hypoxia Induces Epithelial-Mesenchymal Transition in Colorectal Cancer Cells through Ubiquitin-specific Protease 47-mediated Stabilization of Snail: A Potential Role of Sox9. *Sci. Rep.* 7, 15918. doi:10.1038/s41598-017-15139-5

Everett, R. D., Meredith, M., Orr, A., Cross, A., Kathoria, M., and Parkinson, J. (1997). A Novel Ubiquitin-specific Protease Is Dynamically Associated with the PML Nuclear Domain and Binds to a Herpesvirus Regulatory Protein. *EMBO J.* 16, 566–577. doi:10.1093/emboj/16.3.566

Glickman, M. H., and Ciechanover, A. (2002). The Ubiquitin-Proteasome Proteolytic Pathway: Destruction for the Sake of Construction. *Physiol. Rev.* 82, 373–428. doi:10.1152/physrev.00027.2001

Henry, K. W., Wyce, A., Lo, W. S., Duggan, L. J., Emre, N. C., Kao, C. F., et al. (2003). Transcriptional Activation *via* Sequential Histone H2B Ubiquitylation and Deubiquitylation, Mediated by SAGA-Associated Ubp8. *Genes Dev.* 17, 2648–2663. doi:10.1101/gad.1144003

Hoeller, D., and Dikic, I. (2009). Targeting the Ubiquitin System in Cancer Therapy. *Nature* 458, 438–444. doi:10.1038/nature07960

Hou, J., Zhao, R., Xia, W., Chang, C. W., You, Y., Hsu, J. M., et al. (2020). PD-L1-mediated Gasdermin C Expression Switches Apoptosis to Pyroptosis in Cancer Cells and Facilitates Tumour Necrosis. *Nat. Cel Biol* 22, 1264–1275. doi:10.1038/s41556-020-0575-z

Hou, X., Wang, Z., Ding, F., He, Y., Wang, P., Liu, X., et al. (2019). Taurine Transporter Regulates Adipogenic Differentiation of Human Adipose-Derived Stem Cells through Affecting Wnt/β-Catenin Signaling Pathway. *Int. J. Biol. Sci.* 15, 1104–1112. doi:10.7150/ijbs.31794

Hubbard, K., Catalano, J., Puri, R. K., and Gnatt, A. (2008). Knockdown of TFIIS by RNA Silencing Inhibits Cancer Cell Proliferation and Induces Apoptosis. *BMC Cancer* 8, 133. doi:10.1186/1471-2407-8-133

Hussain, S., Zhang, Y., and Galardy, P. J. (2009). DUBs and Cancer: the Role of Deubiquitinating Enzymes as Oncogenes, Non-oncogenes and Tumor Suppressors. *Cell Cycle* 8, 1688–1697. doi:10.4161/cc.8.11.8739

Ito, T., Arimitsu, N., Takeuchi, M., Kawamura, N., Nagata, M., Saso, K., et al. (2006). Transcription Elongation Factor S-II Is Required for Definitive Hematopoiesis. *Mol. Cel Biol* 26, 3194–3203. doi:10.1128/MCB.26.8.3194-3203.2006

Kazim, N., Adhikari, A., Oh, T. J., and Davie, J. (2020). The Transcription Elongation Factor TCEA3 Induces Apoptosis in Rhabdomyosarcoma. *Cell Death Dis* 11, 67. doi:10.1038/s41419-020-2258-x

Kennedy, R. D., and D'Andrea, A. D. (2006). DNA Repair Pathways in Clinical Practice: Lessons from Pediatric Cancer Susceptibility Syndromes. *J. Clin. Oncol.* 24, 3799–3808. doi:10.1200/JCO.2005.05.4171

Kettenberger, H., Armache, K. J., and Cramer, P. (2003). Architecture of the RNA Polymerase II-TFIIS Complex and Implications for mRNA Cleavage. *Cell* 114, 347–357. doi:10.1016/s0092-8674(03)00598-1

Komander, D., Clague, M. J., and Urbé, S. (2009). Breaking the Chains: Structure and Function of the Deubiquitinases. *Nat. Rev. Mol. Cel Biol* 10, 550–563. doi:10.1038/nrm2731

Markowitz, S. D., and Bertagnolli, M. M. (2009). Molecular Origins of Cancer: Molecular Basis of Colorectal Cancer. *N. Engl. J. Med.* 361, 2449–2460. doi:10.1056/NEJMra0804588

Melino, G. (2005). Discovery of the Ubiquitin Proteasome System and its Involvement in Apoptosis. *Cell Death Differ* 12, 1155–1157. doi:10.1038/sj.cdd.4401740

Nijman, S. M., Luna-Vargas, M. P., Velds, A., Brummelkamp, T. R., Dirac, A. M., Sixma, T. K., et al. (2005). A Genomic and Functional Inventory of Deubiquitinating Enzymes. *Cell* 123, 773–786. doi:10.1016/j.cell.2005.11.007

Oliveira, A. M., Hsi, B. L., Weremowicz, S., Rosenberg, A. E., Dal Cin, P., Joseph, N., et al. (2004). USP6 (Tre2) Fusion Oncogenes in Aneurysmal Bone Cyst. *Cancer Res.* 64, 1920–1923. doi:10.1158/0008-5472.can-03-2827

Pan, B., Yang, Y., Li, J., Wang, Y., Fang, C., Yu, F. X., et al. (2020). USP47-mediated Deubiquitination and Stabilization of YAP Contributes to the Progression of Colorectal Cancer. *Protein Cell* 11, 138–143. doi:10.1007/s13238-019-00674-w

Park, K. S., Cha, Y., Kim, C. H., Ahn, H. J., Kim, D., Ko, S., et al. (2013). Transcription Elongation Factor Tcea3 Regulates the Pluripotent Differentiation Potential of Mouse Embryonic Stem Cells *via* the Lefty1-Nodal-Smad2 Pathway. *Stem Cells* 31, 282–292. doi:10.1002/stem.1284

Parsons, J. L., DianovaII, Khoronenkova, S. V., Edelmann, M. J., Kessler, B. M., and Dianov, G. L. (2011). USP47 Is a Deubiquitylating Enzyme that Regulates Base Excision Repair by Controlling Steady-State Levels of DNA Polymerase β. *Mol. Cel* 41, 609–615. doi:10.1016/j.molcel.2011.02.016

Piao, J., Tashiro, A., Nishikawa, M., Aoki, Y., Moriyoshi, E., Hattori, A., et al. (2015). Expression, Purification and Enzymatic Characterization of a Recombinant Human Ubiquitin-specific Protease 47. *J. Biochem.* 158, 477–484. doi:10.1093/jb/mvv063

Sako-Kubota, K., Tanaka, N., Nagae, S., Meng, W., and Takeichi, M. (2014). Minus End-Directed Motor KIFC3 Suppresses E-Cadherin Degradation by Recruiting USP47 to Adherens Junctions. *Mol. Biol. Cel* 25, 3851–3860. doi:10.1091/mbc.E14-07-1245

Shi, J., Gao, W., and Shao, F. (2017). Pyroptosis: Gasdermin-Mediated Programmed Necrotic Cell Death. *Trends Biochem. Sci.* 42, 245–254. doi:10.1016/j.tibs.2016.10.004

Sun, H., Ou, B., Zhao, S., Liu, X., Song, L., Liu, X., et al. (2019). USP11 Promotes Growth and Metastasis of Colorectal Cancer *via* PPP1CA-mediated Activation of ERK/MAPK Signaling Pathway. *EBioMedicine* 48, 236–247. doi:10.1016/j.ebiom.2019.08.061

Varshavsky, A. (1997). The Ubiquitin System. *Trends Biochem. Sci.* 22, 383–387. doi:10.1016/s0968-0004(97)01122-5

Wang, Q., Wang, Y., Ding, J., Wang, C., Zhou, X., Gao, W., et al. (2020). A Bioorthogonal System Reveals Antitumour Immune Function of Pyroptosis. *Nature* 579, 421–426. doi:10.1038/s41586-020-2079-1

Wei, Z., Song, J., Wang, G., Cui, X., Zheng, J., Tang, Y., et al. (2018). Deacetylation of Serine Hydroxymethyl-Transferase 2 by SIRT3 Promotes Colorectal Carcinogenesis. *Nat. Commun.* 9, 4468. doi:10.1038/s41467-018-06812-y

Xu, X., Huang, A., Cui, X., Han, K., Hou, X., Wang, Q., et al. (2019a). Ubiquitin Specific Peptidase 5 Regulates Colorectal Cancer Cell Growth by Stabilizing Tu Translation Elongation Factor. *Theranostics* 9, 4208–4220. doi:10.7150/thno.33803

Xu, X., Li, S., Cui, X., Han, K., Wang, J., Hou, X., et al. (2019b). Inhibition of Ubiquitin Specific Protease 1 Sensitizes Colorectal Cancer Cells to DNA-Damaging Chemotherapeutics. *Front. Oncol.* 9, 1406. doi:10.3389/fonc.2019.01406

Yu, L., Dong, L., Wang, Y., Liu, L., Long, H., Li, H., et al. (2019). Reversible Regulation of SATB1 Ubiquitination by USP47 and SMURF2 Mediates colon Cancer Cell Proliferation and Tumor Progression. *Cancer Lett.* 448, 40–51. doi:10.1016/j.canlet.2019.01.039

Yun, S. I., Hong, H. K., Yeo, S. Y., Kim, S. H., Cho, Y. B., and Kim, K. K. (2020). Ubiquitin-Specific Protease 21 Promotes Colorectal Cancer Metastasis by Acting as a Fra-1 Deubiquitinase. *Cancers (Basel)* 12. doi:10.3390/cancers12010207

Yun, S. I., Kim, H. H., Yoon, J. H., Park, W. S., Hahn, M. J., Kim, H. C., et al. (2015). Ubiquitin Specific Protease 4 Positively Regulates the WNT/β-catenin Signaling in Colorectal Cancer. *Mol. Oncol.* 9, 1834–1851. doi:10.1016/j.molonc.2015.06.006

Conflict of Interest: The authors declare that the research was conducted in the absence of any commercial or financial relationships that could be construed as a potential conflict of interest.

Publisher's Note: All claims expressed in this article are solely those of the authors and do not necessarily represent those of their affiliated organizations, or those of the publisher, the editors and the reviewers. Any product that may be evaluated in this article, or claim that may be made by its manufacturer, is not guaranteed or endorsed by the publisher.

frontiers in Oncology

ORIGINAL RESEARCH
published: 28 September 2021
doi: 10.3389/fonc.2021.745918

Smoking, DNA Methylation, and Breast Cancer: A Mendelian Randomization Study

Haibo Tang[1], *Desong Yang*[2], *Chaofei Han*[3*] *and Ping Mu*[4*]

[1] Department of Metabolic and Bariatric Surgery, The Third Xiangya Hospital, Central South University, Changsha, China, [2] Department of Thoracic Surgery II, Hunan Cancer Hospital and The Affiliated Cancer Hospital of Xiangya School of Medicine, Central South University, Changsha, China, [3] Department of Burn and Plastic Surgery, The Third Xiangya Hospital, Central South University, Changsha, China, [4] Department of Physiology, Shenyang Medical College, Shenyang, China

OPEN ACCESS

Edited by:
Yi-Chao Zheng,
Zhengzhou University, China

Reviewed by:
Zhiru Wang,
Zhengzhou University, China
Jian Huang,
Imperial College London, United Kingdom
Yao Wang,
Zhejiang University, China

***Correspondence:**
Ping Mu
pingmu@symc.edu.cn
Chaofei Han
491616@163.com

Specialty section:
This article was submitted to Cancer Genetics, a section of the journal Frontiers in Oncology

Received: *30 July 2021*
Accepted: *01 September 2021*
Published: *28 September 2021*

Citation:
Tang H, Yang D, Han C and Mu P (2021) Smoking, DNA Methylation, and Breast Cancer: A Mendelian Randomization Study. Front. Oncol. 11:745918. doi: 10.3389/fonc.2021.745918

Background: Smoking was strongly associated with breast cancer in previous studies. Whether smoking promotes breast cancer through DNA methylation remains unknown.

Methods: Two-sample Mendelian randomization (MR) analyses were conducted to assess the causal effect of smoking-related DNA methylation on breast cancer risk. We used 436 smoking-related CpG sites extracted from 846 middle-aged women in the ARIES project as exposure data. We collected summary data of breast cancer from one of the largest meta-analyses, including 69,501 cases for ER+ breast cancer and 21,468 cases for ER– breast cancer. A total of 485 single-nucleotide polymorphisms (SNPs) were selected as instrumental variables (IVs) for smoking-related DNA methylation. We further performed an MR Steiger test to estimate the likely direction of causal estimate between DNA methylation and breast cancer. We also conducted colocalization analysis to evaluate whether smoking-related CpG sites shared a common genetic causal SNP with breast cancer in a given region.

Results: We established four significant associations after multiple testing correction: the CpG sites of cg2583948 [OR = 0.94, 95% CI (0.91–0.97)], cg0760265 [OR = 1.07, 95% CI (1.03–1.11)], cg0420946 [OR = 0.95, 95% CI (0.93–0.98)], and cg2037583 [OR =1.09, 95% CI (1.04–1.15)] were associated with the risk of ER+ breast cancer. All the four smoking-related CpG sites had a larger variance than that in ER+ breast cancer (all $p < 1.83 \times 10^{-11}$) in the MR Steiger test. Further colocalization analysis showed that there was strong evidence (based on PPH4 > 0.8) supporting a common genetic causal SNP between the CpG site of cg2583948 [with *IMP3* expression (PPH4 = 0.958)] and ER+ breast cancer. There were no causal associations between smoking-related DNA methylation and ER– breast cancer.

Conclusions: These findings highlight potential targets for the prevention of ER+ breast cancer. Tissue-specific epigenetic data are required to confirm these results.

Keywords: Mendelian randomization (MR), smoking, DNA methylation, breast cancer, causal inference

INTRODUCTION

In the latest global cancer data released by the International Agency for Research on Cancer (IARC), breast cancer has been confirmed as the most commonly diagnosed cancer in women (https://www.iarc.who.int/). The data indicated that one in every four cancer cases diagnosed is breast cancer, and one in every six cancer deaths is breast cancer in women in 2020. Breast cancer caused 685,000 deaths in 2020, and it became the fifth leading cause of cancer mortality worldwide. It has been confirmed that cigarette smoking, one of the most important environmental risk factors, represents a significant effect on breast cancer risk (1–4).

Cigarette smoking was reported to induce reactive oxygen species (ROS), oxidative stress, and DNA methylation, which play vital roles in carcinogenesis (5, 6). The changes in DNA methylation profiles have been detected between smokers and nonsmokers in various cancers (6–8), and the effect of cigarette smoking on the DNA methylation patterns of breast tumors has also been revealed by using a cancer-focused array (9), whereas cancer-focused array only provides the correlation analysis, which could not avoid the interference of confounding factors and reverse causality. In contrast to previous studies with the above limitations, Mendelian randomization (MR) offers an opportunity to efficiently and reliably assess the causal effects between smoking-related DNA methylation patterns and breast cancer risk.

MR is considered as "nature's randomized control trial" (10), using genetic variants significantly associated with the exposure of interest to explore causal effects on the outcomes (11), which is similar to random different interventions in randomized controlled trials (RCTs). We performed a two-sample MR study to evaluate the effect magnitude and direction of smoking-related methylation on the risk of breast cancer.

METHODS

Study Design

The design of our study is shown in **Figure 1**. Firstly, we identified genetic variants as IVs for smoking-related methylation. Secondly, we collected the complete summary data from the large-scale genome-wide association studies (GWASs) for breast cancer. Thirdly, we performed a two-sample MR with two basic MR methods [e.g., Wald ratio for only one SNP and inverse-variance weighted (IVW) for two SNPs]. Fourthly, we conducted an MR Steiger test and a colocalization to evaluate the causal direction and identify the shared SNP between DNA methylation and breast cancer.

Data for Exposure

We collected summary data of smoking-related DNA methylation from the ARIES (Accessible Resource for Integrated Epigenomics Studies) project, which used the Illumina Infinium HumanMethylation450 (HM450) BeadChip to generate epigenetic data on cord blood and peripheral blood samples from 1,018 mother–offspring pairs at five time points (birth, childhood, adolescence, antenatal period, and middle age) (12). A recent study considered those methylation quantitative trait loci (mQTLs) identified in the middle-age time point among women in ARIES (mean age = 47.5 years, $n = 846$) and found 474 smoking-related CpG sites proxied by at least one mQTL (96% for cis, 4% for trans). Of these, 406 CpGs (86%) were proxied by a single SNP (13). On this basis, we further screened valid IVs according to the following criteria: (1) we selected SNPs as IVs using a p-value threshold of 5×10^{-8} (IV assumption 1, **Supplementary Figure S1**); (2) we included SNPs that have definitive allele information especially effect allele and its frequency; and (3) only cis-mQTLs (referring to genetic variants that act on local genes) were included in this study because trans-mQTLs (referring to genetic variants that act on distant genes and genes locating at different chromosomes) may lead to significant bias through horizontal pleiotropy. F statistic represents the strength of the relationship between IVs and VAT. Generally, $F > 10$ may attenuate bias produced by weak IVs (14).

Data for Outcomes

We collected summary data of breast cancer from the largest available GWAS summary statistics to date, a meta-analysis of 67

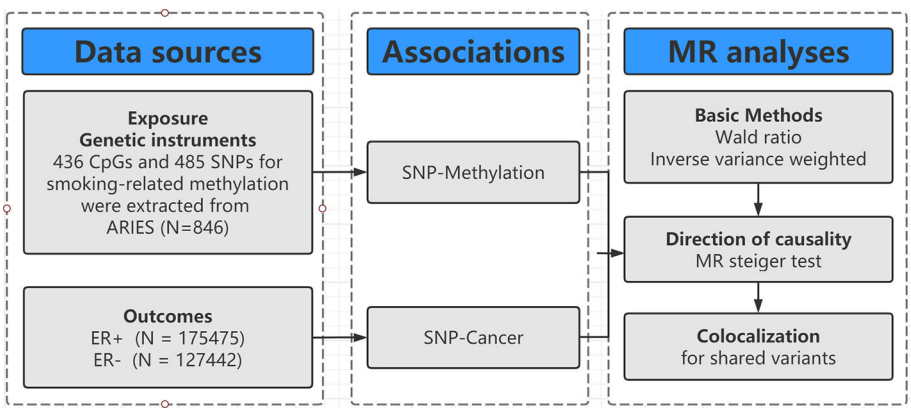

FIGURE 1 | Flowchart of Mendelian randomization framework in this study. SNP indicates single-nucleotide polymorphism; ER, estrogen receptor; MR, mendelian randomization.

studies including 69,501 ER+ and 21,648 ER− cases, and 105,974 controls for breast cancer (15). Of these, most studies were population-based case–control studies, or case–control studies nested within population-based cohorts. All studies provided the participants' status and age at diagnosis, and the majority provided additional clinical data and lifestyle factors, which have been curated and incorporated into the Breast Cancer Association Consortium (BCAC). All participating studies were approved by their respective ethics review board, and all subjects provided informed consent.

Statistical Analysis

Two-Sample Mendelian Randomization

As shown in **Supplementary Figure S1**, we calculated the effect of every single SNP using the basic model: $\beta_{\text{causal effect}} = \beta_{ZY}/\beta_{ZX}$ (β_{ZX} and β_{ZY} represent the regression coefficient on smoking-related DNA methylation and breast cancer, respectively). Generally, a valid instrument should satisfy three assumptions (**Supplementary Figure S1**): (1) must be truly associated with smoking-related methylation passing genome-wide significance ($p < 5 \times 10^{-8}$); (2) not associated with confounders of DNA methylation or breast cancer; and (3) should only be associated to the breast cancer through the smoking-related DNA methylation.

To evaluate the causal effects of smoking-related DNA methylation on the risk of breast cancer, we conducted a two-sample MR analysis (16) using two MR methods, including Wald ratio for only one SNP and IVW (17). The IVW is a conventional method to obtain an MR estimate performing a meta-analysis of each Wald ratio for multiple SNPs. The IVW could provide the strongest statistical power when none of the assumptions are violated.

Sensitivity Analyses

It is possible that smoking-related DNA methylation may have a causal effect on breast cancer. Another possibility concerns reverse causation, whereby SNPs used as proxies for DNA methylation have their primary effect through breast cancer rather than through DNA methylation. For this, we performed the MR Steiger test (18) to estimate the likely direction of effect between DNA methylation and breast cancer.

In addition, for smoking-related DNA methylation (CpG sites) where there was evidence supporting a causal relationship on breast cancer, we applied colocalization analysis to investigate whether the SNP responsible for influencing smoking-related DNA methylation at each CpG site was the same SNP influencing changes to breast cancer risk. As recommended by the developers of the colocalization, a posterior probability of hypothesis (PPH, exposure, and outcome are associated and share a single causal SNP) of 80% or higher was considered evidence of colocalization.

In our study, most CpG sites were proxied by a single SNP, so it was difficult to evaluate horizontal pleiotropy using conventional methods like evaluation of MR-Egger regression intercept. We conducted a phenome-wide association test (19) to assess the relationships of IVs with potential confounders of breast cancer such as body mass index, age at menarche or menopause, and alcohol usage. We also performed a Cochran's Q-test for CpG sites proxied by at least two SNPs (20).

Based on the analyses as mentioned above, we could conclusively establish a robustly causal association when satisfying the following conditions: (1) the results of Wald ratio or IVW reached the multiple comparisons adjusted *p*-value (*q*-value after false discovery rate) < 0.05; (2) the MR Steiger test showed a direction of effect from smoking-related DNA methylation to breast cancer; and (3) colocalization analysis supported the idea that smoking-related DNA methylation and breast cancer shared a common genetic causal SNP in a given region.

MR analyses and the MR Steiger test were performed in R (version 4.0.3) with the R package "TwoSampleMR" (21), and colocalization analysis was performed using the R package "Coloc" (22). The false discovery rate was calculated by the R package "fdrtool". The *p*-values were two-sided, and the statistical significance was set at the level of adjusted *p*-value < 0.05 after false discovery rate correction.

RESULTS

Participant Characteristics and Instruments

The characteristics of the participants from the ARIES project for smoking-related DNA methylation and meta-analysis for breast cancer are shown in **Table 1**. After screening, 485 SNPs were obtained for 436 CpG sites (all cis-mQTLs) (**Supplementary Table S1**), with *F* statistics ranging from 19 to 952, reflecting a strong instrument strength for smoking-related DNA methylation. All the participants had an identical genetic background (all Europeans), as a consistent selection in exposure data, and to our knowledge, there was no sample overlap between the exposure and outcome GWASs.

Main Results of Two-Sample MR

To assess the causal effect of DNA methylation at smoking-related CpG sites on breast cancer, we extracted the identified

TABLE 1 | Characteristics of smoking-related methylation datasets and breast cancer.

Exposure	Data source	CpG	*F*	Cases/Controls	Sample size	Population
Smoking-related methylation	ARIES	436	19–952	NA	846	European
Outcomes	**Consortium**	**Studies**		**Cases/Controls**	**Sample size**	**Population**
ER+ breast cancer	BCAC	67		69,501/105,974	175,475	European
ER– breast cancer	BCAC	67		21,468/105,974	127,442	European

ARIES indicates Accessible Resource for Integrated Epigenomics Studies; ER, estrogen receptor; BCAC, Breast Cancer Association Consortium; NA, not applicable.

SNPs for mQTLs in the GWAS summary data from BCAC Consortium and conducted a two-sample MR. The top 10 results are shown in **Table 2** (full results in **Supplementary Tables S2**, **S3**). For ER+ breast cancer, we observed four CpG-cancer effect estimates that survived in multiple comparisons test (q-value after false discovery rate < 0.05): using rs8035987 as an instrument, we found that the smoking-related DNA methylation level of cg2583948 was associated with the risk of ER+ breast cancer [OR = 0.94, 95% CI (0.91–0.97)]. Similarly, the CpG sites of cg0760265 [OR = 1.07, 95% CI (1.03–1.11)], cg0420946 [OR = 0.95, 95% CI (0.93–0.98)], and cg2037583 [OR =1.09, 95% CI (1.04–1.15)] showed causal effects on ER+ breast cancer risk. For ER− breast cancer, we found no significant smoking-related CpG sites after false discovery rate correction. Moreover, in these four smoking-related CpG sites identified in ER+ breast cancer, only cg25839482 showed a nominally significant effect on ER− breast cancer risk [OR =0.92, 95% CI (0.88–0.96)], but failed to pass the multiple test correction (q-value = 0.085) (**Figure 2**).

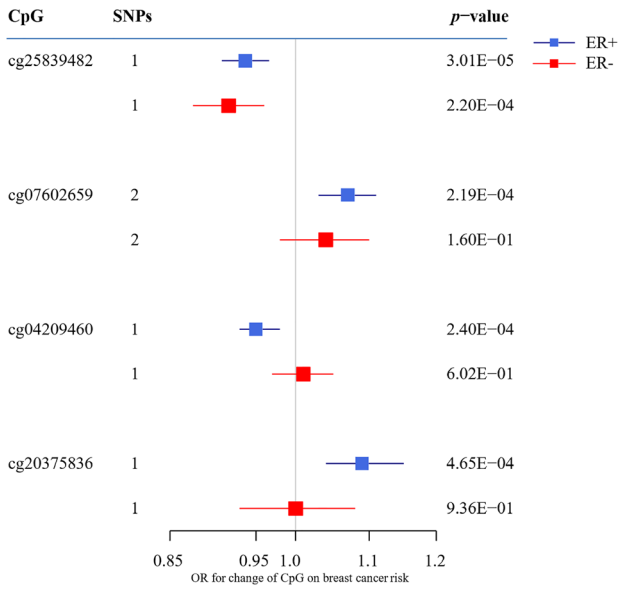

FIGURE 2 | The association between CpG sites (passing the multiple testing correction) and the breast cancer risk. OR indicates odds ratio; ER, estrogen receptor; MR, mendelian randomization.

Sensitivity Analyses

By calculating the variance explained in the smoking-related CpG sites and breast cancer subtypes by the instrumenting SNPs, and testing the difference of variance between exposure and outcome, we found that all four smoking-related CpG sites had a larger variance than that in ER+ breast cancer (all $p < 1.83\times 10^{-11}$), suggesting a forward causal direction from smoking-related DNA methylation to breast cancer risk (**Table 3**). Further colocalization analysis provided the posterior probability of five hypotheses (PP.H0–H4), supporting the idea that the CpG site of cg2583948 and ER+ breast cancer shared a common SNP (PP.H0–H3 < 0.05, and PP.H4 = 0.958) (**Table 3**). Although the PP.H4 of cg04209460 was close to the threshold of 0.8, PP.H1 was not satisfied (PP.H1 = 0.212, H1

TABLE 2 | Two-sample Mendelian randomization estimations showing the effect of smoking-related methylation on the risk of breast cancer subtypes (top ten CpGs according to p-value).

CpG	Chr	Position	Method	SNPs	Odds ratio	95% CI		p-value	q-value	Gene	Power
ER+											
cg2583948	15	75931953	Wald ratio	1	0.94	0.91	0.97	3.01E-05	**1.03E-02**	*IMP3*	1.00
cg0760265*	17	80844196	IVW	2	1.07	1.03	1.11	2.19E-04	**2.68E-02**	*TBCD*	0.91
cg0420946	17	4711018	Wald ratio	1	0.95	0.93	0.98	2.40E-04	**2.74E-02**	*PLD2*	1.00
cg2037583	13	99135543	Wald ratio	1	1.09	1.04	1.15	4.65E-04	**3.99E-02**	*STK24*	0.97
cg1227506	1	45279329	Wald ratio	1	0.93	0.89	0.97	8.06E-04	5.34E-02	*BTBD19*	0.93
cg2607605*	5	421317	IVW	2	1.05	1.02	1.08	1.04E-03	5.95E-02	*AHRR*	0.79
cg1782334	10	80848143	Wald ratio	1	1.04	1.02	1.07	1.62E-03	7.78E-02	*ZMIZ1*	1.00
cg0156570	14	103245090	Wald ratio	1	1.09	1.03	1.14	2.19E-03	9.07E-02	*TRAF3*	0.97
cg1870825	22	39545030	Wald ratio	1	0.96	0.94	0.99	2.82E-03	1.01E-01	*CBX7*	0.97
cg0318838	2	233245886	Wald ratio	1	0.93	0.88	0.97	3.39E-03	1.09E-01	*ALPP*	0.87
ER-											
cg2583948	15	75931953	Wald ratio	1	0.92	0.88	0.96	2.20E-04	8.47E-02	*IMP3*	0.98
cg1882444	15	89154058	Wald ratio	1	0.94	0.91	0.98	2.10E-03	3.64E-01	*MIR7-2*	0.97
cg1261648	11	62379063	Wald ratio	1	0.87	0.79	0.96	3.31E-03	4.25E-01	*ROM1*	0.97
cg2761893	8	71581788	Wald ratio	1	1.13	1.04	1.23	5.33E-03	4.91E-01	*XKR9*	0.99
cg2670350	2	113404661	Wald ratio	1	0.93	0.88	0.99	1.30E-02	5.77E-01	*SLC20A1*	0.91
cg1693695	17	57915665	Wald ratio	1	0.91	0.85	0.98	1.44E-02	5.84E-01	*TMEM49*	0.90
cg1782334	10	80848143	Wald ratio	1	1.05	1.01	1.09	1.60E-02	5.91E-01	*ZMIZ1*	0.96
cg1345216	13	96204518	Wald ratio	1	1.09	1.02	1.18	1.76E-02	5.96E-01	*CLDN10*	0.82
cg2403312	16	30485383	Wald ratio	1	1.04	1.01	1.07	1.81E-02	5.98E-01	*ITGAL*	0.84
cg1858406	2	64975916	Wald ratio	1	0.91	0.84	0.98	1.98E-02	6.02E-01		0.78

Bold font indicates the estimation passed the FDR test.

CI indicates confidence interval; IVW, Inverse variance weighted; ER, estrogen receptor; SNP, single nucleotide polymorphism. Statistical power was calculated by a web tool (https://shiny.cnsgenomics.com/mRnd/) (23).

** Cochran's Q-test for cg0760265 (Q-statistics, 0.19; p = 0.66) and cg2607605 (Q-statistics, 0.05; p = 0.83).*

TABLE 3 | MR Steiger directionality test and colocalization for four top findings in ER+ breast cancer.

CpG	PP.H0	PP.H1	PP.H2	PP.H3	PP.H4	Steiger *p*-value	Evidence
ER+ breast cancer							
cg2583948	4.38E-27	4.19E-02	1.00E-28	0	9.58E-01	1.01E-34	Strong
cg07602659	3.43E-07	8.83E-01	8.13E-11	9.29E-05	1.17E-01	1.86E-21	Weak
cg04209460	5.52E-43	2.12E-01	2.05E-45	0	7.88E-01	1.92E-57	Moderate
cg20375836	5.82E-06	3.67E-01	1.01E-08	0	6.33E-01	1.83E-11	Weak

ER indicates estrogen receptor; PP, posterior probability.

represents only the CpG site that has a genetic association in the given region). There was no evidence that the CpG sites of cg07602659 and cg20375836 shared a common SNP with ER+ breast cancer. Moreover, a phenome-wide association study suggested that cg20375836 is associated with body mass index (p = 5.86E-07) (**Supplementary Table S4**), which has been proved to be a significant risk factor of breast cancer.

DISCUSSION

In this study, we performed MR analyses to test if genetic evidence supported a causal relationship of smoking-related DNA methylation with breast cancer risk. Our MR results showed that DNA methylation may be a vital bridge linking smoking and breast cancer, especially for the subtype of ER+ breast cancer.

The associations between smoking and DNA methylation have been established based on epigenome-wide association analyses (24–26). A recent MR study assessing the role of genome-wide DNA methylation between smoking and risk of lung cancer identified 75 significant CpG sites from the Trøndelag Health Study (HUNT) (27). The top DNA methylation sites around or within genes, such as *AHRR*, *F2RL3*, *RARA*, *MGAT3*, *GPR15*, and *PRSS23*, were proved to be associated with smoking. Of these, DNA methylation at cg05575921 in the *AHRR* gene has been found to be most strongly influenced by smoking in previous studies, but most restricted to lung cancer or chronic obstructive pulmonary disease. Only a few studies have investigated the association between DNA methylation and breast cancer risk, indicating that both DNA hypo-methylation and DNA hyper-methylation may be significantly associated with breast cancer (28).

However, we failed to extract instrumental SNPs for the DNA methylation at cg05575921 in our study. When we used two SNPs (rs72711366 and rs77454118) to proxy the CpG site of cg2607605 (with *AHRR* expression), the effect of methylation on the risk of ER+ breast cancer achieved a nominal significance but did not pass the multiple testing threshold (OR = 1.05, 95% CI [1.02–1.08], p = 1.04E-03, q = 5.95E-02). We finally identified the DNA methylation at cg2583948, which locates at the promoter region of *IMP3* and inhibits *IMP3* expression (29), as a crucial mediator between smoking and ER+ breast cancer. The *IMP3* gene encodes the human and mouse homologs of the yeast U3 snoRNP-associated protein Imp3 (30). The protein Imp3 localizes to nucleoli and interacts with the U3 snoRNA, and is essential for the early cleavage steps in pre-rRNA processing (31). As reported in a previous study, pre-rRNA processing plays a key role in ribosome synthesis, which leads to cell growth and represents specific hallmarks of cancer cells (32). Furthermore, increasing evidence indicates the existence of a strong relationship between the aberrant rRNA synthesis and the development of cancers: on the one hand, altered rRNA processing may reduce the stability of the *p53* gene, causing *p53* to lose its tumor suppressor function; on the other hand, abnormal ribosomal biosynthesis causes altered translation and may result in increased translation of oncogenes and impaired translation of tumor suppressor genes (33). Overexpression of *IMP3* was found in colorectal cancer tissue, and downregulation of *IMP3* suppressed the protein translation rates and cell growth in colorectal cancer cells (34). However, few studies focused on the relationship of *IMP3* expression with other cancer types including breast cancer. Therefore, further large-scale epigenetic and basic studies are required to confirm this new finding.

In addition, we observed a distinct effect between DNA methylation and different subtypes of breast cancer. Compared with ER– breast cancer, DNA methylation seemed to play a more important role in linking smoking and ER+ breast cancer. This was consistent with findings from prior studies, reporting that different subtypes of breast cancer display different patterns of DNA methylation. Specifically, ER+/luminal breast cancer is characterized by a remarkably higher frequency of DNA methylation compared to ER–/basal-like tumors, and a large amount of genes are differentially methylated in different breast cancer subtypes (35, 36). Taken together, these findings suggest that DNA methylation profiles could be more active in ER+ breast cancer, resulting in more mediation effects linking smoking behavior and the risk of ER+ breast cancer.

In this study, modification of cg25839482 for the *IMP3* gene was first reported to be associated with breast cancer using two-sample MR combined with colocalization analysis. There are still several shortages in our study. One is the relatively small sample sizes for smoking-related DNA methylation, which provides a limited statistical power. Second is the deficiency of tissue-specific data because the DNA methylation level in blood cannot accurately reflect the methylation level in the breast tissue. Third, the samples of the methylation cohort are middle-aged women, while the samples from the breast cancer cohort are a whole age group. The difference in age between the two cohorts may lead to bias.

CONCLUSIONS

In summary, our MR results provided evidence that DNA methylation modification in blood, especially the CpG site of

cg2583948, seems to represent a causal pathway linking smoking and the ER+ breast cancer risk, other than ER− breast cancer, which offers a novel insight into probing potential mechanisms and intervention targets for different breast cancer subtypes.

DATA AVAILABILITY STATEMENT

The original contributions presented in the study are included in the article/**Supplementary Material**. Further inquiries can be directed to the corresponding authors.

AUTHOR CONTRIBUTIONS

HT: Data collection, formal analysis, statistical analysis, and writing—original draft. DY: Data collection and formal analysis. CH and PM: Methodology, writing—review and editing, and supervision. All authors contributed to the article and approved the submitted version.

FUNDING

This work was supported by Hunan Cancer Hospital Climb Plan (ZX2020005).

SUPPLEMENTARY MATERIAL

The Supplementary Material for this article can be found online at: https://www.frontiersin.org/articles/10.3389/fonc.2021.745918/full#supplementary-material

Supplementary Figure S1 | Instrumental variable (IV) assumptions of Mendelian randomization.

REFERENCES

1. Gaudet MM, Carter BD, Brinton LA, Falk RT, Gram IT, Luo J, et al. Pooled Analysis of Active Cigarette Smoking and Invasive Breast Cancer Risk in 14 Cohort Studies. *Int J Epidemiol* (2017) 46:881–93. doi: 10.1093/ije/dyw288
2. Dossus L, Boutron-Ruault MC, Kaaks R, Gram IT, Vilier A, Fervers B, et al. Active and Passive Cigarette Smoking and Breast Cancer Risk: Results From the EPIC Cohort. *Int J Cancer* (2014) 134:1871–88. doi: 10.1002/ijc.28508
3. Karlsson A, Ellonen A, Irjala H, Väliaho V, Mattila K, Nissi L, et al. Impact of Deep Learning-Determined Smoking Status on Mortality of Cancer Patients: Never Too Late to Quit. *ESMO Open* (2021) 6:100175. doi: 10.1016/j.esmoop.2021.100175
4. Nicolas M, Grandal B, Dubost E, Kassara A, Guerin J, Toussaint A, et al. Breast Cancer (BC) Is a Window of Opportunity for Smoking Cessation: Results of a Retrospective Analysis of 1234 BC Survivors in Follow-Up Consultation. *Cancers (Basel)* (2021) 13:2423. doi: 10.3390/cancers13102423
5. Caliri AW, Tommasi S, Besaratinia A. Relationships Among Smoking, Oxidative Stress, Inflammation, Macromolecular Damage, and Cancer. *Mutat Res* (2021) 787:108365. doi: 10.1016/j.mrrev.2021.108365
6. Silva CP, Kamens HM. Cigarette Smoke-Induced Alterations in Blood: A Review of Research on DNA Methylation and Gene Expression. *Exp Clin Psychopharmacol* (2021) 29:116–35. doi: 10.1037/pha0000382
7. Huynh K. Inflammation: Targeting Inflammatory Pathways to Treat Atherosclerosis and Cancer. *Nat Rev Cardiol* (2017) 14:629. doi: 10.1038/nrcardio.2017.152
8. Chen Z, Wen W, Cai Q, Long J, Wang Y, Lin W, et al. From Tobacco Smoking to Cancer Mutational Signature: A Mediation Analysis Strategy to Explore the Role of Epigenetic Changes. *BMC Cancer* (2020) 20:880. doi: 10.1186/s12885-020-07368-1
9. Conway K, Edmiston SN, Parrish E, Bryant C, Tse CK, Swift-Scanlan T, et al. Breast Tumor DNA Methylation Patterns Associated With Smoking in the Carolina Breast Cancer Study. *Breast Cancer Res Treat* (2017) 163:349–61. doi: 10.1007/s10549-017-4178-8
10. Thanassoulis G, O'donnell CJ. Mendelian Randomization: Nature's Randomized Trial in the Post–Genome Era. *JAMA* (2009) 301:2386–8. doi: 10.1001/jama.2009.812
11. Smith GD, Ebrahim S. 'Mendelian Randomization': Can Genetic Epidemiology Contribute to Understanding Environmental Determinants of Disease? *Int J Epidemiol* (2003) 32:1–22. doi: 10.1093/ije/dyg070
12. Relton CL, Gaunt T, McArdle W, Ho K, Duggirala A, Shihab H, et al. Data Resource Profile: Accessible Resource for Integrated Epigenomic Studies (ARIES). *Int J Epidemiol* (2015) 44:1181–90. doi: 10.1093/ije/dyv072
13. Jamieson E, Korologou-Linden R, Wootton RE, Guyatt AL, Battram T, Burrows K, et al. Smoking, DNA Methylation, and Lung Function: A Mendelian Randomization Analysis to Investigate Causal Pathways. *Am J ; Hum Genet* (2020) 106:315–26. doi: 10.1016/j.ajhg.2020.01.015
14. Burgess S, Thompson SG. Avoiding Bias From Weak Instruments in Mendelian Randomization Studies. *Int J Epidemiol* (2011) 40:755–64. doi: 10.1093/ije/dyr036
15. Allen RJ, Guillen-Guio B, Oldham JM, Ma SF, Dressen A, Paynton ML, et al. Genome-Wide Association Study of Susceptibility to Idiopathic Pulmonary Fibrosis. *Am J Respir Crit Care Med* (2020) 201:564–74. doi: 10.1164/rccm.201905-1017OC
16. Burgess S, Scott RA, Timpson NJ, Davey Smith G, Thompson SG. Using Published Data in Mendelian Randomization: A Blueprint for Efficient Identification of Causal Risk Factors. *Eur J Epidemiol* (2015) 30:543–52. doi: 10.1007/s10654-015-0011-z
17. Johnson T, Uk S. Efficient Calculation for Multi-SNP Genetic Risk Scores. *Am Soc Hum Genet Annual Meeting* (2012).
18. Hemani G, Tilling K, Davey Smith G. Orienting the Causal Relationship Between Imprecisely Measured Traits Using GWAS Summary Data. *PloS Genet* (2017) 13:e1007081. doi: 10.1371/journal.pgen.1007081
19. Kamat MA, Blackshaw JA, Young R, Surendran P, Burgess S, Danesh J, et al. Phenoscanner V2: An Expanded Tool for Searching Human Genotype-Phenotype Associations. *Bioinformatics* (2019) 35:4851–3. doi: 10.1093/bioinformatics/btz469
20. Bowden J, Davey Smith G, Burgess S. Mendelian Randomization With Invalid Instruments: Effect Estimation and Bias Detection Through Egger Regression. *Int J Epidemiol* (2015) 44:512–25. doi: 10.1093/ije/dyv080
21. Hemani G, Zheng J, Elsworth B, Wade KH, Haberland V, Baird D, et al. The MR-Base Platform Supports Systematic Causal Inference Across the Human Phenome. *Elife* (2018) 7:e34408. doi: 10.7554/eLife.34408
22. Wallace C. Statistical Testing of Shared Genetic Control for Potentially Related Traits. *Genet Epidemiol* (2013) 37:802–13. doi: 10.1002/gepi.21765
23. Brion M-JA, Shakhbazov K, Visscher PM. Calculating Statistical Power in Mendelian Randomization Studies. *Int J Epidemiol* (2012) 42:1497–501. doi: 10.1093/ije/dyt179
24. Sun YV, Smith AK, Conneely KN, Chang Q, Li W, Lazarus A, et al. Epigenomic Association Analysis Identifies Smoking-Related DNA Methylation Sites in African Americans. *Hum Genet* (2013) 132:1027–37. doi: 10.1007/s00439-013-1311-6
25. Shenker NS, Polidoro S, van Veldhoven K, Sacerdote C, Ricceri F, Birrell MA, et al. Epigenome-Wide Association Study in the European Prospective Investigation Into Cancer and Nutrition (EPIC-Turin) Identifies Novel Genetic Loci Associated With Smoking. *Hum Mol Genet* (2013) 22:843–51. doi: 10.1093/hmg/dds488
26. Breitling LP, Yang R, Korn B, Burwinkel B, Brenner H. Tobacco-Smoking-Related Differential DNA Methylation: 27K Discovery and Replication. *Am J Hum Genet* (2011) 88:450–7. doi: 10.1016/j.ajhg.2011.03.003

27. Sun YQ, Richmond RC, Suderman M, Min JL, Battram T, Flatberg A, et al. Assessing the Role of Genome-Wide DNA Methylation Between Smoking and Risk of Lung Cancer Using Repeated Measurements: The HUNT Study. *Int J Epidemiol* (2021). doi: 10.1093/ije/dyab044
28. Conway K, Edmiston SN, May R, Kuan PF, Chu H, Bryant C, et al. DNA Methylation Profiling in the Carolina Breast Cancer Study Defines Cancer Subclasses Differing in Clinicopathologic Characteristics and Survival. *Breast Cancer Res* (2014) 16:450. doi: 10.1186/s13058-014-0450-6
29. Yang Y, Wu L, Shu X-O, Cai Q, Shu X, Li B, et al. Genetically Predicted Levels of DNA Methylation Biomarkers and Breast Cancer Risk: Data From 228 951 Women of European Descent. *J Natl Cancer Institute* (2020) 112:295–304. doi: 10.1093/jnci/djz109
30. Kornprobst M, Turk M, Kellner N, Cheng J, Flemming D, Koš-Braun I, et al. Architecture of the 90S Pre-Ribosome: A Structural View on the Birth of the Eukaryotic Ribosome. *Cell* (2016) 166:380–93. doi: 10.1016/j.cell.2016.06.014
31. Granneman S, Gallagher JE, Vogelzangs J, Horstman W, van Venrooij WJ, Baserga SJ, et al. The Human Imp3 and Imp4 Proteins Form a Ternary Complex With Hmpp10, Which Only Interacts With the U3 Snorna in 60-80S Ribonucleoprotein Complexes. *Nucleic Acids Res* (2003) 31:1877–87. doi: 10.1093/nar/gkg300
32. Pecoraro A, Pagano M, Russo G, Russo A. Ribosome Biogenesis and Cancer: Overview on Ribosomal Proteins. *Int J Mol Sci* (2021) 22:5496. doi: 10.3390/ijms22115496
33. Penzo M, Montanaro L, Treré D, Derenzini M. The Ribosome Biogenesis-Cancer Connection. *Cells* (2019) 8:55. doi: 10.3390/cells8010055
34. Liu Y, Xu W, Xu X, Tan Z, Xu J, Ma L, et al. Loss of BRMS2 Induces Cell Growth Inhibition and Translation Capacity Reduction in Colorectal Cancer Cells. *Am J Cancer Res* (2021) 11:930–44.
35. Győrffy B, Bottai G, Fleischer T, Munkácsy G, Budczies J, Paladini L, et al. Aberrant DNA Methylation Impacts Gene Expression and Prognosis in Breast Cancer Subtypes. *Int J Cancer* (2016) 138:87–97. doi: 10.1002/ijc.29684
36. Holm K, Hegardt C, Staaf J, Vallon-Christersson J, Jönsson G, Olsson H, et al. Molecular Subtypes of Breast Cancer Are Associated With Characteristic DNA Methylation Patterns. *Breast Cancer Res* (2010) 12:R36. doi: 10.1186/bcr2590

Conflict of Interest: The authors declare that the research was conducted in the absence of any commercial or financial relationships that could be construed as a potential conflict of interest.

Publisher's Note: All claims expressed in this article are solely those of the authors and do not necessarily represent those of their affiliated organizations, or those of the publisher, the editors and the reviewers. Any product that may be evaluated in this article, or claim that may be made by its manufacturer, is not guaranteed or endorsed by the publisher.

frontiers in Pharmacology

ORIGINAL RESEARCH
published: 29 September 2021
doi: 10.3389/fphar.2021.706240

Lysophosphatidic Acid–Induced EGFR Transactivation Promotes Gastric Cancer Cell DNA Replication by Stabilizing Geminin in the S Phase

*Haile Zhao†, Gezi Gezi†, Xiaoxia Tian†, Peijun Jia, Morigen Morigen and Lifei Fan**

State Key Laboratory of Reproductive Regulation & Breeding of Grassland Livestock, School of Life Sciences, Inner Mongolia University, Hohhot, China

Geminin, an inhibitor of the DNA replication licensing factor, chromatin licensing and DNA replication factor (Cdt) 1, is essential for the maintenance of genomic integrity. As a multifunctional protein, geminin is also involved in tumor progression, but the molecular details are largely unknown. Here, we found that lysophosphatidic acid (LPA)–induced upregulation of geminin was specific to gastric cancer cells. LPA acted *via* LPA receptor (LPAR) 3 and matrix metalloproteinases (MMPs) signaling to transactivate epidermal growth factor receptor (EGFR) (Y1173) and thereby stabilize geminin expression level during the S phase. LPA also induced the expression of deubiquitinating protein (DUB) 3, which prevented geminin degradation. These results reveal a novel mechanism underlying gastric cancer progression that involves the regulation of geminin stability by LPA-induced EGFR transactivation and provide potential targets for the signaling pathway and tumor cell–specific inhibitors.

Keywords: LPA, EGFR, transactivation, DNA replication, geminin

OPEN ACCESS

Edited by:
Yi-Chao Zheng,
Zhengzhou University, China

Reviewed by:
Orsola di Martino,
Washington University in St. Louis, United States
Lukasz Opalinski,
University of Wroclaw, Poland

****Correspondence:***
Lifei Fan
lifei.fan@imu.edu.cn

†These authors have contributed equally to this work and share first authorship

Specialty section:
This article was submitted to Experimental Pharmacology and Drug Discovery, a section of the journal Frontiers in Pharmacology

Received: *07 May 2021*
Accepted: *13 August 2021*
Published: *29 September 2021*

Citation:
Zhao H, Gezi G, Tian X, Jia P, Morigen M and Fan L (2021) Lysophosphatidic Acid–Induced EGFR Transactivation Promotes Gastric Cancer Cell DNA Replication by Stabilizing Geminin in the S Phase. Front. Pharmacol. 12:706240. doi: 10.3389/fphar.2021.706240

INTRODUCTION

Precise control of DNA replication is critical for maintaining genomic integrity. To this end, both eukaryotic and prokaryotic cells have evolved various mechanisms to ensure that nuclear DNA is completely replicated at the right time, right place, and only once per cell division (Machida et al., 2005; Zhou et al., 2020). Initiation of DNA replication is strictly regulated in eukaryotes, as reinitiation at any starting origin leads to cell death or genomic rearrangement, which causes serious physiologic consequences, including cancer. The regulatory mechanism involves suppression of chromatin licensing and DNA replication factor (Cdt)1 function by geminin, proteasome-mediated Cdt1 degradation in the S phase, and cyclin-dependent kinase (CDK)–mediated inhibition of transcription initiation (Miotto and Struhl, 2010; Wong et al, 2010; Diffley, 2011; Ballabeni et al, 2013).

Geminin directly binds to Cdt1 and inhibits pre-replicative complex formation to prevent aneuploidy and re-replication (McGarry and Kirschner, 1998; Wohlschlegel et al., 2000). The precise control of geminin levels throughout the cell cycle mainly depends on ubiquitin-mediated proteasomal degradation. Geminin levels fluctuate throughout the cell cycle and the protein is degraded in late mitosis/G1 phase by the anaphase-promoting complex/cyclosome (APC/C) ubiquitin ligase complex to facilitate origin licensing (Wohlschlegel et al., 2000). In contrast, geminin accumulates in early S, G2, and early M phases as a result of APC/C ubiquitin ligase

complex inhibition, ensuring that pre-replicative complex formation is blocked (Ballabeni et al., 2004). A recent study reported that in the late S phase, the microRNA miR-571 reduced geminin protein level via the Cdk2–c-Myc–miR-571 axis independent of the APC/C inducing DNA replication efficiency and S-phase cell-cycle progression (Zhang et al., 2019). In the early M phase, Aurora-A phosphorylates geminin at Thr25 to prevent its degradation by APC/C during mitosis (Tsunematsu et al., 2013). Deubiquitinating protein (DUB)3 and ubiquitin-specific peptidase (USP) 7 also increase geminin levels by preventing its ubiquitination (Hernández-Pérez et al., 2017).

Geminin is a multifunctional protein that plays important roles in DNA replication and transcriptional/epigenetic regulation and is frequently deregulated in human cancers. The upregulation of geminin in various malignancies was shown to be correlated with tumor cell proliferation, invasion, and metastasis (Gonzalez et al., 2004; Petropoulou et al., 2008; Emmett and O'Shea, 2012; Rajan et al., 2013; Sato et al., 2013; Hills and Diffley, 2014; Yagi et al., 2014; Zhang et al., 2017; Ryan et al, 2019; Alaeddini and Etemad-Moghadam, 2020; Lewis and Stracker, 2021). Tumor cells depend on geminin to prevent excess DNA replication from triggering DNA damage–induced apoptosis. Knockdown of geminin resulted in DNA re-replication and apoptosis in malignant cancer cells, whereas normal and immortalized cells were unaffected (Zhu and Depamphilis, 2009). Aberrant geminin expression has been linked to DNA replication damage, aneuploidy, and genomic instability, all of which are associated with a precancerous state and malignant transformation (Petropoulou et al., 2008; Champeris Tsaniras et al., 2018). Thus, geminin is considered as an oncogene, although its mechanism of action in tumorigenesis is not fully understood.

The tumor microenvironment (TME) includes various cell types and extracellular components. Communication between tumor cells and the TME involves cell–cell and cell-extracellular matrix (ECM) adhesion, as well as cellular responses to soluble molecules (Wu and Dai, 2016). The TME is implicated in tumor initiation, progression, and metastasis. Soluble extracellular components such as lysophospholipase D autotaxin (ATX) and its product lysophosphatidic acid (LPA) are key factors in cancer progression. *In vitro* and *in vivo* studies have shown that increased ATX/LPA signaling contributes to cancer initiation and progression (Mills and Moolenaar, 2003; Leblanc and Peyruchaud, 2014; Lee et al., 2015). LPA stimulates cell proliferation, migration, and survival through activation of G protein–coupled receptors (GPCRs). Both LPA receptor (LPAR) family members and ATX are aberrantly expressed in various malignancies, including breast, ovarian, and prostate cancers, hepatocellular carcinoma multiforme, and melanoma (Lee et al., 2015). The context of LPA biology is complex as it involves not only several distinct GPCRs, but also cross-talk with receptor tyrosine kinase signaling via matrix metalloproteinase (MMP) activation (Gschwind et al., 2002; Köse, 2017). Epidermal growth factor receptor (EGFR) transactivation by GPCRs was shown to induce mitogen-activated protein kinase (MAPK) signaling and gene expression, stimulate DNA synthesis, and regulate cell-cycle progression (Daub et al., 1996; Kalmes et al., 2000; Alsahafi et al, 2020); and transactivation of EGFR by LPA and sphingosine-1-phosphate has been linked to the pathophysiology of human cancer (Gschwind et al., 2002; Deng et al, 2004; Sukocheva et al., 2006; Tveteraas et al, 2016), although the mechanisms are yet to be elucidated clearly.

LPA is significantly elevated in the plasma and ascites of gastric cancer patients with peritoneal carcinomatosis compared to healthy individuals (Zeng et al., 2017). Submucosal connective tissue–type mast cells are a source of LPA in the gastrointestinal tract (Mori et al., 2007). LPA stimulates gastric cancer cell migration and invasion *via* various effectors (Murray et al., 2008; Ren et al., 2019; Shida et al., 2008), as well as cell proliferation by upregulating sphingosine kinase (SPHK) 1 transcription (Ramachandran et al., 2010). However, it is unclear whether LPA affects DNA replication in gastric cancer.

In this study, we investigated the role and mechanism of action of geminin and LPA in gastric cancer. Our results indicated that geminin functions as a regulator of gastric cancer progression. Depletion of geminin induced DNA re-replication in gastric cancer cells. Meanwhile, LPA induced the upregulation of geminin protein and induced EGFR transactivation via an MMP-dependent pathway, which was partly responsible for stabilizing geminin in the early S phase and promoting DNA replication. These data indicate that the cross-talk between LPA and EGFR signaling pathway regulates DNA replication in gastric cancer cells by controlling geminin levels.

MATERIALS AND METHODS

Cell Culture

Gastric cancer cells (MKN45 and BGC-803) were maintained in RPMI 1,640 medium (Gibco) supplemented with 10% fetal bovine serum (BI) and 1% (vol/vol) penicillin/streptomycin/L-Glutamin (Gibco). Human gastric mucosal epithelial cells (GES-1) were maintained in DMEM (High glucose, Gibco) supplemented with 10% (vol/vol) fetal bovine serum (BI) and 1% (vol/vol) penicillin/streptomycin/L-Glutamin (Gibco). All cells were cultured at 37°C and 5% CO_2 in a humidified atmosphere (Thermo Fisher Scientific, MA, United States). To synchronize cells in the G1/S-phase, the cells were cultured in serum-free medium for 24 h.

Reagents and Inhibitors

Reagents and inhibitors were purchased from the following suppliers: LPA (SIGMA), DMSO (SIGMA), BB94 (SIGMA), BSA (SIGMA), Ki16425 (SELLECK), AG1478 (SELLECK), LY294002 (SELLECK), and Rapamycin (SELLECK).

RNA Interference

To knockdown endogenous geminin expression, the cells were transfected with 50 nM siRNA that targets human geminin using Lipofectamine 2000 (Thermo Fisher Scientific, MA, United States). Three oligos of siGEM were mixed in equal proportions. Short interfering oligoribonucleotide for luciferase (non-targeting

siRNA, siGL/siNC/sitrl) was used as a control. Both of them were used as previously described (Zhu et al., 2004; Zhu and Depamphilis, 2009) and obtained from Sangon Biotech (Shanghai, China) and their sequences are listed in **Supplementary Table 1**. Knockdown efficiency of endogenous geminin expression was confirmed by Western blotting using an antibody against geminin.

To knockdown endogenous $LPAR_3$ expression, the cells were transfected with 50 nM siRNA that targets human $LPAR_3$ using Lipofectamine 2000. Nontargeting siRNA (sitrl) was used as a control. The custom-synthesized siRNA sequences were ordered from Sangon and their sequences are listed in **Supplementary Table 1**. Knockdown efficiency of endogenous $LPAR_3$ expression was confirmed by quantitative real-time (qRT)-PCR.

To knockdown endogenous DUB3 expression, the cells were transfected with 50 nM siRNA that targets human DUB3 using Lipofectamine 2000. Nontargeting siRNA (siNC) was used as a control. Both of them were used as previously described (Hernández-Pérez et al., 2017). The custom-synthesized siRNA sequences were ordered from Sangon and their sequences are listed in **Supplementary Table 1**. Knockdown efficiency of endogenous DUB3 expression was confirmed by western blotting using an antibody against DUB3.

Flow Cytometry Analysis of Cell Cycle

Cell-cycle progression under different conditions was evaluated by flow cytometry. After treatment, cells were harvested by digestion with 0.05% trypsin, washed twice with ice-cold 1× phosphate-buffered saline (1x PBS), and then fixed overnight at −20°C in 70% ethanol. The next day, the cells were washed with 1x PBS and incubated with 50 μg/ml propidium iodide (PI) and 50 μg/ml RNase A in 1x PBS on ice for 30 min in the dark. Flow cytometry was performed on a FACSCalibur system (BD Biosciences, San Jose, CA, United States) with CELLQuest v3.3 software (BD Biosciences), and cell-cycle distribution was analyzed with ModFit LT v3.0 software (Verity Software House, Topsham, ME, United States).

RNA Extraction, Reverse Transcription PCR, and qRT-PCR

Total RNA was extracted from cells using TRIzol (TransGen Biotech, Beijing, China) according to the manufacturer's instructions. TransScript One-Step gDNA Removal and cDNA Synthesis SuperMix (TransGen Biotech) was used to generate cDNA template, and qRT-PCR was performed with the TransStart Tip Green qPCR SuperMix (TransGen Biotech) on a LightCycler 480 II system (Roche, Basel, Switzerland). The mRNA expression levels of target genes were calculated relative to that of β-actin. The primers were obtained from Sangon and their sequences are listed in **Supplementary Table 2**.

Western Blotting and Immunoprecipitation

Cells were lysed with lysis buffer (250 mM Tris [pH 6.8], 20 mM DL-dithiothreitol, 150 mM bromophenol blue, 10% [v/v] glycerol, and 1% sodium dodecyl sulfate [SDS]). Immunoprecipitation was performed as described in this article. Proteins in the cell lysates were separated by SDS–polyacrylamide gel electrophoresis and electrotransferred to a semi-dry membrane (Bio-Rad, Hercules, CA, United States), then incubated with antibodies and exposed to Pierce ECL Western Blotting Substrate (Thermo Fisher Scientific) for visualization of protein bands. The relative amounts of geminin and other proteins were quantified by densitometry using the ChemiDoc XRS system (Bio-Rad) and normalized in that of β-tubulin. The geminin/tubulin Western blotting signal ratios were calculated using Image Lab Version 5.2.1 (Bio-Rad) for each time point. Densitometry of three independent experiments was performed, normalized to tubulin, and expressed as a ratio of the control lane of each group. The following antibodies were used: Geminin rabbit polyclonal antibody (Proteintech), EGFR-specific rabbit polyclonal antibody (Proteintech), rabbit anti-DUB3 polyclonal antibody (Proteintech), mouse anti-β-tubulin monoclonal antibody (Transgen), anti-phosphotyrosine antibody (abcam), goat anti-rabbit IgG (Transgen), and goat anti-mouse IgG (Transgen). In Western blotting, dilution ratio for all primary antibodies was 1:1,000 and 1:25,000 for all secondary antibodies. For the immunoprecipitation assay, the antibody was used at 1:100 dilution.

Immunofluorescence Analysis and Confocal Microscopy

Cells grown on glass coverslips in a 12-well plate were fixed in 4% paraformaldehyde (PFA) for 15 min, permeabilized with Triton X-100 for 5 min, and incubated in sodium borohydride for 10 min. They were then incubated with rabbit anti-geminin antibody (1:200) in 1x PBS containing 1% bovine serum albumin (BSA) for 1 h at room temperature (RT). Cells were washed 5 times with 1x PBS, incubated with Alexa Fluor 488–conjugated goat anti-rabbit IgG (H + L) secondary antibody (1:200; Invitrogen, Carlsbad, CA, United States) in 1x PBS containing 1% BSA for 45 min at RT in the dark, followed by washing twice with 1x PBS. DNA was visualized by staining with 4',6-diamidino-2-phenylindole (1:5,000 in water; Invitrogen). Cells were visualized with a laser scanning confocal microscope (LSM 710; CarlZeiss, Wetzlar, Germany).

Cell Viability Staining

Gastric cancer cells were cultured on sterile glass coverslips in a 12-well plate, and after the transfections of siGL or siGEM, all cells were cultured for 2 days. Cells were visualized by using Live & Dead Viability/Cytotoxicity Assay Kit for Animal Cells (KeyGEN BioTECH, China). Cells were then visualized by using laser scanning confocal microscope (CarlZeiss LSM 710).

Cell Proliferation Assay

Cells were seeded on a 96-well plate with 2,000 cells for each well and grown in 200 μl serum-free medium with 0.1% DMSO, 10 μM LPA, or 10 ng/ml EGF. The medium was changed every 2 days. 20 μl of Cell Counting Kit-8 (CCK-8) was provided to every well for 1.5 h. The plate was then read using a spectrophotometric microtiter plate reader (EPOCH) set at a dual wavelength of 450 nm. Bromodeoxyuridine (BrdU) is incorporated into newly synthesized DNA strands of actively

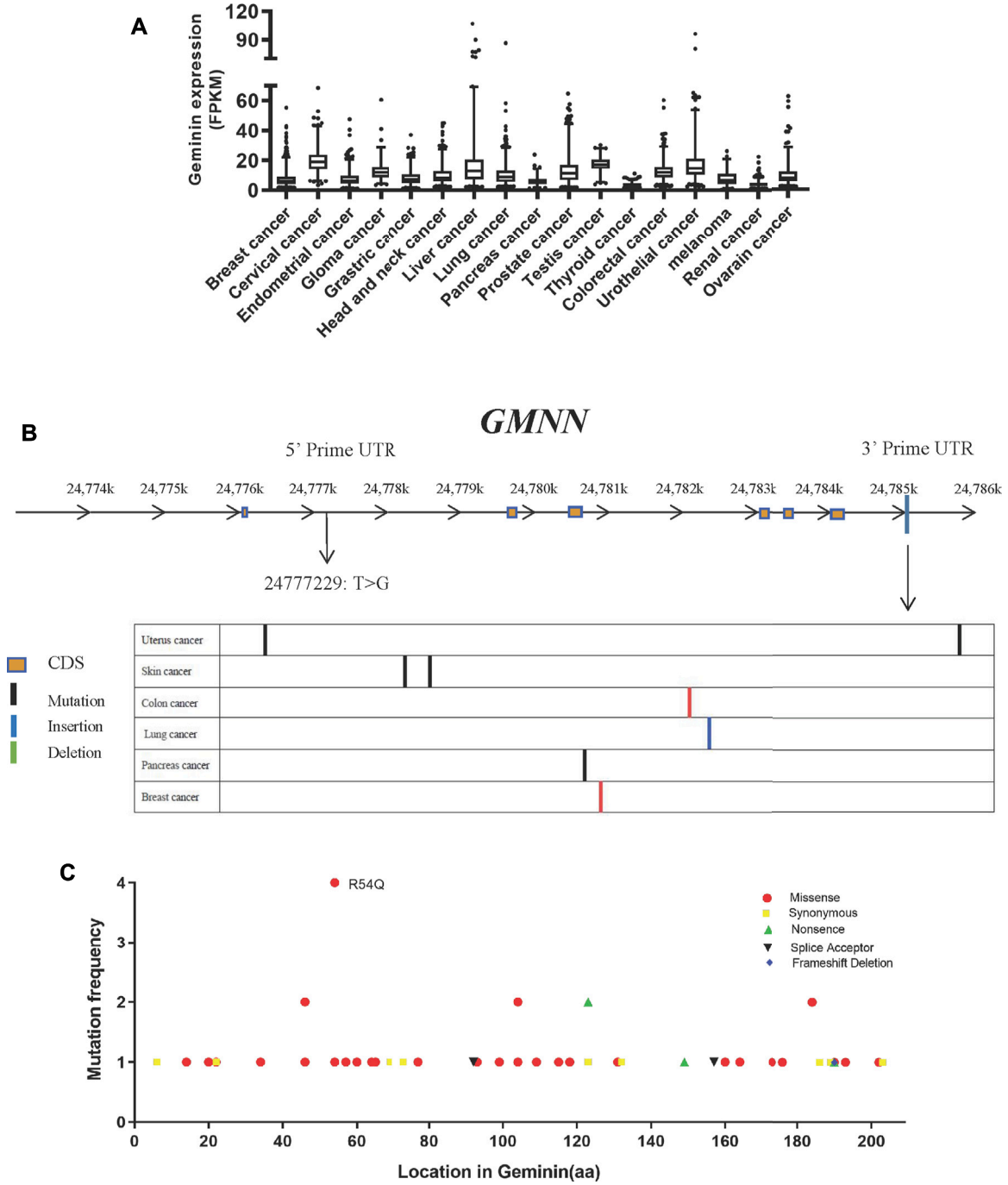

FIGURE 1 | Mutation of geminin is non-predominant in human cancer. **(A)** RNA expression of geminin in 17 cancer types. **(B)** Location of mutation sites in *GMNN* gene. **(C)** Summary of geminin mutations across different tumor types from TCGA.

proliferating cells (Abcam, ab126556, BrdU Cell Proliferation ELISA Kit [colorimetric]).

Statistical Analyses

All statistical analyses were processed using GraphPad Prism v8.0 software. Quantitative analyses from three independent experiments (mean ± SD) are shown. More than two groups were analyzed for data by ANOVA test and Dunnett's multiple comparisons test under the assumption of normality. In data with two groups, unpaired Student's t-tests were used under the assumption of normality. In general, at least three independent biological replicates were carried out for each experiment. $^{*}p < 0.05$, $^{**}p < 0.01$, and $^{***}p < 0.001$ were considered statistical significance.

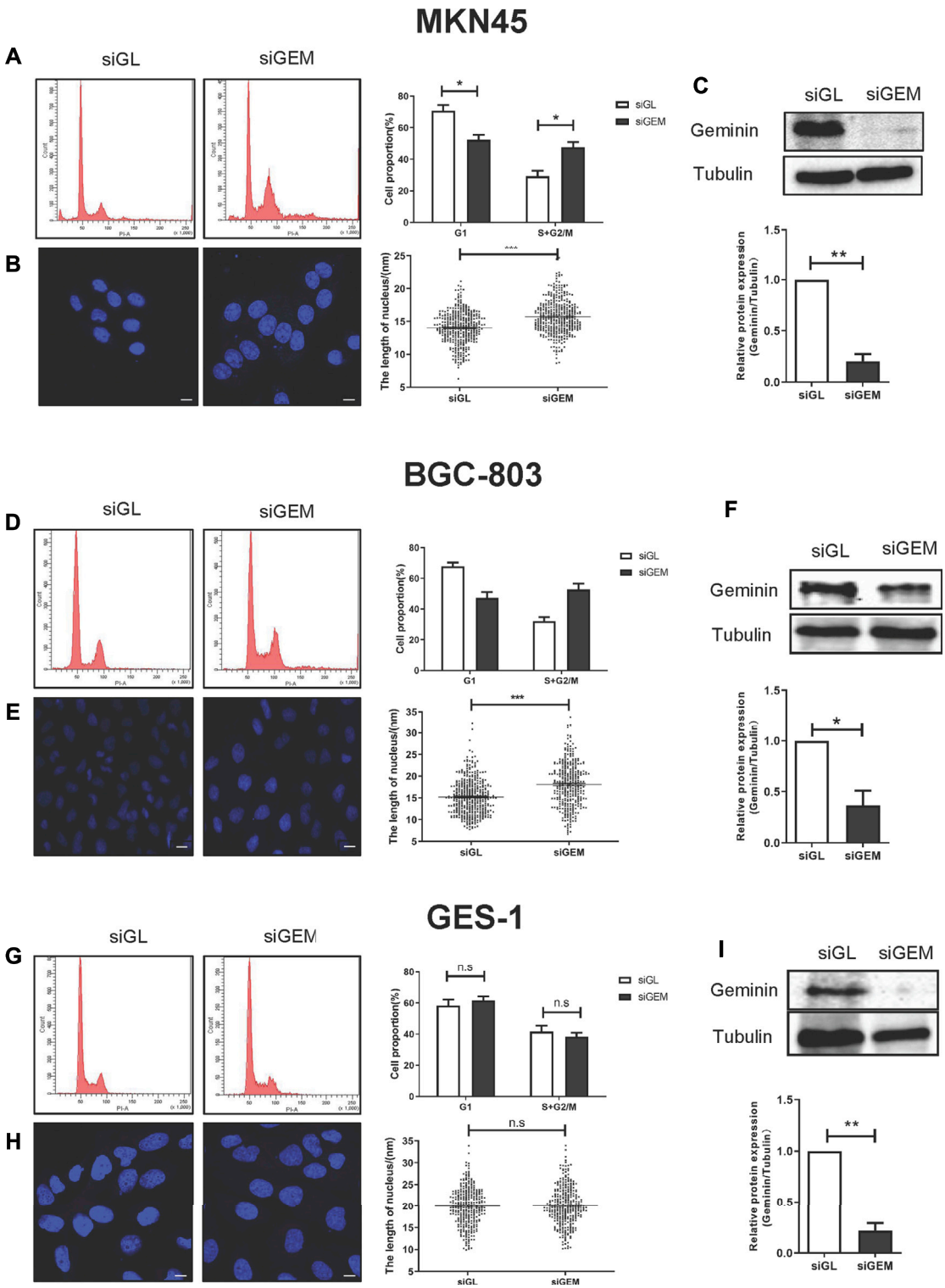

FIGURE 2 | Depletion of geminin induces DNA re-replication in gastric cancer cells but not in normal gastric epithelial cells. Two gastric cancer cells (MKN45 and BGC-803) and normal epithelial cells (GES-1) were transfected with siGL or siGEM. After 48-h posttransfection, the cells were harvested and stained with PI to quantify DNA content by FACS analysis **(A, D, G)** or with DAPI to visualize nuclei by LSM **(B, E, H)**. Geminin and tubulin were detected by Western blotting **(C, F, I)**. Densitometry of three independent experiments was performed, normalized to tubulin, and expressed as a ratio of siGL, respectively, mean ± SD, $^{*}p < 0.05$, $^{**}p < 0.01$, $^{***}p < 0.001$ (T test).

URLs

The Cancer Genome Atlas (TCGA), http://cancergenome.nih.gov/. Human Protein Atlas (HPA), http://www.proteinatlas.org/.

RESULTS

Geminin is Not Frequently Mutated in Human Cancers

To explore the genetic abnormalities affecting the gene encoding geminin (*GMNN*) in human cancers comprehensively, we searched public databases including the TCGA and HPA (Uniform Resource Locators, URLs). The *GMNN* mRNA expression level was similar across 17 cancer types (**Figure 1A**), indicating that the gene has no cell or tissue specificity, consistent with its function as a regulatory protein that is expressed during the proliferative phase of the cell cycle.

In TCGA, whole-genome sequencing results, 57 mutations in the *GMNN* gene were identified in 13 cancer types. The mutations gave rise to 51 variants of geminin, many of which were discretely distributed. Most of the 57 mutations were located in the exon region, while one was located in the 5′ untranslated region (UTR) (T > G at the chromosome position 24777229) and eight were present in the 3′ UTR (**Figure 1B**). There were only missense or synonymous mutations at the N terminus of the protein, whereas deletions, nonsense mutation, and splice site mutations were also observed at the C terminus (**Figure 1C**). An arginine at amino acid position 54 was more susceptible to glutamine substitution than other amino acids (**Figure 1C**). Thus, mutations in the *GMNN* gene are not widespread in human cancers. As cells alter the expression of replication factors to conquer replicative stress in the early stages of tumorigenesis, mutations in replication factors are rare.

Depletion of Geminin Selectively Induces DNA Re-Replication in Gastric Cancer Cells

SiRNAs targeting *GMNN* (siGEM) were shown to induce DNA re-replication in colorectal carcinoma, head and neck squamous cell carcinomas (HNSCCs), and breast cancer (Zhu et al., 2004; Zhu and Depamphilis, 2009). However, this effect varied according to cell type: immortalized cells derived from normal tissues and some cancer cell lines (e.g., cervix adenocarcinoma cells HeLa, skin melanoma cells A375 and WM-266-4) were resistant to DNA re-replication induced by *GMNN* knockdown (Zhu and Depamphilis, 2009). We examined the effect of geminin depletion in gastric cancer using three gastric cell lines (MKN45, BGC-803, and GES-1 cells). Two days after transfection with siGEM, the proportion of gastric cancer cells MKN45 and BGC-803 in the S + G2/M phase was increased compared to the cells transfected with a control siRNA (siGL) (**Figures 2A,D**), and it was accompanied by an increase in the number of giant nuclei observed by laser scanning confocal microscopy (**Figures 2B,E**) and downregulation of geminin expression (**Figures 2C,F**). Depletion of geminin had no effect on the viability and proliferation of MKN45 and BGC-803 cells (**Supplementary Figure 1**).

We examined whether depletion of geminin had the same effect on GES-1 cells, a normal gastric epithelial cell line. As expected, siGEM reduced geminin expression (**Figure 2I**) but no changes were observed in the proportion of cells in the S + G2/M phase (**Figure 2G**) or in the fraction of cells with giant nuclei (**Figure 2H**). Thus, depletion of geminin induces DNA re-replication in gastric cancer cells but not in normal gastric epithelial cells.

LPA Selectively Triggers the Upregulation of Geminin in Gastric Cancer Cells

LPA is a GPCR agonist which can modulate cell proliferation (Gschwind et al., 2002), migration (Guo et al., 2015), and invasion (Gschwind et al., 2003) *via* multiple signaling pathways. Abnormalities in LPA signal transduction can lead to cancer development and metastasis (Mills and Moolenaar, 2003). To investigate the role of LPA in gastric cancer, MKN45, BGC-803, and GES-1 cells were treated with LPA, and geminin protein level was evaluated by Western blotting. 10 μM LPA treatment could induce a significant increase in the geminin expression (**Figures 3B,E**). LPA stimulation caused a transient upregulation of geminin in the early S phase (0–2 h) in MKN45 cells (**Figure 3A**) and BGC-803 cells (**Figure 3D**) but not GES-1 cells (**Figure 3G**). Prior to LPA treatment, the cells were serum starved and maintained in a quiescent state, and 1% BSA was added to the medium to preserve the biological activity of LPA. To exclude the effect of BSA on geminin expression, we evaluated the changes in the protein level following incubation for 0.5 h in the presence or absence of 1% BSA. As expected, BSA did not affect geminin protein levels in gastric cancer cells (**Figures 3C,F**). These results indicate that LPA specifically increases geminin protein level in gastric cancer cells.

As a DNA replication factor, geminin shuttles among the nucleus, nucleoplasm, and cytoplasm (McGarry and Kirschner, 1998). In normal human gastric tissue, geminin was localized in the cytoplasm and cytoplasmic membrane of all tissues and was detected in the nucleus only in 67% of samples *via* IHC. In contrast, geminin was detected in the nucleus of 81.8% of tumor tissue samples, with exclusive nuclear localization in 72.73% (data were obtained from HPA, **Supplementary Figure 2A**).

To investigate whether LPA affects cytoplasmic–nuclear trafficking of geminin in gastric cancer, we examined geminin localization at different time points after LPA treatment. In quiescent cells treated with DMSO, geminin was mainly detected in the cytoplasm, and nuclear localization increased with prolonged LPA treatment (**Supplementary Figure 2B**). Thus, in gastric cancer cells, LPA stimulation promotes nucleus transfer of geminin, which can be a useful diagnostic marker.

LPA Enhances Geminin Stability Through Deubiquitinating Enzyme DUB3 in Gastric Cancer Cells

APC/C controls geminin degradation, while DUB3 is also known to regulate geminin protein stability (Hernández-Pérez et al., 2017). The latter was confirmed by overexpressing transfected

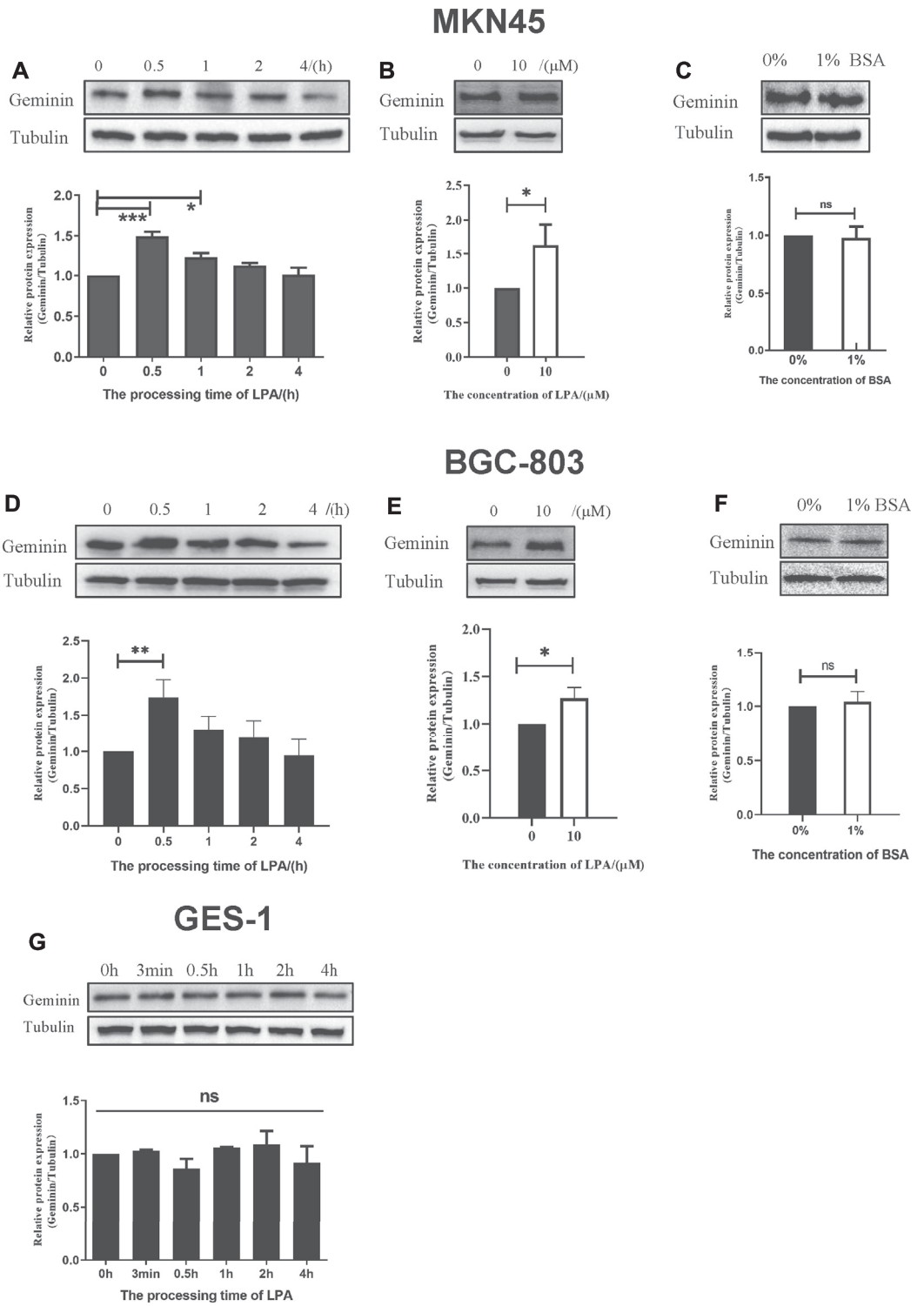

FIGURE 3 | LPA selectively triggers the upregulation of geminin in gastric cancer cells. **(A, D, G)** G1/S–arrested cells were treated with LPA time gradient. **(B, E)** Protein level of geminin with or without 10 μM LPA treatment. **(C, F)** G1/S–arrested cells were under the treatment with or without 1% BSA. Densitometry of three independent experiments was performed, normalized to tubulin and expressed as a ratio of 0 h or 0 μM, respectively. Mean ± SD, $^{*}p < 0.05$, $^{**}p < 0.01$ (ANOVA test and Dunnett's multiple comparisons test)

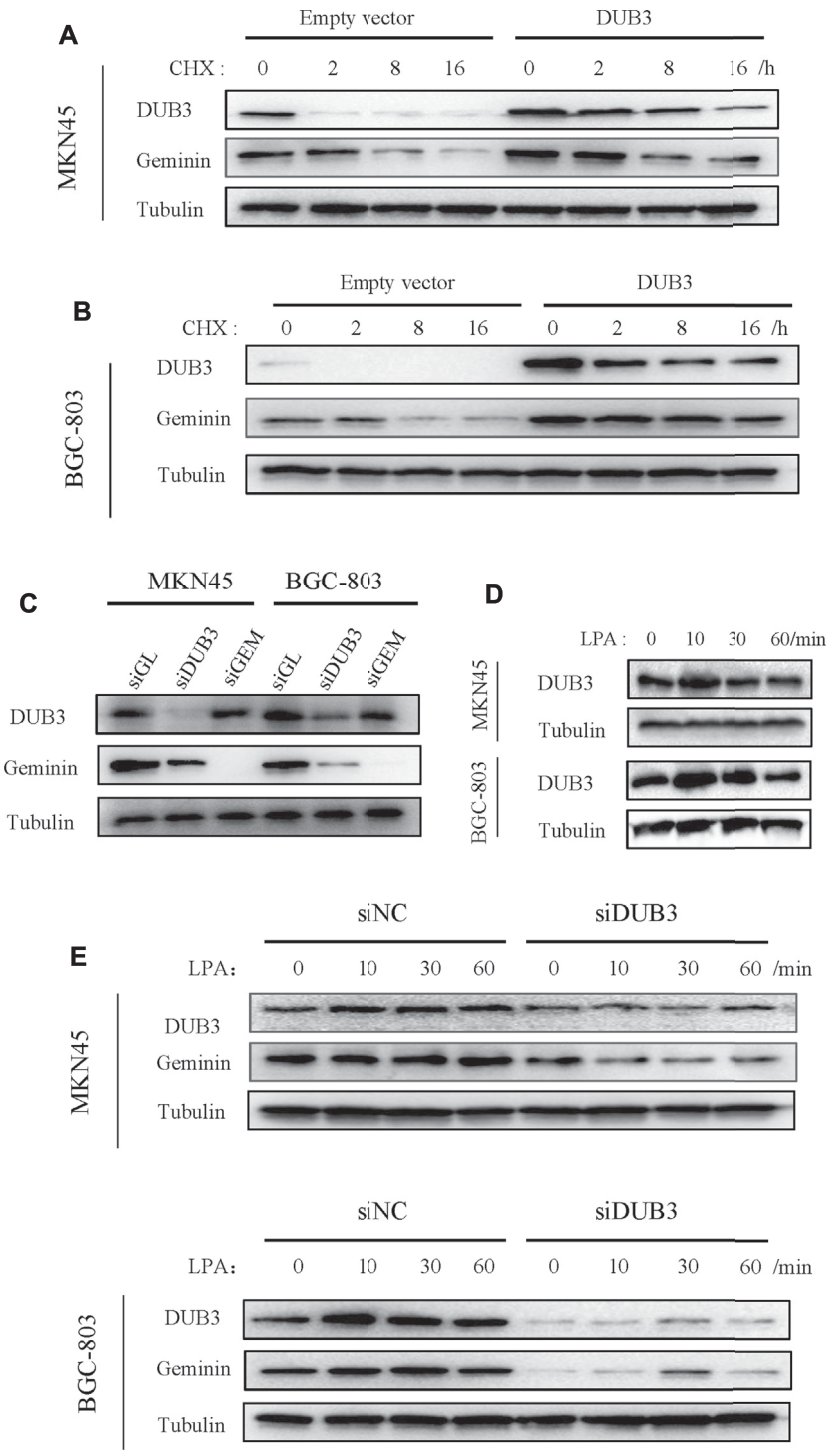

FIGURE 4 | LPA potentiates geminin stability through DUB3 in gastric cancer cells. **(A, B)** Gastric cancer cells MKN45 **(A)** and BGC-803 **(B)** were transfected with the indicated vectors (empty vector; DUB3, a vector that contains *Homo sapiens* ubiquitin-specific peptidase 17-like family member 2 [USP17L2] mRNA [DUB3]), and incubated with cycloheximide (CHX, 50 μg/ml) for the indicated time points. Western blotting analysis with the indicated antibodies. **(C)** Two gastric cancer cells (MKN45 and BGC-803) were transfected with the indicated siRNA. Cell lysates were analyzed by Western blotting. **(D)** Two gastric cancer cells were treated with LPA time gradient, and cell lysates were analyzed by Western blotting. **(E)** Two gastric cancer cells (MKN45 and BGC-803) were transfected with the indicated siRNA, together with LPA time gradient treatment, and cell lysates were analyzed by Western blotting.

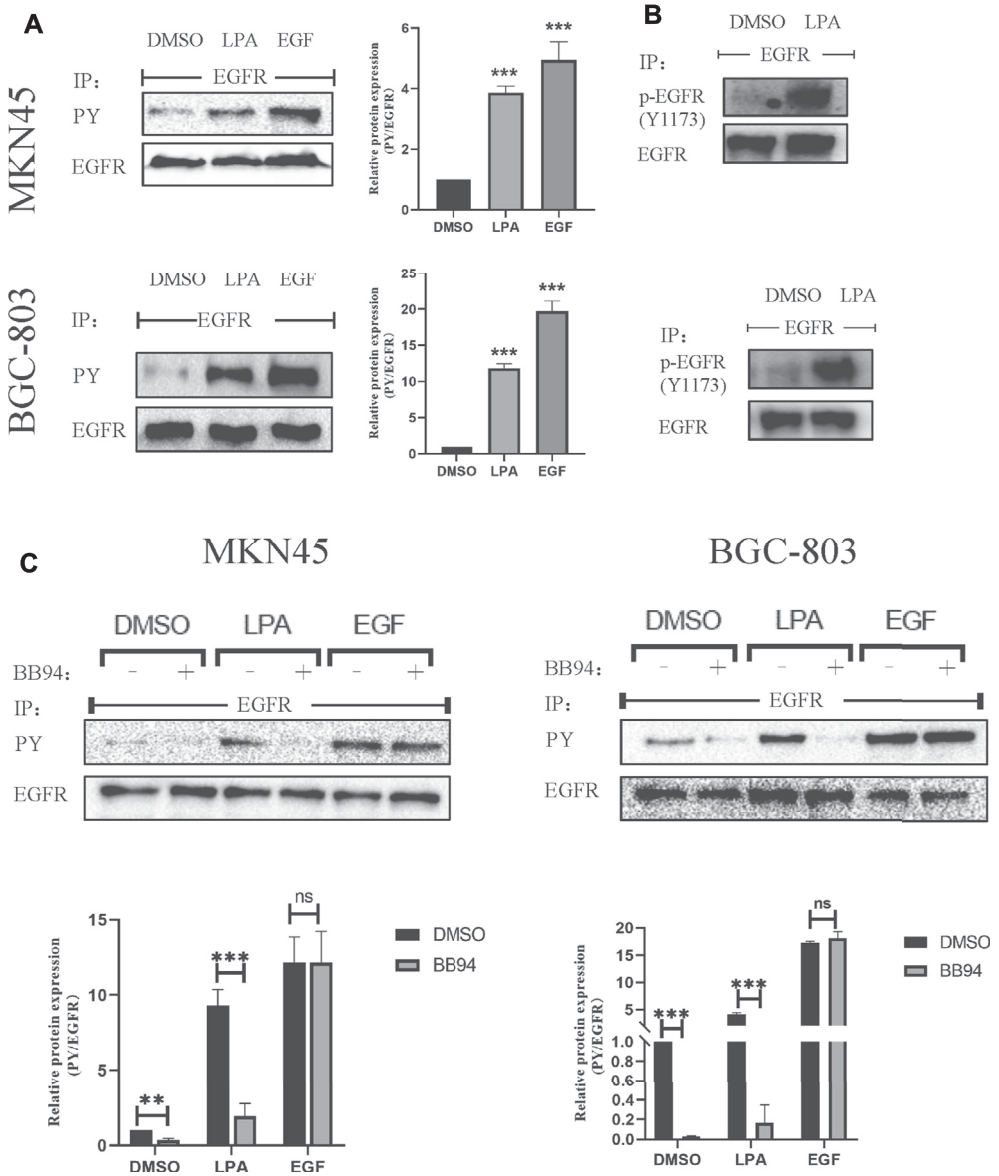

FIGURE 5 | LPA stimulates EGFR transactivation in gastric cancer cells. **(A–B)** Tyrosine-phosphorylated EGFR (**(A)**, PY) and Y1173-phosphorylated EGFR **(B)** level after treated with 0.1% DMSO (vehicle), 10 μM LPA, or 10 ng/ml EGF for 3 min. **(C)** Tyrosine-phosphorylated EGFR levels after pretreated with 0.1% DMSO or 10 μM BB94 for 30 min and stimulated with 10 μM LPA. Densitometry of three independent experiments was performed normalized to tubulin and expressed as a ratio of DMSO; mean ± SD, $^{**}p < 0.01$ (ANOVA test and Dunnette's multiple comparisons test).

DUB3 in gastric cancer cells, which were then treated with cycloheximide to block new protein synthesis, followed by measuring geminin protein levels. DUB3 increased geminin stability compared to that of the control empty vector (**Figures 4A,B**). Conversely, *DUB3* knockdown significantly decreased geminin protein levels in MKN45 and BGC-803 cells (**Figure 4C**).

To investigate the relationship between LPA-induced upregulation of geminin and its deubiquitination by DUB3, we assessed the expression levels of DUB3 protein following LPA stimulation by Western blotting. DUB3 was upregulated in MKN45 and BGC-803 cells, with peak expression 10 min after LPA treatment (**Figure 4D**); meanwhile, geminin protein levels reached a maximum within 1 h (**Figure 3**). Next, the changes of DUB3 and geminin protein expression after the depletion of DUB3 together with LPA stimulation were observed. Indeed, *DUB3* knockdown significantly affected geminin stability (**Figure 4E**). These results suggest that LPA enhances the stability of geminin in gastric cancer cells by inducing its deubiquitination through DUB3.

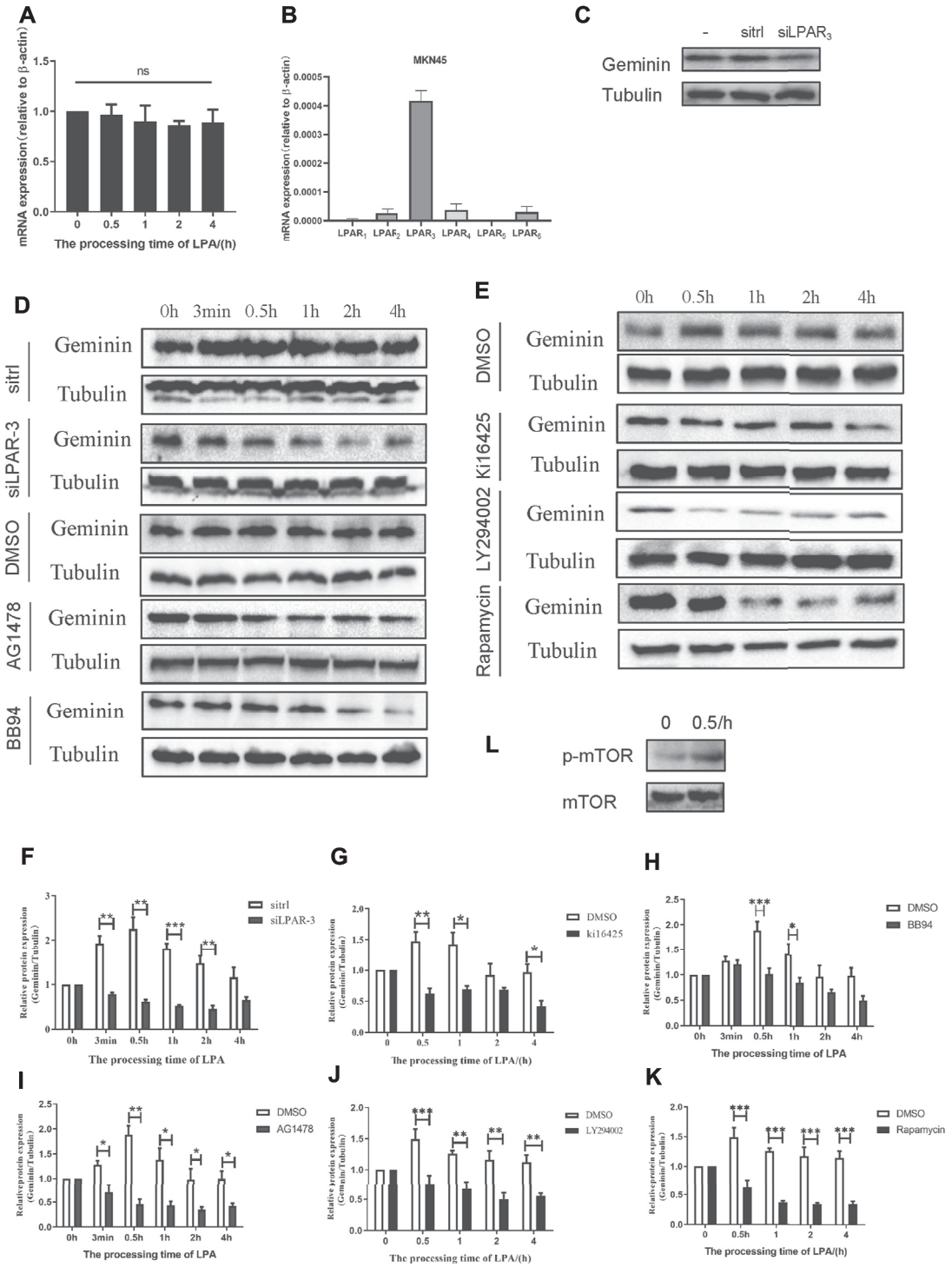

FIGURE 6 | LPA potentiates geminin stability through $LPAR_3/MMP_S$/EGFR/PI3K/mTOR signaling axis in MKN45 cells. **(A)** mRNA expression of geminin under 10 μM LPA time gradient. Densitometry of three independent experiments was performed normalized to actin and expressed as ratio of 0 h; mean ± SD (ANOVA test and Dunnett's multiple comparisons test). **(B)** mRNA expression of LPARI-6 in MKN45 cells. **(C)** Geminin protein levels after transfected with or without sitrl/siLPAR3 for 6 h, and the cells were cultured for another 48 h in the total medium until harvested. **(D–E)** Gemimin protein level after pretreated with DMSO (vehicle, 0.1%), Kil6425 (10 μM), BB94 (10 μM), AG1478 (250 nM), LY294002 (10 μM), or rapamycin (100 nM) for 30 min, and stimulated with 10 μM LPA time gradient. In siRNA-silencing experiments, cells were transfected with either siGL or siGEM for 6 h and then cultured for another 48 h. **(F–K)** Quantification of geminin protein levels in **(D)** and **(E)**. Densitometry of three independent experiments was performed normalized to tubulin and expressed as a ratio of control group; mean ± SD, $^{*}p < 0.05$, $^{**}p < 0.01$, $^{***}p < 0.001$ (ANOVA test and Dunnette's multiple comparisons test). **(L)** Activation level of mTOR and p-mTOR (Ser2448) under 10 μM LPA treatment.

LPA Stimulates EGFR Transactivation *via* an MMP-Dependent Pathway in Gastric Cancer Cells

LPA can induce an intracellular transactivated mechanism, and it is thought to activate GPCR-regulated transmembrane MMPs at the cell surface, leading to EGFR transactivation via a classic autocrine mechanism (Daub et al., 1996; Prenzel et al., 1999). To determine whether LPA is involved in EGFR transactivation in gastric cancer, we first examined the changes in EGFR phosphotyrosine level upon LPA (10 μM) stimulation. In two of the tested gastric cancer cell lines, tyrosine phosphorylation of EGFR was increased in the presence of LPA. In contrast, the vehicle DMSO had little effect, although EGF-induced EGFR autophosphorylation was obviously enhanced (**Figure 5A**). Moreover, LPA treatment increased phosphorylation at Y1173, a well-known transphosphorylation site for EGFR activation (**Figure 5B**). These results provide evidence for the cross-talk linking between GPCR with EGFR signal pathway in gastric cancer cells.

MMPs mediate the cross-talk between GPCR and EGFR in HEK-293 cells (Prenzel et al., 1999) and HNSCCs cells (Gschwind et al., 2002). We therefore examined whether MMPs is involved in LPA-induced EGFR transactivation in MKN45 and BGC-803 cells in the absence or presence of the MMP inhibitor batimastat (BB94). BB94 (10 μM) completely blocked the EGFR transactivation induced by LPA treatment, whereas EGF-induced EGFR autophosphorylation was unaffected (**Figure 5C**). In addition, BB94 also affected the basic EGFR autophosphorylation in gastric cancer, perhaps by modulating the activity of basic EGFR ligand (**Figure 5C**). These results indicate that LPA induces EGFR transactivation in gastric cancer via an MMP-dependent mechanism.

LPA Potentiates Geminin Stability *via* the LPAR3/MMPs/EGFR/PI3K/mTOR Signaling

We showed that LPA treatment increased geminin protein levels in gastric cancer cells during the S phase. To elucidate the signaling pathway(s) involved, we examined the mRNA level of *GMNN* under the time gradient treatment of LPA by qRT-PCR. Unlike the effect on geminin protein level, *GMNN* transcript level was not altered by LPA treatment in MKN45 cells (**Figure 6A**) and BGC-803 cells (**Supplementary Figure 3A**).

Of the six LPARs, LPAR1, LPAR2, and LPAR3 are most widely studied. To identify the LPAR(s) involved in LPA-induced EGFR transactivation in gastric cancer, we evaluated the mRNA levels of various LPARs by qRT-PCR and found that LPAR3 was more highly expressed than the others (**Figure 6B**; **Supplementary Figure 3B**). Knockdown of *LPAR3* reduced the protein level of geminin that was increased by LPA treatment (**Figures 6D,F**), whereas no change in geminin expression was observed in gastric cancer cells that were transfected with a control siRNA (sitrl) or siLPAR3 in the absence of LPA (**Figure 6C**). To confirm the role of LPAR3 in LPA-meditated geminin upregulation, we evaluated geminin protein levels in gastric cancer cells treated with the LPAR1/3 inhibitor Ki16425 by Western blotting. Ki16425 (10 μM) completely abrogated the increase in geminin protein expression induced by LPA in MKN45 cells (**Figures 6E,G**) and BGC-803 cells (**Supplementary Figures 3C,D**), whereas the vehicle DMSO (0.1%) had no effect, indicating that LPA regulates geminin stability through LPAR3.

To investigate the relationship between the stabilization of geminin and EGFR transactivation induced by LPA, we measured geminin protein levels in cells treated with DMSO, the MMP inhibitor BB94 (10 μM), or the EGFR inhibitor AG1478 (250 nM) by Western blotting. Gastric cancer cells were synchronized with serum-free medium for 24 h and then pretreated with a vehicle or inhibitors for 30 min before treatment with LPA (10 μM) for different times. Inhibitors treatment completely abrogated the upregulation of geminin protein under LPA stimulation in MKN45 cells (**Figures 6D,H,I**) and BGC-803 cells (**Supplementary Figures 3C,E,F**), while DMSO had no effect, indicating that LPA regulates geminin stability via EGFR transactivation signal pathway.

GPCR-induced EGFR transactivation is known to activate the Ras-MAPK pathway in some cell lines, including GT1-7, COS-7, and HEK-293 cells (Shah et al., 2003). However, inhibiting MAPK signaling using MAPK kinase (MEK) or extracellular signal-regulated kinase (ERK) inhibitors did not attenuate LPA-induced geminin upregulation (data not shown). We investigated the downstream factor(s) of EGFR involved in LPA-mediated geminin stabilization, and found that in both MKN45 and BGC-803 cells LPA treatment increased Phospho-mTOR (Ser2448) level (**Figure 6L**; **Supplementary Figure 3I**). Moreover, the PI3K inhibitor LY294002 (10 μM) and mTOR inhibitor Rapamycin (100 nM) notably eliminated the upregulation of geminin protein stimulated with LPA in MKN45 cells (**Figures 6E,J,K**) and BGC-803 cells (**Supplementary Figures 3C,G,H**), whereas DMSO had no effect. Thus, LPA enhances geminin stability *via* the LPAR3/MMPs/EGFR/PI3K/mTOR signaling axis in gastric cancer.

LPA Mediates S-Phase Cell-Cycle Progression *via* the $LPAR_3$/MMPs/EGFR/PI3K/mTOR Signaling

Cell cycle–related proteins other than geminin such as cell division cycle (Cdc)6, Cdt1, minichromosome maintenance complex component (Mcm)2, Mcm7, and Mcm10 did not respond to LPA stimulation in preliminary experiment (data not shown); however, the expression of the cell cycle–related protein P27 was upregulated (**Figure 7C**; **Supplementary Figure 4C**). Given our observation, LPA stabilized geminin via the LPAR3/MMPs/EGFR/PI3K/mTOR signaling axis in gastric cancer cells, we examined whether this pathway modulated cell-cycle progression. Gastric cancer cells were synchronized with serum-free medium for 24 h, and G1/S–arrested cells were pretreated with vehicle or inhibitor as described above for 30 min and then stimulated with LPA (10 μM) in a time gradient. The cells harvested and stained with PI and DNA

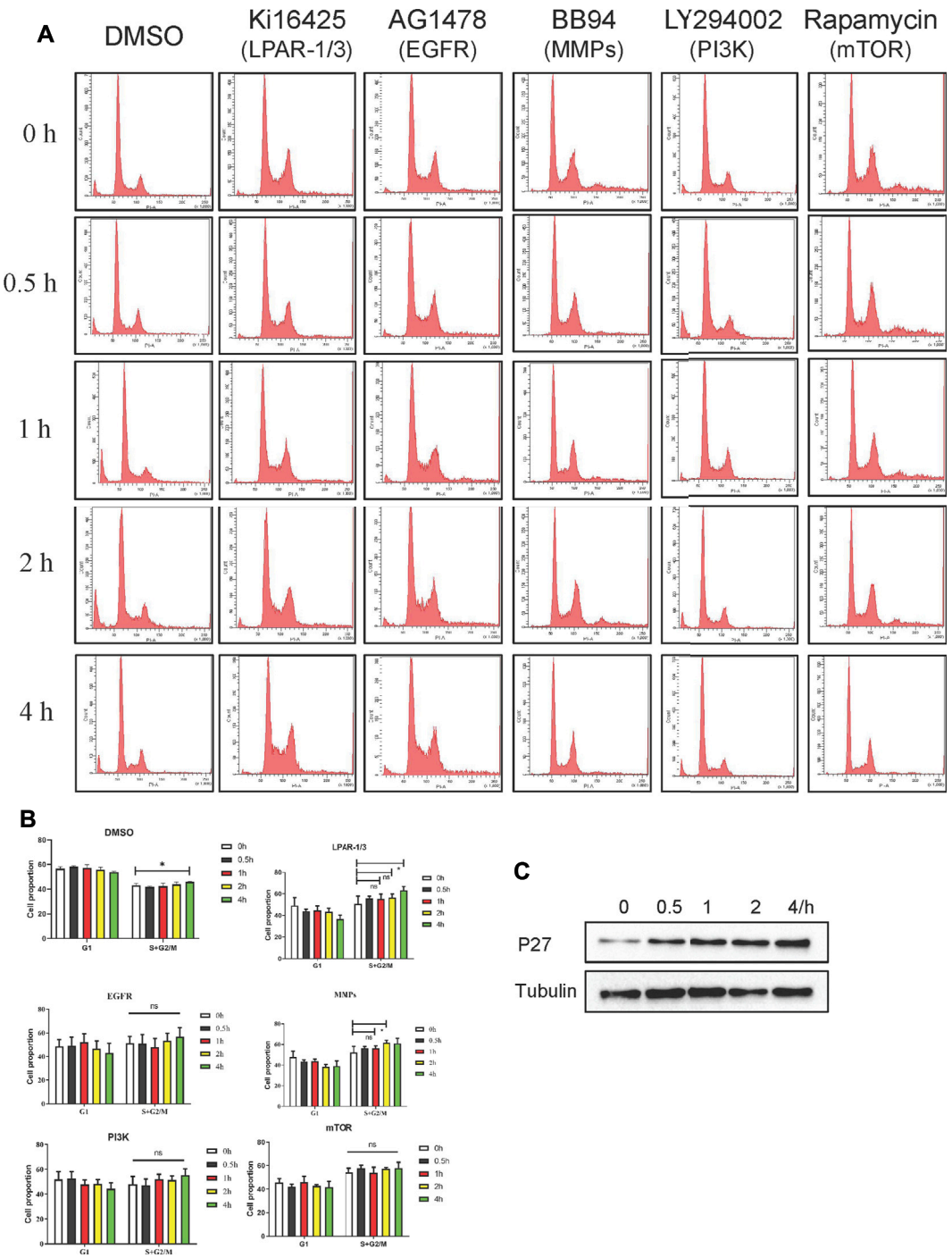

FIGURE 7 | LPA induces S phase cell-cycle progression through $LPAR_3$/MMP_S/EGFR/PI3K/mTOR signaling axis in MKN45 cells. **(A)** Quiescent cells were pretreated with DMSO (vehicle 0.1%), Kil6425 (10 μM), BB94 (10 μM), AG1478 (250 nM), LY294002 (10 μM), or rapamycin (100 nM) for 30 min and stimulated with 10 μM LPA up to 4 h. After the treatment, the cells were harvested and stained with PI to analyze the quality of DNA content by FACS analysis. **(B)** Qualification of DNA content in **(A)**, mean ± SD, $n = 3$. *$p < 0.05$, ANOVA test and Dunette's multiple comparisons test were used for data analysis. **(C)** Expression of p27 after LPA time grade stimulation.

content were quantified by flow cytometry. In both MKN45 and BGC-803 cells, inhibitor treatment did not alter the S and G2/M phase fractions compared to the cells treated with DMSO (**Figures 7A,B**; **Supplementary Figures 4A,B**). Thus, LPA promotes S-phase cell-cycle progression in gastric cancer cells via the LPAR3/MMPs/EGFR/PI3K/mTOR signaling axis.

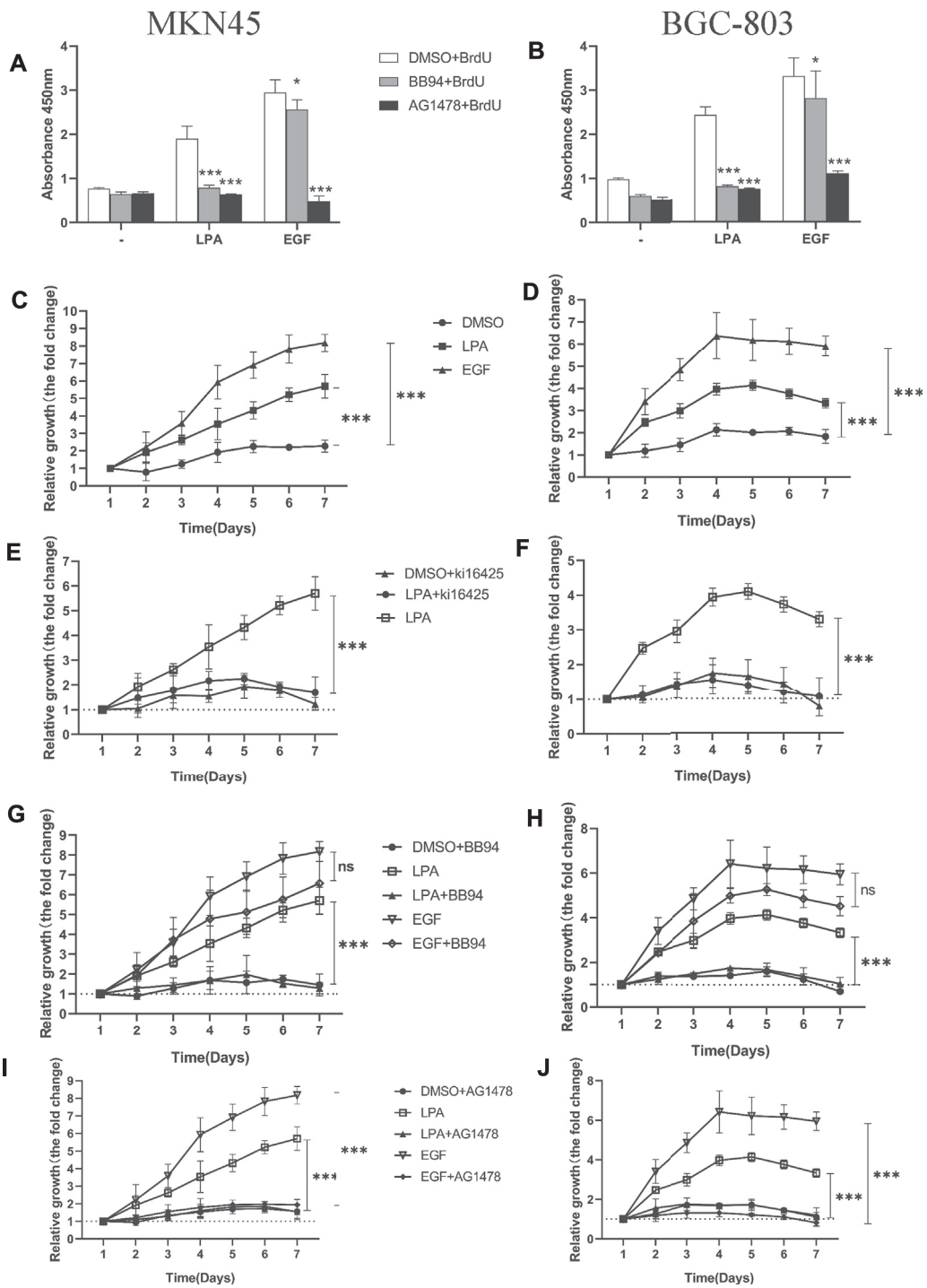

FIGURE 8 | Kil6425, BB94, and AG1478 inhibit LPA-induced efficient DNA synthesis and cell proliferation in gastric cancer cells. **(A–B)** LPA-induced efficient DNA synthesis after pretreated with inhibitors for 30 min and grown in the ligands (0.1% DMSO, 10 μM LPA, or 10 ng/ml EGF) for 4 days. **(C–D)** Cell proliferation of gastric cancer cells with ligands. **(E–J)** Cell proliferation of gastric cancer cells after pretreated with inhibitors for 30 min and grown in the ligand. In qualifications, the cell growth were calculated using GraphPad Prism v8.0 software at each time point, and the fold is compared relative to the level at 1 day, respectively, mean ± SD, n=3, $^{*}p < 0.05$, $^{***}p < 0.001$ (ANOVA test and Dunnette's multiple comparisons test).

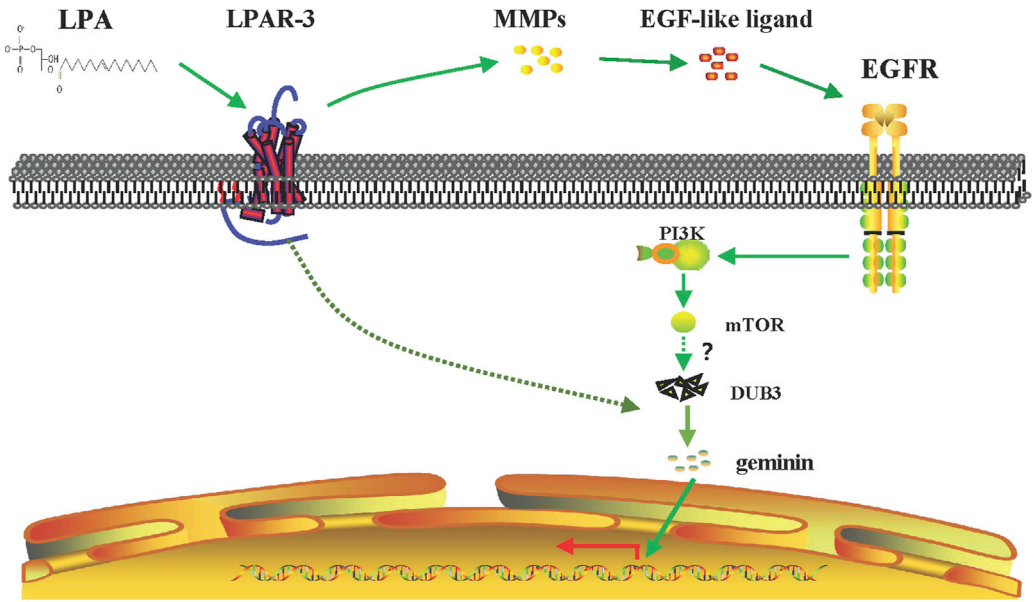

FIGURE 9 | Signaling pathway of LPA-mediated DNA replication initiation. LPA work through $LPAR_3$ to transactive EGFR by MMPs and to increase the expression of geminin protein level in the S phase through PI3K/mTOR signaling pathway. Meanwhile, LPA stimulation induces upregulation of DUB3 in a short time, inhibiting the ubiquitination degradation of geminin protein and enhancing its stability, and then positively regulating the DNA replication initiation of gastric cancer cells.

MMPs-Dependent Tansactivation of EGFR is Critical for LPA-Induced Efficient DNA Synthesis and Cell Proliferation in Gastric Cancer Cells

To quantify the efficiency of DNA synthesis in response to LPA stimulation, we evaluated the ratio of DNA synthesis by measuring BrdU incorporation using ELISA assay. In both MKN45 and BGC-803 cells, BB94 and AG1478 notably abrogated DNA synthesis induced by LPA, respectively (**Figures 8A,B**). Furthermore, AG1478 notably eliminated DNA synthesis upon exogenous EGF stimulation (**Figures 8A,B**). It is surprising to observe that BB94 also reduced DNA synthesis induced by exogenous EGF in gastric cancer cells. This suggested that exogenous EGF stimulation may result in enhancing the shedding of endogenous EGFR ligands in gastric cancer as observed in HNSCCs (Gschwind et al., 2002; O-charoenrat et al., 2001). Taken together, these data strongly indicate that LPA-induced efficient DNA synthesis is dependent on metalloprotease function in gastric cancer.

An increase in cell proliferation is another hallmark of tumorigenesis. We investigated whether MMPs or EGFR inhibition influences LPA-induced efficient cell proliferation in gastric cancer cells with the CCK-8 assay. Treatment with LPA or EGF enhanced efficient cell proliferation in MKN45 (**Figure 8C**) and BGC-803 cells (**Figure 8D**); this was blocked by the LPAR1/3 inhibitor Ki16425 (**Figures 8E,F**) and by BB94 (**Figures 8G,H**) and AG1478 (**Figures 8I,J**). Notably, BB94 had no effect in EGF-induced cell proliferation (**Figures 8G,H**). These results demonstrate that LPAR3, MMPs, and EGFR activities are required for LPA-induced efficient DNA synthesis and cell proliferation in gastric cancer.

DISCUSSION

In this study, we showed that geminin mutations are not widespread in human cancers, consistent with its function as a regulatory protein. Depletion of geminin selectively induced DNA re-replication in gastric cancer cells but not in normal gastric epithelial cells, whereas LPA treatment induced the upregulation of geminin protein in the S phase in gastric cancer cells. Notably, LPA stimulated EGFR transactivation via an MMPs-dependent mechanism in gastric cancer, which was partly responsible for enhancing geminin stability in the S phase and promoting DNA replication. On the other hand, LPA also induced the rapid upregulation of DUB3; thereby, indirectly stabilizing geminin by preventing its degradation. These data indicate that the cross-talk between LPA and EGFR signaling regulates DNA replication by stabilizing geminin level in the S phase to promote gastric cancer progression (**Figure 9**).

The survival of tumor cells depends on their interaction with components of the TME including ECM, surrounding vasculature, other non-malignant cells, and signaling molecules (Quail and Joyce, 2013). Perturbation of the TME promotes cancer cell transformation and invasion of other tissues, facilitating cancer progression (Roy and Walsh, 2014). Many cancers are characterized by overexpression of LPA, which is also present in the ECM (Nouh et al., 2009). There is increasing evidence that LPA is an important factor in the TME which promotes tumor growth, migration, invasion, metastasis, and angiogenesis. LPA was found to stimulate cell migration and invasion

mainly via LPAR1-3 (Shida et al., 2008; Ren et al., 2019); however, the role of LPA/LPARs in DNA replication has not been reported. Here, we show for the first time that LPA promotes DNA replication by up-regulating geminin protein in gastric cancer cells. As an oncogene, geminin is overexpressed in tumors, which is linked to the prognosis of colon, rectal, and breast cancers (Montanari et al., 2005; Hernández-Pérez et al., 2017; Zhang et al., 2017). The expression of geminin is cell cycle–dependent, and the protein is synthesized during the S phase with a half-life of 3–4 h (Kulartz et al., 2003). We demonstrated that LPA treatment increased geminin expression in the S phase in gastric cancer cells. This effect depends on cellular context, as LPA was shown to induce the upregulation of geminin in gastric and ovarian cancer cells but not in breast cancer cell line MCF-7 that frequently overexpress the protein (data not shown), although the reasons for this difference are not clear. Deregulation of geminin has been reported in different human cancers and is associated with DNA replication and metastasis (Hernández-Pérez et al., 2017; Zhang et al., 2017). Our data establish a novel link between geminin-regulated DNA replication and tumor progression; an elevated level of LPA in the TME of gastric cancer cells enhanced the stability of geminin in the S phase, which promoted rapid DNA replication and tumor progression.

Identifying patient subpopulations that would benefit from a personalizing targeted therapeutic regimen is important for improving clinical outcomes. Mutations in specific genes can alter the proliferative potential of tumor cells. Although we found that mutations or deletions of the *GMNN* gene were not prevalent in human cancers, the R54Q mutation in geminin protein was detected at a high frequency, and other potentially significant sites that may be phosphorylated under different circumstances are Thr25, S32, S60 (Tsunematsu et al., 2013) S45, and S49 (Kulartz et al., 2003), although the physiologic relevance of these modifications remains to be determined.

Mutations in replication factors are rare in cancer; tumor cells have adopted other strategies to alter the levels of replication factors to induce replicative stress. Geminin is downregulated in G0/G1 phases by APC/C E3 ubiquitin ligase (McGarry and Kirschner, 1998) in association with polycomb group complex 1 and the RDCOX complex (containing Scmh1Hoxb4/Hoxa9), which are associated with E3 ubiquitin ligase core complex Roc1/Ddb1/Cul4a (Ohno et al., 2013). Recent study certifies that DUB3 and USP7 were shown to control geminin protein stability in breast cancer (Hernández-Pérez et al., 2017); our results demonstrate that DUB3 also regulates geminin protein stability in gastric cancer.

Activation or inhibition of protein tyrosine phosphorylation signaling networks can lead to consequent changes in gene transcription and translation. We identified a novel signaling axis that modulates geminin expression through LPA-induced EGFR (Y1173) transactivation in gastric cancer cells. EGFR initiates a signaling cascade that leads to DNA synthesis and cell proliferation; and EGFR and PI3K initiate malignant transformation of cancer cells by activating other pathways such as Myc and Rb-E2F, which in turn leads to the formation of cyclinD/Cdk4 and cyclinE/Cdk2 complexes (Read et al., 2009). In the early S phase, Cdk2 phosphorylates c-Myc and promotes its association with the promoter of miR-571, thereby inhibiting its expression. miR-571 targets *GMNN* mRNA, and its downregulation is associated with the accumulation of geminin protein (Zhang et al., 2019). This may elucidate one possible signaling event downstream of LPA-induced geminin upregulation. Aurora-A phosphorylates geminin on Thr25 to protect it from APC/C-dependent proteolysis during the early M phase, and the binding of geminin to Cdt1 protects the latter from ubiquitylation and proteolysis (Tsunematsu et al., 2013). We investigated whether LPA stimulation leads to geminin phosphorylation, but were unable to identify the phosphorylation site by mass spectrometry analysis (data not shown). Further studies are needed to identify the kinase acting downstream of EGFR that phosphorylates and thereby stabilizes geminin.

GPCR and EGFR are two pivotal families of drug targets, given that GPCR-induced transactivation of EGFR has been linked to cancer development (Köse, 2017), through the activation of MAPK signaling, stimulation of cell migration, and regulation of cell-cycle progression. We provided evidence that LPA-induced EGFR transactivation in gastric cancer cells promoted efficient DNA synthesis, cell-cycle progression through the S phase, and cell proliferation. Based on these findings, disrupting the cross-talk between the two receptors might be a potential therapeutic strategy for the treatment of gastric cancer.

DATA AVAILABILITY STATEMENT

The raw data supporting the conclusions of this article will be made available by the authors, without undue reservation.

AUTHOR CONTRIBUTIONS

HZ, GE, XT, and PJ were responsible for conducting experiments, acquisition of data, and analysis. HZ carried out Western blotting analysis and molecular biological studies *in vitro*. XT performed the statistical analysis and some functional experiments. PJ provided technical and material support for immunofluorescent staining and some functional experiments. LF and MO were responsible for designing the experiments, research supervision, and drafted the article. All authors read and approved the final article.

FUNDING

This work was supported by grants from the National Natural Science Foundation of China (NSFC Grant no. 31960162 to LF), the Program for Young Talents of Science and Technology in Universities of Inner Mongolia Autonomous Region (Grant no. NJYT-17-B03 to LF), and the Natural Science Foundation of Inner Mongolia (Grant no. 2017MS0331 to LF).

SUPPLEMENTARY MATERIAL

The Supplementary Material for this article can be found online at: https://www.frontiersin.org/articles/10.3389/fphar.2021.706240/full#supplementary-material

REFERENCES

Alaeddini, M., and Etemad-Moghadam, S. (2020). Cell Kinetic Markers in Cutaneous Squamous and Basal Cell Carcinoma of the Head and Neck. *Braz. J. Otorhinolaryngol* doi:10.1016/j.bjorl.2020.07.010

Alsahafi, E. N., Thavaraj, S., Sarvestani, N., Novoplansky, O., Elkabets, M., Ayaz, B., et al. (2020). EGFR Overexpression Increases Radiotherapy Response in HPV-Positive Head and Neck Cancer through Inhibition of DNA Damage Repair and HPV E6 Downregulation. *Cancer Lett.* 498, 80–97. doi:10.1016/j.canlet.2020.10.035

Ballabeni, A., Melixetian, M., Zamponi, R., Masiero, L., Marinoni, F., and Helin, K. (2004). Human Geminin Promotes Pre-RC Formation and DNA Replication by Stabilizing CDT1 in Mitosis. *EMBO J.* 23, 3122–3132. doi:10.1038/sj.emboj.7600314

Ballabeni, A., Zamponi, R., Moore, J. K., Helin, K., and Kirschner, M. W. (2013). Geminin Deploys Multiple Mechanisms to Regulate Cdt1 before Cell Division Thus Ensuring the Proper Execution of DNA Replication. *Proc. Natl. Acad. Sci. U S A.* 110, E2848–E2853. doi:10.1073/pnas.1310677110

Champeris Tsaniras, S., Villiou, M., Giannou, A. D., Nikou, S., Petropoulos, M., Pateras, I. S., et al. (2018). Geminin Ablation *In Vivo* Enhances Tumorigenesis through Increased Genomic Instability. *J. Pathol.* 246, 134–140. doi:10.1002/path.5128

Daub, H., Weiss, F. U., Wallasch, C., and Ullrich, A. (1996). Role of Transactivation of the EGF Receptor in Signalling by G-Protein-Coupled Receptors. *Nature* 379, 557–560. doi:10.1038/379557a0

Deng, W., Poppleton, H., Yasuda, S., Makarova, N., Shinozuka, Y., Wang, D. A., et al. (2004). Optimal Lysophosphatidic Acid-Induced DNA Synthesis and Cell Migration but Not Survival Require Intact Autophosphorylation Sites of the Epidermal Growth Factor Receptor. *J. Biol. Chem.* 279, 47871–47880. doi:10.1074/jbc.M405443200

Diffley, J. F. (2011). Quality Control in the Initiation of Eukaryotic DNA Replication. *Philos. Trans. R. Soc. Lond. B Biol. Sci.* 366, 3545–3553. doi:10.1098/rstb.2011.0073

Emmett, L. S., and O'Shea, K. S. (2012). Geminin Is Required for Epithelial to Mesenchymal Transition at Gastrulation. *Stem Cell Dev* 21, 2395–2409. doi:10.1089/scd.2011.0483

Gonzalez, M. A., Tachibana, K. E., Chin, S. F., Callagy, G., Madine, M. A., Vowler, S. L., et al. (2004). Geminin Predicts Adverse Clinical Outcome in Breast Cancer by Reflecting Cell-Cycle Progression. *J. Pathol.* 204, 121–130. doi:10.1002/path.1625

Gschwind, A., Hart, S., Fischer, O. M., and Ullrich, A. (2003). TACE Cleavage of Proamphiregulin Regulates GPCR-Induced Proliferation and Motility of Cancer Cells. *EMBO J.* 22, 2411–2421. doi:10.1093/emboj/cdg231

Gschwind, A., Prenzel, N., and Ullrich, A. (2002). Lysophosphatidic Acid-Induced Squamous Cell Carcinoma Cell Proliferation and Motility Involves Epidermal Growth Factor Receptor Signal Transactivation. *Cancer Res.* 62, 6329–6336.

Guo, L., He, P., No, Y. R., and Yun, C. C. (2015). Krüppel-like Factor 5 Incorporates into the β-catenin/TCF Complex in Response to LPA in colon Cancer Cells. *Cell Signal* 27, 961–968. doi:10.1016/j.cellsig.2015.02.005

Hernández-Pérez, S., Cabrera, E., Salido, E., Lim, M., Reid, L., Lakhani, S. R., et al. (2017). DUB3 and USP7 De-ubiquitinating Enzymes Control Replication Inhibitor Geminin: Molecular Characterization and Associations with Breast Cancer. *Oncogene* 36, 4817. doi:10.1038/onc.2017.220

Hills, S. A., and Diffley, J. F. (2014). DNA Replication and Oncogene-Induced Replicative Stress. *Curr. Biol.* 24, R435–R444. doi:10.1016/j.cub.2014.04.012

Kalmes, A., Vesti, B. R., Daum, G., Abraham, J. A., and Clowes, A. W. (2000). Heparin Blockade of Thrombin-Induced Smooth Muscle Cell Migration Involves Inhibition of Epidermal Growth Factor (EGF) Receptor Transactivation by Heparin-Binding EGF-like Growth Factor. *Circ. Res.* 87, 92–98. doi:10.1161/01.RES.87.2.92

Köse, M. (2017). GPCRs and EGFR - Cross-Talk of Membrane Receptors in Cancer. *Bioorg. Med. Chem. Lett.* 27, 3611–3620. doi:10.1016/j.bmcl.2017.07.002

Kulartz, M., Kreitz, S., Hiller, E., Damoc, E. C., Przybylski, M., and Knippers, R. (2003). Expression and Phosphorylation of the Replication Regulator Protein Geminin. *Biochem. Biophys. Res. Commun.* 305, 412–420. doi:10.1016/S0006-291X(03)00773-3

Leblanc, R., and Peyruchaud, O. (2016). Metastasis: New Functional Implications of Platelets and Megakaryocytes. *Blood* 128 (1), 24–31. doi:10.1182/blood-2016-01-636399

Lee, S. C., Fujiwara, Y., and Tigyi, G. J. (2015). Uncovering Unique Roles of LPA Receptors in the Tumor Microenvironment. *Receptors Clin. Investig.* 2. doi:10.14800/rci.440

Lewis, M., and Stracker, T. H. (2021). Transcriptional Regulation of Multiciliated Cell Differentiation. *Semin. Cel Developmental Biol.* 110, 51–60. doi:10.1016/j.semcdb.2020.04.007

Machida, Y. J., Hamlin, J. L., and Dutta, A. (2005). Right Place, Right Time, and Only once: Replication Initiation in Metazoans. *Cell* 123, 13–24. doi:10.1016/j.cell.2005.09.019

McGarry, T. J., and Kirschner, M. W. (1998). Geminin, an Inhibitor of DNA Replication, Is Degraded During Mitosis. *Cell.* 93 (6), 1043–1053. doi:10.1016/s0092-8674(00)81209-x

Mills, G. B., and Moolenaar, W. H. (2003). The Emerging Role of Lysophosphatidic Acid in Cancer. *Nat. Rev. Cancer* 3, 582–591. doi:10.1038/nrc1143

Miotto, B., and Struhl, K. (2010). HBO1 Histone Acetylase Activity Is Essential for DNA Replication Licensing and Inhibited by Geminin. *Mol. Cel* 37, 57–66. doi:10.1016/j.molcel.2009.12.012

Montanari, M., Boninsegna, A., Faraglia, B., Coco, C., Giordano, A., Cittadini, A., and Sgambato, A. (2005). Increased Expression of Geminin Stimulates the Growth of Mammary Epithelial Cells and is a Frequent Event in Human Tumors. *J. Cell. Physiol.* 202, 215–222. doi:10.1002/jcp.20120

Mori, K., Kitayama, J., Aoki, J., Kishi, Y., Shida, D., Yamashita, H., et al. (2007). Submucosal Connective Tissue-type Mast Cells Contribute to the Production of Lysophosphatidic Acid (LPA) in the Gastrointestinal Tract through the Secretion of Autotaxin (ATX)/lysophospholipase D (lysoPLD). *Virchows Arch.* 451, 47–56. doi:10.1007/s00428-007-0425-4

Murray, D., Horgan, G., Macmathuna, P., and Doran, P. (2008). NET1-mediated RhoA Activation Facilitates Lysophosphatidic Acid-Induced Cell Migration and Invasion in Gastric Cancer. *Br. J. Cancer* 99, 1322–1329. doi:10.1038/sj.bjc.6604688

Nouh, M. A., Wu, X. X., Okazoe, H., Tsunemori, H., Haba, R., Abou-Zeid, A. M., et al. (2009). Expression of Autotaxin and Acylglycerol Kinase in Prostate Cancer: Association with Cancer Development and Progression. *Cancer Sci.* 100, 1631–1638. doi:10.1111/j.1349-7006.2009.01234.x

O-Charoenrat, P., Rhys-Evans, P. H., and Eccles, S. A. (2001). Expression of Matrix Metalloproteinases and Their Inhibitors Correlates with Invasion and Metastasis in Squamous Cell Carcinoma of the Head and Neck. *Arch. Otolaryngol.-Head Neck Surg.* 127 (7), 813–820.

Ohno, H., Shinoda, K., Ohyama, K., Sharp, L. Z., Kajimura, S., et al. (2013). EHMT1 Controls Brown Adipose Cell Fate and Thermogenesis Through the PRDM16 Complex. *Nature* 504, 163–167. doi:10.1038/nature12652

Petropoulou, C., Kotantaki, P., Karamitros, D., and Taraviras, S. (2008). Cdt1 and Geminin in Cancer: Markers or Triggers of Malignant Transformation? *Front. Biosci.* 13, 4485–4494. doi:10.2741/3018

Prenzel, N., Zwick, E., Daub, H., Leserer, M., Abraham, R., Wallasch, C., et al. (1999). EGF Receptor Transactivation by G-Protein-Coupled Receptors Requires Metalloproteinase Cleavage of proHB-EGF. *Nature* 402, 884–888. doi:10.1038/47260

Quail, D. F., and Joyce, J. A. (2013). Microenvironmental Regulation of Tumor Progression and Metastasis. *Nat. Med.* 19, 1423–1437. doi:10.1038/nm.3394

Ramachandran, S., Shida, D., Nagahashi, M., Fang, X., Milstien, S., Takabe, K., et al. (2010). Lysophosphatidic Acid Stimulates Gastric Cancer Cell Proliferation via ERK1-dependent Upregulation of Sphingosine Kinase 1 Transcription. *FEBS Lett.* 584, 4077–4082. doi:10.1016/j.febslet.2010.08.035

Read, R. D., Cavenee, W. K., Furnari, F. B., and Thomas, J. B. (2009). A drosophila Model for EGFR-Ras and PI3K-dependent Human Glioma. *Plos Genet.* 5, e1000374. doi:10.1371/journal.pgen.1000374

Ren, Z., Zhang, C., Ma, L., Zhang, X., Shi, S., Tang, D., et al. (2019). Lysophosphatidic Acid Induces the Migration and Invasion of SGC-7901 Gastric Cancer Cells through the LPA2 and Notch Signaling Pathways. *Int. J. Mol. Med.* 44, 67–78. doi:10.3892/ijmm.2019.4186

Roy, D. M., and Walsh, L. A. (2014). Candidate Prognostic Markers in Breast Cancer: Focus on Extracellular Proteases and Their Inhibitors. *Breast Cancer (Dove Med. Press.* 6, 81–91. doi:10.2147/BCTT.S46020

Ryan, D., Koziol, J., and ElShamy, W. M. (2019). Targeting AXL and RAGE to Prevent Geminin Overexpression-Induced Triple-Negative Breast Cancer Metastasis. *Sci. Rep.* 9, 19150. doi:10.1038/s41598-019-55702-w

Sato, K., Tanaka, S., Mitsunori, Y., Mogushi, K., Yasen, M., Aihara, A., et al. (2013). Contrast-enhanced Intraoperative Ultrasonography for Vascular Imaging of

Hepatocellular Carcinoma: Clinical and Biological Significance. *Hepatology (Baltimore, Md)* 57, 1436–1447. doi:10.1002/hep.26122

Shah, B. H., Soh, J. W., and Catt, K. J. (2003). Dependence of Gonadotropin-Releasing Hormone-Induced Neuronal MAPK Signaling on Epidermal Growth Factor Receptor Transactivation. *J. Biol. Chem.* 278, 2866–2875. doi:10.1074/jbc.M208783200

Shida, D., Fang, X., Kordula, T., Takabe, K., Lépine, S., Alvarez, S. E., et al. (2008). Cross-talk between LPA1 and Epidermal Growth Factor Receptors Mediates Up-Regulation of Sphingosine Kinase 1 to Promote Gastric Cancer Cell Motility and Invasion. *Cancer Res.* 68, 6569–6577. doi:10.1158/0008-5472.CAN-08-0411

Sukocheva, O. (2006). Estrogen Transactivates egfr via the Sphingosine 1-Phosphate Receptor edg-3: The Role of Sphingosine Kinase-1. *J. Cell Biol.* 173 (2), 301–310. doi:10.1083/jcb.200506033

Sundara Rajan, S., Hanby, A. M., Horgan, K., Thygesen, H. H., and Speirs, V. (2013). The Potential Utility of Geminin as a Predictive Biomarker in Breast Cancer. *Breast Cancer Res. Treat.* 143, 91–98. doi:10.1007/s10549-013-2786-5

Tsunematsu, T., Takihara, Y., Ishimaru, N., Pagano, M., Takata, T., and Kudo, Y. (2013). Aurora-A Controls Pre-replicative Complex Assembly and DNA Replication by Stabilizing Geminin in Mitosis. *Nat. Commun.* 4, 1885. doi:10.1038/ncomms2859

Tveteraas, I. H., Aasrum, M., Brusevold, I. J., Ødegård, J., Christoffersen, T., and Sandnes, D. (2016). Lysophosphatidic Acid Induces Both EGFR-dependent and EGFR-independent Effects on DNA Synthesis and Migration in Pancreatic and Colorectal Carcinoma Cells. *Tumour Biol.* 37, 2519–2526. doi:10.1007/s13277-015-4010-1

Wohlschlegel, J. A., Dwyer, B. T., Dhar, S. K., Cvetic, C., Walter, J. C., and Dutta, A. (2000). Inhibition of Eukaryotic DNA Replication by Geminin Binding to Cdt1. *Science* 290, 2309–2312. doi:10.1126/science.290.5500.2309

Wong, P. G., Glozak, M. A., Cao, T. V., Vaziri, C., Seto, E., and Alexandrow, M. (2010). Chromatin Unfolding by Cdt1 Regulates MCM Loading via Opposing Functions of HBO1 and HDAC11-Geminin. *Cell Cycle* 9, 4351–4363. doi:10.4161/cc.9.21.13596

Wu, T., and Dai, Y. (2017). Tumor Microenvironment and Therapeutic Response. *Cancer Lett.* 387, 61–68. doi:10.1016/j.canlet.2016.01.043

Yagi, T., Inoue, N., Yanai, A., Murase, K., Imamura, M., Miyagawa, Y., et al. (2014). Prognostic Significance of Geminin Expression Levels in Ki67-High Subset of Estrogen Receptor-Positive and HER2-Negative Breast Cancers. *Breast Cancer (Tokyo, Japan)* 23, 224–230. doi:10.1007/s12282-014-0556-9

Zeng, R., Li, B., Huang, J., Zhong, M., Li, L., Duan, C., et al. (2017). Lysophosphatidic Acid Is a Biomarker for Peritoneal Carcinomatosis of Gastric Cancer and Correlates with Poor Prognosis. *Genet. Test. Mol. Biomarkers* 21, 641–648. doi:10.1089/gtmb.2017.0060

Zhang, L., Cai, M., Gong, Z., Zhang, B., Li, Y., Guan, L., et al. (2017). Geminin Facilitates FoxO3 Deacetylation to Promote Breast Cancer Cell Metastasis. *J. Clin. Invest.* 127, 2159–2175. doi:10.1172/JCI90077

Zhang, Y., Li, Z., Hao, Q., Tan, W., Sun, J., Li, J., et al. (2019). The Cdk2-C-Myc-miR-571 Axis Regulates DNA Replication and Genomic Stability by Targeting Geminin. *Cancer Res. 0020.2019* 79, 4896–4910. doi:10.1158/0008-5472.CAN-19-0020

Zhou, Y., Pozo, P. N., Oh, S., Stone, H. M., and Cook, J. G. (2020). Distinct and Sequential Re-replication Barriers Ensure Precise Genome Duplication. *Plos Genet.* 16, e1008988. doi:10.1371/journal.pgen.1008988

Zhu, W., Chen, Y., and Dutta, A. (2004). Rereplication by Depletion of Geminin Is Seen Regardless of P53 Status and Activates a G2/M Checkpoint. *Mol. Cel Biol* 24, 7140–7150. doi:10.1128/MCB.24.16.7140-7150.2004

Zhu, W., and Depamphilis, M. L. (2009). Selective Killing of Cancer Cells by Suppression of Geminin Activity. *Cancer Res.* 69, 4870–4877. doi:10.1158/0008-5472.CAN-08-4559

Conflict of Interest: The authors declare that the research was conducted in the absence of any commercial or financial relationships that could be construed as a potential conflict of interest.

Publisher's Note: All claims expressed in this article are solely those of the authors and do not necessarily represent those of their affiliated organizations, or those of the publisher, the editors and the reviewers. Any product that may be evaluated in this article, or claim that may be made by its manufacturer, is not guaranteed or endorsed by the publisher.

frontiers in Pharmacology

ORIGINAL RESEARCH
published: 27 October 2021
doi: 10.3389/fphar.2021.723729

Ilicicolin A Exerts Antitumor Effect in Castration-Resistant Prostate Cancer Via Suppressing EZH2 Signaling Pathway

Lang Guo[1†], Xiaowei Luo[2†], Ping Yang[3†], Yanting Zhang[2], Jialuo Huang[4], Hong Wang[4], Yinfeng Guo[4], Weifeng Huang[4], Zhiqiang Chen[1], Shusheng Wang[1], Junjian Wang[5], Jinping Lei[4], Songtao Xiang[1]* and Yonghong Liu[2,6]**

[1]Department of Urology, The Second Affiliated Hospital of Guangzhou University of Chinese Medicine, Second Clinical Medical College, Guangzhou University of Chinese Medicine, Guangzhou, China, [2]Institute of Marine Drugs/Guangxi Key Laboratory of Marine Drugs, Guangxi University of Chinese Medicine, Nanning, China, [3]Department of Pathology, Sun Yat-sen University Cancer Center, State Key Laboratory of Oncology in South China; Collaborative Innovation Center for Cancer Medicine, Guangzhou, China, [4]School of Pharmaceutical Sciences, Sun Yat-sen University, Guangzhou, China, [5]Guangdong Provincial Key Laboratory of New Drug Design and Evaluation, School of Pharmaceutical Sciences, Sun Yat-sen University, Guangzhou, China, [6]CAS Key Laboratory of Tropical Marine Bio-resources and Ecology/Guangdong Key Laboratory of Marine Materia Medica, South China Sea Institute of Oceanology, Chinese Academy of Sciences, Guangzhou, China

OPEN ACCESS

Edited by:
Zhi Shi,
Jinan University, China

Reviewed by:
Dinglan Wu,
Southern Medical University, China
Min Huang,
Shanghai Institute of Materia Medica (CAS), China

***Correspondence:**
Jinping Lei
leijp@mail.sysu.edu.cn
Songtao Xiang
tonyxst@gzucm.edu.cn
Yonghong Liu
yonghongliu@scsio.ac.cn

[†]These authors have contributed equally to this work

Specialty section:
This article was submitted to Experimental Pharmacology and Drug Discovery, a section of the journal Frontiers in Pharmacology

Received: *11 June 2021*
Accepted: *13 October 2021*
Published: *27 October 2021*

Citation:
Guo L, Luo X, Yang P, Zhang Y, Huang J, Wang H, Guo Y, Huang W, Chen Z, Wang S, Wang J, Lei J, Xiang S and Liu Y (2021) Ilicicolin A Exerts Antitumor Effect in Castration-Resistant Prostate Cancer Via Suppressing EZH2 Signaling Pathway. Front. Pharmacol. 12:723729. doi: 10.3389/fphar.2021.723729

The Polycomb protein enhancer of zeste homolog 2 (EZH2) has critical roles in prostate cancer (PCa) progression and drug-resistance, which remains an obstacle for PCa treatment. Enzalutamide (ENZ) is a second-generation androgen receptor antagonist employed for treatment of metastatic castration-resistant prostate cancer A considerable proportion of tumors eventually develop resistance during treatment. Thus, agents that can overcome resistance to PCa are needed urgently. Ilicicolin A (Ili-A), an ascochlorin derivative isolated from the coral-derived fungus *Acremonium sclerotigenum* GXIMD 02501, shows antiproliferative activity in human PCa cells, but its mechanism of action against Castration-resistant prostate cancer is not known. Herein, RNA-sequencing showed the EZH2 pathway to be involved in PCa proliferation. Ili-A at low doses reduced the protein level of EZH2, leading to transcriptional change. Interestingly, Ili-A suppressed the binding of EZH2 to promoter regions in AR/serine/threonine polo-like kinase-1/aurora kinase A. Moreover, Ili-A could enhance the anticancer activity of enzalutamide in CRPC cancer models. These data suggest that Ili-A could be used in combination with enzalutamide to treat CRPC.

Keywords: ascochlorin derivatives, enhancer of zeste homolog 2, enzalutamide, castration-resistant prostate cancer (CRPC), androgen receptor

INTRODUCTION

Cancer of the prostate gland, known commonly as "prostate cancer" (PCa), is the most commonly diagnosed cancer in men living in the United States PCa is responsible for ~10% of all cancer-related deaths in men (Siegel et al., 2021). In China, PCa is the sixth most commonly diagnosed malignancy among men, it accounts for 3.35% of malignant tumors, and represents 2.1% of the total cancer-related mortality in men (Chen et al., 2016). During the past decade, surgery or androgen-deprivation therapy has become the first-line treatment for PCa patients (Litwin and Tan, 2017).

However, a proportion of patients fail to respond to medical castration initially, and nearly all patients who undergo androgen-deprivation therapy will progress eventually to metastatic castration-resistant prostate cancer (mCRPC). Taxane-based chemotherapies, next-generation antiandrogens, and biosynthesis inhibitors, such as enzalutamide (also named MDV3100), abiraterone acetate, and cabazitaxel, have been administered to patients who developed mCRPC (Litwin and Tan, 2017; Oudard et al., 2017; Thakur et al., 2018).

Enzalutamide is an androgen receptor (AR) antagonist that blocks several key steps in the AR signaling pathway: androgen binding to the AR, nuclear translocation of activated AR, and binding of activated AR with DNA (Tran et al., 2009; Baciarello and Sternberg, 2016; Scott, 2018). Despite the clinical efficacy of these drugs in mCRPC patients, the almost inevitable emergence of drug resistance hampers a definitive cure, possibly due to amplification or gain-of-function somatic mutations of AR, aberrant posttranslational modification of the AR protein, alternative splicing events that result in hyperactive receptors, and cofactor dysregulation and/or intracrine androgen synthesis (Watson et al., 2015). Considerable effort has been made on improving these weaknesses, but an efficient and efficacious method is lacking.

Microbial natural products and their derivatives are important sources for drug discovery (Choi et al., 2018). Most antibiotics in clinical practice are unmodified or modified derivatives of natural products produced by microorganisms to kill competing bacteria, and have been isolated originally from environmental sources (Liu et al., 2020). Therefore, it may be possible to search for "natural" anti-tumor components. Intriguingly, ilicicolin A (Ili-A) is an ascochlorin derivative isolated from theBeibu Gulf coral-derived fungus *Acremonium sclerotigenum* GXIMD 02501. Ili-A has been reported to be a promising anti-tumor drug in recent studies (Nirma et al., 2015; Sorres et al., 2018).

Aberrant methylation of DNA and histone modification are hallmarks of several cancer types. It has become evident that genes encoding epigenetic modifiers play a crucial role in normal development and cancer progression, and inhibitors of DNA methyltransferases, histone deacetylases thus methyltransferases are widely used in cancer therapy (Kovač et al., 2018). One type of histone methyltransferase, enhancer of zeste homolog 2 (EZH2), is an enzymatic catalytic subunit of polycomb-repressive complex 2 (PRC2), which catalyzes trimethylation of histone H3 at lysine 27 (H3K27me3) through its core components EZH1/EZH2, EED and SUZ12, and silences its target genes. EZH2 is overexpressed in many cancer types, such as cancer of the endometrium (Roh et al., 2020; Smith et al., 2019), and prostate gland (Varambally et al., 2008; Eich et al., 2020). AR, an important therapeutic target in PCa, remain highly expressed even when the tumor progressed to advanced stage. Previous study showed that EZH2 interacts directly with AR and activates them, which leads to regulation of AR expression and downstream targets (Liu et al., 2019). Inhibition of EZH2 expression enhances the efficacy of enzalutamide in enzalutamide-resistant PCa cells (Bai et al., 2019). Previous study identified the role of EZH2 in aggressive PCa, and suggested that EZH2 serves as a target of PCa treatment (Sellers and Loda, 2002). Here, we found that Ili-A inhibited the transactivation activity of AR and their downstream targets. A low dose of Ili-A inhibited the growth of CRPC cells and enhance the anticancer activity of enzalutamide in CRPC cancer models. Thus, combination of Ili-A with enzalutamide could be add in treatment strategy for CRPC.

MATERIALS AND METHODS

Cell Culture and Chemicals

22Rv1 was from American Type Culture Collection (ATCC, Manassas, VA, United States). C4-2B was from UroCor Inc. (Oklahoma City, OK, United States). C4-2B and 22Rv1 cells were cultured in RPMI 1640 medium (Senrui, Zhejiang, China). All culture media were supplemented with 10% fetal bovine serum and 1% penicillin/streptomycin (Gibco, Grand Island, NY, United States). Cells were cultured at 37°C in a humidified incubator containing 5% CO_2. Ilicicolin A (Ili A) was isolated from the Beibu Gulf coral-derived fungus *Acremonium sclerotigenum* GXIMD 02501. The strain GXIMD 02501 was fermented on a nutrient-limited culture medium (10 g soluble starch, 1 g bacterial peptone, 20 g sea salt, and 1 L H2O) inoculating at room temperature with 1 L × 160 Erlenmeyer flasks. In brief, ilicicolin A was isolated from its EtOAc extract (20 g) by various chromatographic methods, including silica gel, reversed-phase silica gel C18, and semi-preparative HPLC. It was determined to have ≥95% purity by analytical HPLC. The chemical structure of ili A was further determined by comparing the spectroscopic data (**Supplementary Figure S3**) with the literature (Sorres et al., 2018). Other chemicals were purchased from Sigma Aldrich (St. Louis, MO, United States) unless specified otherwise.

Cell Viability

Cells were seeded in 96-well plates at 500–1,000 cells per well (optimum density for growth) in a total volume of 100 μL of media. Serially diluted compounds in 250 μL of media were added 50 μL to the cells per well 24 h later. After 4 days of incubation, Cell-Titer GLO reagents (Promega Corp., Madison, WI, United States) were added, and luminescence was measured on GLOMAX microplate luminometer (Promega Corp.) according to the manufacturer's instructions. The results were presented as percentages and vehicle-treated cells set at 100. The estimated *in vitro* IC_{50} values were calculated using GraphPad Prism seven software.

Colony Formation

For colony-formation assays, 500 cells were seeded in a six-well plate and cultured for 10–14 days in a 37°C incubator; the medium was changed and the test compound added every 3 days. Cells were fixed in 4% paraformaldehyde for 15 min. Then, the plate was washed thrice with phosphate-buffered saline (PBS). Cell colonies were stained with crystal violet for 15 min. The number of colonies was counted after washing thrice with PBS. Colony-formation assays were carried out in triplicate, and all experiments were repeated three times.

RT-qPolymerase Chain Reaction

Total RNA was extracted from cells in 6-well plates. cDNA was prepared according to the manufacturer's protocol. PCR was performed on a BIO-RAD CFX96™ (BIO-RAD, San Diego, CA, United States) in the presence of SYBR Green. After the fluorescence values were collected, a melting-curve analysis was performed. The experiments were performed with data presented as mean standard deviation (SD). The sequences of primers for the RT-qPCR analysis are listed in **Supplementary Table S1**.

Cell Lysates and Western Blot Analysis

The 22Rv1, C4-2B, and C4-2B/ENZR cells were treated with the vehicle or different concentrations of ilicicolin A (Ili-A) or ENZ for 48 h before being harvested for a Western blot analysis. The cells were lysed in RIPA buffer plus 1% PMSF (Phenylmethylsulfonyl fluoride) and then were separated on a denaturing polyacrylamide gel according to the manufacturer's instructions. The proteins were transferred to a PVDF (Polyvinylidene fluoride) membrane and were blocked for 1 h in a 5% nonfat milk solution (Trisbuffered saline, 0.1% Tween (TBS-T), 5% nonfat dry milk). Finally, the signal was detected using a BIO-RAD imager. All the antibodies used in this study are described in the **Supplementary Table S2**.

Chromatin Immunoprecipitation Assay

Crude chromatin solutions of C4-2B cells were cleared with protein-A beads (Invitrogen, Carlsbad, CA, United States) that had been precoated with preimmune serum (i.e., serum extracted before immunization) for 2 h at 4°C. Then, the precleared chromatin solutions were incubated overnight at 4°C with antibodies (listed in **Supplemental Material**) before precipitation with protein-A beads that had been preblocked with bovine serum albumin and sonicated salmon-sperm DNA. For reChIP, the immunoprecipitated complexes from the first ChIP were eluted with dithiothreitol (20 mM) for 30 min at 37°C with brief vortex-mixing, diluted 50 times with ChIP buffer, cleared by centrifugation, and incubated with antibodies for secondary ChIP overnight at 4°C. The immunoprecipitated DNA was analyzed by real-time reverse transcription-quantitative polymerase chain reaction (RT-qPCR) with SYBR® Green on an iCycler® (Thermo Fisher, Waltham, MA, United States). Enrichment of genomic DNA is presented as the percent recovery relative to the input. The primers are listed in **Supplementary Table S1**.

EZH2 Activity Assessed Step

Dilute EZH2 enzyme, SAM(S-(5′-Adenosyl)-L-methionine chloride), compounds and peptide substrate in Assay Buffer just before use. Add 4 μL of inhibitor, 2 μL of enzyme to the wells of a white OptiPlate-384 and incubate for 10 min at room temperature. Subsequently, add 4 μL of H3 (1–50) K27 me0-biotin peptide/SAM mix to the reaction system. Cover the plate with TopSeal-A film and incubate at room temperature for 4 h. Prepare a 2X mix of anti-H3K27me3-Eu(K) at 0.225 μg/ml and SA-XL 665 at 10 ng/μL, respectively, in Detection Buffer. Add 10 μL of detection mixture (2X) to the plate. Cover with TopSeal-A film and incubate in subdued light for 1 h at room temperature. Remove plate sealer and read fluorescence emission at 665 and 620 nm wavelengths on an HTRF compatible reader. The resultant data were analyzed with GraphPad Prism.

Molecular Docking

The crystal structure of human PRC2 (Protein Data Bank (PDB) code: 5WG6), which includes the EZH2 subunit, was downloaded from PDB (www.pdb.org/) and used for molecular docking. Preparation of the protein structure (protonation-state adjustment, water deletion, addition of disulfide bonds and hydrogen atoms) was undertaken using Maestro 11.6.013 (Schrodinger, New York, NY, United States). The ligand was also prepared by Maestro, and the "Glide" docking program in Maestro was used for docking studies. The designed molecule Ili-A was first docked into the catalytic region of EZH2 using Glide SP mode. Then, the predicted binding mode was redocked further into this region by Glide XP mode. For docking and redocking using Glide, the grid was defined using a 30-A box centered on the N atom of residue TRP624 in the catalytic site of EZH2. All other parameters were kept as default. PyMOL (DeLano Scientific, Palo Alto, CA, United States) was used to obtain the three-dimensional structure of the docking model.

Ribonucleic Acid Sequencing Data Analysis

C4-2B cells were treated with vehicle or the small molecule Ili-A (5, 10 μM), for 48 h before RNA extraction. RNA-sequencing libraries were from 1 μg of total RNA, which was extracted using the Total RNA Isolation kit from Tiangen (Beijing, China) and reverse-transcribed with reverse transcriptase M-MLV according to manufacturer (TaKaRa Biotechnology, Shiga, Japan) instructions. Libraries were validated with a bioanalyzer (2,100 series; Agilent Technologies, Palo Alto, CA, United States). Sequencing was done on a MGISEQ 2000 SE 50 system (BGI Tech, Wuhan, China). First, we used Trim Galore (www.bioinformatics.babraham.ac.uk/)! to automate quality and adapter trimming, as well as quality control, for FastQ files. Then, the FastQ-formatted sequence data were analyzed using a standard BWA-Bowtie 2-Cufflinks workflow. Briefly, sequence reads were mapped to the reference human-genome assembly (GRCh37/hg19) with BWA and Bowtie 2. Subsequently, the Cufflinks package 62 was applied for transcript assembly, quantification of normalized gene and isoform expression in fragments per kilobase of exon model per million mapped reads (FPKM), and testing for differential expression (Cuff diff). To avoid spurious fold levels resulting from low expression values, only those genes with expression FPKM >1 for the vehicle control cell or treated cells (but not necessarily both), were included. Change in expression of ≥1.5-fold (increase or decrease) was clustered with the k-means clustering algorithm in Cluster 63. The cluster was displayed with Tree View.

Animal Experiments

For establishing the prostate cancer xenograft tumors, Four-week-old male NOD/SCID mice (body weight 18 g) were purchased from Zhongshan Biomedical Research Institute of Sun Yat-Sen University (Zhongshan, China). Briefly, the mice were injected with 10×10^7 22Rv1 cells in 100 μL PBS/Matrigel (1: 1), and implanted subcutaneously into the dorsal flank of the mice. When the tumor volume was reached about 50 mm^3, the mice

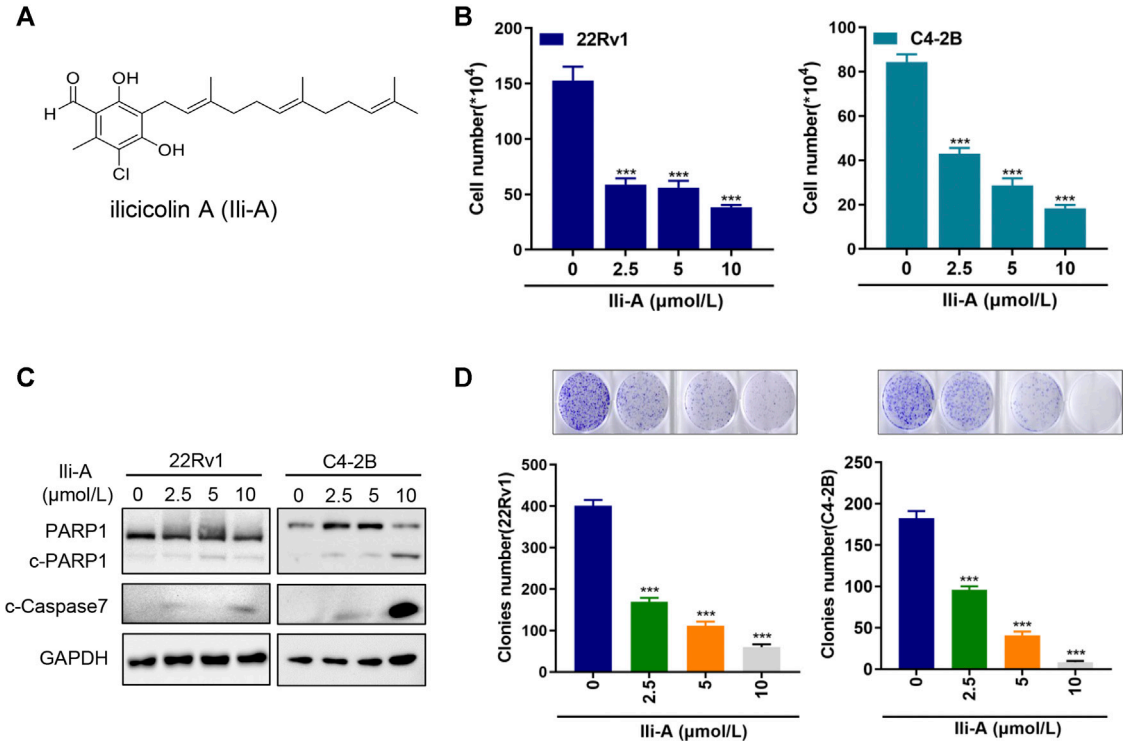

FIGURE 1 | Ili-A inhibits survival of castration-resistant prostate cancer cells and induces their apoptosis. **(A)** Chemical structure of Ili-A. **(B)** 22Rv1 cells and C4-2B cells were treated with vehicle or Ili-A as indicated. After 96 h, the total number of viable cells was counted with a cell counter. **(C)** Immunoblotting of the indicated proteins in 22Rv1 and C4-2B cells treated with vehicle or Ili-A for 48 h. **(D)** 22Rv1 cells and C4-2B cells were treated with vehicle (DMSO) or the indicated concentrations of Ili-A for 12 days, after which colony formation was counted.

were grouped randomly. Then mice were divided into four groups (n = 8) randomly and treated intraperitoneally (i.p.) with 100 μL of either vehicle (DMSO and sesame oil, 1:50, Sigma, St. Louis, MO, United States), 10 mg/kg Ilicicolin A (Ili-A) (six times a week), 10 mg/kg Enzalutamide (six times a week) or a combination of 10 mg/kg Ilicicolin A (Ili-A) (six times a week) and 10 mg/kg Enzalutamide (six times a week). Tumor volume and body weight were measured three times per week. Tumor growth was monitored by calipers with volume calculated using the equation $\pi/6$ (length × width^2). The mice were sacrificed at the end of the studies. Tumors were collected and immediately stored in liquid nitrogen or fixed in formalin solution. The procedures were approved by the Institutional Animal Care and Use Committee of Sun Yat-Sen University (Guangzhou, China).

Animal Experiments

For establishing the prostate cancer xenograft tumors, Four-week-old male NOD/SCID mice (body weight 18 g) were purchased from Zhongshan Biomedical Research Institute of Sun Yat-Sen University (Zhongshan, China). Briefly, the mice were injected with 10× 10^7 22Rv1 cells in 100 μL PBS/Matrigel (1: 1), and implanted subcutaneously into the dorsal flank of the mice. When the tumor volume was reached about 50 mm^3, the mice were grouped randomly. Then mice were divided into four groups (n = 8) randomly and treated intraperitoneally (i.p.) with 100 μL of either vehicle (DMSO and sesame oil, 1:50, Sigma, St. Louis, MO, United States), 10 mg/kg Ilicicolin A (Ili-A) (six times a week), 10 mg/kg Enzalutamide (six times a week) or a combination of 10 mg/kg Ilicicolin A (Ili-A) (six times a week) and 10 mg/kg Enzalutamide (six times a week). Tumor volume and body weight were measured three times per week. Tumor growth was monitored by calipers with volume calculated using the equation $\pi/6$ (length × width^2). The mice were sacrificed at the end of the studies. Tumors were collected and immediately stored in liquid nitrogen or fixed in formalin solution. The procedures were approved by the Institutional Animal Care and Use Committee of Sun Yat-Sen University (Guangzhou, China).

Statistical Analyses

Analyses were conducted with Prism 7 (GraphPad, San Diego, CA, United States). Differences between two groups were analyzed by Student's t-test. $p < 0.05$ was considered significant. The results are expressed as the mean ± standard deviation (SD).

RESULTS

Ili-A Inhibits the Survival of Castration-Resistant Prostate Cancer Cells and Induces Their Apoptosis

We wished to search for drug candidates for CRPC treatment in humans. We screened a chemical library containing 30 natural compounds from marine microorganisms for their activity in

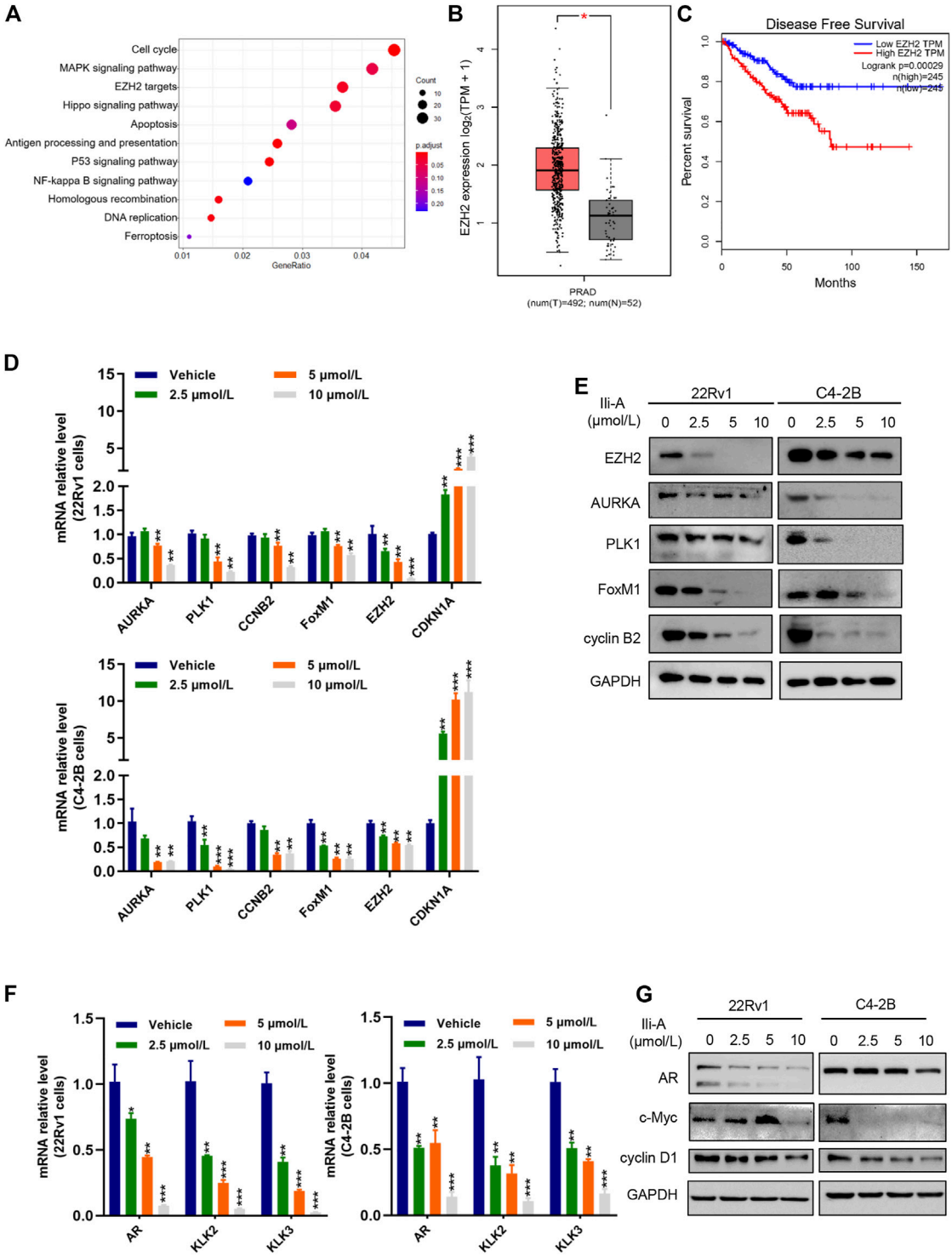

FIGURE 2 | RNA-sequencing shows that the EZH2 pathway is involved in the proliferation of prostate cancer cells. **(A)** Bubble chart showing enrichment of the most significantly changed genes in the signaling pathways of C4-2B cells. **(B)** Gene expression of EZH2 expression in human prostate cancer in TCGA and matched normal prostate-gland tissues in TCGA using log2 (TPM +1) for log scale. **(C)** EZH2 mRNA expression was correlated inversely with survival from prostate cancer. Kaplan–Meier plots are based on analyses of data from prostate-cancer patients in TCGA using GEPIA. **(D)** RT-qPCR showing expression of the indicated cyclin genes in 22Rv1 cells and C4-2B cells treated with vehicle or Ili-A for 48 h. **(E)** Immunoblotting showing expression of the indicated cyclin proteins in 22Rv1 cells and C4-2B cells treated with vehicle or Ili-A for 48 h. **(F)** RT-qPCR showing expression of the AR downstream genes in 22Rv1 cells and C4-2B cells treated with vehicle or Ili-A for 48 h. **(G)** Immunoblotting showing expression of AR downstream proteins in 22Rv1 cells and C4-2B cells treated with vehicle or Ili-A for 48 h.

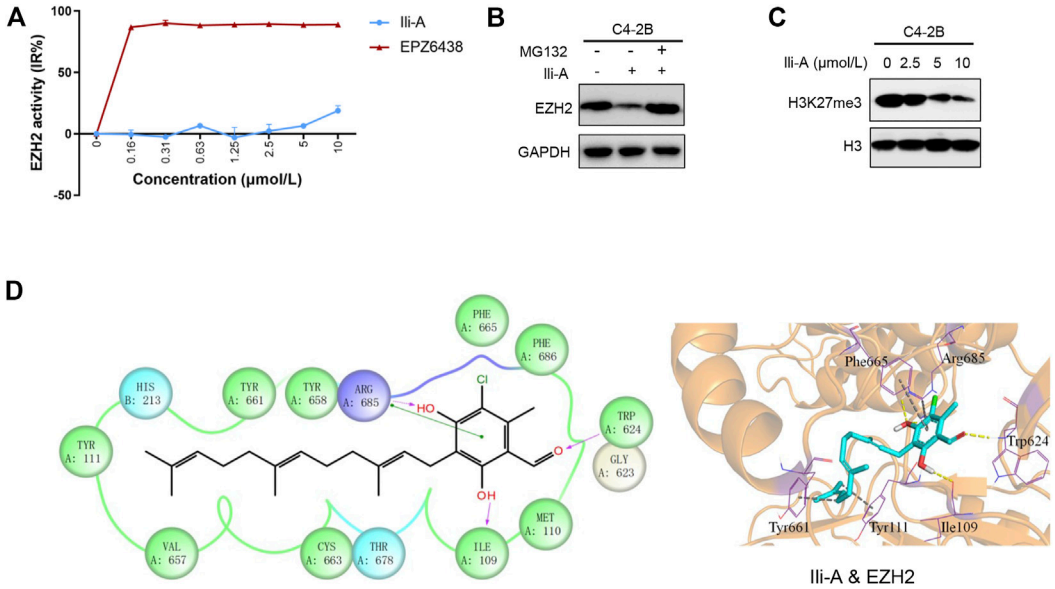

FIGURE 3 | Ili-A inhibits expression of EZH2-mediated signaling. **(A)** Biochemical inhibition of full-length human EZH2 by compound Ili-A and EPZ6438. **(B)** Immunoblotting showing an EZH2 protein-degraded pathway in C4-2B cells treated with vehicle or Ili-A for 18 h and MG132 for an additional 6 h. **(C)** Immunoblotting showing bulk histone methylation for H3K27me3 on acid-extracted histones in C4-2B cells treated with vehicle or Ili-A for 48 h. **(D)** Binding mode of Ili-A in the catalytic region of EZH2 by molecular docking. The hydrogen bonds are labeled by yellow dashed lines, and the hydrophobic interaction is shown as gray dashed lines.

growth inhibition of CRPC cell lines (C4-2B and 22Rv1) (**Supplementary Figures S1A,B**). Chemical structure of Ili-A (**Figure 1A**) and showed a strong chemotherapeutic effect in C4-2B cells and 22Rv1 cells at nanomolar concentrations (**Figure 1B**). Ili-A could induce expression of apoptosis-related proteins such as cleaved- Poly [ADP-ribose] polymerase (PARP)-1 and cleaved-caspase 7 (**Figure 1C**). A similar result was observed for formation of cell colonies (**Figure 1D**).

Ili-A Inhibits Expression of a EZH2-Mediated Signaling Pathway

We added Ili-A to C4-2B cells and extracted RNA. The amplified PCR product was sent for sequencing. Using the Kyoto Encyclopedia of Genes and Genomes (KEGG) database, we discovered that 11 pathways were enriched significantly among PCa genes. Of these, EZH2-targeting pathways were mainly enriched (**Figure 2A**). Based on the *Cancer* Genome Atlas database, EZH2 was overexpressed in PCa (**Figure 2B**) and associated significantly with an unfavorable prognosis of patients (**Figure 2C**). EZH2 has a pivotal role in the development and progression of PCa, so next we examined whether Ili-A could inhibit survival of CRPC cells by blocking EZH2 signaling. Ili-A significantly inhibited expression of EZH2 at mRNA and protein levels in a dose-dependent manner (**Figures 2D,E**). Ili-A deceased expression of proteins associated with cellular proliferation and the cell cycle, such as cyclin B2 and serine/threonine polo-like kinase (PLK)1. To investigate AR function by EZH2, we examined if Ili-A could repress AR transcription by blocking EZH2 signaling. Ili-A significantly inhibited expression of AR signaling at mRNA and protein levels in a dose-dependent manner (**Figures 2F,G**).

Ili-A Degrades EZH2 Protein by Promoting the Ubiquitin–Proteasome Pathway

We investigated the functional importance of EZH2 expression in the EZH2 signaling pathway by characterizing the inhibition effect of Ili-A on EZH2 activity. Surprisingly, EZH2 activity was uninhibited even after administration of Ili-A in nanomolar concentrations (**Figure 3A**). However, protein expression of EZH2 was decreased according to western blotting, by conduct MG132 (proteasome inhibitor), EZH2 protein expression was recovered. Hence, Ili-A may mediate EZH2 signaling by degrading EZH2 protein and promoting the ubiquitin–proteasome pathway (**Figure 3B**).

EZH2 is an important catalytic subunit of the PRC2 complex. It contains a SET catalytic domain, which is a methyltransferase domain that functions as exogenous methyl group identification through covalent reaction in combination of catalytic histone H3 lysine 9 and 27 occurred three methylation (H3K9me3 and H3K27me3). EZH2 is a key tumor-suppressor gene that induces chromatin densification and epigenetic silence, then leads to tumorigenesis. Thus, we also examined the trimethylation of H3K27me3. We discovered that inhibition of EZH2 expression with Ili-A decreased H3K27me3 expression in C4-2B cells (**Figure 3C**). To further understand the inhibition mechanism of human EZH2 with Ili-A at the molecular level, we undertook molecular docking to investigate the detailed interactions between Ili-A and EZH2. Ili-A was docked into the split catalytic region of EZH2 comprising the SET

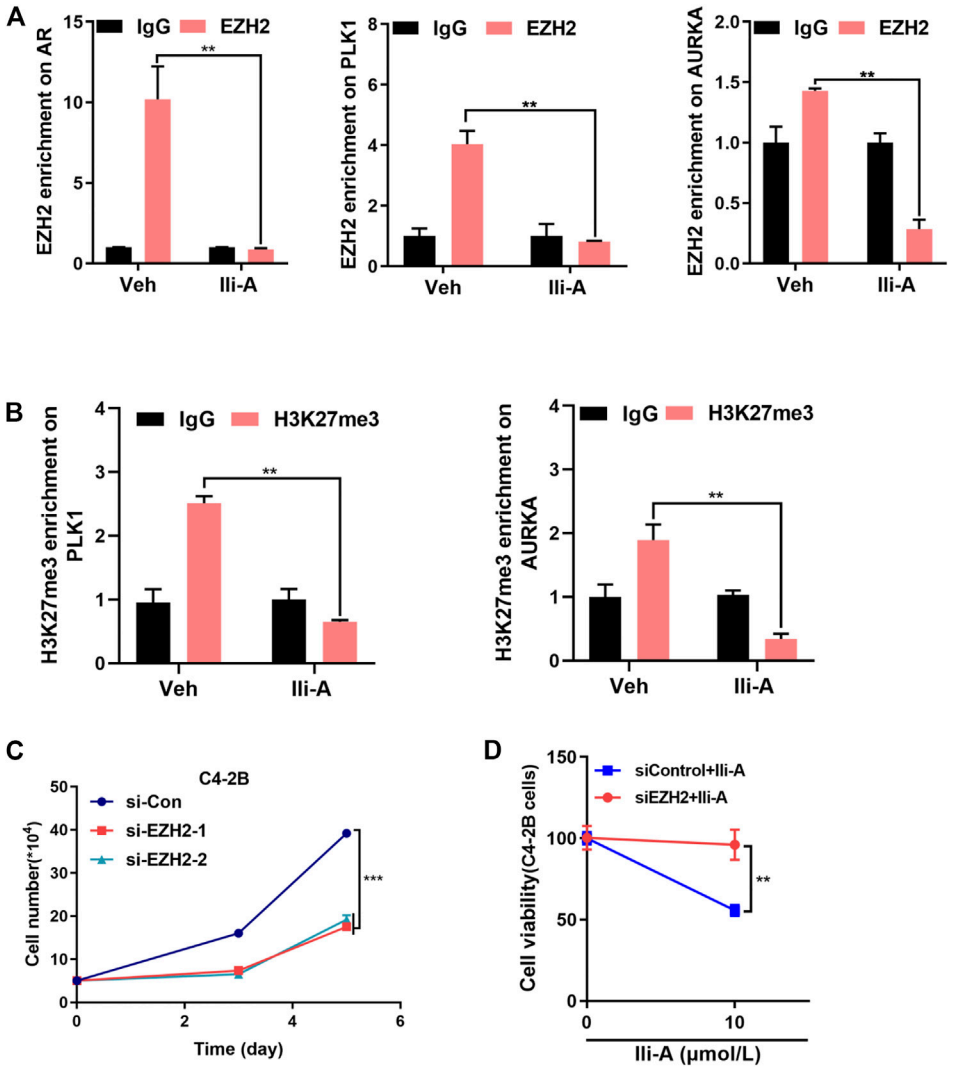

FIGURE 4 | Ili-A decreases expression of EZH2 target genes by inhibiting EZH2 expression. **(A)** ChIP-qPCR of the relative enrichment of EZH2 at *AR*, *PLK1* and *AURKA* promoters in C4-2B cells treated with vehicle or Ili-A for 48 h **(bottom)**. "Fold change" denotes the indicated enrichment of *AR*, *PLK1*, and *AURKA* under the influence of Ili-A compared with IgG enrichment in cells treated with vehicle control set as 1. **(B)** ChIP-qPCR of the relative enrichment of H3K27me3 at *PLK1* and *AURKA* promoters in C4-2B cells treated with vehicle or Ili-A for 48 h **(bottom)**. Fold change denotes the indicated enrichment on *PLK1* and *AURKA* under the influence of Ili-A compared with IgG enrichment in cells treated with vehicle set as control. **(C)** C4-2B cells were transfected with EZH2 or control siRNA for 72 and 120 h, and the total number of viable cells was counted with a cell counter. **(D)** C4-2B cells were transfected with EZH2 or control siRNA for 48 h and treated with vehicle or Ili-A for an additional 24 h. Cells were harvested to determine cell growth by counting the number of viable cells.

domain (residues 623–625 and 657–686) and SET activation loop (SAL; residues 109–111) (**Figure 3D**) (Bratkowski et al., 2018). Ili-A could bind tightly to the catalytic region of EZH2 in a similar manner to that seen with pyridone inhibitors (**Figure 3D**). The carbonyl oxygen of the phenyl head of Ili-A formed a hydrogen bond with main-chain amide of Trp624, so Ili-A could compete with S-adenosylmethionine (SAM) binding to the same residue (Trp624) of EZH2. In addition, the two hydroxyl groups in the phenyl head of Ili-A could form a hydrogen bond with Arg685 in the drug-binding pocket and Ile109 in the SAL region, respectively. Furthermore, the alkane tail of Ili-A extended to the SET/SAL gate comprising Tyr661 and Tyr111, and could form strong hydrophobic interactions with the benzene ring of these two residues. Therefore, our molecular-docking results indicated that Ili-A could act as a novel EZH2 inhibitor and compete with SAM for EZH2 binding as general pyridone-containing inhibitors.

Ili-A Decreases Expression of EZH2 Target Genes via the EZH2 Signaling Pathway

ChIP-qPCR showed that Ili-A strongly reduced EZH2 occupancy on *AR*/*PLK1*/*AURKA* promoter sites (**Figure 4A**). Given that EZH2 causes methylation of H3K27me3, our data showed that Ili-A reduced H3K27me3 occupancy on *PLK1*/*AURKA* promoter sites (**Figure 4B**).

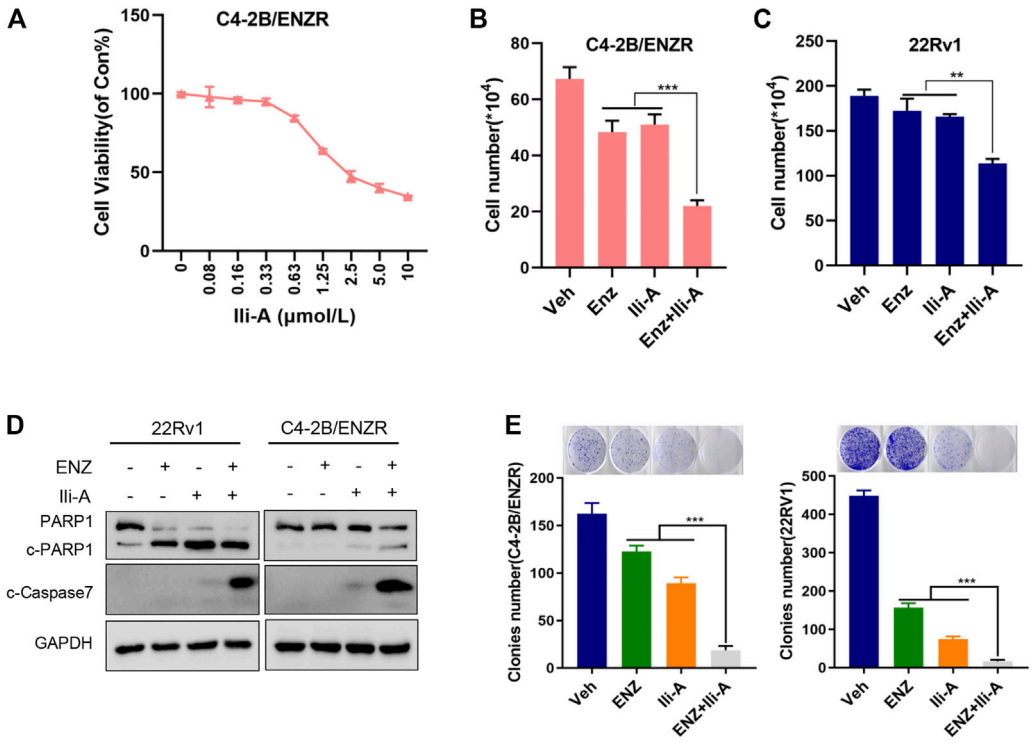

FIGURE 5 | Cotreatment of Ili-A and enzalutamide (ENZ) suppresses cell growth and induces apoptosis in CRPC cells. **(A)** Cell proliferation was assessed using the CellTiter-Glo assay after 96 h of treatment with Ili-A in C4-2B/ENZR cells at the indicated doses. **(B,C)** Cell numbers were counted with a cell counter after 96 h of treatment with Ili-A (1.25 μM), enzalutamide (ENZ; 10 μM) or Ili-A (1.25 μM) plus ENZ (10 μM) in 22Rv1 cells and C4-2B/ENZR cells. **(D)** Western blots demonstrating apoptotic markers following treatment with vehicle, Ili-A (1.25 μM), enzalutamide (ENZ; 10 μM) or Ili-A (1.25 μM) plus ENZ (10 μM) in 22Rv1 cells and C4-2B/ENZR cells. **(E)** Cell proliferation as assessed using a colony-formation assay after 12 days of treatment with Ili-A (1.25 μM), enzalutamide (ENZ; 10 μM) or Ili-A (1.25 μM) plus ENZ (10 μM) in 22Rv1 cells and C4-2B/ENZR cells.

We wished to ascertain if silencing of EZH2 expression would block inhibition of Ili-A and affect cell survival. First, we used EZH2 small interfering (si)RNA to silence EZH2 expression specifically. Ili-A-induced inhibition of cell survival was attenuated significantly in EZH2 siRNA-treated cells compared with that in control cells (**Figures 4C,D**). Collectively, these results suggested that Ili-A could inhibit proliferation of CRPC cells by inhibiting EZH2 expression-mediated target-gene expression.

Ili-A Sensitizes Castration-Resistant Prostate Cancer Cells to Enzalutamide Induced Cell Death *In Vitro*

To further explore the effects of Ili-A on CRPC cells, we generated an enzalutamide-resistant PCa cell line C4-2B/ENZR (C4-2 enzalutamide-resistant) by continuous culture of C4-2 cells in a medium containing enzalutamide for 7 months. C4-2B/ENZR cells showed more resistance to enzalutamide than the parental C4-2 cells. Interestingly, we found that the viability of C4-2B/ENZR cells was reduced significantly by Ili-A treatment in a dose-dependent manner (**Figure 5A**). This observation indicated that Ili-A: 1) could overcome the enzalutamide-induced resistance of PCa cells; 2) could combine with enzalutamide against CRPC. To support this hypothesis and explore the combined effects of these two agents, we treated 22Rv1 cells with Ili-A (1.25 μM) in the presence or absence of enzalutamide (10 μM) for 4 days. Combination of Ili-A and enzalutamide had a stronger inhibitory effect on the viability of 22Rv1 cells than that observed with treatment of Ili-A alone or enzalutamide alone (**Figure 5B**). Similar results were observed in the enzalutamide-resistant cell line C4-2B/ENZR (**Figure 5C**). Interestingly, co-treatment also induced higher expression of the cleaved products of two well-known markers of apoptosis, cleaved-PARP-1 and cleaved-caspase 7, in 22Rv1 cells and C4-2B/ENZR cells (**Figure 5D**), indicating that such combined treatment might be more toxic to CRPC cells than monotherapy. Moreover, co-treatment with Ili-A and enzalutamide had a stronger inhibitory effect on the colony-forming ability of 22Rv1 cells and C4-2B/ENZR cells (**Figure 5E**). Taken together, these results indicated that Ili-A may have a synergistic effect with enzalutamide against PCa cells *in vitro*.

Ili-A Inhibits Growth of Castration-Resistant Prostate Cancer Tumors and Potentiates the Anti-Tumor Effect of Enzalutamide *In Vivo*

To investigate the anti-tumor effects of co-treatment of Ili-A and enzalutamide *in vivo*, 22Rv1 cells were used to establish an animal

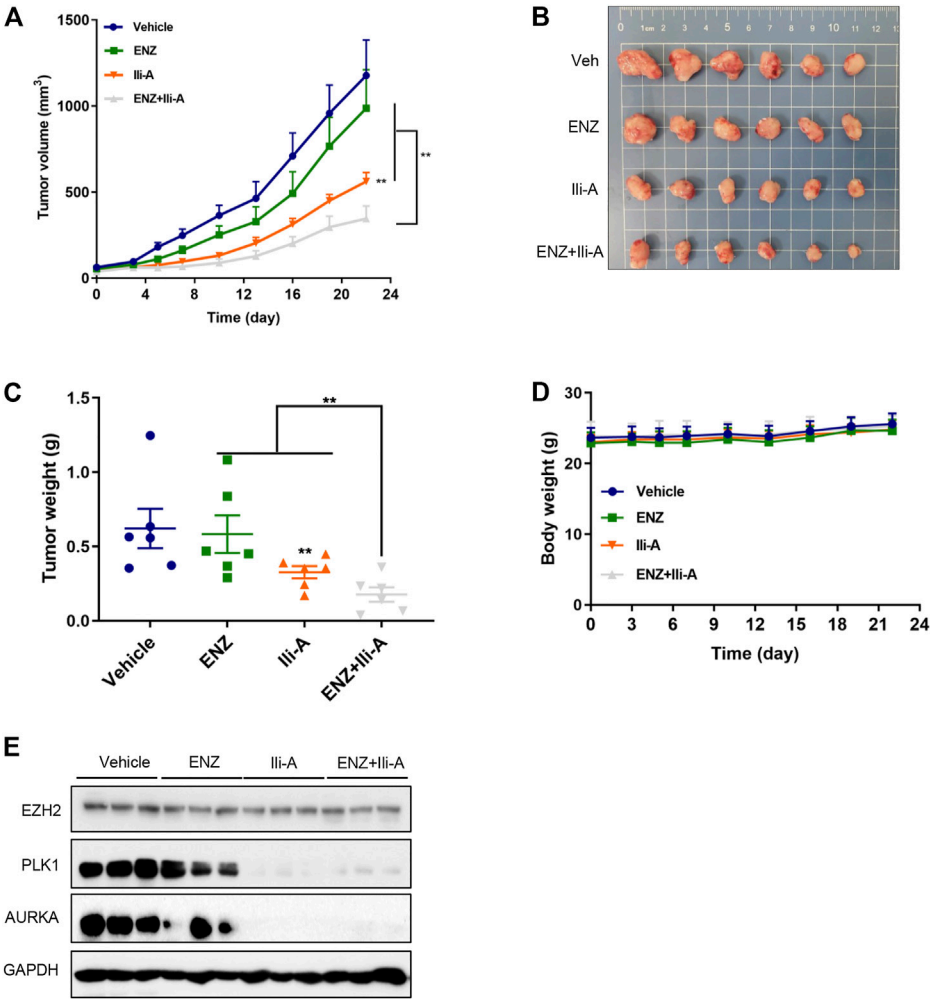

FIGURE 6 | Ili-A enhances the anti-tumor effects of enzalutamide *in vivo*. Mice bearing 22Rv1 xenografts (n = 8 mice per group) received vehicle, Ili-A (10 mg/kg, i. p.), ENZ (10 mg/kg, i. p.) or a combination of Ili-A and ENZ, as indicated, six times per week. **(A)** Tumor volume in different groups (tumor volume was measured twice every week). **(B)** Images of xenograft tumors harvested at day-22. **(C)** Weight of xenograft tumors in different groups. **(D)** Body weight of Mice in different groups. **(E)** Western blotting was done to detect EZH2 and target proteins in tumors undergoing monotherapy or combination with Ili-A and enzalutamide.

xenograft model of CRPC. Male nude mice bearing 22Rv1 xenografts were randomized and treated with Ili-A (10 mg/kg; six times per week), enzalutamide (10 mg/kg; six times per week), or both, for 3 weeks. Tumor volume and bodyweight were monitored twice or thrice a week. At the end of 3 weeks, mice were sacrificed and xenografts were harvested for further investigation. After 3 weeks of combined treatment with Ili-A and enzalutamide, the volumes and weight of xenograft tumors decreased dramatically compared with the moderate effect of Ili-A alone and the slight effect of enzalutamide alone (**Figures 6A–C**). Photographs of the heart, spleen, and kidneys showed no visible change after drug treatment (**Supplementary Figure S2**). The three treatment groups suppressed tumor growth to different extents but did not elicit a significant effect on bodyweight (**Figure 6D**). Moreover, *EZH2*/*PLK1*/*AURKA* expression was strongly suppressed in the co-treatment group (**Figure 6E**). These results indicated that Ili-A could enhance the anti-cancer effect of enzalutamide on CRPC cells *in vivo*.

DISCUSSION

Despite significant progress in anti-androgen therapies for CRPC, as a second-generation AR antagonist, enzalutamide has been widely used in treatment of advanced prostate cancer. However, the acquired resistance to these therapies is inevitable, which restricts treatment efficacy. Thus, the discovery of new therapeutic targets against CRPC resistance is an urgent and unmet need. In this study, we showed that EZH2 plays an important role in the development of PCa and enzalutamide resistance. We demonstrated that Ili-A could be a novel EZH2 antagonist that exerts anti-tumor effects against CRPC *in vitro* and *in vivo* and capable of enhance the anticancer activity of enzalutamide in CRPC cancer models. Mechanistically, we demonstrated that Ili-A exerts its effect by inhibiting EZH2 expression and AR activation. These findings were highly consistent in our prostate cancer cell models *in vitro* and 22Rv1 xenograft mice models *in vivo*, suggesting that

combination of Ili-A and enzalutamide would be more efficient in treating patients with advanced prostate cancer, especially the ones with enzalutamide-resistant cancer.

Several naturally occurring antagonists, mainly derived from marine microorganisms, have shown potent anti-tumor activity. Chemical activities in growth inhibition of C4-2B cells and 22Rv1 cells show that Ili-A displayed chemotherapeutic effect in C4-2B cells and 22Rv1 cells at nanomolar concentrations. C4-2B cells were treated with Ili-A, and RNA-sequencing carried out. Use of the KEGG database revealed that EZH2-targeting pathways were the main ones enriched. Given its crucial roles in the development and progression of PCa, EZH2 could be a novel therapeutic target for CRPC.

It is well established that up-regulation of EZH2 is closely correlated with the progression of advanced PCa and unfavorable outcome, but the EZH2 inhibitors-based treatment is basically ineffective for PCa (Deb et al., 2013). EZH2 and other PRC2 components are transcriptional repressors that methylate H3K27 and condense chromatin conformation. Scholars have reported that EZH2 can repress multiple downstream targets (e.g., *KDM6A*, *GIT1*) directly by binding to their promoter regions contributed to the progression of urothelial bladder carcinoma (Ler et al., 2017; Yang et al., 2020). In CRPC cells, PLK1 is a regulator of several cell-cycle events: mitotic entry, formation of bipolar spindles, and cytokinesis (Strebhardt, 2010). *AURKA* is a serine/threonine protein kinase crucial for formation of mitotic spindles and chromosome segregation (Willems et al., 2018). By directly binding to the promoter region of *PLK1* and *AURKA*, EZH2 serves as a regulatory transcriptional factor in regulation of the expression of *PLK1* and *AURKA* and subsequently induce proliferation of PCa. In our study, we observed that Ili-A could reduce EZH2 protein and mRNA level and the expression of the downstream *AURKA*/PLK1 gene, which contribute to the anti-tumor effects against CRPC.

Compounds capable of degrading EZH2 protein (similar to knockdown of EZH2 expression) might greatly outperform enzymatic EZH2 inhibitors, and would have higher specificity in blocking the dual roles of EZH2. RNA-sequencing results also supported the notion of activation of AR targets via induction of EZH2 expression.

The ubiquitin–proteasome system (UPS) is the most prominent pathway for modulation of cellular EZH2 protein homeostasis. Ili-A decreased EZH2 protein levels in prostate cancer cells via accelerated degradation of EZH2. While MG132, a proteasome inhibitor, could reverse this effect. These results suggested that Ili-A could accelerate the degradation of EZH2 in prostate cancer cells through the proteasome pathway. We demonstrated that Ili-A suppressed expression of the EZH2 target genes *PLK1* and *AURKA* markedly, and inhibited the growth of PCa cells significantly via EZH2 degradation. Previous study demonstrated that EZH2 inhibitors such as EPZ and GSK126, though effective in blocking the enzymatic roles of EZH2, could not suppress EZH2-mediated activation of AR. Instead, they inadvertently increased AR expression (Ku et al., 2017). Our ChIP-PCR results indicated that EZH2 activates AR via its direct occupancy at the AR promoter, and promote an AR-dependent transcriptional network. Ili-A could repress EZH2 and other PRC2 components that methylate H3K27 and condense chromatin conformation. Inhibited expression of EZH2 decreased AR expression markedly at transcriptional and protein levels, and reduced expression of AR-activated genes, such as *KLK2* and *KLK3*.

Enzalutamide is a second-line AR antagonist used against CRPC. However, enzalutamide resistance is an urgent problem in treatment of PCa, which is induced mainly by AR point mutations, AR overexpression, and constitutively active AR splice variants (Visakorpi et al., 1995; Borgmann et al., 2018). Therapeutic strategies have focused on the combination of other reagents with enzalutamide for CRPC treatment (Han et al., 2017). In addition, several compounds have been shown to diminish drug resistance if added to enzalutamide treatment *in vitro* or *in vivo*, such as the CXCR7 inhibitor CCX771 (Luo et al., 2018), and AZD5363 (Toren et al., 2015), which targets the phosphoinositide 3-kinase/protein kinase B pathway. Studies have shown that EZH2 has a critical role in acquisition of enzalutamide-resistance in CRPC cells and drives enzalutamide-resistance (Varambally et al., 2002). Targeting EZH2 could overcome enzalutamide resistance in PCa cells. GSK126 combined with enzalutamide inhibits proliferation and colony formation of enzalutamide-resistant CRPC cells dramatically. In prostate cancer, EZH2 activates AR gene transcription through direct occupancy at its promoter.

Previous study demonstrated the effect of GSK126 and enzalutamide on disruption of EZH2 directly binds to androgen receptor (AR) in coordinating the activities of PRC2 complex and playing a central role in the interaction with H3K27 and enhancing H3K27me3 in CRPC cells (Liu et al., 2019); whereas silencing of EZH2 significantly decreased AR and the expression of downstream targets such as *PSA* and *TMPRSS2*. Furthermore, short-hairpin RNA-mediated depletion of EZH2 can enhance the efficacy of enzalutamide treatment in enzalutamide-resistant CRPC cells and xenograft tumors (Bai et al., 2019). Thus, beyond its transcriptional repressor function, EZH2 also acts as an activator for AR and its downstream targets facilitating growth of CRPC cells. Our studies demonstrate that combination treatment with Ili-A and enzalutamide dissociates the association between AR and members of the EZH2 downstream targets.

However, the EZH2 inhibitors-based treatment is basically ineffective against PCa, which limits its clinical application. Two EZH2 inhibitors, EPZ-6438 and GSK126, showed preliminary benefits in some hematological malignances with constitutive enzymatic activity of EZH2 (McCabe et al., 2012; Kurmasheva et al., 2017). Although the up-regulation of EZH2 is associated with advanced PCa and poor prognosis, the EZH2 inhibitors-based treatment is basically ineffective for PCa (Deb et al., 2013). Moreover, by employing 22Rv1 cell line-derived PCa xenograft models, we further revealed that Ili-A enhance the anticancer activity of enzalutamide in CRPC cancer models. This signifies that combined targeting of EZH2 and AR is an effective treatment option for CRPC.

CONCLUSION

We demonstrated that Ili-A could be employed for CRPC therapy. Ili-A showed efficacious activity against PCa cells by abrogating EZH2/AR-mediated processes, and demonstrated a synergistic anti-PCa effect with enzalutamide *in vivo*. Taken together, these data suggest that Ili-A, a novel EZH2 inhibitor, could combine with enzalutamide and serve as a new therapeutic strategy for CRPC.

DATA AVAILABILITY STATEMENT

The datasets presented in this study can be found in online repositories. The names of the repository/repositories and accession number(s) can be found below: NCBI (accession: GSE182064).

ETHICS STATEMENT

The animal study was reviewed and approved by Institutional Animal Care and Use Committee of Sun Yat-Sen University (Guangzhou, China).

AUTHOR CONTRIBUTIONS

LG and XL were responsible for doing the experiments and drafting the manuscript. YZ undertook extraction of compounds. JH and HW carried out some cell-model experiments. YG and WH offered help for molecular docking. ZC and SW provided technical and material support. JW and PY provided helpful discussions and reviewed the manuscript. JL, SX and YL were responsible for designing the study and supervising the experiments. All authors approved the final version of the manuscript.

FUNDING

This research was funded by the National Natural Science Foundation of China (81872891, 22007019, U20A20101), Guangdong Natural Science Funds for Distinguished Young Scholar (2019B151502016), Guangzhou Basic and Applied Basic Research Foundation (202002020082), Key-Area Research and Development Program of Guangdong Province (2020B1111110003), Fundamental Research Funds for the Central Universities (19ykzd23), the Natural Science Foundation of Guangxi (2020GXNSFGA297002), the Special Fund for Bagui Scholarsof Guangxi (05019055), and Science and Technology Planning Project of Guangdong Province (2017A050506042).

ACKNOWLEDGMENTS

The study protocol was approved by the Animal Care and Use Committee of Sun Yat-Sen University (Guangzhou, China).

SUPPLEMENTARY MATERIAL

The Supplementary Material for this article can be found online at: https://www.frontiersin.org/articles/10.3389/fphar.2021.723729/full#supplementary-material

REFERENCES

Baciarello, G., and Sternberg, C. N. (2016). Treatment of Metastatic Castration-Resistant Prostate Cancer (mCRPC) with Enzalutamide. *Crit. Rev. Oncol. Hematol.* 106, 14–24. doi:10.1016/j.critrevonc.2016.07.005

Bai, Y., Zhang, Z., Cheng, L., Wang, R., Chen, X., Kong, Y., et al. (2019). Inhibition of Enhancer of Zeste Homolog 2 (EZH2) Overcomes Enzalutamide Resistance in Castration-Resistant Prostate Cancer. *J. Biol. Chem.* 294 (25), 9911–9923. doi:10.1074/jbc.RA119.008152

Borgmann, H., Lallous, N., Ozistanbullu, D., Beraldi, E., Paul, N., Dalal, K., et al. (2018). Moving towards Precision Urologic Oncology: Targeting Enzalutamide-Resistant Prostate Cancer and Mutated Forms of the Androgen Receptor Using the Novel Inhibitor Darolutamide (ODM-201). *Eur. Urol.* 73 (1), 4–8. doi:10.1016/j.eururo.2017.08.012

Bratkowski, M., Yang, X., and Liu, X. (2018). An Evolutionarily Conserved Structural Platform for PRC2 Inhibition by a Class of Ezh2 Inhibitors. *Sci. Rep.* 8 (1), 9092. doi:10.1038/s41598-018-27175-w

Chen, W., Zheng, R., Baade, P. D., Zhang, S., Zeng, H., Bray, F., et al. (2016). Cancer Statistics in China, 2015. *CA Cancer J. Clin.* 66 (2), 115–132. doi:10.3322/caac.21338

Choi, S. S., Katsuyama, Y., Bai, L., Deng, Z., Ohnishi, Y., and Kim, E. S. (2018). Genome Engineering for Microbial Natural Product Discovery. *Curr. Opin. Microbiol.* 45, 53–60. doi:10.1016/j.mib.2018.02.007

Deb, G., Thakur, V. S., and Gupta, S. (2013). Multifaceted Role of EZH2 in Breast and Prostate Tumorigenesis: Epigenetics and beyond. *Epigenetics* 8 (5), 464–476. doi:10.4161/epi.24532

Eich, M. L., Athar, M., Ferguson, J. E., 3rd, and Varambally, S. (2020). EZH2-Targeted Therapies in Cancer: Hype or a Reality. *Cancer Res.* 80 (24), 5449–5458. doi:10.1158/0008-5472.Can-20-2147

Han, Y., Huang, W., Liu, J., Liu, D., Cui, Y., Huang, R., et al. (2017). Triptolide Inhibits the AR Signaling Pathway to Suppress the Proliferation of Enzalutamide Resistant Prostate Cancer Cells. *Theranostics* 7 (7), 1914–1927. doi:10.7150/thno.17852

Kovač, K., Sauer, A., Mačinković, I., Awe, S., Finkernagel, F., Hoffmeister, H., et al. (2018). Tumour-associated Missense Mutations in the dMi-2 ATPase Alters Nucleosome Remodelling Properties in a Mutation-specific Manner. *Nat. Commun.* 9 (1), 2112. doi:10.1038/s41467-018-04503-2

Ku, S. Y., Rosario, S., Wang, Y., Mu, P., Seshadri, M., Goodrich, Z. W., et al. (2017). Rb1 and Trp53 Cooperate to Suppress Prostate Cancer Lineage Plasticity, Metastasis, and Antiandrogen Resistance. *Science* 355 (6320), 78–83. doi:10.1126/science.aah4199

Kurmasheva, R. T., Sammons, M., Favours, E., Wu, J., Kurmashev, D., Cosmopoulos, K., et al. (2017). Initial Testing (Stage 1) of Tazemetostat (EPZ-6438), a Novel EZH2 Inhibitor, by the Pediatric Preclinical Testing Program. *Pediatr. Blood Cancer* 64 (3). doi:10.1002/pbc.26218

Ler, L. D., Ghosh, S., Chai, X., Thike, A. A., Heng, H. L., Siew, E. Y., et al. (2017). Loss of Tumor Suppressor KDM6A Amplifies PRC2-Regulated Transcriptional Repression in Bladder Cancer and Can Be Targeted through Inhibition of EZH2. *Sci. Transl Med.* 9 (378). doi:10.1126/scitranslmed.aai8312

Litwin, M. S., and Tan, H. J. (2017). The Diagnosis and Treatment of Prostate Cancer: A Review. *Jama* 317 (24), 2532–2542. doi:10.1001/jama.2017.7248

Liu, Q., Wang, G., Li, Q., Jiang, W., Kim, J. S., Wang, R., et al. (2019). Polycomb Group Proteins EZH2 and EED Directly Regulate Androgen Receptor in Advanced Prostate Cancer. *Int. J. Cancer* 145 (2), 415–426. doi:10.1002/ijc.32118

Liu, Y., Liu, Y., Du, Z., Zhang, L., Chen, J., Shen, Z., et al. (2020). Skin Microbiota Analysis-Inspired Development of Novel Anti-infectives. *Microbiome* 8 (1), 85. doi:10.1186/s40168-020-00866-1

Luo, Y., Azad, A. K., Karanika, S., Basourakos, S. P., Zuo, X., Wang, J., et al. (2018). Enzalutamide and CXCR7 Inhibitor Combination Treatment Suppresses Cell Growth and Angiogenic Signaling in Castration-Resistant Prostate Cancer Models. *Int. J. Cancer* 142 (10), 2163–2174. doi:10.1002/ijc.31237

McCabe, M. T., Ott, H. M., Ganji, G., Korenchuk, S., Thompson, C., Van Aller, G. S., et al. (2012). EZH2 Inhibition as a Therapeutic Strategy for Lymphoma with EZH2-Activating Mutations. *Nature* 492 (7427), 108–112. doi:10.1038/nature11606

Nirma, C., Eparvier, V., and Stien, D. (2015). Antibacterial Ilicicolinic Acids C and D and Ilicicolinal from Neonectria Discophora SNB-CN63 Isolated from a Termite Nest. *J. Nat. Prod.* 78 (1), 159–162. doi:10.1021/np500080m

Oudard, S., Fizazi, K., Sengeløv, L., Daugaard, G., Saad, F., Hansen, S., et al. (2017). Cabazitaxel versus Docetaxel as First-Line Therapy for Patients with Metastatic Castration-Resistant Prostate Cancer: A Randomized Phase III Trial-FIRSTANA. *J. Clin. Oncol.* 35 (28), 3189–3197. doi:10.1200/jco.2016.72.1068

Roh, J. W., Choi, J. E., Han, H. D., Hu, W., Matsuo, K., Nishimura, M., et al. (2020). Clinical and Biological Significance of EZH2 Expression in Endometrial Cancer. *Cancer Biol. Ther.* 21 (2), 147–156. doi:10.1080/15384047.2019.1672455

Scott, L. J. (2018). Enzalutamide: A Review in Castration-Resistant Prostate Cancer. *Drugs* 78 (18), 1913–1924. doi:10.1007/s40265-018-1029-9

Sellers, W. R., and Loda, M. (2002). The EZH2 Polycomb Transcriptional Repressor-Aa Marker or Mover of Metastatic Prostate Cancer? *Cancer Cell* 2 (5), 349–350. doi:10.1016/s1535-6108(02)00187-3

Siegel, R. L., Miller, K. D., Fuchs, H. E., and Jemal, A. (2021). Cancer Statistics, 2021. *CA A. Cancer J. Clin.* 71 (1), 7–33. doi:10.3322/caac.21654

Smith, H. W., Hirukawa, A., Sanguin-Gendreau, V., Nandi, I., Dufour, C. R., Zuo, D., et al. (2019). An ErbB2/c-Src axis Links Bioenergetics with PRC2 Translation to Drive Epigenetic Reprogramming and Mammary Tumorigenesis. *Nat. Commun.* 10 (1), 2901. doi:10.1038/s41467-019-10681-4

Sorres, J., Sabri, A., Brel, O., Stien, D., and Eparvier, V. (2018). Ilicicolinic Acids and Ilicicolinal Derivatives from the Fungus Neonectria Discophora SNB-CN63 Isolated from the Nest of the Termite Nasutitermes Corniger Found in French Guiana Show Antimicrobial Activity. *Phytochemistry* 151, 69–77. doi:10.1016/j.phytochem.2018.04.003

Strebhardt, K. (2010). Multifaceted polo-like Kinases: Drug Targets and Antitargets for Cancer Therapy. *Nat. Rev. Drug Discov.* 9 (8), 643–660. doi:10.1038/nrd3184

Thakur, A., Roy, A., Ghosh, A., Chhabra, M., and Banerjee, S. (2018). Abiraterone Acetate in the Treatment of Prostate Cancer. *Biomed. Pharmacother.* 101, 211–218. doi:10.1016/j.biopha.2018.02.067

Toren, P., Kim, S., Cordonnier, T., Crafter, C., Davies, B. R., Fazli, L., et al. (2015). Combination AZD5363 with Enzalutamide Significantly Delays Enzalutamide-Resistant Prostate Cancer in Preclinical Models. *Eur. Urol.* 67 (6), 986–990. doi:10.1016/j.eururo.2014.08.006

Tran, C., Ouk, S., Clegg, N. J., Chen, Y., Watson, P. A., Arora, V., et al. (2009). Development of a Second-Generation Antiandrogen for Treatment of Advanced Prostate Cancer. *Science* 324 (5928), 787–790. doi:10.1126/science.1168175

Varambally, S., Cao, Q., Mani, R. S., Shankar, S., Wang, X., Ateeq, B., et al. (2008). Genomic Loss of microRNA-101 Leads to Overexpression of Histone Methyltransferase EZH2 in Cancer. *Science* 322 (5908), 1695–1699. doi:10.1126/science.1165395

Varambally, S., Dhanasekaran, S. M., Zhou, M., Barrette, T. R., Kumar-Sinha, C., Sanda, M. G., et al. (2002). The Polycomb Group Protein EZH2 Is Involved in Progression of Prostate Cancer. *Nature* 419 (6907), 624–629. doi:10.1038/nature01075

Visakorpi, T., Hyytinen, E., Koivisto, P., Tanner, M., Keinänen, R., Palmberg, C., et al. (1995). *In Vivo* amplification of the Androgen Receptor Gene and Progression of Human Prostate Cancer. *Nat. Genet.* 9 (4), 401–406. doi:10.1038/ng0495-401

Watson, P. A., Arora, V. K., and Sawyers, C. L. (2015). Emerging Mechanisms of Resistance to Androgen Receptor Inhibitors in Prostate Cancer. *Nat. Rev. Cancer* 15 (12), 701–711. doi:10.1038/nrc4016

Willems, E., Dedobbeleer, M., Digregorio, M., Lombard, A., Lumapat, P. N., and Rogister, B. (2018). The Functional Diversity of Aurora Kinases: a Comprehensive Review. *Cell Div.* 13, 7. doi:10.1186/s13008-018-0040-6

Yang, S., Chen, J., Lv, B., Zhang, J., Li, D., Huang, M., et al. (2020). Decreased Long Non-coding RNA lincFOXF1 Indicates Poor Progression and Promotes Cell Migration and Metastasis in Osteosarcoma. *J. Cel Mol Med.* 24 (21), 12633–12641. doi:10.1111/jcmm.15828

Conflict of Interest: The authors declare that the research was conducted in the absence of any commercial or financial relationships that could be construed as a potential conflict of interest.

Publisher's Note: All claims expressed in this article are solely those of the authors and do not necessarily represent those of their affiliated organizations, or those of the publisher, the editors and the reviewers. Any product that may be evaluated in this article, or claim that may be made by its manufacturer, is not guaranteed or endorsed by the publisher.

frontiers in Pharmacology

ORIGINAL RESEARCH
published: 18 November 2021
doi: 10.3389/fphar.2021.767187

Predicting the Prognosis of Esophageal Adenocarcinoma by a Pyroptosis-Related Gene Signature

Ruijie Zeng[1,2†], Shujie Huang[2,3†], Xinqi Qiu[4†], Zewei Zhuo[1], Huihuan Wu[1], Lei Jiang[5], Weihong Sha[1]* and Hao Chen[1]**

[1]Department of Gastroenterology, Guangdong Provincial People's Hospital, Guangdong Academy of Medical Sciences, Guangzhou, China, [2]Shantou University Medical College, Shantou, China, [3]Department of Thoracic Surgery, Guangdong Provincial People's Hospital, Guangdong Academy of Medical Sciences, Guangzhou, China, [4]Zhuguang Community Healthcare Center, Guangzhou, China, [5]Guangdong Provincial Geriatrics Institute, Guangdong Provincial People's Hospital, Guangdong Academy of Medical Sciences, Guangzhou, China

OPEN ACCESS

Edited by:
Yi-Chao Zheng,
Zhengzhou University, China

Reviewed by:
Li-Juan Zhao,
Zhengzhou University, China
William K. K. Wu,
Chinese University of Hong Kong, China

***Correspondence:**
Lei Jiang
jianglei@smu.edu.cn
Weihong Sha
shaweihong@gdph.org.cn
Hao Chen
chenhao@gdph.org.cn

†These authors have contributed equally to this work

Specialty section:
This article was submitted to Experimental Pharmacology and Drug Discovery, a section of the journal Frontiers in Pharmacology

Received: 30 August 2021
Accepted: 22 October 2021
Published: 18 November 2021

Citation:
Zeng R, Huang S, Qiu X, Zhuo Z, Wu H, Jiang L, Sha W and Chen H (2021) Predicting the Prognosis of Esophageal Adenocarcinoma by a Pyroptosis-Related Gene Signature. Front. Pharmacol. 12:767187. doi: 10.3389/fphar.2021.767187

Esophageal adenocarcinoma (EAC) is a highly malignant type of digestive tract cancers with a poor prognosis despite therapeutic advances. Pyroptosis is an inflammatory form of programmed cell death, whereas the role of pyroptosis in EAC remains largely unknown. Herein, we identified a pyroptosis-related five-gene signature that was significantly correlated with the survival of EAC patients in The Cancer Genome Atlas (TCGA) cohort and an independent validation dataset. In addition, a nomogram based on the signature was constructed with novel prognostic values. Moreover, the downregulation of *GSDMB* within the signature is notably correlated with enhanced DNA methylation. The pyroptosis-related signature might be related to the immune response and regulation of the tumor microenvironment. Several inhibitors including GDC-0879 and PD-0325901 are promising in reversing the altered differentially expressed genes in high-risk patients. Our findings provide insights into the involvement of pyroptosis in EAC progression and are promising in the risk assessment as well as the prognosis for EAC patients in clinical practice.

Keywords: pyroptosis, esophageal adenocarcinoma, prognosis, methylation, tumor microenvironment

INTRODUCTION

Esophageal cancer is one of the most common malignancies worldwide, accounting for approximately 604,100 new cases and 544,076 deaths per year over the world (Sung et al., 2021). Esophageal adenocarcinoma (EAC) and esophageal squamous cell carcinoma (ESCC) composite the principle histologic subtypes of esophageal cancer, in which the incidence of EAC in western countries has increased dramatically in the last decades (Klingelhöfer et al., 2019). Despite therapeutic advances in surgery, radiotherapy, chemotherapy, and targeted drugs, the 5-year survival of esophageal cancer remains less than 20% (Alsop and Sharma, 2016). In consequence, biomarkers and effective models are urgently needed to predict the prognosis of EAC and provide insights into targeted therapy.

Pyroptosis is a proinflammatory form of regulated cell death, relying on the enzymatic activity of inflammatory proteases that belong to the caspase family (Vande Walle and Lamkanfi, 2016). Pyroptosis is featured with swift plasma-membrane rupture and subsequent release of proinflammatory intracellular contents, which is distinct from apoptosis (Bergsbaken et al., 2009). Studies evaluating the role of pyroptosis in neurological, infectious, autoimmune, cardiovascular, and oncologic disorders have been

emerging in recent years (Yu et al., 2021). Activation of the canonical inflammasome pathway is the basis of pyroptosis, in which pattern-recognition receptors (PRRs), for example, Toll-like receptors (TLRs), nucleotide-binding oligomerization domain-like receptors (NLRs), and absent in melanoma 2 like-receptors (ALRs) recognize pathogen-associated molecular patterns (PAMPs) or nonpathogen-related damage-associated molecular patterns (DAMPs) to activate inflammasomes and facilitate caspase-1 activation (Xia et al., 2019). Direct activation of caspase-4/5/11 under lipopolysaccharide (LPS) is involved in the noncanonical pyroptosis pathway, which is independent of the inflammasome complex (Shi et al., 2014). The gasdermin (GSDM) family proteins serve as the main mediators of pyroptosis, which are proteolytically activated by proteases and induce the formation of plasma membrane pores, leading to cell swelling and lysis (Van Opdenbosch and Lamkanfi, 2019; Tsuchiya, 2020). Due to the pivotal role of GSDM family proteins, pyroptosis is defined by some researchers as gasdermin-mediated programmed cell death (Shi et al., 2017).

However, despite the fact that research is emerging in ESCC, the role of pyroptosis in esophageal cancer remains largely unknown, and none of the previous publications have comprehensively evaluated the pyroptosis-related genes in EAC. Therefore, we performed a comprehensive evaluation of pyroptosis-related genes in EAC, in order to develop a pyroptosis-gene-based modality to predict the prognosis of the patients, and provide insights into the correlations between pyroptosis and tumor immune microenvironment.

MATERIALS AND METHODS

Datasets

The RNA-sequencing (RNA-seq) data of 87 patients (78 with EAC; 9 normal samples) and the corresponding clinical information from The Cancer Genome Atlas (TCGA) database were retrieved on May 20, 2021 (https://portal.gdc.cancer.gov/repository). The DNA microarray and clinical features of the validation cohort were downloaded from the Gene Expression Omnibus (GEO) database (https://www.ncbi.nlm.nih.gov/geo/, ID: GSE13898). The initial inclusion criteria were as follows: 1) patients with EAC; 2) patients with clear data for overall survival and survival status; and 3) patients with available gene expression data. The exclusion criteria were as follows: 1) patients with ESCC; 2) patients with incomplete data for overall survival, survival status; and 3) patients without gene expression data. As described in the following sections, further analysis based on clinicopathological characteristics was performed in patients with complete clinical data including age, gender, and stage. Patients with survival time of less than 30 days were excluded.

Identification of Differentially Expressed Genes in Pyroptosis-Related Gene Set

The 58 pyroptosis-related genes were derived from prior literature and the Gene Ontology (GO) term pyroptosis (ID: GO0070269; **Supplementary Table S1**) (Man and Kanneganti, 2015; Wang and

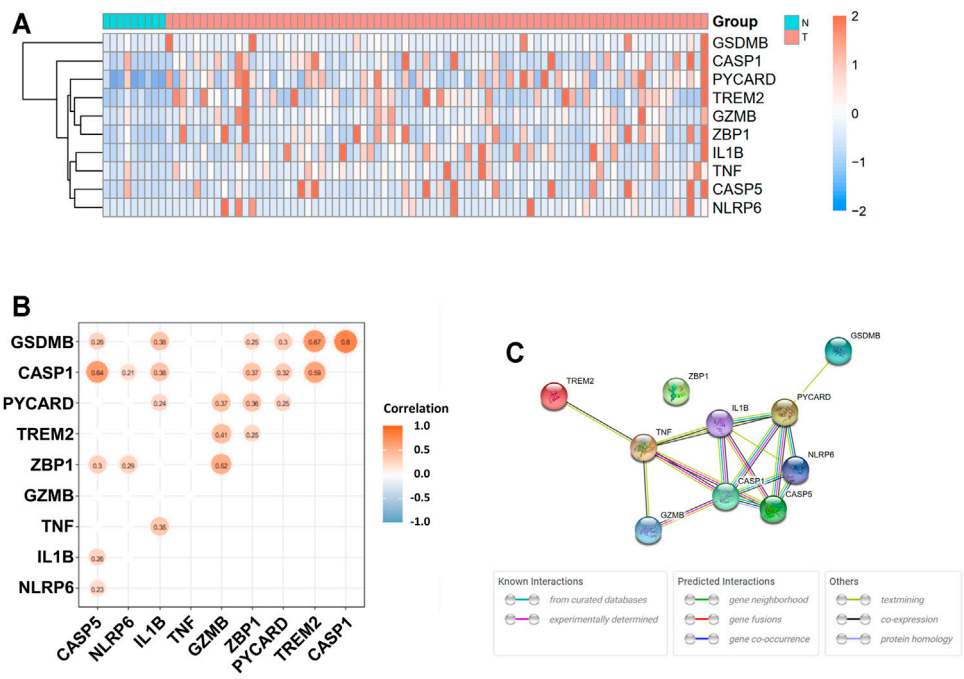

FIGURE 1 | Expressions of 10 differentially expressed pyroptosis-related genes and interaction. **(A)** Heatmap of gene expression between the tumor (T, red color) and normal (N, blue color) groups. Higher expression: red color. Lower expression: blue color. **(B)** Correlation network of 10 differentially expressed pyroptosis-related genes. Nonsignificant correlations ($p > 0.05$) were not shown in the figure. Orange: higher levels of correlation; blue: lower levels of correlation. **(C)** Protein–protein interaction (PPI) network of proteins encoded by selected genes.

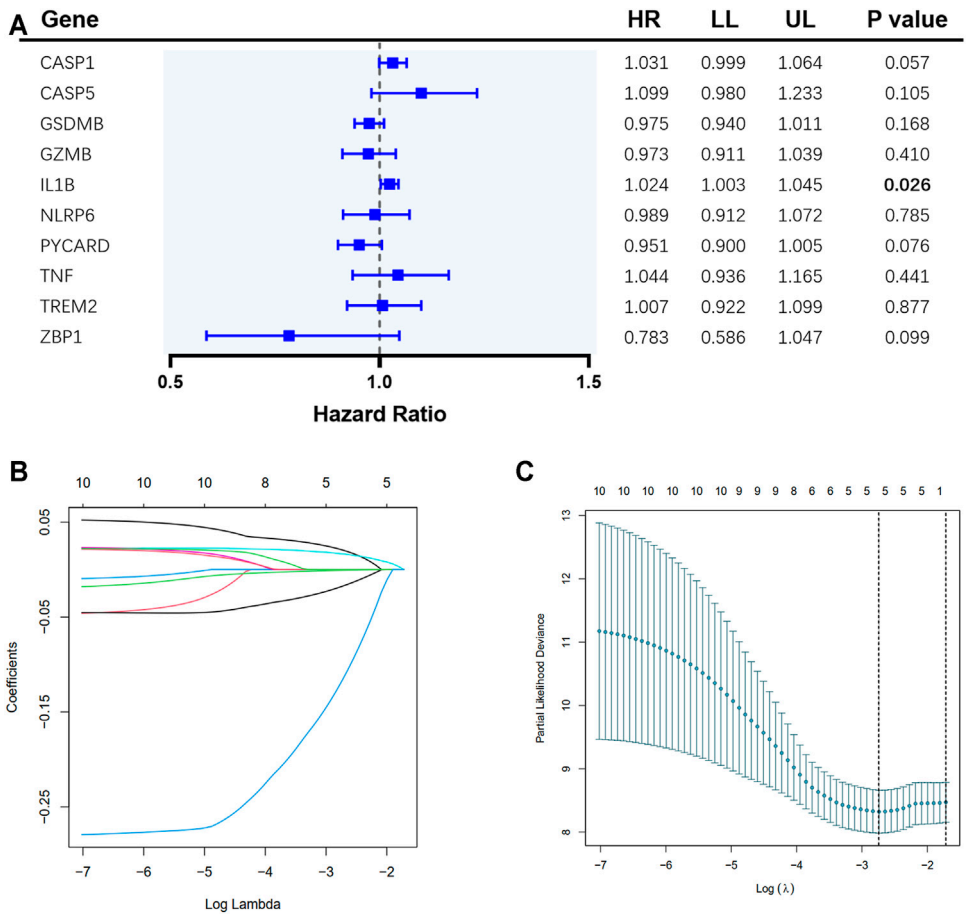

FIGURE 2 | Construction of pyroptosis-related gene risk signature in the TCGA cohort. **(A)** Univariate Cox regression analysis of overall survival (OS) for the selected genes. **(B)** LASSO regression of the 10 selected genes. **(C)** Cross-validation for tuning the parameter selection in LASSO regression.

Yin, 2017; Karki and Kanneganti, 2019; Xia et al., 2019). The microarray data from the GSE13898 cohort were normalized using the quantile normalization method, and the expression levels of genes were transformed to a $\log_2$ base for further analysis (Kim et al., 2010). The package "limma" was used to explore DEGs with the threshold of p value <0.05 (Ritchie et al., 2015). Probes with missing information for gene expressions in >20% samples were removed. The correlations of selected genes were evaluated by the "ggcorrplot" package (Kassambara and Kassambara, 2019). Protein–protein interaction (PPI) networks were created by Search Tool for the Retrieval of Interacting Genes (STRING) and the "igraph" package (Csardi and Nepusz, 2006; Szklarczyk et al., 2019).

Development and Validation of the Pyroptosis-Correlated Gene Prediction Model for Prognosis

Cox regression analysis was employed to evaluate the value of pyroptosis-related genes for prognosis. The DEGs were identified for further analysis. The LASSO Cox regression analysis was employed to construct a refined model for prognosis using the R package "glmnet" (Friedman et al., 2010). The calculation of the risk score was performed using the following formula: risk score = $\sum_{(n=1)}^{i} Coef\ i * Xi$ (Coef i indicates the coefficient, and Xi indicates the gene expression levels after standardization). The EAC patients were classified into low- and high-risk groups based on the median risk score, and Kaplan–Meier analysis was used to compare the overall survival (OS) between the two groups. Principal component analysis (PCA) was used to assess the separability of the two groups by the "prcomp" function. The R packages "survival," "survminer," "timeROC," and "riskRegression" were utilized for receiver operating characteristic (ROC) curve graphing and area under curve (AUC) calculation for 1, 2, and 5 years (Blanche et al., 2013; Therneau and Lumley, 2015; Kassambara et al., 2017; Ozenne et al., 2017). A nomogram model with clinical features including stage and risk score was constructed by the R packages "rms," "foreign," and "survival" (Therneau and Lumley, 2015; Harrell et al., 2017; Team et al., 2020). The calibration curve and detrended correspondence analysis (DCA) were performed using the "rms" package (Harrell et al., 2017). An EAC cohort (GSE13898) from the GEO database was used for validation, and the risk score was calculated by the same methods described

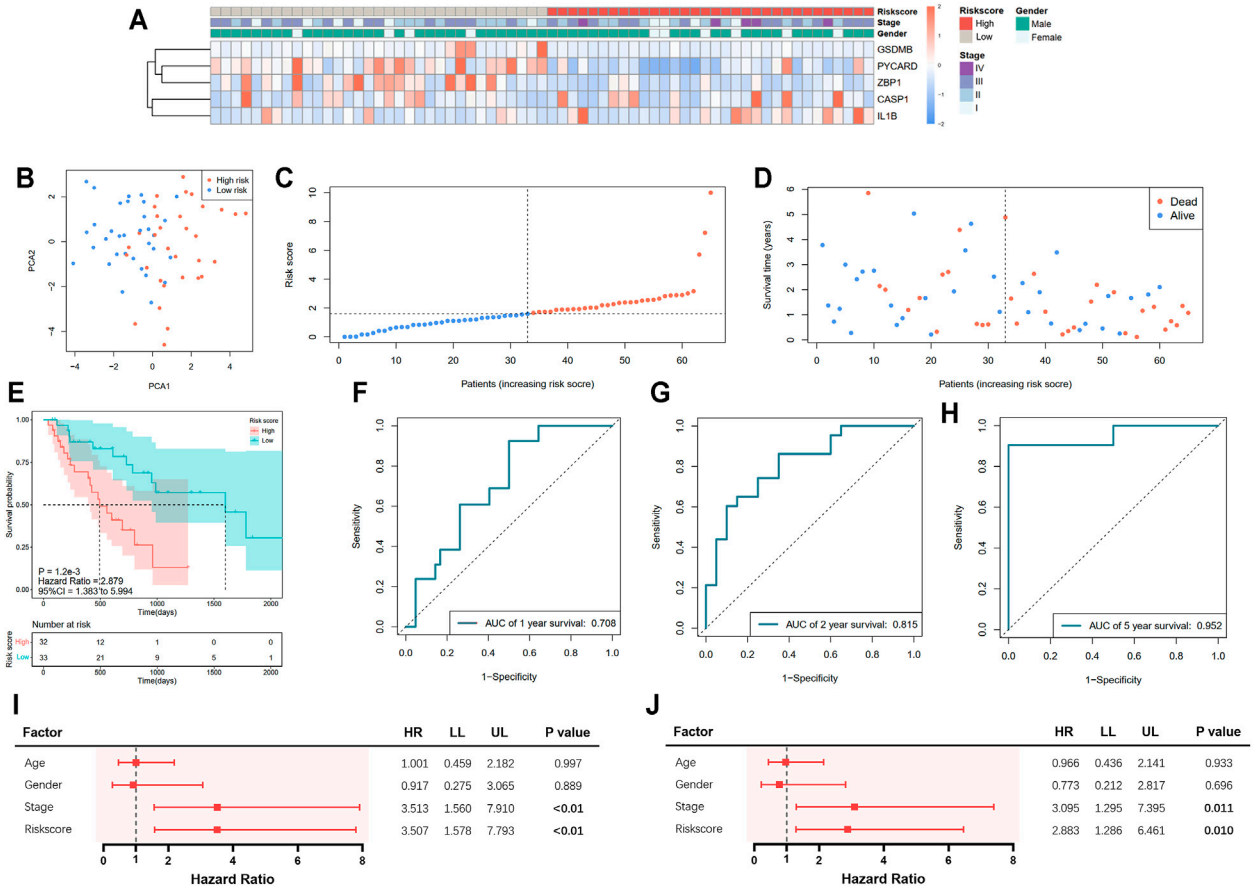

FIGURE 3 | Prediction of prognosis using the pyroptosis-related five-gene signature in the TCGA cohort. **(A)** Heatmap of five selected gene expressions with clinical features ordered by risk score (red: higher expression; blue: lower expression). **(B)** Principal component analysis (PCA) of the risk groups. **(C)** Distribution of patients according to risk scores. **(D)** Survival time and status of patients. **(E)** Kaplan–Meier curves for the survival of patients in the low- and high-risk groups. **(F–H)** Receiver operating characteristic (ROC) curve for 1-, 2-, and 5-year survival of patients. **(I)** Univariate Cox analysis. **(J)** Multivariate Cox analysis.

above to divide the cohort into two subgroups (low risk and high risk).

Prognostic Analysis of the Variables

Clinical data (age, gender, and stage) were extracted from patients in the TCGA and GSE13898 cohorts. The clinicopathological characteristics of EAC patients with complete data for further analysis were described in **Supplementary Table S2**. Variables including gender, stage, and risk score were analyzed in the regression model by univariate and multivariate Cox regression analysis.

Methylation Analysis

For the genes included in the signature, the cBio Cancer Genomics Portal (cBioPortal) database (http://www.cbioportal.org/) was used for exploring the correlation between methylation alterations and gene expressions in the TCGA esophageal adenocarcinoma cohort. The MEXPRESS database (http://mexpress.be/) was utilized for further assessment of the correlation between the precise genomic location of DNA methylation and altered levels of gene expression. $p < 0.05$ and $R^2 > 0.25$ were considered as significant correlation.

Tumor Microenvironment Analysis

The Tumor Immune Estimation Resource (TIMER) database (https://cistrome.shinyapps.io/timer/) was utilized to assess the correlation between tumor-infiltrating immune cells and expressions of selected genes (Li et al., 2017). Estimation Resource (TIMER) was used to compare the immune scores of the four subtypes. The CIBERSORT algorithm was used to further explore the composition and differences in the fraction of 22 immune cell types between two subgroups classified by risk scores (Chen et al., 2018).

Enrichment Analysis

Patients with EAC in the TCGA cohort were divided into two groups based on the median risk score. The DEGs between the low- and high-risk groups were extracted by $|\log2FC| \geq 1$ and p value <0.05. GO and Kyoto Encyclopedia of Genes and Genomes (KEGG) pathway enrichment was performed by the R package

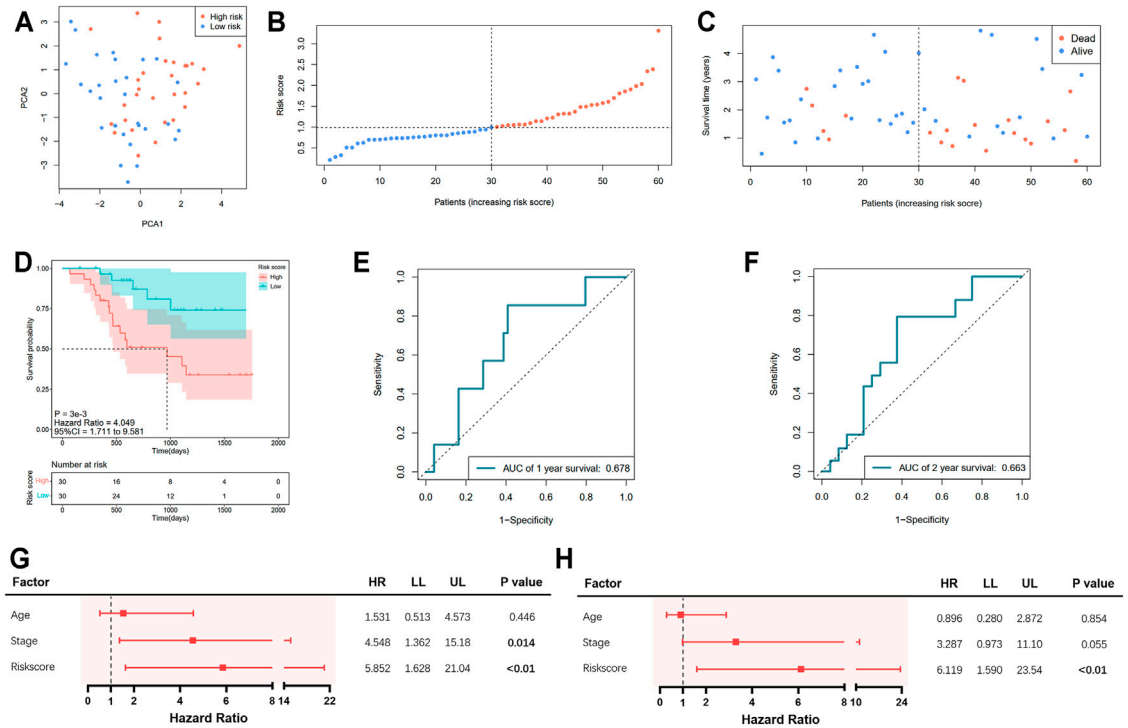

FIGURE 4 | Validation of the pyroptosis-related five-gene signature in the GSE13898 cohort. **(A)** Principal component analysis (PCA) of the risk groups. **(B)** Distribution of patients according to risk scores. **(C)** Survival time and status of patients. **(D)** Kaplan–Meier curves for the survival of patients in the low- and high-risk groups. **(E, F)** Receiver operating characteristic (ROC) curve for 1-, 2-, and 5-year survival of patients. **(G)** Univariate Cox analysis. **(H)** Multivariate Cox analysis.

"clusterProfiler," and the results were visualized using the "GOplot" package (Yu et al., 2012; Walter et al., 2015).

Connectivity Map Analysis

CMap analysis was performed and visualized in https://clue.io/ (Lamb et al., 2006), The top 150 upregulated and downregulated genes were selected according to the |logFC| values of DEGs for CMap analysis to identify a shortlist of drugs. According to the pattern-matching algorithms, positive scores indicate the induction effect of the small molecules on the signature, while negative scores indicate the inhibition effect. The drugs were further selected based on the negative scores.

Statistical Analysis

Statistical analyses were performed by R (version 4.1.0). Student's t-test was applied to compare the differences in gene expression between tumor and normal tissues, while categorical variables were compared using Pearson's chi-square test. The OS of patients between low- and high-risk groups were compared by the Kaplan–Meier method with log-rank test. The Cox regression analysis was performed to evaluate the independent prognostic factors for survival. The Wilcoxon test was used to compare the immune cell infiltration between groups.

Code Availability

The R code used in this study is available from the corresponding author upon reasonable request.

RESULTS

Identification of DEGs Between EAC and Normal Tissues

The expression levels of 58 pyroptosis-correlated genes were examined in the TCGA data of 78 EAC and 9 normal tissues. Ten DEGs were identified (|log2FC| ≥ 1 and p value <0.05), and all of them (*CASP1, CASP5, GSDMB, GZMB, IL1B, NLRP6, PYCARD, TNF, TREM2,* and *ZBP1*) were upregulated in the tumor group. The expression profiles of DEGs were demonstrated in **Figure 1A** (red color represents a higher expression level; blue color represents a lower expression level). **Figure 1B** showed the correlation network of DEGs in the TCGA data, indicating that GSDMB expressions are strongly correlated with CASP1 ($r = 0.80$, $p < 0.05$) and TREM2 ($r = 0.67$, $p < 0.05$) expressions. In addition, the expression of CASP1 is significantly correlated with that of CASP5 ($r = 0.64$, $p < 0.05$). The PPIs of DEGs were presented in **Figure 1C**, in which the interaction score was set as 0.4. The correlation between CASP1 and CASP5 was consistent in the protein level.

Construction of Prognostic Model Based on DEGs

A total of 65 EAC patients with available survival data were included in our study. Univariate Cox regression analysis was initially performed to assess the prognostic value of DEGs

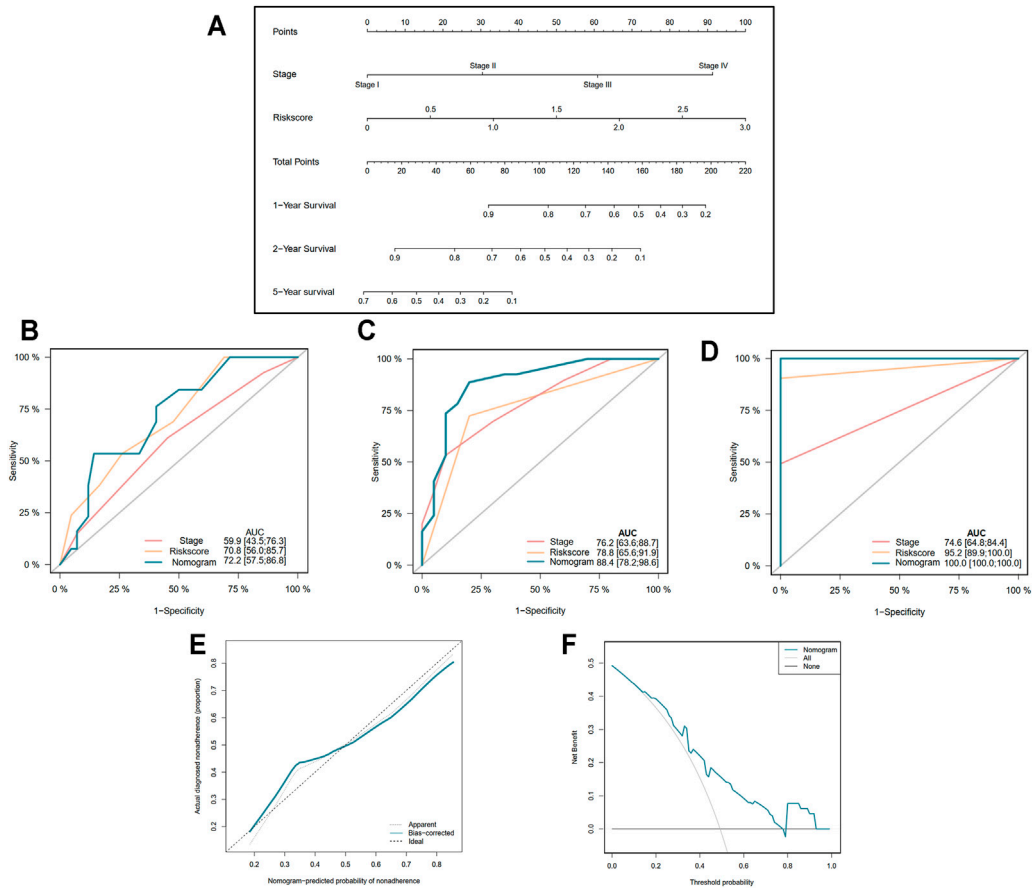

FIGURE 5 | Construction of nomogram based on the pyroptosis-related five-gene signature. **(A)** Nomogram for predicting 1-, 2-, and 5-year survival of EAC patients. **(B–D)** Receiver operating characteristic (ROC) curve evaluating the efficiency of nomogram for 1-, 2-, and 5-year survival of patients. **(E)** Calibration curve of nomogram. **(F)** Decision curve analysis (DCA) curve of the nomogram.

(**Figure 2A**). Among them, six genes (*CASP1, CASP5, GSDMB, IL1B, PYCARD*, and *ZBP1*) were with p value <0.2, and higher expressions of *CASP1, CASP5,* and *IL1B* were associated with increased risk (HR > 1), while upregulated expressions of *GSDMB, PYCARD,* and *ZBP1* were correlated with lower risk (HR < 1). Subsequently, LASSO Cox regression analysis retrieved five genes for prognostic model construction based on the optimum λ value (**Figures 2B,C**). The calculation of the risk score was as follows: Risk score = (0.042 × exp*CASP1*) + (−0.025 × exp*GSDMB*) + (0.021 × expIL1B) + (−0.037 × exp*PYCARD*) + (−0.243 × exp*ZBP1*). According to the calculated median risk score, 65 patients were divided into two groups (32 in the high-risk group and 33 in the low-risk group), and the clinical information is shown in **Figure 3A**. The PCA illustrated that patients were well divided into two clusters (**Figure 3B**). The distributions of the risk score and survival time are shown in **Figures 3C,D**. The OS of the high-risk group was significantly worse than that of the low-risk group (p = 0.0012, **Figure 3E**). ROC analysis of the risk model indicated that the AUC for 1, 2, and 5-year survival was 0.708, 0.815, and 0.952, respectively (**Figures 3F–H**). Both of the univariate and multivariate Cox regression analyses showed that the pyroptosis-related gene signature independently predicted the prognosis of EAC patients (**Figures 3I,J**).

Verification of the Gene Signature by the External Dataset

Information of 60 EAC patients from the GSE13898 dataset of GEO with available survival data was used for the validation of the gene signature. The expressions of the available differentially expressed pyroptosis-related genes are shown in **Supplementary Figure S1**. The patients were subdivided into the low- and high-risk groups, respectively, as described above. PCA illustrated well the separation of patients between the two groups (**Figure 4A**). The distribution of the risk score and the survival time is demonstrated in **Figures 4B,C**. Patients in the low-risk group were with significantly higher survival rates than those in the high-risk group (p = 0.003; **Figure 4D**). According to the ROC curve, the 1- and 2-year survival prediction models were with AUCs of 0.678 and 0.663 (**Figures 4E,F**), respectively, while the 5-year survival prediction model could not be generated due to insufficient data. The risk score in our model could also serve as an

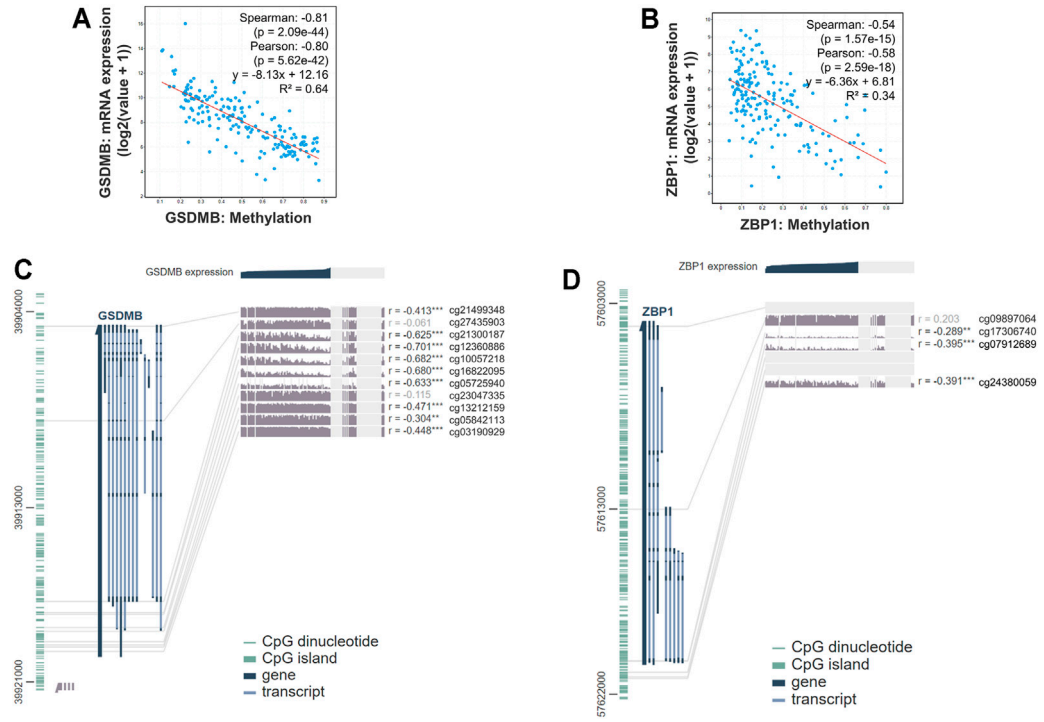

FIGURE 6 | Gene expression and methylation status in EAC. The correlation between *GSDMB* **(A)** and *ZBP1* **(B)** methylation with RNA expressions by analysis using the cBioPortal database. Detailed information on methylated probes of *GSDMB* **(C)** and *ZBP1* **(D)** by analysis using the MEXPRESS database.

independent prognostic factor in the validation cohort (**Figures 4G,H**).

Construction of Nomogram Based on the Gene Signature and Clinical Data

In order to more precisely predict the prognosis of EAC patients, the TNM stage was used to construct a nomogram model as shown in **Figure 5A** (C-index = 0.764 ± 0.046). The AUCs of the nomogram for predicting 1-, 2-, and 5-year survival were 0.722, 0.884, and 1.000, respectively (**Figures 5B–D**). The calibration curve indicated an ideal prediction of the nomogram (**Figure 5E**). **Figure 5F** shows that when the nomogram-predicted probability ranged from 15% to 80%, the nomogram provided extra value relative to the treat-all-patients scheme or the treat-none scheme.

The Expressions of GSDMB and ZBP1 Within the Signature Are Downregulated by Hypermethylation

Epigenetic regulations including DNA methylation affect gene expression and modulate various cellular responses in tumorigenesis. Therefore, we further explored the mechanisms that might be involved in controlling the expressions of genes involved in the signature. We found that the RNA expressions of *GSDMB* (Spearman: −0.81, p = 2.09e-44; Pearson: −0.80, p = 5.62e-42, R^2 = 0.64) and *ZBP1* (Spearman: −0.54, p = 1.57e-15; Pearson: −0.58, p = 2.59e-18, R^2 = 0.34) were significantly correlated with the DNA methylation status (**Figures 6A,B**), whereas the association between RNA expressions of *CASP1, IL1B*, and *PYCARD* and DNA methylation was nonsignificant (**Supplementary Figure S2**). Analysis by the MEXPRESS database further identified the detailed information of the methylated probes and their correlation with *GSDMB* (**Figure 6C**) and *ZBP1* (**Figure 6D**) RNA expressions, suggesting that the expressions of *GSDMB* and *ZBP1* could be regulated by epigenetic mechanisms.

Differential Expression Analysis Reveals Immune-Correlated Pathways

A total of 527 DEGs between the low- and high-risk groups were extracted according to the threshold described above. A total of 310 genes were downregulated in the high-risk group, while 217 genes were upregulated in the low-risk group. On the basis of the DEGs, GO enrichment and KEGG pathway analyses were performed. The results from GO enrichment analysis demonstrated that the DEGs were mainly associated with the regulation of cytokine production, cytokine activity, and humoral immune response pathways (**Figures 7A,B**) in the TCGA cohort. KEGG pathway analysis showed that the DEGs were principally associated with the cytokine–cytokine receptor interaction and IL-17 signaling pathways (**Figures 7C,D**) in the TCGA cohort. Detailed information for the deregulated pathways is shown in **Supplementary Figures**

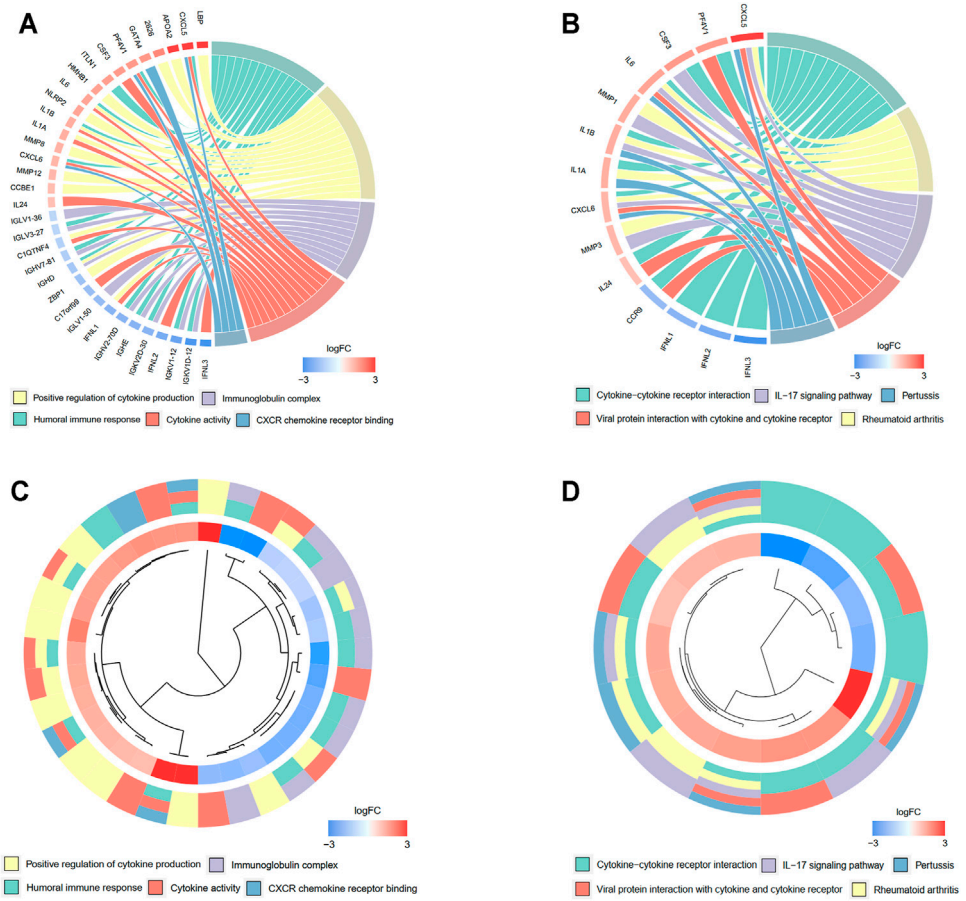

FIGURE 7 | Functional enrichment analysis of differentially regulated genes (DEGs) between low- and high-risk groups. **(A, B)** Chord plot demonstrating the linkage of genes and assigned term by GO **(A)** and KEGG **(B)** pathway enrichment analysis. **(C, D)** Cluster plot of the expression profiles. The inner ring shows the color-coded logFC, while the outer ring illustrates the assigned functional terms by GO **(C)** and KEGG **(D)** pathway enrichment analysis.

TABLE 1 | List of the five most significant small molecular compounds to potentially reverse altered expression of differentially expressed genes (DEGs) in the high-risk group.

Name	Score	Description	Target	MOA
GDC-0879	−93.76	RAF inhibitor	BRAF	RAF inhibitor
PD-0325901	−91.95	MEK inhibitor	MAP2K1, MAP2K2	MEK inhibitor, MAP kinase inhibitor, Protein kinase inhibitor
VER-155008	−89.75	HSP inhibitor	HSPA1A	HSP inhibitor
torin-2	−87.13	MTOR inhibitor	MTOR	MTOR inhibitor
GR-206	−86.62	Aryl hydrocarbon receptor ligand	—	Aryl hydrocarbon receptor ligand

MOA, mechanisms of action; MEK, mitogen-activated protein kinase kinase; MAP, mitogen-activated protein; HSP, heat shock protein; MTOR, mammalian target of rapamycin.

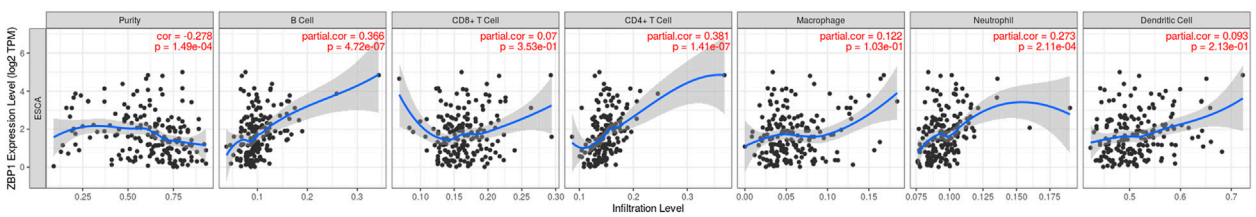

FIGURE 8 | Correlations between immune cells and selected genes. ZBP1 and immune cells in esophageal cancer.

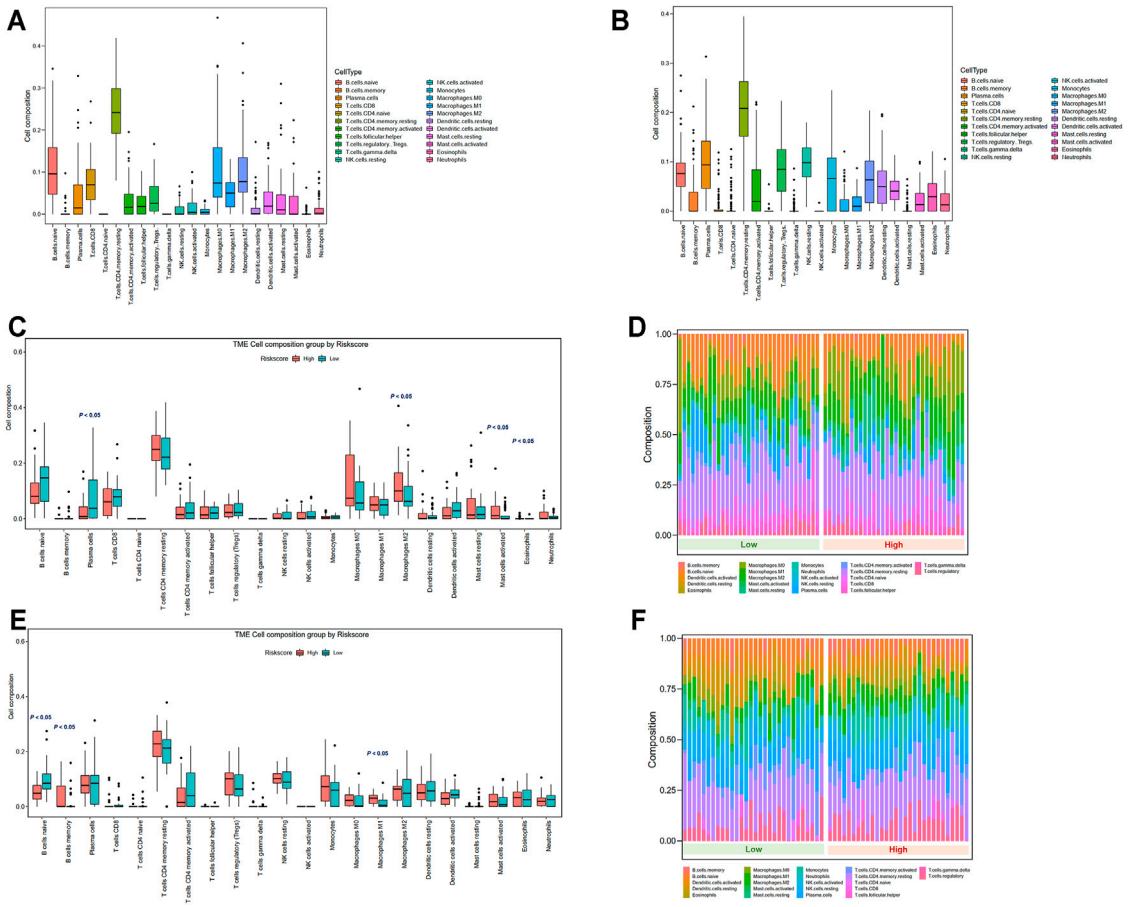

FIGURE 9 | Tumor microenvironment immune cell composition in low- and high-risk groups. **(A)** Overview of immune cell composition in the TCGA cohort. **(B)** Overview of immune cell composition in the GSE13898 cohort. **(C, D)** Differences in immune cell composition in the TCGA cohort classified by risk groups by Wilcoxon test. **(E, F)** Differences in immune cell composition in the GSE13898 cohort classified by risk groups by Wilcoxon test.

S3A–D. Similarly, the GO analysis in the GSE13898 cohort demonstrated that immune-related pathways, including neutrophil activation for immune response, neutrophil-mediated immunity, and cytokine and chemokine receptor binding pathways, were deregulated between the two groups divided by the risk score (**Supplementary Figures S4A, 3B**). The DEGs in the GSE13898 cohort were also associated with the IL-17 signaling pathway (**Supplementary Fig. S4C, 3D**).

Pyroptosis-Related Gene Signature Is Related to the Immune Status of EAC

The CMap analysis was performed to screen for small-molecular drugs that are able to revert the pyroptosis signature-related pathways, which contribute to a high-risk state. A total of 730 drugs with negative scores were identified (**Supplementary Table S3**). The RAF inhibitor GDC-0879 (score: −93.76), mitogen-activated protein kinase kinase (MEK) inhibitor PD-0325901 (score: −91.95), heat shock protein (HSP) inhibitor VER-155008 (score: −89.75), mitogen-activated protein (MTOR) inhibitor torin-2 (score: −87.13), and aryl hydrocarbon receptor ligand GR-206 (score: −86.62) were the top five small-molecular drugs based on inhibition scores (**Table 1**).

Pyroptosis-Related Gene Signature Is Related to the Immune Status of EAC

To explore the correlation between the selected pyroptosis-related genes and gene-based signature with the immune microenvironment of EAC, analysis by the TIMER database for each gene was initially performed. The results indicated that *ZBP1* expression was most significantly correlated with the infiltration signature of esophageal cancer, in which infiltrations of B cells (correlation coefficient = 0.366, p = 4.72e-07) and $CD4^+$ T cells (correlation coefficient = 0.381, p = 1.41e-07) were with the most remarkable correlations (**Figure 8A**, **Supplementary Figure S5**). In addition, somatic copy number alterations of *ZBP1* were correlated with the infiltration levels of B cells, $CD8^+$ T cells, macrophages, and dendritic cells (**Figure 8B**).

The variations in the abundance of immune cell infiltration between low- and high-risk groups were further explored. The

immune cells were analyzed in the TCGA (**Supplementary Table S4**) and GSE13898 cohorts (**Supplementary Table S5**). The overview of immune cell compositions is illustrated in **Figure 9A** for the TCGA cohort and in **Figure 9B** for the GSE13898 cohort. The high-risk group in the TCGA cohort possessed significantly higher infiltration levels of M2 macrophages, activated mast cells, and eosinophils, whereas the infiltration levels of plasma cells were significantly lower (**Figures 9C,D**). By contrast, the infiltration levels of memory B cells and M1 macrophages were upregulated in the high-risk group of the GSE13898 cohort, while those of naïve B cells were significantly downregulated (**Figures 9E,F**).

DISCUSSION

Cell death serves as an essential barrier against the development of cancer, and pyroptosis is one of the major forms of programmed cell death (Bertheloot et al., 2021). However, the role of pyroptosis in EAC remains largely unclear. In the present study, we comprehensively evaluated the pyroptosis-related gene profiles in EAC and constructed a novel five-gene risk signature (*CASP1, GSDMB, IL1B, PYCARD,* and *ZBP1*) by LASSO Cox regression analysis. The five-gene signature showed good performance for predicting EAC prognosis in both the internal and external validation cohorts. Within the signature, *GSDMB* expression is distinctly correlated with the methylation status. Further enrichment analyses revealed that the DEGs between the low- and high-risk groups were correlated with immune-related pathways. The RAF inhibitor GDC-0879 and the MEK inhibitor PD-0325901 might be promising in reverting the pyroptosis-related pathways in the high-risk EAC patients. Tumor immune microenvironment analyses indicated that high-risk patients had decreased levels of infiltrating active immune cells and higher proportions of quiescent immune-cell infiltration.

For the components within the signature, Gasdermin B (GSDMB) belongs to the GSDM family and is more broadly expressed compared to other GSDM family members (Saeki et al., 2009). The cleavage of GSDMB induced by lymphocyte-derived granzyme A triggers pyroptosis (Zhou et al., 2020). Therefore, the downregulation of *GSDMB* is associated with poorer prognosis of the patients. Caspase 1 encoded by *CASP1* is a member of the caspase family, which is activated by inflammasomes and induces pyroptosis (Miao et al., 2011). By contrast, caspase 1 can direct T cell-independent tumor proliferation and correlates with a poorer prognosis (Zeng et al., 2018). Interleukin 1 beta (IL-1β) is a proinflammatory cytokine involved in pyroptosis. CASP-1 directly cleaves GSMD and precursor cytokines into pro-IL-1β, which initiates pyroptosis and maturation of IL-1β, respectively (Man et al., 2017). IL-1β has pro-tumorigenic effects by promoting proliferation, migration, metastasis, and angiogenesis (Gelfo et al., 2020; Rébé and Ghiringhelli, 2020). In the present study, *CASP1* and *IL1B* upregulation is associated with a worse prognosis of EAC patients. Apoptosis-associated speck-like protein containing a CARD (ASC/PYCARD) is encoded by the *PYCARD* gene and contains a caspase activation and recruitment domain (CARD) for binding and facilitating the activation of caspase 1 (Bergsbaken et al., 2009). The dual role of the inflammasome adaptor PYCARD is identified in cancer cells, and therefore, PYCARD can be associated with lower cancer risks (Protti and De Monte, 2020). Z-DNA-binding protein 1 (ZBP1)-NLR Family Pyrin Domain Containing 3 (NLRP3) is critical in inducing pyroptosis by leading to cytokine maturation and GSDMD cleavage (Zheng and Kanneganti, 2020). *ZBP1* expression was found to reduce tumor cell motility and chemotaxis, which decreased the potential of metastasis of tumor cells (Lapidus et al., 2007). ZBP1 stabilizes intercellular connections and focal adhesions, which suppresses breast cancer cell invasion (Gu et al., 2012). *PYCARD* and *ZBP1* were identified as downregulated in the high-risk EAC populations. Therefore, inflammasome components might exert different effects in tumor development and progression depending on the biological context, and further investigations are needed.

Epigenetic regulation mechanisms, particularly DNA methylation, modify gene expression and regulate various cellular responses in cancer including proliferation, invasion, apoptosis, and senescence (Cheng et al., 2019). Our study reveals that *GSDMB* promoter hypermethylation most notably induces decreased expression levels, indicating that methylation is essential for the regulation of pyroptosis in EAC. In recent years, epigenetic drugs are emerging, and hundreds of clinical trials are ongoing for investigating the effects of anti-DNA methylation therapies (Cheng et al., 2019). Therefore, our results suggest that epigenetics-targeted therapy is a promising strategy for future anticancer therapeutics in part by modulating the pyroptosis-related genes. Nomograms are promising for use in clinical practice for evaluating the prognosis of EAC patients, in which the survival can be predicted using specific parameters. As indicated by the ROC curves, the nomogram demonstrates high predictive accuracy and sensitivity. Compared to the conventional TNM staging and a previously developed ferroptosis-related gene signature (AUC = 0.744) in EAC (Zhu et al., 2021), the pyroptosis-related gene signature-based nomogram, which integrates gene expression profiles and clinical parameters, more effectively predicts the prognosis of EAC patients. In addition, the prognostic value of our signature is better than the DNA repair-based gene signature (AUC = 0.759) in esophageal cancer (Wang et al., 2021). The prognostic value for 3- and 5-year survival is also higher than a recently developed signature based on nine immune-related genes for esophageal cancer (AUC = 0.826) (Zhang et al., 2021). The use of nomogram based on integrated information can facilitate the prediction of prognosis, clinical decision-making, and patient counseling (Bobdey et al., 2018).

The tumor immune microenvironment is diverge and complex, which contributes to tumorigenesis and modulates the effects of immunotherapy to a large extent. Current studies on lymphocytes in tumor immunity predominantly focus on T cells, while the protective effect of B cells has also been revealed (Wang et al., 2019). By contrast, mast cells have been reported to induce cancer growth (Maciel et al., 2015). Activated T cells, natural killer cells, and macrophages are potent suppressors that mediate the tumor microenvironment and exert antitumor functions (Lin et al.,

2013; Nurieva et al., 2019; Cózar et al., 2021). Although some of the comparisons were not statistically different and might be contributed by the limited number of samples in both cohorts, accumulation of immune cells that promote cancer in the tumor microenvironment was generally observed in the high-risk group in both the TCGA and GEO cohorts, while the compositions of tumor-protective immune cells were reduced compared to the low-risk group.

The strength of our study is that a systemic analysis was performed based on the TCGA and GEO cohorts, and the pyroptosis-related genes were assessed for the first time. Limitations also exist in our study. Current publicly available datasets are limited in both number and size, and therefore, validation of our prediction model in large-scale EAC cohorts could be performed in future studies. In addition, based on the information of our study, further *in vitro* and *in vivo* studies could be conducted to evaluate the function and mechanisms of pyroptotic regulation in EAC. Despite the limitations, our study has provided a comprehensive overview of pyroptosis-related gene profiles in EAC.

In summary, we identified differentially expressed pyroptosis-related genes and developed a novel five-gene pyroptosis signature that significantly correlates with the survival of EAC patients. The pyroptosis-based signature is an independent prognostic factor and performs better than the TNM stage, which is promising for clinical application. Moreover, GSDMB expression is notably correlated with methylation status, and the signature is related to antitumor immunity in the tumor microenvironment. Modulating pyroptosis, epigenetic mechanisms, and immune microenvironment by drug discovery might be promising for improving the prognosis of patients. Further studies exploring the regulating patterns are warranted.

DATA AVAILABILITY STATEMENT

The datasets presented in this study can be found in online repositories. The names of the repository/repositories and accession number(s) can be found in the article/**Supplementary Material**.

AUTHOR CONTRIBUTIONS

RZ and SH acquired the data, performed the analysis, and wrote the manuscript. XQ was involved in the analysis, data interpretation, and revision of the manuscript. ZZ and HW participated in data analysis. HC, WS, and LJ were involved in study design, supervision, and acquiring funding.

FUNDING

This work is supported by the National Natural Science Foundation of China (grant numbers 82171698, 82170561, 81741067, and 81300279), the Natural Science Foundation for Distinguished Young Scholars of Guangdong Province (grant number 2021B1515020003), and the Climbing Program of Introduced Talents and High-Level Hospital Construction Project of Guangdong Provincial People's Hospital (grant numbers DFJH201803, KJ012019099, KJ012021143, and KY012021183).

ACKNOWLEDGMENTS

The authors thank Prof. Ju-Seog Lee for kindly providing the data of the GSE13898 cohort.

SUPPLEMENTARY MATERIAL

The Supplementary Material for this article can be found online at: https://www.frontiersin.org/articles/10.3389/fphar.2021.767187/full#supplementary-material

REFERENCES

Alsop, B. R., and Sharma, P. (2016). Esophageal Cancer. *Gastroenterol. Clin. North. Am.* 45, 399–412. doi:10.1016/j.gtc.2016.04.001

Bergsbaken, T., Fink, S. L., and Cookson, B. T. (2009). Pyroptosis: Host Cell Death and Inflammation. *Nat. Rev. Microbiol.* 7, 99–109. doi:10.1038/nrmicro2070

Bertheloot, D., Latz, E., and Franklin, B. S. (2021). Necroptosis, Pyroptosis and Apoptosis: an Intricate Game of Cell Death. *Cell Mol Immunol* 18, 1106–1121. doi:10.1038/s41423-020-00630-3

Blanche, P., Dartigues, J. F., and Jacqmin-Gadda, H. (2013). Estimating and Comparing Time-dependent Areas under Receiver Operating Characteristic Curves for Censored Event Times with Competing Risks. *Stat. Med.* 32, 5381–5397. doi:10.1002/sim.5958

Bobdey, S., Mair, M., Nair, S., Nair, D., Balasubramaniam, G., and Chaturvedi, P. (2018). A Nomogram Based Prognostic Score that Is superior to Conventional TNM Staging in Predicting Outcome of Surgically Treated T4 Buccal Mucosa Cancer: Time to Think beyond TNM. *Oral Oncol.* 81, 10–15. doi:10.1016/j.oraloncology.2018.04.002

Chen, B., Khodadoust, M. S., Liu, C. L., Newman, A. M., and Alizadeh, A. A. (2018). "Profiling Tumor Infiltrating Immune Cells with CIBERSORT," in *Cancer Systems Biology* (Clifton, NJ: Springer), 243–259. doi:10.1007/978-1-4939-7493-1_12

Cheng, Y., He, C., Wang, M., Ma, X., Mo, F., Yang, S., et al. (2019). Targeting Epigenetic Regulators for Cancer Therapy: Mechanisms and Advances in Clinical Trials. *Signal. Transduct Target. Ther.* 4, 62–39. doi:10.1038/s41392-019-0095-0

Cózar, B., Greppi, M., Carpentier, S., Narni-Mancinelli, E., Chiossone, L., and Vivier, E. (2021). Tumor-infiltrating Natural Killer Cells. *Cancer Discov.* 11, 34–44. doi:10.1158/2159-8290.CD-20-0655

Csardi, G., and Nepusz, T. (2006). The Igraph Software Package for Complex Network Research. *InterJournal, complex Syst.* 1695, 1–9.

Friedman, J., Hastie, T., and Tibshirani, R. (2010). Regularization Paths for Generalized Linear Models *via* Coordinate Descent. *J. Stat. Softw.* 33, 1–22. doi:10.18637/jss.v033.i01

Gelfo, V., Romaniello, D., Mazzeschi, M., Sgarzi, M., Grilli, G., Morselli, A., et al. (2020). Roles of IL-1 in Cancer: From Tumor Progression to Resistance to Targeted Therapies. *Int. J. Mol. Sci.* 21, 6009. doi:10.3390/ijms21176009

Gu, W., Katz, Z., Wu, B., Park, H. Y., Li, D., Lin, S., et al. (2012). Regulation of Local Expression of Cell Adhesion and Motility-Related mRNAs in Breast Cancer Cells by IMP1/ZBP1. *J. Cel Sci* 125, 81–91. doi:10.1242/jcs.086132

Harrell, F. E., Jr, Harrell, M. F. E., Jr, and Hmisc, D. (2017). *Package 'rms'*. Vanderbilt University 229. Available at: http://CRAN.R-project.org/package = rms 2017.

Karki, R., and Kanneganti, T. D. (2019). Diverging Inflammasome Signals in Tumorigenesis and Potential Targeting. *Nat. Rev. Cancer* 19, 197–214. doi:10.1038/s41568-019-0123-y

Kassambara, A., and Kassambara, M. A. (2019). *Package 'ggcorrplot'. R Package.* version 0.1 3. Available at: https://cran.r-project.org/package=ggcorrplot.

Kassambara, A., Kosinski, M., Biecek, P., and Fabian, S. (2017). Survminer: Drawing Survival Curves Using'ggplot2. R. Package Version 0.3 1. Available at: https://cran.r-project.org/web/packages/ggplot2.

Kim, S. M., Park, Y. Y., Park, E. S., Cho, J. Y., Izzo, J. G., Zhang, D., et al. (2010). Prognostic Biomarkers for Esophageal Adenocarcinoma Identified by Analysis of Tumor Transcriptome. *PloS one* 5, e15074. doi:10.1371/journal.pone.0015074

Klingelhöfer, D., Zhu, Y., Braun, M., Brüggmann, D., Schöffel, N., and Groneberg, D. A. (2019). A World Map of Esophagus Cancer Research: a Critical Accounting. *J. Transl Med.* 17, 150. doi:10.1186/s12967-019-1902-7

Lamb, J., Crawford, E. D., Peck, D., Modell, J. W., Blat, I. C., Wrobel, M. J., et al. (2006). The Connectivity Map: Using Gene-Expression Signatures to Connect Small Molecules, Genes, and Disease. *science* 313, 1929–1935. doi:10.1126/science.1132939

Lapidus, K., Wyckoff, J., Mouneimne, G., Lorenz, M., Soon, L., Condeelis, J. S., et al. (2007). ZBP1 Enhances Cell Polarity and Reduces Chemotaxis. *J. Cel Sci.* 120, 3173–3178. doi:10.1242/jcs.000638

Li, T., Fan, J., Wang, B., Traugh, N., Chen, Q., Liu, J. S., et al. (2017). TIMER: A Web Server for Comprehensive Analysis of Tumor-Infiltrating Immune Cells. *Cancer Res.* 77, e108–e110. doi:10.1158/0008-5472.CAN-17-0307

Lin, Y. C., Mahalingam, J., Chiang, J. M., Su, P. J., Chu, Y. Y., Lai, H. Y., et al. (2013). Activated but Not Resting Regulatory T Cells Accumulated in Tumor Microenvironment and Correlated with Tumor Progression in Patients with Colorectal Cancer. *Int. J. Cancer* 132, 1341–1350. doi:10.1002/ijc.27784

Maciel, T. T., Moura, I. C., and Hermine, O. (2015). The Role of Mast Cells in Cancers. *F1000prime Rep.* 7, 09. doi:10.12703/P7-09

Man, S. M., and Kanneganti, T. D. (2015). Regulation of Inflammasome Activation. *Immunol. Rev.* 265, 6–21. doi:10.1111/imr.12296

Man, S. M., Karki, R., and Kanneganti, T. D. (2017). Molecular Mechanisms and Functions of Pyroptosis, Inflammatory Caspases and Inflammasomes in Infectious Diseases. *Immunol. Rev.* 277, 61–75. doi:10.1111/imr.12534

Miao, E. A., Rajan, J. V., and Aderem, A. (2011). Caspase-1-induced Pyroptotic Cell Death. *Immunol. Rev.* 243, 206–214. doi:10.1111/j.1600-065X.2011.01044.x

Nurieva, R. I., Liu, Z., Gangadharan, A., Bieerkehazhi, S., Zhao, Y.-Z., Alekseev, A., et al. (2019). Function of T Follicular Helper Cells in Anti-tumor Immunity. *Am. Assoc. Immnol.* 202 (1 Supplement), 138.18.

Ozenne, B., Sørensen, A. L., Scheike, T., Torp-Pedersen, C., and Gerds, T. A. (2017). riskRegression: Predicting the Risk of an Event Using Cox Regression Models. *R. J.* 9, 440–460. doi:10.32614/rj-2017-062

Protti, M. P., and De Monte, L. (2020). Dual Role of Inflammasome Adaptor ASC in Cancer. *Front Cel Dev Biol.* 8, 40. doi:10.3389/fcell.2020.00040

Rébé, C., and Ghiringhelli, F. (2020). Interleukin-1β and Cancer. *Cancers (Basel)* 12, 1791. doi:10.3390/cancers12071791

Ritchie, M. E., Phipson, B., Wu, D., Hu, Y., Law, C. W., Shi, W., et al. (2015). Limma powers Differential Expression Analyses for RNA-Sequencing and Microarray Studies. *Nucleic Acids Res.* 43, e47. doi:10.1093/nar/gkv007

Saeki, N., Usui, T., Aoyagi, K., Kim, D. H., Sato, M., Mabuchi, T., et al. (2009). Distinctive Expression and Function of Four GSDM Family Genes (GSDMA-D) in normal and Malignant Upper Gastrointestinal Epithelium. *Genes Chromosomes Cancer* 48, 261–271. doi:10.1002/gcc.20636

Shi, J., Gao, W., and Shao, F. (2017). Pyroptosis: Gasdermin-Mediated Programmed Necrotic Cell Death. *Trends Biochem. Sci.* 42, 245–254. doi:10.1016/j.tibs.2016.10.004

Shi, J., Zhao, Y., Wang, Y., Gao, W., Ding, J., Li, P., et al. (2014). Inflammatory Caspases Are Innate Immune Receptors for Intracellular LPS. *Nature* 514, 187–192. doi:10.1038/nature13683

Sung, H., Ferlay, J., Siegel, R. L., Laversanne, M., Soerjomataram, I., Jemal, A., et al. (2021). Global Cancer Statistics 2020: GLOBOCAN Estimates of Incidence and Mortality Worldwide for 36 Cancers in 185 Countries. *CA Cancer J. Clin.* 71, 209–249. doi:10.3322/caac.21660

Szklarczyk, D., Gable, A. L., Lyon, D., Junge, A., Wyder, S., Huerta-Cepas, J., et al. (2019). STRING V11: Protein-Protein Association Networks with Increased Coverage, Supporting Functional Discovery in Genome-wide Experimental Datasets. *Nucleic Acids Res.* 47, D607–d613. doi:10.1093/nar/gky1131

Team, R. C., Bivand, R., Carey, V. J., Debroy, S., Eglen, S., Guha, R., et al. (2020). *Package 'foreign'*. Available at: https://cran.r-project.org/web/packages/foreign.

Therneau, T. M., and Lumley, T. (2015). Package 'survival. *R. Top. Doc.* 128, 28–33.

Tsuchiya, K. (2020). Inflammasome-associated Cell Death: Pyroptosis, Apoptosis, and Physiological Implications. *Microbiol. Immunol.* 64, 252–269. doi:10.1111/1348-0421.12771

Van Opdenbosch, N., and Lamkanfi, M. (2019). Caspases in Cell Death, Inflammation, and Disease. *Immunity* 50, 1352–1364. doi:10.1016/j.immuni.2019.05.020

Vande Walle, L., and Lamkanfi, M. (2016). Pyroptosis. *Curr. Biol.* 26, R568–r572. doi:10.1016/j.cub.2016.02.019

Walter, W., Sánchez-Cabo, F., and Ricote, M. (2015). GOplot: an R Package for Visually Combining Expression Data with Functional Analysis. *Bioinformatics* 31, 2912–2914. doi:10.1093/bioinformatics/btv300

Wang, B., and Yin, Q. (2017). AIM2 Inflammasome Activation and Regulation: A Structural Perspective. *J. Struct. Biol.* 200, 279–282. doi:10.1016/j.jsb.2017.08.001

Wang, L., Li, X., Zhao, L., Jiang, L., Song, X., Qi, A., et al. (2021). Identification of DNA-Repair-Related Five-Gene Signature to Predict Prognosis in Patients with Esophageal Cancer. *Pathol. Oncol. Res.* 27, 25. doi:10.3389/pore.2021.596899

Wang, S. S., Liu, W., Ly, D., Xu, H., Qu, L., and Zhang, L. (2019). Tumor-infiltrating B Cells: Their Role and Application in Anti-tumor Immunity in Lung Cancer. *Cel Mol Immunol.* 16, 6–18. doi:10.1038/s41423-018-0027-x

Xia, X., Wang, X., Cheng, Z., Qin, W., Lei, L., Jiang, J., et al. (2019). The Role of Pyroptosis in Cancer: Pro-cancer or Pro-"host. *Cell Death Dis.* 10, 650. doi:10.1038/s41419-019-1883-8

Yu, G., Wang, L. G., Han, Y., and He, Q. Y. (2012). clusterProfiler: an R Package for Comparing Biological Themes Among Gene Clusters. *OMICS* 16, 284–287. doi:10.1089/omi.2011.0118

Yu, P., Zhang, X., Liu, N., Tang, L., Peng, C., and Chen, X. (2021). Pyroptosis: Mechanisms and Diseases. *Signal. Transduct Target. Ther.* 6, 128. doi:10.1038/s41392-021-00507-5

Zeng, Q., Fu, J., Korrer, M., Gorbounov, M., Murray, P. J., Pardoll, D., et al. (2018). Caspase-1 from Human Myeloid-Derived Suppressor Cells Can Promote T Cell-independent Tumor Proliferation. *Cancer Immunol. Res.* 6, 566–577. doi:10.1158/2326-6066.CIR-17-0543

Zhang, Z., Chen, C., Fang, Y., Li, S., Wang, X., Sun, L., et al. (2021). Development of a Prognostic Signature for Esophageal Cancer Based on Nine Immune Related Genes. *BMC Cancer* 21, 113. doi:10.1186/s12885-021-07813-9

Zheng, M., and Kanneganti, T. D. (2020). The Regulation of the ZBP1-NLRP3 Inflammasome and its Implications in Pyroptosis, Apoptosis, and Necroptosis (PANoptosis). *Immunol. Rev.* 297, 26–38. doi:10.1111/imr.12909

Zhou, Z., He, H., Wang, K., Shi, X., Wang, Y., Su, Y., et al. (2020). Granzyme A from Cytotoxic Lymphocytes Cleaves GSDMB to Trigger Pyroptosis in Target Cells. *Science* 368. doi:10.1126/science.aaz7548

Zhu, L., Yang, F., Wang, L., Dong, L., Huang, Z., Wang, G., et al. (2021). Identification the Ferroptosis-Related Gene Signature in Patients with Esophageal Adenocarcinoma. *Cancer Cel Int* 21, 124. doi:10.1186/s12935-021-01821-2

Conflict of Interest: The authors declare that the research was conducted in the absence of any commercial or financial relationships that could be construed as a potential conflict of interest.

Publisher's Note: All claims expressed in this article are solely those of the authors and do not necessarily represent those of their affiliated organizations, or those of the publisher, the editors and the reviewers. Any product that may be evaluated in this article, or claim that may be made by its manufacturer, is not guaranteed or endorsed by the publisher.

frontiers in Pharmacology

REVIEW
published: 22 November 2021
doi: 10.3389/fphar.2021.771588

Acetylation in Tumor Immune Evasion Regulation

Jun Lu[1,2†], *Xiang He*[2,3†], *Lijuan Zhang*[4†], *Ran Zhang*[1*] *and Wenzheng Li*[4*]

[1]Hunan Normal University School of Medicine, Changsha, China, [2]Key Laboratory of Molecular Radiation Oncology Hunan Province, Changsha, China, [3]Xiangya Cancer Center, Xiangya Hospital, Central South University, Changsha, China, [4]Department of Radiology, Xiangya Hospital, Central South University, Changsha, China

Acetylation is considered as one of the most common types of epigenetic modifications, and aberrant histone acetylation modifications are associated with the pathological process of cancer through the regulation of oncogenes and tumor suppressors. Recent studies have shown that immune system function and tumor immunity can also be affected by acetylation modifications. A comprehensive understanding of the role of acetylation function in cancer is essential, which may help to develop new therapies to improve the prognosis of cancer patients. In this review, we mainly discussed the functions of acetylase and deacetylase in tumor, immune system and tumor immunity, and listed the information of drugs targeting these enzymes in tumor immunotherapy.

Keywords: acetylated modifications, tumor immunity, acetylases, deacetylases, cancer immunotherapy

OPEN ACCESS

Edited by:
Yi-Chao Zheng,
Zhengzhou University, China

Reviewed by:
Ercan Cacan,
Gaziosmanpaşa University, Turkey
Dapeng Dai,
Beijing Hospital, China

***Correspondence:**
Wenzheng Li
wenzhen727@163.com
Ran Zhang
ZR13971@hunnu.edu

†These authors have contributed equally to this work and share first authorship

Specialty section:
This article was submitted to Experimental Pharmacology and Drug Discovery, a section of the journal Frontiers in Pharmacology

Received: *06 September 2021*
Accepted: *05 November 2021*
Published: *22 November 2021*

Citation:
Lu J, He X, Zhang L, Zhang R and Li W (2021) Acetylation in Tumor Immune Evasion Regulation. Front. Pharmacol. 12:771588. doi: 10.3389/fphar.2021.771588

INTRODUCTION

The main driving force for tumor initiation and progression are not only the alterations in cancer cells but also the influences of immune system and tumor immune microenvironments (Bindea et al., 2013; Jones et al., 2019). As an important hallmark of cancer, tumor cells evade immune surveillance by suppressing the immune system and having low immunogenicity (Peng et al., 2019; Gao et al., 2020). For example, aberrant expression of immune checkpoints (ICs) components, such as the programmed cell death protein 1 (PD-1), cytotoxic T lymphocyte-associated protein 4 (CTLA-4), T-cell immunoglobulin and mucin domain-containing lymphocyte activation gene 3 (LAG-3), and LAG-3 with Ig and ITIM structural domains T-cell immune receptors (TIGIT), creates an immune destructive environment that promotes tumor cells escape immune destructions (Saleh et al., 2020). *Cancer* immunotherapies such as cancer vaccines, adoptive T-cell therapy (ACT), and immune checkpoint blockade (ICB), which kills cancer cells through employing the body's own immune system, have achieved encouraging progress within the last decade (Wang S. et al., 2019). Despite these breakthroughs, only 10–30% of patients respond to and benefit from them, and the underlying reasons of these low benefits are due to the development of primary and acquired drug resistance, low response frequency of some cancers, and the heterogeneity of tumors (Sharma et al., 2017). Therefore, the urgent question is how to enhance patient responsivity and benefit from immunotherapy by targeting tumor cells or modulating tumor immune microenvironment.

Recently, there is growing evidence showing that epigenetic modification is essential to regulation of tumor immunity and immunotherapy, which provides a possible target for improving the outcome of immunotherapy. Epigenetic gene regulation, which alters gene expression and function without involving alterations in DNA sequences, is an important regulatory process in cellular biology. Several types of epigenetic modification were identified such as DNA methylation, histone modification, miRNA regulation, genomic imprinting, and chromosome remodeling, among which acetylation is considered one of the most common types of epigenetic modification (Lawrence et al.,

TABLE1 | Function of HATs related to tumor immunity in different cell types.

Protein	Cell type	Target	Function	References
PCAF	Tregs	Foxp3	acetylate Foxp3 to impair Tregs function	Liu et al. (2019c)
	Macrophages	TNF-α, IL-6 and CXCL10	inhibit the inflammatory response of M1 macrophages	Wang et al. (2021)
	CD4 and CD8 T Cells	Foxp3	reduce tumor volume and improves anti-tumor immunity	Liu et al. (2019c)
GCN5	Tregs	ISG	regulate the development of T regulatory cells and the transcription of ISG expression	Au-Yeung and Horvath, (2018)
	Tregs	Foxp3	*in vivo* deletion inhibit Treg and Teff cells function	Liu et al. (2019c)
	iNKT Cells	--	promote iNKT cells development	Wang et al. (2017)
	Head and Neck Squamous Cell Carcinoma	H3K27	activate transcription of PD-L1 and galectin-9 to evade tumor immunity	Ma et al. (2020)
p300/CBP	Tregs	Foxp3	protect the function of Foxp3+ Tregs and suppress anti-tumor immunity	Liu et al. (2013) Liu et al. (2014)
	T and B Cells	IL2 and IL10	promote Treg differentiation by inducing T and B cells to secrete the pro-inflammatory cytokines IL2 and IL10	Castillo et al. (2019)
	Immunosuppressive Cells	--	promote tumor progression by protecting the function of immunosuppressive cells in tumor microenvironments	Liu et al. (2013) de Almeida Nagata et al. (2019)
	Liver *Cancer*	MEF2D	induce PD-L1 expression in liver cancer by acetylation of MEF2D to impair $CD8^+$ T cell-mediated anti-tumor immunity	Xiang et al. (2020) Guo et al. (2021)
	CTL	MHC-I	regulate tumor cell immunogenicity	Zhou et al. (2021)
Tip60	Tregs	Foxp3	promote FOXP3 mediated inhibition and T cell mediated suppression	Li et al. (2007)
	Tregs	Usp7	control Treg function and limit tumor progression	Wang et al. (2016)
HAT1	Pancreatic *Cancer*	--	transcriptional upregulation of PD-L1 in tumor cells	Fan et al. (2019)

Abbreviations: Treg, regulatory T cells; TNF, tumor necrosis factor; IL, interleukin; CXCL, C-X-C motif chemokine ligand; ISG, IFN-stimulated gene; NK, natural killer cell; CTL, cytotoxic T cell; MHC, major histocompatibility class; Usp, ubiquitin-specific protease.

2016). Histone acetylation is mediated by histone acetyltransferase (HAT), while deacetylation is mediated by histone deacetylase (HDAC). Acetylation of histones alters the secondary structure of the histone tail, leading to relaxation of the chromatin structure by increasing the distance between DNA and histones, opening up tracts of DNA and allowing for increased binding of transcription factor complexes to gene promoter sequences, thereby upregulating transcription (Kouzarides, 2007; Lawrence et al., 2016). In contrast, histone deacetylation usually promotes chromatin condensation and down-regulates the transcriptional level of related genes, and is usually accompanied by an increase in histone methylation of the same residue.

Besides, there is growing evidence that abnormal histone acetylation modification is related to the pathological process of cancer through regulating the expression of oncogenes and tumor suppressors (Audia and Campbell, 2016). For instance, previous studies have shown that changes in histone acetylation level, especially the loss of acetylated Lys16 of histone H4, is related to the development of many cancers and is a common feature in human tumor cells (Fraga et al., 2005). Due to the critical role of acetylation in tumorigenesis, several drugs targeting HDAC have been developed to treat cancer. Furthermore, recent studies have shown acetylation modification is essential for immune system function and tumor immunity.

Therefore, in view of the effects of acetylation modification on tumor cells and immune system, as well as the clinical use of the HATs and HDACs inhibitors, it is worth exploring whether HATs and HDACs could influence immunotherapy efficacy by altering the tumor immune microenvironment through acetylation regulation on tumor cells or immune cells, and whether targeting these enzymes may improve the efficacy of immunotherapy. In this review, we focus on how HATs and HDACs modulate tumor immunity and discuss the potential application of drugs targeting these enzymes to improve the outcome of immunotherapy.

HATS IN TUMOR IMMUNITY REGULATION

There are three major HAT subfamilies in human: the GCN5-related N-acetyltransferase (GNAT) subfamily including PCAF and GCN5; the MYST subfamily including TIP60, MOZ, MORF, MOF and HBO1; the p300 subfamily including p300, CBP. Besides these enzymes, HATs also include TAT1, ESCO1, ESCO2 and HAT1 (Narita et al., 2019). In addition to acetylated histones, HATs can also directly acetylate a range of transcription factors such as C/EBPα, FOXO1, and p53, resulting in the regulation of transcription factor activity and thereby regulation of cancer progression (Sheikh and Akhtar, 2019). At present, only a portion of HATs have been shown to be involved in tumor immunity regulation (**Table 1**).

P300/CBP-Associated Factor

P300/CBP-associated factor (PCAF), also named lysine acetyltransferase 2B (KAT2B) (Liu T. et al., 2019), is a HAT that mainly acetylates H3 histones, as well as a number of non-histone proteins that coordinate carcinogenic and tumor suppressive processes (Wang LT. et al., 2020). Previous studies have shown that the expression of PCAF is reduced as a tumor suppressor in esophageal, breast, ovarian, colorectal and

TABLE 2 | Function of HADCs related to tumor immunity in different cell types.

Protein	Cell type	Target	Function	References
HDAC1	Gastric *Cancer*	STAT1	enhance the expression of JAK2, *p*-JAK1, *p*-JAK2, and p-STAT1 and promote the nucleus translocation of STAT1	Deng et al. (2018)
	Cervical *Cancer* and GBM	Keap1	repress membrane expression of MHCII	Wijdeven et al. (2018)
	NSCLC	Sp1	repress the activity of sp1 to impair the membrane expression of cd1d	Yang et al. (2012)
	Macrophages	miR-146a	induces tumor associated macrophages to adopt the M1-like phenotype	Gao et al. (2015) Ji et al. (2019)
	Tregs	IL-2 and the IFN- γ promoter	participate in the formation of the CoRest which promote function of Treg	Xiong et al. (2020)
HDAC2	Multiple Cell Lines	PD-L1	deacetylate PD-L1 to promote the nuclear translocation of PD-L1 which enhance the expression of PD-L1 and MHC I	Gao et al. (2020)
	Melanoma	ISG promoter	deacetylates IFN-stimulated genes (ISG) promoter at H4K16 to enhances the infiltration of tumor lymphocytes	Zhang et al. (2015)
	Macrophages	c-Jun promoter	repress the expression of c-Jun	Fang et al. (2018) Wu et al. (2019)
HDAC3	Melanoma	Runx3	inhibits the cytotoxicity of CD8+T cells and recognition ability of NK cells	Fiegler et al. (2013) Tay et al. (2020)
	Monocytes and Mø	--	inhibit LPS induced cytokine secretion	Ghiboub et al. (2020)
	Breast *Cancer* and Colorectal *Cancer*	--	down-regulate PD-L1 expression via HDAC3/p300-mediated NF-κB signaling	Lucas et al. (2018) Wang et al. (2020a)
	B-cell Lymphoma	PD-L1 promoter	repress PD-L1 expression via being recruited to the PD-L1 promoter by the transcriptional inhibitor BCL6	Deng et al. (2019)
	Pancreatic *Cancer*	--	enhance PD-L1 expression through STAT3 signaling pathway	Hu et al. (2019)
HDAC4	Brain Astrocytes	liver X receptor	HDAC4 impairs LXR-Induced suppression of STAT1 binding to promoters and downstream inflammatory gene expression	Lee et al. (2009)
	Cervical *Cancer*	IFN-α–stimulated promoter	promote type I interferon signaling via recruiting STAT2 to IFN-α–stimulated promoters	Kalbasi and Ribas, (2020)
HDAC5	CD4+T Cells	Foxp3	positively related to the transformation of Treg and the production of IFN γ	Xiao et al. (2016)
	Macrophages	MKL1	impair TNF-α induced pro inflammatory gene transcription	Li et al. (2017)
	Macrophages	SOCS3	recruit CCR2+ macrophages to promote macrophages to reaggregate into tumor	Hou et al. (2020)
HDAC6	APCs	IL-10 promoter	recruit to immunosuppressive cytokine IL-10 promoter with STAT3	Cheng et al. (2014b)
	Macrophages	--	inhibit the expression of IFN γ and IL-2	Knox et al. (2019b)
	GBM and Melanoma	STAT3	promote the recruitment and activation of STAT3 to enhance the expression of PD-L1	M et al. (2016) Liu et al. (2019a)
	HCC	Foxo1	reduce the expression of PD-L1 and inhibit Foxo1 nuclear translocation to limit TH17 pathogenicity	Qiu et al. (2020)
	Melanoma	--	up-regulate the expression of tumor-associated antigens and MHC-I	Woan et al. (2015)
HDAC7	Pre-B Cells	MEF2C	repress transdifferentiation of Pre-B cells into macrophages	Barneda-Zahonero et al. (2013)
	CD4 T Cells	Nur77 and Irf4	repress the IFN-γ production and $CD4^+$ T cells proliferation	Myers et al. (2017)
	Macrophages	PKM2	deacetylate PKM2 to increase the expression of IL-1β	Das Gupta et al. (2020)
HDAC8	Melanoma	PD-L1 promoter	prevent transcription factors to bind to PD-L1 promoter	Wang et al. (2018b)
	HCC	--	repress intra tumoral CD8+T cell infiltration	Yang et al. (2021e)
	Keratinocytes	--	increases proinflammatory gene expression	Sanford et al. (2016)
HDAC9	CCRC	--	activates immune cell infiltration and increase expression of immunological molecules such as PD-L1, CTLA4 and LAG3	Fu et al. (2020b)
	NSCLC	--	promote the CD8+DC infiltration of the TME and DC antigen presentation	Ning et al. (2020)
	Macrophages	TBK1	enhance the kinase activity of TBK1 to activate antivirus innate immunity	Li et al. (2016b)
	NSCLC	--	positively correlated with the expression of PD-L1	Liu et al. (2020c)
HDAC10				
	HCC	CXCL10 promoter	recruit EZH2 to CXCL10 promoter to inhibit CXCL10 expression thus repressing NK cell migration	Bugide et al. (2021)
	APC	IL-10 promoter	interacts with the IL-10 promoter to repress IL-10 expression	Villagra et al. (2009)
HDAC11				
	MDSCs	C/EBPβ promoter	repress expression of C/EBPβ to inhibit immunosuppressive arginase and iNOS	Chen et al. (2021)
	T Cells	Eomesodermin and Tbx21 promoter	repress transcription factors Eomesodermin and Tbx21 to reduce the production of inflammatory cytokine and effector molecule	Woods et al. (2017)
Sirt1	Th1/17 Cells	Foxo1	enhance the activity of Foxo1 to promotes the expression of Klf2 and Ccr7 genes	Chatterjee et al. (2018)
	Tregs	Foxp3	promote the proteasomal degradation of Foxp3 via deacetylating Foxp3 to repress Treg activation	van Loosdregt et al. (2010)

(Continued on following page)

TABLE 2 | (*Continued*) Function of HADCs related to tumor immunity in different cell types.

Protein	Cell type	Target	Function	References
	Mesenchymal Stem Cells	p65	deacetylate p65 to reduce the expression of iNOS which impair the immunosuppressive ability of MSCs	Zhou et al. (2019)
	Mesenchymal Stem Cells	--	induce IFN γ and CXCL10 expression to recruit NK cells	Yu et al. (2016b) Ye et al. (2020)
	NSCLC	Snail	deacetylate and stabilize transcriptional factor Snail to inhibits transcription of Axin2 which leads to enhanced binding of β-catenin/TCF to PD-L1 promoter	Yu et al. (2016a)
	HCC	--	promoted M1 macrophage polarization via NF-κB signaling	Chen et al. (2015)
Sirt2	T Cells	GSK3 β	promote aerobic oxidation in CD8+T and differentiation of CD8+T cells into TEM	Jiang et al. (2020)
	NK Cells	--	promotes Erk1/2 and p38 MAPK signaling in activated NK cells	Chen et al. (2019a)
	Multiple Malignant Myeloid Cells	CDK9	enhance IFN signaling via deacetylating CDK9 which promote STAT1 phosphorylation at Ser-727	Kosciuczuk et al. (2019)
Sirt3	Prostate *Cancer*	--	reduce the infiltration of $CD4^+$ T cells, macrophages and neutrophils via decreasing the level of CCL8 and CXCL2	Fu et al. (2020a)
	Mø	NLRC4	deacetylates NLRC4 to promote its activation which promotes inflammasome activation	Guan et al. (2021)
Sirt4	Tregs	--	inhibit FoxP3, anti-inflammatory cytokines IL-10, TGFβ and AMPK signaling to impair the anti-inflammatory function of Treg	Lin et al. (2019)
Sirt5	CCRC	--	promote immune cell infiltration	Lu et al. (2021)
Sirt6	Breast *Cancer*	IκB	deacetylate IκB to suppresses the expression of PD-L1	Song et al. (2020)
	Pancreatic *Cancer*	--	increased the production of TNF and IL8 which leads to pro-inflammatory and pro-angiogenic phenotype	Vanamee and Faustman, (2017)
Sirt7	Breast *Cancer*	--	positively correlated with the expression of IRF5 and PD1, M1 macrophages and depletes T cells	Li et al. (2016a)
	HCC	MEF2D	deacetylate MEF2D to inhibit its binding to PD-L1 promoter	Castillo et al. (2019)

Abbreviations: STAT, signal transducer and activator of transcription; JAK, janus kinase; NSCLC, Non-small-cell carcinoma; Treg, Regulatory T cell; IL, interleukin; IFN, interferon; PD-L1, programmed death-ligand 1; ISG, IFN-stimulated gene; LPS, lipopolysaccharides; NF-κB, nucleus factor κ-light-chain enhancer of activated B cells; PKM, pyruvate kinase M2; CTLA, cytotoxic T lymphocyte-associated protein; LAG, lymphocyte activation gene; Foxo, forkhead box O; APCs, antigen-presenting cells.

pancreatic cancers, and that loss of PCAF expression is associated with poor prognosis in gastric cancer and may serve as a potential biomarker for invasive and aggressive tumors (Brasacchio et al., 2018). For example, it acts as a suppressor of HCC progression by promoting apoptosis through acetylation of glioma-associated oncogene homolog-1 (Gli1), histone H4 and the phosphatase and tensin homolog deleted on chromosome 10 (PTEN). On the contrary, PCAF was reported to be highly expressed in HCCs and to promote tumor progression via acetylation of phosphoglycerate kinase 1 (PGK1), pyruvate kinase M2 (PKM2), and glyceraldehyde-3-phosphate dehydrogenase (GAPDH), which subsequentially induces the Warburg effect and activates Akt signaling (Zheng et al., 2013; Wang T. et al., 2018).

With its modulatory effects on tumors, PCAF can also regulate immune system function. In a study of Foxp3+ Treg cells, PCAF was found to contribute to the inhibition of Treg cells apoptosis in response to TCR stimulation and to increase inducible Tregs (iTregs) production via IL-2 and TGF-β. In addition, PCAF acetylates Foxp3 to impair Treg cells function (Liu Y. et al., 2019). Another study has shown that overexpression of PCAF significantly suppressed the expression of pro-inflammatory genes TNF-α, IL-6 and CXCL10, suggesting that PCAF is a potential negative regulator of the inflammatory response of M1 macrophages (Wang et al., 2021).

There is limited evidence reporting the role of PCAF in tumor immunity regulation. A study reported that in lung adenocarcinoma tumor growth was compromised in $PCAF^{-/-}$ mice, with reduced infiltration of CD4+Foxp3+ Treg cells but increased infiltration of host CD8 T cells, indicating that targeting PCAF reduces tumor volume and improves anti-tumor immunity (Liu Y. et al., 2019). More research on the role of PACF in tumor immunity in other cancer types is needed in the future.

GCN5

General control non-depressible 5 (GCN5) mainly responsible for acetylation of H3K27, is the first histone acetyltransferase to be characterized in saccharomyces cerevisiae. GCN5 is highly expressed in a variety of human cancers and promotes cancer progression by participating in the acetylation of many non-histone proteins (Haque et al., 2021). An example is in prostate cancer, where upregulated GCN5 downregulates Egr-1 expression via the PI3K/PTEN/Akt signaling pathway, negatively affecting IL-6-induced prostate cancer cell metastasis and epithelial-mesenchymal transition (EMT) (Shao et al., 2018).

In the immune system, GCN5 was reported to regulate the development of Treg cells and the transcription of interferon (IFN)-stimulated gene (ISG) expression (Au-Yeung and Horvath, 2018). In Foxp3+ Treg cells, GCN5 deletion has no effect on Treg *in vitro* but inhibits Treg function *in vivo*, and impairs T-effector (Teff) cells function (Liu Y. et al., 2019). For invariant natural killer T (iNKT) cells, the deficiency of GCN5 blocks its development (Wang et al., 2017).

TABLE 3 | Information of drugs targeted to acetylase and deacetylase.

Drugs	Target enzymes	IC50	Clinical trials stage	References
E7386	--	--	Phase1	
PRI-724	--	--	Phase1-2	
A485	p300-BHC	9.8 nM	--	Lasko et al. (2017)
	CBP-BHC	2.6 nM	--	Lasko et al. (2017)
Panobinostat (LBH589)	HDAC1	2.5 nM	Phase1-4	Li et al. (2020a)
	HDAC2	13.2 nM		
	HDAC3	2.1 nM		
	HDAC4	203 nM		
	HDAC5	531 nM		
	HDAC7	531 nM		
	HDAC8	277 nM		
	HDAC9	5.7 nM		
Chidamide (CS055/HBI-8000)	HDACs	0.296 ± 0.0417 μM,112 ± 20 nM	Phase1-4	Lu et al. (2017) Chen et al. (2019b)
Trichostatin-A (TSA)	HDACs	0.0125 ± 0.0012 μM	Phase1-4	Chen et al. (2019b)
ACY738	HDACs	1.7 nM	--	Jochems et al. (2014)
Nexturastat A	--	--	--	
Mocetinostat (MGCD0103)	HDAC1	142 nM	Phase1-2	Atadja, (2009)
	HDAC2	147 nM		
	HDAC3	205 nM		
	HDAC4	>30000 nM		
	HDAC5	1889 nM		
	HDAC6	>30000 nM		
	HDAC7	>30000 nM		
	HDAC8	28167 nM		
	HDAC9	1177 nM		
	HDAC10	54.9 nM		
	HDAC11	104 nM		
Mocetinostat (MGCD0103)	HDACs	2.76 ± 1.98 μM	Phase1-2	Gorshkov et al. (2019)
Domatinostat (4SC-202)	--	--	Phase1-2	
Valproic acid (VPA)	HDAC1	0.7–1 mM	Phase1-4	Gurvich et al. (2004)
	HDAC2	0.7–1 mM		
	HDAC3	0.7–1 mM		
	HDAC4	1–1.5 mM		
	HDAC5	1–1.5 mM		
	HDAC7	1–1.5 mM		
Tacedinaline (CI994)	--	--	Phase2-3	
CXD101	HDAC1	63 nM	Phase1-2	Eyre et al. (2019)
	HDAC2	570 nM		
	HDAC3	550 nM		
AR42	--	--	Phase1	
Belinostat(PDX101)	HDAC1	17.6 nM	Phase1-2	Atadja, (2009)
	HDAC2	33.3 nM		
	HDAC3	21.1 nM		
	HDAC4	1,236 nM		
	HDAC5	76.3 nM		
	HDAC6	14.5 nM		
	HDAC7	598 nM		
	HDAC8	157 nM		
	HDAC9	44.2 nM		
	HDAC10	31.3 nM		
	HDAC11	44.2 nM		

Abbreviations: P300-BHC, E1A binding protein p300-bromodomain-HAT-C/H3; CBP-BHC, cyclic-AMP, response element binding protein-bromodomain-HAT-C/H3.

At present, studies on the role of GCN5 in tumor immunity are still relatively few. Overexpression of GCN5 and PCAF in solid tumors *in vivo* enhances immune surveillance and associated NKG2D-dependent tumor cell death (Hu et al., 2021). Knockdown of GCN5 and PCAF in osteosarcoma and lung cancer resulted impaired induction of the natural killer group 2D (NKG2D) ligand Rae-1 by IL-12 and the chemotherapeutic agent doxorubicin as inhibition of NKG2D ligand expression was associated with tumor cell death and accelerated tumor progression (Hu et al., 2017). On the contrary, in head and neck squamous cell carcinoma, GCN5 acetylates H3K27, which activates transcription of PD-L1 and

galectin-9 to evade tumor immunity (Ma et al., 2020). More research is needed to explain this opposite trend and to provide more precise strategies for cancer therapy.

p300/CBP

p300 (E1A binding protein p300) and CBP[CREB] (cyclic-AMP response element binding protein) binding proteins are considered functional homologs, sharing 63% homology at the amino acid level and exhibiting high structural similarity and functional redundancy (Ogryzko et al., 1996; Iyer et al., 2004; He et al., 2021). p300/CBP as a vital transcriptional co-activator and HAT contributes to a variety of cellular activities and plays a role in immune-mediated diseases and cancers through chromatin remodeling and gene activation (Karamouzis et al., 2007; Dancy and Cole, 2015). Overexpression or mutations of p300/CBP are found in malignant tumor, such as prostate and breast cancers (Bouchal et al., 2011; Hickey et al., 2021).

Previous studies have found that p300 and CBP are essential for the development and function of Foxp3+ Treg cells. Inhibition of p300 and CBP impairs Foxp3+ Treg cells function and furthers antitumor immunity (Liu et al., 2013; Liu et al., 2014). p300/CBP promotes Treg differentiation by inducing T and B cells to secrete the pro-inflammatory cytokines IL2 and IL10 (Castillo et al., 2019). It was observed that Treg was reduced in follicular lymphoma in tissues carrying CBP/p300 loss-of-function mutations (Castillo et al., 2019). In breast and lung cancers, p300/CBP inhibition can restrict tumor progression by impairing the function of immunosuppressive cells such as regulatory T cells and MDSCs in tumor microenvironments (Liu et al., 2013; de Almeida Nagata et al., 2019).

Several studies reported p300 can induce the expression of PD-L1 in liver cancer to impair $CD8^+$ T cell-mediated anti-tumor immunity (Xiang et al., 2020; Guo et al., 2021), probably via acetylation of myocyte enhancer factor 2D (MEF2D). Furthermore, targeting p300/CBP by small molecular inhibitors such as E7386 and A485 could remarkably enhance the efficacy of PD-L1 blockade therapy in prostate and breast cancers in preclinical mouse models (Liu J. et al., 2020; Yamada et al., 2021). Additionally, p300 has been reported to regulate tumor cell immunogenicity, p300 ablations prevent chemotherapy-induced processing and presentation of major histocompatibility class I (MHC-I) antigens and abrogating the rejection of low MHC-I-expressing tumors by reinvigorated CD8 cytotoxic T cells (CTLs) (Zhou et al., 2021).

Tip60

Tat-interactive protein 60-kDa (Tip60, also known as KAT5) is one of the MYST subfamily of HATs and was originally identified as a tat-interacting protein widely involved in DNA damage repair, cellular activity and carcinogenesis (Zhang et al., 2017; McGuire et al., 2019). The regulatory function of Tip60 on cancer is dependent on cancer types. As a tumor suppressor in most cancers such as breast cancer (Bassi et al., 2016), gastric cancer (Sakuraba et al., 2011) and advanced stage colorectal cancer (Mattera et al., 2009), downregulation of Tip60 leads to defective DNA repair inducing the accumulation of genetic mutations that can cause tumor progression (Bassi et al., 2016). On the contrary, Tip60 promotes prostate cancer progression via acetylation of androgen receptor (AR) to augment AR signaling (Halkidou et al., 2003; Shiota et al., 2010; Coffey et al., 2012).

Tip60 was found to be essential for the survival of thymic and peripheral Treg cells (Xiao et al., 2014). Overexpression of Tip60 promoted FOXP3-mediated transcriptional repression, suggesting that enhancing its function would alter T cell-mediated transcriptional inhibition (Li et al., 2007). For tumor immunity, studies have shown that Tip60 plays a critical role in fostering acetylation, dimerization and function in Treg cells, leading to tumor suppression. Accordingly, targeting ubiquitin-specific protease (Usp) 7, which controls Treg function primarily by stabilizing expression and promoting multimerization of Tip60 and Foxp3, limits tumor progression (Wang et al., 2016).

HAT1

Histone acetyltransferase 1 (HAT1), also known as KAT1, was the first identified HAT (Poziello et al., 2021), and is a type of B histone acetyltransferase responsible for acetylating newly synthesized histones (Yang G. et al., 2021). As an oncogene, HAT1 is overexpressed and related to poor prognosis in a variety of solid tumors, such as HCCs (Jin et al., 2017), nasopharyngeal carcinoma (Miao et al., 2018), and pancreatic cancer (Fan et al., 2019), and can be a therapeutic target (Carafa et al., 2018). This may be due to the fact that HAT1 is involved in chromatin assembly and DNA damage repair, and its alterations can induce tumor development, invasion and metastasis (Poziello et al., 2021). HAT1 is also a transcription factor that upregulates the expression of various genes such as Bcl2L12 and Fas, and promotes cancer cell proliferation (Fan et al., 2019).

Despite being the first HAT to be discovered, HAT1 is still one of the least studied enzymes of its class (Poziello et al., 2021). In pancreatic cancer, HAT1 was shown to function as an important regulator in cancer immunity through transcriptional upregulation of PD-L1 in tumor cells, indicating that HAT1 could be used as a novel diagnostic and prognostic marker in immune checkpoint blockade therapy (Fan et al., 2019).

HISTONE DEACETYLASES IN TUMOR IMMUNITY REGULATION

Based on the homologies between HDAC and yeast deacetylases, HDACs can be divided into four sub-classes: Class I HDACs (HDAC1, 2, 3 and 8), which are similar to yeast Rpd3, are widely expressed *in vivo* and mainly located in the nucleus. Class II HDACs (HDAC4, 5, 6, 7, 9 and 10) have been studied that expressed in the cytoplasm and nucleus and distributed specifically in tissues. Class III HDACs (Sirt1-7) are similar to yeast Sir2, and its enzyme activity requires NAD+. Class IV HDAC (HDAC11) is homologous to yeast Rpd3 and Hda1. (Li and Seto, 2016). Studies have reported that more than 75% of human cancer tissues possess highly expressed class I HDACs (Nakagawa et al., 2007), besides, high expression of HDACs and low acetylation of histones are common in cancer cells (Cacan

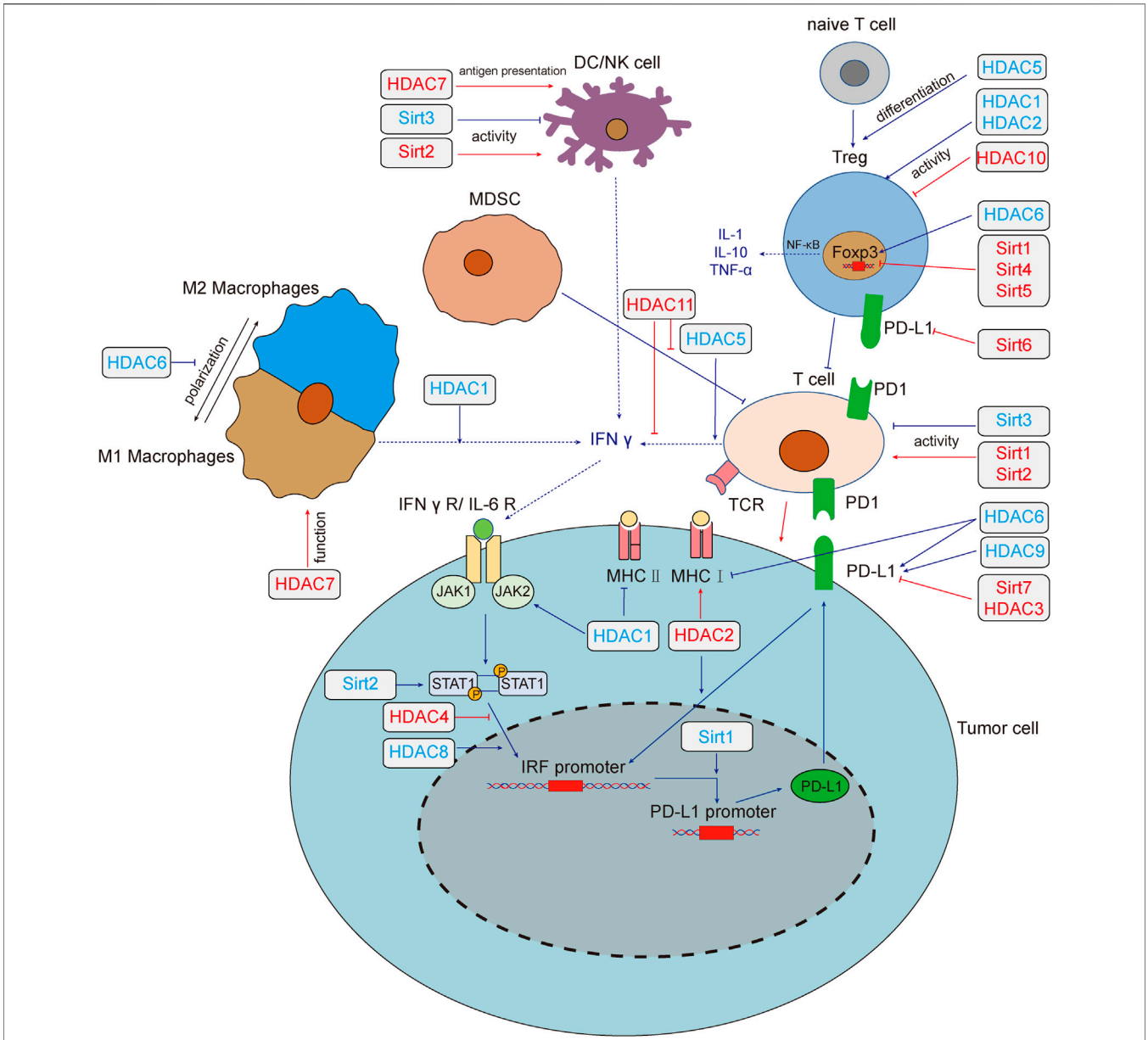

FIGURE 1 | HADCs regulate tumor immunity and tumor immune microenvironment. Deacetylase regulates tumor immune response through multiple pathways. HDAC1,3,4,6,8,9 and Sirt1,2,6,7 regulate the expression of PD-L1 by regulating the IFN signaling pathway. HDAC1,2,6 regulates the expression of MHC, which affect the recognition of tumor cells by T cells. Sirt1, 2, 3 affect tumor immunity by changing the activity of T cells, HDAC1, 2, 10 could affect the function of Treg cells, and HDAC5 promotes the differentiation of naive T cells into Treg cells. Sirt2,3 could affect the activity of NK cells. HDAC7 both enhances the anti-tumor function of macrophages and the antigen presentation function of DC cells. HDAC1, 5, 6, 11 and Sirt1, 4, 5 modulate the tumor microenvironment by affecting the secretion of cytokines. Red lines and text colors represent the promoting effects of tumor immunity, while blue represents the tumor immunosuppression effects. Dotted lines indicate the regulation and function of cytokines. Abbreviations: T cell, T lymphocyte; NK, natural killer cell; DC, dendritic cells; MDSC, myeloid-derived suppressor cell; IFN-γ, interferon-γ; IFNγ R, interferon-γ receptor; IL, interleukin; JAK, Janus kinase; STAT, signal transducer and activator of transcription; TNF-α, tumor necrosis factor-α; Treg, regulatory T cell; IRF, interferon regulatory factor; PD-L1, programmed death-ligand 1; MHC, major histocompatibility complex; Sirt, sirtuins; HDAC, histone deacetylases.

et al., 2014; Cacan, 2016; Alqinyah et al., 2017). The regulatory role of HDACs on tumor immunity was summarized in **Figure 1**.

Histone Deacetylase Family

The HDAC family is a histone deacetylase subfamily that contains HDAC1-11, whose activity is independent of NAD+. It has been observed in multiple cancers that HDACs promotes the proliferation of cancer cells by reducing the expression of the cyclin-dependent kinase inhibitor p21 or TGF-β, in addition, Class I HDACs can also promote cancer cell metastasis by inhibiting the expression of E-cadherin (Glozak and Seto, 2007).

HDAC family plays an important regulatory role in immune cells via its histone deacetylation activity. For instance, the effects of HDACs have been reflected in all aspects of T cells, including T cell development, peripheral immature T cell pool formation, T cell activation and differentiation into effector T cells, activation of regulatory T (Treg) cells, secretion of cytokines, and T cell immune function (Kumari et al., 2013; Cacan, 2017; Ellmeier and Seiser, 2018). Besides, ample evidences have indicated that HDACs regulate the macrophage development, differentiation, polarization, and activation through a variety of signal pathways (Mohammadi et al., 2018).

In addition, HDAC also participates in immunomodulatory networks in cancer cells such as STAT and NF-κB, which not only regulate the expression of molecules in the signal pathway but also controls the nucleus translocation and degradation of STAT and NF-κB signal molecules (Villagra et al., 2010). Target HDACs can increase the expression of antigen presentation molecules such as MHC I, MHC II, CD40 or promote their translocation (Maeda et al., 2000; Khan et al., 2008). HDAC inhibitors can also increase the expression of PD-L1 in tumor cells, and the combination of HDAC inhibitors and PD-1 blockers can delay tumor progression and improve survival rate (Woods et al., 2015).

HDAC1

HDAC1, belonging to Class I, regulates N-terminal lysine residue deacetylation of histones to regulate gene transcription, cell cycle, growth, and apoptosis (Willis-Martinez et al., 2010). HDAC1 were significantly up-regulated in gastric cancer and could promote tumorigenesis and inhibit apoptosis (Yu et al., 2019). In addition, several recent studies have shown that HDAC1 inhibition is beneficial to the therapy of cancer, thus highlighting the cancer promoting function of HDAC1.

HDAC1/2 are required for normal T-cell development (Dovey et al., 2013), and HDAC1 regulates T cell-mediated autoimmunity by regulating CD4+T cells trafficking (Hamminger et al., 2021). Inhibition of HDAC1 promoted acetylation of histone H3/H4 in IFN-β1 promoter, and enhanced phosphorylation of interferon regulatory factor (IRF) 3 and its binding to the IFN-β promoter, which could lead to an anti-tumor immune response of macrophages microenvironment (Mounce et al., 2014; Meng et al., 2016). In addition, the role of HDAC1 in immune cells polarization has been highlighted. Several studies have shown that HDAC1 directly up-regulating the expression of miR-146a in macrophages, which induces tumor associated macrophages (TAMs) to adopt the M1-like phenotype. Besides, HDAC1 inhibition could promote the shift of microglia from M1 to M2 (Gao et al., 2015; Ji et al., 2019).

Mounting evidence shows that HDAC1 could regulate the expression of immune checkpoint molecules. HDAC1 inhibition could suppress the expression of PD-L1 induced by the IFN-γ signal pathway via down-regulating nucleus translocation of JAK2-mediated STAT1 in gastric cancer cells (Deng et al., 2018). In addition, the inhibition of HDAC1 could upregulate membrane expression of MHCⅡin cervical cancer and glioblastoma multiforme cells, and enhance the expression of CD1d in NSCLC cells (Yang et al., 2012; Wijdeven et al., 2018). HDAC1 also affects tumor immunity by regulating the secretion of cytokines. The CoREST complex, composed of HDAC1/2, LSD1, and scaffolding proteins Rcor1 and Rcor2, regulates a variety of immune and inflammatory responses. Targeting HDAC1/2 inhibits the binding of CoREST with IL-2 and the IFN-γ promoter, thereby promoting their expression, inhibiting the function of Treg, and enhancing anti-tumor immunity (Xiong et al., 2020).

HDAC2

Similar to HDAC1 in structure, HDAC2 has been shown vital in cardiac hypertrophy, Alzheimer's disease, Parkinson's and cancer (Kramer, 2009). HDAC2 inactivation can inhibit tumor cell growth and activate apoptosis by activating p53 and Bax (Jung et al., 2012). HDAC2 enhances proinflammatory cytokine production in LPS-stimulated macrophages by impairing the expression of c-Jun which are essential for the negative regulation of the inflammatory response (Wu et al., 2019) and inhibits the expression of plasminogen activator inhibitor 1 (PAI-1), TNF, and macrophage inflammatory protein-2 (MIP-2) in macrophage cells (Fang et al., 2018). Besides, studies have shown that HDAC2 enhances the infiltration of tumor lymphocytes and inhibits IL6 through its histone deacetylation function (Zhang et al., 2015; Xu et al., 2019).

P300-mediated PD-L1 acetylation at K263 inhibits the nucleus translocation of PD-L1, whereas HDAC2 deacetylate PD-L1 K263 and promote nucleus translocation of PD-L1. In the nucleus, PD-L1 interact with RelA and IRF proteins to form a positive feedback pathway to promote immune escape. Besides, treatment with HDAC2 inhibitors can also induce interferon type III related genes IL28A and IL28B, to activate STAT1 and increase the expression of MHC class I antigen presenting genes, thus achieving an improved immunotherapeutic effect (Gao et al., 2020).

HDAC3

HDAC3 plays an important role in apoptosis, cell progress, and DNA damage repair (Sarkar et al., 2020). In colorectal cancer and triple-negative breast cancer, the level of HDAC3 was upregulated. HDAC3 promotes the proliferation of colorectal cancer cells, HCC cells and glioma cells and inhibits the apoptosis of prostate cancer cells (Tong et al., 2020).

HDAC3 inhibition was reported to inhibit lipopolysaccharides (LPS) induced cytokine secretion in monocytes and M1 macrophages (Ghiboub et al., 2020). HDAC3 was reported to reduce the ratios of $CD4^+$ and $CD8^+$ T cells infiltration in

colorectal carcinoma through upregulating B7x expression, which is related to a poor prognosis (Li et al., 2020b). HDAC3 inhibits the cytotoxicity of CD8+T cells and recognition ability of NK cells in melanoma cells by inhibiting genes encoding necessary cytotoxic proteins and key transcription factors (Fiegler et al., 2013; Tay et al., 2020).

Interestingly, depend on the cancer type, there are opposite reports on the regulation of PD-L1 by HDAC3. Studies have found that expression of PD-L1 is negatively correlated with HDAC3, suggesting that HDAC3 is a key inhibitor of PD-L1 transcription. Drugs targeting HDAC3 like resveratrol and pioglitazone upregulate PD-L1 expression in NSCLC, breast and colorectal cancer (Lucas et al., 2018; Wang H. et al., 2020). In B-cell lymphoma, HDAC3 is recruited to the PD-L1 promoter by the transcriptional inhibitor BCL6. In addition, HDAC3 inhibitors can also indirectly reduce the level of DNA methyltransferase 1 protein and activate PD-L1 transcription. HDAC3 inhibition combined with anti-PD-1/PD-L1 therapy can significantly improve the efficacy of B-cell lymphoma treatment (Deng et al., 2019). However, one study showed that the HDAC3/STAT3 pathway transcriptionally regulates PD-L1 expression in pancreatic ductal adenocarcinoma, and HDAC3 inhibitors reduce the protein and mRNA levels of PD-L1 in pancreatic cancer cells (Hu et al., 2019).

HDAC4

HDAC4, in class II, plays an important role in cell cycle progression and developmental events (Wang et al., 2014). HDAC4 was inhibited by miR-155 in human diffuse large B cell lymphoma (DLBCL) cells, resulting in up-regulation of downstream genes and induction of uncontrolled cell proliferation (Sandhu et al., 2012).

As an important signal pathway regulating tumor immunity, IFN signal promotes the phosphorylation of STAT and binds to the transcription factor interferon regulatory factor1 (IRF1) which promotes expression of PD-L1 (Kalbasi and Ribas, 2020). Although there is no direct report on the relationship between HDAC4 and tumor immunity, studies believe that HDAC4 can affect IFN signal. HDAC4 was reported to form a trimer with liver X receptor (LXR)α and pSTAT1, which block the binding of pSTAT1 to the promoter and inhibit the expression of d IRF1, TNF-α, and IL-6 in brain astrocytes (Lee et al., 2009). In cervical cancer cell line, HDAC4 was reported to promote type I interferon signaling via recruiting STAT2 to IFN-α–stimulated promoters (Lu et al., 2019).

HDAC5

HDAC5 is highly expressed in many tumors such as NSCLC, and melanoma but lowly expressed in gastric cancer (Yang J. et al., 2021). Several studies have shown that HDAC5 enhance the invasion and metastasis of neuroblastoma, pancreatic cancer and lung cancer. In addition, HDAC5 also inhibits the proliferation of tumor cells, which may be mediated by TGF-β (Yang J. et al., 2021).

HDAC5 has been reported to repress the production of proinflammatory cytokine in macrophages via TNF-α signaling (Li et al., 2017) and play an inhibitory role in regulating tumor microenvironments. HDAC5 deficient CD4+T cells lack the ability to transform into Tregs, while CD8+T cells impairs the ability to produce IFN- γ without HDAC5, which may offset the immune benefit resulting from decreased Treg function (Xiao et al., 2016). HDAC5-driven escape tumors exhibit a significant transition from neutrophils to macrophages. HDAC5 inhibits suppressor of cytokine signaling 3 (SOCS3), which leads to an increase of C-C motif chemokine ligand 2 (CCL2), recruits CCR2+ macrophages, promotes macrophages to reaggregate into tumor microenvironments, and promotes tumor recurrence (Cheng et al., 2014a; Hou et al., 2020).

HDAC6

HDAC6 protein is related to tumorigenesis, cell survival and metastasis of cancer cells (Aldana-Masangkay and Sakamoto, 2011). In breast cancer, HDAC6 promotes cell movement by acting on the nonhistone substrates, which enhance tumor cell movement, metastasis, and invasion. In addition, the expression of HDAC6 is closely related to endocytosis, and inhibits EGFR transport and degradation through α-tubulin deacetylation, thus activating cell proliferation through the downstream pathway of EGFR in NSCLC (Li et al., 2018).

HDAC6 and STAT3 form a complex and are recruited together to the immunosuppressive cytokine IL-10 promoter in antigen-presenting cells (APCs) to promote immune tolerance (Cheng et al., 2014b). In addition, NextA, a selective HDAC6 inhibitor, was found to increase the proportion of M1/M2 macrophages in tumor microenvironments, promoting IFN-γ and IL-2 levels and transformation of tumor microenvironments from “cold” to “hot”, thus enhancing the efficacy of immune checkpoint blocking therapy (Knox et al., 2019b).

HDAC6 has been also reported the two opposite regulation of PD-L1 in different tumor types. Several studies have reported that inhibition of HDAC6 decreases expression of PD-L1 in glioblastoma and melanoma. Selective inhibition of HDAC6 reduces the immunosuppressive activity of PD-L1 and leads to the recovery of host antitumor activity. A study suggested these effects may be mediated by recruitment and activation of STAT3 (M et al., 2016; Liu JR. et al., 2019). However, another study showed targeting HDAC6 can increase expression of PD-L1 and promote immunotherapy efficacy. Meanwhile, HDAC6 binds to cytoplasmic Foxo1 at K242 and deacetylates Foxo1 to weak the stability of Foxo1 and inhibit nucleus translocation, which limits IL-17–producing helper T (TH17) pathogenicity and antitumor effect in hepatocellular carcinoma (Qiu et al., 2020). Targeting HDAC6 in melanoma can up-regulate the expression of tumor-associated antigens and MHC-I molecules leading to enhance anti-tumor immunity (Woan et al., 2015).

HDAC7, 8, 9, 10, 11

Although the studies of HDAC7, 8, 9, 10 and 11 in tumorigenesis and progress have been widely reported, there is still a lack of research on their role in tumor immunity. Thereby, we summarize and describe the function of these enzymes in this part. HDAC7, 9, 10 belongs to the class II HDACs, HDAC8

belongs to the class I HDACs, and HDAC11 is the only class IV HDAC, all of them affect the initial and progress of tumors in different ways. HDAC7 is considered a regulator of apoptosis in developing thymocytes (Dequiedt et al., 2003) and promoted cell proliferation through regulation of c-myc (Zhu et al., 2011). HDAC8 has been reported to promote the proliferation of hepatocellular carcinoma and inhibit apoptosis. On the contrary, targeting of HDAC8 inhibits the proliferation of lung cancer cell lines (Chakrabarti et al., 2015). HDAC9 is upregulated in various tumors such as glioblastoma, medulloblastoma (Yang C. et al., 2021). HDAC10 function as a tumor suppressor in stem-like lung adenocarcinoma and has been shown to interact with HDAC2 (Fischer et al., 2002; Li et al., 2020c). Notably, HDAC11 as the smallest HDAC isotype possesses very low deacetylase activity. Studies have shown that HDAC11 is highly expressed in prostate cancer, ovarian cancer, breast cancer, and NSCLC. Besides, targeting HDAC11 can enhance chemosensitivity (Liu SS. et al., 2020; Nunez-Alvarez and Suelves, 2021).

HDAC7, 8, 9, 10, 11 regulates immune function via affecting the polarization, antigen presentation, infiltration and activation of immune cells via various mechanisms. Previous studies have shown that HDAC7 and HDAC9 are involved in immune response mediated by immune effector cells. HDAC7 blocks the induction of genes that involved in macrophage immunity, phagocytosis, inflammation and cytokine production (Barneda-Zahonero et al., 2013). Besides, in uterine macrophages, HDAC9 deficiency promotes M2 macrophage polarization (Liu et al., 2021). HDAC9 also enhance immune response via enhancing dendritic cell antigen presentation and CD8+T cell TME infiltration (Ning et al., 2020). In addition, HDAC10 and HDAC11 promote the inhibition of immune response by immune regulatory cells. HDAC10 deletion Treg exhibited a stronger immune inhibitory effect and represses inflammation after intracerebral hemorrhage (Dahiya et al., 2020). MDSCs without HDAC11 exhibit stronger inhibitory activity against CD8+T cells via inducing high level of immunosuppressive enzymes expressed in CD8+T cells (Chen et al., 2021).

In addition, the secretion of cytokines is also an important apparent regulatory function of these enzymes. HADC7 represses the production of IFN-γ and promotes $CD4^+$ T cells proliferation, as well as increasing the expression of the proinflammatory cytokine IL-1β in macrophage (Myers et al., 2017; Das Gupta et al., 2020). Similarly, in T cells, HDAC11 knockout increases the expression of transcription factors Eomesodermin and Tbx21, which reduce the production of inflammatory cytokines and increase the expression of IFN-γ (Woods et al., 2017). Besides, HDAC11 can bind to the promoter of IL-10 to inhibit IL-10 expression and induce inflammatory antigen-presenting cells to activate primordial antigen-specific CD4+T cells (Villagra et al., 2009).

In terms of tumor immunity, HDAC8, 9, and 10 have been reported to be related to the expression of immune checkpoint. HDAC8 can promote tumor immunity by inhibiting the expression of PD-L1. In melanoma cells, HDAC8 competitively inhibits the transcription factor to bind the PD-L1 promoter, thus inhibiting the expression of PD-L1 (Wang YF. et al., 2018). However, opposite studies have shown that HDAC8 inhibition increases the expression of NKG2D ligand in glioma cells which enhanced the recognition ability and cytotoxicity of NK cells, and activates immune cells in hepatocellular carcinoma resulting in an effective and lasting response to ICB (Yang W. et al., 2021; Mormino et al., 2021). On the contrary, HDAC9 and HDAC10 are opposite to HDAC8 in up-regulating PD-L1. One study has suggested that HDAC9 can significantly promote infiltration of immune cells and increase expression of immunological molecules such as PD-L1, CTLA4 and LAG3 in clear cell renal cell carcinoma (Fu Y. et al., 2020). In addition, the expression of HDAC10 in NSCLC was positively correlated with the expression of PD-L1, and the level of PD-L1 is significantly higher than paracancerous tissues, indicating a poor prognosis (Liu X. et al., 2020). Besides, HDAC10 inhibits NK cell-mediated antitumor immunity in hepatocellular carcinoma via recruiting EZH2 to block the CXCL10 promoter (Bugide et al., 2021).

Sirtuin Family

The mammalian Sirtuin protein family is a homologue of Sir2, which can regulate various processes in mammalian cells and play a crucial part in regulating aging, metabolism, gene transcription, and stress responses (such as neurodegeneration, diabetes, cardiovascular disease and many types of cancer) (Michan and Sinclair, 2007). Sirtuins plays an indispensable role in tumorigenesis and development through cellular effects to genomic instability (regulation of cell cycle, DNA repair, cell survival and apoptosis), such as modulating cancer-related metabolism and changing the tumor microenvironment. There are few studies available. (Palmirotta et al., 2016).

Sirt1

Sirt1 (Sirtuin 1) mainly locates in the nucleus, and can removes acetyl groups from proteins. Sirt1 can inhibit transcription by directly deacetylating histones H1 lys26, H3 lys9、lys14, and H4 lys16 and by recruiting other ribozymes to chromatin to promote histone and DNA methylation changes that regulate chromatin function (Vaquero et al., 2004).

At present, the research of Sirt1 in tumor immunity is gradually in-depth. In T cells, Sirt1 enhances the activity of Foxo1 by deacetylating Foxo1, and promotes the expression of *Klf2* and *Ccr7* genes, thereby improving the anti-tumor immune response of T cells (Chatterjee et al., 2018). Additionally, the deacetylation of FoxP3 induced by Sirt1 is critical to the immunosuppressive function of Treg, resulting in Foxp3 degradation and reduced Treg cell number and activity (van Loosdregt et al., 2010). Sirt1 could enhance the tumor killing ability of macrophages, and deacetylate K310 of the p65 subunit in NF-κB, thereby increasing the infiltration of CD8+T cells in tumors or increasing the expression of CXCL10, so as to recruit NK cells and macrophages into tumor microenvironments (Yu et al., 2016a; Yu et al., 2016b; Zhou et al., 2019; Ye et al., 2020). Sirt1 can enhance the activity of NF-κB by promoting the phosphorylation of p65 and IκB, thereby promoting the polarization of M1 in hepatocellular carcinoma (Zhou et al., 2019).

In tumor microenvironments, Sirt1 participates in the immune response by activating the pro-inflammatory pathway (Chen et al., 2015). Pharmacological activation of Sirt1 increases the stability of the transcription factor snail, enhances the binding of β-catenin/TCF to the PD-L1 promoter, and promotes the expression of PD-L1 in NSCLC (Yang M. et al., 2021). Further research is needed on the specific regulation details of Sirt1 in tumor microenvironment.

Sirt2

Sirt2 is the only Sirtuin protein found mainly in the cytoplasm, and it is also expressed in mitochondria and nucleus (Wang Y. et al., 2019). Sirt2 plays an important role in cell differentiation, senescence, infection, inflammation, oxidative stress, and autophagy by regulating the function of important oncogenes, such as Myc and KRAS (Chen et al., 2020). Although there is clear evidence of that Sirt2 is abnormally expressed in various tumors, its causal relationship with tumorigenesis is still unclear, and its effect on the development of different kinds of tumors and its molecular mechanism are still contested (Song et al., 2016; Wang Y. et al., 2019).

Studies have found that the level of Sirt2 is positively correlated with $CD8^+$ effector memory T (TEM) cells in peripheral T lymphocytes from breast cancer patients. Sirt2 can inhibits GSK3 β acetylation in CD8+T cells by promoting aerobic oxidation, which promotes the differentiation of CD8+T cells into TEM (Jiang et al., 2020). In chemically induced hepatocellular carcinoma mice, it has been found that sirt2 was induced in the immune microenvironment of hepatoma cells to enhance the tumor-killing activity of NK cells by promoting mitogen-activated protein kinase (MAPK) in activated NK cells (Chen M. et al., 2019). In addition, Sirt2 can regulate IFN-driven gene transcription by regulating the phosphorylation of Ser-727 on IFN I-dependent STAT1 through deacetylation of CDK9 Lys48 (Kosciuczuk et al., 2019).

Sirt3

Sirt3 plays an important role in mitochondrial function, aging, and carcinogenesis by targeting a series of key regulatory factors and their related pathways in tumors to regulate cell death (Chen et al., 2014). A study has shown that Sirt3 deacetylates NLRC4 to promote its activation, thereby promoting the activation of inflammasomes and mediating the production of the pro-inflammatory cytokine IL-1β in macrophages (Guan et al., 2021).

Blocking Sirt3 and Sirt6 can inhibit the activation of RIPK3 and MLKL in prostate cancer cells, thus enhancing necrotizing apoptosis and promoting infiltration of CD4+T cells, macrophages and neutrophils, so as to inhibit the progression of cancer (Fu W. et al., 2020).

Sirt4

Sirt4 is located in mitochondria and plays an important role in cellular metabolism and tumor biology (Tomaselli et al., 2020). It is mostly regarded as a tumor suppressor gene, and its expression is low in breast, gastric, and colon cancers (Huang and Zhu, 2018). Sirt4 can inhibit FoxP3, anti-inflammatory cytokines IL-10, TGFβ and AMPK signal in Treg cells, which impairs their anti-inflammatory function (Lin et al., 2019).

Sirt5

Sirt5 promotes cancer cell proliferation by targeting a variety of metabolic enzymes including GLS, SHMT2, and PKM2 (Abril et al., 2021). It can maintain histone acetylation and methylation levels in melanoma, thereby promoting the corresponding expression of MITF and c-myc (Milling and Edgar, 2019). It is reported that Sirt5 affects the tumor immune microenvironment through its succinylation function, which is negatively correlated with Treg infiltration in clear cell renal cell carcinoma (Lu et al., 2021).

Sirt6

Sirt6 is a NAD + -dependent histone H3K9 deacetylase that prevents genomic instability, maintains telomere integrity, and regulates metabolic homeostasis and DNA repair (Desantis et al., 2018). It inhibits IGF-Akt and NF-κβ signal transduction by the deacetylation of H3K9 (Sundaresan et al., 2012). High Sirt6 expression levels are observed in the immune system. It may be a possibly a negative regulator of immune cell function and metabolism, which related to neutrophil inactivation and increased the polarization to M2 macrophages (Pillai and Gupta, 2021).

Induction of Sirt6 expression in 4T1 cells inhibits the activation of NF-κB and suppresses the transcription of PD-L1 (Song et al., 2020), which suppresses the proliferation and transcription of PD-L1 in Treg cells (Vanamee and Faustman, 2017). In addition, overexpression of Sirt6 in pancreatic cancer cells increases the production of TNF and IL8 which has nothing to do with the activation of NF-κB, thus leading to pro-inflammatory and pro-angiogenic phenotype (Bauer et al., 2012).

Sirt7

Sirt7 plays an important role in ribosomal biogenesis, cellular stress response, genomic stability, metabolic regulation, aging, and cancer (Ford et al., 2006; Blank and Grummt, 2017; Tang et al., 2021). Compared with other nucleus-localized Sirts, Sirt7 exhibits weaker deacetylase activity. The enzyme activity of Sirt7 targets acetylated H3K18 and succinylated H3K122 (Li L. et al., 2016).

Sirt7 is high expressed in breast cancer, which is an indicator of poor prognosis, and the expression of Sirt7 is positively correlated with the expression of IRF5 and PD1, which increases M1 macrophages, and depletes T cells in the immune environment of breast cancer (Huo et al., 2020). Sirt7 knockout hepatocellular carcinoma cells expressed higher levels of PD-L1 by inhibiting the deacetylation of MEDF2D and reduced T cell infiltration and activation. Moreover, Sirt7 inhibition combined with PD1 blocking therapy can significantly improve the efficacy of hepatocellular carcinoma (Xiang et al., 2020).

TARGETING ACETYLATION IN TUMOR IMMUNOTHERAPY

Immune checkpoint blockades such as anti-PD-1/PD-L1 and anti-CTLA4 have shown promising effects in cancer treatment. However, only few patients benefit from immunotherapy. The combinations of immunotherapy and acetylation-modified drugs (HAT inhibitors and HDAC inhibitors) have attracted more attention in tumor treatment due to the role of acetylases in the regulation of tumor and tumor immunity.

Currently available HAT inhibitors are primarily target CBP and p300, including E7386 (Yamada et al., 2021), PRI-724 (Osawa et al., 2015; Osawa et al., 2019), and A485 (Lasko et al., 2017; Liu J. et al., 2020), which have shown promising effects in improving anti-PD1 immunotherapy. Among them, E7386 (Yamada et al., 2021) and PRI-724 (Osawa et al., 2015; Osawa et al., 2019) inhibit the interaction between CBP and/or β-catenin, which can increase the infiltration of $CD8^+$ T cells. A485 (Lasko et al., 2017; Liu J. et al., 2020) directly targets p300/CBP and inhibits the secretion of exosomal PD-L1.

Correspondingly, partial HDAC inhibitors can also modulate immunotherapies. Some drugs enhance tumor immunity by up regulating PD-L1 in tumor cells, such as Panobinostat(LBH589) (Atadja, 2009; Woods et al., 2015), Chidamide (CS055/HBI-8000) (Ning et al., 2012; Yan et al., 2020; Que et al., 2021), Trichostatin-A (TSA) (Li et al., 2021) and ACY738 (Regna et al., 2016; Maharaj et al., 2020). Other drugs can achieve antitumor immunity by increasing the infiltration of cytotoxic cells, including Nexturastat A (Knox et al., 2019a), Mocetinostat (Boumber et al., 2011; Briere et al., 2018), Domatinostat (4SC-202) (Bretz et al., 2019), Chidamide (CS055/HBI-8000) (Ning et al., 2012; Yan et al., 2020; Que et al., 2021), Valproic acid (VPA) (Xie et al., 2018; Adeshakin et al., 2020), Tacedinaline (CI994) (Berger et al., 1990; el-Beltagi et al., 1993; LoRusso et al., 1996; Burke et al., 2020), CXD10 (Eyre et al., 2019; Blaszczak et al., 2021), Nexturastat A (Knox et al., 2019a), AR42 (Booth et al., 2017) and Trichostatin-A (TSA) (Li et al., 2021), which can improve the infiltration of macrophages, NK cells, and neutrophils. In addition, Mocetinostat (Boumber et al., 2011; Briere et al., 2018), Chidamide (CS055/HBI-8000) (Ning et al., 2012; Yan et al., 2020; Que et al., 2021), Valproic acid (VPA) (Xie et al., 2018; Adeshakin et al., 2020), Trichostatin-A (Li et al., 2021) and Belinostat (PDX101) (Atadja, 2009; Llopiz et al., 2019) can also play an immune regulatory role by reducing the infiltration of immunosuppressive cells such as myeloid-derived suppressor cell (MDSC) and T-regulatory cells (Tregs). Finally, ACY738 (Regna et al., 2016; Maharaj et al., 2020) enhances MHC-restricted antigen presentation by upregulating tumor cell MHC-I expression.

CONCLUSION

Over the last few decades, we have recognized acetylation plays an important role in the regulation of protein function, chromatin structure and gene expression. Research into this field has covered metabolism, immunity, cell cycle, DNA damage repair, apoptosis and autophagy. New discoveries reveal the evidence that acetylation may also influence the tumor immunity through several pathways including regulating the expression and function of immune checkpoint molecules and antigens in tumor cells, as well as processes such as infiltration, secretion of cytokines and antigen presentation by immune cells. Emerging interest in acetylation research has been centered on the use of HAT or HDAC inhibitors that have shown great potential for improving immunotherapeutic outcomes. Further studies should focus on safety and the best way to combine these drugs with various immunotherapies to conquer cancer in the future.

AUTHOR CONTRIBUTIONS

JL, XH and LZ designed and wrote the manuscript. WL and RZ reviewed and critically read the manuscript. All authors read and approved the manuscript.

FUNDING

This work was funded by the Hunan Science and Technology Department Plan Project (2018XK2304), National Natural Science Foundations of China (82,071,895 to WL).

REFERENCES

Abril, Y. L. N., Fernandez, I. R., Hong, J. Y., Chiang, Y. L., Kutateladze, D. A., Zhao, Q., et al. (2021). Pharmacological and Genetic Perturbation Establish SIRT5 as a Promising Target in Breast Cancer. *Oncogene* 40 (9), 1644–1658. doi:10.1038/s41388-020-01637-w

Adeshakin, A. O., Yan, D., Zhang, M., Wang, L., Adeshakin, F. O., Liu, W., et al. (2020). Blockade of Myeloid-Derived Suppressor Cell Function by Valproic Acid Enhanced Anti-PD-L1 Tumor Immunotherapy. *Biochem. Biophys. Res. Commun.* 522 (3), 604–611. doi:10.1016/j.bbrc.2019.11.155

Aldana-Masangkay, G. I., and Sakamoto, K. M. (2011). The Role of HDAC6 in Cancer. *J. Biomed. Biotechnol.* 2011, 875824. doi:10.1155/2011/875824

Alqinyah, M., Maganti, N., Ali, M. W., Yadav, R., Gao, M., Cacan, E., et al. (2017). Regulator of G Protein Signaling 10 (Rgs10) Expression Is Transcriptionally Silenced in Activated Microglia by Histone Deacetylase Activity. *Mol. Pharmacol.* 91 (3), 197–207. doi:10.1124/mol.116.106963

Atadja, P. (2009). Development of the Pan-DAC Inhibitor Panobinostat (LBH589): Successes and Challenges. *Cancer Lett.* 280 (2), 233–241. doi:10.1016/j.canlet.2009.02.019

Au-Yeung, N., and Horvath, C. M. (2018). Histone H2A.Z Suppression of Interferon-Stimulated Transcription and Antiviral Immunity Is Modulated by GCN5 and BRD2. *iScience* 6, 68–82. doi:10.1016/j.isci.2018.07.013

Audia, J. E., and Campbell, R. M. (2016). Histone Modifications and Cancer. *Cold Spring Harb Perspect. Biol.* 8 (4), a019521. doi:10.1101/cshperspect.a019521

Barneda-Zahonero, B., Román-González, L., Collazo, O., Rafati, H., Islam, A. B., Bussmann, L. H., et al. (2013). HDAC7 Is a Repressor of Myeloid Genes Whose Downregulation Is Required for Transdifferentiation of Pre-B Cells into Macrophages. *Plos Genet.* 9 (5), e1003503. doi:10.1371/journal.pgen.1003503

Bassi, C., Li, Y. T., Khu, K., Mateo, F., Baniasadi, P. S., Elia, A., et al. (2016). The Acetyltransferase Tip60 Contributes to Mammary Tumorigenesis by Modulating DNA Repair. *Cell Death Differ* 23 (7), 1198–1208. doi:10.1038/cdd.2015.173

Bauer, I., Grozio, A., Lasiglié, D., Basile, G., Sturla, L., Magnone, M., et al. (2012). The NAD+-dependent Histone Deacetylase SIRT6 Promotes Cytokine Production and Migration in Pancreatic Cancer Cells by Regulating Ca2+ Responses. *J. Biol. Chem.* 287 (49), 40924–40937. doi:10.1074/jbc.M112.405837

Berger, M. R., Richter, H., Seelig, M. H., Eibl, H., and Schmähl, D. (1990). New Cytostatics-Mmore Activity and Less Toxicity. *Cancer Treat Rev.* 17 (2-3), 143–154. doi:10.1016/0305-7372(90)90039-i

Bindea, G., Mlecnik, B., Tosolini, M., Kirilovsky, A., Waldner, M., Obenauf, A. C., et al. (2013). Spatiotemporal Dynamics of Intratumoral Immune Cells Reveal the Immune Landscape in Human Cancer. *Immunity* 39 (4), 782–795. doi:10.1016/j.immuni.2013.10.003

Blank, M. F., and Grummt, I. (2017). The Seven Faces of SIRT7. *Transcription* 8 (2), 67–74. doi:10.1080/21541264.2016.1276658

Blaszczak, W., Liu, G., Zhu, H., Barczak, W., Shrestha, A., Albayrak, G., et al. (2021). Immune Modulation Underpins the Anti-cancer Activity of HDAC Inhibitors. *Mol. Oncol.* 1, 1. doi:10.1002/1878-0261.12953

Booth, L., Roberts, J. L., Poklepovic, A., Kirkwood, J., and Dent, P. (2017). HDAC Inhibitors Enhance the Immunotherapy Response of Melanoma Cells. *Oncotarget* 8 (47), 83155–83170. doi:10.18632/oncotarget.17950

Bouchal, J., Santer, F. R., Höschele, P. P., Tomastikova, E., Neuwirt, H., and Culig, Z. (2011). Transcriptional Coactivators P300 and CBP Stimulate Estrogen Receptor-Beta Signaling and Regulate Cellular Events in Prostate Cancer. *Prostate* 71 (4), 431–437. doi:10.1002/pros.21257

Boumber, Y., Younes, A., and Garcia-Manero, G. (2011). Mocetinostat (MGCD0103): a Review of an Isotype-specific Histone Deacetylase Inhibitor. *Expert Opin. Investig. Drugs* 20 (6), 823–829. doi:10.1517/13543784.2011.577737

Brasacchio, D., Busuttil, R. A., Noori, T., Johnstone, R. W., Boussioutas, A., and Trapani, J. A. (2018). Down-regulation of a Pro-apoptotic Pathway Regulated by PCAF/ADA3 in Early Stage Gastric Cancer. *Cell Death Dis* 9 (5), 442. doi:10.1038/s41419-018-0470-8

Bretz, A. C., Parnitzke, U., Kronthaler, K., Dreker, T., Bartz, R., Hermann, F., et al. (2019). Domatinostat Favors the Immunotherapy Response by Modulating the Tumor Immune Microenvironment (TIME). *J. Immunother. Cancer* 7 (1), 294. doi:10.1186/s40425-019-0745-3

Briere, D., Sudhakar, N., Woods, D. M., Hallin, J., Engstrom, L. D., Aranda, R., et al. (2018). The Class I/IV HDAC Inhibitor Mocetinostat Increases Tumor Antigen Presentation, Decreases Immune Suppressive Cell Types and Augments Checkpoint Inhibitor Therapy. *Cancer Immunol. Immunother.* 67 (3), 381–392. doi:10.1007/s00262-017-2091-y

Bugide, S., Gupta, R., Green, M. R., and Wajapeyee, N. (2021). EZH2 Inhibits NK Cell-Mediated Antitumor Immunity by Suppressing CXCL10 Expression in an HDAC10-dependent Manner. *Proc. Natl. Acad. Sci. U S A.* 118 (30). doi:10.1073/pnas.2102718118

Burke, B., Eden, C., Perez, C., Belshoff, A., Hart, S., Plaza-Rojas, L., et al. (2020). Inhibition of Histone Deacetylase (HDAC) Enhances Checkpoint Blockade Efficacy by Rendering Bladder Cancer Cells Visible for T Cell-Mediated Destruction. *Front Oncol.* 10, 699. doi:10.3389/fonc.2020.00699

Cacan, E., Ali, M. W., Boyd, N. H., Hooks, S. B., and Greer, S. F. (2014). Inhibition of HDAC1 and DNMT1 Modulate RGS10 Expression and Decrease Ovarian Cancer Chemoresistance. *PLoS One* 9 (1), e87455. doi:10.1371/journal.pone.0087455

Cacan, E. (2017). Epigenetic-mediated Immune Suppression of Positive Co-stimulatory Molecules in Chemoresistant Ovarian Cancer Cells. *Cell Biol Int* 41 (3), 328–339. doi:10.1002/cbin.10729

Cacan, E. (2016). Histone Deacetylase-1-Mediated Suppression of FAS in Chemoresistant Ovarian Cancer Cells. *Anticancer Res.* 36 (6), 2819–2826.

Carafa, V., Nebbioso, A., Cuomo, F., Rotili, D., Cobellis, G., Bontempo, P., et al. (2018). RIP1-HAT1-SIRT Complex Identification and Targeting in Treatment and Prevention of Cancer. *Clin. Cancer Res.* 24 (12), 2886–2900. doi:10.1158/1078-0432.CCR-17-3081

Castillo, J., Wu, E., Lowe, C., Srinivasan, S., McCord, R., Wagle, M. C., et al. (2019). CBP/p300 Drives the Differentiation of Regulatory T Cells through Transcriptional and Non-transcriptional Mechanisms. *Cancer Res.* 79 (15), 3916–3927. doi:10.1158/0008-5472.CAN-18-3622

Chakrabarti, A., Oehme, I., Witt, O., Oliveira, G., Sippl, W., Romier, C., et al. (2015). HDAC8: a Multifaceted Target for Therapeutic Interventions. *Trends Pharmacol. Sci.* 36 (7), 481–492. doi:10.1016/j.tips.2015.04.013

Chatterjee, S., Daenthanasanmak, A., Chakraborty, P., Wyatt, M. W., Dhar, P., Selvam, S. P., et al. (2018). CD38-NAD+Axis Regulates Immunotherapeutic Anti-tumor T Cell Response. *Cell Metab* 27 (1), 85–e8. doi:10.1016/j.cmet.2017.10.006

Chen, G., Huang, P., and Hu, C. (2020). The Role of SIRT2 in Cancer: A Novel Therapeutic Target. *Int. J. Cancer* 147 (12), 3297–3304. doi:10.1002/ijc.33118

Chen, J., Cheng, F., Sahakian, E., Powers, J., Wang, Z., Tao, J., et al. (2021). HDAC11 Regulates Expression of C/EBPβ and Immunosuppressive Molecules in Myeloid-Derived Suppressor Cells. *J. Leukoc. Biol.* 109 (5), 891–900. doi:10.1002/JLB.1A1119-606RRR

Chen, M., Xu, M., Zhu, C., Wang, H., Zhao, Q., and Zhou, F. (2019a). Sirtuin2 Enhances the Tumoricidal Function of Liver Natural Killer Cells in a Mouse Hepatocellular Carcinoma Model. *Cancer Immunol. Immunother.* 68 (6), 961–971. doi:10.1007/s00262-019-02337-5

Chen, X., Lu, Y., Zhang, Z., Wang, J., Yang, H., and Liu, G. (2015). Intercellular Interplay between Sirt1 Signalling and Cell Metabolism in Immune Cell Biology. *Immunology* 145 (4), 455–467. doi:10.1111/imm.12473

Chen, X., Zhao, S., Li, H., Wang, X., Geng, A., Cui, H., et al. (2019b). Design, Synthesis and Biological Evaluation of Novel Isoindolinone Derivatives as Potent Histone Deacetylase Inhibitors. *Eur. J. Med. Chem.* 168, 110–122. doi:10.1016/j.ejmech.2019.02.032

Chen, Y., Fu, L. L., Wen, X., Wang, X. Y., Liu, J., Cheng, Y., et al. (2014). Sirtuin-3 (SIRT3), a Therapeutic Target with Oncogenic and Tumor-Suppressive Function in Cancer. *Cell Death Dis* 5, e1047. doi:10.1038/cddis.2014.14

Cheng, F., Lienlaf, M., Perez-Villarroel, P., Wang, H. W., Lee, C., Woan, K., et al. (2014a). Divergent Roles of Histone Deacetylase 6 (HDAC6) and Histone Deacetylase 11 (HDAC11) on the Transcriptional Regulation of IL10 in Antigen Presenting Cells. *Mol. Immunol.* 60 (1), 44–53. doi:10.1016/j.molimm.2014.02.019

Cheng, F., Lienlaf, M., Wang, H. W., Perez-Villarroel, P., Lee, C., Woan, K., et al. (2014b). A Novel Role for Histone Deacetylase 6 in the Regulation of the Tolerogenic STAT3/IL-10 Pathway in APCs. *J. Immunol.* 193 (6), 2850–2862. doi:10.4049/jimmunol.1302778

Coffey, K., Blackburn, T. J., Cook, S., Golding, B. T., Griffin, R. J., Hardcastle, I. R., et al. (2012). Characterisation of a Tip60 Specific Inhibitor, NU9056, in Prostate Cancer. *PLoS One* 7 (10), e45539. doi:10.1371/journal.pone.0045539

Dahiya, S., Beier, U. H., Wang, L., Han, R., Jiao, J., Akimova, T., et al. (2020). HDAC10 Deletion Promotes Foxp3+ T-Regulatory Cell Function. *Sci. Rep.* 10 (1), 424. doi:10.1038/s41598-019-57294-x

Dancy, B. M., and Cole, P. A. (2015). Protein Lysine Acetylation by P300/CBP. *Chem. Rev.* 115 (6), 2419–2452. doi:10.1021/cr500452k

Das Gupta, K., Shakespear, M. R., Curson, J. E. B., Murthy, A. M. V., Iyer, A., Hodson, M. P., et al. (2020). Class IIa Histone Deacetylases Drive Toll-like Receptor-Inducible Glycolysis and Macrophage Inflammatory Responses via Pyruvate Kinase M2. *Cell Rep* 30 (8), 2712–e8. e2718. doi:10.1016/j.celrep.2020.02.007

de Almeida Nagata, D. E., Chiang, E. Y., Jhunjhunwala, S., Caplazi, P., Arumugam, V., Modrusan, Z., et al. (2019). Regulation of Tumor-Associated Myeloid Cell Activity by CBP/EP300 Bromodomain Modulation of H3K27 Acetylation. *Cell Rep* 27 (1), 269–e4. e264. doi:10.1016/j.celrep.2019.03.008

Deng, R., Zhang, P., Liu, W., Zeng, X., Ma, X., Shi, L., et al. (2018). HDAC Is Indispensable for IFN-γ-Induced B7-H1 Expression in Gastric Cancer. *Clin. Epigenetics* 10 (1), 153. doi:10.1186/s13148-018-0589-6

Deng, S., Hu, Q., Zhang, H., Yang, F., Peng, C., and Huang, C. (2019). HDAC3 Inhibition Upregulates PD-L1 Expression in B-Cell Lymphomas and Augments the Efficacy of Anti-PD-L1 Therapy. *Mol. Cancer Ther.* 18 (5), 900–908. doi:10.1158/1535-7163.MCT-18-1068

Dequiedt, F., Kasler, H., Fischle, W., Kiermer, V., Weinstein, M., Herndier, B. G., et al. (2003). HDAC7, a Thymus-specific Class II Histone Deacetylase, Regulates Nur77 Transcription and TCR-Mediated Apoptosis. *Immunity* 18 (5), 687–698. doi:10.1016/s1074-7613(03)00109-2

Desantis, V., Lamanuzzi, A., and Vacca, A. (2018). The Role of SIRT6 in Tumors. *Haematologica* 103 (1), 1–4. doi:10.3324/haematol.2017.182675

Dovey, O. M., Foster, C. T., Conte, N., Edwards, S. A., Edwards, J. M., Singh, R., et al. (2013). Histone Deacetylase 1 and 2 Are Essential for normal T-Cell Development and Genomic Stability in Mice. *Blood* 121 (8), 1335–1344. doi:10.1182/blood-2012-07-441949

el-Beltagi, H. M., Martens, A. C., Lelieveld, P., Haroun, E. A., and Hagenbeek, A. (1993). Acetyldinaline: a New Oral Cytostatic Drug with Impressive Differential Activity against Leukemic Cells and normal Stem Cells-Ppreclinical Studies in a Relevant Rat Model for Human Acute Myelocytic Leukemia. *Cancer Res.* 53 (13), 3008–3014.

Ellmeier, W., and Seiser, C. (2018). Histone Deacetylase Function in CD4+ T Cells. *Nat. Rev. Immunol.* 18 (10), 617–634. doi:10.1038/s41577-018-0037-z

Eyre, T. A., Collins, G. P., Gupta, A., Coupe, N., Sheikh, S., Whittaker, J., et al. (2019). A Phase 1 Study to Assess the Safety, Tolerability, and Pharmacokinetics of CXD101 in Patients with Advanced Cancer. *Cancer* 125 (1), 99–108. doi:10.1002/cncr.31791

Fan, P., Zhao, J., Meng, Z., Wu, H., Wang, B., Wu, H., et al. (2019). Overexpressed Histone Acetyltransferase 1 Regulates Cancer Immunity by Increasing Programmed Death-Ligand 1 Expression in Pancreatic Cancer. *J. Exp. Clin. Cancer Res.* 38 (1), 47. doi:10.1186/s13046-019-1044-z

Fang, W. F., Chen, Y. M., Lin, C. Y., Huang, H. L., Yeh, H., Chang, Y. T., et al. (2018). Histone Deacetylase 2 (HDAC2) Attenuates Lipopolysaccharide (LPS)-induced Inflammation by Regulating PAI-1 Expression. *J. Inflamm. (Lond)* 15, 3. doi:10.1186/s12950-018-0179-6

Fiegler, N., Textor, S., Arnold, A., Rölle, A., Oehme, I., Breuhahn, K., et al. (2013). Downregulation of the Activating NKp30 Ligand B7-H6 by HDAC Inhibitors Impairs Tumor Cell Recognition by NK Cells. *Blood* 122 (5), 684–693. doi:10.1182/blood-2013-02-482513

Fischer, D. D., Cai, R., Bhatia, U., Asselbergs, F. A., Song, C., Terry, R., et al. (2002). Isolation and Characterization of a Novel Class II Histone Deacetylase, HDAC10. *J. Biol. Chem.* 277 (8), 6656–6666. doi:10.1074/jbc.M108055200

Ford, E., Voit, R., Liszt, G., Magin, C., Grummt, I., and Guarente, L. (2006). Mammalian Sir2 Homolog SIRT7 Is an Activator of RNA Polymerase I Transcription. *Genes Dev.* 20 (9), 1075–1080. doi:10.1101/gad.1399706

Fraga, M. F., Ballestar, E., Villar-Garea, A., Boix-Chornet, M., Espada, J., Schotta, G., et al. (2005). Loss of Acetylation at Lys16 and Trimethylation at Lys20 of Histone H4 Is a Common Hallmark of Human Cancer. *Nat. Genet.* 37 (4), 391–400. doi:10.1038/ng1531

Fu, W., Li, H., Fu, H., Zhao, S., Shi, W., Sun, M., et al. (2020a). The SIRT3 and SIRT6 Promote Prostate Cancer Progression by Inhibiting Necroptosis-Mediated Innate Immune Response. *J. Immunol. Res.* 2020, 8820355. doi:10.1155/2020/8820355

Fu, Y., Piao, C., Zhang, Z., Zhu, Y., Sun, S., Bi, J., et al. (2020b). Decreased Expression and Hypomethylation of HDAC9 lead to Poor Prognosis and Inhibit Immune Cell Infiltration in clear Cell Renal Cell Carcinoma. *Urol. Oncol.* 38 (9), 740–e9. e749. doi:10.1016/j.urolonc.2020.03.006

Gao, J., Wang, D., Liu, D., Liu, M., Ge, Y., Jiang, M., et al. (2015). Tumor Necrosis Factor-Related Apoptosis-Inducing Ligand Induces the Expression of Proinflammatory Cytokines in Macrophages and Re-educates Tumor-Associated Macrophages to an Antitumor Phenotype. *Mol. Biol. Cell* 26 (18), 3178–3189. doi:10.1091/mbc.E15-04-0209

Gao, Y., Nihira, N. T., Bu, X., Chu, C., Zhang, J., Kolodziejczyk, A., et al. (2020). Acetylation-dependent Regulation of PD-L1 Nuclear Translocation Dictates the Efficacy of Anti-PD-1 Immunotherapy. *Nat. Cell Biol* 22 (9), 1064–1075. doi:10.1038/s41556-020-0562-4

Ghiboub, M., Zhao, J., Li Yim, A. Y. F., Schilderink, R., Verseijden, C., van Hamersveld, P. H. P., et al. (2020). HDAC3 Mediates the Inflammatory Response and LPS Tolerance in Human Monocytes and Macrophages. *Front Immunol.* 11, 550769. doi:10.3389/fimmu.2020.550769

Glozak, M. A., and Seto, E. (2007). Histone Deacetylases and Cancer. *Oncogene* 26 (37), 5420–5432. doi:10.1038/sj.onc.1210610

Gorshkov, K., Sima, N., Sun, W., Lu, B., Huang, W., Travers, J., et al. (2019). Quantitative Chemotherapeutic Profiling of Gynecologic Cancer Cell Lines Using Approved Drugs and Bioactive Compounds. *Transl Oncol.* 12 (3), 441–452. doi:10.1016/j.tranon.2018.11.016

Guan, C., Huang, X., Yue, J., Xiang, H., Shaheen, S., Jiang, Z., et al. (2021). SIRT3-mediated Deacetylation of NLRC4 Promotes Inflammasome Activation. *Theranostics* 11 (8), 3981–3995. doi:10.7150/thno.55573

Guo, L., Li, H., Fan, T., Ma, Y., and Wang, L. (2021). Synergistic Efficacy of Curcumin and Anti-programmed Cell Death-1 in Hepatocellular Carcinoma. *Life Sci.* 279, 119359. doi:10.1016/j.lfs.2021.119359

Gurvich, N., Tsygankova, O. M., Meinkoth, J. L., and Klein, P. S. (2004). Histone Deacetylase Is a Target of Valproic Acid-Mediated Cellular Differentiation. *Cancer Res.* 64 (3), 1079–1086. doi:10.1158/0008-5472.can-03-0799

Halkidou, K., Gnanapragasam, V. J., Mehta, P. B., Logan, I. R., Brady, M. E., Cook, S., et al. (2003). Expression of Tip60, an Androgen Receptor Coactivator, and its Role in Prostate Cancer Development. *Oncogene* 22 (16), 2466–2477. doi:10.1038/sj.onc.1206342

Hamminger, P., Marchetti, L., Preglej, T., Platzer, R., Zhu, C., Kamnev, A., et al. (2021). Histone Deacetylase 1 Controls CD4+ T Cell Trafficking in Autoinflammatory Diseases. *J. Autoimmun.* 119, 102610. doi:10.1016/j.jaut.2021.102610

Haque, M. E., Jakaria, M., Akther, M., Cho, D. Y., Kim, I. S., and Choi, D. K. (2021). The GCN5: its Biological Functions and Therapeutic Potentials. *Clin. Sci. (Lond)* 135 (1), 231–257. doi:10.1042/CS20200986

He, Z. X., Wei, B. F., Zhang, X., Gong, Y. P., Ma, L. Y., and Zhao, W. (2021). Current Development of CBP/p300 Inhibitors in the Last Decade. *Eur. J. Med. Chem.* 209, 112861. doi:10.1016/j.ejmech.2020.112861

Hickey, T. E., Selth, L. A., Chia, K. M., Laven-Law, G., Milioli, H. H., Roden, D., et al. (2021). The Androgen Receptor Is a Tumor Suppressor in Estrogen Receptor-Positive Breast Cancer. *Nat. Med.* 27 (2), 310–320. doi:10.1038/s41591-020-01168-7

Hou, P., Kapoor, A., Zhang, Q., Li, J., Wu, C. J., Li, J., et al. (2020). Tumor Microenvironment Remodeling Enables Bypass of Oncogenic KRAS Dependency in Pancreatic Cancer. *Cancer Discov.* 10 (7), 1058–1077. doi:10.1158/2159-8290.CD-19-0597

Hu, G., He, N., Cai, C., Cai, F., Fan, P., Zheng, Z., et al. (2019). HDAC3 Modulates Cancer Immunity via Increasing PD-L1 Expression in Pancreatic Cancer. *Pancreatology* 19 (2), 383–389. doi:10.1016/j.pan.2019.01.011

Hu, J., Bernatchez, C., Zhang, L., Xia, X., Kleinerman, E. S., Hung, M. C., et al. (2017). Induction of NKG2D Ligands on Solid Tumors Requires Tumor-specific CD8+ T Cells and Histone Acetyltransferases. *Cancer Immunol. Res.* 5 (4), 300–311. doi:10.1158/2326-6066.CIR-16-0234

Hu, J., Xia, X., Zhao, Q., and Li, S. (2021). Lysine Acetylation of NKG2D Ligand Rae-1 Stabilizes the Protein and Sensitizes Tumor Cells to NKG2D Immune Surveillance. *Cancer Lett.* 502, 143–153. doi:10.1016/j.canlet.2020.12.002

Huang, G., and Zhu, G. (2018). Sirtuin-4 (SIRT4), a Therapeutic Target with Oncogenic and Tumor-Suppressive Activity in Cancer. *Onco Targets Ther.* 11, 3395–3400. doi:10.2147/OTT.S157724

Huo, Q., Li, Z., Cheng, L., Yang, F., and Xie, N. (2020). SIRT7 Is a Prognostic Biomarker Associated with Immune Infiltration in Luminal Breast Cancer. *Front Oncol.* 10, 621. doi:10.3389/fonc.2020.00621

Iyer, N. G., Ozdag, H., and Caldas, C. (2004). p300/CBP and Cancer. *Oncogene* 23 (24), 4225–4231. doi:10.1038/sj.onc.1207118

Ji, J., Wang, J., Yang, J., Wang, X. P., Huang, J. J., Xue, T. F., et al. (2019). The Intranuclear SphK2-S1p Axis Facilitates M1-To-M2 Shift of Microglia via Suppressing HDAC1-Mediated KLF4 Deacetylation. *Front Immunol.* 10, 1241. doi:10.3389/fimmu.2019.01241

Jiang, C., Liu, J., Guo, M., Gao, X., Wu, X., Bai, N., et al. (2020). The NAD-dependent Deacetylase SIRT2 Regulates T Cell Differentiation Involved in Tumor Immune Response. *Int. J. Biol. Sci.* 16 (15), 3075–3084. doi:10.7150/ijbs.49735

Jin, X., Tian, S., and Li, P. (2017). Histone Acetyltransferase 1 Promotes Cell Proliferation and Induces Cisplatin Resistance in Hepatocellular Carcinoma. *Oncol. Res.* 25 (6), 939–946. doi:10.3727/096504016X14809827856524

Jochems, J., Boulden, J., Lee, B. G., Blendy, J. A., Jarpe, M., Mazitschek, R., et al. (2014). Antidepressant-like Properties of Novel HDAC6-Selective Inhibitors with Improved Brain Bioavailability. *Neuropsychopharmacology* 39 (2), 389–400. doi:10.1038/npp.2013.207

Jones, P. A., Ohtani, H., Chakravarthy, A., and De Carvalho, D. D. (2019). Epigenetic Therapy in Immune-Oncology. *Nat. Rev. Cancer* 19 (3), 151–161. doi:10.1038/s41568-019-0109-9

Jung, K. H., Noh, J. H., Kim, J. K., Eun, J. W., Bae, H. J., Xie, H. J., et al. (2012). HDAC2 Overexpression Confers Oncogenic Potential to Human Lung Cancer Cells by Deregulating Expression of Apoptosis and Cell Cycle Proteins. *J. Cell Biochem* 113 (6), 2167–2177. doi:10.1002/jcb.24090

Kalbasi, A., and Ribas, A. (2020). Tumour-intrinsic Resistance to Immune Checkpoint Blockade. *Nat. Rev. Immunol.* 20 (1), 25–39. doi:10.1038/s41577-019-0218-4

Karamouzis, M. V., Konstantinopoulos, P. A., and Papavassiliou, A. G. (2007). Roles of CREB-Binding Protein (CBP)/p300 in Respiratory Epithelium Tumorigenesis. *Cell Res* 17 (4), 324–332. doi:10.1038/cr.2007.10

Khan, A. N., Gregorie, C. J., and Tomasi, T. B. (2008). Histone Deacetylase Inhibitors Induce TAP, LMP, Tapasin Genes and MHC Class I Antigen Presentation by Melanoma Cells. *Cancer Immunol. Immunother.* 57 (5), 647–654. doi:10.1007/s00262-007-0402-4

Knox, T., Sahakian, E., Banik, D., Hadley, M., Palmer, E., Noonepalle, S., et al. (2019a). Author Correction: Selective HDAC6 Inhibitors Improve Anti-PD-1 Immune Checkpoint Blockade Therapy by Decreasing the Anti-inflammatory Phenotype of Macrophages and Down-Regulation of Immunosuppressive Proteins in Tumor Cells. *Sci. Rep.* 9 (1), 14824. doi:10.1038/s41598-019-51403-6

Knox, T., Sahakian, E., Banik, D., Hadley, M., Palmer, E., Noonepalle, S., et al. (2019b). Selective HDAC6 Inhibitors Improve Anti-PD-1 Immune Checkpoint Blockade Therapy by Decreasing the Anti-inflammatory Phenotype of Macrophages and Down-Regulation of Immunosuppressive Proteins in Tumor Cells. *Sci. Rep.* 9 (1), 6136. doi:10.1038/s41598-019-42237-3

Kosciuczuk, E. M., Mehrotra, S., Saleiro, D., Kroczynska, B., Majchrzak-Kita, B., Lisowski, P., et al. (2019). Sirtuin 2-mediated Deacetylation of Cyclin-dependent Kinase 9 Promotes STAT1 Signaling in Type I Interferon Responses. *J. Biol. Chem.* 294 (3), 827–837. doi:10.1074/jbc.RA118.005956

Kouzarides, T. (2007). Chromatin Modifications and Their Function. *Cell* 128 (4), 693–705. doi:10.1016/j.cell.2007.02.005

Krämer, O. H. (2009). HDAC2: a Critical Factor in Health and Disease. *Trends Pharmacol. Sci.* 30 (12), 647–655. doi:10.1016/j.tips.2009.09.007

Kumari, A., Cacan, E., Greer, S. F., and Garnett-Benson, C. (2013). Turning T Cells on: Epigenetically Enhanced Expression of Effector T-Cell Costimulatory Molecules on Irradiated Human Tumor Cells. *J. Immunother. Cancer* 1, 17. doi:10.1186/2051-1426-1-17

Lasko, L. M., Jakob, C. G., Edalji, R. P., Qiu, W., Montgomery, D., Digiammarino, E. L., et al. (2017). Discovery of a Selective Catalytic P300/CBP Inhibitor that Targets Lineage-specific Tumours. *Nature* 550 (7674), 128–132. doi:10.1038/nature24028

Lawrence, M., Daujat, S., and Schneider, R. (2016). Lateral Thinking: How Histone Modifications Regulate Gene Expression. *Trends Genet.* 32 (1), 42–56. doi:10.1016/j.tig.2015.10.007

Lee, J. H., Park, S. M., Kim, O. S., Lee, C. S., Woo, J. H., Park, S. J., et al. (2009). Differential SUMOylation of LXRalpha and LXRbeta Mediates Transrepression of STAT1 Inflammatory Signaling in IFN-Gamma-Stimulated Brain Astrocytes. *Mol. Cell* 35 (6), 806–817. doi:10.1016/j.molcel.2009.07.021

Li, B., Samanta, A., Song, X., Iacono, K. T., Bembas, K., Tao, R., et al. (2007). FOXP3 Interactions with Histone Acetyltransferase and Class II Histone Deacetylases Are Required for Repression. *Proc. Natl. Acad. Sci. U S A.* 104 (11), 4571–4576. doi:10.1073/pnas.0700298104

Li, L., Shi, L., Yang, S., Yan, R., Zhang, D., Yang, J., et al. (2016a). SIRT7 Is a Histone Desuccinylase that Functionally Links to Chromatin Compaction and Genome Stability. *Nat. Commun.* 7, 12235. doi:10.1038/ncomms12235

Li, T., Zhang, C., Hassan, S., Liu, X., Song, F., Chen, K., et al. (2018). Histone Deacetylase 6 in Cancer. *J. Hematol. Oncol.* 11 (1), 111. doi:10.1186/s13045-018-0654-9

Li, X., Jiang, Y., Peterson, Y. K., Xu, T., Himes, R. A., Luo, X., et al. (2020a). Design of Hydrazide-Bearing HDACIs Based on Panobinostat and Their P53 and FLT3-ITD Dependency in Antileukemia Activity. *J. Med. Chem.* 63 (10), 5501–5525. doi:10.1021/acs.jmedchem.0c00442

Li, X., Su, X., Liu, R., Pan, Y., Fang, J., Cao, L., et al. (2021). HDAC Inhibition Potentiates Anti-tumor Activity of Macrophages and Enhances Anti-PD-L1-mediated Tumor Suppression. *Oncogene* 40 (10), 1836–1850. doi:10.1038/s41388-020-01636-x

Li, X., Zhang, Q., Ding, Y., Liu, Y., Zhao, D., Zhao, K., et al. (2016b). Methyltransferase Dnmt3a Upregulates HDAC9 to Deacetylate the Kinase TBK1 for Activation of Antiviral Innate Immunity. *Nat. Immunol.* 17 (7), 806–815. doi:10.1038/ni.3464

Li, Y., Liu, Y., Zhao, N., Yang, X., Li, Y., Zhai, F., et al. (2020b). Checkpoint Regulator B7x Is Epigenetically Regulated by HDAC3 and Mediates Resistance to HDAC Inhibitors by Reprogramming the Tumor Immune Environment in Colorectal Cancer. *Cell Death Dis* 11 (9), 753. doi:10.1038/s41419-020-02968-y

Li, Y., and Seto, E. (2016). HDACs and HDAC Inhibitors in Cancer Development and Therapy. *Cold Spring Harb Perspect. Med.* 6 (10). doi:10.1101/cshperspect.a026831

Li, Y., Zhang, X., Zhu, S., Dejene, E. A., Peng, W., Sepulveda, A., et al. (2020c). HDAC10 Regulates Cancer Stem-like Cell Properties in KRAS-Driven Lung Adenocarcinoma. *Cancer Res.* 80 (16), 3265–3278. doi:10.1158/0008-5472.CAN-19-3613

Li, Z., Qin, H., Li, J., Yu, L., Yang, Y., and Xu, Y. (2017). HADC5 Deacetylates MKL1 to Dampen TNF-α Induced Pro-inflammatory Gene Transcription in Macrophages. *Oncotarget* 8 (55), 94235–94246. doi:10.18632/oncotarget.21670

Lin, W., Chen, W., Liu, W., Xu, Z., and Zhang, L. (2019). Sirtuin4 Suppresses the Anti-neuroinflammatory Activity of Infiltrating Regulatory T Cells in the Traumatically Injured Spinal Cord. *Immunology* 158 (4), 362–374. doi:10.1111/imm.13123

Liu, J., He, D., Cheng, L., Huang, C., Zhang, Y., Rao, X., et al. (2020a). p300/CBP Inhibition Enhances the Efficacy of Programmed Death-Ligand 1 Blockade Treatment in Prostate Cancer. *Oncogene* 39 (19), 3939–3951. doi:10.1038/s41388-020-1270-z

Liu, J. R., Yu, C. W., Hung, P. Y., Hsin, L. W., and Chern, J. W. (2019a). High-selective HDAC6 Inhibitor Promotes HDAC6 Degradation Following Autophagy Modulation and Enhanced Antitumor Immunity in Glioblastoma. *Biochem. Pharmacol.* 163, 458–471. doi:10.1016/j.bcp.2019.03.023

Liu, S. S., Wu, F., Jin, Y. M., Chang, W. Q., and Xu, T. M. (2020b). HDAC11: a Rising star in Epigenetics. *Biomed. Pharmacother.* 131, 110607. doi:10.1016/j.biopha.2020.110607

Liu, T., Wang, X., Hu, W., Fang, Z., Jin, Y., Fang, X., et al. (2019b). Epigenetically Down-Regulated Acetyltransferase PCAF Increases the Resistance of Colorectal Cancer to 5-Fluorouracil. *Neoplasia* 21 (6), 557–570. doi:10.1016/j.neo.2019.03.011

Liu, X., Wang, Y., Zhang, R., Jin, T., Qu, L., Jin, Q., et al. (2020c). HDAC10 Is Positively Associated with PD-L1 Expression and Poor Prognosis in Patients with NSCLC. *Front Oncol.* 10, 485. doi:10.3389/fonc.2020.00485

Liu, Y., Bao, C., Wang, L., Han, R., Beier, U. H., Akimova, T., et al. (2019c). Complementary Roles of GCN5 and PCAF in Foxp3+ T-Regulatory Cells. *Cancers (Basel)* 11 (4). doi:10.3390/cancers11040554

Liu, Y., Du, M., and Lin, H. Y. (2021). Histone Deacetylase 9 Deficiency Exaggerates Uterine M2 Macrophage Polarization. *J. Cell Mol Med* 25 (16), 7690–7708. doi:10.1111/jcmm.16616

Liu, Y., Wang, L., Han, R., Beier, U. H., Akimova, T., Bhatti, T., et al. (2014). Two Histone/protein Acetyltransferases, CBP and P300, Are Indispensable for Foxp3+ T-Regulatory Cell Development and Function. *Mol. Cell Biol* 34 (21), 3993–4007. doi:10.1128/MCB.00919-14

Liu, Y., Wang, L., Predina, J., Han, R., Beier, U. H., Wang, L. C., et al. (2013). Inhibition of P300 Impairs Foxp3$^+$ T Regulatory Cell Function and Promotes Antitumor Immunity. *Nat. Med.* 19 (9), 1173–1177. doi:10.1038/nm.3286

Llopiz, D., Ruiz, M., Villanueva, L., Iglesias, T., Silva, L., Egea, J., et al. (2019). Enhanced Anti-tumor Efficacy of Checkpoint Inhibitors in Combination with the Histone Deacetylase Inhibitor Belinostat in a Murine Hepatocellular Carcinoma Model. *Cancer Immunol. Immunother.* 68 (3), 379–393. doi:10.1007/s00262-018-2283-0

LoRusso, P. M., Demchik, L., Foster, B., Knight, J., Bissery, M. C., Polin, L. M., et al. (1996). Preclinical Antitumor Activity of CI-994. *Invest New Drugs* 14 (4), 349–356. doi:10.1007/BF00180810

Lu, D., Yan, J., Wang, L., Liu, H., Zeng, L., Zhang, M., et al. (2017). Design, Synthesis, and Biological Evaluation of the First C-Met/HDAC Inhibitors Based on Pyridazinone Derivatives. *ACS Med. Chem. Lett.* 8 (8), 830–834. doi:10.1021/acsmedchemlett.7b00172

Lu, W., Che, X., Qu, X., Zheng, C., Yang, X., Bao, B., et al. (2021). Succinylation Regulators Promote Clear Cell Renal Cell Carcinoma by Immune Regulation and RNA N6-Methyladenosine Methylation. *Front Cell Dev Biol* 9, 622198. doi:10.3389/fcell.2021.622198

Lu, Y., Stuart, J. H., Talbot-Cooper, C., Agrawal-Singh, S., Huntly, B., Smid, A. I., et al. (2019). Histone Deacetylase 4 Promotes Type I Interferon Signaling, Restricts DNA Viruses, and Is Degraded via Vaccinia Virus Protein C6. *Proc. Natl. Acad. Sci. U S A.* 116 (24), 11997–12006. doi:10.1073/pnas.1816399116

Lucas, J., Hsieh, T. C., Halicka, H. D., Darzynkiewicz, Z., and Wu, J. M. (2018). Upregulation of PD-L1 E-xpression by R-esveratrol and P-iceatannol in B-reast

and C-olorectal C-ancer C-ells O-ccurs via HDAC3/p300-mediated NF-κB S-ignaling. *Int. J. Oncol.* 53 (4), 1469–1480. doi:10.3892/ijo.2018.4512

M, L., P, K., M, S., J, P., K V, W., C, L., et al. (2016). Essential Role of HDAC6 in the Regulation of PD-L1 in Melanoma. *Mol. Oncol.* 10 (5), 735–750. doi:10.1016/j.molonc.2015.12.012

Ma, H., Chang, H., Yang, W., Lu, Y., Hu, J., and Jin, S. (2020). A Novel IFNα-Induced Long Noncoding RNA Negatively Regulates Immunosuppression by Interrupting H3K27 Acetylation in Head and Neck Squamous Cell Carcinoma. *Mol. Cancer* 19 (1), 4. doi:10.1186/s12943-019-1123-y

Maeda, T., Towatari, M., Kosugi, H., and Saito, H. (2000). Up-regulation of Costimulatory/adhesion Molecules by Histone Deacetylase Inhibitors in Acute Myeloid Leukemia Cells. *Blood* 96 (12), 3847–3856. doi:10.1182/blood.v96.12.3847.h8003847_3847_3856

Maharaj, K., Powers, J. J., Mediavilla-Varela, M., Achille, A., Gamal, W., Quayle, S., et al. (2020). HDAC6 Inhibition Alleviates CLL-Induced T-Cell Dysfunction and Enhances Immune Checkpoint Blockade Efficacy in the Eμ-TCL1 Model. *Front Immunol.* 11, 590072. doi:10.3389/fimmu.2020.590072

Mattera, L., Escaffit, F., Pillaire, M. J., Selves, J., Tyteca, S., Hoffmann, J. S., et al. (2009). The p400/Tip60 Ratio Is Critical for Colorectal Cancer Cell Proliferation through DNA Damage Response Pathways. *Oncogene* 28 (12), 1506–1517. doi:10.1038/onc.2008.499

McGuire, A., Casey, M. C., Shalaby, A., Kalinina, O., Curran, C., Webber, M., et al. (2019). Quantifying Tip60 (Kat5) Stratifies Breast Cancer. *Sci. Rep.* 9 (1), 3819. doi:10.1038/s41598-019-40221-5

Meng, J., Liu, X., Zhang, P., Li, D., Xu, S., Zhou, Q., et al. (2016). Rb Selectively Inhibits Innate IFN-β Production by Enhancing Deacetylation of IFN-β Promoter through HDAC1 and HDAC8. *J. Autoimmun.* 73, 42–53. doi:10.1016/j.jaut.2016.05.012

Miao, B. P., Zhang, R. S., Yang, G., Sun, J. J., Tang, Y. Y., Liang, W. F., et al. (2018). Histone Acetyltransferase 1 up Regulates Bcl2L12 Expression in Nasopharyngeal Cancer Cells. *Arch. Biochem. Biophys.* 646, 72–79. doi:10.1016/j.abb.2018.03.040

Michan, S., and Sinclair, D. (2007). Sirtuins in Mammals: Insights into Their Biological Function. *Biochem. J.* 404 (1), 1–13. doi:10.1042/BJ20070140

Milling, S., and Edgar, J. M. (2019). How T'reg-ulate Healing of the Injured Spinal Cord? *Immunology* 158 (4), 253–254. doi:10.1111/imm.13148

Mohammadi, A., Sharifi, A., Pourpaknia, R., Mohammadian, S., and Sahebkar, A. (2018). Manipulating Macrophage Polarization and Function Using Classical HDAC Inhibitors: Implications for Autoimmunity and Inflammation. *Crit. Rev. Oncol. Hematol.* 128, 1–18. doi:10.1016/j.critrevonc.2018.05.009

Mormino, A., Cocozza, G., Fontemaggi, G., Valente, S., Esposito, V., Santoro, A., et al. (2021). Histone-deacetylase 8 Drives the Immune Response and the Growth of Glioma. *Glia* 69 (11), 2682–2698. doi:10.1002/glia.24065

Mounce, B. C., Mboko, W. P., Kanack, A. J., and Tarakanova, V. L. (2014). Primary Macrophages Rely on Histone Deacetylase 1 and 2 Expression to Induce Type I Interferon in Response to Gammaherpesvirus Infection. *J. Virol.* 88 (4), 2268–2278. doi:10.1128/JVI.03278-13

Myers, D. R., Lau, T., Markegard, E., Lim, H. W., Kasler, H., Zhu, M., et al. (2017). Tonic LAT-HDAC7 Signals Sustain Nur77 and Irf4 Expression to Tune Naive CD4 T Cells. *Cell Rep* 19 (8), 1558–1571. doi:10.1016/j.celrep.2017.04.076

Nakagawa, M., Oda, Y., Eguchi, T., Aishima, S., Yao, T., Hosoi, F., et al. (2007). Expression Profile of Class I Histone Deacetylases in Human Cancer Tissues. *Oncol. Rep.* 18 (4), 769–774. doi:10.3892/or.18.4.769

Narita, T., Weinert, B. T., and Choudhary, C. (2019). Functions and Mechanisms of Non-histone Protein Acetylation. *Nat. Rev. Mol. Cell Biol* 20 (3), 156–174. doi:10.1038/s41580-018-0081-3

Ning, Y., Ding, J., Sun, X., Xie, Y., Su, M., Ma, C., et al. (2020). HDAC9 Deficiency Promotes Tumor Progression by Decreasing the CD8+ Dendritic Cell Infiltration of the Tumor Microenvironment. *J. Immunother. Cancer* 8 (1). doi:10.1136/jitc-2020-000529

Ning, Z. Q., Li, Z. B., Newman, M. J., Shan, S., Wang, X. H., Pan, D. S., et al. (2012). Chidamide (CS055/HBI-8000): a New Histone Deacetylase Inhibitor of the Benzamide Class with Antitumor Activity and the Ability to Enhance Immune Cell-Mediated Tumor Cell Cytotoxicity. *Cancer Chemother. Pharmacol.* 69 (4), 901–909. doi:10.1007/s00280-011-1766-x

Núñez-Álvarez, Y., and Suelves, M. (2021). HDAC11: a Multifaceted Histone Deacetylase with Proficient Fatty Deacylase Activity and its Roles in Physiological Processes. *FEBS J.* 23, 1. doi:10.1111/febs.15895

Ogryzko, V. V., Schiltz, R. L., Russanova, V., Howard, B. H., and Nakatani, Y. (1996). The Transcriptional Coactivators P300 and CBP Are Histone Acetyltransferases. *Cell* 87 (5), 953–959. doi:10.1016/s0092-8674(00)82001-2

Osawa, Y., Kojika, E., Nishikawa, K., Kimura, M., Osakaya, S., Miyauchi, H., et al. (2019). Programmed Cell Death Ligand 1 (PD-L1) Blockade Attenuates Metastatic colon Cancer Growth in cAMP-Response Element-Binding Protein (CREB)-binding Protein (CBP)/β-catenin Inhibitor-Treated Livers. *Oncotarget* 10 (32), 3013–3026. doi:10.18632/oncotarget.26892

Osawa, Y., Oboki, K., Imamura, J., Kojika, E., Hayashi, Y., Hishima, T., et al. (2015). Inhibition of Cyclic Adenosine Monophosphate (cAMP)-Response Element-Binding Protein (CREB)-binding Protein (CBP)/β-Catenin Reduces Liver Fibrosis in Mice. *EBioMedicine* 2 (11), 1751–1758. doi:10.1016/j.ebiom.2015.10.010

Palmirotta, R., Cives, M., Della-Morte, D., Capuani, B., Lauro, D., Guadagni, F., et al. (2016). Sirtuins and Cancer: Role in the Epithelial-Mesenchymal Transition. *Oxid Med. Cell Longev* 2016, 3031459. doi:10.1155/2016/3031459

Peng, M., Mo, Y., Wang, Y., Wu, P., Zhang, Y., Xiong, F., et al. (2019). Neoantigen Vaccine: an Emerging Tumor Immunotherapy. *Mol. Cancer* 18 (1), 128. doi:10.1186/s12943-019-1055-6

Pillai, V. B., and Gupta, M. P. (2021). Is Nuclear Sirtuin SIRT6 a Master Regulator of Immune Function? *Am. J. Physiol. Endocrinol. Metab.* 320 (3), E399–E414. doi:10.1152/ajpendo.00483.2020

Poziello, A., Nebbioso, A., Stunnenberg, H. G., Martens, J. H. A., Carafa, V., and Altucci, L. (2021). Recent Insights into Histone Acetyltransferase-1: Biological Function and Involvement in Pathogenesis. *Epigenetics* 16 (8), 838–850. doi:10.1080/15592294.2020.1827723

Qiu, W., Wang, B., Gao, Y., Tian, Y., Tian, M., Chen, Y., et al. (2020). Targeting Histone Deacetylase 6 Reprograms Interleukin-17-Producing Helper T Cell Pathogenicity and Facilitates Immunotherapies for Hepatocellular Carcinoma. *Hepatology* 71 (6), 1967–1987. doi:10.1002/hep.30960

Que, Y., Zhang, X.-L., Liu, Z.-X., Zhao, J.-J., Pan, Q.-Z., Wen, X.-Z., et al. (2021). Frequent Amplification of HDAC Genes and Efficacy of HDAC Inhibitor Chidamide and PD-1 Blockade Combination in Soft Tissue Sarcoma. *J. Immunother. Cancer* 9 (2), e001696. doi:10.1136/jitc-2020-001696

Regna, N. L., Vieson, M. D., Luo, X. M., Chafin, C. B., Puthiyaveetil, A. G., Hammond, S. E., et al. (2016). Specific HDAC6 Inhibition by ACY-738 Reduces SLE Pathogenesis in NZB/W Mice. *Clin. Immunol.* 162, 58–73. doi:10.1016/j.clim.2015.11.007

Sakuraba, K., Yokomizo, K., Shirahata, A., Goto, T., Saito, M., Ishibashi, K., et al. (2011). TIP60 as a Potential Marker for the Malignancy of Gastric Cancer. *Anticancer Res.* 31 (1), 77–79.

Saleh, R., Toor, S. M., Sasidharan Nair, V., and Elkord, E. (2020). Role of Epigenetic Modifications in Inhibitory Immune Checkpoints in Cancer Development and Progression. *Front Immunol.* 11, 1469. doi:10.3389/fimmu.2020.01469

Sandhu, S. K., Volinia, S., Costinean, S., Galasso, M., Neinast, R., Santhanam, R., et al. (2012). miR-155 Targets Histone Deacetylase 4 (HDAC4) and Impairs Transcriptional Activity of B-Cell Lymphoma 6 (BCL6) in the Eμ-miR-155 Transgenic Mouse Model. *Proc. Natl. Acad. Sci. U S A.* 109 (49), 20047–20052. doi:10.1073/pnas.1213764109

Sanford, J. A., Zhang, L. J., Williams, M. R., Gangoiti, J. A., Huang, C. M., and Gallo, R. L. (2016). Inhibition of HDAC8 and HDAC9 by Microbial Short-Chain Fatty Acids Breaks Immune Tolerance of the Epidermis to TLR Ligands. *Sci. Immunol.* 1 (4), 1. doi:10.1126/sciimmunol.aah4609

Sarkar, R., Banerjee, S., Amin, S. A., Adhikari, N., and Jha, T. (2020). Histone Deacetylase 3 (HDAC3) Inhibitors as Anticancer Agents: A Review. *Eur. J. Med. Chem.* 192, 112171. doi:10.1016/j.ejmech.2020.112171

Shao, G., Liu, Y., Ma, T., Zhang, L., Yuan, M., and Zhao, S. (2018). GCN5 Inhibition Prevents IL-6-induced Prostate Cancer Metastases through PI3K/PTEN/Akt Signaling by Inactivating Egr-1. *Biosci. Rep.* 38 (6), 1. doi:10.1042/BSR20180816

Sharma, P., Hu-Lieskovan, S., Wargo, J. A., and Ribas, A. (2017). Primary, Adaptive, and Acquired Resistance to Cancer Immunotherapy. *Cell* 168 (4), 707–723. doi:10.1016/j.cell.2017.01.017

Sheikh, B. N., and Akhtar, A. (2019). The many Lives of KATs - Detectors, Integrators and Modulators of the Cellular Environment. *Nat. Rev. Genet.* 20 (1), 7–23. doi:10.1038/s41576-018-0072-4

Shiota, M., Yokomizo, A., Masubuchi, D., Tada, Y., Inokuchi, J., Eto, M., et al. (2010). Tip60 Promotes Prostate Cancer Cell Proliferation by Translocation of Androgen Receptor into the Nucleus. *Prostate* 70 (5), 540–554. doi:10.1002/pros.21088

Song, H. Y., Biancucci, M., Kang, H. J., O'Callaghan, C., Park, S. H., Principe, D. R., et al. (2016). SIRT2 Deletion Enhances KRAS-Induced Tumorigenesis *In Vivo* by Regulating K147 Acetylation Status. *Oncotarget* 7 (49), 80336–80349. doi:10.18632/oncotarget.12015

Song, L., Chen, X., Mi, L., Liu, C., Zhu, S., Yang, T., et al. (2020). Icariin-induced Inhibition of SIRT6/NF-Kb Triggers Redox Mediated Apoptosis and Enhances Anti-tumor Immunity in Triple-Negative Breast Cancer. *Cancer Sci.* 111 (11), 4242–4256. doi:10.1111/cas.14648

Sundaresan, N. R., Vasudevan, P., Zhong, L., Kim, G., Samant, S., Parekh, V., et al. (2012). The Sirtuin SIRT6 Blocks IGF-Akt Signaling and Development of Cardiac Hypertrophy by Targeting C-Jun. *Nat. Med.* 18 (11), 1643–1650. doi:10.1038/nm.2961

Tang, M., Tang, H., Tu, B., and Zhu, W. G. (2021). SIRT7: a sentinel of Genome Stability. *Open Biol.* 11 (6), 210047. doi:10.1098/rsob.210047

Tay, R. E., Olawoyin, O., Cejas, P., Xie, Y., Meyer, C. A., Weng, Q. Y., et al. (2020). Hdac3 Is an Epigenetic Inhibitor of the Cytotoxicity Program in CD8 T Cells. *J. Exp. Med.* 217 (7), 1. doi:10.1084/jem.20191453

Tomaselli, D., Steegborn, C., Mai, A., and Rotili, D. (2020). Sirt4: A Multifaceted Enzyme at the Crossroads of Mitochondrial Metabolism and Cancer. *Front Oncol.* 10, 474. doi:10.3389/fonc.2020.00474

Tong, L., Liang, H., Zhuang, H., Liu, C., and Zhang, Z. (2020). The Relationship between HDAC3 and Malignant Tumors: A Mini Review. *Crit. Rev. Eukaryot. Gene Expr.* 30 (3), 279–284. doi:10.1615/CritRevEukaryotGeneExpr.2020034380

van Loosdregt, J., Vercoulen, Y., Guichelaar, T., Gent, Y. Y., Beekman, J. M., van Beekum, O., et al. (2010). Regulation of Treg Functionality by Acetylation-Mediated Foxp3 Protein Stabilization. *Blood* 115 (5), 965–974. doi:10.1182/blood-2009-02-207118

Vanamee, É. S., and Faustman, D. L. (2017). TNFR2: A Novel Target for Cancer Immunotherapy. *Trends Mol. Med.* 23 (11), 1037–1046. doi:10.1016/j.molmed.2017.09.007

Vaquero, A., Scher, M., Lee, D., Erdjument-Bromage, H., Tempst, P., and Reinberg, D. (2004). Human SirT1 Interacts with Histone H1 and Promotes Formation of Facultative Heterochromatin. *Mol. Cell* 16 (1), 93–105. doi:10.1016/j.molcel.2004.08.031

Villagra, A., Cheng, F., Wang, H. W., Suarez, I., Glozak, M., Maurin, M., et al. (2009). The Histone Deacetylase HDAC11 Regulates the Expression of Interleukin 10 and Immune Tolerance. *Nat. Immunol.* 10 (1), 92–100. doi:10.1038/ni.1673

Villagra, A., Sotomayor, E. M., and Seto, E. (2010). Histone Deacetylases and the Immunological Network: Implications in Cancer and Inflammation. *Oncogene* 29 (2), 157–173. doi:10.1038/onc.2009.334

Wang, H., Fu, C., Du, J., Wang, H., He, R., Yin, X., et al. (2020a). Enhanced Histone H3 Acetylation of the PD-L1 Promoter via the COP1/c-Jun/HDAC3 axis Is Required for PD-L1 Expression in Drug-Resistant Cancer Cells. *J. Exp. Clin. Cancer Res.* 39 (1), 29. doi:10.1186/s13046-020-1536-x

Wang, L., Kumar, S., Dahiya, S., Wang, F., Wu, J., Newick, K., et al. (2016). Ubiquitin-specific Protease-7 Inhibition Impairs Tip60-dependent Foxp3+ T-Regulatory Cell Function and Promotes Antitumor Immunity. *EBioMedicine* 13, 99–112. doi:10.1016/j.ebiom.2016.10.018

Wang, L. T., Liu, K. Y., Jeng, W. Y., Chiang, C. M., Chai, C. Y., Chiou, S. S., et al. (2020b). PCAF-mediated Acetylation of ISX Recruits BRD4 to Promote Epithelial-Mesenchymal Transition. *EMBO Rep.* 21 (2), e48795. doi:10.15252/embr.201948795

Wang, S., He, Z., Wang, X., Li, H., and Liu, X. S. (2019a). Antigen Presentation and Tumor Immunogenicity in Cancer Immunotherapy Response Prediction. *Elife* 8, 1. doi:10.7554/eLife.49020

Wang, T., Yao, W., Shao, Y., Zheng, R., and Huang, F. (2018a). PCAF fine-tunes Hepatic Metabolic Syndrome, Inflammatory Disease, and Cancer. *J. Cell Mol Med* 22 (12), 5787–5800. doi:10.1111/jcmm.13877

Wang, X., Li, H., Chen, S., He, J., Chen, W., Ding, Y., et al. (2021). P300/CBP-associated Factor (PCAF) Attenuated M1 Macrophage Inflammatory Responses Possibly through KLF2 and KLF4. *Immunol. Cell Biol* 99 (7), 724–736. doi:10.1111/imcb.12455

Wang, Y., Yang, J., Hong, T., Chen, X., and Cui, L. (2019b). SIRT2: Controversy and Multiple Roles in Disease and Physiology. *Ageing Res. Rev.* 55, 100961. doi:10.1016/j.arr.2019.100961

Wang, Y., Yun, C., Gao, B., Xu, Y., Zhang, Y., Wang, Y., et al. (2017). The Lysine Acetyltransferase GCN5 Is Required for iNKT Cell Development through EGR2 Acetylation. *Cell Rep* 20 (3), 600–612. doi:10.1016/j.celrep.2017.06.065

Wang, Y. F., Liu, F., Sherwin, S., Farrelly, M., Yan, X. G., Croft, A., et al. (2018b). Cooperativity of HOXA5 and STAT3 Is Critical for HDAC8 Inhibition-Mediated Transcriptional Activation of PD-L1 in Human Melanoma Cells. *J. Invest Dermatol.* 138 (4), 922–932. doi:10.1016/j.jid.2017.11.009

Wang, Z., Qin, G., and Zhao, T. C. (2014). HDAC4: Mechanism of Regulation and Biological Functions. *Epigenomics* 6 (1), 139–150. doi:10.2217/epi.13.73

Wijdeven, R. H., van Luijn, M. M., Wierenga-Wolf, A. F., Akkermans, J. J., van den Elsen, P. J., Hintzen, R. Q., et al. (2018). Chemical and Genetic Control of IFNγ-Induced MHCII Expression. *EMBO Rep.* 19 (9), 1. doi:10.15252/embr.201745553

Willis-Martinez, D., Richards, H. W., Timchenko, N. A., and Medrano, E. E. (2010). Role of HDAC1 in Senescence, Aging, and Cancer. *Exp. Gerontol.* 45 (4), 279–285. doi:10.1016/j.exger.2009.10.001

Woan, K. V., Lienlaf, M., Perez-Villaroel, P., Lee, C., Cheng, F., Knox, T., et al. (2015). Targeting Histone Deacetylase 6 Mediates a Dual Anti-melanoma Effect: Enhanced Antitumor Immunity and Impaired Cell Proliferation. *Mol. Oncol.* 9 (7), 1447–1457. doi:10.1016/j.molonc.2015.04.002

Woods, D. M., Sodré, A. L., Villagra, A., Sarnaik, A., Sotomayor, E. M., and Weber, J. (2015). HDAC Inhibition Upregulates PD-1 Ligands in Melanoma and Augments Immunotherapy with PD-1 Blockade. *Cancer Immunol. Res.* 3 (12), 1375–1385. doi:10.1158/2326-6066.CIR-15-0077-T

Woods, D. M., Woan, K. V., Cheng, F., Sodré, A. L., Wang, D., Wu, Y., et al. (2017). T Cells Lacking HDAC11 Have Increased Effector Functions and Mediate Enhanced Alloreactivity in a Murine Model. *Blood* 130 (2), 146–155. doi:10.1182/blood-2016-08-731505

Wu, C., Li, A., Hu, J., and Kang, J. (2019). Histone Deacetylase 2 Is Essential for LPS-Induced Inflammatory Responses in Macrophages. *Immunol. Cell Biol* 97 (1), 72–84. doi:10.1111/imcb.12203

Xiang, J., Zhang, N., Sun, H., Su, L., Zhang, C., Xu, H., et al. (2020). Disruption of SIRT7 Increases the Efficacy of Checkpoint Inhibitor via MEF2D Regulation of Programmed Cell Death 1 Ligand 1 in Hepatocellular Carcinoma Cells. *Gastroenterology* 158 (3), 664–e24. doi:10.1053/j.gastro.2019.10.025

Xiao, H., Jiao, J., Wang, L., O'Brien, S., Newick, K., Wang, L. C., et al. (2016). HDAC5 Controls the Functions of Foxp3(+) T-Regulatory and CD8(+) T Cells. *Int. J. Cancer* 138 (10), 2477–2486. doi:10.1002/ijc.29979

Xiao, Y., Nagai, Y., Deng, G., Ohtani, T., Zhu, Z., Zhou, Z., et al. (2014). Dynamic Interactions between TIP60 and P300 Regulate FOXP3 Function through a Structural Switch Defined by a Single Lysine on TIP60. *Cell Rep* 7 (5), 1471–1480. doi:10.1016/j.celrep.2014.04.021

Xie, Z., Ago, Y., Okada, N., and Tachibana, M. (2018). Valproic Acid Attenuates Immunosuppressive Function of Myeloid-Derived Suppressor Cells. *J. Pharmacol. Sci.* 137 (4), 359–365. doi:10.1016/j.jphs.2018.06.014

Xiong, Y., Wang, L., Di Giorgio, E., Akimova, T., Beier, U. H., Han, R., et al. (2020). Inhibiting the Coregulator CoREST Impairs Foxp3+ Treg Function and Promotes Antitumor Immunity. *J. Clin. Invest* 130 (4), 1830–1842. doi:10.1172/JCI131375

Xu, P., Ye, S., Li, K., Huang, M., Wang, Q., Zeng, S., et al. (2019). NOS1 Inhibits the Interferon Response of Cancer Cells by S-Nitrosylation of HDAC2. *J. Exp. Clin. Cancer Res.* 38 (1), 483. doi:10.1186/s13046-019-1448-9

Yamada, K., Hori, Y., Inoue, S., Yamamoto, Y., Iso, K., Kamiyama, H., et al. (2021). E7386, a Selective Inhibitor of the Interaction between β-Catenin and CBP, Exerts Antitumor Activity in Tumor Models with Activated Canonical Wnt Signaling. *Cancer Res.* 81 (4), 1052–1062. doi:10.1158/0008-5472.CAN-20-0782

Yan, Z., Yao, S., Liu, Y., Zhang, J., Li, P., Wang, H., et al. (2020). Durable Response to Sintilimab and Chidamide in a Patient with Pegaspargase- and Immunotherapy-Resistant NK/T-Cell Lymphoma: Case Report and Literature Review. *Front Oncol.* 10, 608304. doi:10.3389/fonc.2020.608304

Yang, C., Croteau, S., and Hardy, P. (2021a). Histone Deacetylase (HDAC) 9: Versatile Biological Functions and Emerging Roles in Human Cancer. *Cell Oncol.* 44, 997–1017. doi:10.1007/s13402-021-00626-9

Yang, G., Yuan, Y., Yuan, H., Wang, J., Yun, H., Geng, Y., et al. (2021b). Histone Acetyltransferase 1 Is a Succinyltransferase for Histones and Non-histones and Promotes Tumorigenesis. *EMBO Rep.* 22 (2), e50967. doi:10.15252/embr.202050967

Yang, J., Gong, C., Ke, Q., Fang, Z., Chen, X., Ye, M., et al. (2021c). Insights into the Function and Clinical Application of HDAC5 in Cancer Management. *Front Oncol.* 11, 661620. doi:10.3389/fonc.2021.661620

Yang, M., Li, Z., Tao, J., Hu, H., Li, Z., Zhang, Z., et al. (2021d). Resveratrol Induces PD-L1 Expression through Snail-Driven Activation of Wnt Pathway in Lung Cancer Cells. *J. Cancer Res. Clin. Oncol.* 147 (4), 1101–1113. doi:10.1007/s00432-021-03510-z

Yang, P. M., Lin, P. J., and Chen, C. C. (2012). CD1d Induction in Solid Tumor Cells by Histone Deacetylase Inhibitors through Inhibition of HDAC1/2 and Activation of Sp1. *Epigenetics* 7 (4), 390–399. doi:10.4161/epi.19373

Yang, W., Feng, Y., Zhou, J., Cheung, O. K., Cao, J., Wang, J., et al. (2021e). A Selective HDAC8 Inhibitor Potentiates Antitumor Immunity and Efficacy of Immune Checkpoint Blockade in Hepatocellular Carcinoma. *Sci. Transl Med.* 13 (588), 1. doi:10.1126/scitranslmed.aaz6804

Ye, F., Jiang, J., Zong, C., Yang, X., Gao, L., Meng, Y., et al. (2020). Sirt1-Overexpressing Mesenchymal Stem Cells Drive the Anti-tumor Effect through Their Pro-inflammatory Capacity. *Mol. Ther.* 28 (3), 874–888. doi:10.1016/j.ymthe.2020.01.018

Yu, Y., Liu, Y., Zong, C., Yu, Q., Yang, X., Liang, L., et al. (2016a). Mesenchymal Stem Cells with Sirt1 Overexpression Suppress Breast Tumor Growth via Chemokine-dependent Natural Killer Cells Recruitment. *Sci. Rep.* 6, 35998. doi:10.1038/srep35998

Yu, Y., Zhang, Q., Meng, Q., Zong, C., Liang, L., Yang, X., et al. (2016b). Mesenchymal Stem Cells Overexpressing Sirt1 Inhibit Prostate Cancer Growth by Recruiting Natural Killer Cells and Macrophages. *Oncotarget* 7 (44), 71112–71122. doi:10.18632/oncotarget.12737

Yu, Z., Zeng, J., Liu, H., Wang, T., Yu, Z., and Chen, J. (2019). Role of HDAC1 in the Progression of Gastric Cancer and the Correlation with lncRNAs. *Oncol. Lett.* 17 (3), 3296–3304. doi:10.3892/ol.2019.9962

Zhang, Q., Zhao, K., Shen, Q., Han, Y., Gu, Y., Li, X., et al. (2015). Tet2 Is Required to Resolve Inflammation by Recruiting Hdac2 to Specifically Repress IL-6. *Nature* 525 (7569), 389–393. doi:10.1038/nature15252

Zhang, X., Wu, J., and Luan, Y. (2017). Tip60: Main Functions and its Inhibitors. *Mini Rev. Med. Chem.* 17 (8), 675–682. doi:10.2174/1389557516666160923125031

Zheng, X., Gai, X., Ding, F., Lu, Z., Tu, K., Yao, Y., et al. (2013). Histone Acetyltransferase PCAF Up-Regulated Cell Apoptosis in Hepatocellular Carcinoma via Acetylating Histone H4 and Inactivating AKT Signaling. *Mol. Cancer* 12 (1), 96. doi:10.1186/1476-4598-12-96

Zhou, B., Yang, Y., and Li, C. (2019). SIRT1 Inhibits Hepatocellular Carcinoma Metastasis by Promoting M1 Macrophage Polarization via NF-Kb Pathway. *Onco Targets Ther.* 12, 2519–2529. doi:10.2147/OTT.S195234

Zhou, Y., Bastian, I. N., Long, M. D., Dow, M., Li, W., Liu, T., et al. (2021). Activation of NF-Kb and P300/CBP Potentiates Cancer Chemoimmunotherapy through Induction of MHC-I Antigen Presentation. *Proc. Natl. Acad. Sci. USA* 118 (8), e2025840118. doi:10.1073/pnas.2025840118

Zhu, C., Chen, Q., Xie, Z., Ai, J., Tong, L., Ding, J., et al. (2011). The Role of Histone Deacetylase 7 (HDAC7) in Cancer Cell Proliferation: Regulation on C-Myc. *J. Mol. Med. (Berl)* 89 (3), 279–289. doi:10.1007/s00109-010-0701-7

Conflict of Interest: The authors declare that the research was conducted in the absence of any commercial or financial relationships that could be construed as a potential conflict of interest.

Publisher's Note: All claims expressed in this article are solely those of the authors and do not necessarily represent those of their affiliated organizations, or those of the publisher, the editors and the reviewers. Any product that may be evaluated in this article, or claim that may be made by its manufacturer, is not guaranteed or endorsed by the publisher.

GLOSSARY

HAT histone acetyltransferase
HDAC histone deacetylase
ICs immune checkpoints
PD-1 programmed cell death protein 1
PD-L1 programmed death-ligand 1
CTLA-4 cytotoxic T lymphocyte-associated protein 4
LAG lymphocyte activation gene
ACT adoptive T-cell therapy
ICB immune checkpoint blockade
MHC major histocompatibility class
CTLs cytotoxic T cells
IL interleukin
Tregs regulatory T cells
IRF interferon regulatory factor
IFN interferon
TNF tumor necrosis factor
NK natural killer cell
Sirt Sirtuin
NF- κ B nucleus factor κ-light-chain enhancer of activated B cells
CXCL C-X-C motif chemokine ligand
EMT epithelial-mesenchymal transition
MDSCs myeloid-derived suppressor cells
NSCLC Non-small-cell carcinoma
Lys lysine
Ser serine
JAK Janus kinase
STAT signal transducer and activator of transcription
TAM tumor associated macrophage
CoREST repressor element 1 silencing transcription factor corepressor
DLBCL diffuse large B cell lymphoma
Foxo forkhead box O
NCOR2 nucleus receptor co-repressor 2
EZH enhancer of zeste homolog 2
APC antigen-presenting cell
TEM effector memory T
RIPK receptor interacting protein kinase
MLKL mixed lineage kinase domain like pseudokinase
TGF transforming growth factor
AMPK AMP-activated protein kinase
GBM glioblastoma

frontiers in Pharmacology

REVIEW
published: 25 November 2021
doi: 10.3389/fphar.2021.779779

Roles of Major RNA Adenosine Modifications in Head and Neck Squamous Cell Carcinoma

Xing-xing Huo[1,2†], Shu-jie Wang[2†], Hang Song[3†], Ming-de Li[1], Hua Yu[4], Meng Wang[2], Hong-xiao Gong[1], Xiao-ting Qiu[1], Yong-fu Zhu[1] and Jian-ye Zhang[5]**

[1]Experimental Center of Clinical Research, Scientific Research Department, The First Affiliated Hospital of Anhui University of Chinese Medicine, Hefei, China, [2]Anhui Province Key Laboratory of Medical Physics and Technology, Institute of Health and Medical Technology, Hefei Institutes of Physical Science, Chinese Academy of Sciences, Hefei, China, [3]Department of Biochemistry and Molecular Biology, School of Integrated Chinese and Western Medicine, Anhui University of Chinese Medicine, Hefei, China, [4]Institute of Chinese Medical Sciences, State Key Laboratory of Quality Research in Chinese Medicine, University of Macau, Macao, China, [5]Key Laboratory of Molecular Target and Clinical Pharmacology and the State Key Laboratory of Respiratory Disease, School of Pharmaceutical Sciences and the Fifth Affiliated Hospital, Guangzhou Medical University, Guangzhou, China

OPEN ACCESS

Edited by:
Yingjie Zhang,
Shandong University, China

Reviewed by:
Yan Liu,
Nanjing Normal University, China
Cristina Barbagallo,
University of Catania, Italy

***Correspondence:**
Yong-fu Zhu
zyf240@ahtcm.edu.cn
Jian-ye Zhang
jianyez@163.com

[†]These authors have contributed equally to this work.

Specialty section:
This article was submitted to Experimental Pharmacology and Drug Discovery, a section of the journal Frontiers in Pharmacology

Received: 19 September 2021
Accepted: 09 November 2021
Published: 25 November 2021

Citation:
Huo X-x, Wang S-j, Song H, Li M-d, Yu H, Wang M, Gong H-x, Qiu X-t, Zhu Y-f and Zhang J-y (2021) Roles of Major RNA Adenosine Modifications in Head and Neck Squamous Cell Carcinoma. Front. Pharmacol. 12:779779. doi: 10.3389/fphar.2021.779779

Head and neck squamous cell carcinoma (HNSCC) is the sixth most common cancer malignancy worldwide and is known to have poor prognosis. The pathogenesis behind the development of HNSCC is not fully understood. Modifications on RNA are involved in many pathophysiological processes, such as tumor development and inflammation. Adenosine-related RNA modifications have shown to be linked to cancer and may play a role in cancer occurrence and development. To date, there are at least 170 different chemical RNA modifications that modify coding and non-coding RNAs (ncRNAs). These modifications affect RNA stability and transcription efficiency. In this review, we focus on the current understanding of the four major RNA adenosine modifications (N^6-Methyladenosine, N^1-Methyladenosine, Alternative Polyadenylation Modification and A-to-I RNA editing) and their potential molecular mechanisms related to HNSCC development and progression. We also touch on how these RNA modifications affect treatment of HNSCCs.

Keywords: RNA modification, N 6-methyladenosine, N 1-methyladenosine, alternative polyadenylation, adenosine-to-inosine editing, head and neck squamous cell carcinoma, immunotherapy

INTRODUCTION

Head and neck squamous cell carcinoma (HNSCCs) mainly occurs in the mucosal epithelium of the oral cavity, pharynx or larynx. It is the sixth most common cancer worldwide, with over 800,000 cases diagnosed annually and an increasing incidence (Ferlay et al., 2019; Sung et al., 2021). Exposure to tobacco-derived carcinogens, excessive alcohol consumption, human papillomavirus and EBV are some of the triggers associated with HNSCC (Johnson et al., 2020). The molecular mechanisms behind HNSCC pathogenesis and development have not been fully elucidated. In recent years, advances in molecular biology expanded the understanding of epigenetics, especially post-transcriptional modifications of RNA, which play important roles in cell fate determination, proliferation, metabolism and many pathological processes.

New messenger RNA (mRNA) transcripts require additional processing and modifications before translation and protein synthesis. RNA modifications regulate most steps of gene expression, from indirectly controlling DNA transcription through transcription factors, to

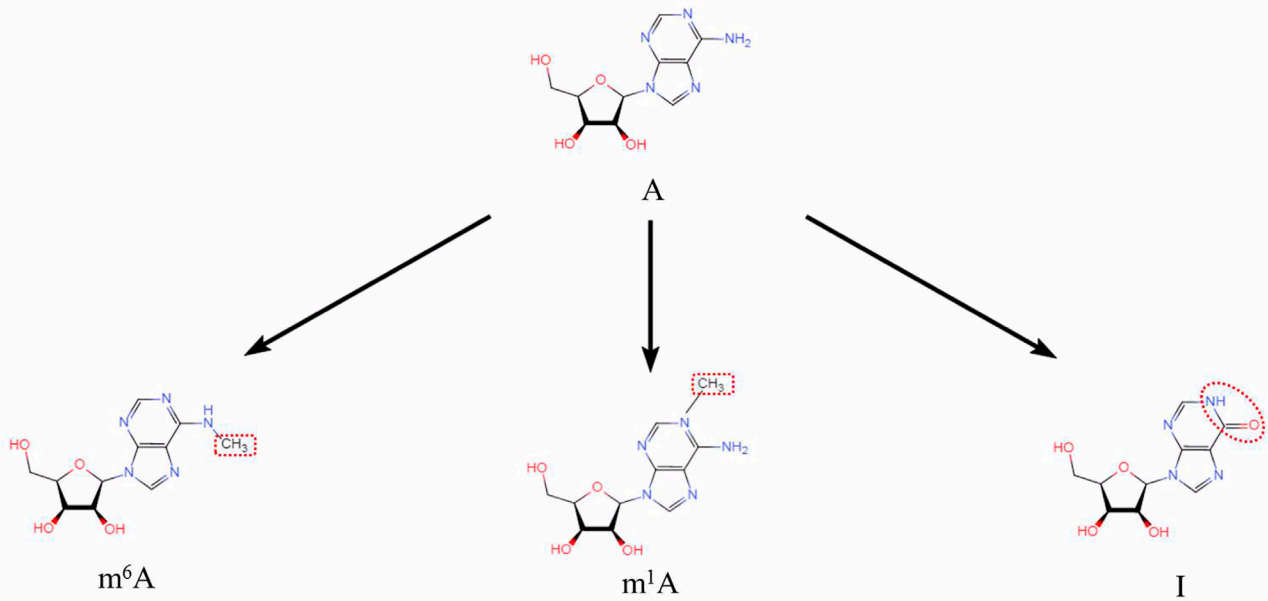

FIGURE 1 | Three adenine-associated RNA modifications (N^6-methyladenosine (m^6A), N^1-methyladenosine (m^1A) and Adenosine to Inosine (A to I)). Chemical structures of three adenine-associated RNA modifications are shown.

directly affecting mRNA translation (Delaunay and Frye, 2019). Many RNA modifications have been uncovered thanks to next generation sequencing technologies. Some RNA modifications are difficult to study since there may be an inability to distinguish between certain nucleotides (Li et al., 2019c). To date, there are at least 170 different chemical RNA modifications known to modify coding and non-coding RNAs (ncRNAs) (Ramanathan et al., 2016; Xu et al., 2017; Dimitrova et al., 2019). The heavy nucleotide adenine is the most commonly modified in RNA. In this review, we focus on adenine-associated RNA modifications, including m^6A methylation, m^1A methylation, A-to-I RNA editing (**Figure 1**) and APA (**Figure 2**). We also discuss adenine-associated RNA modifications in regulating gene expression in HNSCC.

ADENINE-RELATED RNA MODIFICATIONS

N^6-Methyladenosine Modifications

m^6A is the most abundant and well-defined internal modification in mRNA. Methylation of the sixth nitrogen atom of RNA base A affects RNA stability and translation efficiency (**Figure 3**). This modification is programmed by m^6A-methyltransferases, including methyltransferase-like 3 (METTL3), methyltransferase-like 14 (METTL14), WTAP, RNA-binding motif protein 15 (RBM15), RNA-binding motif protein 15B (RBM15B), ZC3H13 and KIAA1429.

N6-Methyladenosine Writers

The m^6A modification process undergoes first-order catalysis involving the two methyltransferase complexes (writers) METTL14 and METTL3. METTL3 coverts adenosine to m^6A through its methyltransferase domain, and METTL14 is responsible for the recognition of RNA substrates. ZC3H13, RBM15 and VIRMA are also incorporated into the methyltransferase complex to regulate METTL14 and METTL3 functions.

N6-Methyladenosine Erasers

The deposition of N^6-methyladenosine on RNA is reversible through coordination of methyltransferases and demethylases. Fat mass and obesity-associated protein (FTO) and AlkB homolog 5 (ALKBH5) have been identified as members of non-heme Fe (II)/α -ketoglutarate-dependent dioxygenases. AlkB homolog 3 (ALKBH3), another member of the family, preferentially acts on m^6A in tRNAs. The mechanisms where m^6A methylation selectively and dynamically targets specific regions of the transcriptome are not fully understood. It is anticipated that additional m^6A demethylases will be discovered.

N6-Methyladenosine Readers

m^6A modifications are unique recognition elements that bind proteins to readers and drive biochemical processes that occur in labeled RNA. The RNA-binding domain or the YTH domain contains YTH-domain proteins 1 and 2 family members (YTHDF1, YTHDF2, YTHDF3, YTHDC1 and YTHDC2). More recently, other readers have been identified, including insulin-like growth factor 2 mRNA-binding proteins (IGF2BP1, IGF2BP2, and IGF2BP3) and heterogeneous ribonucleic proteins (HNRNPC and HNRNPA2/B1). These proteins are highly expressed in different cancers and are involved in various molecular mechanisms. These proteins are not always dependent on the recognition of m^6A.

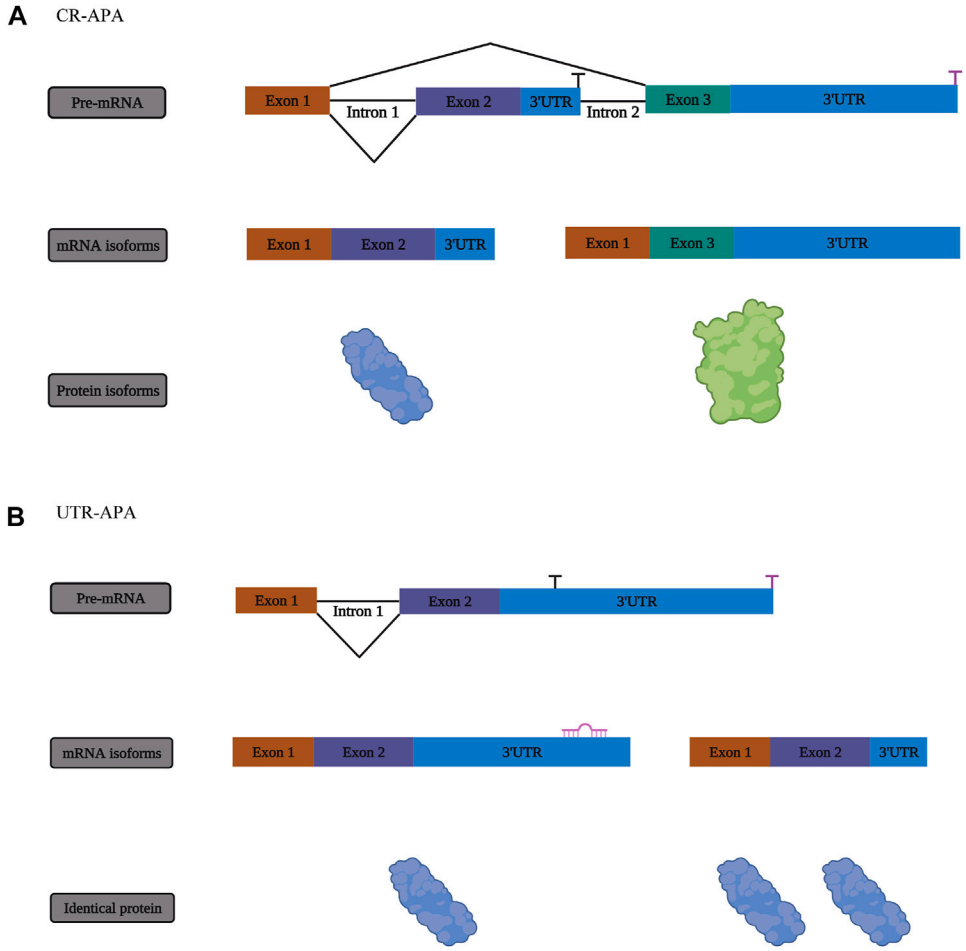

FIGURE 2 | The mechanism of alternative polyadenylation (APA). **(A)** One form of APA, termed coding region alternative polyadenylation (CR-APA), occurs when the alternative polyA sites (PASs) are located within exons or introns. **(B)** Another form of APA is known as untranslated region alternative polyadenylation (UTR-APA) when alternative PASs are located in different regions of the 3′-UTR, resulting in the identical protein isoforms.

N^1-Methyladenosine Modifications

m^1A is a reversible modification produced when a methyl group attaches to the N^1 position of adenosine. TRMT61A, TRMT61B, TRMT10C and TRMT6 have the ability to generate m^1A modifications. It carries a positive charge when in physiological conditions and blocks the Watson–Crick interface, alters the structure of RNA, regulates protein-RNA interactions and affects the tertiary structure of ribosomes and translation (Shi et al., 2019). In mammals, the abundance of m^1A in tRNAs and rRNAs is significantly greater than the abundance of mRNAs. Most m^1A sites are located in the 5′-untranslated region (5′-UTR) of RNA (Dominissini et al., 2016). This modification affects both the occurrence and development of tumors by regulating gene expression and related biological processes.

N^1-Methyladenosine Writers

m^1A "writers" contain a methyltransferase complex, including TRMT6, TRMT61A, TRMT10C and TRMT61B (Safra et al., 2017; Dai et al., 2018). In eukaryotes, m^1A methyltransferases consist of TRMT6 and TRMT61A responsible for m^1A58 modifications of cytoplasmic tRNAs (Ozanick et al., 2005). TRMT6 plays a key role in tRNA binding (Anderson et al., 2000). Studies have shown that TRMT10C and TRMT61B catalytic sites are located at positions 9 and 58 of human mt-tRNAs, respectively (Chujo and Suzuki, 2012; Vilardo et al., 2012). These positions on mt-tRNAs also coincide with the presence of m^1A modifications (Ozanick et al., 2005). In addition, the tRNA m^1A enzyme also modifies m^1A modifications in mRNAs. For example, TRMT6/61A programs m^1A sites in some nuclear mRNAs with GUUCRA tRNA-like motifs, while TRMT61B methylates half of the known m^1A sites in mt-mRNAs (Li et al., 2017). Safra et al. also revealed that position 1374 of the mt-mRNA ND5 can be programmed into m^1A by TRMT10C (Safra et al., 2017). Additional m^1A mRNA enzymes may be discovered in the future.

N^1-Methyladenosine Erasers

m^1A "erasers," such as m^1A demethylase, remove methyl groups from m^1A. ALKBH1 and ALKBH3 both exert m^1A demethylase activity and act as "erasers". Li et al. proposed that ALKBH1 and ALKBH3, both members of the ALKB family, participate in

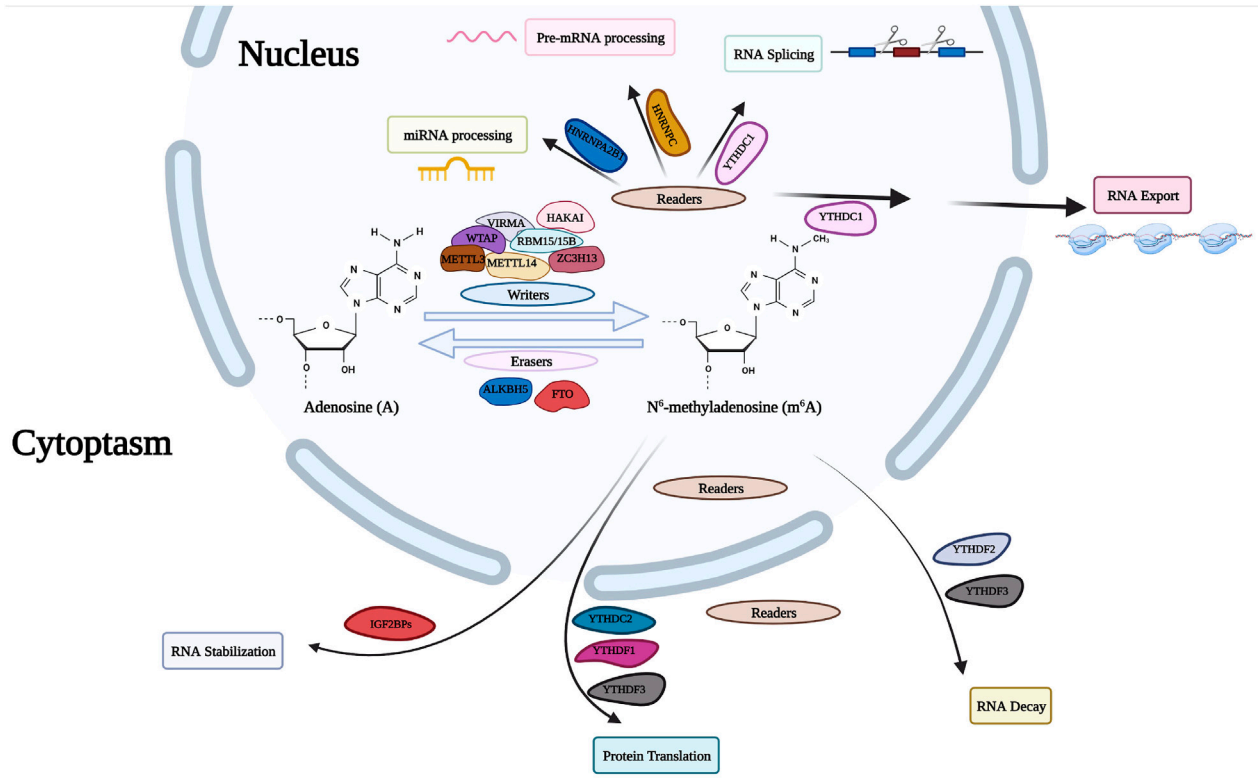

FIGURE 3 | m^{6}A RNA modifying process. The RNA modification of m^{6}A is performed by the writer proteins with a polymer complex containing WTAP, HAKAI, METTL3, METTL14, ZC3H13, RBM15, and VIRMA, while the modification can be removed by the eraser proteins (FTO and ALKBH5). The modification is identified by reader proteins including YT521B homology (YTH) domain-containing protein family, HNRNP family and IGF2BPs. WTAP, Wilms Tumor 1 Associated Protein; HAKAI, Cbl Proto-Oncogene Like 1; METTL3, methyltransferase Like 3; METTL14, methyltransferase Like 14; ZC3H13, Zinc Finger CCCH-Type Containing 13; RBM15, RNA Binding Motif Protein 15; VIRMA, Vir Like m^{6}A methyltransferase Associated; FTO, Fat Mass And Obesity-Associated Protein; ALKBH5, AlkB Homolog 5; HNRNP, Heterogeneous Nuclear Ribonucleoprotein; IGF2BP, Insulin Like Growth Factor 2 MRNA Binding Protein.

demethylation of m^{1}A sites in RNA (Li et al., 2016). Knocking out ALKBH1 increases m^{1}A methylation (Liu et al., 2016). Knockout of ALKBH3 increases m^{1}A levels in tRNAs and reduces protein synthesis in cancer cells (Ueda et al., 2017).

N^1-Methyladenosine Readers

The known "readers" for m^{1}A methylation include YTHDF1, YTHDF2, YTHDF3 and YTHDC1, which decode m^{1}A methylation markers and regulate m^{1}A-related functions by mediating post-transcriptional regulation (Dai et al., 2018). A recent study revealed YTHDF1-3 and YTHDC1 as m^{1}A readers, but not YTHDC2 (Dai et al., 2018). Electrophoretic mobility studies indicated that the YTH domain of YTHDF1-3 and YTHDC1 binds to RNA with m^{1}A modifications. In contrast, the YTH domain of YTHDC2 does not appear to bind to RNA with m^{1}A modification. Proteins containing an YTH domain recognize m^{1}A modifications, proving that YTHDF1-3 and YTHDC1 may be readers of m^{1}A modifications. However, there is limited research on m^{1}A "readers", and more m^{1}A "readers" are expected to be uncovered in the future.

Alternative Polyadenylation Modifications

Transcripts containing 3′-untranslation (3'-UTR) or coding regions of different lengths are generated through alternative polyadenylation (APA) when poly (A) tails are added or removed to different sites on RNA (Sandberg et al., 2008; Tian and Manley, 2017; Ikeda et al., 2020) (**Figures 2A,B**). Different transcripts have variable 3′-UTR lengths as a result of polyA sites, which contributes to polymorphisms (Pan et al., 2008; Wang et al., 2008; Xia et al., 2014). During embryonic development, APA is present at large amounts on mRNA. The most common form present in differentiated cells is the long 3′-UTR version (Grassi et al., 2018).

APA can affect the transcription in multiple ways (Lin et al., 2012). First, APA changes the position of protein products, adjusting metabolism (Berkovits and Mayr, 2015). Second, some APAs are tissue-specific and quickly respond to signals to regulate gene expression (Passacantilli et al., 2017). Furthermore, APA plays an important role in post-transcriptional splicing and can produce abnormal protein isoforms (Meyer et al., 2017; Ma et al., 2018; Zhu et al., 2018). In addition, upstream mechanisms, such as RNA processing factors and binding proteins, regulate APA and ultimately downstream biological processes (Zheng and Tian, 2014).

The proximal poly (A) site is used to form mRNAs with short 3 UTRs in highly proliferating cells (Ji and Tian, 2009). Studies

have shown that NUDT21 plays an important role in bladder cancer. NUDT21 regulates the expression of ANXA2 and LIMK2 through Wnt/beta-catenin and NF-kappaB signaling pathways. ANXA2 and LIMK2 act by APA (Wang et al., 2019a). Among the various risk factors related to the occurrence and development of cancer, APA is an important endogenous factor directly triggering malignant phenotypes. Specific APA events are closely related to the occurrence of malignant tumors and autoimmune diseases (Rajasekar et al., 2020). For example, high levels APA in cancer cells are often accompanied by loss of 3′-UTR inhibitory elements, indicating that APA plays a universal role in oncogene activation (Gruber and Zavolan, 2019). By studying the regulatory factors or mediators during the APA process, new diagnostic criteria or therapeutic targets for cancer and other diseases may be identified.

Adenosine-to-Inosine Editing

Epigenetic and post transcriptional mechanisms play important roles in gene expression and normal physiology editing is a post-transcriptional mechanism that changes the sequence of transcriptional RNA through post transcriptional modifications (Simpson and Emeson, 1996).

The most common form of RNA editing in higher eukaryotes includes A-to-I RNA editing, which occurs in double stranded RNA (dsRNA) where adenosine (A) forms inosine (I) through hydrolytic deamination (Roth et al., 2019). A-to-I editing alters amino acid sequences and affects other transcriptional processes, thereby promoting tumorigenesis and tumor progression through site-specific modifications of tumor-associated genes (Chen et al., 2017b; Hong et al., 2018; Xu et al., 2019a; Han et al., 2020). Adenosine deaminase (ADARs), including ADAR1, ADAR2 and ADAR3, catalyze this reaction (Valente and Nishikura, 2005; Yao et al., 2019). The ADAR family all contain a highly conserved C-terminal catalytic deaminase domain and several N-terminal dsRNA binding domains (Zinshteyn and Nishikura, 2009). The mammalian ADAR family consists of three structurally conserved members, ADAR1, ADAR2 and ADAR3 (Bass, 2002). ADAR1 and ADAR2 are expressed in most tissues and their catalytic activity has been observed for a while (Lehmann and Bass, 2000; Wong et al., 2001). ADAR3 is highly expressed in the central nervous system (Chen et al., 2000; Wang et al., 2019b). The ADAR1 protein has both a long (P150) and short (P110) isoform. ADAR1p110 is predominantly found in the nucleus, whereas ADAR1p150 is found in both the nucleus and cytoplasm. ADAR1p150 expression is driven by an interferon inducible promoter and is upregulated in situations of cellular stress or viral infection (Patterson and Samuel, 1995). ADAR1 plays an important role in A-to-I RNA editing and influences cancer development (Qin et al., 2014; Heraud-Farlow et al., 2019; Vlachogiannis et al., 2021). ADAR2 is present in the nucleus of cells and ADAR2 along with ADAR1 may both influence the function of neurons (Behm et al., 2017; Hosaka et al., 2019). ADAR3 exists as a monomer *in vitro* and is specifically expressed only in brain tissue, which may explain why it is thought to be catalytically inactive (Chen et al., 2000; Nishikura, 2010).

ADENINE-RELATED RNA MODIFICATION REGULATION IN HEAD AND NECK SQUAMOUS CELL CARCINOMA

The Role of N^6-Methyladenosine in Head and Neck Squamous Cell Carcinoma

Presently, it is generally believed that m^{6}A methylation modifications play key roles in the occurrence and development of carcinomas. Most studies indicate that an increase of m^{6}A methylation levels promotes tumor growth, development and treatment resistance (**Figure 4**). Here, we review recent articles studying m^{6}A modifications in head and neck carcinoma. A summary of these compiled studies are presented in **Table 1**.

N6-Methyladenosine Writers in Head and Neck Squamous Cell Carcinoma

METTL3 is a common writer for m^{6}A methylation. It is highly expressed in gastric, bladder, colorectal and pancreatic cancers as well as, glioblastoma and other tumors. High levels of METTL3 indicate a poor prognosis for gastric cancer (Li et al., 2019a; Li et al., 2019b; Han et al., 2019; Xia et al., 2019; Yue et al., 2019; Zhao and Cui, 2019; Wang et al., 2020a). METTL3 also plays an important role in head and neck carcinoma. A study by Wu et al. found that METTL3 regulates the m^{6}A methylation levels of circCUX1 and increases its stability in hypopharyngeal squamous cell carcinoma patients resistant to radiotherapy. The circCUX1 further inhibits caspase1 expression, reduces the release of inflammatory factors and increases the tolerability of tumor cells to radiotherapy. Knockout of circCUX1 increases the sensitivity of hypopharyngeal cancer cells to radiotherapy (Wu et al., 2021). Similarly, Ai et al. confirmed that METTL3 is highly expressed in oral squamous cell carcinoma (OSCC). METTL3 writes m^{6}A modifications in PRMT5 and PD-L1 and promotes the progression of OSCC by increasing m^{6}A editing (Ai et al., 2021). Interestingly, Liu et al. also found that the expression of METTL3 in two OSCC cohorts was significantly higher than in normal adjacent tissues, which was associated with a poor prognosis. METTL3 promotes proliferation, migration and invasion of OSCC *cells in vitro* by mediating m^{6}A modifications in the 3′-UTR of BMI1 mRNAs. METTL3 also cooperates with IGF2BP1 to promote the translation of BMI1 in OSCC. The METTL3-m^{6}A-BMI1 axis may serve as a therapeutic target or prognostic biomarker for OSCC (Liu et al., 2020). Meng et al. found that METTL3 was highly expressed in nasopharyngeal carcinoma (NPC) tissues, with increasing levels of expression associated with tumor stage. METTL3 is associated with the vitality and migration ability of NPC cells. In terms of mechanism, METTL3 binds and mediates m^{6}A modifications on EZH2 mRNAs, inhibiting EZH2 expression and upregulating CDKN1C expression. This increases the malignancy and promotes the development of NPC (Meng et al., 2020). We speculate that the METTL3-EZH2-CDKN1C regulatory axis may be closely related to NPC, and m^{6}A methylation modifications affect its activation.

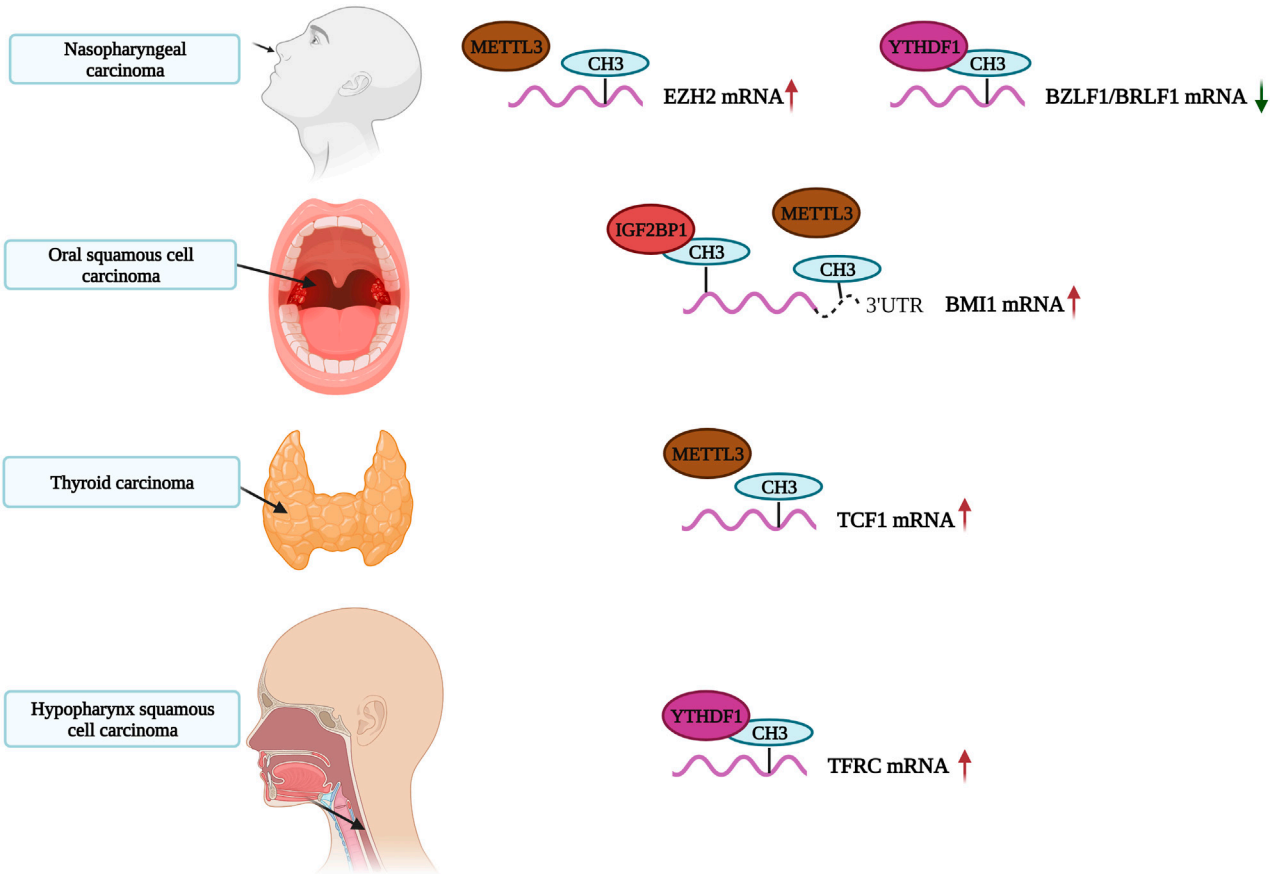

FIGURE 4 | The role of m^{6}A in Head and Neck Carcinoma. The m^{6}A-modified RNA play an important role in the occurrence and development of Head and Neck Carcinoma.

METTL3 and METTL14 also mediate m^{6}A modifications. Ban et al. found that METTL3 and METTL14 stabilize or even increase the expression of LNCAROD in HNSCC cells through m^{6}A modifications. LNCAROD binds to YBX1 and HSPA1A proteins, and its overexpression enhances the proliferation and migration of HNSCC cells. The dysregulation of m^{6}A methylation may cause abnormal expression of LNCAROD in HNSCC (Ban et al., 2020). In laryngeal squamous cell carcinoma (LSCC) patients, the expression of is significantly increased RBM15, indicating a poor prognosis. RBM15 mediates m^{6}A modifications of TMBIM6, and stabilizes the expression of TMBIM6 through IGF2BP3, thereby promoting LSCC (Wang et al., 2021b). Arumugam et al. reported that the expression levels of KIAA1429 in HNSCC tissues were significantly higher than in normal tissues. The increase of KIAA1429 expression is closely related to HNSCC metastasis. KIAA1429 (VIRMA), an m^{6}A writer, is frequently amplified and mutated (8%), which promotes the overexpression of KIAA1429 mRNA. Therefore, the methylation level of KIAA1429 (VIRMA) may be closely related to HNSCC (Arumugam et al., 2021). Similarly, there is evidence that KIAA1429 is a highly expressed m^{6}A regulatory gene in HNSCC (Zhao and Cui, 2019; Paramasivam et al., 2021). Unfortunately, these studies did not explore these relevant mechanisms in depth.

N6-Methyladenosine Readers in Head and Neck Squamous Cell Carcinoma

The IGF2BP family promotes tumor progression by reading m^{6}A-modified oncogenic mRNA. IGF2BP2 plays a key role in the progression of many cancers. Studies have shown that the overexpression of IGF2BP2 predicts poor prognosis of patients with colorectal cancer, acute myeloid leukemia and metaplastic breast cancer (He et al., 2018; Wang et al., 2020a). Upregulation of IGF2BP2 in pancreatic cancer may influence cell proliferation through the PI3K/Akt signaling pathway (Xu et al., 2019b). It has been confirmed that SNPs in IGF2BP2 and IGF2BP3 promote lymph node metastasis in esophagogastric junction adenocarcinoma (Chen et al., 2018). IGF2BP2 has also been linked to the occurrence and development of head and neck carcinoma. Paramasivam et al. pointed out that nearly half of HNSCC patients show significant changes in m^{6}A regulatory genes (Paramasivam et al., 2021). Among the aforementioned patients, nearly half of the patients showed increased expression of IGF2BP2, and the expression of the most common oncogene in

TABLE 1 | Regulation of m^{6}A modification in HNSCC.

m6A Regulators	Target	Regulation in HNSCC	Function	Mechanisms
METTL3 Wu et al. (2021); Arumugam et al. (2021); Ai et al. (2021)	Circux1 Wu et al. (2021)	Up	writer	METTL3 promotes the m6A methylation level of Circux1 and increases the stability of its expression in hypopharyngeal squamous cell carcinoma (HPSCC) Wu et al. (2021)
	PRMT5 and PD-L1 Ai et al. (2021)	Up	writer	METTL3 can promote the progress of OSCC by increasing the m6A editing degree of PRMT5 and PD-L1 Ai et al., 2021
METTL3 and METTL14	LNCAROD	Up	writer	METTL3 and METTL14 can stabilize the expression of LNCAROD in HNSCC cells through m6A modification Ban et al., 2020
RBM15	TMBIM6	Up	writer	RBM15 mediates the m6A modification of TMBIM6 and stabilizes the expression of TMBIM6 through IGF2BP3 Wang et al. (2021b)
KIAA1429 (VIRMA)	KIAA1429	Up	writer	KIAA1429 (VIRMA) can be used as a "writer" of m6A to help overexpression of KIAA1429 mRNA Arumugam et al., 2021
IGF2BP family (IGF2BP1, IGF2BP2 Geng et al., 2021; Paramasivam et al., 2021, IGF2BP3)	HMGA2 TK1 HDGF FSCN1 MKI67 CD44	Up	reader	The IGF2BP family promotes tumor progression by reading m6A-modified oncogenic mRNA Paramasivam et al., 2021
YTHDF1 Ye et al., 2020; Zhou et al., 2020 YTHDF2 Zhou et al., 2020 YTHDF3 Arumugam et al., 2021		Up	reader	The YTHDF1 methyltransferase domain can bind to the 3′UTR and 5′UTR of TRFC mRNA to promote m6A modification and translation of TFRC mRNA Ye et al., 2020
YTHDC2 Zhou et al., 2020			reader	
ALKBH5 Shriwas et al., 2020	FOXM1, NANOG (Shriwas et al., 2020)	Up	eraser	DDX3 directly regulates ALKBH5 to eliminate m6A methylation in the new transcripts of FOXM1 and NANOG Shriwas et al., 2020
FTO Zhou et al., 2020; Paramasivam et al., 2021			eraser	
	GRHL3-AS1, AL121845.4, AC116914.2, AL513190.1	Down		GRHL3-AS1, AL121845.4, AC116914.2, AL513190.1 have a protective effect on HNSCC patients

TABLE 2 | Immunotherapeutic methods and targets of HNSCCs.

Remedy	Regulation of target	Target	Mechanisms
CRISPR/Cas9 (HuR-CRISPR)	Knockout	HuR (ELAVL1)	The multifunctional nanoparticles Wang et al. designed can achieve targeted delivery of HuR CRISPR and epirubicin, and significantly improved the symptoms of mice bearing SAS tumors Wang et al. (2021a)
CRISPR-dCas9	Reactivate	ZAR1	Epigenetic therapy through the CRISPR-dCas9 method can accurately target and reactivate zygote arrest 1 (ZAR1), allowing it to regain its role as a tumor suppressor Deutschmeyer and Richter, (2020)
Immune Checkpoint Inhibitor (TIGIT)	Block	CD155	Blocking TIGIT/CD155 combined with PD-L1 monoclonal antibody treatment can significantly improve the efficacy of HNSCC Mao et al., 2021
Immune Checkpoint Inhibitor	Conjunct	P53	Adenoviral p53 can work in conjunction with immune checkpoint inhibitors to jointly exert anti-cancer effects Sobol et al., 2021
Immune Checkpoint Inhibitor	Inhibition	PD-1/ PD-L1	ICIs have good anti-tumor activity against R/M HNSCC Lee et al., 2021
Type I interferon	Promote	ADAR1	Type I interferon treatment can increase the amount and degree of RNA editing in esophageal squamous cell carcinoma cell lines Zhang et al., 2017
anti-OX40 neoadjuvant	Activate	CD4$^+$ and CD8$^+$ T cell	Patients with advanced HNSCC can receive anti-OX40 neoadjuvant treatment before surgery, which is not only safe, but can also increase the activation and proliferation of CD4$^+$ and CD8$^+$ T cells in the blood and tumors Duhen et al., 2021

HNSCC patients increased with higher levels of IGF2BP2. Similarly, Geng et al. reported that IGF2BP2 is increased in HNSCC and serves as an m^{6}A regulatory gene (Geng et al., 2021). This shows that IGF2BP2 is closely related to the occurrence and development of HNSCC. Deng et al. showed that IGF2BP2 is upregulated in HNSCC tissues, and its high

expression is associated with poor prognosis, playing a key role in HNSCC progression (Deng et al., 2020). Wang et al. also found that IGF2BP2 is highly expressed in papillary thyroid cancer (PTC) tissues and is closely related to the poor prognosis of PTC patients. The risk score of the m^{6}A-related IGF2BP2 signature can be used as an independent prognostic factor of PTC, which helps predict the disease-free survival of PTC patients (Wang et al., 2020d). This evidence indicates that the IGF2BP family may act as a key regulatory node, positively regulating the pathogenesis of HNSCC through m^{6}A methylation modifications.

A recent study showed that the m^{6}A reader YTH N6-methyladenosine RNA-binding protein 1 (YTHDF1) promotes the degradation of BZLF1 and BRLF1 by recruiting the RNA degrading proteins ZAP, DDX17 and DCP2. YTHDF1 ultimately inhibits EBV infection and lytic replication. This process is dependent on XRN1. Xia et al. speculated that EBV introduces m^{6}A modifications into host cells to destabilize BZLF1 and BRLF1, thereby inhibiting lytic replication and maintaining the incubation period of the virus (Xia et al., 2021). Previously, Ye et al. demonstrated that high expression of YTHDF1 increases m^{6}A modifications on TFRC mRNA to promote iron accumulation in hypopharyngeal squamous cell carcinoma (HPSCC). These modifications on TFRC mRNA have also influence tumor occurrence and proliferation. At the same time, YTHDF1 and iron-related genes (FTH1 and TFRC) are significantly upregulated in tumor tissues (Ye et al., 2020). Therefore, YTHDF1 may serve as a potential therapeutic target for HNSCC.

YTHDC2 is an m^{6}A reader protein (Kretschmer et al., 2018). It is a tumor suppressor gene reduced in HNSCC tissues that is closely associated with prognosis and immune infiltration levels (Li et al., 2020a).

N6-Methyladenosine Erasers in Head and Neck Squamous Cell Carcinoma

Only two m^{6}A erasers, including FTO and ALKBH5, have been uncovered so far (Zhao and Cui, 2019; Zhou et al., 2020; Paramasivam et al., 2021). FTO, a m^{6}A demethylase associated with human obesity, reverses m^{6}A modifications (Jia et al., 2011). Shriwas et al. found that the m^{6}A demethylase ALKBH5 is directly regulated by the DEAD-box RNA helicase 3 (DDX3), erasing m^{6}A methylation in new FOXM1 and NANOG transcripts and causes chemotherapy resistance (Shriwas et al., 2020). FTO regulates the proliferation and migration of cervical cancer cells by modifying E2F1 and Myc transcripts (Zou et al., 2019). However, there is no related work investigating the role of FTO as an m^{6}A eraser in HNSCC.

Bioinformatics Reveal N6-Methyladenosine Methylation Regulatory Genes

Of the expression of many m^{6}A regulatory genes, including writers (METTL3, METTL14, WTAP, ZC3H13 and RBM15), erasers (ALKBH5 and FTO), and readers (YTHDF1, YTHDF2, YTHDF3, YTHDC1, IGF2BP1 and IGF2BP3) were found to be significantly increased in HNSCC tissues (Feng et al., 2021; Paramasivam et al., 2021). Deng et al. pointed out that the expression of m^{6}A methylation regulatory genes is significantly related to the prognosis of HNSCC (Deng et al., 2021). Zhou et al. identified 10 m^{6}A regulators and those high expression levels of ALKBH5, FTO, METTL14, WTAP, YTHDC1, YTHDF1 and YTHDF2 predict poor prognosis for HNSCC patients. The expression level of YTHDC2 was also found to be directly proportional to patient prognosis (Zhou et al., 2020). However, this study also performed a preliminary analysis and further studies are needed. Feng et al. used bioinformatic methods to screen 4 m^{6}A-modified differentially expressed lncRNAs between high-risk group and low-risk group cancer groups. Interestingly, results showed that the expression levels of these four m^{6}A-modified lncRNAs were reduced in the high-risk group. The higher the m^{6}A-modified lncRNA expression level, the higher the survival rate of HNSCC patients. In other words, these four m^{6}A-modified lncRNAs showed protective effects for HNSCC patients (Feng et al., 2021). This finding differs from public opinion, but indicates that the biological role of m^{6}A methylation modifications in HNSCC requires further exploration. Other relevant bioinformatic analyses show similar findings (Zhao and Cui, 2019; Li et al., 2020a; Huang et al., 2020). These studies identified key genes as potential aspects for future research and treatment (Yi et al., 2020).

The Role of N^1-Methyladenosine in Head and Neck Squamous Cell Carcinoma

There are limited studies investigating the role of m^{1}A modifications in cancer as well its role in HNSCC. Some studies revealed that m^{1}A methylation modifications influence different cancers including hepatocellular carcinoma (HCC), lung cancer, colorectal cancer and pancreatic cancer (Wang et al., 2020; Shi et al., 2020; Xie et al., 2020). In addition, Li et al. found that expression of m^{1}A regulatory factors are significantly altered in cancer patients and are closely related to changes in carcinogenic pathways and overall survival rate (Li et al., 2021).

Zhao et al. comprehensively analyzed TCGA data for diagnosed with esophageal carcinoma (ESCA), liver hepatocellular carcinoma (LIHC), stomach adenocarcinoma (STAD), pancreatic adenocarcinoma (PAAD) and colorectal adenocarcinoma (COAD)). Expression of m^{1}A regulators, such as writers (TRMT6, TRMT61A and TRMT10C), erasers (ALKBH1, ALKBH3) and readers (YTHDF1-3, YTHDC1), were significantly changed in all gastrointestinal cancers analyzed.

The expression levels of m^{1}A regulatory genes are significantly higher in HCC than in normal tissues. In addition, the expression levels of TRMT6, TRMT61A and TRMT10C, as well as ALKBH3 and YTHDF2, are higher in patients with late-stage tumors (G1-G3) (Zhao et al., 2019). Shi et al. also found that the expression of m^{1}A-related regulatory genes, such as TRMT6, TRMT61A, TRMT10C and YTHDF1, are helpful in assessing risk and survival prediction of HCC patients. A significant correlation between YTHDF1 and TRMT6 was identified in their study.

YTHDF1, which acts as m^6A modification reader, also acts as m^1A modified RNA binding protein, playing an important role in regulating m^1A methylation modifications. TRMT6 forms a methyltransferase complex with TRMT61A to catalyze the methylation of the N^1 position of adenosine residues in mRNAs. Increased expression of TRMT6 is associated with poor prognosis (Shi et al., 2020). Meanwhile, Zhao et al. found that some GC patients show alterations in m^1A regulatory factors, including mutations, copy number amplifications or deep deletions. The change frequency of TRMT6 is nearly 1.8%, and the mutation frequency of the YTHDF1 and YTHDF3 readers is highest amongst GC patients, reaching 6 and 5%, respectively (Zhao et al., 2019). This is consistent with findings by Shi et al. Their studies revealed that copy number variations (CNV) have a higher frequency in m^1A-related regulatory genes. The differential expression of 10 m^1A-related regulatory genes, such as the reader YTHDF1, can be used as prognostic indicators (Shi et al., 2020). Based on these observations, there is reason to believe that YTHDF1 can be used as a reader along with TRMT6 and TRMT61A to jointly regulate m^1A methylation in HCC. Interestingly, Wang et al. also observed dysregulation in m^1A regulatory factors in gynecological cancers. TRMT10C was found to be highly expressed in ovarian and cervical cancers and being associated with a poor prognosis. TRMT10C inhibits the proliferation and migration of ovarian and cervical cancer cells (Wang et al., 2020c). Therefore, it is reasonable to believe that TRMT10C can also be used as a biomarker for predicting the prognosis of patients with gynecological cancers. m^1A modification-related genes may affect the expression of oncogenes through m^1A methylation and may be involved in the progression of HNSCC.

These differences are also present in PAAD but only at a moderate level compared with HCC (Shi et al., 2020). Zheng et al. also found that changes of m^1A regulatory genes in PAAD are associated with cancer stage. Some of these genes serve as writers or readers and have a high mutational frequency. CNV has also been found to have a high frequency of mutations. Meanwhile, changes in the YTHDF1 and TRMT61A genes were found in two PAAD samples. Even though high expression levels of YTHDF1 and YTHDF2 were found to be associated with the poor prognosis of PAAD patients (Chen et al., 2017a), it is not clear whether this is due tom^{1}A regulation. The m^1A-related writers, erasers and readers are differentially expressed depending on the stage. Low expression of the ALKBH1 eraser predicts poor prognosis of PAAD patients (Zheng et al., 2021). ALKBH1 contains both m^1A and m^6A demethylase activities (Wu et al., 2016; Kawarada et al., 2017). Wang et al. found that ALKBH1, YTHDF1, TRMT6, TRMT10C and TRMT61B are elevated in endometrial cancers (Wang et al., 2020c). Therefore, overexpression of ALKBH1 most likely reverses methylation and inhibits tumor development. Shi et al. identified that m^1A modifications are increased in COAD tissues, accompanied by down-regulation in lncRNA expression levels relative to normal adjacent tissues (Shi et al., 2021). Meanwhile, three different m^1A modification patterns identified by Gao et al. significantly affect relapse-free survival, overall survival and the number of tumor microenvironment infiltration cells in COAD patients. In addition, Pan et al. found that m^1A regulatory factor expression levels significantly differed between lung squamous cell carcinoma and normal tissues (Pan et al., 2021).

This evidence proves that m^1A methylation modifications play important roles in gastrointestinal, gynecological and lung cancers. m^1A methylation modifications also influence the occurrence and development of HNSCC.

The Role of Alternative Polyadenylation in Head and Neck Squamous Cell Carcinoma

APA induces 3′-UTR shortening and it has been considered a specific feature of tumorigenesis and involved in the development of HNSCC.

CPSF plays an important role in processing the 3′-processing complex. Core 3′-processing factors include protein complexes (CPSF, CSTF, CFI and CFII) and several single proteins. CPSF1 is the largest subunit of the protein complex (Murthy and Manley, 1995) that recognizes polyadenylation signals and regulates APA (Martin et al., 2012; MacDonald, 2019). Sakai et al. identified 13 candidate spliceosome genes significantly altered in HNSCC. In these candidate genes, a higher number of alternative splicing events (ASEs) were identified with CPSF1 was overexpressed. This promoted the growth of HNSCC cells. In addition, junction analysis showed that abnormal expression of CPSF1 is related to ASEs of cancer-related genes, such as LAMC2, UBE2C, AKT2, AKT2, BOK, MAP4 and FANCD2. Therefore, it was speculated that CPSF1 overexpression leads to abnormal splicing of oncogenes and promotes tumor occurrence and development (Sakai et al., 2020). Interestingly, there is evidence that CPSF1 promotes tumor development by regulating APA events in triple-negative breast cancer (TNBC). Wang et al. determined that CPSF1 and PABPN1 are the main C/P factors that regulate APA events. Knockout of CPSF1 or PABPN1 reverses APA events of tumor-related genes in TNBCs, inhibits tumor cell proliferation, promotes apoptosis and redistributes the cell cycle (Wang et al., 2020b). This indicates that the mechanism by which APA regulates TNBC cell proliferation may be achieved by changing core processing factor (CPSF1 and PABPN1) levels. We speculate that CPSF1 may affect tumors development and group through the APA pathway.

PABPN1 may also act as the core factor of APA regulation. Poly (A) tails grow to ~250 nucleotides. PABPN1 binds to poly (A) and breaks the connection between CPSF and poly (A) polymerase, thereby controlling the length of the poly (A) tail (Wahle, 1995; Kuhn et al., 2009; Eckmann et al., 2011). Xiang et al. proved that PABPN1 is a key factor regulating the APA profile of many cancers (Xiang et al., 2018). Ichinose et al. found that PABPN1 acts as an APA inhibitor. Deletion of PABPN1 induces APA events, leading to microRNA-mediated gene regulation and causing the release of cancer cells (Ichinose et al., 2014). In summary, we speculate that CPSF1 and PABPN1 serve as key regulatory factors to increase APA events and promote HNSCC development.

In addition, we believe that some oncogenes alter the length of 3′-UTR through APA events, thereby evading gene suppression and promoting the growth of HNSCC (Martin et al., 2012; Missan

et al., 2015). It has been demonstrated in NPC that the oncogene FND3CB increases proximal polyadenylation sites through APA events, resulting in shorter 3′-UTRs. This evades miRNA-mediated gene suppression (Li et al., 2020b). The same mechanism of action has also been identified in bladder cancer (Xiong et al., 2019) and HCC (Sun et al., 2017; Tan et al., 2018). Meanwhile, 195 genes were also identified in NPC and their tandem 3′-UTR lengths were significantly different between NPC and the control group (Xu et al., 2018). In esophageal squamous cell carcinomas, 903 genes related to adhesion junctions and the cell cycle shortened the 3′-UTR, and the distal PolyA site was used by 917 genes (Sun et al., 2014). This difference may be caused by APA-mediated gene expression regulation. In summary, APA may play a key role in the occurrence and development of HNSCC.

The Role of Adenosine-to-Inosine Editing in Head and Neck Squamous Cell Carcinoma

Currently, there are only a few studies directly investigating A-to-I RNA editing in HNSCC. One reason for this may be due to limited detection technology in identifying A-to-I editing sites. Previous studies have shown A-to-I RNA editing (R334G) in the tumor suppressor gene prox1 present in 4 of 8 esophageal cancer cases, indicating that A-to-I RNA editing may be closely related to the progression of this cancer (Yoshimoto et al., 2007). Hochberg et al. identified two A-to-I editing sites in insulin-like growth factor-binding protein-7 (IGFBP7) transcripts. In the normal epidermis, IGFBP7 transcripts are highly edited, but this editing is significantly reduced in basal cell and squamous cell carcinomas. Edited IGFBP7 inhibits the proliferation of keratinocytes and induces their senescence. These results indicate that A-to-I RNA editing in IGFBP7 maintains the balance between normal skin proliferation and aging, and its reduction may promote the occurrence and development of carcinoma (Hochberg et al., 2013). A recent study showed that A-to-I SLC22A3 RNA editing resulted in a decrease in SLC22A3 gene expression and led to lymph node metastasis in ESCC cases. This process almost only occurs in familial high-risk individuals, making them susceptible to ESCC, but does not occur in sporadic ESCC cases. The A-to-I transcript editing event (A261 at exon 1) that resulted in the substitution of asparagine (Asn)-aspartate (Asp) amino acids may be related to ESCC susceptibility (Fu et al., 2017). However, this study later discovered that the RNA editing enzyme ADAR2 is a familial ESCC susceptibility gene, suggesting that ADAR plays a central role in A-to-I RNA editing. Adenosine deaminase catalysis that acts on the RNA (ADARs) family plays an important role in A-to-I RNA editing. Therefore, most current research is focused on ADARs.

ADAR1 as a Foe

ADAR1 may be closely related to the occurrence and development of HNSCC. Zhang et al. showed that ADAR1 expression is related to STAT1, STAT2 and IRF9, and the abundance of ADAR1 protein is related to the activation of JAK/STAT pathway induced by type I interferons. The activation of JAK/STAT pathway regulates the expression of ADAR1, which leads to an abnormal RNA editing spectrum in ESCC (Zhang et al., 2017). Interestingly, Qin et al. found that ADAR1 was overexpressed in ESCC and that it predicted a poor prognosis. Over-editing of AZIN1 information catalyzed by ADAR1 makes carcinomas more aggressive. This study confirmed that ADAR1 can be used as an oncogene, and the excessive A-to-I editing mediated by it promotes the development of ESCC (Qin et al., 2014). In summary, ADAR1 may be closely related to the occurrence and development of ESCC. A-to-I RNA editing mediated by ADAR1 may promote ESCC. In addition, there is evidence that ADAR1 plays an important biological function in oral squamous cell carcinoma (OSCC). Liu et al. found that ADAR1 is over-expressed in OSCC and positively correlates with migration, invasion and EMT. ADAR1 may combine with dicer to increase the expression of oncogenic miRNAs, affect cell migration and invasion, promote carcinoma growth and reduce patient survival (Bo et al., 2019). Ma et al. found that ADAR binds to forkhead box D1 antisense RNA 1 (FOXD1-AS1) and FOXD1 in OSCC cells, to enhances the stability of FOXD1 mRNA, thereby promoting the occurrence and development of OSCC (Ma et al., 2021). This evidence indicates that ADAR1 is involved in A-to-I RNA editing to promote the occurrence and development of HNSCC. An increase in A-to-I RNA editing will lead to increased proliferation and migration, which indicates a poor prognosis for HNSCC patients.

ADAR2: Friend or Foe?

Behm et al. found that mice do not survive to adulthood in the absence of the active editing enzymes ADAR1 or ADAR2. As neurons mature, the number of interactions between ADAR2 and nuclear isomerase Pin1 increases, which contributes to the stability of ADAR2 protein and helps mouse neurons develop and mature (Behm et al., 2017). Terajima et al. showed that ADAR2 mediated A-to-I RNA editing critically contributes to light induced circadian clock phase shifts in the suprachiasmatic nucleus of the mouse hypothalamus (Terajima et al., 2018). However, Agranat et al. identified arginine/glycine sites of SON mRNA as ADAR2 dependent sites. They also detected multiple circular RNAs with ADAR2 dependent sites in SH-SY5Y cells and culture medium. These RNAs with ADAR2 dependent sites may serve as biomarkers for amyotrophic lateral sclerosis (Agranat et al., 2010). As previously mentioned, Fu et al. determined that ADAR2 is a familial ESCC susceptibility gene and that SLC22A3 is a tumor suppressor gene. ADAR2 is overexpressed in familial normal esophageal tissues, which increases the A-to-I RNA editing of the SLC22A3 gene and reduces the expression of the SLC22A3 gene, thereby increasing the susceptibility of ESCC (Fu et al., 2017). Interestingly, Chen et al. believe that overexpression of ADAR2 inhibits the growth and induces apoptosis by editing and stabilizing IGFBP7 in ESCC. Knockout of ADAR2 in carcinoma cells with high expression of ADAR2 inhibits tumor cell apoptosis (Chen et al., 2017d). This is contrary to the view of Fu et al., which suggests that overexpression of ADAR2 promotes tumor growth (Fu et al., 2017). Therefore, additional studies are needed to identify the true roles of ADAR2.

ADAR3: A Potential Friend

The biological role of ADAR3 has been studied over recent years. Wang et al. found that ADAR3 binds to two activity-dependent immediate-early genes in response to brain stimulation that encode the 3′-UTRs of the mRNAs early growth response 1 (EGR1) and bispecific phosphatase 1 (DUSP1), thereby regulating the transcription levels of DUSP1 and EGR1. This result suggests that ADAR3 may play a new role in brain function (Wang et al., 2019b). ADAR3 was also found to be related to Q/R locus editing. The Q/R site refers to the codon modification site of the glutamate receptor ionotropic AMPA 2 (GRIA2). GRIA2 is an adenosine in glutamate receptor subunit B transcripts. In glioblastoma, the reduction of GRIA2 transcript editing leads to cell migration and tumor invasion. However, Oakes et al. detected that ADAR3 expression was higher in glioblastoma compared to adjacent brain tissues. Meanwhile, they found that ADAR3 directly binds to GRIA2 precursor-mRNAs in astrocytes and astrocytoma cell lines. Overexpression of ADAR3 inhibits the RNA editing of the GRIA2 Q/R site, thus inhibiting tumor migration (Oakes et al., 2017). Interestingly, ADAR3 was also found to negatively correlate with the prognosis of low-grade gliomas, and positively correlate with GRIA2 (Q607R) editing. Zhang et al. believe that ADAR3 may inhibit the growth of glioma cells, and its high expression serves as a prognosis for patients with low-grade gliomas (Zhang et al., 2018). Therefore, the presence of ADAR3 may indicate a good prognosis for cancer patients.

ADENINE-RELATED RNA MODIFICATIONS AND HEAD AND NECK SQUAMOUS CELL CARCINOMA THERAPY

The current treatment methods for HNSCC mainly include a combination of surgery, radiotherapy, chemotherapy, organ-sparing neoadjuvant radiotherapy and chemotherapy. There is an extreme treatment plan for recurrent or metastatic HNSCC (R/M HNSCC) cases that combines platinum, fluorouracil and cetuximab chemotherapy (Vermorken et al., 2008). This can increase the survival rate of patients (the risk of death ratio (HR) is 0.80, $p = 0.04$) (Leon et al., 2005; Stewart et al., 2009; Vermorken et al., 2014), but the efficacy of R/M HNSCC patients who are resistant to platinum-containing chemotherapy is limited. Also, many patients cannot tolerate the side effects caused by radiotherapy and chemotherapy. Therefore, it is necessary to find new immunotherapy targets.

HuR (ELAVL1) is an RNA-binding protein that plays a positive role in regulating tumor survival and invasion. Wang et al. proposed that knockout of HuR through CRISPR/Cas9 (HuR-CRISPR) inhibits tumor progression. Multifunctional nanoparticles can achieve targeted delivery of HuR CRISPR and epirubicin, and significantly improved the symptoms of mice bearing SAS tumors (Wang et al., 2021a). However, related research is still at the stage of animal experiments, and further research is needed to determine whether it can be applied to the clinic.

Programmed cell death protein-1 (PD-1/CD279) is an important immune checkpoint expressed by T cells. It can be coupled with the programmed death ligand PD-L1 (B7-H1/CD274) expressed by tumor cells and inhibit the activation of T cells and the anti-tumor response, evading immune system clearance. Immune checkpoint inhibitors (ICIs) can block the inhibitory immune checkpoint pathway, thereby reactivating anti-tumor immune activity. Common ICIs include PD-1/PD-L1 inhibitors that can specifically bind to PD-L1 on tumor cells and block the inhibitory immune checkpoint pathway (Gong et al., 2018). TIGIT is a new immune checkpoint molecule that binds to CD155 with high affinity (Yu et al., 2009). It can deliver immunosuppressive signals by binding to CD155 in competition with CD226 (dNaM-1). Liang et al. showed that CD155 (+) PD-L1 (+) bone marrow mesenchymal stem cells are enriched in the tumor microenvironment. Blocking TIGIT/CD155 combined with PD-L1 monoclonal antibody treatment can significantly improve the efficacy of HNSCC (Mao et al., 2021). Meanwhile, *Liu et al.* proposed that the expression of PD-L1 in HNSCC cytology samples is highly consistent with matched histological samples (Liu et al., 2021). Lee et al. also believe that ICIs show good anti-tumor activity against R/M HNSCC (Lee et al., 2021). Therefore, ICIs can be used for the treatment of HNSCC, and PD-1/PD-L1 inhibitors may play a positive role in promoting this treatment.

In addition, there are other immunotherapy approaches for HNSCC, such as p53 targeted therapy. Adenoviral p53 can work in conjunction with immune checkpoint inhibitors to jointly exert anti-cancer effects (Sobol et al., 2021). Type I interferon treatment can increase the amount and degree of RNA editing in ESCC cell lines (Zhang et al., 2017). Epigenetic therapy using the CRISPR-dCas9 method accurately targets and reactivates zygote arrest 1 (ZAR1), allowing it to regain its role as a tumor suppressor (Deutschmeyer and Richter, 2020). Patients with advanced HNSCC can receive anti-OX40 neoadjuvant treatment before surgery. It not only is safe, but can also increase the activation and proliferation of $CD4^+$ and $CD8^+$ T cells in the blood and tumors (Duhen et al., 2021) (**Table 2**). Therefore, we have reason to believe that the future treatment of HNSCC will be more accurate and effective.

DISCUSSION

RNA editing refers to post-transcriptional changes in RNA sequences. RNA modifications play key roles in the occurrence of various cancers, but the specific mechanisms are still unclear. These modifications may act as tumor-promoting factors to promote tumor growth, while it can also be used as inhibitors to limit the occurrence of tumors.

Presently, RNA editing research in HNSCC can be summarized into the following four mechanisms: 1) The number of RNA editing changes. An increase in the number of RNA edits can be observed in some cancers, but it does not cause overexpression of oncogenes. The may be due to the presence of these editing sites in normal tissues as well (Takahashi et al., 2006; Chen et al., 2013). 2) So far, most reported RNA edits are located in introns and 3′-UTRs, and there is almost no RNA edits present in the coding region (Zhang et al., 2016; Liu et al., 2019). These transcriptional "noises," once

thought to have no biological functions, have been shown to play a key role in some biological activities of eukaryotes, such as chromatin modification, post-transcriptional processing and nuclear transport (Ponting and Belgard, 2010; Nagano and Fraser, 2011; Lee, 2012; Shi et al., 2013). Some studies related to APA events have shown that some oncogenes have changes in the length of 3′-UTRs through APA events, thereby avoiding gene suppression and promoting tumor occurrence. A study reveals that m^6A demethylase ALKBH5 is directly regulated by DDX3 which leads to decreased m^6A methylation in FOXM1 and NANOG nascent transcript that contribute to chemoresistance (Shriwas et al., 2020). This mode of RNA editing has been studied (Murthy and Manley, 1995; Sun et al., 2014; Missan et al., 2015; Sun et al., 2017; Li et al., 2020b). 3) Even though tumor samples show simultaneous increases or decreases in RNA editing levels, changes in RNA editing in specific sites related to tumorigenesis show the opposite trend (Han et al., 2015; Paz-Yaacov et al., 2015). For example, breast cancer shows a significant increase in RNA editing at the transcriptome level, but in the specific editing sites affecting breast cancer, the RNA editing drops below 10% (Fumagalli et al., 2015). IGFBP7 transcripts are highly edited in the normal epidermis, while this editing is significantly reduced in basal cell and squamous cell carcinomas (Hochberg et al., 2013); 4) A-to-I is regulated by the ADAR enzyme RNA editing, thereby regulating the editing level of oncogenes and regulating the development of cancer (Qiao et al., 2014; Chen et al., 2017c; Chen et al., 2017d; Dong et al., 2018; Caponio et al., 2019; Yu et al., 2019). For example, ADAR1 can mediate the increase of A-to-I editing, resulting in over-editing of AZIN1 and promoting the development of ESCC (Qin et al., 2014).

In summary, recent studies have revealed RNA editing events in HNSCC. However, there is still very little known about the specific mechanisms of RNA modification to control cancer progression and drug resistance. Currently, investigators have been able to study the editing of non-coding regions using high throughput sequencing technology. At the same time, they have also found that non-coding regions have the highest levels of complexity. As a result, we started to explore the expression regulation of miRNAs and lncRNAs from a new perspective. This new concept breaks traditional thinking, which believes that unedited sequences or biomarkers must be linked to downstream targets through certain mechanisms. The mechanism by which RNA editing regulates the occurrence and development of cancer is still unclear. Research on the pathophysiological functions of RNA modifications in cancer is still in the early stages of research and there is still a long way to go. However, there is increasing evidence that the dysregulation of RNA editing central mediators (such as ADAR) contributes to the progression of cancer. Therefore, future work should focus on how to translate these modifications into available treatment options and how to relate these modifying behaviors to diagnosis and prognosis.

AUTHOR CONTRIBUTIONS

J-YZ and HS conceived and designed the study. X-XH, S-JW, M-DL, H-XG and X-TQ collected data and aided in writing the manuscript. HS, HY, MW and Y-FZ edited the manuscript. All authors read and approved the final manuscript.

FUNDING

This study was supported by the National Natural Science Foundation of China (No. 81802103, 81803938), Project of High-Level Talents in AHUTCM (Project code: 2019rcZD001), Excellent Young Scholars Project of Natural Science Foundation of Anhui Province in China(Grant Nos.2108085Y29), Open project of the Key Laboratory of Regenerative Biology, Chinese Academy of Sciences and Opening Project of Zhejiang Provincial Preponderant and Characteristic Subject of Key University (Chinese Traditional Medicine), Zhejiang Chinese Medical University (No.ZYXZD2019004). We thank the study participants and research staff for their contributions and commitment to this study. Figures are created with BioRender.com.

REFERENCES

Agranat, L., Sperling, J., and Sperling, R. (2010). A Novel Tissue-specific Alternatively Spliced Form of the A-To-I RNA Editing Enzyme ADAR2. *RNA Biol.* 7, 253–262. doi:10.4161/rna.7.2.11568

Ai, Y., Liu, S., Luo, H., Wu, S., Wei, H., Tang, Z., et al. (2021). METTL3 Intensifies the Progress of Oral Squamous Cell Carcinoma via Modulating the m6A Amount of PRMT5 and PD-L1. *J. Immunol. Res.* 2021, 6149558. doi:10.1155/2021/6149558

Anderson, J., Phan, L., and Hinnebusch, A. G. (2000). The Gcd10p/Gcd14p Complex Is the Essential Two-Subunit tRNA(1-methyladenosine) Methyltransferase of *Saccharomyces cerevisiae*. *Proc. Natl. Acad. Sci. U S A.* 97, 5173–5178. doi:10.1073/pnas.090102597

Arumugam, P., George, R., and Jayaseelan, V. P. (2021). Aberrations of m6A Regulators Are Associated with Tumorigenesis and Metastasis in Head and Neck Squamous Cell Carcinoma. *Arch. Oral Biol.* 122, 105030. doi:10.1016/j.archoralbio.2020.105030

Ban, Y., Tan, P., Cai, J., Li, J., Hu, M., Zhou, Y., et al. (2020). LNCAROD Is Stabilized by m6A Methylation and Promotes Cancer Progression via Forming a Ternary Complex with HSPA1A and YBX1 in Head and Neck Squamous Cell Carcinoma. *Mol. Oncol.* 14, 1282–1296. doi:10.1002/1878-0261.12676

Bass, B. L. (2002). RNA Editing by Adenosine Deaminases that Act on RNA. *Annu. Rev. Biochem.* 71, 817–846. doi:10.1146/annurev.biochem.71.110601.135501

Behm, M., Wahlstedt, H., Widmark, A., Eriksson, M., and Öhman, M. (2017). Accumulation of Nuclear ADAR2 Regulates Adenosine-To-Inosine RNA Editing during Neuronal Development. *J. Cel Sci* 130, 745–753. doi:10.1242/jcs.200055

Berkovits, B. D., and Mayr, C. (2015). Alternative 3' UTRs Act as Scaffolds to Regulate Membrane Protein Localization. *Nature* 522, 363–367. doi:10.1038/nature14321

Bo, R., Liu, Z., Zhang, J., Gu, P., Ou, N., Sun, Y., et al. (2019). Mechanism of Lycium Barbarum Polysaccharides Liposomes on Activating Murine Dendritic Cells. *Carbohydr. Polym.* 205, 540–549. doi:10.1016/j.carbpol.2018.10.057

Caponio, V. C. A., Troiano, G., Botti, G., Pedicillo, M. C., Lo Russo, L., Mastrangelo, F., et al. (2019). Overexpression of ADAR1 into the Cytoplasm Correlates with a Better Prognosis of Patients with Oral Squamous Cells Carcinoma. *J. Oral Pathol. Med.* 48, 108–114. doi:10.1111/jop.12808

Chen, C. X., Cho, D. S., Wang, Q., Lai, F., Carter, K. C., and Nishikura, K. (2000). A Third Member of the RNA-specific Adenosine Deaminase Gene Family,

ADAR3, Contains Both Single- and Double-Stranded RNA Binding Domains. *RNA* 6, 755–767. doi:10.1017/s1355838200000170

Chen, J., Sun, Y., Xu, X., Wang, D., He, J., Zhou, H., et al. (2017a). YTH Domain Family 2 Orchestrates Epithelial-Mesenchymal Transition/proliferation Dichotomy in Pancreatic Cancer Cells. *Cell Cycle* 16, 2259–2271. doi:10.1080/15384101.2017.1380125

Chen, L., Li, Y., Lin, C. H., Chan, T. H., Chow, R. K., Song, Y., et al. (2013). Recoding RNA Editing of AZIN1 Predisposes to Hepatocellular Carcinoma. *Nat. Med.* 19, 209–216. doi:10.1038/nm.3043

Chen, S., Qiu, H., Liu, C., Wang, Y., Tang, W., and Kang, M. (2018). Relationship between IGF2BP2 and IGFBP3 Polymorphisms and Susceptibility to Non-small-cell Lung Cancer: a Case-Control Study in Eastern Chinese Han Population. *Cancer Manag. Res.* 10, 2965–2975. doi:10.2147/CMAR.S169222

Chen, W., He, W., Cai, H., Hu, B., Zheng, C., Ke, X., et al. (2017b). A-to-I RNA Editing of BLCAP Lost the Inhibition to STAT3 Activation in Cervical Cancer. *Oncotarget* 8, 39417–39429. doi:10.18632/oncotarget.17034

Chen, Y., Wang, H., Lin, W., and Shuai, P. (2017c). ADAR1 Overexpression Is Associated with Cervical Cancer Progression and Angiogenesis. *Diagn. Pathol.* 12, 12. doi:10.1186/s13000-017-0600-0

Chen, Y. B., Liao, X. Y., Zhang, J. B., Wang, F., Qin, H. D., Zhang, L., et al. (2017d). ADAR2 Functions as a Tumor Suppressor via Editing IGFBP7 in Esophageal Squamous Cell Carcinoma. *Int. J. Oncol.* 50, 622–630. doi:10.3892/ijo.2016.3823

Chujo, T., and Suzuki, T. (2012). Trmt61B Is a Methyltransferase Responsible for 1-methyladenosine at Position 58 of Human Mitochondrial tRNAs. *RNA* 18, 2269–2276. doi:10.1261/rna.035600.112

Dai, X., Wang, T., Gonzalez, G., and Wang, Y. (2018). Identification of YTH Domain-Containing Proteins as the Readers for N1-Methyladenosine in RNA. *Anal. Chem.* 90, 6380–6384. doi:10.1021/acs.analchem.8b01703

Delaunay, S., and Frye, M. (2019). RNA Modifications Regulating Cell Fate in Cancer. *Nat. Cel Biol* 21, 552–559. doi:10.1038/s41556-019-0319-0

Deng, X., Jiang, Q., Liu, Z., and Chen, W. (2020). Clinical Significance of an m6A Reader Gene, IGF2BP2, in Head and Neck Squamous Cell Carcinoma. *Front. Mol. Biosci.* 7, 68. doi:10.3389/fmolb.2020.00068

Deng, Y., Li, K., Tan, F., and Liu, H. (2021). Gene Model Related to m6A Predicts the Prognostic Effect of Immune Infiltration on Head and Neck Squamous Cell Carcinoma. *J. Oncol.* 2021, 1814266. doi:10.1155/2021/1814266

Deutschmeyer, V. E., and Richter, A. M. (2020). The ZAR1 Protein in Cancer; from Epigenetic Silencing to Functional Characterisation and Epigenetic Therapy of Tumour Suppressors. *Biochim. Biophys. Acta Rev. Cancer* 1874, 188417. doi:10.1016/j.bbcan.2020.188417

Dimitrova, D. G., Teysset, L., and Carré, C. (2019). RNA 2'-O-Methylation (Nm) Modification in Human Diseases. *Genes (Basel)* 10, 117. doi:10.3390/genes10020117

Dominissini, D., Nachtergaele, S., Moshitch-Moshkovitz, S., Peer, E., Kol, N., Ben-Haim, M. S., et al. (2016). The Dynamic N(1)-methyladenosine Methylome in Eukaryotic Messenger RNA. *Nature* 530, 441–446. doi:10.1038/nature16998

Dong, X., Chen, G., Cai, Z., Li, Z., Qiu, L., Xu, H., et al. (2018). CDK13 RNA Over-editing Mediated by ADAR1 Associates with Poor Prognosis of Hepatocellular Carcinoma Patients. *Cell Physiol Biochem* 47, 2602–2612. doi:10.1159/000491656

Duhen, R., Ballesteros-Merino, C., Frye, A. K., Tran, E., Rajamanickam, V., Chang, S. C., et al. (2021). Neoadjuvant Anti-OX40 (MEDI6469) Therapy in Patients with Head and Neck Squamous Cell Carcinoma Activates and Expands Antigen-specific Tumor-Infiltrating T Cells. *Nat. Commun.* 12, 1047. doi:10.1038/s41467-021-21383-1

Eckmann, C. R., Rammelt, C., and Wahle, E. (2011). Control of Poly(A) Tail Length. *WIREs RNA* 2, 348–361. doi:10.1002/wrna.56

Feng, Z. Y., Gao, H. Y., and Feng, T. D. (2021). Immune Infiltrates of m6A RNA Methylation-Related lncRNAs and Identification of PD-L1 in Patients with Primary Head and Neck Squamous Cell Carcinoma. *Front Cel Dev Biol* 9, 672248. doi:10.3389/fcell.2021.672248

Ferlay, J., Colombet, M., Soerjomataram, I., Mathers, C., Parkin, D. M., Piñeros, M., et al. (2019). Estimating the Global Cancer Incidence and Mortality in 2018: GLOBOCAN Sources and Methods. *Int. J. Cancer* 144, 1941–1953. doi:10.1002/ijc.31937

Fu, L., Qin, Y. R., Ming, X. Y., Zuo, X. B., Diao, Y. W., Zhang, L. Y., et al. (2017). RNA Editing of SLC22A3 Drives Early Tumor Invasion and Metastasis in Familial Esophageal Cancer. *Proc. Natl. Acad. Sci. U S A.* 114, E4631–E4640. doi:10.1073/pnas.1703178114

Fumagalli, D., Gacquer, D., Rothé, F., Lefort, A., Libert, F., Brown, D., et al. (2015). Principles Governing A-To-I RNA Editing in the Breast Cancer Transcriptome. *Cell Rep* 13, 277–289. doi:10.1016/j.celrep.2015.09.032

Geng, X., Zhang, Y., Zeng, Z., Zhu, Z., Wang, H., Yu, W., et al. (2021). Molecular Characteristics, Prognostic Value, and Immune Characteristics of m6A Regulators Identified in Head and Neck Squamous Cell Carcinoma. *Front. Oncol.* 11, 629718. doi:10.3389/fonc.2021.629718

Gong, J., Chehrazi-Raffle, A., Reddi, S., and Salgia, R. (2018). Development of PD-1 and PD-L1 Inhibitors as a Form of Cancer Immunotherapy: a Comprehensive Review of Registration Trials and Future Considerations. *J. Immunother. Cancer* 6, 8. doi:10.1186/s40425-018-0316-z

Grassi, E., Santoro, R., Umbach, A., Grosso, A., Oliviero, S., Neri, F., et al. (2018). Choice of Alternative Polyadenylation Sites, Mediated by the RNA-Binding Protein Elavl3, Plays a Role in Differentiation of Inhibitory Neuronal Progenitors. *Front Cel Neurosci* 12, 518. doi:10.3389/fncel.2018.00518

Gruber, A. J., and Zavolan, M. (2019). Alternative Cleavage and Polyadenylation in Health and Disease. *Nat. Rev. Genet.* 20, 599–614. doi:10.1038/s41576-019-0145-z

Han, J., An, O., Hong, H., Chan, T. H. M., Song, Y., Shen, H., et al. (2020). Suppression of Adenosine-To-Inosine (A-To-I) RNA Editome by Death Associated Protein 3 (DAP3) Promotes Cancer Progression. *Sci. Adv.* 6, eaba5136. doi:10.1126/sciadv.aba5136

Han, J., Wang, J. Z., Yang, X., Yu, H., Zhou, R., Lu, H. C., et al. (2019). METTL3 Promote Tumor Proliferation of Bladder Cancer by Accelerating Pri-miR221/222 Maturation in m6A-dependent Manner. *Mol. Cancer* 18, 110. doi:10.1186/s12943-019-1036-9

Han, L., Diao, L., Yu, S., Xu, X., Li, J., Zhang, R., et al. (2015). The Genomic Landscape and Clinical Relevance of A-To-I RNA Editing in Human Cancers. *Cancer Cell* 28, 515–528. doi:10.1016/j.ccell.2015.08.013

He, X., Li, W., Liang, X., Zhu, X., Zhang, L., Huang, Y., et al. (2018). IGF2BP2 Overexpression Indicates Poor Survival in Patients with Acute Myelocytic Leukemia. *Cel Physiol Biochem* 51, 1945–1956. doi:10.1159/000495719

Heraud-Farlow, J. E., Chalk, A. M., and Walkley, C. R. (2019). Defining the Functions of Adenosine-To-Inosine RNA Editing through Hematology. *Curr. Opin. Hematol.* 26, 241–248. doi:10.1097/MOH.0000000000000514

Hochberg, M., Gilead, L., Markel, G., Nemlich, Y., Feiler, Y., Enk, C. D., et al. (2013). Insulin-like Growth Factor-Binding Protein-7 (IGFBP7) Transcript: A-To-I Editing Events in normal and Cancerous Human Keratinocytes. *Arch. Dermatol. Res.* 305, 519–528. doi:10.1007/s00403-013-1338-5

Hong, H., An, O., Chan, T. H. M., Ng, V. H. E., Kwok, H. S., Lin, J. S., et al. (2018). Bidirectional Regulation of Adenosine-To-Inosine (A-To-I) RNA Editing by DEAH Box Helicase 9 (DHX9) in Cancer. *Nucleic Acids Res.* 46, 7953–7969. doi:10.1093/nar/gky396

Hosaka, T., Yamashita, T., Teramoto, S., Hirose, N., Tamaoka, A., and Kwak, S. (2019). ADAR2-dependent A-To-I RNA Editing in the Extracellular Linear and Circular RNAs. *Neurosci. Res.* 147, 48–57. doi:10.1016/j.neures.2018.11.005

Huang, G. Z., Wu, Q. Q., Zheng, Z. N., Shao, T. R., Chen, Y. C., Zeng, W. S., et al. (2020). M6A-related Bioinformatics Analysis Reveals that HNRNPC Facilitates Progression of OSCC via EMT. *Aging (Albany NY)* 12, 11667–11684. doi:10.18632/aging.103333

Ichinose, J., Watanabe, K., Sano, A., Nagase, T., Nakajima, J., Fukayama, M., et al. (2014). Alternative Polyadenylation Is Associated with Lower Expression of PABPN1 and Poor Prognosis in Non-small Cell Lung Cancer. *Cancer Sci.* 105, 1135–1141. doi:10.1111/cas.12472

Ikeda, T., Saito-Takatsuji, H., Yoshitomi, Y., and Yonekura, H. (2020). Role of Arginine Methylation in Alternative Polyadenylation of VEGFR-1 (Flt-1) Pre-mRNA. *Int. J. Mol. Sci.* 21, 6460. doi:10.3390/ijms21186460

Ji, Z., and Tian, B. (2009). Reprogramming of 3' Untranslated Regions of mRNAs by Alternative Polyadenylation in Generation of Pluripotent Stem Cells from Different Cell Types. *PLoS One* 4, e8419. doi:10.1371/journal.pone.0008419

Jia, G., Fu, Y., Zhao, X., Dai, Q., Zheng, G., Yang, Y., et al. (2011). N6-methyladenosine in Nuclear RNA Is a Major Substrate of the Obesity-Associated FTO. *Nat. Chem. Biol.* 7, 885–887. doi:10.1038/nchembio.687

Johnson, D. E., Burtness, B., Leemans, C. R., Lui, V. W. Y., Bauman, J. E., and Grandis, J. R. (2020). Head and Neck Squamous Cell Carcinoma. *Nat. Rev. Dis. Primers* 6, 92. doi:10.1038/s41572-020-00224-3

Kawarada, L., Suzuki, T., Ohira, T., Hirata, S., Miyauchi, K., and Suzuki, T. (2017). ALKBH1 Is an RNA Dioxygenase Responsible for Cytoplasmic and Mitochondrial tRNA Modifications. *Nucleic Acids Res.* 45, 7401–7415. doi:10.1093/nar/gkx354

Kretschmer, J., Rao, H., Hackert, P., Sloan, K. E., Höbartner, C., and Bohnsack, M. T. (2018). The m6A Reader Protein YTHDC2 Interacts with the Small Ribosomal Subunit and the 5'-3' Exoribonuclease XRN1. *RNA* 24, 1339–1350. doi:10.1261/rna.064238.117

Kühn, U., Gündel, M., Knoth, A., Kerwitz, Y., Rüdel, S., and Wahle, E. (2009). Poly(A) Tail Length Is Controlled by the Nuclear Poly(A)-binding Protein Regulating the Interaction between Poly(A) Polymerase and the Cleavage and Polyadenylation Specificity Factor. *J. Biol. Chem.* 284, 22803–22814. doi:10.1074/jbc.M109.018226

Lee, J. T. (2012). Epigenetic Regulation by Long Noncoding RNAs. *Science* 338, 1435–1439. doi:10.1126/science.1231776

Lee, Y. G., Chang, H., Keam, B., Chun, S. H., Park, J., Park, K. U., et al. (2021). Outcomes and Biomarkers of Immune Checkpoint Inhibitor Therapy in Patients with Refractory Head and Neck Squamous Cell Carcinoma: KCSG HN18-12. *Cancer Res. Treat.* 53, 671–677. doi:10.4143/crt.2020.824

Lehmann, K. A., and Bass, B. L. (2000). Double-stranded RNA Adenosine Deaminases ADAR1 and ADAR2 Have Overlapping Specificities. *Biochemistry* 39, 12875–12884. doi:10.1021/bi001383g

León, X., Hitt, R., Constenla, M., Rocca, A., Stupp, R., Kovács, A. F., et al. (2005). A Retrospective Analysis of the Outcome of Patients with Recurrent And/or Metastatic Squamous Cell Carcinoma of the Head and Neck Refractory to a Platinum-Based Chemotherapy. *Clin. Oncol. (R Coll. Radiol.* 17, 418–424. doi:10.1016/j.clon.2005.02.014

Li, F., Yi, Y., Miao, Y., Long, W., Long, T., Chen, S., et al. (2019a). N6-Methyladenosine Modulates Nonsense-Mediated mRNA Decay in Human Glioblastoma. *Cancer Res.* 79, 5785–5798. doi:10.1158/0008-5472.CAN-18-2868

Li, J., Zhang, C., Yuan, X., and Cao, Y. (2021). Molecular Characteristics of N1-Methyladenosine Regulators and Their Correlation with Overall Cancer Survival. *DNA Cel Biol* 40, 513–522. doi:10.1089/dna.2020.6214

Li, T., Hu, P. S., Zuo, Z., Lin, J. F., Li, X., Wu, Q. N., et al. (2019b). METTL3 Facilitates Tumor Progression via an m6A-igf2bp2-dependent Mechanism in Colorectal Carcinoma. *Mol. Cancer* 18, 112. doi:10.1186/s12943-019-1038-7

Li, X., Xiong, X., Wang, K., Wang, L., Shu, X., Ma, S., et al. (2016). Transcriptome-wide Mapping Reveals Reversible and Dynamic N(1)-methyladenosine Methylome. *Nat. Chem. Biol.* 12, 311–316. doi:10.1038/nchembio.2040

Li, X., Xiong, X., Zhang, M., Wang, K., Chen, Y., Zhou, J., et al. (2017). Base-Resolution Mapping Reveals Distinct m1A Methylome in Nuclear- and Mitochondrial-Encoded Transcripts. *Mol. Cel* 68, 993–e9. doi:10.1016/j.molcel.2017.10.019

Li, Y., Zheng, J. N., Wang, E. H., Gong, C. J., Lan, K. F., and Ding, X. (2020a). The m6A Reader Protein YTHDC2 Is a Potential Biomarker and Associated with Immune Infiltration in Head and Neck Squamous Cell Carcinoma. *PeerJ* 8, e10385. doi:10.7717/peerj.10385

Li, Y. Q., Chen, Y., Xu, Y. F., He, Q. M., Yang, X. J., Li, Y. Q., et al. (2020b). FNDC3B 3'-UTR Shortening Escapes from microRNA-Mediated Gene Repression and Promotes Nasopharyngeal Carcinoma Progression. *Cancer Sci.* 111, 1991–2003. doi:10.1111/cas.14394

Li, Z., Zhao, P., and Xia, Q. (2019c). Epigenetic Methylations on N6-Adenine and N6-Adenosine with the Same Input but Different Output. *Int. J. Mol. Sci.* 20, 2931. doi:10.3390/ijms20122931

Lin, Y., Li, Z., Ozsolak, F., Kim, S. W., Arango-Argoty, G., Liu, T. T., et al. (2012). An In-Depth Map of Polyadenylation Sites in Cancer. *Nucleic Acids Res.* 40, 8460–8471. doi:10.1093/nar/gks637

Liu, F., Clark, W., Luo, G., Wang, X., Fu, Y., Wei, J., et al. (2016). ALKBH1-Mediated tRNA Demethylation Regulates Translation. *Cell* 167, 816–e16. doi:10.1016/j.cell.2016.09.038

Liu, L., Wu, Y., Li, Q., Liang, J., He, Q., Zhao, L., et al. (2020). METTL3 Promotes Tumorigenesis and Metastasis through BMI1 m6A Methylation in Oral Squamous Cell Carcinoma. *Mol. Ther.* 28, 2177–2190. doi:10.1016/j.ymthe.2020.06.024

Liu, X., Fu, Y., Huang, J., Wu, M., Zhang, Z., Xu, R., et al. (2019). ADAR1 Promotes the Epithelial-To-Mesenchymal Transition and Stem-like Cell Phenotype of Oral Cancer by Facilitating Oncogenic microRNA Maturation. *J. Exp. Clin. Cancer Res.* 38, 315. doi:10.1186/s13046-019-1300-2

Liu, Z., Williams, M., Stewart, J., Glisson, B. S., Fuller, C., and Roy-Chowdhuri, S. (2021). Evaluation of Programmed Death Ligand 1 Expression in Cytology to Determine Eligibility for Immune Checkpoint Inhibitor Therapy in Patients with Head and Neck Squamous Cell Carcinoma. *Cancer Cytopathol.* doi:10.1002/cncy.22501

Ma, W., Chen, C., Liu, Y., Zeng, M., Meyers, B. C., Li, J., et al. (2018). Coupling of microRNA-Directed Phased Small Interfering RNA Generation from Long Noncoding Genes with Alternative Splicing and Alternative Polyadenylation in Small RNA-Mediated Gene Silencing. *New Phytol.* 217, 1535–1550. doi:10.1111/nph.14934

Ma, Y., Han, J., and Luo, X. (2021). FOXD1-AS1 Upregulates FOXD1 to Promote Oral Squamous Cell Carcinoma Progression. *Oral Dis.* doi:10.1111/odi.14002

Macdonald, C. C. (2019). Tissue-specific Mechanisms of Alternative Polyadenylation: Testis, Brain, and beyond (2018 Update). *Wiley Interdiscip. Rev. RNA* 10, e1526. doi:10.1002/wrna.1526

Mao, L., Xiao, Y., Yang, Q. C., Yang, S. C., Yang, L. L., and Sun, Z. J. (2021). TIGIT/CD155 Blockade Enhances Anti-PD-L1 Therapy in Head and Neck Squamous Cell Carcinoma by Targeting Myeloid-Derived Suppressor Cells. *Oral Oncol.* 121, 105472. doi:10.1016/j.oraloncology.2021.105472

Martin, G., Gruber, A. R., Keller, W., and Zavolan, M. (2012). Genome-wide Analysis of Pre-mRNA 3' End Processing Reveals a Decisive Role of Human Cleavage Factor I in the Regulation of 3' UTR Length. *Cel Rep* 1, 753–763. doi:10.1016/j.celrep.2012.05.003

Meng, Q. Z., Cong, C. H., Li, X. J., Zhu, F., Zhao, X., and Chen, F. W. (2020). METTL3 Promotes the Progression of Nasopharyngeal Carcinoma through Mediating M6A Modification of EZH2. *Eur. Rev. Med. Pharmacol. Sci.* 24, 4328–4336. doi:10.26355/eurrev_202004_21014

Meyer, K., Köster, T., Nolte, C., Weinholdt, C., Lewinski, M., Grosse, I., et al. (2017). Adaptation of iCLIP to Plants Determines the Binding Landscape of the Clock-Regulated RNA-Binding Protein AtGRP7. *Genome Biol.* 18, 204. doi:10.1186/s13059-017-1332-x

Missan, D. S., Mitchell, K., Subbaram, S., and Dipersio, C. M. (2015). Integrin α3β1 Signaling through MEK/ERK Determines Alternative Polyadenylation of the MMP-9 mRNA Transcript in Immortalized Mouse Keratinocytes. *PLoS One* 10, e0119539. doi:10.1371/journal.pone.0119539

Murthy, K. G., and Manley, J. L. (1995). The 160-kD Subunit of Human Cleavage-Polyadenylation Specificity Factor Coordinates Pre-mRNA 3'-end Formation. *Genes Dev.* 9, 2672–2683. doi:10.1101/gad.9.21.2672

Nagano, T., and Fraser, P. (2011). No-nonsense Functions for Long Noncoding RNAs. *Cell* 145, 178–181. doi:10.1016/j.cell.2011.03.014

Nishikura, K. (2010). Functions and Regulation of RNA Editing by ADAR Deaminases. *Annu. Rev. Biochem.* 79, 321–349. doi:10.1146/annurev-biochem-060208-105251

Oakes, E., Anderson, A., Cohen-Gadol, A., and Hundley, H. A. (2017). Adenosine Deaminase that Acts on RNA 3 (ADAR3) Binding to Glutamate Receptor Subunit B Pre-mRNA Inhibits RNA Editing in Glioblastoma. *J. Biol. Chem.* 292, 4326–4335. doi:10.1074/jbc.M117.779868

Ozanick, S., Krecic, A., Andersland, J., and Anderson, J. T. (2005). The Bipartite Structure of the tRNA m1A58 Methyltransferase from *S. cerevisiae* Is Conserved in Humans. *RNA* 11, 1281–1290. doi:10.1261/rna.5040605

Pan, J., Huang, Z., and Xu, Y. (2021). m5C RNA Methylation Regulators Predict Prognosis and Regulate the Immune Microenvironment in Lung Squamous Cell Carcinoma. *Front. Oncol.* 11, 657466. doi:10.3389/fonc.2021.657466

Pan, Q., Shai, O., Lee, L. J., Frey, B. J., and Blencowe, B. J. (2008). Deep Surveying of Alternative Splicing Complexity in the Human Transcriptome by High-Throughput Sequencing. *Nat. Genet.* 40, 1413–1415. doi:10.1038/ng.259

Paramasivam, A., George, R., and Priyadharsini, J. V. (2021). Genomic and Transcriptomic Alterations in m6A Regulatory Genes Are Associated with Tumorigenesis and Poor Prognosis in Head and Neck Squamous Cell Carcinoma. *Am. J. Cancer Res.* 11, 3688–3697.

Passacantilli, I., Panzeri, V., Bielli, P., Farini, D., Pilozzi, E., Fave, G. D., et al. (2017). Alternative Polyadenylation of ZEB1 Promotes its Translation during Genotoxic Stress in Pancreatic Cancer Cells. *Cell Death Dis* 8, e3168. doi:10.1038/cddis.2017.562

Patterson, J. B., and Samuel, C. E. (1995). Expression and Regulation by Interferon of a Double-stranded-RNA-specific Adenosine Deaminase from Human Cells: Evidence for Two Forms of the Deaminase. *Mol. Cel Biol* 15, 5376–5388. doi:10.1128/mcb.15.10.5376

Paz-Yaacov, N., Bazak, L., Buchumenski, I., Porath, H. T., Danan-Gotthold, M., Knisbacher, B. A., et al. (2015). Elevated RNA Editing Activity Is a Major Contributor to Transcriptomic Diversity in Tumors. *Cel Rep* 13, 267–276. doi:10.1016/j.celrep.2015.08.080

Ponting, C. P., and Belgard, T. G. (2010). Transcribed Dark Matter: Meaning or Myth? *Hum. Mol. Genet.* 19, R162–R168. doi:10.1093/hmg/ddq362

Qiao, J. J., Chan, T. H., Qin, Y. R., and Chen, L. (2014). ADAR1: a Promising New Biomarker for Esophageal Squamous Cell Carcinoma? *Expert Rev. Anticancer Ther.* 14, 865–868. doi:10.1586/14737140.2014.928595

Qin, Y. R., Qiao, J. J., Chan, T. H., Zhu, Y. H., Li, F. F., Liu, H., et al. (2014). Adenosine-to-inosine RNA Editing Mediated by ADARs in Esophageal Squamous Cell Carcinoma. *Cancer Res.* 74, 840–851. doi:10.1158/0008-5472.CAN-13-2545

Rajasekar, V., Geo, V. E., Martin, L. J., and Nagalingam, B. (2020). The Combined Effect of Low Viscous Biofuel and EGR on NO-Smoke Tradeoff in a Biodiesel Engine-An Experimental Study. *Environ. Sci. Pollut. Res. Int.* 27, 17468–17480. doi:10.1007/s11356-019-05449-8

Ramanathan, A., Robb, G. B., and Chan, S. H. (2016). mRNA Capping: Biological Functions and Applications. *Nucleic Acids Res.* 44, 7511–7526. doi:10.1093/nar/gkw551

Roth, S. H., Levanon, E. Y., and Eisenberg, E. (2019). Genome-wide Quantification of ADAR Adenosine-To-Inosine RNA Editing Activity. *Nat. Methods* 16, 1131–1138. doi:10.1038/s41592-019-0610-9

Safra, M., Sas-Chen, A., Nir, R., Winkler, R., Nachshon, A., Bar-Yaacov, D., et al. (2017). The m1A Landscape on Cytosolic and Mitochondrial mRNA at Single-Base Resolution. *Nature* 551, 251–255. doi:10.1038/nature24456

Sakai, A., Ando, M., Fukusumi, T., Ren, S., Liu, C., Qualliotine, J., et al. (2020). Aberrant Expression of CPSF1 Promotes Head and Neck Squamous Cell Carcinoma via Regulating Alternative Splicing. *PLoS One* 15, e0233380. doi:10.1371/journal.pone.0233380

Sandberg, R., Neilson, J. R., Sarma, A., Sharp, P. A., and Burge, C. B. (2008). Proliferating Cells Express mRNAs with Shortened 3' Untranslated Regions and Fewer microRNA Target Sites. *Science* 320, 1643–1647. doi:10.1126/science.1155390

Shi, H., Wei, J., and He, C. (2019). Where, when, and How: Context-dependent Functions of RNA Methylation Writers, Readers, and Erasers. *Mol. Cel* 74, 640–650. doi:10.1016/j.molcel.2019.04.025

Shi, L., Chen, W., Zhang, Z., Chen, J., and Xue, M. (2021). N1-methyladenosine Profiling of Long Non-coding RNA in Colorectal Cancer. *IUBMB Life* 73, 1235. doi:10.1002/iub.2534

Shi, Q., Xue, C., Yuan, X., He, Y., and Yu, Z. (2020). Gene Signatures and Prognostic Values of m1A-Related Regulatory Genes in Hepatocellular Carcinoma. *Sci. Rep.* 10, 15083. doi:10.1038/s41598-020-72178-1

Shi, X., Sun, M., Liu, H., Yao, Y., and Song, Y. (2013). Long Non-coding RNAs: a New Frontier in the Study of Human Diseases. *Cancer Lett.* 339, 159–166. doi:10.1016/j.canlet.2013.06.013

Shriwas, O., Priyadarshini, M., Samal, S. K., Rath, R., Panda, S., Das Majumdar, S. K., et al. (2020). DDX3 Modulates Cisplatin Resistance in OSCC through ALKBH5-Mediated m6A-Demethylation of FOXM1 and NANOG. *Apoptosis* 25, 233–246. doi:10.1007/s10495-020-01591-8

Simpson, L., and Emeson, R. B. (1996). RNA Editing. *Annu. Rev. Neurosci.* 19, 27–52. doi:10.1146/annurev.ne.19.030196.000331

Sobol, R. E., Menander, K. B., Chada, S., Wiederhold, D., Sellman, B., Talbott, M., et al. (2021). Analysis of Adenoviral P53 Gene Therapy Clinical Trials in Recurrent Head and Neck Squamous Cell Carcinoma. *Front. Oncol.* 11, 645745. doi:10.3389/fonc.2021.645745

Stewart, J. S., Cohen, E. E., Licitra, L., Van Herpen, C. M., Khorprasert, C., Soulieres, D., et al. (2009). Phase III Study of Gefitinib Compared with Intravenous Methotrexate for Recurrent Squamous Cell Carcinoma of the Head and Neck [corrected]. *J. Clin. Oncol.* 27, 1864–1871. doi:10.1200/JCO.2008.17.0530

Sun, M., Ding, J., Li, D., Yang, G., Cheng, Z., and Zhu, Q. (2017). NUDT21 Regulates 3'-UTR Length and microRNA-Mediated Gene Silencing in Hepatocellular Carcinoma. *Cancer Lett.* 410, 158–168. doi:10.1016/j.canlet.2017.09.026

Sun, M., Ju, H., Zhou, Z., and Zhu, R. (2014). Pilot Genome-wide Study of Tandem 3' UTRs in Esophageal Cancer Using High-Throughput Sequencing. *Mol. Med. Rep.* 9, 1597–1605. doi:10.3892/mmr.2014.2003

Sung, H., Ferlay, J., Siegel, R. L., Laversanne, M., Soerjomataram, I., Jemal, A., et al. (2021). Global Cancer Statistics 2020: GLOBOCAN Estimates of Incidence and Mortality Worldwide for 36 Cancers in 185 Countries. *CA Cancer J. Clin.* 71, 209–249. doi:10.3322/caac.21660

Takahashi, M., Yoshimoto, T., Shimoda, M., Kono, T., Koizumi, M., Yazumi, S., et al. (2006). Loss of Function of the Candidate Tumor Suppressor Prox1 by RNA Mutation in Human Cancer Cells. *Neoplasia* 8, 1003–1010. doi:10.1593/neo.06595

Tan, S., Li, H., Zhang, W., Shao, Y., Liu, Y., Guan, H., et al. (2018). NUDT21 Negatively Regulates PSMB2 and CXXC5 by Alternative Polyadenylation and Contributes to Hepatocellular Carcinoma Suppression. *Oncogene* 37, 4887–4900. doi:10.1038/s41388-018-0280-6

Terajima, H., Yoshitane, H., Yoshikawa, T., Shigeyoshi, Y., and Fukada, Y. (2018). A-to-I RNA Editing Enzyme ADAR2 Regulates Light-Induced Circadian Phase-Shift. *Sci. Rep.* 8, 14848. doi:10.1038/s41598-018-33114-6

Tian, B., and Manley, J. L. (2017). Alternative Polyadenylation of mRNA Precursors. *Nat. Rev. Mol. Cel Biol* 18, 18–30. doi:10.1038/nrm.2016.116

Ueda, Y., Ooshio, I., Fusamae, Y., Kitae, K., Kawaguchi, M., Jingushi, K., et al. (2017). AlkB Homolog 3-mediated tRNA Demethylation Promotes Protein Synthesis in Cancer Cells. *Sci. Rep.* 7, 42271. doi:10.1038/srep42271

Valente, L., and Nishikura, K. (2005). ADAR Gene Family and A-To-I RNA Editing: Diverse Roles in Posttranscriptional Gene Regulation. *Prog. Nucleic Acid Res. Mol. Biol.* 79, 299–338. doi:10.1016/S0079-6603(04)79006-6

Vermorken, J. B., Mesia, R., Rivera, F., Remenar, E., Kawecki, A., Rottey, S., et al. (2008). Platinum-based Chemotherapy Plus Cetuximab in Head and Neck Cancer. *N. Engl. J. Med.* 359, 1116–1127. doi:10.1056/NEJMoa0802656

Vermorken, J. B., Psyrri, A., Mesía, R., Peyrade, F., Beier, F., De Blas, B., et al. (2014). Impact of Tumor HPV Status on Outcome in Patients with Recurrent And/or Metastatic Squamous Cell Carcinoma of the Head and Neck Receiving Chemotherapy with or without Cetuximab: Retrospective Analysis of the Phase III EXTREME Trial. *Ann. Oncol.* 25, 801–807. doi:10.1093/annonc/mdt574

Vilardo, E., Nachbagauer, C., Buzet, A., Taschner, A., Holzmann, J., and Rossmanith, W. (2012). A Subcomplex of Human Mitochondrial RNase P Is a Bifunctional Methyltransferase-Eextensive Moonlighting in Mitochondrial tRNA Biogenesis. *Nucleic Acids Res.* 40, 11583–11593. doi:10.1093/nar/gks910

Vlachogiannis, N. I., Sachse, M., Georgiopoulos, G., Zormpas, E., Bampatsias, D., Delialis, D., et al. (2021). Adenosine-to-inosine Alu RNA Editing Controls the Stability of the Pro-inflammatory Long Noncoding RNA NEAT1 in Atherosclerotic Cardiovascular Disease. *J. Mol. Cel Cardiol* 160, 111–120. doi:10.1016/j.yjmcc.2021.07.005

Wahle, E. (1995). Poly(A) Tail Length Control Is Caused by Termination of Processive Synthesis. *J. Biol. Chem.* 270, 2800–2808. doi:10.1074/jbc.270.6.2800

Wang, C. S., Chang, C. H., Tzeng, T. Y., Lin, A. M., and Lo, Y. L. (2021a). Gene-editing by CRISPR-Cas9 in Combination with Anthracycline Therapy via Tumor Microenvironment-Switchable, EGFR-Targeted, and Nucleus-Directed Nanoparticles for Head and Neck Cancer Suppression. *Nanoscale Horiz* 6, 729–743. doi:10.1039/d1nh00254f

Wang, E. T., Sandberg, R., Luo, S., Khrebtukova, I., Zhang, L., Mayr, C., et al. (2008). Alternative Isoform Regulation in Human Tissue Transcriptomes. *Nature* 456, 470–476. doi:10.1038/nature07509

Wang, K., Jiang, L., Zhang, Y., and Chen, C. (2020a). Progression of Thyroid Carcinoma Is Promoted by the m6A Methyltransferase METTL3 through Regulating m6A Methylation on TCF1. *Onco Targets Ther.* 13, 1605–1612. doi:10.2147/OTT.S234751

Wang, L., Lang, G. T., Xue, M. Z., Yang, L., Chen, L., Yao, L., et al. (2020b). Dissecting the Heterogeneity of the Alternative Polyadenylation Profiles in Triple-Negative Breast Cancers. *Theranostics* 10, 10531–10547. doi:10.7150/thno.40944

Wang, Q., Zhang, Q., Huang, Y., and Zhang, J. (2020c). m1A Regulator TRMT10C Predicts Poorer Survival and Contributes to Malignant Behavior in Gynecological Cancers. *DNA Cel Biol* 39, 1767–1778. doi:10.1089/dna.2020.5624

Wang, W., Xiong, Y., Ding, X., Wang, L., Zhao, Y., Fei, Y., et al. (2019a). Cathepsin L Activated by Mutant P53 and Egr-1 Promotes Ionizing Radiation-Induced EMT in Human NSCLC. *J. Exp. Clin. Cancer Res.* 38, 61. doi:10.1186/s13046-019-1054-x

Wang, X., Fu, X., Zhang, J., Xiong, C., Zhang, S., and Lv, Y. (2020d). Identification and Validation of m6A RNA Methylation Regulators with Clinical Prognostic

Value in Papillary Thyroid Cancer. *Cancer Cel Int* 20, 203. doi:10.1186/s12935-020-01283-y

Wang, X., Tian, L., Li, Y., Wang, J., Yan, B., Yang, L., et al. (2021b). RBM15 Facilitates Laryngeal Squamous Cell Carcinoma Progression by Regulating TMBIM6 Stability through IGF2BP3 Dependent. *J. Exp. Clin. Cancer Res.* 40, 80. doi:10.1186/s13046-021-01871-4

Wang, Y., Chung, D. H., Monteleone, L. R., Li, J., Chiang, Y., Toney, M. D., et al. (2019b). RNA Binding Candidates for Human ADAR3 from Substrates of a Gain of Function Mutant Expressed in Neuronal Cells. *Nucleic Acids Res.* 47, 10801–10814. doi:10.1093/nar/gkz815

Wong, S. K., Sato, S., and Lazinski, D. W. (2001). Substrate Recognition by ADAR1 and ADAR2. *RNA* 7, 846–858. doi:10.1017/s135583820101007x

Wu, P., Fang, X., Liu, Y., Tang, Y., Wang, W., Li, X., et al. (2021). N6-methyladenosine Modification of circCUX1 Confers Radioresistance of Hypopharyngeal Squamous Cell Carcinoma through Caspase1 Pathway. *Cel Death Dis* 12, 298. doi:10.1038/s41419-021-03558-2

Wu, T. P., Wang, T., Seetin, M. G., Lai, Y., Zhu, S., Lin, K., et al. (2016). DNA Methylation on N(6)-adenine in Mammalian Embryonic Stem Cells. *Nature* 532, 329–333. doi:10.1038/nature17640

Xia, T., Wu, X., Cao, M., Zhang, P., Shi, G., Zhang, J., et al. (2019). The RNA m6A Methyltransferase METTL3 Promotes Pancreatic Cancer Cell Proliferation and Invasion. *Pathol. Res. Pract.* 215, 152666. doi:10.1016/j.prp.2019.152666

Xia, T. L., Li, X., Wang, X., Zhu, Y. J., Zhang, H., Cheng, W., et al. (2021). N(6)-methyladenosine-binding Protein YTHDF1 Suppresses EBV Replication and Promotes EBV RNA Decay. *EMBO Rep.* 22, e50128. doi:10.15252/embr.202050128

Xia, Z., Donehower, L. A., Cooper, T. A., Neilson, J. R., Wheeler, D. A., Wagner, E. J., et al. (2014). Dynamic Analyses of Alternative Polyadenylation from RNA-Seq Reveal a 3'-UTR Landscape across Seven Tumour Types. *Nat. Commun.* 5, 5274. doi:10.1038/ncomms6274

Xiang, Y., Ye, Y., Lou, Y., Yang, Y., Cai, C., Zhang, Z., et al. (2018). Comprehensive Characterization of Alternative Polyadenylation in Human Cancer. *J. Natl. Cancer Inst.* 110, 379–389. doi:10.1093/jnci/djx223

Xie, S., Chen, W., Chen, K., Chang, Y., Yang, F., Lin, A., et al. (2020). Emerging Roles of RNA Methylation in Gastrointestinal Cancers. *Cancer Cel Int* 20, 585. doi:10.1186/s12935-020-01679-w

Xiong, M., Chen, L., Zhou, L., Ding, Y., Kazobinka, G., Chen, Z., et al. (2019). NUDT21 Inhibits Bladder Cancer Progression through ANXA2 and LIMK2 by Alternative Polyadenylation. *Theranostics* 9, 7156–7167. doi:10.7150/thno.36030

Xu, L., Liu, X., Sheng, N., Oo, K. S., Liang, J., Chionh, Y. H., et al. (2017). Three Distinct 3-methylcytidine (m3C) Methyltransferases Modify tRNA and mRNA in Mice and Humans. *J. Biol. Chem.* 292, 14695–14703. doi:10.1074/jbc.M117.798298

Xu, X., Wang, Y., Mojumdar, K., Zhou, Z., Jeong, K. J., Mangala, L. S., et al. (2019a). A-to-I-edited miRNA-379-5p Inhibits Cancer Cell Proliferation through CD97-Induced Apoptosis. *J. Clin. Invest.* 129, 5343–5356. doi:10.1172/JCI123396

Xu, X., Yu, Y., Zong, K., Lv, P., and Gu, Y. (2019b). Up-regulation of IGF2BP2 by Multiple Mechanisms in Pancreatic Cancer Promotes Cancer Proliferation by Activating the PI3K/Akt Signaling Pathway. *J. Exp. Clin. Cancer Res.* 38, 497. doi:10.1186/s13046-019-1470-y

Xu, Y. F., Li, Y. Q., Liu, N., He, Q. M., Tang, X. R., Wen, X., et al. (2018). Differential Genome-wide Profiling of Alternative Polyadenylation Sites in Nasopharyngeal Carcinoma by High-Throughput Sequencing. *J. Biomed. Sci.* 25, 74. doi:10.1186/s12929-018-0477-6

Yao, L., Wang, H., Song, Y., Dai, Z., Yu, H., Yin, M., et al. (2019). Large-scale Prediction of ADAR-Mediated Effective Human A-To-I RNA Editing. *Brief Bioinform* 20, 102–109. doi:10.1093/bib/bbx092

Ye, J., Wang, Z., Chen, X., Jiang, X., Dong, Z., Hu, S., et al. (2020). YTHDF1-enhanced Iron Metabolism Depends on TFRC m6A Methylation. *Theranostics* 10, 12072–12089. doi:10.7150/thno.51231

Yi, L., Wu, G., Guo, L., Zou, X., and Huang, P. (2020). Comprehensive Analysis of the PD-L1 and Immune Infiltrates of m6A RNA Methylation Regulators in Head and Neck Squamous Cell Carcinoma. *Mol. Ther. Nucleic Acids* 21, 299–314. doi:10.1016/j.omtn.2020.06.001

Yoshimoto, T., Takahashi, M., Nagayama, S., Watanabe, G., Shimada, Y., Sakasi, Y., et al. (2007). RNA Mutations of Prox1 Detected in Human Esophageal Cancer Cells by the Shifted Termination Assay. *Biochem. Biophys. Res. Commun.* 359, 258–262. doi:10.1016/j.bbrc.2007.05.071

Yu, J., Zhang, C., Yu, Q., Yu, H., and Zhang, B. (2019). ADAR1 P110 Enhances Adhesion of Tumor Cells to Extracellular Matrix in Hepatocellular Carcinoma via Up-Regulating ITGA2 Expression. *Med. Sci. Monit.* 25, 1469–1479. doi:10.12659/MSM.911944

Yu, X., Harden, K., Gonzalez, L. C., Francesco, M., Chiang, E., Irving, B., et al. (2009). The Surface Protein TIGIT Suppresses T Cell Activation by Promoting the Generation of Mature Immunoregulatory Dendritic Cells. *Nat. Immunol.* 10, 48–57. doi:10.1038/ni.1674

Yue, B., Song, C., Yang, L., Cui, R., Cheng, X., Zhang, Z., et al. (2019). METTL3-mediated N6-Methyladenosine Modification Is Critical for Epithelial-Mesenchymal Transition and Metastasis of Gastric Cancer. *Mol. Cancer* 18, 142. doi:10.1186/s12943-019-1065-4

Zhang, J., Chen, Z., Tang, Z., Huang, J., Hu, X., and He, J. (2017). RNA Editing Is Induced by Type I Interferon in Esophageal Squamous Cell Carcinoma. *Tumour Biol.* 39, 1010428317708546. doi:10.1177/1010428317708546

Zhang, L., Yang, C. S., Varelas, X., and Monti, S. (2016). Altered RNA Editing in 3' UTR Perturbs microRNA-Mediated Regulation of Oncogenes and Tumor-Suppressors. *Sci. Rep.* 6, 23226. doi:10.1038/srep23226

Zhang, Y., Wang, K., Zhao, Z., Sun, S., Zhang, K., Huang, R., et al. (2018). ADAR3 Expression Is an Independent Prognostic Factor in Lower-Grade Diffuse Gliomas and Positively Correlated with the Editing Level of GRIA2Q607R. *Cancer Cel Int* 18, 196. doi:10.1186/s12935-018-0695-8

Zhao, X., and Cui, L. (2019). Development and Validation of a m6A RNA Methylation Regulators-Based Signature for Predicting the Prognosis of Head and Neck Squamous Cell Carcinoma. *Am. J. Cancer Res.* 9, 2156–2169.

Zhao, Y., Zhao, Q., Kaboli, P. J., Shen, J., Li, M., Wu, X., et al. (2019). m1A Regulated Genes Modulate PI3K/AKT/mTOR and ErbB Pathways in Gastrointestinal Cancer. *Transl Oncol.* 12, 1323–1333. doi:10.1016/j.tranon.2019.06.007

Zheng, D., and Tian, B. (2014). RNA-binding Proteins in Regulation of Alternative Cleavage and Polyadenylation. *Adv. Exp. Med. Biol.* 825, 97–127. doi:10.1007/978-1-4939-1221-6_3

Zheng, Q., Yu, X., Zhang, Q., He, Y., and Guo, W. (2021). Genetic Characteristics and Prognostic Implications of m1A Regulators in Pancreatic Cancer. *Biosci. Rep.* 41, 337. doi:10.1042/bsr20210337

Zhou, X., Han, J., Zhen, X., Liu, Y., Cui, Z., Yue, Z., et al. (2020). Analysis of Genetic Alteration Signatures and Prognostic Values of m6A Regulatory Genes in Head and Neck Squamous Cell Carcinoma. *Front. Oncol.* 10, 718. doi:10.3389/fonc.2020.00718

Zhu, Y., Wang, X., Forouzmand, E., Jeong, J., Qiao, F., Sowd, G. A., et al. (2018). Molecular Mechanisms for CFIm-Mediated Regulation of mRNA Alternative Polyadenylation. *Mol. Cel* 69, 62–e4. doi:10.1016/j.molcel.2017.11.031

Zinshteyn, B., and Nishikura, K. (2009). Adenosine-to-inosine RNA Editing. *Wires Syst. Biol. Med.* 1, 202–209. doi:10.1002/wsbm.10

Zou, D., Dong, L., Li, C., Yin, Z., Rao, S., and Zhou, Q. (2019). The m6A Eraser FTO Facilitates Proliferation and Migration of Human Cervical Cancer Cells. *Cancer Cel Int* 19, 321. doi:10.1186/s12935-019-1045-1

Conflict of Interest: The authors declare that the research was conducted in the absence of any commercial or financial relationships that could be construed as a potential conflict of interest.

Publisher's Note: All claims expressed in this article are solely those of the authors and do not necessarily represent those of their affiliated organizations, or those of the publisher, the editors and the reviewers. Any product that may be evaluated in this article, or claim that may be made by its manufacturer, is not guaranteed or endorsed by the publisher.

GLOSSARY

3' -UTR 3′-untranslation regions
5′-UTR 5′-untranslated region
ADARs Adenosine deaminase acting on RNA
A-to-I editing Adenosine-to-Inosine Editing
ALKBH5 AlkB homolog 5
ALKBH3 AlkB homolog 3
ASEs Alternative splicing events
APA Alternative Polyadenylation
R Arginine
EGR1 Arly growth response 1
Asn Asparagine
Asp Aspartate
COAD Colorectal Adenocarcinoma
CNV Copy number variations
DDX3 DEAD-box RNA helicase 3
dsRNA Double stranded RNA
DUSP1 Dual specificity phosphatase 1
ESCA Esophageal carcinoma
ESCC Esophageal squamous cell carcinoma
FTO Fat mass and obesity-associated protein
FOXD1-AS1 Forkhead box D1 antisense RNA 1
GRIA2 Glutamate receptor ionotropic AMPA 2
HNSCCs Head and neck squamous cell carcinoma
R/M HNSCC Head and neck squamous cell carcinoma
HCC Hepatocellular carcinoma
HPSCC Hypopharyngeal squamous cell carcinoma
ICIs Immune checkpoint inhibitors
IGFBP7 Insulin-like growth factor-binding protein-7
LSCC Laryngeal squamous cell carcinoma
LIHC Liver Hepatocellular carcinoma
mRNA Messenger RNA
METTL3 Methyltransferase-like 3
METTL14 Methyltransferase-like 14
m^1A N1-Methyladenosine
m^6A N6-Methyladenosine
NPC Nasopharyngeal carcinoma
ncRNAs Non-coding RNAs
NSCLC Non-small cell lung cancer
OSCC Oral squamous cell carcinoma
PAAD Pancreatic Adenocarcinoma
PTC Papillary thyroid cancer
PD-1/CD279 Programmed cell death protein-1
RBM15 RNA-binding motif protein 15
RBM15B RNA-binding motif protein 15B
STAD Stomach Adenocarcinoma
TNBC Triple-negative breast cancer
ZAR1 Zygote arrest 1

frontiers in Pharmacology

ORIGINAL RESEARCH
published: 27 January 2022
doi: 10.3389/fphar.2021.785981

Characterization of Kinesin Family Member 2C as a Proto-Oncogene in Cervical Cancer

Jing Yang[1†], Zimeng Wu[1†], Li Yang[1,2,3], Ji-Hak Jeong[4], Yuanhang Zhu[1], Jie Lu[1], Baojin Wang[1,2], Nannan Wang[1], Yan Wang[1], Ke Shen[1] and Ruiqing Li[1]*

[1]*Department of Obstetrics and Gynecology, The Third Affiliated Hospital of Zhengzhou University, Zhengzhou, China,* [2]*Henan International Joint Laboratory of Ovarian Malignancies, Zhengzhou, China,* [3]*Zhengzhou Key Laboratory of Endometrial Disease Prevention and Treatment, Zhengzhou, China,* [4]*Research Institute of Pharmaceutical Sciences, College of Pharmacy, Kyungpook National University, Daegu, South Korea*

Kinesin family member 2C (*KIF2C*) is known as an oncogenic gene to regulate tumor progression and metastasis. However, its pan-cancer analysis has not been reported. In this study, we comprehensively analyzed the characteristics of *KIF2C* in various cancers. We found that *KIF2C* was highly expressed and corresponded to a poor prognosis in various cancers. We also found a significant correlation between KIF2C and clinicopathological characteristics, particularly in cervical cancer, which is the most common gynecological malignancy and is the second leading cause of cancer-related deaths among women worldwide. *KIF2C* mutation is strongly associated with the survival rate of cervical cancer, and *KIF2C* expression was significantly upregulated in cervical cancer tissues and cervical cancer cells. Moreover, *KIF2C* promoted cervical cancer cells proliferation, invasion, and migration *in vitro* and as well increased tumor growth *in vivo*. *KIF2C* knockdown promotes the activation of the p53 signaling pathway by regulating the expression of related proteins. The rescue assay with KIF2C and p53 double knockdown partially reversed the inhibitory influence of KIF2C silencing on cervical cancer processes. In summary, our study provided a relatively comprehensive description of *KIF2C* as an oncogenic gene and suggested *KIF2C* as a therapeutic target for cervical cancer.

Keywords: KIF2C, cervical cancer, P53 signaling pathway, molecularly targeted therapy, pan-cancer analysis

OPEN ACCESS

Edited by:
Yingjie Zhang,
Shandong University, China

Reviewed by:
Haiyan Zhu,
First Affiliated Hospital of Wenzhou Medical University, China
Zhenyao Chen,
Fudan University, China

****Correspondence:***
Li Yang
zdsfyyangli@163.com

†These authors have contributed equally to this work

Specialty section:
This article was submitted to Experimental Pharmacology and Drug Discovery, a section of the journal Frontiers in Pharmacology

Received: *29 September 2021*
Accepted: *21 December 2021*
Published: *27 January 2022*

Citation:
Yang J, Wu Z, Yang L, Jeong J-H, Zhu Y, Lu J, Wang B, Wang N, Wang Y, Shen K and Li R (2022) Characterization of Kinesin Family Member 2C as a Proto-Oncogene in Cervical Cancer. Front. Pharmacol. 12:785981. doi: 10.3389/fphar.2021.785981

INTRODUCTION

Kinesin family member 2C (*KIF2C*), also known as mitotic centromere associated kinesin (*MCAK*), is the most representative member of the kinesin family-13 (Kinesin-13) (Ritter et al., 2015). It participates in the functions of microtubules and regulates mitosis and cell cycle, involving in the disaggregation and formation of secondary spindles and the separation of chromosomes (DeLuca et al., 2006; Ganguly et al., 2008; Hedrick et al., 2008; Huang et al., 2009). Because *KIF2C* is involved in the regulation of tumor development, proliferation, and metastasis, it has been considered as a candidate promoting factor for breast cancer, liver cancer, lung cancer, bladder cancer, colon cancer, and other cancers (Bai et al., 2019; Wei et al., 2020; Yang et al., 2020). Shi et al. reported that *KIF2C* is activated by the Wnt/β-catenin signaling pathway and plays a key role in mTORC1 signal transduction and hepatocellular carcinoma progression through its interaction with *TbC1D7* (Wei et al., 2020). Gan et al. (2019) revealed that *KIF2C* has a carcinogenic effect in non-small

TABLE 1 | TCGA cancer types analyzed.

Cancer type	Full name	Number
ACC	Adrenocortical carcinoma	79
BLCA	Bladder urothelial carcinoma	408
BRCA	Breast invasive carcinoma	1,100
CESC	Cervical squamous-cell carcinoma and endocervical adeno-carcinoma	306
CHOL	Cholangiocarcinoma	36
COAD	Colon adenocarcinoma	287
DLBC	Lymphoid neoplasm diffuse large B-cell lymphoma	48
ESCA	Esophageal carcinoma	185
GBM	Glioblastoma multiforme	166
HNSC	Head and neck squamous cell carcinoma	522
KICH	Kidney chromophobe	66
KIRC	Kidney renal clear cell carcinoma	534
KIRP	Kidney renal papillary cell carcinoma	291
LAML	Acute myeloid leukemia	173
LGG	Brain lower-grade glioma	530
LIHC	Liver hepatocellular carcinoma	373
LUAD	Lung adenocarcinoma	517
LUSC	Lung squamous cell carcinoma	501
MESO	Mesothelioma	87
OV	Ovarian serous cystadenocarcinoma	307
PAAD	Pancreatic adeno-carcinoma	179
PCPG	Pheochromocytoma and paraganglioma	184
PRAD	Prostate adenocarcinoma	498
READ	Rectum adenocarcinoma	95
SARC	Sarcoma	263
SKCM	Skin cutaneous melanoma	472
STAD	Stomach adenocarcinoma	415
TGCT	Testicular germ-cell tumors	156
THCA	Thyroid carcinoma	509
THYM	Thymoma	120
UCEC	Uterine corpus endometrial carcinoma	370
UCS	Uterine carcinosarcoma	57
UVM	Uveal melanoma	80

cell lung cancer and is negatively regulated by miR-325-3p. Yang et al. (2020) showed that *circRGNEF* promotes the occurrence and development of bladder cancer by directly targeting miR-548 and upregulating the expression of *KIF2C*.

Cervical cancer is one of the most common gynecological malignancies with high morbidity and mortality, and it is the second leading cause of cancer-related deaths among all female malignant tumors (Siegel et al., 2021). The most common pathological type of cervical cancer is cervical squamous cell carcinoma (Zhao et al., 2019). When cervical cancer patients are diagnosed and treated in the early tumor stage, the chance of survival can be increased and may push the 5-year survival rate to reach as high as 90% (Das, 2021). However, the early symptoms of cervical cancer are not obvious, and 70% of cervical cancer patients are in the middle and late stages of the disease when they are diagnosed with cancer before receiving treatment. Additionally, approximately 31% of cervical cancers relapse after the treatment, and most of the recurrence occurs within 2 years after the initial diagnosis (Zhao and Qiao, 2019; Brisson et al., 2020). The treatment of recurrent cervical cancer is very difficult, and its prognosis is very poor, causing the 1-year survival rate to be only 8–12% (Cohen et al., 2019). Therefore, early treatment provides life-saving, and more and more attention has been paid to finding meaningful therapy targets for cervical cancer.

In the present study, we used The Cancer Genome Atlas (TCGA) project and Gene Expression Omnibus databases to conduct a pan-cancer analysis of *KIF2C* for the first time, including gene expression, survival status, and genetic alteration. Interestingly, we identified *KIF2C* that has a significant value for the research in cervical cancer. Hence, we experimentally confirm that KIF2C expression was increased in cervical cancer tissues and cervical cancer cells. Through *in vivo* experiments, *KIF2C* was found to play an important role in the development of cervical cancer. In addition, RNA sequencing analysis of cervical cancer cells with *KIF2C* knockdown showed that differentially expressed genes were enriched in the p53 signaling pathway. Further analysis of the expression of proteins in the p53 signaling pathway showed that the knockdown of *KIF2C* could induce the activation of the p53 signaling pathway. Beyond this, rescue experiments demonstrated that knockdown of p53 partially reversed the inhibitory influence of knockdown KIF2C silencing on cervical cancer processes. Our findings provide new insights into the functional and mechanistic link between the *KIF2C* and P53 signaling pathways in cervical cancer, which might help discover adjuvant therapy for patients with cervical cancer.

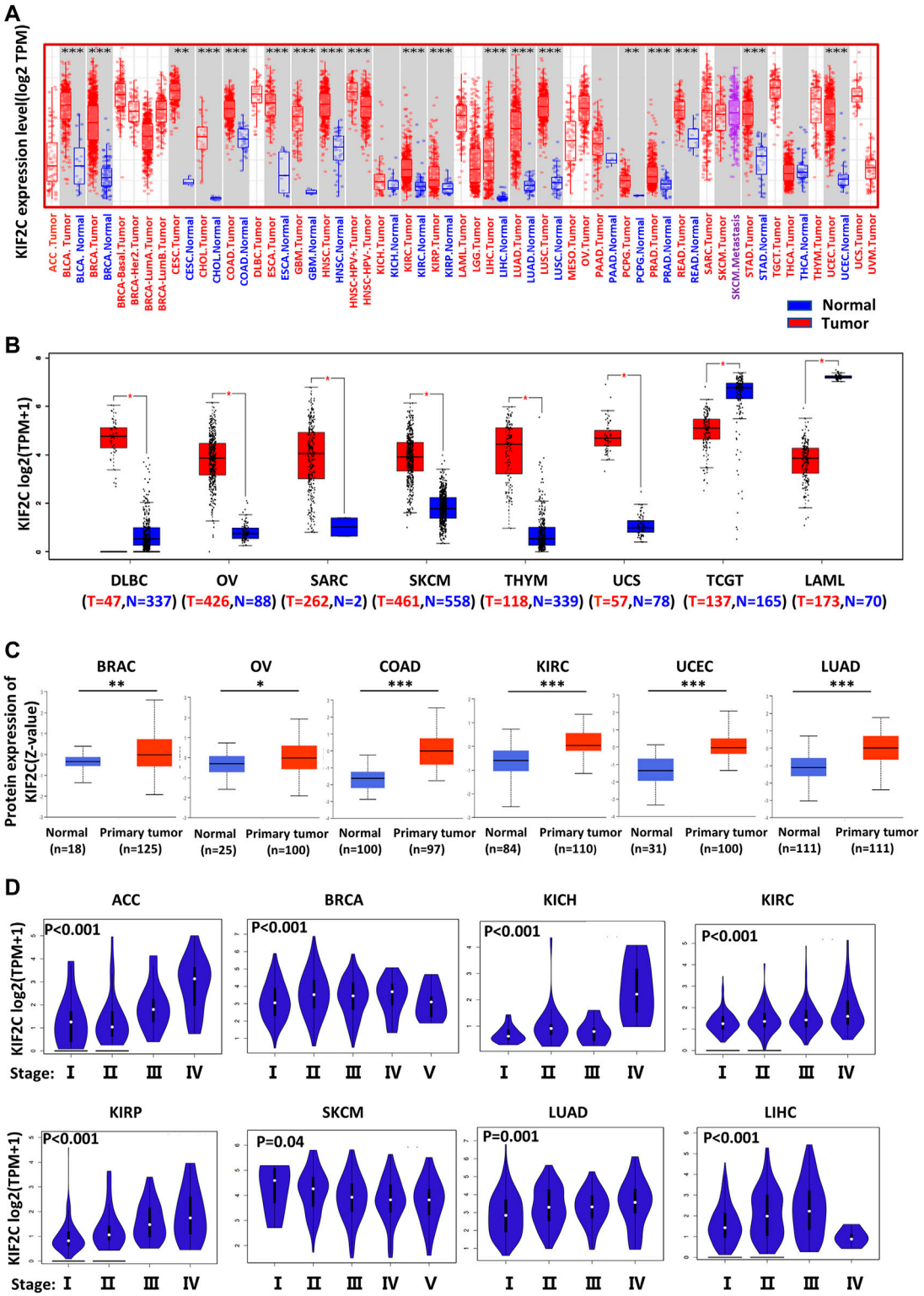

FIGURE 1 | Different expression of *KIF2C* in various tumors and pathological stages. **(A)** *KIF2C* expression in 33 tumor types and paracancer tissues determined by TIMER. **(B)** Tumor types of DLBC, OV, SARC, SKCM, THYM, UCS, TGCT, and LAML were analyzed by box plot, for which corresponding normal tissues of GTEx database were included as controls. **(C)** Diagrams of quantified proteins analyzed by Clinical Proteomic Tumor Analysis Consortium in BRAC, OV, COAD, KIRC, UCEC, and LUAD. **(D)** Expression of *KIF2C* in different tumor stages. Log2 (TPM+1) was applied for log-scale. $^{*}p < 0.05$; $^{**}p < 0.01$; $^{***}p < 0.001$.

MATERIALS AND METHODS

Gene Expression Analysis

The KIF2C expression of tumor and adjacent normal tissues profile was analyzed using the TIMER 2.0 database (https://cistrome.shinyapps.io/timer/), a bioinformatics tool for analyzing and visualizing TCGA (Li et al., 2020a). The 33 TCGA cancer types analyzed are shown in **Table 1**. The gene expression levels are represented as log2 transcript per million (TPM) values. For some tumor tissues without normal tissues, normal expression comparison analyses, the TPM of the given genes from TCGA, and matched GETx (Genotype-Tissue Expression) normal tissue RNA sequencing (RNA-seq) datasets were visualized by GEPIA2 (http://gepia2.cancer-pku.cn/#analysis) (Tang et al., 2017). The cutoff for significance was chosen at $p = 0.01$. The tumor pathological staging map was also obtained from GEPIA2. TPM values were calculated, and the expression levels of genes were presented using the Log2 (TPM + 1) scale.

Protein expression of KIF2C was evaluated using the UALCAN online analysis software (http://ualcan.path.uab.edu/index.html), which is a comprehensive web resource for analyzing cancer-omics data including Clinical Proteomic Tumor Analysis Consortium analysis in various tumor types (Chen et al., 2019).

Survival Analysis

The correlation between KIF2C messenger RNA (mRNA) expression and overall survival (OS) and disease-free survival (DFS) was predicted using the PrognoScan database (http://www.abren.net/PrognoScan/) and GEPIA2. PrognoScan database is also a collection of publicly available cancer microarray datasets and a tool for assessing the biological relationships between gene expression and prognosis, providing a convenient platform to evaluate potential tumor markers and therapeutic targets (Mizuno et al., 2009). The threshold was set as a Cox p-value < 0.05.

Genetic Alteration Analysis

Genomic alteration data were analyzed through the cBio Cancer Genomics Portal (http://cbioportal.org) (Cerami et al., 2012; Gao et al., 2013), which collects multidimensional cancer genomics dataset. We observed the alteration frequency and mutation type of all 33 tumors. We also obtain the data on the overall disease-free, progression-free, and DFS differences for TCGA cancer cases with or without *KIF2C* genetic alteration.

The Human Protein Atlas

HPA provides tissue and cell distribution information of 26,000 human proteins (Uhlén et al., 2015). In this database, researchers used highly specific antibodies and immunoassay techniques to detect the expression of each protein in 64 cell lines, 48 human normal tissues, and 20 tumor tissues in detail. In this study, we conducted HPA to observe the localization of KIF2C in cells and compare the protein expression of KIF2C between normal tissue and carcinoma tissue.

LinkedOmics Database

The LinkedOmics database 8 (http://linkedomics.org) (Vasaikar et al., 2018) is an online open-access powerful bioinformatics platform, which includes multi-omics information and clinical data involving 11,158 patients and 32 cancer types in TCGA project. We used the Linkedomics platform to analyze the relationship between the expression level of KIF2C in TCGA database and the clinical–pathological characteristics of patients.

Tissue Collection and Immunohistochemistry

Tissue specimens were obtained from patients who underwent hysterectomy and pathological diagnosis in the Department of Pathology of The Third Affiliated Hospital of Zhengzhou University (Zhengzhou, China) from 2017 to 2021. Paraffin-embedded histological specimens of 35 cervical squamous tissue samples, 25 cervical adenocarcinoma tissue samples, and 40 normal cervical tissues samples were sectioned (thickness 5 μm). All the patients had not received any antitumor therapy before their diagnoses. The project was approved by the Medical Ethics Committee of the Third Affiliated Hospital of Zhengzhou University (ethics approval number: 2021-080-01) and performed in accordance with the principles of the Declaration of Helsinki.

Immunohistochemistry and scoring criteria were performed as described (Soumaoro et al., 2004). Briefly, the tissue sections were deparaffinized in xylene, rehydrated in graded ethanol, and soaked in distilled water. After heat-mediated citric acid antigen retrieval, the tissue sections were incubated with the primary antibody for KIF2C (DF7348, rabbit antihuman, 1:100, Affinity) and Ki-67 (ab92742, rabbit antihuman, 1:500, Abcam) at 4°C overnight and incubated with horseradish peroxidase-conjugated antibody for 60 min at room temperature. Staining was developed by incubating with diaminobenzidine. Finally, these processed tissue sections were observed under a microscope and then counterstained with hematoxylin. The results were scored independently by two pathologists. A total score of >3 points was considered a high expression, and ≤3 points was considered low expression.

Cell Culture

Cervical cancer cell lines SiHa, HeLa, C33a, and Caski and normal cervical cell line HCerEpic were borrowed from the relevant research group with our laboratory. All cells were cultured in Dulbecco's modified Eagle's medium (Solarbio, SuoLaibao Technology Co., Ltd.) supplemented with 10% fetal bovine serum (Gibco, Thermo Fisher Scientific, Inc.) and incubated at 37°C in a moist atmosphere containing 5% CO_2.

Knockdown of KIF2C by Lentivirus Transfection

When C33a and SiHa cells reached 20–30% confluence on the day of transfection, two lentiviral stocks (named GV248-shKIF2C and GV248-shCon, purchased from Genechem, Shanghai, China) were transduced into the cells with HitransG A, respectively. Stable cell lines were screened with 0.25 μg/ml puromycin. The cells were collected when 80–90% of the cells with green fluorescence were grown under a fluorescence

microscope, then quantitative real-time polymerase chain reaction (qRT-PCR) and Western blot analysis were used to analyze the level of *KIF2C* expression.

Knockout of p53 by CRISPR-Cas9

CRISPR/Cas9 p53 knockdown and its control plasmids were kindly provided by Dr. Qi Zhang; then, the plasmids were transfected into SiHa-sh-KIF2C and SiHa-sh-NC cervical cancer cells, respectively. The cells were transfected using JetPrime transfection reagent (Polyplus transfection, Illkirch, France) according to the manufacturer's protocol; then, Western blot analysis was used to analyze the level of p53 expression.

Overexpression of KIF2C by Plasmid

For overexpression, the plasmid (vector name: GV657) for human KIF2C and negative control were synthesized by Genechem (Shanghai, China), then transfected into Caski cell using JetPrime transfection reagent (Polyplus transfection, Illkirch, France) according to the manufacturer's protocol using 1=μl of JetPrime for 1 μg of plasmid DNA. After being transfected with 24 h, the protein was collected, and Western blotting was used to verify the transfection efficiency.

Quantitative Real-Time Polymerase Chain Reaction Analysis

According to the supplier's instructions, synthesis of complementary DNA by extracting 1 μg total RNA with Trizol (Cwbio, Beijing, China) and SYBR reverse transcription reagent (US Everbright Inc., Suzhou, China). The ratio of target glyceraldehyde 3-phosphate dehydrogenase expressed the relative expression of target gene mRNA. The sequences for the primers are as follows:

GADPH, Forword, 5′-TGACTTCAACAGCGACACCCA-3′;
Reverse, 5′-CACCCTGTTGCTGTAGCCAAA-3′;
KIF2C, Forword, 5′-GGAGGAGAAGGCTATGGAAGA-3′;
Reverse, 5′-TCGCAGGGCTGAGAAATG-3′.

The relative gene expression was normalized to control by the $2^{-\Delta\Delta CT}$ method.

Western Blot Analysis

Total proteins from cells were extracted with radioimmunoprecipitation assay lysis buffer (Solarbio, SuoLaibao Technology Co., Ltd.). Western blot analysis was carried out by first electrophoresing the proteins through a sodium dodecyl sulfate–polyacrylamide gel electrophoresis gel and subsequently transferring to 0.45-μm polyvinylidene fluoride membrane (Millipore, Ireland). Immunoblotting was performed using antibodies against indicated proteins: *KIF2C* (DF7348, rabbit antihuman, 1:1,000, Affinity), *p21* (10355-1-AP, rabbit antihuman, 1:1,000, Proteintech), *p53* (sc126, mouse antihuman, 1:, Santa), *Bax* (50599-2-Ig, rabbit antihuman, 1: 5,000, Proteintech), *bcl-2* (60178-1-Ig, mouse antihuman, 1:2,000, Proteintech), and GADPH (bs2188R, rabbit antihuman, 1:5,000, Bioss). Glyceraldehyde 3-phosphate dehydrogenase was used as an endogenous control. The transferred membranes were blocked with 5% milk for 2 h and then incubated with the indicated primary antibody overnight at 4°C. Then, the membranes were incubated with the appropriate secondary antibodies (1:9,000) at room temperature for 1 h. Finally, the electrogenerated chemiluminescence solution (A:B = 1:1) was added onto the membrane, and the front of the membrane was placed on the glass plate. The GelView 6000Plus was used to process the pictures after exposure.

Cell Proliferation Assay

The successfully transfected cervical cancer cells (C33a, SiHa, and Caski) were inoculated in 96-well plates with 4×10^3 cells per well. A 10-μl CCK-8 solution (US Everbright Inc., Suzhou, China) was added to each well after plating for 12, 24, 48, 72, and 96 h. When the cells were further incubated for 3 h, a microboard reader (Thermo Scientific) was used to measure the spectrometric absorbance at the wavelengths of 450 nm.

Colony Formation Assay

After transfection, the cells were inoculated in six-well plates with 600 per well and cultured 2 weeks. Colonies were fixed with methanol for 20 min and subsequently stained with 0.1% crystal violet for 30 min. Colonies with more than 60 cells were defined as positive.

Migration and Invasion Assay

For this assay, serum-free C33a, SiHa, and Caski cells were seeded to the upper chamber with 5×10^4 cells in 100 μl, and the medium containing 20% fetal bovine serum was used as a chemoattractant in the lower chamber. After incubating for 36 h, migrated cells were fixed by formaldehyde and stained with crystal violet. For invasion assay, cells were also suspended in serum-free medium and counted and seeded in the upper chamber at a concentration of 5 × 104 cells in 100 μl; the only difference was spreading the Matrigel Basement Membrane Matrix (BD Bioscience, United States) on the upper chamber before adding the cells. The number of migrated and invaded cells was captured and calculated using a microscope.

RNA-Sequencing and Data Analysis

Total RNAs were extracted from successfully transfected cervical cancer cells using Trizol reagent (Cwbio, Beijing, China). After a primary test for RNA quality and integrity, the sequencing samples were finally sequenced on Novaseq 6000 sequencer (Illumina) with PE150 model. The raw sequencing data were mapped to the human genome using STRA 2.5 software. Reads mapped to the exon regions of each gene were counted by featureCounts, and then reads per kilobase of transcript per million reads mapped was calculated. Differentially expressed (p-value cutoff of 0.05; the fold-change cutoff of 2) genes between groups were identified using the edgeR package. For further precise analysis, Gene Ontology (GO) analysis and Kyoto Encyclopedia of Genes and Genomes (KEGG) enrichment analysis for differentially expressed genes were conducted by KOBAS 2.1 software (p-value < 0.05; false discovery rate <

0.05). The RNA sequencing analysis and data analysis were performed with the help of Seqhealth cooperation (Wuhan, China). RNA-seq data have been deposited to National Center for Biotechnology Information Sequence Read Archive (Sequence Read Archive accession: PRJNA767113).

In Vivo Experiments

Four- to 5-week-old female BALB/c nude mice (SPF Biotechnology Co., Ltd., Beijing, China) were used in this study. The control and experimental cervical cancer cells (2×10^6) were transplanted to establish the subcutaneous xenograft model. Tumor volumes were measured every 7 days. After 4 weeks, the mice were killed, and tumor weight was examined. The tumor volumes were calculated by the formula: tumor volume = length × width^2/2. Animal research was approved by the Animal Care and Use Committee of Zhengzhou University and was conducted in accordance with the Animal Care Guidelines of Zhengzhou University.

Statistical Analysis

Statistical analysis of all data was done using SPSS 26.0 software. The measurement data with normal distribution was exhibited as the mean ± standard deviation. The statistical significance between the two groups was compared with the two-tailed Student's t-test. Pearson's chi-square test analyzed the association between KIF2C expression and clinicopathological features. $p < 0.05$ was considered statistically significant. All cell experiments had three repetitions.

RESULTS

Database Analysis for KIF2C Expression in Various Cancers

In the TIMER database, we investigated the expression of KIF2C in pan-cancer. The GEPIA2 database supplemented part of cancers without normal samples. The results are shown in **Figures 1A,B**. As expected, KIF2C expression was significantly increased in most tumor tissues compared with normal tissues, including TCGT and LAML. However, there was no significant difference between tumor and normal tissues in ACC and LGG. As there were no normal samples studied in either dataset, an analysis could not be performed for MESO and UVM. In addition, the protein expression level of KIF2C was also shown in a similar manner. Clinical Proteomic Tumor Analysis Consortium analysis showed that the protein expression of KIF2C was higher in primary tissues of BRAC, OV, COAD, KIRC, UCEC, and LUAD compared with those in normal tissues (**Figure 1C**). All the results were statistically significant ($p < 0.05$). Next, we used the UALCAN database to analyze the correlation between *KIF2C* mRNA expression and clinicopathological stages. Expression of *KIF2C* was highly associated with advanced clinical stage (**Figure 1D**) of ACC ($p < 0.001$), BRCA ($p < 0.001$), KICH ($p < 0.001$), KIRC ($p < 0.001$), KIRP ($p < 0.001$), SKCM ($p = 0.04$), LUAD ($p = 0.001$), and LIHC ($p < 0.001$) but not others.

Survival Analysis for KIF2C in Various Cancers

Next, we investigated *KIF2C* prognostic value using PrognoScan and GEPIA2 database. In PrognoScan, high *KIF2C* expression is associated with worse OS [hazard ratio (HR) = 1.45, Cox $p = 0.000964$] and disease-specific survival (DSS, HR = 2.2, Cox $p = 0.000025$) in bladder cancer (**Figures 2A,B**), with worse OS (HR = 4.35, Cox $p = 0.000473$) in brain cancer (**Figure 2C**), with worse OS (HR = 1.39, COX $p = 0.047079$), distant metastasis-free survival (HR = 4.98, COX $p = 0.003309$), DFS (HR = 6.19, COX $p = 0.001105$), and recurrence-free survival (RFS, HR = 4.98, COX $p = 0.000259$) in breast cancer (**Figures 2D–G**), with worse distant relapse-free survival (HR = 2.33, COX $p = 0.000006$) in soft tissue cancer (**Figure 2H**), with worse OS (HR = 3.6, COX $p = 0.042603$), RFS (HR = 2.41, COX $p = 0.000001$) in lung cancer (**Figures 2I,J**) and with worse OS (HR = 9.01, COX $p = 0.000058$) in skin cancer (**Figure 2K**). Conversely, KIF2C high expression is associated with good DFS (HR = 0.53, COX $p = 0.013566$) in colorectal cancer (**Figure 2L**). For blood cancer (**Figures 2M,N**), *KIF2C* presented the opposite manner in OS (HR = 0.53, COX $p = 0.017$) and DSS (HR = 2.53, COX $p = 0.000363$). For other cancers, no statistically significant associations were observed.

To further explore the prognostic value of *KIF2C*, we performed the survival analysis using Kaplan–Meier curves from the GEPIA2. As shown in **Figure 3A**, higher *KIF2C* expression was associated with poor OS in ACC ($p < 0.001$), KICH ($p = 0.018$), KIRC ($p = 0.006$), KIRP ($p = 0.0017$), LGG ($p < 0.001$), LIHC ($p < 0.001$), LUAD ($p = 0.016$), MESO ($p < 0.001$), PAAD ($p = 0.02$), SKCM ($p = 0.01$), and PRAD ($p = 0.049$), whereas higher KIF2C expression was linked to better prognosis in THYM ($p = 0.034$). As for DFS (**Figure 3B**), high KIF2C expression was significantly associated with worse DFS in ACC ($p < 0.001$), KIRC ($p = 0.0018$), KIRP ($p < 0.001$), LGG ($p < 0.001$), PAAD ($p < 0.001$), LIHC ($p < 0.001$), PRAD ($p = 0.00011$), THCA ($p = 0.03$), and MESO ($p = 0.016$). These results suggested that higher KIF2C was associated with worse prognosis.

Analysis of Genetic Alteration for KIF2C in Various Cancers

KIF2C mutations and copy number alterations were investigated using the cBioPortal database. The genetic alteration includes mutation, amplification, deep deletion, and multiple alterations. Notably, the highest mutation frequency (>6%) was observed in UCEC (**Figure 4A**). The amplification type of CNA was the major type in the OV, which showed an alteration frequency of ~4% (**Figure 4A**). The predominant mutation type in PGPC was a deep deletion that resulted in a frameshift (**Figure 4A**). All COAD and LAML cases with genetic alteration had a mutation of *KIF2C* (**Figure 4A**). In addition, the amplification of *KIF2C* was present in all SARC, MESO, and LIHC cases (**Figure 4A**). The information of *KIF2C* genetic alteration is presented in **Figure 4B**. The missense mutation was the only type of genetic alteration of *KIF2C*. In addition, we also explored the potential association between *KIF2C* genetic alteration and

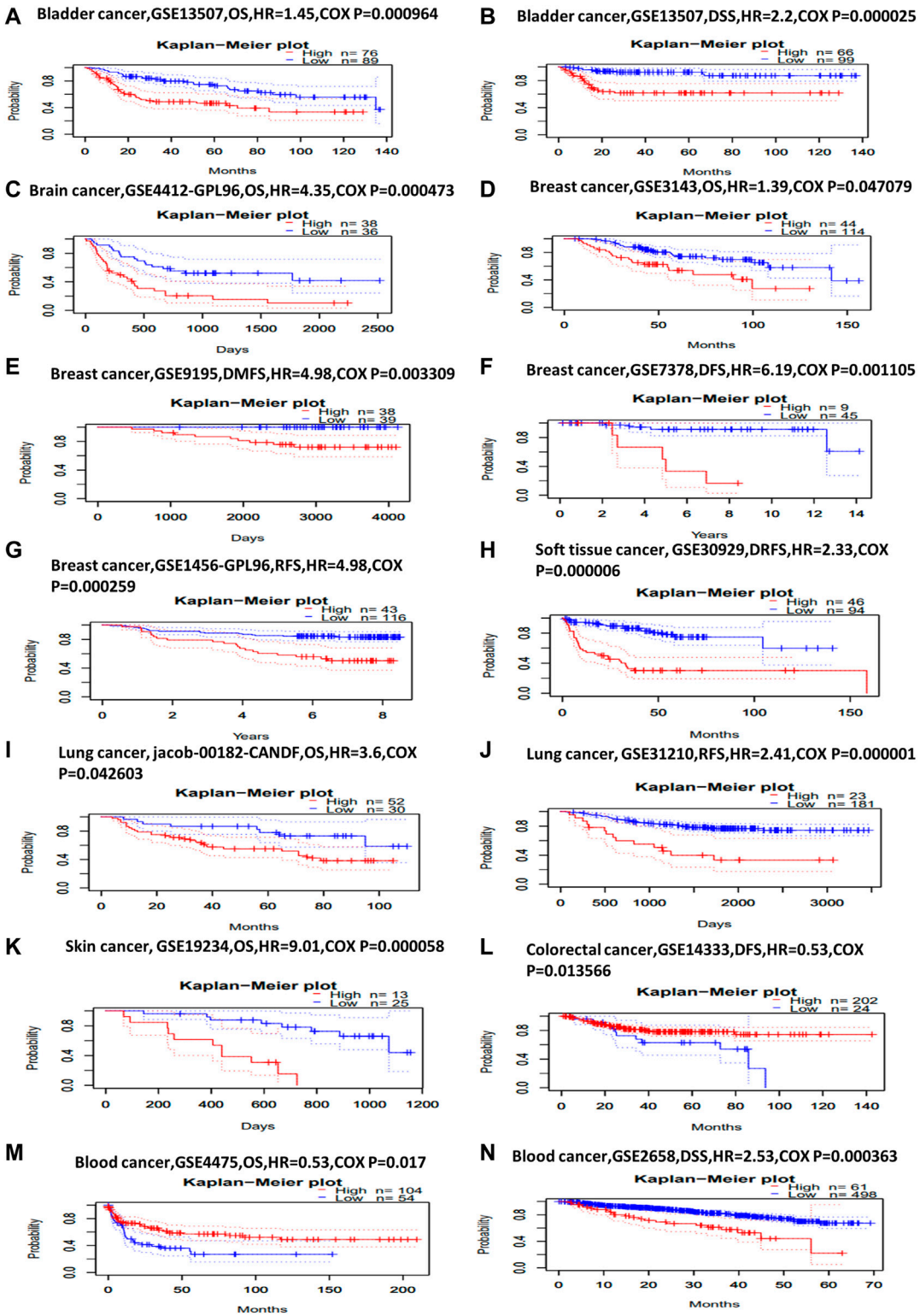

FIGURE 2 | Kaplan–Meier survival curves comparing high and low expression of *KIF2C* in different cancer types in PrognoScan. **(A)** OS (*n* = 165) in bladder cancer cohort GSE13507. **(B)** DSS (*n* = 165) in bladder cancer cohort GSE13507. **(C)** OS (*n* = 74) in brain cancer cohort GSE4412-GPL96. **(D)** OS (*n* = 158) in breast cancer cohort GSE3143. **(E)** Distant metastasis-free survival (*n* = 77) in breast cancer cohort GSE9195. **(F)** DFS (*n* = 54) in breast cancer cohort GSE7378. **(G)** RFS (*n* = 159) in breast cancer cohort GSE1456-GPL96. **(H)** Distant relapse-free survival (*n* = 140) in soft-tissue cancer cohort GSE30929. **(I)** OS (*n* = 82) in lung cancer cohort jacob-00182-CANDF. **(J)** RFS (*n* = 204) in lung cancer cohort GSE31210. **(K)** OS (*n* = 38) in skin cancer cohort GSE19234. **(L)** DFS (*n* = 226) in colorectal cancer cohort GSE14333. **(M)** OS (*n* = 158) in blood cancer cohort GSE4475. **(N)** DSS (*n* = 559) in blood cancer cohort GSE2658.

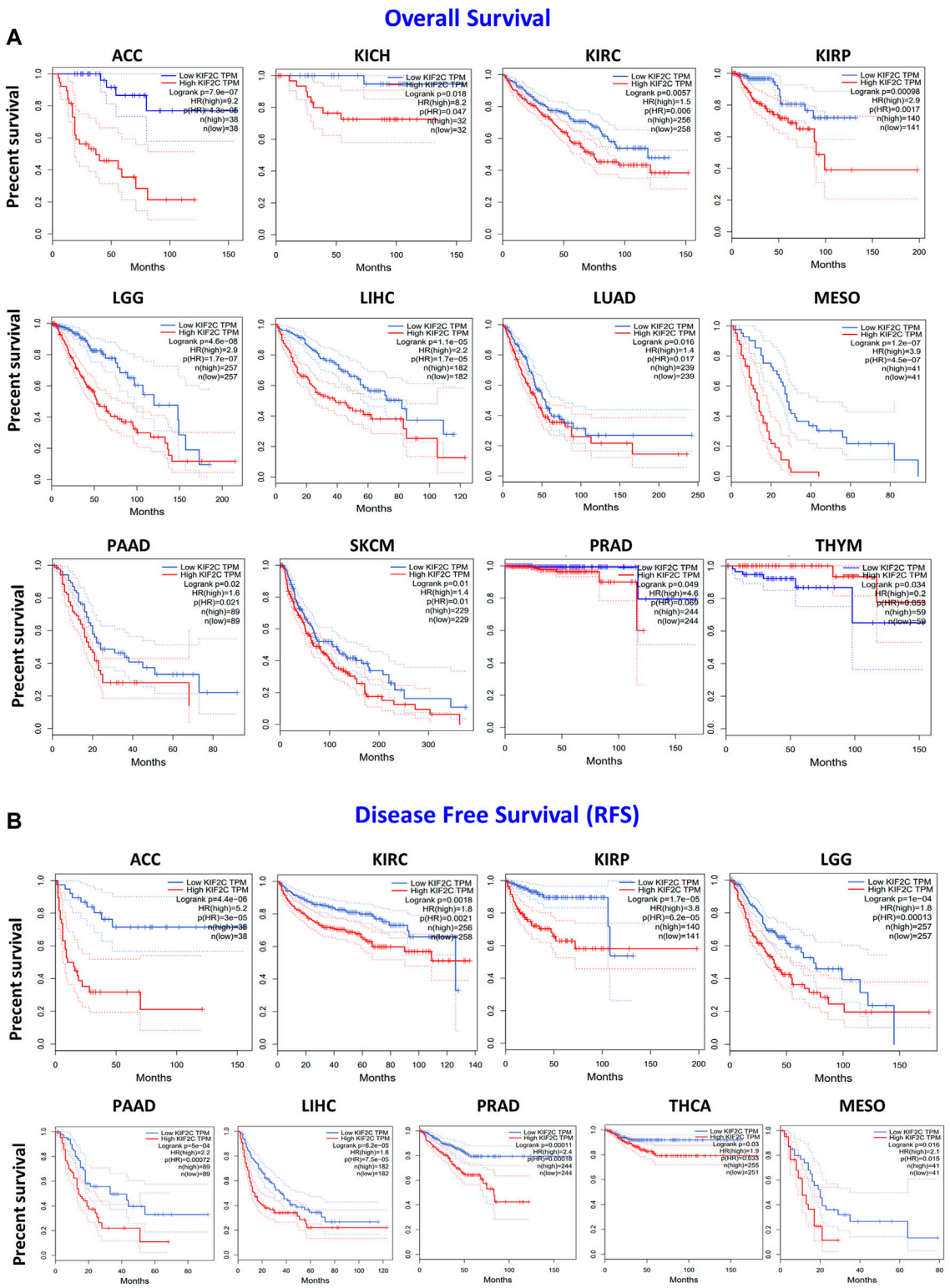

FIGURE 3 | *KIF2C* expression and its association with survival in cancers based on TCGA data analysis. GEPIA2 software was used to analyze **(A)** overall survival rate and **(B)** disease-free survival rate of different tumors in TCGA. Survival plots and Kaplan–Meier curves showing positive results.

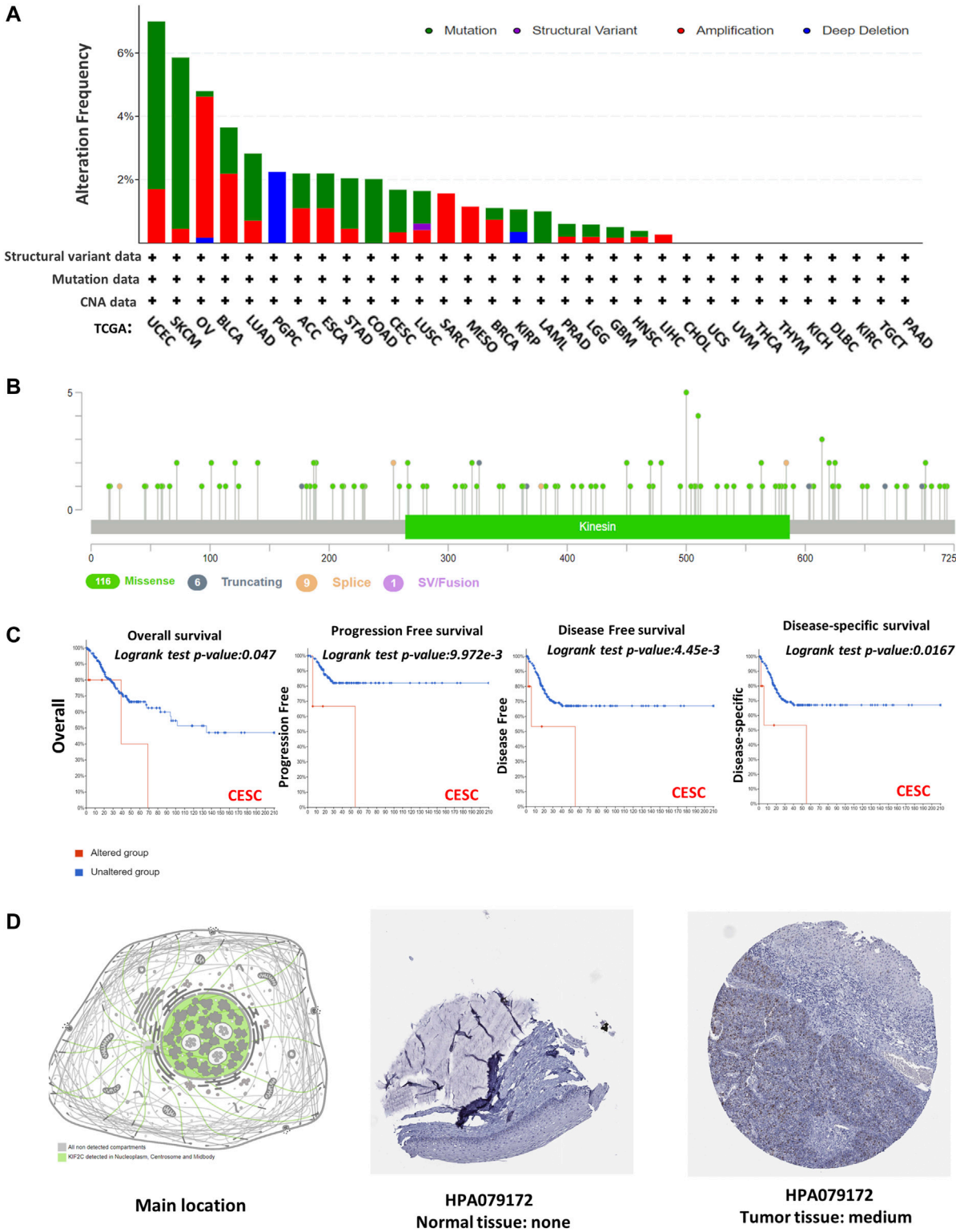

FIGURE 4 | Mutation feature and tissue protein expression of KIF2C in different tumors of TCGA. Mutation features data were obtained using cBioPortal. Alteration frequencies with **(A)** mutation type and **(B)** mutation site are shown. **(C)** Using cBioPortal tool, we analyzed potential correlation between mutation status and overall, disease-specific, disease-free, and progression-free survivals of CESC. Nuclear localization of KIF2C and immunohistochemical results in CESC are shown in **(D).**

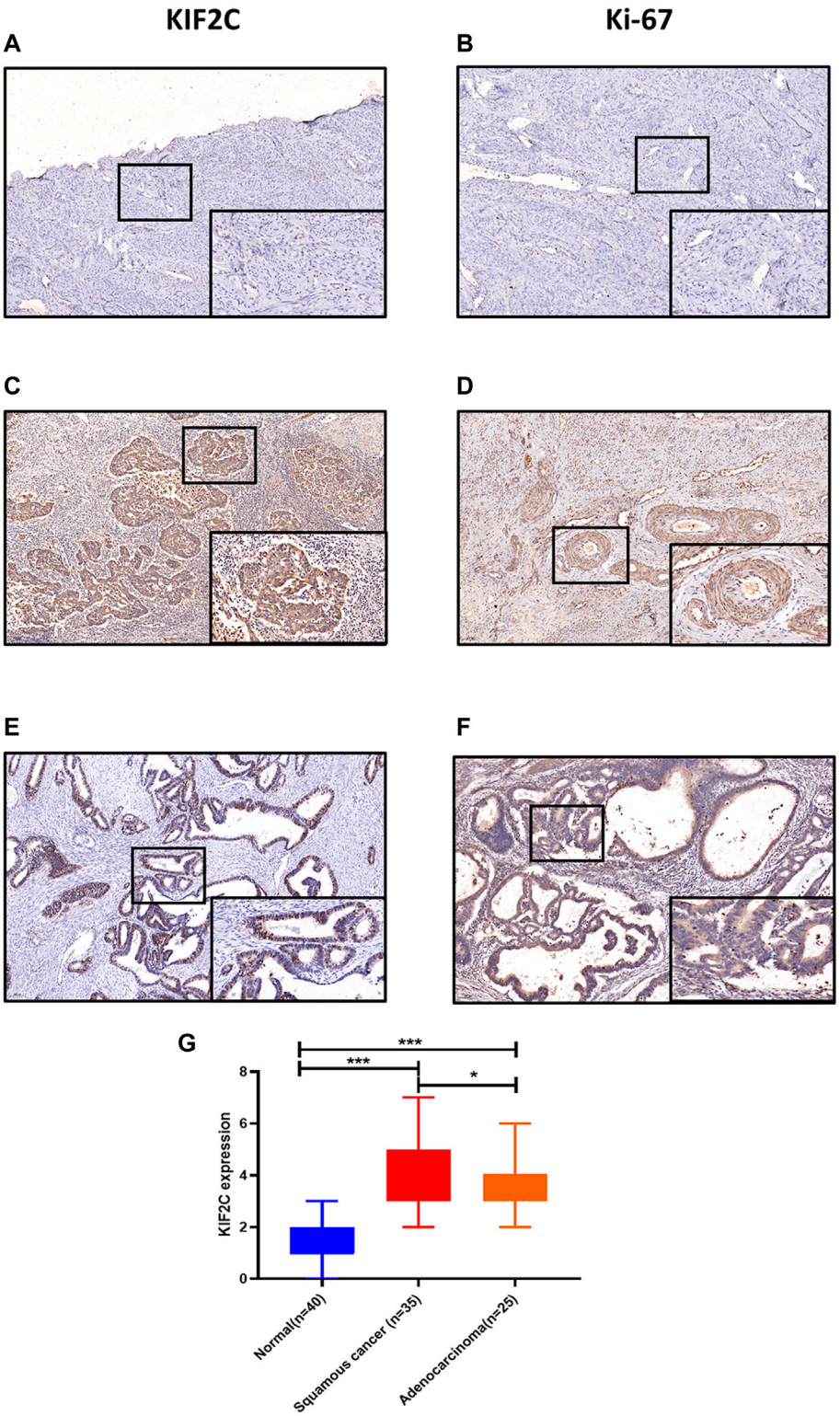

FIGURE 5 | KIF2C was highly expressed in cervical cancer tissues. **(A, B)** Immunohistochemical staining of KIF2C and Ki-67 in normal cervical tissues. **(C, D)** Immunohistochemical staining of KIF2C and Ki-67 in cervical squamous cell carcinoma tissues. **(E,F)** Immunohistochemical staining of KIF2C and Ki-67 in cervical adenocarcinoma tissues. (Insets) Regions with higher magnification. **(G)** Immunohistochemical intensity scores of KIF2C staining in 100 specimens. $^{*}p < 0.05$, $^{**}p < 0.01$; $^{***}p < 0.001$.

TABLE 2 | Relationship between KIF2C and clinicopathological characteristics in cervical cancer patients.

Infuence factors	Cases	KIF2C		*p* value
		Positive	Negative	
Age (years)				0.305
< 40	84	38	46	
≥40	220	114	106	
TNM stage				0.603
I-II	211	108	103	
III-IV	30	14	16	
FIGO stage				0.182
I-II	231	108	123	
III-IV	66	37	29	
Lymphatic metastasis				0.252
Yes	60	36	24	
No	133	68	65	
Distant metastasis				0.126
Yes	10	3	7	
No	116	64	52	
Cancer type				0.006
Adenocarcinoma	52	17	35	
Squamous cell carcinoma	252	135	117	

Chi-square test was used for statistical analysis.
FIGO, 2018 International Federation of Gynecology and Obstetrics; TNM, tumor–nodes–metastases

clinical survival rate in various cancers. The CESC patients with KIF2C genetic alteration had poor prognosis in OS (**Figure 4C**, $p = 0.047$), progression-free survival (**Figure 4C**, $p < 0.001$), DFS (**Figure 4C**, $p < 0.001$), and DSS (**Figure 4C**, $p = 0.0167$). We also used the HPA to investigate the intracellular location and tissue protein expression levels of KIF2C. We found that KIF2C was mostly localized in both cellular nucleus and cytosol (**Figure 4D**), and it was only detected in CESC tissues (**Figure 4D**). These results suggested that *KIF2C* could be a potential therapeutic target in CESC.

KIF2C Was Highly Expressed in CESC Tissue Sample

To explore the possibility of KIF2C as a therapeutic target of cervical cancer, we first detected its expression in human tissues. Findings showed that KIF2C was upregulated in cervical cancer tissues compared with normal tissues (**Figures 5A,C,E**). Not only that, the expression of KIF2C was higher in squamous cervical carcinoma than cervical adenocarcinoma. All three differences were statistically significant ($p < 0.05$, **Figure 5G**). Besides, we also found that the expression of KIF2C has a similar expression pattern with Ki-67 in cervical tissues (**Figures 5B,D,F**). This suggested that the expression of KIF2C may be related to the active proliferation of cancer cells.

Correlation Between *KIF2C* and Clinicopathological Features in Cervical Cancer

To investigate the clinical relevance of KIF2C in cervical cancer, 304 cervical cancer cases from TCGA were analyzed. The results showed that KIF2C expression was correlated with the type of cervical cancer ($p < 0.05$), whereas it was not directly correlated with age, tumor–nodes–metastases stage, 2018 International Federation of Gynecology and Obstetrics stage, lymphatic metastasis, and distant metastasis (**Table 2**).

Establishment of *KIF2C* Knockdown or Overexpression Cells Using Cervical Cancer Cell Lines

Because we found that *KIF2C* was clinically relevant in cervical cancer in the discussion earlier, we examined the KIF2C expression in various cervical cancer and normal cell lines, including C33a, HeLa, SiHa, Caski, and HCerEpic cell lines. We analyzed mRNA and protein levels of KIF2C using qRT-PCR and Western blot assay in those cells. The results showed that the mRNA or protein levels of KIF2C in C33a, HeLa, and SiHa cells were higher than those in HCerEpic cells (**Figures 6A–C**). The two cell lines (SiHa and C33a) with the highest KIF2C expression and Caski cell, which had a relatively low level of KIF2C expression, were used for subsequent experiments. To further investigate the role of KIF2C in cervical cancer, we established the stable KIF2C knockdown cell lines using the short hairpin RNA lentiviral system. We confirmed the knockdown efficiency using Western blot, qRT-PCR (**Figures 6D–I**), and green fluorescent protein (**Figure 6J**) in SiHa and C33a cells. For overexpression, the Caski cell was transfected with KIF2C plasmid, and the transfection efficiency was verified with Western blot (**Figure 6K,L**).

KIF2C Knockdown Inhibited the Tumorigenicity of Cervical Cancer Cells

To explore the role of *KIF2C* in cervical cancer cells, we examined the cell viability using CCK-8 assay and clone formation assay in SiHa or C33a cells. The viability of sh-KIF2C SiHa or C33a cells was significantly decreased compared with that of control cells (**Figure 7A**). These results indicated that the *KIF2C* knockdown inhibited the proliferation of cervical cancer cells. Next, we investigated the role of KIF2C on *in vitro* tumorigenicity in SiHa and C33a cells. The clonal colonies of sh-KIF2C SiHa and C33a cells were also significantly decreased compared with those of control cells (**Figure 7B**). We then examined whether *KIF2C* knockdown could affect the migration and invasion in SiHa and C33a cells. Results showed that the numbers of migrated or invaded cells in *KIF2C* knockdown groups were significantly lower than those in control groups (**Figure 7C**). These results indicated that *KIF2C* knockdown suppresses the migration and invasion of cervical cancer cells.

KIF2C Overexpression Promoted the Tumorigenicity of Cervical Cancer Cells

To further probe the role of *KIF2C* in cervical cancer cells, we transfected the *KIF2C* overexpression plasmid into the Caski cell line. CCK-8 assay and clone formation experiment were used to detect the cell viability and clone formation ability. For the CCK-8

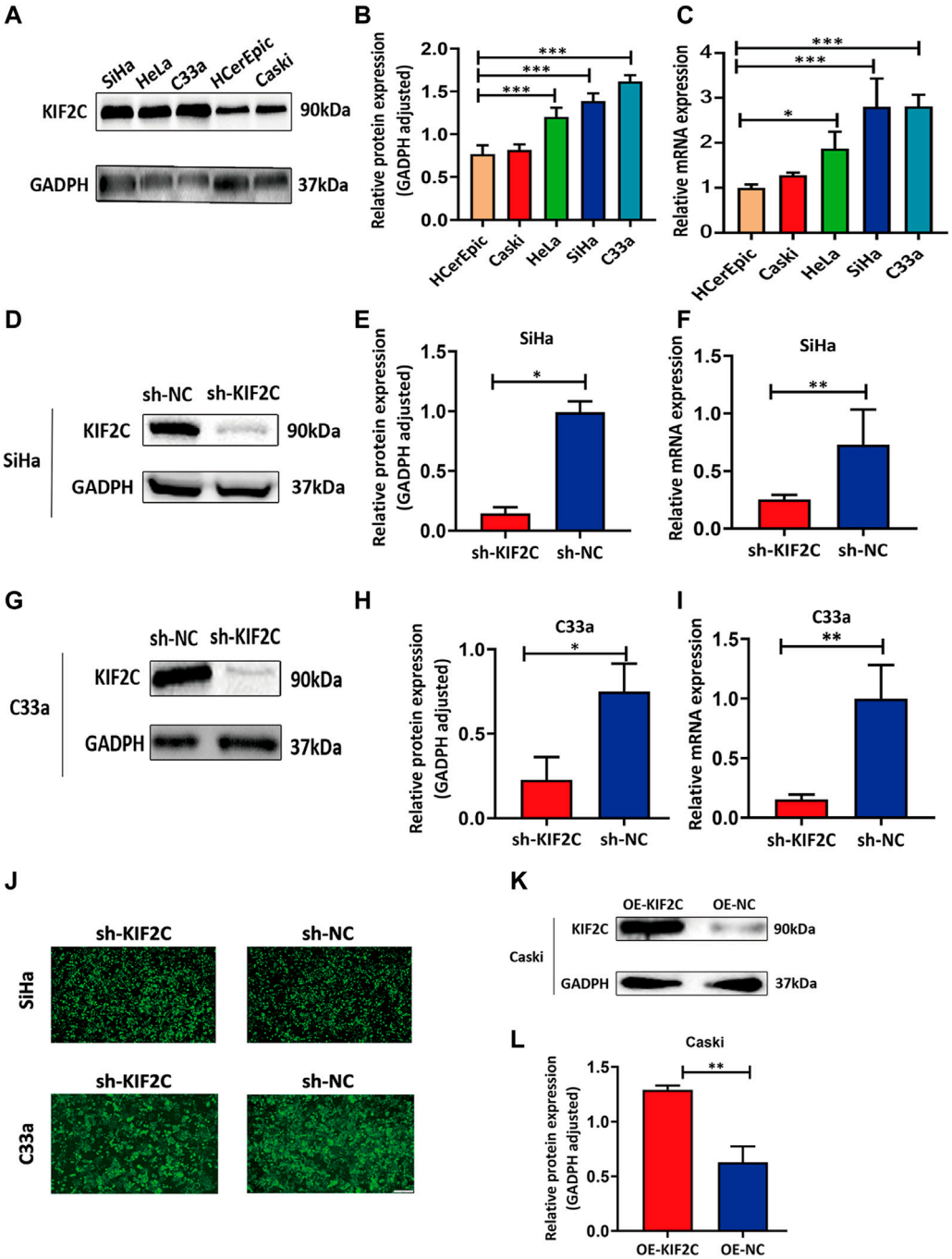

FIGURE 6 | Establishment of *KIF2C* knockdown and overexpression cell lines using cervical cancer cell lines. **(A)** Gray value of KIF2C protein band in SiHa, HeLa, Caski, C33a and HCerEpic; **(B)** relative protein expression of KIF2C in SiHa, HeLa, Caski, C33a, and HCerEpic; **(C)** relative mRNA expression of *KIF2C* in SiHa, HeLa, Caski, C33a, and HCerEpic; **(D)** gray value of KIF2C protein band in SiHa after transfection; **(E)** relative protein expression of KIF2C in SiHa after transfection; **(F)** relative mRNA expression of *KIF2C* in SiHa after transfection; gray value, protein and relative mRNA expression of *KIF2C* in C33a after transfection are shown in **Figures 5G–I**; **(J)** green fluorescence indicated a transfection efficiency greater than 80%; **(K)** gray value of KIF2C protein band in Caski after transfecting *KIF2C* overexpressed plasmid; **(L)** relative protein expression of *KIF2C* in Caski after transfecting overexpressed plasmid. $^{*}p < 0.05$; $^{**}p < 0.01$; $^{***}p < 0.001$.

assay, the results showed the cell viability was significantly increased in the *KIF2C* overexpression groups compared with the control groups (**Figure 8A**). For the clone formation experiment, the clonogenic ability of Caski cells, which overexpressed *KIF2C*, was significantly increased (**Figure 8B**). All findings indicated that *KIF2C* overexpression could promote cell proliferation. By the same token, a transwell assay was performed to examine cell migration and invasion ability, and

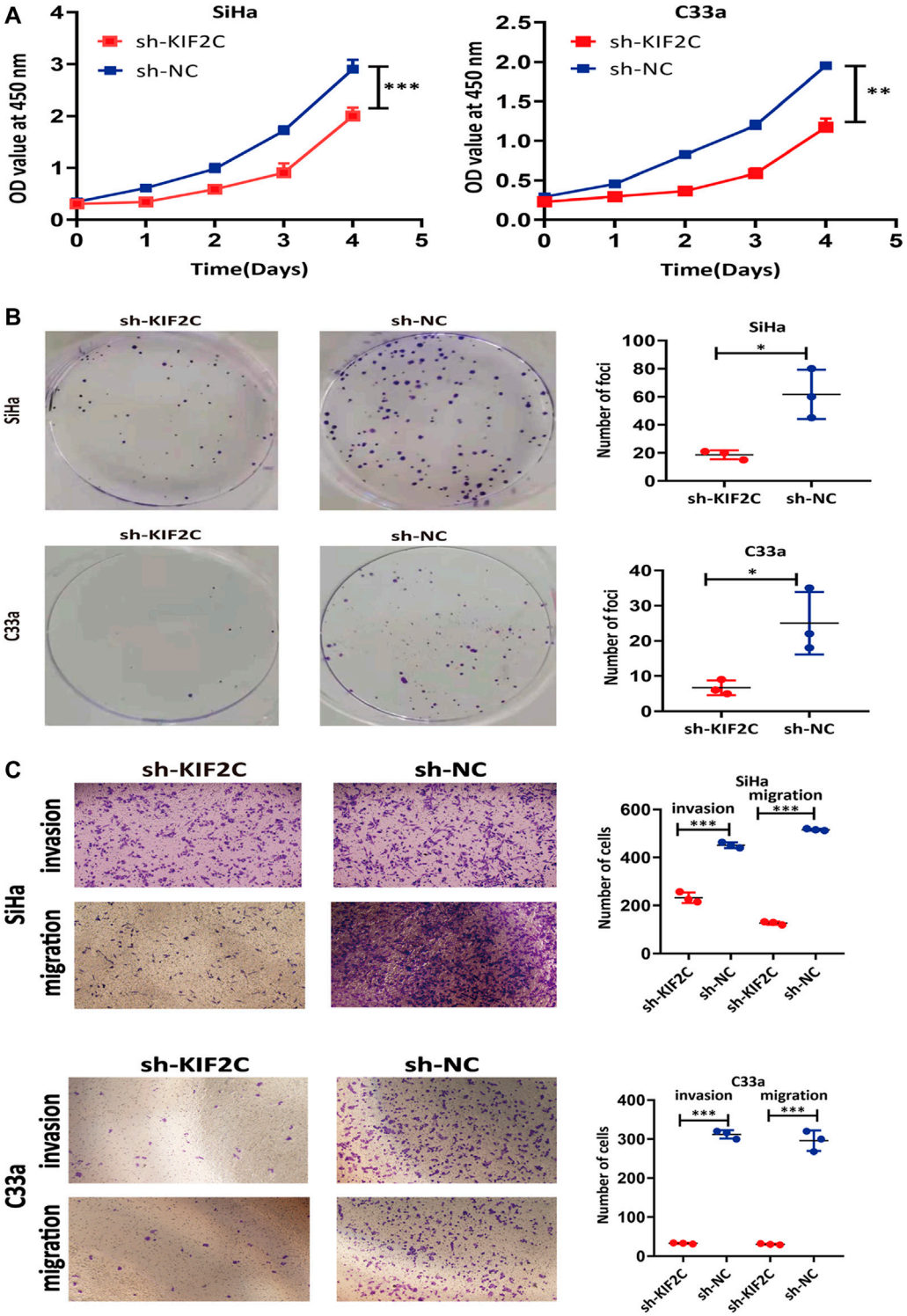

FIGURE 7 | *KIF2C* knockdown inhibited tumorigenicity of cervical cancer cells. CCK-8 assay **(A)** and colony formation assay **(B)** were used to evaluate ability of cell proliferation in cervical cancer cells with *KIF2C* knockdown; dot plots in right showed results of quantitative analyses. **(C)** Migration and invasion of cervical cancer cells were determined after *KIF2C* knockdown and quantification of number of cells in migration and invasion. $^{*}p < 0.05$; $^{**}p < 0.01$; $^{***}p < 0.001$.

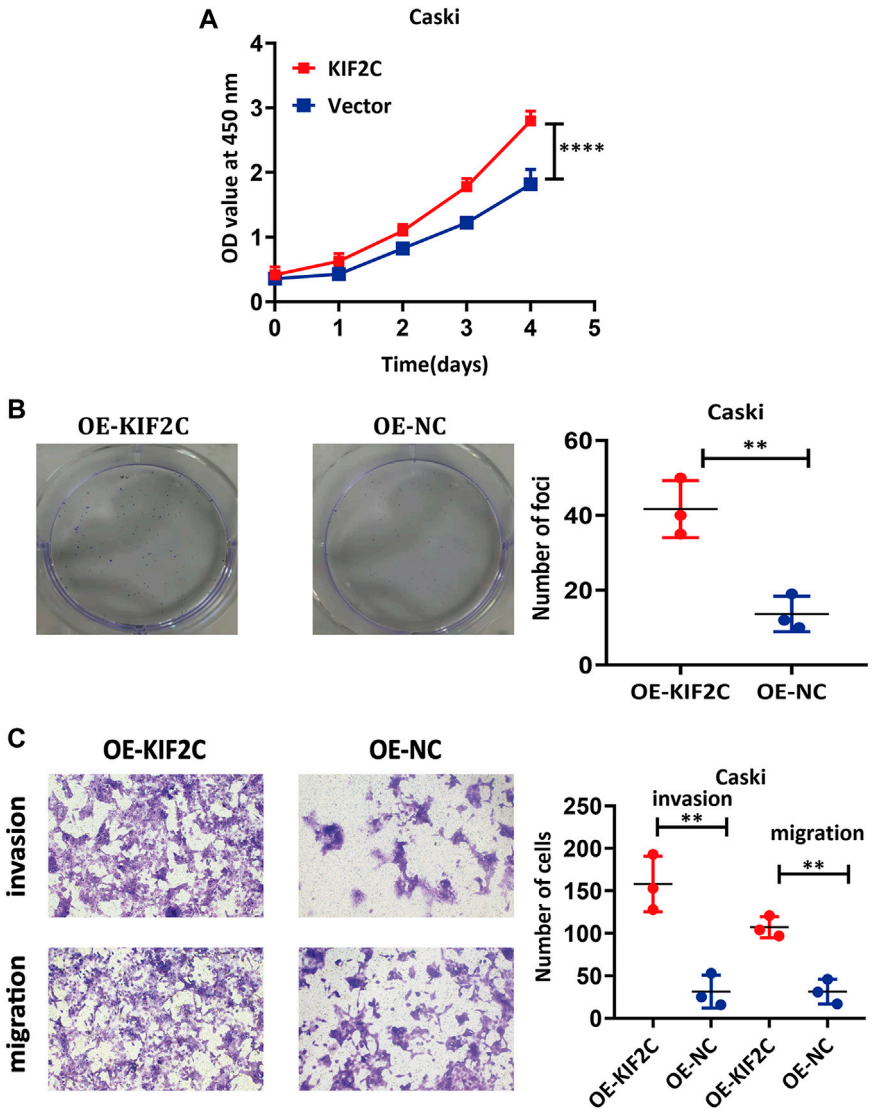

FIGURE 8 | *KIF2C* overexpression promoted tumorigenicity of cervical cancer cells. CCK-8 assay **(A)** and colony formation assay **(B)** were used to evaluate ability of cell proliferation in cervical cancer cells with *KIF2C* overexpression; dot plots in right showed results of quantitative analyses. **(C)** Migration and invasion of cervical cancer cells were determined after *KIF2C* overexpression and quantification of number of cells in migration and invasion. $^{**}p < 0.01$; $^{***}p < 0.001$.

the results demonstrated that *KIF2C* overexpression can remarkably improve the migration and invasion ability of cervical cancer cells (**Figure 8C**).

KIF2C Knockdown Regulated Differential Gene Expression

To gain a deeper insight into the mechanism of *KIF2C* expression, we used RNA-seq analysis. We screened the differentially expressed genes using sh-KIF2C SiHa and sh-NC SiHa. Under the screening criteria, which were false discovery rate < 0.05 and | log2FC| >1.5, a total of 349 differentially expressed genes (104 upregulated and 245 downregulated genes) were analyzed (**Figure 9A**). The results were presented as a heat map, in which blue was the downregulated genes and red was the upregulated genes (**Figure 9B**). Then, we subjected the 349 genes to GO and KEGG analyses. The results of the GO analysis showed the main pathways in which the upregulated genes were involved in protein transport into membrane raft, protein transport within the lipid bilayer, negative regulation of signal transduction, negative regulation of signaling, etc. (**Figure 9C**). In addition, it also showed the main pathways in which the downregulated genes were involved in xenobiotic glucuronidation, negative regulation of cellular glucuronidation, regulation of glucuronosyltransferase activity, immune system process, and other signaling pathways (**Figure 9D**). The results of the KEGG analysis revealed that the upregulated genes were mainly enriched in mucin-type O-glycan biosynthesis, leukocyte transendothelial migration, cell adhesion molecules (CAMs), phagosome, etc. (**Figure 9E**),

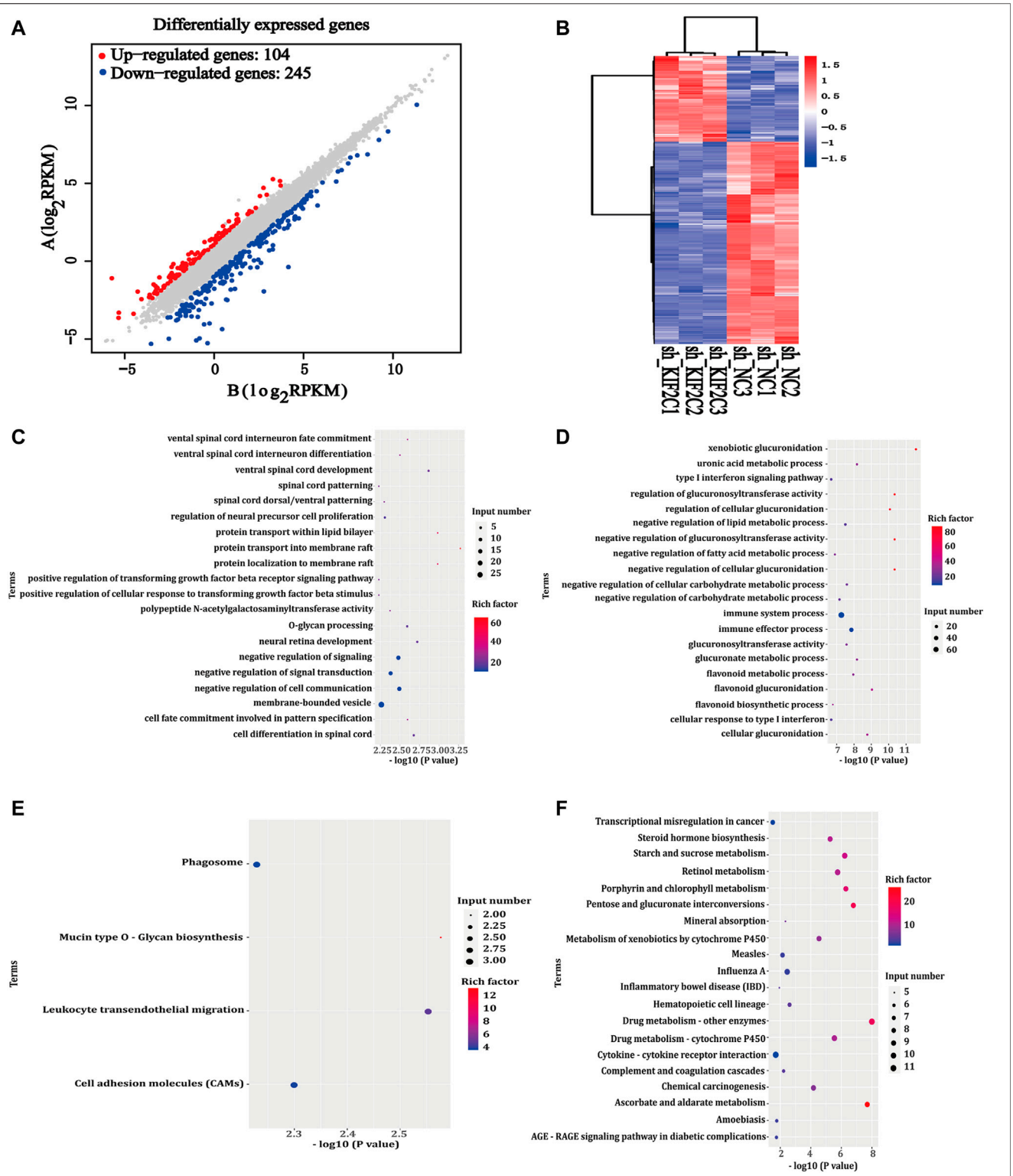

FIGURE 9 | Differentially expressed genes of *KIF2C*. **(A)** Scatter plot of differentially expressed genes between comparison groups; gray dots represent not differentially expressed genes, blue dots represent differentially downregulated genes, and red dots represent differentially upregulated genes; **(B)** leftmost image is overall hierarchical clustering diagram of all differentially expressed genes in all comparison groups, clustered by reads per kilobase of transcript per million reads mapped value, red represents high-expressed genes, and blue represents low-expressed genes. x-axis represents different samples, and y-axis represents gene names; **(C,D)** GO enrichment map of upregulated/downregulated genes; **(E,F)** KEGG enrichment map of upregulated/downregulated genes.

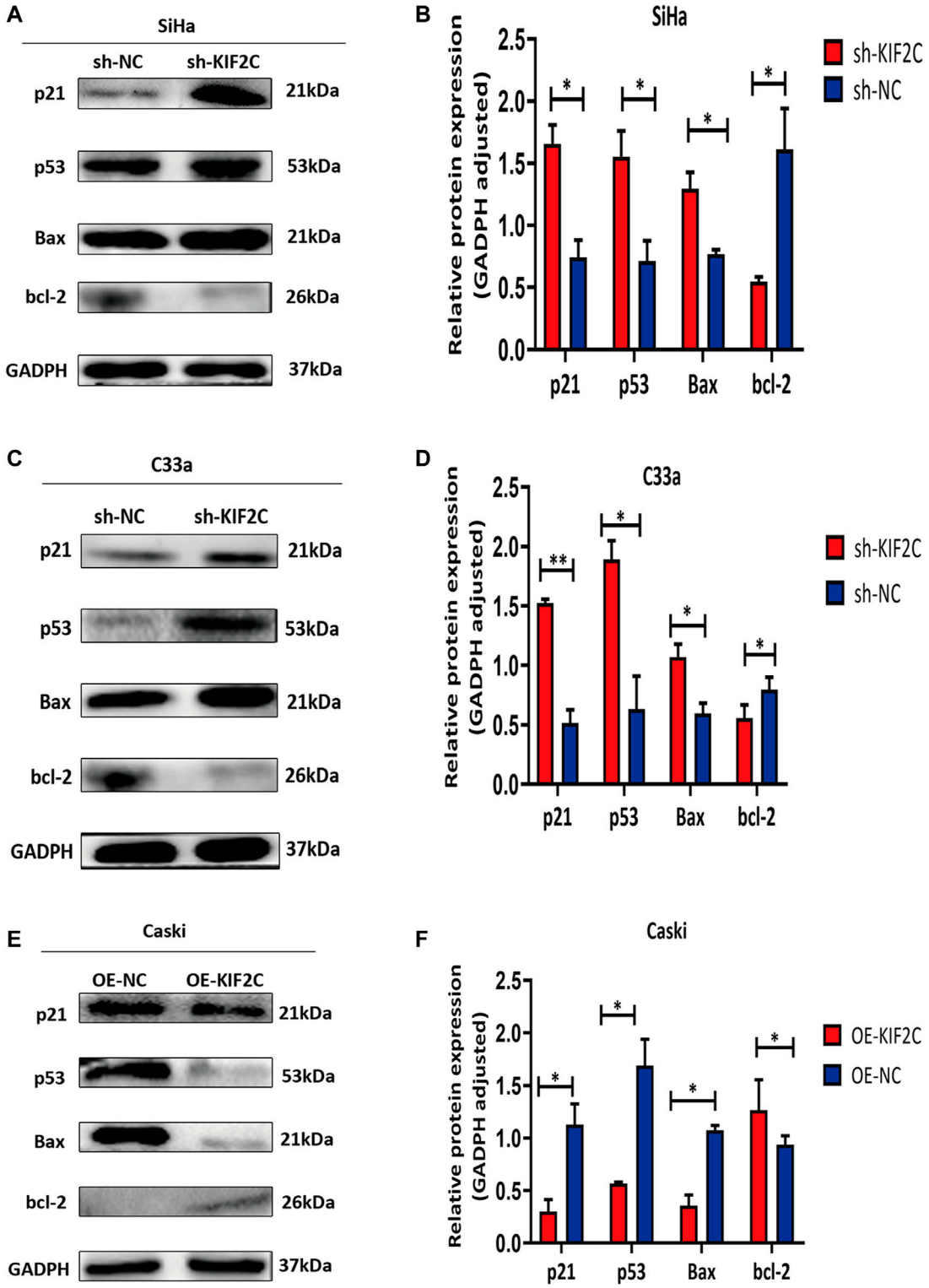

FIGURE 10 | *KIF2C* knockdown promoted activation of p53 signaling pathway. Relative protein expression levels of p21, p53, and Bax were significantly increased, whereas those of bcl-2 was significantly decreased in SiHa **(A,B)** and C33a **(C,D)** cells with KIF2 knockdown. However, expression of proteins mentioned earlier exhibited an opposite trend in presence of KIF2C overexpression **(E,F)**. *$p < 0.05$, **$p < 0.01$.

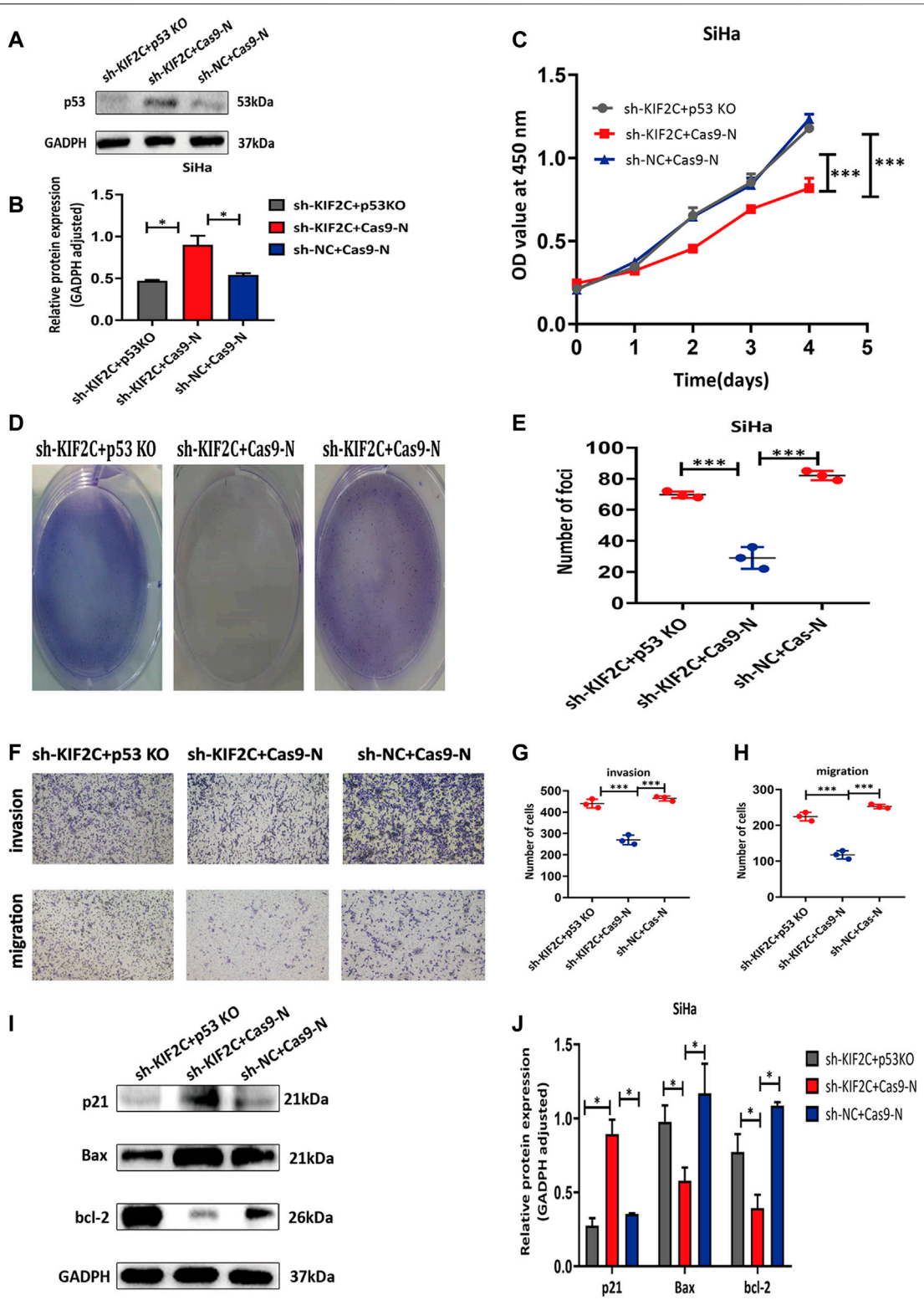

FIGURE 11 | p53 knockdown rescued inhibitory effects of KIF2C in cervical cancer. **(A)** Gray value of p53 protein band in SiHa after transfection; **(B)** relative protein expression of p53 in SiHa after transfection; knockdown of p53 partially reversed KIF2C induced inhibition of proliferation in SiHa cells determined by CCK-8 assay **(C)** and colony formation assay **(D,E)**; knockdown of p53 partially reversed KIF2C induced suppression of invasion and migration **(F)**; bar graphs in **(G,H)** show results of quantitative analyses. **(I)** Gray value of p21, Bax, and bcl-2 protein band in SiHa after transfection; **(J)** relative protein expression of p21, bax, and bcl-2 in SiHa after transfection. $^{*}p < 0.05$; $^{**}p < 0.01$; $^{***}p < 0.001$.

whereas the downregulated genes were mainly enriched in drug metabolism-other enzymes, ascorbate and aldarate metabolism, pentose and glucuronate interconversions, and other related pathways (**Figure 9F**).

KIF2C Promoted Cervical Cancer Progression Through the p53 Signaling Pathway

To further experimentally validate the specific mechanism by which *KIF2C* regulates cervical carcinogenesis, we deeply analyzed the KEGG pathway and found that its differentially expressed genes were enriched in the p53 signaling pathway (**Supplementary Table S1**). There have been some studies showing that alteration of the p53 signaling pathway is involved in the development of cervical cancer. Given that, we further analyzed the expression of proteins involved in the p53 signaling pathways, including p21, p53, bcl-2, and bax. In SiHa and C33a cells with KIF2C knockdown, the expression of p21, p53, and bax proteins was significantly increased, whereas the expression of bcl-2 protein significantly decreased (**Figures 10A–D**). However, the expression of the proteins mentioned earlier exhibited an opposite trend in the presence of the overexpressed KIF2C (**Figures 10E,F**). These results indicated that KIF2C might promote cervical cancer progression through the p53 signaling pathway.

p53 Knockdown Rescued the Inhibitory Effects of *KIF2C* Knockdown in Cervical Cancer

For additionally exploring the associations of *KIF2C* with p53 signaling pathways, the p53 CRISPR/Cas9 knockout plasmid and control CRISPR/Cas9 plasmid were transfected into the SiHa cell with *KIF2C* stable knockdown. Transfection efficiency was verified using Western blot assay (**Figures 11A,B**). The outcome revealed that p53 knockdown reversed the prohibiting effect of *KIF2C*-silenced on cell proliferation (**Figures 11C–E**), migration, and invasion (**Figures 11F–H**). Besides, we also found that the tendency of p21 and Bax showed the same trend with p53; the level of bcl-2 showed the opposite results (**Figures 11I,J**). All these data detailed that *KIF2C* might induce cervical cancer cells growth, invasion, and migration by regulating the p53 signaling pathway.

KIF2C Knockdown Suppressed Cervical Tumor Growth in Mouse Models

To assess the role of *KIF2C* in mouse xenograft models, we subcutaneously inoculated SiHa and C33a cells in the flanks of nude mice. We continuously monitored the tumor growth and measured the volume and weight of tumors for 4 weeks. We found that tumor growth of the sh-KIF2C group was significantly decreased compared with that of the control group (**Figure 12A**). In addition, the volume and weight of tumors of the sh-KIF2C group were lower than those of the control group (**Figures 12B,C**). These results indicated that *KIF2C* knockdown played a tumor-suppressive role *in vivo*.

DISCUSSION

KIF2C belongs to the kinesin superfamily proteins, which participate in microtubule depolymerization, microfilament binding to centromere sites, and chromosome segregation, thus regulating the mitotic process of cells (Ritter et al., 2015). Based on its biological function, *KIF2C* has been suggested to have tumor-promoting properties. Previous studies have reported that *KIF2C* is overexpressed in a variety of cancer types. Shimo et al. (2008) used complementary DNA microarray coupled with laser microbeam microdissection gene chip and laser microbeam technology to detect the genomic expression of 81 breast cancers, from which they found that *KIF2C* is a type of *trans*-activated gene. Their further research also showed that KIF2C is highly expressed in breast cancer tissues and other cell lines. Through bioinformatics analysis, Li et al. (2020b) revealed that *KIF2C* is highly expressed in breast cancer and is involved in the worst OS, RFS, and distant metastasis-free survival of breast cancer. In addition to breast cancer, *KIF2C* is also found to be highly expressed in gastric cancer. Nakamura et al. (2007) reported that the expression level of *KIF2C* in gastric cancer tissues is significantly higher than that in adjacent tissues and is significantly correlated with lymph node invasion, lymph node metastasis, and poor prognosis. Moreover, gastric cancer cell lines transfected with the *KIF2C* gene were verified to have a higher proliferation rate and migration capabilities *in vitro*.

In this study, we performed a series of bioinformatics analyses to identify *KIF2C* gene features in pan-cancer. We analyzed the expression characteristics of *KIF2C* according to the TIMER dataset, TCGA dataset, and GEPIA2 dataset. We found that *KIF2C* was frequently abnormally expressed in various types of cancer. *KIF2C* expression was upregulated in many tumor tissues (BLCA, BRCA, CESC, CHOL, COAD, DLBC, ESCA, GBM, HNSC, KIRC, KIRP, LIHC, LUAD, LUSC, OV, PAAD, PCPG, PRAD, READ, SARC, SKCM, STAD, THYM, UCEC, and UCS) compared with the corresponding normal tissues. However, *KIF2C* expression was downregulated in tumor tissues (e.g., TCGT, LAML). Thus, the difference in *KIF2C* expression in various cancers suggested that it might have different biological functions in different types of cancers. Moreover, high expression levels of *KIF2C* were associated with the poor prognosis of most cancers, which strongly suggested that *KIF2C* was a potential prognostic biomarker for tumor treatment. Tumorigenesis is a complex phenomenon, which is often caused by gene mutations (Fan et al., 2021). Based on this, we then studied the characteristics of *KIF2C* gene mutation. The results demonstrated that the main mutation type of *KIF2C* was missense mutation, which was also the most common oncogenic mutation type (Brown et al., 2014). This may indicate that *KIF2C* was closely related to the development of tumors to some extent. Interestingly, we found that the mutation of *KIF2C* was closely related to the survival rate of CESC, which suggested that *KIF2C* might be a potential therapeutic target of CESC. At the same time, immunohistochemical results in public datasets also showed that KIF2C was only highly expressed in cervical cancer tissue. This prompted us to investigate further the biological function of

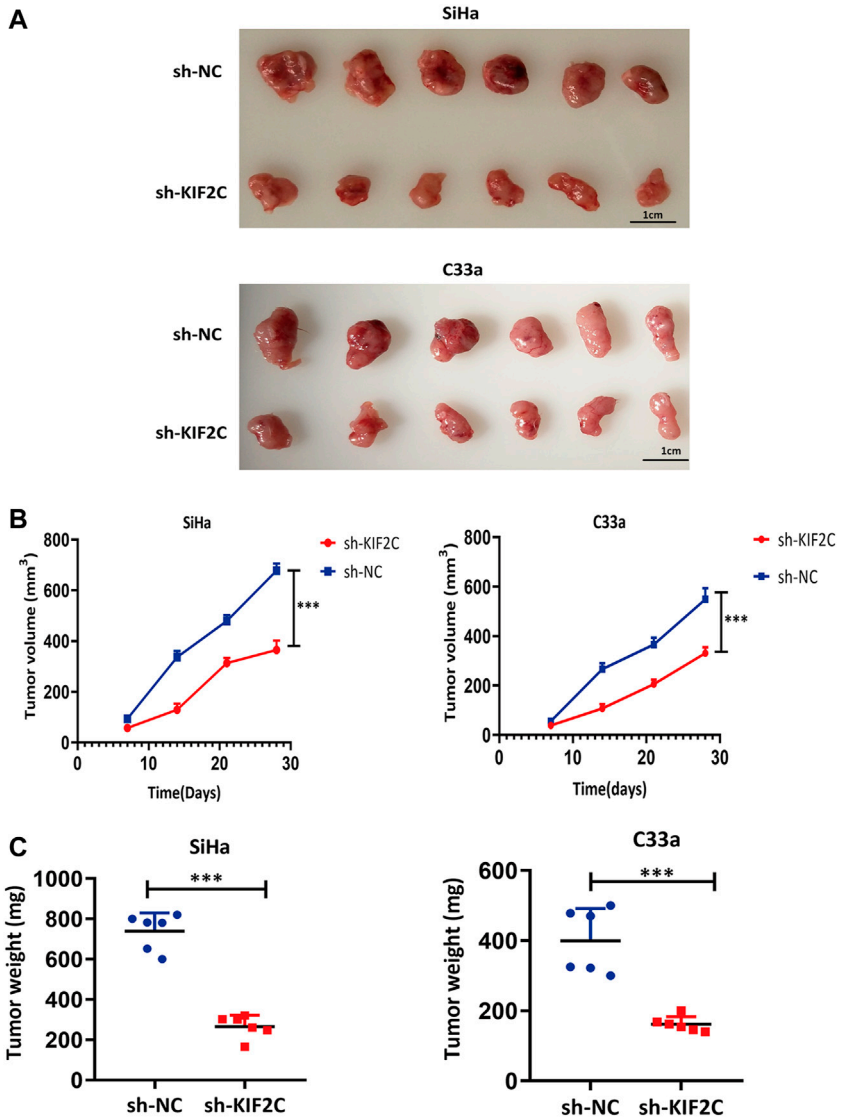

FIGURE 12 | *KIF2C* knockdown suppressed tumor growth *in vivo*. **(A)** Photos of tumor samples from mice; **(B)** curve of tumor volume in mice; **(C)** scatter graph of tumor weight. ***$p < 0.001$.

KIF2C in cervical cancer, which might provide new druggable targets and novel possibilities for cervical cancer therapy.

To explore these possibilities, we first studied the expression of KIF2C in human tissues. Immunohistochemical staining showed that KIF2C was highly expressed in cervical cancer tissues. More than that, there were some similarities in expression levels between Ki-67 and KIF2C. This suggested a latent relationship for KIF2C with the proliferation of cervical cancer. To further investigate the correlation between KIF2C and clinicopathological characteristics, we performed a statistical analysis using the raw data from TCGA database. We found that the expression of KIF2C was dependent on the tumor types, whereas it had no direct correlation with tumor stage, lymph node invasion, and distant metastasis. Therefore, we assumed that *KIF2C* might be involved in the occurrence and development of cervical carcinoma. KIF2C was highly expressed in most cervical cancer cells. Downregulation of the *KIF2C* expression could significantly inhibit the biological functions of cervical cancer cell lines both *in vitro* and *in vivo*. In contrast, the overexpression of *KIF2C* had the opposite effects. These results also suggest that *KIF2C* may be a potential gene contributing to cervical carcinoma development.

The *p53* gene is a tumor suppressor gene that has the highest correlation with human tumorigenesis among genes that have been discovered so far (Levine, 2020). The gene exerts its growth inhibitory effect by activating and interacting with a variety of signaling pathways (Kasteri et al., 2018). As a key transcription factor, p53 has been found to be inactive at both gene and protein levels in a variety of human cancers. Its upregulation in cancer cells may prevent the proliferation of cancer cells by promoting cell cycle arrest and apoptosis (Wang et al., 2015). For example, *SNRPB* can promote the occurrence and development of cervical

cancer by inhibiting the expression of *p53* (Zhu et al., 2020). In addition, in cervical cancer, *ISG15* can upregulate and activate *p53*, which in turn causes the inhibition of proliferation and growth of cancer cells (Zhou et al., 2017). Kong et al. (2015) have reported that *VTRNA2-1-5p* is a direct regulator of *p53*; the inhibition of *VTRNA2-1-5p* can reduce the invasion, proliferation, and tumorigenicity of cervical cancer cells and can increase cell apoptosis and *p53* expression. Furthermore, because *p53* plays a central role in cellular emergency response, deletion or mutation of the *p53* gene can lead to the dysfunctions of upstream regulators or downstream effectors in cancer cells (Miedl et al., 2020). The development of therapy based on the p53 pathway has always faced a huge challenge. Many strategies targeting the p53 pathway have been developed, including the restoration of p53 function, the inhibition of p53-MDM2 interaction, and the conversion of mutant *p53* into wild-type *p53* by gene therapy, the targeting of p53 family proteins, the elimination of mutant *p53*, and the development of p53-based vaccines (Ladds and Laín, 2019). Herein, we found that the downregulation of *KIF2C* causes the activation of the p53 signaling pathway, whereas the upregulation of *KIF2C* inhibits the activation of the p53 signaling pathway. To further confirm the mechanisms by which *KIF2C* regulates cervical cancer formation and development, we applied p53 CRISPR/Cas9 knockout plasmid in Siha cells to rescue the phenotype induced by KIF2C. Indeed, the knockdown of p53 partially reversed the oncogenic effects of KIF2C. Thus, we assumed that *KIF2C* might promote the development of cervical cancer by inhibiting the activation of the p53 signaling pathway. Whether or not this finding can lead to the development of a therapeutic strategy targeting the p53 pathway of cervical cancer, it provides clues and directions for targeted therapy and combined radiotherapy and chemotherapy of cervical cancer, which will be the main topics for our future research.

CONCLUSION

In summary, the results of this pan-cancer analysis showed that the abnormal expression of *KIF2C* was associated with poor prognosis of different cancer types. We also found that *KIF2C* promoted cervical cancer cell proliferation by suppressing the p53 signaling pathway. These findings suggest the potential use of *KIF2C* as a therapeutic target for the treatment of cervical cancer.

DATA AVAILABILITY STATEMENT

The datasets presented in this study can be found in online repositories. The names of the repository/repositories and accession number(s) can be found in the article/ **Supplementary Material**.

ETHICS STATEMENT

The studies involving human participants were reviewed and approved by the Medical Ethics Committee of the Third Affiliated Hospital of Zhengzhou University (ethics approval number: 2021-080-01). Written informed consent for participation was not required for this study in accordance with the national legislation and the institutional requirements. The animal study was reviewed and approved by the Animal Center of Zhengzhou University.

AUTHOR CONTRIBUTIONS

LY designed the study. JY and ZW performed the experiments and wrote the manuscript. J-HJ and BW modified the language. YW, NW, KS, and RL contributed to the analysis of the data. YZ and JL reviewed and edited the manuscript. All authors read and approved the manuscript.

SUPPLEMENTARY MATERIAL

The Supplementary Material for this article can be found online at: https://www.frontiersin.org/articles/10.3389/fphar.2021.785981/full#supplementary-material

REFERENCES

Bai, Y., Xiong, L., Zhu, M., Yang, Z., Zhao, J., and Tang, H. (2019). Co-Expression Network Analysis Identified KIF2C in Association with Progression and Prognosis in Lung Adenocarcinoma. *Cancer Biomark* 24 (3), 371–382. doi:10.3233/cbm-181512

Brisson, M., Kim, J. J., Canfell, K., Drolet, M., Gingras, G., Burger, E. A., et al. (2020). Impact of HPV Vaccination and Cervical Screening on Cervical Cancer Elimination: a Comparative Modelling Analysis in 78 Low-Income and Lower-Middle-Income Countries. *Lancet* 395 (10224), 575–590. doi:10.1016/s0140-6736(20)30068-4

Brown, S. D., Warren, R. L., Gibb, E. A., Martin, S. D., Spinelli, J. J., Nelson, B. H., et al. (2014). Neo-antigens Predicted by Tumor Genome Meta-Analysis Correlate with Increased Patient Survival. *Genome Res.* 24 (5), 743–750. doi:10.1101/gr.165985.113

Cerami, E., Gao, J., Dogrusoz, U., Gross, B. E., Sumer, S. O., Aksoy, B. A., et al. (2012). The cBio Cancer Genomics portal: an Open Platform for Exploring Multidimensional Cancer Genomics Data. *Cancer Discov.* 2 (5), 401–404. doi:10.1158/2159-8290.Cd-12-0095

Chen, F., Chandrashekar, D. S., Varambally, S., and Creighton, C. J. (2019). Pan-Cancer Molecular Subtypes Revealed by Mass-Spectrometry-Based Proteomic Characterization of More Than 500 Human Cancers. *Nat. Commun.* 10 (1), 5679. doi:10.1038/s41467-019-13528-0

Cohen, P. A., Jhingran, A., Oaknin, A., and Denny, L. (2019). Cervical Cancer. *Lancet* 393 (10167), 169–182. doi:10.1016/s0140-6736(18)32470-x

Das, M. (2021). WHO Launches Strategy to Accelerate Elimination of Cervical Cancer. *Lancet Oncol.* 22 (1), 20–21. doi:10.1016/s1470-2045(20)30729-4

DeLuca, J. G., Gall, W. E., Ciferri, C., Cimini, D., Musacchio, A., and Salmon, E. D. (2006). Kinetochore Microtubule Dynamics and Attachment Stability Are Regulated by Hec1. *Cell* 127 (5), 969–982. doi:10.1016/j.cell.2006.09.047

Fan, T., Lu, Z., Liu, Y., Wang, L., Tian, H., Zheng, Y., et al. (2021). A Novel Immune-Related Seventeen-Gene Signature for Predicting Early Stage Lung Squamous Cell Carcinoma Prognosis. *Front. Immunol.* 12, 665407. doi:10.3389/fimmu.2021.665407

Gan, H., Lin, L., Hu, N., Yang, Y., Gao, Y., Pei, Y., et al. (2019). KIF2C Exerts an Oncogenic Role in Nonsmall Cell Lung Cancer and Is Negatively Regulated by miR-325-3p. *Cell Biochem. Funct.* 37 (6), 424–431. doi:10.1002/cbf.3420

Ganguly, A., Bhattacharya, R., and Cabral, F. (2008). Cell Cycle Dependent Degradation of MCAK: Evidence against a Role in Anaphase Chromosome Movement. *Cell Cycle* 7 (20), 3187–3193. doi:10.4161/cc.7.20.6814

Gao, J., Aksoy, B. A., Dogrusoz, U., Dresdner, G., Gross, B., Sumer, S. O., et al. (2013). Integrative Analysis of Complex Cancer Genomics and Clinical Profiles Using the cBioPortal. *Sci. Signal.* 6 (269), pl1. doi:10.1126/scisignal.2004088

Hedrick, D. G., Stout, J. R., and Walczak, C. E. (2008). Effects of Anti-microtubule Agents on Microtubule Organization in Cells Lacking the Kinesin-13 MCAK. *Cell Cycle* 7 (14), 2146–2156. doi:10.4161/cc.7.14.6239

Huang, S. M., Mishina, Y. M., Liu, S., Cheung, A., Stegmeier, F., Michaud, G. A., et al. (2009). Tankyrase Inhibition Stabilizes Axin and Antagonizes Wnt Signalling. *Nature* 461 (7264), 614–620. doi:10.1038/nature08356

Kasteri, J., Das, D., Zhong, X., Persaud, L., Francis, A., Muharam, H., et al. (2018). Translation Control by P53. *Cancers (Basel)* 10 (5), 133. doi:10.3390/cancers10050133

Kong, L., Hao, Q., Wang, Y., Zhou, P., Zou, B., and Zhang, Y. X. (2015). Regulation of P53 Expression and Apoptosis by Vault RNA2-1-5p in Cervical Cancer Cells. *Oncotarget* 6 (29), 28371–28388. doi:10.18632/oncotarget.4948

Ladds, M. J. G. W., and Laín, S. (2019). Small Molecule Activators of the P53 Response. *J. Mol. Cel. Biol.* 11 (3), 245–254. doi:10.1093/jmcb/mjz006

Levine, A. J. (2020). p53: 800 Million Years of Evolution and 40 Years of Discovery. *Nat. Rev. Cancer* 20 (8), 471–480. doi:10.1038/s41568-020-0262-1

Li, T., Fu, J., Zeng, Z., Cohen, D., Li, J., Chen, Q., et al. (2020a). TIMER2.0 for Analysis of Tumor-Infiltrating Immune Cells. *Nucleic Acids Res.* 48, W509–W514. doi:10.1093/nar/gkaa407

Li, T. F., Zeng, H. J., Shan, Z., Ye, R. Y., Cheang, T. Y., Zhang, Y. J., et al. (2020b). Overexpression of Kinesin Superfamily Members as Prognostic Biomarkers of Breast Cancer. *Cancer Cel Int* 20, 123. doi:10.1186/s12935-020-01191-1

Miedl, H., Dietrich, B., Kaserer, K., and Schreiber, M. (2020). The 40bp Indel Polymorphism Rs150550023 in the MDM2 Promoter Is Associated with Intriguing Shifts in Gene Expression in the P53-MDM2 Regulatory Hub. *Cancers (Basel)* 12 (11), 3363. doi:10.3390/cancers12113363

Mizuno, H., Kitada, K., Nakai, K., and Sarai, A. (2009). PrognoScan: a New Database for Meta-Analysis of the Prognostic Value of Genes. *BMC Med. Genomics* 2, 18. doi:10.1186/1755-8794-2-18

Nakamura, Y., Tanaka, F., Haraguchi, N., Mimori, K., Matsumoto, T., Inoue, H., et al. (2007). Clinicopathological and Biological Significance of Mitotic Centromere-Associated Kinesin Overexpression in Human Gastric Cancer. *Br. J. Cancer* 97 (4), 543–549. doi:10.1038/sj.bjc.6603905

Ritter, A., Kreis, N. N., Louwen, F., Wordeman, L., and Yuan, J. (2015). Molecular Insight into the Regulation and Function of MCAK. *Crit. Rev. Biochem. Mol. Biol.* 51 (4), 228–245. doi:10.1080/10409238.2016.1178705

Shimo, A., Tanikawa, C., Nishidate, T., Lin, M. L., Matsuda, K., Park, J. H., et al. (2008). Involvement of Kinesin Family Member 2C/mitotic Centromere-Associated Kinesin Overexpression in Mammary Carcinogenesis. *Cancer Sci.* 99 (1), 62–70. doi:10.1111/j.1349-7006.2007.00635.x

Miller, K. D., Ortiz, A. P., Pinheiro, P. S., Bandi, P., Minihan, A., Fuchs, H. E., et al. (2021). Cancer Statistics for the US Hispanic/Latino Population, 2021. *CA Cancer J. Clin.* 71 (1), 466–487. doi:10.3322/caac.21695

Soumaoro, L. T., Uetake, H., Higuchi, T., Takagi, Y., Enomoto, M., and Sugihara, K. (2004). Cyclooxygenase-2 Expression: a Significant Prognostic Indicator for Patients with Colorectal Cancer. *Clin. Cancer Res.* 10 (24), 8465–8471. doi:10.1158/1078-0432.Ccr-04-0653

Tang, Z., Li, C., Kang, B., Gao, G., Li, C., and Zhang, Z. (2017). GEPIA: a Web Server for Cancer and normal Gene Expression Profiling and Interactive Analyses. *Nucleic Acids Res.* 45, W98–W102. doi:10.1093/nar/gkx247

Uhlén, M., Fagerberg, L., Hallström, B., Lindskog, C., Oksvold, P., Mardinoglu, A., et al. (2015). Proteomics. Tissue-Based Map of the Human Proteome. *Science (New York, N.Y.)* 347 (6220), 1260419. doi:10.1126/science.1260419

Vasaikar, S. V., Straub, P., Wang, J., and Zhang, B. (2018). LinkedOmics: Analyzing Multi-Omics Data within and across 32 Cancer Types. *Nucleic Acids Res.* 46, D956–D963. doi:10.1093/nar/gkx1090

Wang, X., Simpson, E. R., and Brown, K. A. (2015). p53: Protection against Tumor Growth beyond Effects on Cell Cycle and Apoptosis. *Cancer Res.* 75 (23), 5001–5007. doi:10.1158/0008-5472.Can-15-0563

Wei, S., Dai, M., Zhang, C., Teng, K., Wang, F., Li, H., et al. (2020). KIF2C: a Novel Link between Wnt/β-Catenin and mTORC1 Signaling in the Pathogenesis of Hepatocellular Carcinoma. *Protein Cell* 12, 788–809. doi:10.1007/s13238-020-00766-y

Yang, C., Li, Q., Chen, X., Zhang, Z., Mou, Z., Ye, F., et al. (2020). Circular RNA circRGNEF Promotes Bladder Cancer Progression via miR-548/KIF2C axis Regulation. *Aging (Albany NY)* 12 (8), 6865–6879. doi:10.18632/aging.103047

Zhao, F., and Qiao, Y. (2019). Cervical Cancer Prevention in China: a Key to Cancer Control. *Lancet* 393 (10175), 969–970. doi:10.1016/s0140-6736(18)32849-6

Zhao, Z., Zhou, S., Li, W., Zhong, F., Zhang, H., Sheng, L., et al. (2019). AIB1 Predicts Tumor Response To Definitive Chemoradiotherapy And Prognosis In Cervical Squamous Cell Carcinoma. *J. Cancer* 10 (21), 5212–5222. doi:10.7150/jca.31697

Zhou, M. J., Chen, F. Z., Chen, H. C., Wan, X. X., Zhou, X., Fang, Q., et al. (2017). ISG15 Inhibits Cancer Cell Growth and Promotes Apoptosis. *Int. J. Mol. Med.* 39 (2), 446–452. doi:10.3892/ijmm.2016.2845

Zhu, L., Zhang, X., and Sun, Z. (2020). SNRPB Promotes Cervical Cancer Progression through Repressing P53 Expression. *Biomed. Pharmacother.* 125, 109948. doi:10.1016/j.biopha.2020.109948

Conflict of Interest: The authors declare that the research was conducted in the absence of any commercial or financial relationships that could be construed as a potential conflict of interest.

Publisher's Note: All claims expressed in this article are solely those of the authors and do not necessarily represent those of their affiliated organizations, or those of the publisher, the editors and the reviewers. Any product that may be evaluated in this article, or claim that may be made by its manufacturer, is not guaranteed or endorsed by the publisher.

frontiers | Frontiers in Pharmacology

ORIGINAL RESEARCH
published: 16 May 2022
doi: 10.3389/fphar.2022.806682

Hypoxia-Induced Upregulation of lncRNA ELFN1-AS1 Promotes Colon Cancer Growth and Metastasis Through Targeting TRIM14 *via* Sponging miR-191-5p

Xu Jing[1], *Lutao Du*[1], *Shuang Shi*[1], *Aijun Niu*[1], *Jing Wu*[2], *Yunshan Wang*[1] *and Chuanxin Wang*[1]*

[1]Department of Clinical Laboratory, The Second Hospital of Shandong University, Jinan, China, [2]Department of Pharmacy, The Second Hospital of Shandong University, Jinan, China

OPEN ACCESS

Edited by:
Ning Wang,
The University of Hong Kong, Hong Kong SAR, China

Reviewed by:
Tianxiang Chen,
First Affiliated Hospital of Xi'an Jiaotong University, China
Davide Barbagallo,
University of Catania, Italy

***Correspondence:**
Chuanxin Wang
cxwang@sdu.edu.cn

Specialty section:
This article was submitted to Experimental Pharmacology and Drug Discovery, a section of the journal Frontiers in Pharmacology

Received: 01 November 2021
Accepted: 14 April 2022
Published: 16 May 2022

Citation:
Jing X, Du L, Shi S, Niu A, Wu J, Wang Y and Wang C (2022) Hypoxia-Induced Upregulation of lncRNA ELFN1-AS1 Promotes Colon Cancer Growth and Metastasis Through Targeting TRIM14 via Sponging miR-191-5p. Front. Pharmacol. 13:806682. doi: 10.3389/fphar.2022.806682

Hypoxia is identified as one of the microenvironmental features of most solid tumors and is involved in tumor progression. In the present research, we demonstrate that lncRNA extracellular leucine rich repeat and fibronectin type III domain-containing 1-antisense RNA 1 (ELFN1-AS1) is upregulated by hypoxia in colon cancer cells. Knockdown of ELFN1-AS1 in hypoxic colon cancer cells can reduce cell proliferation and restore the invasion to non-hypoxic levels. Fluorescence in situ hybridization results show that ELFN1-AS1 is distributed in the cytoplasm of colon cancer cells, so we further analyze the potential targets for ELFN1-AS1 as a competing endogenous RNA (ceRNA). MiR-191-5p contains a binding sequence with ELFN1-AS1 and is downregulated by ELFN1-AS1 in colon cancer cells. Then, there is a binding site between miR-191-5p and the 3′ untranslated region of tripartite motif TRIM 14 (TRIM14). The expression of TRIM14 is inhibited by ELFN1-AS1 siRNA or miR-191-5p mimics in LoVo and HT29 cells. The treatment of the miR-191-5p inhibitor in ELFN1-AS1 knockdown cells can significantly increase cell proliferation and invasion ability. Overexpression of TRIM14 in miR-191-5p-mimic-treated cells can rescue the inhibition of proliferation and invasion caused by miR-191-5p mimics. In conclusion, ELFN1-AS1 operates as a downstream target of hypoxia, promotes proliferation and invasion, and inhibits apoptosis through upregulating TRIM14 by sponging miR-191-5p in the colon cancer cells. Our results enrich our understanding of colon cancer progression and provide potential targets for clinical treatment of colon cancer.

Keywords: ELFN1-AS1, hypoxia, TRIM14, colon cancer, miR-191-5p

INTRODUCTION

Colon cancer is one of the most common malignant tumors in the digestive system, accounting for the third death rate of cancer patients (Siegel et al., 2013). At present, surgery combined with postoperative adjuvant chemotherapy and targeted therapies are mainly used for the treatment of colon cancer, but the therapeutic effect is not satisfactory (Dienstmann et al., 2015). Therefore, it is of great significance to identify and develop new therapeutic targets for colon cancer. Hypoxia is identified as one of the microenvironmental features of most solid tumors (Jing et al., 2019).

Moderate hypoxia may be the initiating factor for genetic instability, malignant transformation, and even metastasis of tumor cells (Manoochehri Khoshinani et al., 2016; Jing et al., 2019). Cells that are not sensitive to apoptosis under hypoxic environments are more invasive and resistant to radiotherapy and chemotherapy. Numerous studies have shown that HIF1α plays a central role in the process of tumor adaptation to hypoxia (Manoochehri Khoshinani et al., 2016). However, its mechanism has not been clarified.

In the present research, we found that lncRNA extracellular leucine rich repeat and fibronectin type III domain-containing 1-antisense RNA 1 (ELFN1-AS1) was upregulated by hypoxia in colon cancer cells. In 2014, ELFN1-AS1 was reported for the first time to be generally highly expressed in tumors but low in normal tissues (Polev et al., 2014). Subsequently, through screening for the key lncRNAs in early-stage colon adenocarcinoma (COAD), Liu et al. found that ELFN1-AS1 was associated with early-stage COAD with a potential diagnostic value (Liu et al., 2018). Furthermore, extracellular vesicles (EVs) from human umbilical cord mesenchymal stem cells (hUCMSCs) transfected with ELFN1-AS1-siRNA could inhibit the progression of COAD (Dong et al., 2019). In the latest research, the high expression of ELFN1-AS1 was found to predict poor prognosis in colon cancer through survival analysis based on The Cancer Genome Atlas (TCGA) database (Chen et al., 2020). However, the specific role and mechanism of ELFN1-AS1 in colon cancer remain unclear. In our research, we clarified that hypoxia promoted the growth and metastasis of tumor cells by upregulating the ELFN1-AS1/miR-191-5p/tripartite motif 14 (TRIM14) axis, providing potential targets for the clinical treatment of colon cancer.

MATERIALS AND METHOD

Tissue Samples

A total of 32 cases of colon cancer tissues and 32 paired control tissues from patients with colon cancer were collected from the second hospital of Shandong University. The samples were snap-frozen in liquid nitrogen and stored at −80 °C until further analysis. All patients signed informed consents.

Cell Culture

The human colon cancer cell lines HCT116, SW480, LoVo, and HT29 were maintained in our laboratory. Dulbecco's modified Eagle's medium with 0.1 mg/ml streptomycin, 100 U/ml penicillin, and 10% fetal bovine serum (Thermo Fisher Scientific, Shanghai, China) were used for cell culture. The hypoxia model was constructed with 5% CO_2 and 95% N_2. Cells in the logarithmic phase were transfected using lipofectamine 2000 (Invitrogen, Carlsbad, CA, United States). ELFN1-AS1 (Transcript: ENST00000415399.1) siRNAs, miR-191-5p mimics, TRIM14 overexpressed plasmids, and scramble sequences were all purchased from RiboBio (Guangzhou, China). The sequences involved in this study are shown as follows: ELFN1-AS1 siRNA, 5′-CCTTTAATCTCTTGCTCAA-3′; control siRNA, 5′-TTCTCCGAACGTGTCACGT-3′; inhibitor control, 5′-GGUUCGUACGUACACUGUUCA-3′; mimic control, 5′-CGGUACGAUCGCGGCGGGAUAUC-3′. 50 nM siRNA was used for transfection. Control siRNA, the inhibitor control, the mimic control, and empty plasmid pcDNA3.1 were used as the scramble for ELFN1-AS1 siRNA, the miR-191-5p inhibitor, miR-191-5p mimics, and TRIM14 overexpressed plasmids, respectively.

Quantitative Reverse Transcription Polymerase Chain Reaction

Total RNA was extracted from LoVo and HT29 cells after the transfection for 24 h using TriQuick Reagent (Solarbio Science and Technology Company, Beijing, China). The cDNA was synthesized using a HiFiScript cDNA Synthesis Kit (CwBio, Beijing, China), and then quantitative reverse transcription polymerase chain reaction (qRT-PCR) was performed using a Fluorescence quantitative PCR kit UltraSYBR Mixture (CwBio, Beijing, China). The primers used in this research were synthesized in GENEWIZ (Suzhou, China). The following primers were used in this research: ELFN1-AS1-F, 5′-GCG CCTCAGCCACAATCGTAATC-3′; ELFN1-AS1-R, 5′-GGG GGCATGCACCAGAGGACT-3′; TRIM14-F, 5′-TATTGCTGA AATACGCGCGC-3′; TRIM14-R, 5′-GTCAACCTCCCAGTA GTGGC-3′; Actin-F, 5′-CCCGAGCCGTGTTTCCT-3′; Actin-R, 5′-GTCCCAGTTGGTGACGATGC-3′. The miRNA Purification Kit (CwBio, Beijing, China), miRNA cDNA Synthesis Kit (CwBio, Beijing, China), and miRNA qPCR Assay Kit (CwBio, Beijing, China) were used for miRNA extraction and detection. The expression of target genes was analyzed using the $2^{-\Delta\Delta CT}$ method. A qRT-PCR instrument (Funglyn Biotech, Toronto, Canada) was used for the detection. Actin was used as an internal control.

Western Blot

The protein levels of genes were detected using western blot analysis. After the transfection for 48 h, the protein was extracted using RIPA buffer and separated on 10% sodium dodecyl sulfate–polyacrylamide gel electrolysis gel. Then, the protein was transferred into a PVDF membrane. After 1 h of the block with 5% non-fat milk, the membrane was incubated with primary antibodies at 4°C overnight and subsequently secondary antibodies at room temperature for 1 h. The primary antibodies anti-HIF1α (20960-1-AP) and anti-TRIM14 (15742-1-AP) were purchased from ProteinTech Group (Chicago, IL, United States). Protein bands were developed using an ECL kit (Solarbio Science and Technology Company, Beijing, China).

Fluorescence *in situ* Hybridization

The distribution of ELFN1-AS1 in HT29 cells was detected by FISH using a Fluorescent *In Situ* Hybridization Kit (RiboBio, Guangzhou, China) following the manufacturer's manual. The probes of ELFN1-AS1 were designed and synthesized by RiboBio (Guangzhou, China). The fluorescence was observed by using a fluorescence microscope (OLYMPUS, Tokyo, Japan).

Cell Viability and Proliferation Assays

CCK8 assay was performed to detect cell viability. After transfection, cells were seeded into a 96-well plate at the concentration of 1000 cells/well. Cells were incubated with 10 μl of CCK8 reagent (Solarbio Science and Technology Ltd., Beijing, China) at 37°C for 1.5 h. Cell viability was measured every 24 h. The OD value was detected at 450 nm.

The proliferation of LoVo and HT29 cells was further determined by colony formation assay. After transfection, 500 cells were seeded in a 6-well plate and incubated at 37°C for 14 days. After fixing with 4% paraformaldehyde, cells were stained with GIMSA for 20 min. The photo of plates was taken, and the colony number of each group was counted in five random fields.

Cell Invasion Assay

The invasive ability of cells was detected using a transwell assay. 100 μl of melted matrigel (Solarbio Science and Technology Ltd., Beijing, China) was added into the upper chamber of the transwell chamber (Invitrogen, Carlsbad, CA, United States) and incubated at 37°C for 4 h. 500 μl of the serum-free medium was added into the lower chamber. Then, 100 μl of the transfected cell suspension (1×10^5 cells, serum-free medium) was added into the upper chamber. After incubation for 24 h, the invasive cells were fixed with 4% paraformaldehyde for 30 min and stained with 0.1% crystal violet for 20 min Five fields of each group were randomly selected and photographed at × 100 magnification. The invasive cells were counted by two independent researchers.

Cell Apoptosis Analysis With a Flow Cytometer

After 24 h of transfection, cells were resuspended with the binding buffer at a density of 1–5 × 10^6 cells/ml. 100 μl of the cell suspension was added into a 5 ml flow tube. 5 μl of Annexin V/FITC (4ABio, Beijing, China) was added into the flow tube, which was subsequently incubated at room temperature for 5 min 10 μl of PI solution was added for detection. Flowjo software was used to analyze the flow results.

Bioinformatics Analysis

The expression and prognosis value of ELFN1-AS1 were obtained through an online TCGA database, GEPIA (http://gepia.cancer-pku.cn/index.html). The differential analysis here is based on 275 colon adenocarcinoma (COAD) and 349 normal tissues. The method for differential analysis is one-way ANOVA. Overall survival analysis was performed using the Log-rank test, a.k.a the Mantel–Cox test, for the hypothesis test.

The sequences of the hypoxic response element (HRE) on the ELFN1-AS1 promoter were predicted on PROMO (http://alggen.lsi.upc.es/cgi-bin/promo_v3/promo/promoinit.cgi?dirDB=TF_8.3). The potential downstream targets of ELFN1-AS1 and miR-191-5p were predicted using Diana tools (DIANA-LncBase v3, https://diana.e-ce.uth.gr/lncbasev3/interactions).

Luciferase Reporter Assay

The binding status of HRE on the ELFN1-AS1 promoter under hypoxia conditions was detected using a luciferase reporter assay. The sequence containing the wild-type (WT)/mutant-type (MUT) HRE on the ELFN1-AS1 promoter was cloned into the reporter vector (Youbio, Hunan, China). Then, the plasmids carrying WT/MUT HRE were transfected into LoVo and HT29 cells. The luciferase activity was measured using a dual-luciferase assay system (MedChemExpress, Monmouth Junction, United States).

To analyze the interaction between miR-191-5p and ELFN1-AS1 or TRIM14, the wild-type (WT)/mutant-type (MUT) ELFN1-AS1 and WT/MUT TRIM14 3′ untranslated region (UTR) were cloned into the reporter vector (Youbio, Hunan, China), respectively. LoVo cells were co-transfected with miR-191-5p mimics and either of the above vectors. The luciferase activity was measured using a dual-luciferase assay system (MedChemExpress, Monmouth Junction, United States). A microplate reader (TECAN, Grodig, Austria) was used for fluorescence detection.

Statistical Analysis

SPSS 18.0 statistical analysis software was used to analyze the results. All data were expressed as mean ± standard deviation (SD). A *t*-test was used for comparison between the two groups, and one-way ANOVA was used for the comparison between the multiple groups with Bonferroni as a post hoc test. A paired *t*-test was used to compare 32 pairs of clinical tissues. Pearson correlation analysis was used to analyze the correlation between groups. $p < 0.05$ was statistically significant.

RESULTS

ELFN1-AS1 is Highly Expressed in Colon Cancer Tissues and Cells

First, the expression and prognosis value of ELFN1-AS1 were obtained through a TCGA database, GEPIA (Tang et al., 2017). As shown in **Figure 1A**, ELFN1-AS1 was markedly upregulated in COAD tissues ($n = 275$) compared with the normal tissues ($n = 349$) ($p < 0.01$). The prognosis of COAD patients with low ELFN1-AS1 levels was better than that of high-ELFN1-AS1 patients ($p = 0.0085$, **Figure 1B**). A total of 32 pairs of clinical tissues of colon cancer were collected from the local hospital, and the ELFN1-AS1 level was detected using qRT-PCR. Our results showed that ELFN1-AS1 was significantly upregulated in colon cancer tissues compared with para-cancerous tissues ($p < 0.001$, **Figure 1C**). Then, the ELFN1-AS1 level was detected in four human colon cancer cell lines, HCT116, SW480, HT29, and LoVo. As shown in **Figure 1D**, the two cell lines with high ELFN1-AS1 levels (HT29 and LoVo) were used for subsequent experiments. Next, the distribution of ELFN1-AS1 in HT29 cells was analyzed by FISH assay. As shown in **Figure 1E**, ELFN1-AS1 was expressed in both the cytoplasm and nucleus, suggesting that ELFN1-AS1 has the potential to function as a competing endogenous RNA (ceRNA) in colon cancer cells.

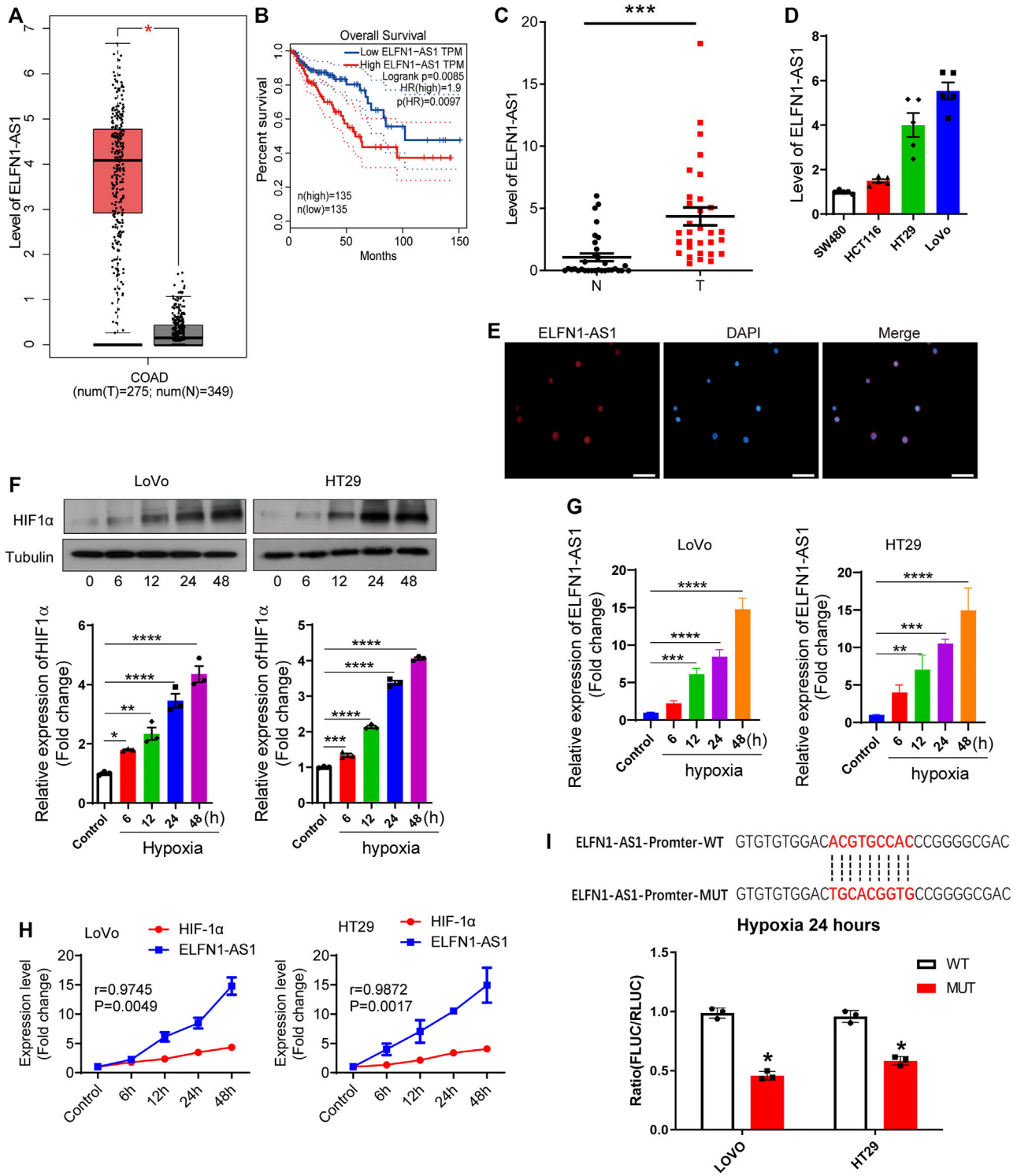

FIGURE 1 | Hypoxia induces overexpression of ELFN1-AS1 in colon cancer. **(A)** Expression level of ELFN1-AS1 in colon adenocarcinoma (COAD) was analyzed on the TCGA database (GEPIA). Compared with the normal tissues ($n = 349$), ELFN1-AS1 was markedly upregulated in COAD tissues ($n = 275$) ($p < 0.01$). The method for differential analysis is one-way ANOVA. **(B)** Prognosis value of ELFN1-AS1 in COAD was analyzed on the TCGA database (GEPIA). The COAD tissues were divided into two groups (low ELFN1-AS1 and high ELFN1-AS1 groups) at a 50% cutoff. Overall survival analysis was performed using the Log-rank test, a.k.a the Mantel–Cox test, for the hypothesis test. **(C)** qRT-PCR was performed to detect the expression of ELFN1-AS1 in 32 pairs of clinical tissues of colon cancer collected from local hospitals. Actin was used as an internal control. A paired *t*-test was used to compare 32 pairs of clinical tissues. **(D)** qRT-PCR was used to determine the ELFN1-AS1 level in four human colon cancer cell lines, HCT116, SW480, HT29, and LoVo. **(E)** Expression and distribution of ELFN1-AS1 in HT29 cells were analyzed by FISH. The

(*Continued*)

FIGURE 1 | red fluorescence and blue fluorescence represent ELFN1-AS1 and the nucleus, respectively. Scale bar 10 μm. **(F)** After 0, 6, 12, 24, and 48 h of hypoxia, the expression of HIF1α was detected using western blot. **(G)** After 0, 6, 12, 24, and 48 h of hypoxia, the expression of ELFN1-AS1 was detected using RT-PCR in LoVo and HT29 cells. **(H)** Correlation between ELFN1-AS1 and HIF-1α was analyzed using Pearson correlation analysis. **(I)** Binding status of HRE on the ELFN1-AS1 promoter under hypoxia conditions was detected using a dual luciferase reporter assay. One-way ANOVA was used for the comparison between the multiple groups with Bonferroni as a post hoc test. All data were representative of three independent experiments. *$p < 0.05$; ***$p < 0.001$; ****$p < 0.0001$.

Hypoxia Upregulates ELFN1-AS1 in Colon Cancer Cells

Subsequently, we investigated the relationship between hypoxia and ELFN1-AS1 expression. LoVo and HT29 cells were incubated at 37°C with 5% CO_2 and 95% N_2 to construct a hypoxia cell model. As shown in **Figure 1F,** HIF1α expression gradually increased in a time-dependent manner in both LoVo and HT29 cells. Then, the expression of ELFN1-AS1 in LoVo and HT29 cells was detected after 24 h of hypoxia using qRT-PCR. As shown in **Figure 1G**, ELFN1-AS1 was significantly upregulated in LoVo and HT29 cells under hypoxia compared with that in routine culture in a time-dependent manner ($p < 0.001$). In addition, Pearson correlation analysis showed that there was a significant positive correlation between the expressions of HIF1α and ELFN1-AS1 in hypoxic LoVo and HT29 cells (**Figure 1H**). The binding status of HRE on the ELFN1-AS1 promoter under hypoxia conditions was detected using a dual luciferase reporter assay. The sequences of HRE on the ELFN1-AS1 promoter were predicted on PROMO (http://alggen.lsi.upc.es/cgi-bin/promo_v3/promo/promoinit.cgi?dirDB=TF_8.3). Plasmids carrying wild and mutant elements were transfected into colon cancer cells. As shown in **Figure 1I**, after 24 h of hypoxia, the fluorescence ratio of the MUT group was significantly lower than that of the WT group, suggesting that hypoxia promoted ELFN1-AS1 transcription through HRE. These results indicated that ELFN1-AS1 might be a downstream target of hypoxia response in colon cancer cells.

ELFN1-AS1 is a Downstream Target of Hypoxia Response in Colon Cancer Cells

According to our results, hypoxia induced the expression of ELFN1-AS1 in LoVo and HT29 cells, suggesting that ELFN1-AS1 may be a downstream factor of hypoxia response. To verify this hypothesis, LoVo and HT29 cells transfected with ELFN1-AS1 siRNA or negative siRNA were incubated under hypoxic conditions (5% CO_2 and 95% N_2) to generate the hypoxia + scramble and hypoxia + siELFN1-AS1 groups, respectively. As shown in **Figure 2A**, siRNA could significantly inhibit the expression of ELFN1-AS1 in both LoVo and HT29 cells compared with the scramble group. Compared with the scramble cells, the cell viability of the hypoxia group was enhanced significantly in both LoVo and HT29 cells. Interestingly, the OD value of LoVo and HT29 cells declined significantly after the transfection of ELFN1-AS1 siRNA under hypoxic conditions (**Figures 2B,C**). The result of the colony formation assay was consistent with CCK8's results. Knockdown of ELFN1-AS1 significantly decreased the colony number in LoVo cells; the colony numbers of LoVo and HT29 cells cultured under hypoxic conditions declined after the transfection of ELFN1-AS1 siRNA (**Figures 2D–F**). In addition, the invasive cell number of LoVo and HT29 cells transfected with ELFN1-AS1 siRNA decreased significantly compared with that of control siRNA; hypoxia increased the invasive cell number, while knockdown of ELFN1-AS1 decreased the invasive cell number to a normal level in LoVo and HT29 cells (**Figures 2G,H**). These results proved that knockdown of ELFN1-AS1 blocked the proliferation and invasion induced by hypoxia in colon cancer cells.

Knockdown of ELFN1-AS1 Induces the Apoptosis in Hypoxic Colon Cancer Cells

Next, the apoptosis of LoVo and HT29 cells was detected using flow cytometry analysis. As shown in **Figure 3**, the percentage of apoptotic cells significantly increased after the transfection of ELFN1-AS1 siRNA in LoVo cells; in HT29 cells, ELFN1-AS1 siRNA also increased the percentage of apoptotic cells compared with the control siRNA. Our data indicated that knockdown of ELFN1-AS1 induced the apoptosis in colon cancer cells.

We further analyzed the apoptosis of LoVo and HT29 cells cultured under hypoxic conditions. As shown in **Figure 3**, after 24 h of hypoxia culturing, the apoptosis of LoVo and HT29 cells was significantly inhibited. However, knockdown of ELFN1-AS1 raised the percentage of apoptotic cells to a normal level in both hypoxic LoVo and HT29 cells. These results proved that ELFN1-AS1 knockdown rescued hypoxia-induced inhibition of apoptosis in colon cancer cells.

ELFN1-AS1 Promotes the Expression of TRIM14 Through Sponging miR-191-5p

ELFN1-AS1 is abundantly distributed in the cytoplasm, suggesting that it may operate as a ceRNA to regulate the expression of downstream targets. Therefore, we predicted the potential downstream targets of ELFN1-AS1 using Diana tools (https://diana.e-ce.uth.gr/lncbasev3/interactions) (Paraskevopoulou et al., 2016). Analysis results showed that there were six miRNAs which contained potential binding sites of ELFN1-AS1, namely, miR-33a-5p, miR-151b, miR-16b-5p, miR-191-5p, miR-877-5p, and miR-28–5p (**Figure 4A**). Then, the expression levels of six potential miRNAs were detected using qRT-PCR in LoVo and HT29 cells. As shown in **Figure 4B**, after ELFN1-AS1 knockdown, the expression of five miRNAs increased significantly (miR-33a-5p, miR-151b, miR-191-5p, miR-877-5p, and miR-28-5p), of which miR-191-5p showed the most significant upward trend. Then, we analyzed the interaction between miR-191-5p and wild or mutant ELFN1-AS1 using the double luciferase reporter

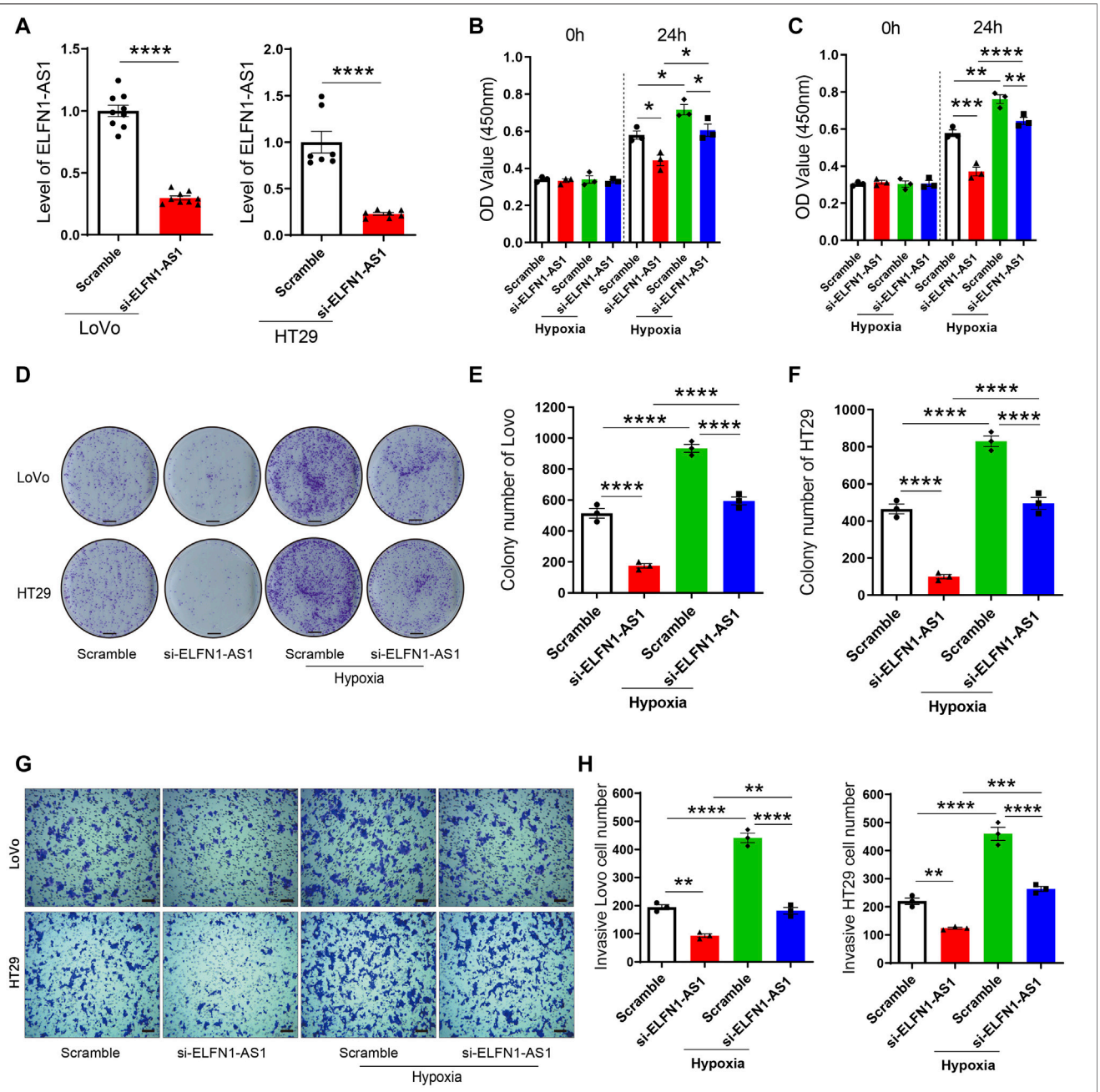

FIGURE 2 | ELFN1-AS1 rescues the proliferation and invasion induced by hypoxia in colon cancer cells. **(A)** ELFN1-AS1-specific siRNAs were transfected into LoVo and HT29 cells with the negative siRNA as a control (Scramble). The ELFN1-AS1 level was detected using qRT-PCR after the transfection for 24 h. A *t*-test was used for this comparison. **(B)** and **(C)** After transfection with ELFN1-AS1 siRNA and empty plasmids, LoVo and HT29 cells were cultured in 5% CO_2 and 95% N_2 to generate the hypoxia + scramble and hypoxia + siELFN1-AS1 groups. Cell viability was detected using CCK8 assay. **(D)** Proliferation of LoVo and HT29 cells was determined using a colony formation assay. The photo of the plates was taken after 14 days of incubation. **(E)** and **(F)** Colony number of each group was counted in five random fields. Scale bar 5 mm. **(G)** Transwell assay was performed to detect the invasion of each group. After 24 h of culture in matrigel chambers, cells were photographed under a microscope at ×100 magnification. Scale bar 100 μ. **(H)** Number of invasive cells was counted in three random fields. One-way ANOVA was used for the comparison between the multiple groups with Bonferroni as a post hoc test. All data were representative of three independent experiments. $^{*}p < 0.05$; $^{**}p < 0.01$; $^{***}p < 0.001$; $^{****}p < 0.0001$.

gene. As shown in **Figure 4C**, miR-191-5p could interact with ELFN1-AS1, which was weakened when the predicted binding site was mutated.

We subsequently analyzed the downstream targets of miR-191-5p. The results showed that there were five genes' 3 'UTR regions (FOXK1, TRIM14, SMC1A, RCC2, and GBP1) in

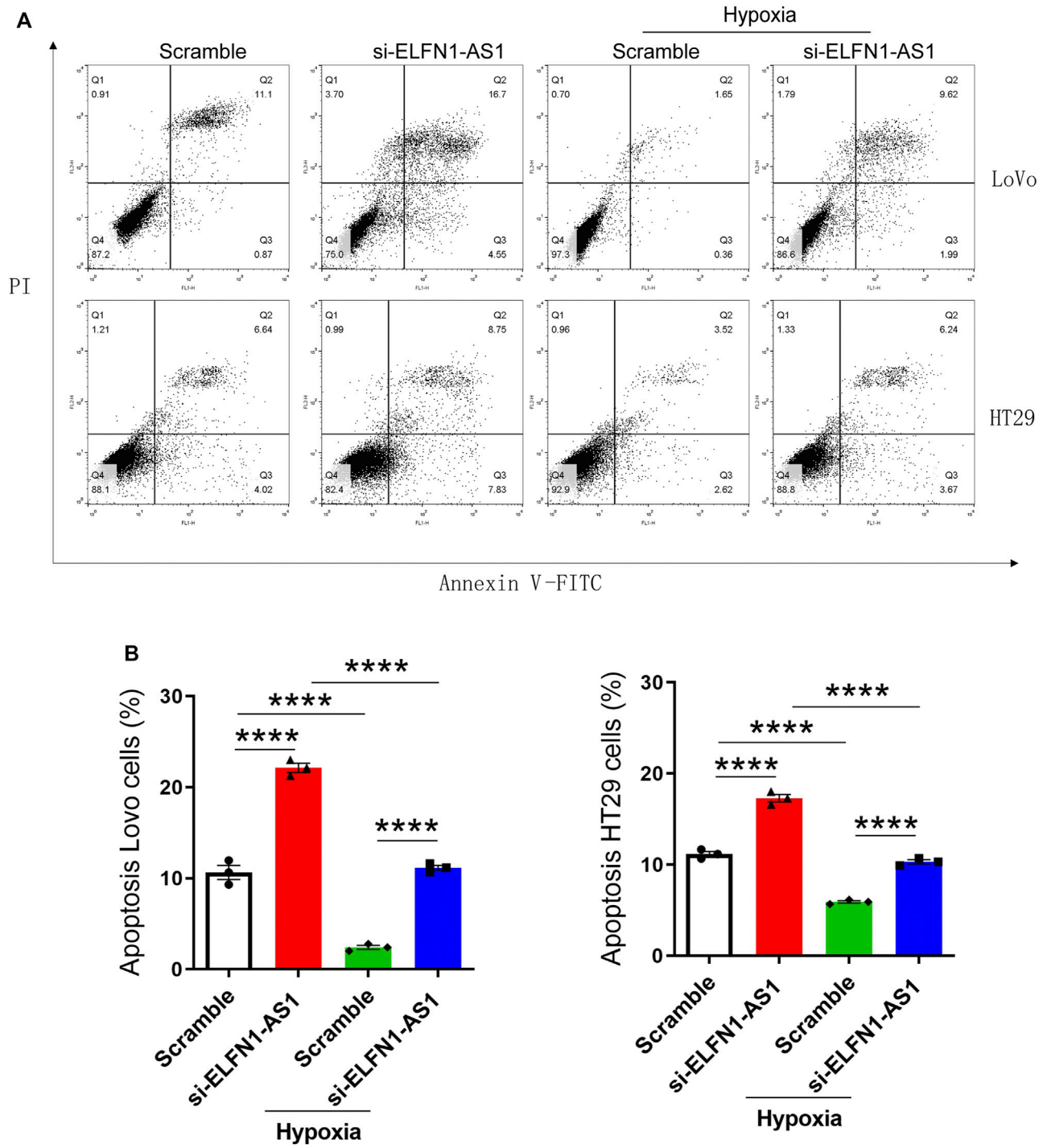

FIGURE 3 | ELFN1-AS1 blocks the inhibition of apoptosis induced by hypoxia in colon cancer cells. **(A)** Flow cytometry analysis was performed to detect the apoptosis in each group after the transfection for 24 h. **(B)** Percentage of apoptotic cells was analyzed using Flowjo software. Analysis was performed using one-way ANOVA with Bonferroni as a post hoc test. All data were representative of three independent experiments. ****$p < 0.0001$.

which there were binding sites of miR-191-5p (**Figure 4D**). The expression of FOXK1, TRIM14, SMC1A, and GBP1 declined significantly in LoVo and HT29 cells transfected with miR-191-5p mimics (**Figure 4E**). TRIM14 showed the most significant downward trend. The combination of miR-191-5p and TRIM14 was confirmed using double luciferase reporter gene analysis. As shown in **Figure 4F**, miR-191-5p could bind to wild-type TRIM14, while mutations at the

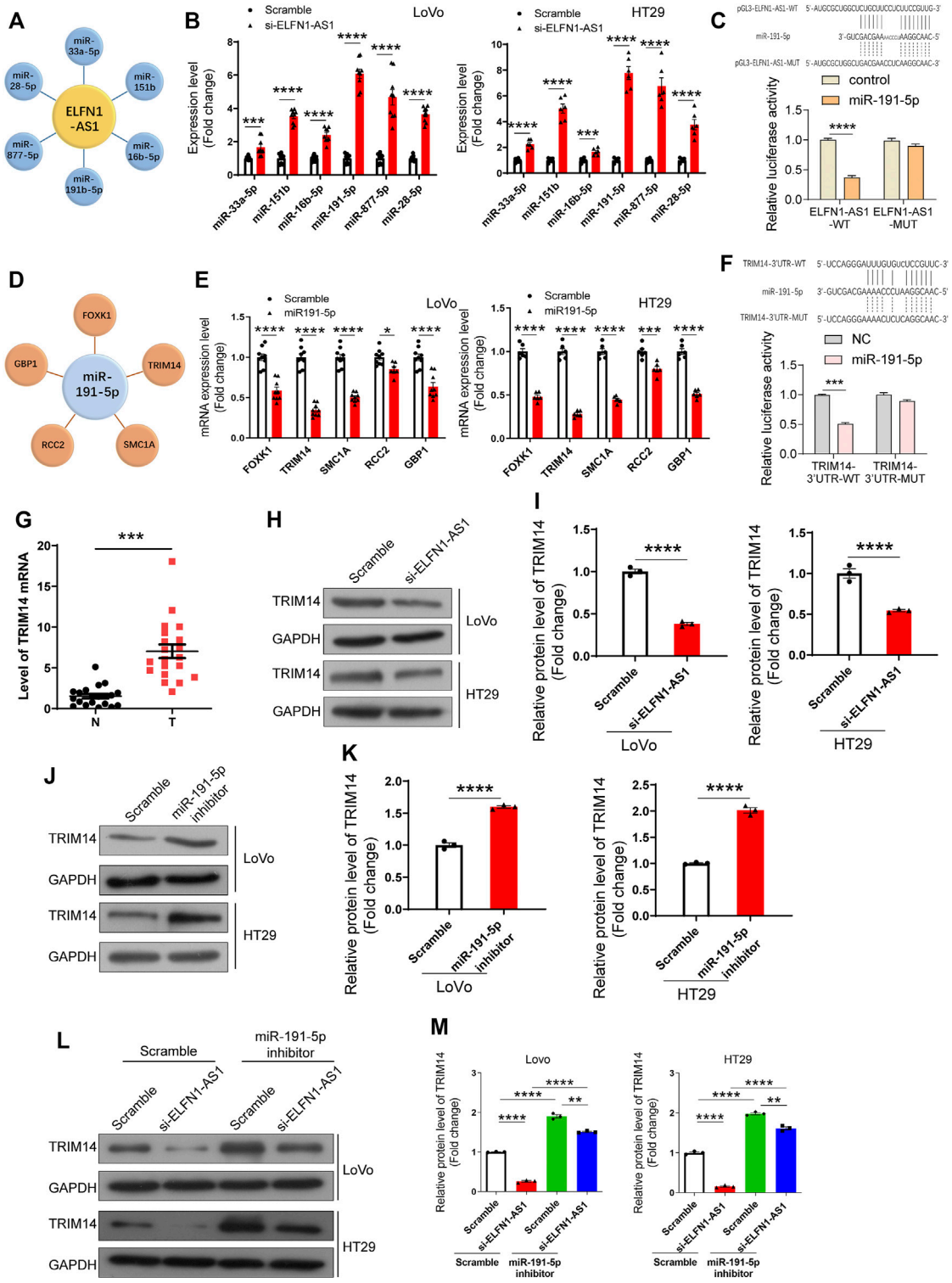

FIGURE 4 | Analysis and verification of ELFN1-AS1's downstream targets in colon cancer cells. **(A)** miRNAs with potential binding sites to ELFN1-AS1 were predicted in Diana tools (https://diana.e-ce.uth.gr/lncbasev3/interactions). **(B)** Six miRNAs (miR-33a-5p, miR-151b, miR-16b-5p, miR-191-5p, miR-877-5p, and miR-28-5p) were detected in ELFN1-AS1 knockdown cells using qRT-PCR. **(C)** Interaction between miR-191-5p and ELFN1-AS1 was detected using luciferase reporter assay. **(D)** Potential downstream targets of miR-191-5p were also analyzed in Diana tools. **(E)** Five genes (FOXK1, TRIM14, SMC1A, RCC2, and GBP1) were verified in HT29 cells transfected with miR-191-5p mimics. **(F)** Interaction between miR-191-5p and TRIM14 was detected using luciferase reporter assay. **(G)** mRNA level of TRIM14 was detected in 32 pairs of clinical tissues of colon cancer using RT-PCR. A paired *t*-test was used for data analysis. **(H)** and **(I)** Protein level of TRIM14

(*Continued*)

FIGURE 4 | was detected using western blot after the transfection of si-ELFN1-AS1. **(J)** and **(K)** Protein level of TRIM14 in miR-191-5p knockdown cells was detected using western blot. **(L)** and **(M)** Expression level of TRIM14 in ELFN1-AS1 and miR-191-5p knockdown cells was detected using western blot. A *t*-test was used for comparison between the two groups, and one-way ANOVA was used for the comparison between the multiple groups with Bonferroni as a post hoc test. All data were representative of three independent experiments. $^{**}p < 0.01$; $^{***}p < 0.001$; $^{****}p < 0.0001$.

predicted site in TRIM14 3′UTR significantly weaken this interaction. Importantly, the mRNA level of TRIM14 was significantly upregulated in 32 colon cancer tissues compared with para-cancerous tissues (**Figure 4G**).

These results suggested that ELFN1-AS1 upregulated the expression of TRIM14 by sponging miR-191-5p in colon cancer cells.

To verify our hypothesis, we further explored the effect of ELFN1-AS1 and miR-191-5p on TRIM14 expression. As shown in **Figures 4H,I**, the protein level of TRIM14 declined significantly in ELFN1-AS1 knocked-down LoVo and HT29 cells. After the treatment with the miR-191-5p inhibitor, the protein level of TRIM14 increased significantly (**Figures 4J,K**). The expression of TRIM14 in ELFN1-AS1 and miR-191-5p knockdown cells increased significantly compared with that of ELFN1-AS1 knockdown cells, while the expression of TRIM14 in ELFN1-AS1 and miR-191-5p knockdown cells increased significantly compared with that of miR-191-5p knockdown cells (**Figures 4L,M**).

TRIM14 rescues the inhibition of the proliferation and invasion induced by ELFN1-AS1 knockdown in colon cancer cells.

According to the above results, ELFN1-AS1 may promote the expression of TRIM14 by sponging miR-191-5p and finally involve in the regulation of tumor cell behavior. We performed rescue experiments to confirm this hypothesis. As shown in **Figure 5A**, the miR-191-5p inhibitor promoted cell viability in both LoVo and HT29 cells. After 24 h of simultaneous knockdown of ELFN1-AS1 and miR-191-5p, cell viability increased significantly compared with that of only ELFN1-AS1 knockdown cells (**Figure 5A**). As shown in **Figure 5B**, TRIM14 overexpression significantly increased the OD450 value; cell viability in TRIM14 overexpression plus miR-191-5p-mimic-treated cells increased significantly compared with that of miR-191-5p-mimic-treated cells. Compared with that of TRIM14 overexpression cells, cell viability declined significantly in TRIM14 overexpression plus miR-191-5p-mimic-treated cells.

miR-191-5p knockdown increased the proliferation. After the simultaneous knockdown of ELFN1-AS1 and miR-191-5p, the proliferation of LoVo and HT29 cells increased compared with that of only ELFN1-AS1 knockdown cells (**Figure 5C**). A similar trend was observed in the transwell assay. The invasive cell number in the knockdown of ELFN1-AS1 and miR-191-5p cells increased significantly compared with that of only ELFN1-AS1 knockdown cells and declined significantly compared with that of only miR-191-5p knockdown cells (**Figure 5D**).

TRIM14 overexpression inhibited the proliferation in miR-191-5p-mimic-treated cells (**Figure 5E**). The invasive cell number in TRIM14 overexpression plus treatment of miR-191-5p-mimic cells increased significantly compared with that of miR-191-5p-mimic-treated cells and declined significantly compared with that of TRIM14 overexpression cells (**Figure 5F**). These results showed that the treatment of the miR-191-5p inhibitor in ELFN1-AS1 knockdown cells can significantly increase cell proliferation and invasion ability, and overexpression of TRIM14 in miR-191-5p-mimic-treated cells can rescue the inhibition of proliferation and invasion caused by miR-191-5p mimics.

DISCUSSION

The hypoxic microenvironment widely exists in solid tumors, which is mainly due to the increased oxygen consumption and decreased oxygen supply caused by microenvironmental obstacles and abnormal functions of tumor blood vessels (Patel and Sant, 2016). In colon cancer, hypoxia induces the production of vascular endothelial growth factor (VEGF), which initiates tumor angiogenesis (Kim et al., 2015; Kawczyk-Krupka et al., 2018). However, due to the abnormality structure of the blood vessels, the tumor hypoxia persists. In the hypoxic microenvironment, colon cancer cells undergo a series of biochemical changes in response to hypoxia, including enhanced anaerobic glycolysis and increased protective stress proteins, which include specific cytokines and growth factors, such as erythropoietin, VEGF glycolytic enzymes, and transcription factors AP-1, NFKB, and HIF1 (Vasilevskaya et al., 2008; Gombos et al., 2011; Ni et al., 2017; Vadde et al., 2017). These factors regulate the function of colon cancer cells by regulating the expression of downstream targets (Costa et al., 2017; Chen et al., 2018a). For example, HIF1-α activates p21 transcription, which blocks the interaction between VHL and HIF1 α, then inhibits the interpretation of HIF1 α, forms a positive feedback regulatory loop, and finally promotes cell growth of colon cancer (Yang et al., 2014).

In the present research, we found that cell hypoxia significantly increased the expression of ELFN1-AS1. Hypoxia promoted proliferation and invasion and inhibited the apoptosis of colon cancer cells. Knocking down ELFN1-AS1 under hypoxic conditions significantly reduced cell proliferation and invasion and increased apoptosis significantly. The specificity and limited dosage of ELFN1-AS1 siRNA avoided the apoptosis caused by excessive siRNA mediated off-target effects. In addition, knockdown of ELFN1-AS1 in conventionally cultured colon cancer cells effectively inhibited cell growth and invasion. These results indicate that ELFN1-AS1 may be a promoter of abnormal proliferation of colon cancer cells and operates as a target in the hypoxic response of tumor cells. At present, ELFN1-AS1 has been found to be upregulated in esophageal cancer and facilitates esophageal cancer progression (Zhang et al., 2019). It is

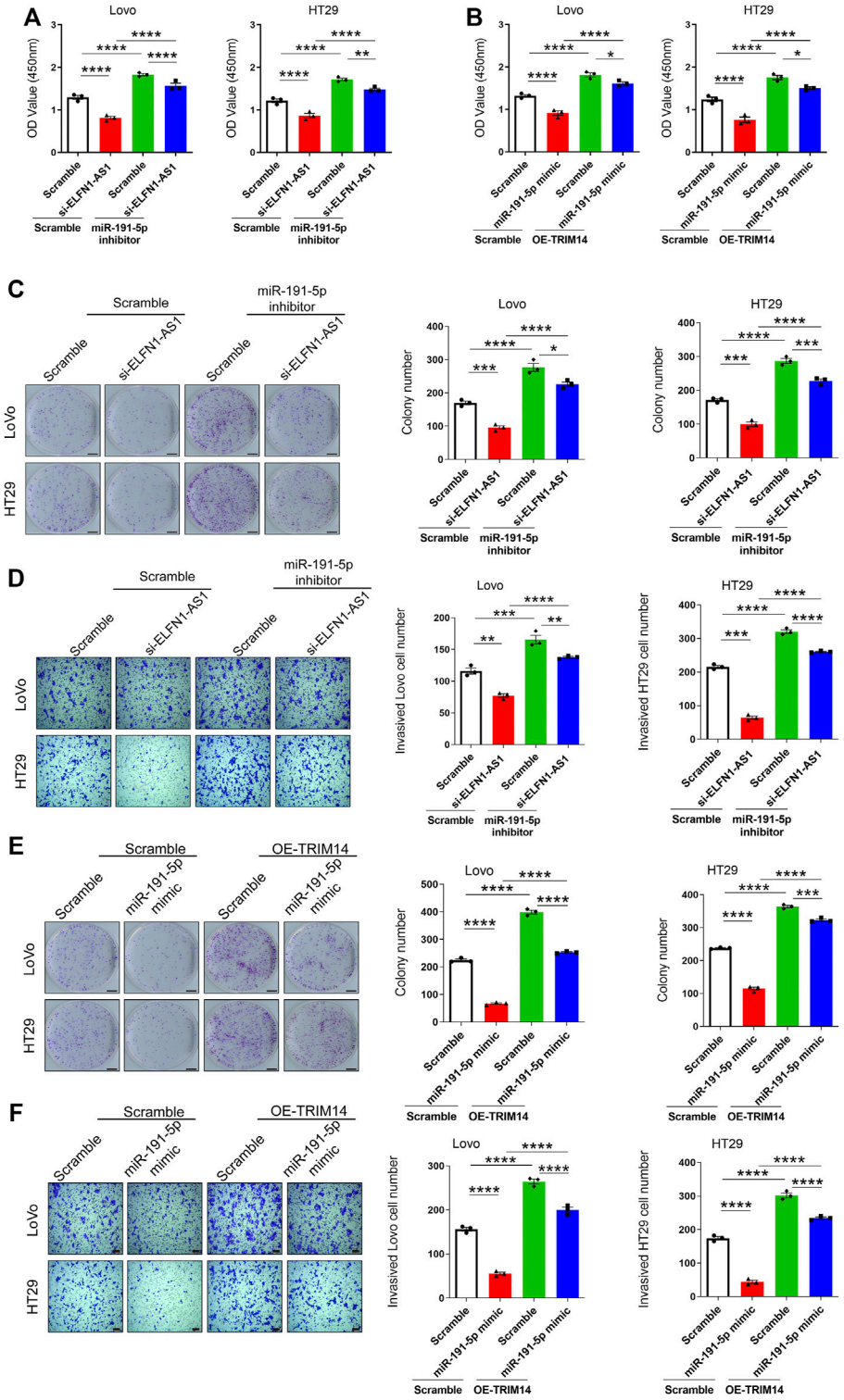

FIGURE 5 | Knockdown of ELFN1-AS1 inhibited the proliferation and invasion by regulating the expression of TRIM14 by targeting miR-191-5p. **(A)** and **(B)** Cell viability was detected using CCK8 assay. **(C)** Colony formation assay was performed to determine the proliferation of LoVo and HT29 cells. The photo of the plates was taken after 14 days of incubation. The colony number of each group was counted in five random fields. Scale bar 5 mm. **(D)** Transwell assay was performed to detect the invasion of each group. After 24 h of culture in matrigel chambers, cells were photographed under a microscope at ×100 magnification. The number of invasive cells was counted in three random fields. Scale bar 100 μ. **(E)** Colony formation assay was performed to determine the proliferation of LoVo and HT29 cells. Scale bar 5 mm. **(F)** Transwell assay was performed to detect the invasion of each group. Scale bar 100 μ. One-way ANOVA was used for the comparison between the multiple groups with Bonferroni as a post hoc test. All data were representative of three independent experiments. *$p < 0.05$; **$p < 0.01$; ***$p < 0.001$; ****$p < 0.0001$.

also reported to be highly expressed in colon cancer and can predict the prognosis of patients (Dong et al., 2019; Chen et al., 2020). However, our understanding of the role and mechanism of ELFN1-AS1 in tumors is still limited.

We found that ELFN1-AS1 was distributed in the cytoplasm and nucleus of colon cancer cells, suggesting that it might operate as ceRNA in the cytoplasm. CeRNAs regulate gene expression by competing with miRNAs and are widely involved in the regulation of tumor growth, metastasis, recurrence, and drug resistance (Salmena et al., 2011; Qi et al., 2015; Wang et al., 2016). In the present study, we demonstrated that ELFN1-AS1, as a ceRNA, competitively adsorbed miR-191-5p to promote the expression of TRIM14 through bioinformatics analysis and cell line verification.

According to current research, miR-191-5p exerts a tumor-suppressive role in lung adenocarcinoma, COAD, and renal cell carcinoma (Chen et al., 2018b; Chen et al., 2018c; Zhou et al., 2020). Chen et al. report that the miR-191-5p level is negatively associated with PD-L1 expression and predicts overall survival (OS) as an independent prognostic factor in COAD (Chen et al., 2018b). However, the downstream targets of miR-191-5p in colon cancer have not been reported. According to our research, overexpression of miR-191-5p inhibited the expression of TRIM14 in LoVo and HT29 cells. TRIM14, as a member of the trim family, has been proved to be upregulated in breast cancer, hepatocellular carcinoma, and oral squamous cell carcinoma and can regulate tumor biological behavior through a variety of signaling pathways (Chen et al., 2016; Wang et al., 2017a; Dong and Zhang, 2018; Hu et al., 2019). Studies have shown that TRIM14 can be regulated by different miRNAs in different tumors. For example, TRIM14 is inhibited by miR-15b and enhances cancer-initiating cell phenotypesoral in tongue squamous cell cancer (Wang et al., 2017b). MiR-195-5p can downregulate the expression of TRIM14 and then promote the progression of gastric cancer by regulating the epithelial–mesenchymal transition process (Wang et al., 2018). In a recent study, TRIM14 is reported to promote migration and invasion by regulating sphingosine kinase 1 (SPHK1) and phosphorylated STAT3 (p-STAT3) in CRC cells (Jin et al., 2018). However, due to the limitations of the experiment, the demonstration of direct ceRNA interactions in this study is limited to a single gene. In a huge ceRNA network, a single lncRNA or miRNA can target numerous genes. Therefore, other miRNAs and genes detected in this study may be potential targets of ELFN1-AS1, and their role remains to be further studied.

In addition, our results showed that HIF1 α was overexpressed under hypoxia in a time-dependent manner. HIF1 α is the main mediator of cell adaptation to hypoxia. In the hypoxic environment, it can enhance the transcription of hypoxia-induced genes and produce a series of physiological effects (Soni and Padwad, 2017; Pezzuto and Carico, 2018). However, we did not explore the effect of intermediate targets of HIF1 α on the resulting ELFN1-AS1/miR-191-5p/TRIM14 pathway, which will be our interest in further study.

In conclusion, ELFN1-AS1 operates as a downstream target of hypoxia to promote proliferation and invasion through upregulating TRIM14 by sponging miR-191-5p in colon cancer cells. Our results enrich the regulatory network of ceRNA and provide potential targets for the clinical treatment of colon cancer.

DATA AVAILABILITY STATEMENT

The original contributions presented in the study are included in the article/Supplementary Material, further inquiries can be directed to the corresponding author.

AUTHOR CONTRIBUTIONS

XJ and LD performed the experiments. XJ analyzed the data and wrote the paper. SS, AN, JW, and YW assisted with the experiments and data analysis. CW helped modify the paper. All authors have edited and approved the final manuscript.

FUNDING

This work was supported by the National Natural Science Foundation of China (no. 81801163), the Doctor Fund of Shandong Natural Science Foundation (no. ZR201807060846), and the China Postdoctoral Science Foundation (no. 2018M640636).

REFERENCES

Chen, J. T., Liu, C. C., Yu, J. S., Li, H. H., and Lai, M. C. (2018). Integrated Omics Profiling Identifies Hypoxia-Regulated Genes in HCT116 colon Cancer Cells. *J. Proteomics* 188, 139–151. doi:10.1016/j.jprot.2018.02.031

Chen, M., Fan, M., Yang, J., and Lang, J. (2020). Identification of Potential Oncogenic Long Non-coding RNA Set as a Biomarker Associated with Colon Cancer Prognosis. *J. Environ. Pathol. Toxicol. Oncol.* 39 (1), 39–49. doi:10.1615/JEnvironPatholToxicolOncol.2020032351

Chen, M., Meng, Q., Qin, Y., Liang, P., Tan, P., He, L., et al. (2016). TRIM14 Inhibits cGAS Degradation Mediated by Selective Autophagy Receptor P62 to Promote Innate Immune Responses. *Mol. Cel* 64 (1), 105–119. doi:10.1016/j.molcel.2016.08.025

Chen, P., Pan, X., Zhao, L., Jin, L., Lin, C., Quan, J., et al. (2018). MicroRNA-191-5p Exerts a Tumor Suppressive Role in Renal Cell Carcinoma. *Exp. Ther. Med.* 15 (2), 1686–1693. doi:10.3892/etm.2017.5581

Chen, X. Y., Zhang, J., Hou, L. D., Zhang, R., Chen, W., Fan, H. N., et al. (2018). Upregulation of PD-L1 Predicts Poor Prognosis and Is Associated with miR-191-5p Dysregulation in colon Adenocarcinoma. *Int. J. Immunopathol Pharmacol.* 32, 2058738418790318. doi:10.1177/2058738418790318

Costa, V., Lo Dico, A., Rizzo, A., Rajata, F., Tripodi, M., Alessandro, R., et al. (2017). MiR-675-5p Supports Hypoxia Induced Epithelial to Mesenchymal Transition in colon Cancer Cells. *Oncotarget* 8 (15), 24292–24302. doi:10.18632/oncotarget.14464

Dienstmann, R., Salazar, R., and Tabernero, J. (2015). Personalizing colon Cancer Adjuvant Therapy: Selecting Optimal Treatments for Individual Patients. *J. Clin. Oncol.* 33 (16), 1787–1796. doi:10.1200/JCO.2014.60.0213

Dong, B., and Zhang, W. (2018). High Levels of TRIM14 Are Associated with Poor Prognosis in Hepatocellular Carcinoma. *Oncol. Res. Treat.* 41 (3), 129–134. doi:10.1159/000485625

Dong, L., Ding, C., Zheng, T., Pu, Y., Liu, J., Zhang, W., et al. (2019). Extracellular Vesicles from Human Umbilical Cord Mesenchymal Stem Cells Treated with siRNA against ELFN1-AS1 Suppress colon Adenocarcinoma Proliferation and Migration. *Am. J. Transl Res.* 11 (11), 6989–6999.

Gombos, Z., Danihel, L., Repiska, V., Acs, G., and Furth, E. (2011). Expression of Erythropoietin and its Receptor Increases in Colonic Neoplastic Progression: the Role of Hypoxia in Tumorigenesis. *Indian J. Pathol. Microbiol.* 54 (2), 273–278. doi:10.4103/0377-4929.81591

Hu, G., Pen, W., and Wang, M. (2019). TRIM14 Promotes Breast Cancer Cell Proliferation by Inhibiting Apoptosis. *Oncol. Res.* 27 (4), 439–447. doi:10.3727/096504018X15214994641786

Jin, Z., Li, H., Hong, X., Ying, G., Lu, X., Zhuang, L., et al. (2018). TRIM14 Promotes Colorectal Cancer Cell Migration and Invasion through the SPHK1/STAT3 Pathway. *Cancer Cel Int* 18, 202. doi:10.1186/s12935-018-0701-1

Jing, X., Yang, F., Shao, C., Wei, K., Xie, M., Shen, H., et al. (2019). Role of Hypoxia in Cancer Therapy by Regulating the Tumor Microenvironment. *Mol. Cancer* 18 (1), 157. doi:10.1186/s12943-019-1089-9

Kawczyk-Krupka, A., Kwiatek, B., Czuba, Z. P., Mertas, A., Latos, W., Verwanger, T., et al. (2018). Secretion of the Angiogenic Factor VEGF after Photodynamic Therapy with ALA under Hypoxia-like Conditions in colon Cancer Cells. *Photodiagnosis Photodyn Ther.* 21, 16–18. doi:10.1016/j.pdpdt.2017.10.020

Kim, D. H., Sung, B., Kang, Y. J., Hwang, S. Y., Kim, M. J., Yoon, J. H., et al. (2015). Sulforaphane Inhibits Hypoxia-Induced HIF-1α and VEGF Expression and Migration of Human colon Cancer Cells. *Int. J. Oncol.* 47 (6), 2226–2232. doi:10.3892/ijo.2015.3200

Liu, J. X., Li, W., Li, J. T., Liu, F., and Zhou, L. (2018). Screening Key Long Non-coding RNAs in Early-Stage colon Adenocarcinoma by RNA-Sequencing. *Epigenomics* 10 (9), 1215–1228. doi:10.2217/epi-2017-0155

Manoochehri Khoshinani, H., Afshar, S., and Najafi, R. (2016). Hypoxia: A Double-Edged Sword in Cancer Therapy. *Cancer Invest.* 34 (10), 536–545. doi:10.1080/07357907.2016.1245317

Ni, T., He, Z., Dai, Y., Yao, J., Guo, Q., and Wei, L. (2017). Oroxylin A Suppresses the Development and Growth of Colorectal Cancer through Reprogram of HIF1α-Modulated Fatty Acid Metabolism. *Cell Death Dis* 8 (6), e2865. doi:10.1038/cddis.2017.261

Paraskevopoulou, M. D., Vlachos, I. S., and Hatzigeorgiou, A. G. (2016). DIANA-TarBase and DIANA Suite Tools: Studying Experimentally Supported microRNA Targets. *Curr. Protoc. Bioinformatics* 55, 12–18. doi:10.1002/cpbi.12

Patel, A., and Sant, S. (2016). Hypoxic Tumor Microenvironment: Opportunities to Develop Targeted Therapies. *Biotechnol. Adv.* 34 (5), 803–812. doi:10.1016/j.biotechadv.2016.04.005

Pezzuto, A., and Carico, E. (2018). Role of HIF-1 in Cancer Progression: Novel Insights. A Review. *Curr. Mol. Med.* 18 (6), 343–351. doi:10.2174/1566524018666181109121849

Polev, D. E., Karnaukhova, I. K., Krukovskaya, L. L., and Kozlov, A. P. (2014). ELFN1-AS1: a Novel Primate Gene with Possible microRNA Function Expressed Predominantly in Human Tumors. *Biomed. Res. Int.* 2014, 398097. doi:10.1155/2014/398097

Qi, X., Zhang, D. H., Wu, N., Xiao, J. H., Wang, X., and Ma, W. (2015). ceRNA in Cancer: Possible Functions and Clinical Implications. *J. Med. Genet.* 52 (10), 710–718. doi:10.1136/jmedgenet-2015-103334

Salmena, L., Poliseno, L., Tay, Y., Kats, L., and Pandolfi, P. P. (2011). A ceRNA Hypothesis: the Rosetta Stone of a Hidden RNA Language? *Cell* 146 (3), 353–358. doi:10.1016/j.cell.2011.07.014

Siegel, R., Naishadham, D., and Jemal, A. (2013). Cancer Statistics, 2013. *CA Cancer J. Clin.* 63 (1), 11–30. doi:10.3322/caac.21166

Soni, S., and Padwad, Y. S. (2017). HIF-1 in Cancer Therapy: Two Decade Long story of a Transcription Factor. *Acta Oncol.* 56 (4), 503–515. doi:10.1080/0284186X.2017.1301680

Tang, Z., Li, C., Kang, B., Gao, G., Li, C., and Zhang, Z. (2017). GEPIA: a Web Server for Cancer and normal Gene Expression Profiling and Interactive Analyses. *Nucleic Acids Res.* 45 (W1), W98–w102. doi:10.1093/nar/gkx247

Vadde, R., Vemula, S., Jinka, R., Merchant, N., Bramhachari, P. V., and Nagaraju, G. P. (2017). Role of Hypoxia-Inducible Factors (HIF) in the Maintenance of Stemness and Malignancy of Colorectal Cancer. *Crit. Rev. Oncol. Hematol.* 113, 22–27. doi:10.1016/j.critrevonc.2017.02.025

Vasilevskaya, I. A., Selvakumaran, M., and O'Dwyer, P. J. (2008). Disruption of Signaling through SEK1 and MKK7 Yields Differential Responses in Hypoxic colon Cancer Cells Treated with Oxaliplatin. *Mol. Pharmacol.* 74 (1), 246–254. doi:10.1124/mol.107.044644

Wang, F., Ruan, L., Yang, J., Zhao, Q., and Wei, W. (2018). TRIM14 Promotes the Migration and Invasion of Gastric Cancer by Regulating Epithelial-to-mesenchymal T-ransition via A-ctivation of AKT S-ignaling R-egulated by miR-195-5p. *Oncol. Rep.* 40 (6), 3273–3284. doi:10.3892/or.2018.6750

Wang, T., Ren, Y., Liu, R., Ma, J., Shi, Y., Zhang, L., et al. (2017). miR-195-5p Suppresses the Proliferation, Migration, and Invasion of Oral Squamous Cell Carcinoma by Targeting TRIM14. *Biomed. Res. Int.* 2017, 7378148. doi:10.1155/2017/7378148

Wang, X., Guo, H., Yao, B., and Helms, J. (2017). miR-15b Inhibits Cancer-Initiating Cell Phenotypes and Chemoresistance of Cisplatin by Targeting TRIM14 in Oral Tongue Squamous Cell Cancer. *Oncol. Rep.* 37 (5), 2720–2726. doi:10.3892/or.2017.5532

Wang, Y., Hou, J., He, D., Sun, M., Zhang, P., Yu, Y., et al. (2016). The Emerging Function and Mechanism of ceRNAs in Cancer. *Trends Genet.* 32 (4), 211–224. doi:10.1016/j.tig.2016.02.001

Yang, F., Zhang, H., Mei, Y., and Wu, M. (2014). Reciprocal Regulation of HIF-1α and lincRNA-P21 Modulates the Warburg Effect. *Mol. Cel* 53 (1), 88–100. doi:10.1016/j.molcel.2013.11.004

Zhang, C., Lian, H., Xie, L., Yin, N., and Cui, Y. (2019). LncRNA ELFN1-AS1 Promotes Esophageal Cancer Progression by Up-Regulating GFPT1 via Sponging miR-183-3p. *Biol. Chem.* 401 (9), 1053–1061. doi:10.1515/hsz-2019-0430

Zhou, L. Y., Zhang, F. W., Tong, J., and Liu, F. (2020). MiR-191-5p Inhibits Lung Adenocarcinoma by Repressing SATB1 to Inhibit Wnt Pathway. *Mol. Genet. Genomic Med.* 8 (1), e1043. doi:10.1002/mgg3.1043

Conflict of Interest: The authors declare that the research was conducted in the absence of any commercial or financial relationships that could be construed as a potential conflict of interest.

Publisher's Note: All claims expressed in this article are solely those of the authors and do not necessarily represent those of their affiliated organizations or those of the publisher, the editors, and the reviewers. Any product that may be evaluated in this article or claim that may be made by its manufacturer is not guaranteed or endorsed by the publisher.

Advantages of publishing in Frontiers

OPEN ACCESS
Articles are free to read for greatest visibility and readership

FAST PUBLICATION
Around 90 days from submission to decision

HIGH QUALITY PEER-REVIEW
Rigorous, collaborative, and constructive peer-review

TRANSPARENT PEER-REVIEW
Editors and reviewers acknowledged by name on published articles

Frontiers
Avenue du Tribunal-Fédéral 34
1005 Lausanne | Switzerland

Visit us: www.frontiersin.org
Contact us: frontiersin.org/about/contact

REPRODUCIBILITY OF RESEARCH
Support open data and methods to enhance research reproducibility

DIGITAL PUBLISHING
Articles designed for optimal readership across devices

FOLLOW US
@frontiersin

IMPACT METRICS
Advanced article metrics track visibility across digital media

EXTENSIVE PROMOTION
Marketing and promotion of impactful research

LOOP RESEARCH NETWORK
Our network increases your article's readership